Complexity

Public Policy Modeling and Applications

Lead Guest Editor: Miguel Fuentes
Guest Editors: Claudio J. Tessone and Bernardo A. Furtado

Public Policy Modeling and Applications

Complexity

Public Policy Modeling and Applications

Lead Guest Editor: Miguel Fuentes
Guest Editors: Claudio Tessone and Bernardo A. Furtado

Editorial Board

Contents

Hindawi
Complexity
Volume 2019, Article ID 4128703, 4 pages
https://doi.org/10.1155/2019/4128703

Editorial

Public Policy Modeling and Applications

Miguel A. Fuentes,[1,2,3] **Claudio J. Tessone**,[4] **and Bernardo A. Furtado**[5,6]

[1]*Santa Fe Institute, 1399 Hyde Park Road, Santa Fe, NM, 87501, USA*
[2]*Instituto de Investigaciones Filosóficas, Bulnes 642, Buenos Aires 1176, Argentina*
[3]*Facultad de Ingeniería y Tecnología, Universidad San Sebastián, Lota 2465, Santiago 7510157, Chile*
[4]*URPP Social Networks, Universität Zürich, Zürich CH-8050, Switzerland*
[5]*Department of Innovation and Infrastructure, Institute for Applied Economic Research, Brasília 70076-900, Brazil*
[6]*National Council of Research, Brasília, Brazil*

Correspondence should be addressed to Miguel A. Fuentes; fuentesmig@gmail.com

Received 27 January 2019; Accepted 27 January 2019; Published 17 February 2019

This special issue brings 18 papers on applied policy modeling where the complex nature of the systems (and intervention techniques) plays a significant role. The issue covers a range of applications from crime, finance and trade, infrastructure, and engineering to health policies. In order to tackle these multifaceted problems, a plethora of methodologies is used: extended econometric approaches, large-scale simulations, and theoretical models for which some results can be derived analytically. This highlights the difficulty of the tasks and the lack of standardized approaches, which also may be seen in a good light as it pinpoints the wide background of the scholars that are approaching these problems. We argue that the current issue gives a good overview of the challenges to be addressed and how the state-of-the-art deals with them. As a final remark, it is worth noticing that the following list of papers is sorted only based on topics—without any underlying judgment.

The special issue opens up with the work by the Guest Editors: "Policy Modeling and Applications: State-of-the-Art and Perspectives." This review focuses on methodologies that are, arguably, at the core of the complex systems science: agent-based modeling, network models, dynamical systems, data mining, and evolutionary game theory. The view of all the chosen methodologies is presented having in mind public policy applications. They illustrate specific experiences of large applied projects in macroeconomics, urban systems, and infrastructure planning.

Two expected results of public policies are fostering economic development and show adaptive capacity in case of disruptions. The latter is linked to the concept of *resilience*. In the research paper by G. Castañeda and O. A. Guerrero, "the Resilience of Public Policies in Economic Development," the authors analyze how the adaptive capacity of the policy-making process generates resilience in the face of disruptions. Further, they develop a computational model, which takes into account different social mechanisms (coevolutionary learning and complex interaction networks) to compute a resilience score against simulated disruptions to the expected evolution. Interestingly, they show that certain policy issues are resilient and others fragile, depending on the context of application.

This special issue also brings two papers that focus explicitly on applied policy from a complex systems perspective. The first—"Infrastructure as a Complex Adaptive System"—by E. J. Oughton et al. advocates the need to coordinate govern planning considering interdependencies among infrastructure sectors. The second paper—"A Case Study of Complex Policy Design"—by Buzuku et al. reinforces the need to integrate policy analysis. The authors of the latter propose methodological steps that should guarantee a systematic analysis that covers the space of possibilities paving optimal paths for policymakers.

The paper by E. J. Oughton et al. makes a case that infrastructure sectors are increasingly becoming more integrated in tandem with advances in digital and technological

enhancements. Further, the authors describe the pervasive effects of the lack of intertwined infrastructure planning over social and economic issues. This description is in tune with the concepts of complex adaptive systems (CAS), mainly, its multitude of decentralized decision-making agents, its emergent phenomena characteristics, and its networked, dynamic connections. The paper then details each feature of systems locking together properties of CAS and infrastructure. Finally, E. J. Oughton et al. illustrate the analysis of the applied version of their system-of-systems to a case study of the United Kingdom. They identify the key decision-makers across government bodies and list four necessary metrics to consider about each sector to foster integration. A family of models under the NISMOD umbrella functions as the coordinator of the systems aiming specifically at long-term planning, risk, and vulnerability analysis and the prevention of cascading failures within extreme events. The paper concludes with a critical review of its contributions and the limitations of the proposal.

The paper by S. Buzuku et al., in turn, advocates systems integrated analysis via creative and analytical methods applied in sequence. The authors claim that so-called wicked problems demand a prior phase of complex understanding before applying optimal analytics. Hence, when the space of possibilities is intractable, systemic methods may contribute to problem-solving. S. Buzuku et al. proposed method combines General Morphological Analysis (GMA) to Design Structure Matrix (DSM) along with an embedded sensitivity analysis and a cross-consistency assessment to enhance goal-oriented policy design. The paper applies the proposed method to a case study of a large industrial wastewater treatment plant in Brazil. The authors claim that the tool systematically served the purpose of guiding and facilitating the process of decision-making among stakeholders and experts. Limitations included the difficult iterative learning process experienced by theme experts and the lack of priority for cluster of resulting policies suggested at the outcome of the process.

The special issue also depicts two agent-based models (ABM) that evaluate details of policy performance features. Both papers try to illuminate and anticipate the response societal groups are more likely to display factoring in internal social mechanisms.

A. Székely et al. present "Countering Protection Rackets Using Legal and Social Approaches: An Agent-Based Test," in which they balance benefits of strong legal measures against coordinated social approaches but also a combination of both. In fact, the authors claim to consider and integrate influence from *Homo Sociologicus* and *Homo Economicus* alike. In the model, the notion of the 'salience of a norm' and its measurement along with a calibration process help make it more theoretically and empirically grounded. In short, the agents of the model are the State (implementing legislation) and the NGO (fostering social norms) acting upon the core, complex-behavior duet of entrepreneur and consumers within the Mafia influence. Validation is achieved via participatory modeling but also through comparative historical data analysis. Although not definitive, results suggest that a combination of legal and social approaches is socially preferable.

H. I. Brugger et al. also investigate features of alternative policy scenarios within (income) groups in "Equity of Incentives: Agent-Based Explorations of How Social Networks Influence the Efficacy of Programs to Promote Solar Adoption." Rather than observing overall increase in solar photovoltaic (PV) adoption, the paper emphasizes unequal distribution of adopters given by segregated network effects. The model theoretically tests different structures of influence on the next adopter. Thus, four alternatives of incentives are tested against extreme levels (low and high) of network segregation. Feed-in tariff keeps fixed rates for energy that is fed into the grid; leasing equipment comes from third parties; and seeding supports initial adopters in given neighborhoods. Alternatively, there is also a comparison with zero incentives. Among the tested cases, feed-in tariffs were the one found to produce larger inequalities among consumers, whereas leasing is in pair with the scenario with no incentive. The author strengthens the argument that underlying network structures may be relevant when designing policy.

The work by R. Azghandi et al., "Minimization of Drug Shortages in Pharmaceutical Supply Chains: A Simulation-Based Analysis of Drug Recall Patterns and Inventory Policies," studies, using a mathematical model, the pharmaceutical supply chain in order to understand the behavior of the drug shortages under different disruption patterns. This problem is of relevance to public policy as it must, in principle, ensure that any drug is available to patients at healthcare centers. This is a problem that official healthcare administrators and other stakeholders of supply chains continue to face. The authors use a mix of simulation modeling and data envelopment analysis approaches.

From a policy and regulatory point of view, understanding the characteristics and instabilities brought by the financial interrelations between variegated actors is fundamental. These interrelations can be represented in terms of a *financial network*. Contrary to stylized models in the former literature, such networks exhibit a nontrivial topology. Their characterization is fundamental, as it is the study of economic processes over them. In Y. Tang et al., "Complexities in Financial Network Topological Dynamics: Modeling of Emerging and Developed Stock Markets," the authors study the interplay between the topological structure of the price correlation network and the emergent market behavior. In their paper, they analyze the stock markets of the two largest world economies (China and USA), unveiling fundamentally different properties in the two stock markets, as also revealed by price movements. While the paper discusses portfolio applications, the authors call for the interpretation from the policy-making point of view.

In this special issue, another agent-based model is introduced to study a specific financial network: that of the interbank exposures. In this setup S. Davidovic et al., in "Liquidity Hoarding in Financial Networks: The Role of Structural Uncertainty," study the dynamics of confidence in the presence of different kinds of shocks. The model is microfounded including the balance sheet of the bank. Interestingly, the authors study the spreading of local impacts

in confidence in cases such as sudden shocks, leading to the system breakdown. With respect to policy-making, the results suggest the importance of rapid bailouts and the need for regulation designed to improve overall transparency in the financial system.

In a similar direction, the problem of fund investment is tackled by X. Yue and X. Sue, in "A Novel Decision-Making Approach to Fund Investments Based on Multigranulation Rough Set." In this paper, a multigranulation rough set decision method is used to construct the fund investment decision information system; then, the fund investment decision information system is reduced at different thresholds, the decision rules are extracted by reduction and the rules are analyzed, and finally the decision rules are given using fund investment.

In a somewhat different venue of research, G.-Y. Shi et al. analyze the stable marriage problem (SMP) and propose a theoretical generalized form for SMP, along with average happiness achieved. Indeed, the paper "Instability in Stable Marriage Problem: Matching Unequally Numbered Men and Women" focuses on the application of GSMP for unequal sized matching groups. The GSMP could be applied to any matching problems such as clients and servers, peers in a P2P network or, more generally, allocation of limited resources across interested users. Their results suggest that the advantages of the active side are typically observed on the Gale-Shapley algorithm reverses on the GSMP when the active side has a higher number of individuals. Further, GSMP suggests that results are highly sensitive to group size.

In a related research line, Y.-X. Kong et al. in "Competition May Increase Social Utility in Bipartite Matching Problem" study again the stable marriage problem and in the context of competition (instead of random matching, as in the original Gale-Shapley formulation). In this context, they introduce a global measure for the social utility. Interestingly, they find that, under this condition, competition increases the overall social utility. They also show imbalances in the size of the two groups can change dramatically with respect to the symmetric case.

In "Congenital and Blood Transfusion Transmission of Chagas Disease: A Framework Using Mathematical Modeling" E. Ramalho et al. study the dynamics of Chagas disease in cases where there is no vector. The importance of this case can be understood in the mobility from places with such vectors, for example, Latin America, to places like Europe. The authors use a ODE-model in order to evaluate the epidemiological effect of control measures. It was applied to demographic data from Spain and sensitivity analysis was performed on model parameters associated with control strategies.

N. M. R. Ahmad et al., in "Analyzing Policymaking for Tuberculosis Control in Nigeria," study one of the major causes of death by an infectious disease worldwide. The authors focus on the tuberculosis control in Nigeria. Using a sophisticated mathematical model they aim to analyze effective strategies that could be used in policy-making to effectively reduce Tuberculosis.

M. Jovanovic et al. in "SOSerbia: Android-Based Software Platform for Sending Emergency Messages" present a platform used in smartphone devices to be used in emergency situation. This platform is experimentally used as a part of the emergency response center at the Ministry of Interior of the Republic of Serbia. In their work they empirically demonstrate how the treatment of complex information in coordination with public forces can be of use in order to be more effective when applying public policy.

K. Yoo and S. Blumsack analyze "the Political Complexity of Regional Electricity Policy Formation." The authors focus on a very important aspect of energy supply: any technological change in electric power systems required from one part physical systems adapts to integrate new technologies and market players but also policies and rules adapt to support that technological integration.

The products produced, imported, and exported by a given country determine its profile. Different representations are possible of this world trade network. It found in the last decade that such profile largely determines the development of nations. Conversely, the set of nations that produce, import, or export specific products are indicators of the complexity involved in its production. In the last years, a wealth of studies has delved into this research direction. In policy-making, prediction is helpful as it can help practitioners to solve practical problems and advise meaningful strategies for the future. In the special issue, H. Liao et al. "Enhancing Countries' Fitness with Recommender Systems on the International Trade Network" analyze the export data of countries within the World trade. They introduce a methodology akin to recommender systems to identify products that correspond to the production capacity of countries, which are however overlooked by them. By a minimalistic modeling they simulate the evolution of country's fitness if changes in the product profile of the country are changed, following the policy recommendation. Interestingly, the recommendation seems to capture the countries' technological evolution by making correct out-of-sample predictions of different economic indicators.

In a related line of research, M.-Y. Zhou et al., in "Quantifying the Robustness of Countries' Competitiveness by Network-Based Methods," deal with quantifying the robustness of countries to fluctuating economic conditions. The long-term aim is to provide policy-makers with indicators of fragility that allow for construction of efficient policies to overcome it. Specifically, the authors develop indicators to characterize the robustness (or stability, as they frame it) of countries against unexpected economic recessions. They resort to different approaches (the celebrated Fitness-Complexity approach and a method of reflections). Interestingly, they find that the characterization through Fitness-Complexity yields countries which have strong robustness against economic crises.

We—as Editors—are glad to have been able to put together a relevant number of papers, from a wide spectrum of disciplines—from economics to sociology and from physics to medicine and engineering—and traditions to a united core of applied policy modeling environment. Clearly, network, agent-based modeling, and mathematical simulations come to fore as preferable tools of the craft. Much is yet to be discussed, mainly, from our perspective, validation,

replication, and comparative studies. We hope you enjoy the diverse contents and methods that are represented in the following collection.

Conflicts of Interest

The authors declare that there are no conflicts of interest regarding the publication of this paper. The editors declare that they have no conflicts of interest regarding the publication of this special issue.

Acknowledgments

Claudio J. Tessone acknowledges the funding provided by the University of Zurich through the University Research Program Social Networks.

Miguel A. Fuentes
Claudio J. Tessone
Bernardo A. Furtado

Hindawi
Complexity
Volume 2019, Article ID 4349823, 15 pages
https://doi.org/10.1155/2019/4349823

Research Article

Equity of Incentives: Agent-Based Explorations of How Social Networks Influence the Efficacy of Programs to Promote Solar Adoption

Heike I. Brugger[1] **and Adam Douglas Henry**[2]

[1]*Fraunhofer ISI, Karlsruhe, Germany*
[2]*University of Arizona, Tucson, AZ, USA*

Correspondence should be addressed to Heike I. Brugger; heike.brugger@isi.fraunhofer.de

Received 19 May 2018; Revised 2 October 2018; Accepted 13 December 2018; Published 3 February 2019

Guest Editor: Miguel Fuentes

Agent-based models are used to explore how social networks influence the effectiveness of governmental programs to promote the adoption of solar photovoltaics (solar PV) by residential households. This paper examines how a common characteristic of social networks, known as network segregation, can dampen the indirect benefits of solar incentive programs that arise from peer effects. Peer effects cause an agent to be more likely to adopt a technology if they are socially connected to other adopters. Due to network segregation, programs that target relatively affluent agents can generate rapid increases in overall adoption levels but at the cost of increasing disparities in access to solar technology between rich and poor communities. These dynamics are explored through theoretical agent-based models of solar adoption within hypothetical social systems. The effectiveness of three types of solar incentive programs, the feed-in tariff, leasing programs, and seeding programs, is explored. Even though these programs promote rapid adoption in the short term, results demonstrate that network segregation can create serious distributional justice problems in the long term for some programs. The distributional justice effects are particularly severe with the feed-in tariff. Overall, this paper provides an illustration of how agent-based models may be used to evaluate and experiment with policy interventions in a virtual space, which enhances the scientific basis of policymaking.

1. Introduction

This paper uses agent-based models (ABM) to evaluate the effectiveness of public policies to promote the adoption of alternative energy technologies by residential households. Of particular interest is the adoption of rooftop solar photovoltaics (PV), or solar panels, which convert sunlight falling on one's rooftop into electricity. Solar PV is one example of a decentralized energy technology with great potential for reducing a given region's dependence on fossil fuels and can therefore contribute positively to sustainability [1]. At the same time, solar PV has a long way to go. Even in markets where rooftop solar is prevalent, such as in Germany and in California, USA, overall market penetration is relatively small [2, 3]. For individuals, solar PV systems represent large investments and carry with them risk and uncertainty. It is in reducing these risks and up-front costs that incentives to install residential solar systems can help promote more widespread adoption and commensurate decarbonization of energy systems.

These considerations underscore the need for public policies that incentivize more widespread interest and adoption of solar PV. While incentive programs come in many shapes and sizes, the essential logic of an incentive program is that it will reduce barriers to adoption for direct recipients of a program benefit, such as those agents that receive tax credits or other subsidies for installing solar PV. Incentive programs also create indirect benefits through peer effects—a phenomenon whereby the adoption behavior of agents increases the probability that other agents in the system will adopt (see, e.g., the diffusion model by [4]). Peer effects work through a variety of mechanisms, such as the exertion of

social influence on nonadopters (e.g., [5, 6]) and the provision of new information about the true costs and benefits of solar through active communication with solar adopters (e.g., [7–9]).

Thus beneficiaries of governmental incentive programs can, through their adoption behavior, increase the probability that other actors in the system will also adopt. At the same time, however, peer effects are naturally limited to a certain group of people around an adopter. Certain incentive programs may perform well in terms of promoting greater distributional energy justice through supporting PV adoption specifically by low-income households, thus increasing the number of social multipliers who put the peer effect into action within this group. Other incentives systematically target more affluent households and thus might increase injustice by spurring a peer effect in a group with less need for a given technology.

In this way, public policies meant to promote solar adoption may create inequalities in the adoption of solar between disparate social groups. These potential inequities are ignored in most formal evaluation of energy policy, which tends to focus on the overall penetration of solar PV, that is, the aggregate number of people who have adopted in a given region. And yet, understanding inequality in access to renewable energy is a crucial research need ([10]; [11, 179]; [12, 435]). This is important in part because solar PV technology carries more than just environmental benefits. Solar PV can also create significant cost savings for households, helping them to be less vulnerable to energy rate increases and fluctuations in availability. Depending on local policies, rooftop solar can even create a revenue stream for households as they sell surplus electricity back to the energy utility. However, these benefits accrue in the long term and becoming a PV adopter generally requires substantial capital investments and financial risk. This makes it difficult for households with modest incomes to enjoy the long-term benefits of solar, potentially creating inequities where the solar PV is exclusively available to wealthy house holds.

1.1. The Need for a Complexity Science Approach to Policy Evaluation. In order to design better public policy for solar PV, it is necessary to evaluate the efficacy of different policy choices given the complex social systems in which these policies unfold, particularly in terms of the degree to which they avoid (or exacerbate) inequities in access to a given technology. Classic tools of policy evaluation are poorly suited for this task. Classic tools tend to extrapolate future scenarios based on past behaviors, assume relatively homogenous and rational agents, and focus on aggregate trends. These approaches largely ignore the complexity that arises through the interplay of individual decision-makers and focus instead of the decisions of a hypothetical "central planner" (see, e.g., [13]).

The use of a network science perspective allows us to study complex system processes through the explicit representation of relations between actors, such as pathways or the interdependence of decision-making. In recent years, a vast body of literature has emerged on diffusion processes in complex networks [14, 15], such as the spread of epidemics [16] or information [17]. We build on this research and extend it to the evaluation of policies that aim to promote a certain technology adoption behavior, explicitly taking into account the interdependencies between decision-makers and the complex social networks in which they are embedded. The peer network influences studied here are nested within the larger study of economic networks, which are themselves an important approach for complex systems analysis (see Emmert-Streib et al., 2018, for a comprehensive review). For tractability, we focus on the purely social influences by which potential adopters learn about the benefits and costs of solar energy. Of course, potential adopters are embedded in a complex economic network of organizations providing adoption incentives and banks providing the capital for necessary upfront investments.

Consequentially, this paper applies a complexity science perspective by explicitly accounting for the diffusion of adoption behavior in complex networks in the evaluation of solar policies, particularly in terms of equity outcomes. One useful tool in the complexity science toolkit is the agent-based model (ABM), which is increasingly recognized as a promising approach to evaluate the effectiveness of public policies where costs and benefits accrue from complex social behaviors. Theoretical ABMs can examine the nonlinear dynamics of solar PV adoption which arise from the behaviors of interconnected, heterogeneous agents, as we see in the real world where solar PV adoption decisions are made. By focusing on the individual decision-maker rather than aggregate trends, ABMs allow for an explicit representation of agents' adaptive capacity [18]. ABMs are increasingly used to develop a more robust understanding of energy demand and the ex-ante evaluation of renewable energy policies [19].

1.2. Roadmap of This Paper. This paper uses a series of theoretical, computational ABMs to compare and evaluate three distinct types of real-world solar incentive programs: the feed-in tariff, leasing programs, and seeding of underserved communities. Of particular interest is the effectiveness of these incentive programs in terms of (i) the overall speed of solar PV adoption in a social system and (ii) the access to solar PV that is afforded to different groups, particularly high- and low-income agents. This second evaluative criterion is a crucial component of the distributional justice issues discussed above. These inequities may be underestimated if an analyst assumes that social networks allow for the positive, indirect benefits of incentive programs to spill over to less affluent communities that face high barriers to solar adoption. In reality, social network structures may inhibit these processes and dampen the indirect benefits of solar incentive programs. In other words, program effectiveness is likely conditional on how social networks are structured within a given market.

Our model compares the effectiveness of incentive programs in terms of aggregate adoption as well as energy justice as called for by Sovacool [10, 2] and illustrates the degree to which the structure of actual social networks—particularly the degree of segregation observed within networks—is likely

to change the relative effectiveness of different policy instruments. Understanding the mechanisms behind the interplay of different network structures and policy instruments is crucial for a transfer of policies from a context with a rather integrated society (such as Germany or California) to a context with a more segregated society (as might be the case in developing countries).

This paper turns next to a discussion of the benefits generated by solar incentive policies, with a particular focus on the indirect benefits derived from peer effects. We discuss how network segregation may create distributional justice concerns in that certain segments of society will accrue disproportionate benefits. We then turn to a focused discussion of the particular types of incentive programs represented in our ABM, as well as expectations based on network theory regarding program effectiveness based on varying degrees of network segregation. The structure of the ABM is discussed afterwards—this is a theoretical model in which agents in a hypothetical social system are randomly exposed to incentive programs and make subsequent adoption decisions. We conclude with an analysis and summary of the results, as well as a discussion of policy implications of this research.

2. Solar Adoption Incentives and the Role of Social Networks

Solar PV adoption dynamics are ultimately the result of decisions made by individuals and households. As with other types of high-cost, emerging technologies, these are not simple decisions [20, 21]. Many factors play into adoption decisions, such as peoples' financial means, peer-group behavior, and attitudes towards green and new technologies (e.g., [6, 173]).

Solar incentive programs seek to intervene in these individual decision-making processes by reducing the various barriers to adoption, whether this means making solar PV more affordable, less uncertain, or more socially desirable. Most programs focus on reducing financial barriers and perceived risks associated with solar. Perceived risk can be decreased through information provision—providing trustworthy information about the true costs and benefits of adopting solar PV. Perceived risk can also be reduced by guaranteeing a reasonable amortization period (e.g., through guaranteed feed-in-tariffs as used, e.g., in Germany and discussed in more detail below). Incentives may decrease financial barriers in two ways: by decreasing the upfront investment costs for purchase and installation of the PV (e.g., through convenient loans or leasing contracts) and by increasing the long-term profitability of a solar system [20, p. 74].

As noted above, these direct benefits of solar incentive programs are complemented by the indirect benefit of making solar PV a more viable or attractive option for potential adopters. It is these indirect benefits—realized through several possible mechanisms—through which a bulk of the benefit of solar incentive programs are likely realized. These mechanisms include, for instance, lowering costs as more individuals adopt. Increasing demand for solar PVs followed by more competitors on the supply side leads to more efficient ways of production and decreasing prices [23]. Of central interest in this paper, however, is the peer effect, where the adoption of solar by a substantial number of early adopters makes it more likely that agents in the (geographical or social) neighborhood adopt solar PV. A number of mechanisms underlie the peer effect, such as increased information provision through one's social network, the creation of social pressures to reduce one's environmental impact, or the showing-off of investments in new technologies. Solar adopters who are well integrated in the network may act as social multipliers by distributing information and being positive role models. For designing just and effective incentives, it is necessary to consider the role that the peer effect and network structures play within the diffusion process of environmental-friendly technologies.

2.1. Networks and Indirect Benefits of Solar Incentive Programs. The idea that social networks enhance the indirect benefits of solar incentive programs is not new; indeed, there is a growing body of research on the interdependencies of environmental consumption decisions by individuals and households. This has been studied in the literature alternatively as peer effects [5, 9, 24], social influence [6, 7], and diffusion of innovations [25–27], all of which underscore the same fundamental lesson that the behavior of any particular agent is determined in part by the behaviors of those they are socially close to.

Varied notions of "closeness" matter for peer effects, such as spatial proximity (e.g., one might tend to adopt the behaviors that are prevalent in the community) or informal social relations (e.g., one might adopt the behaviors of their friends). Whatever the case may be, social closeness may be represented in social systems using the concept of social networks [28, 29]. A network is simply a generic representation of how agents in social systems—commonly referred to as the *nodes*, which may represent individuals, households, formal organizations, or any discrete decision-maker—are related to one another through *linkages*, which represent socially important relationships such as information sharing, friendship, or proximity.

There is a vast literature in the emerging field of network science that seeks to understand how individual behaviors are correlated with one's position in a network [30, 31]. Most relevant to the idea of the peer effect are diffusion models of networks. Generally speaking, these models examine how network nodes adopt the attributes of their neighbors and how certain structures influence the speed with which a particular attribute spreads throughout the network (see [26] for a current overview). These models are applicable to a wide range of phenomena, such as the spread of disease over space and time (see, e.g., [32, 33]), the reaching of a consensus within groups [34, 35], or the adoption of environmental technologies including rooftop solar [5, 36, 37].

The primary characteristic of a network that increases diffusion speeds (and therefore the effectiveness of peer effects) is the closeness of agents within the network [38]. "Closeness" refers to the average distance between any two pairs of network nodes and is related to how many steps

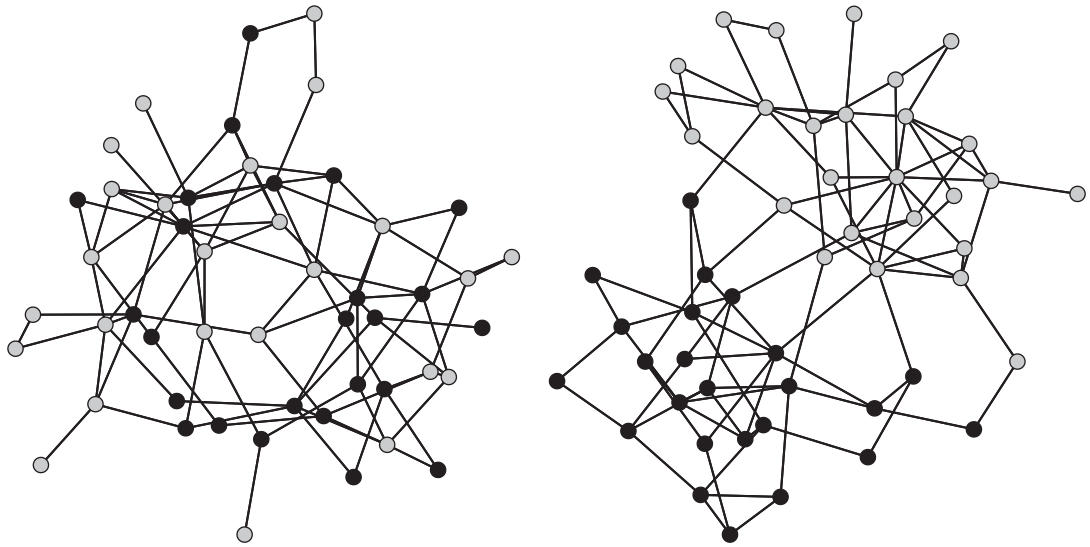

(a) Integrated network (b) Segregated network

Figure 1: Illustrative network structures. *Note: networks generated using ABMs of random network formation in R* [22].

it takes to reach a given node by starting at any particular node. Even relatively slight changes in network structure can dramatically influence the closeness of nodes. For instance, only a few random rewires of a lattice-type network can dramatically increase the overall closeness of nodes and thus increase potential diffusion speed [39, 40].

In this paper, we focus on two particular types of network structures: "integrated" and "segregated" networks (Figure 1, Panels (a) and (b), resp.). In these networks, network actors have a group membership represented by the shading of the nodes. Integrated networks are those where actors are as likely to be connected to actors of their own type as to actors of another type. For diffusion processes in an integrated network, it should make no difference to which group the first adopters belong. In a segregated network, however, actors with the same attributes are much more likely to be connected than actors with different attributes. For instance, actors might be divided along economic characteristics or in terms of attitudes towards new technologies. In the case of segregated networks, diffusion is fastest among the group of the early adopters. However, overcoming the gap between the two groups—and thus achieving widespread adoption—will be much more difficult. Again, the position of the early adopters will be crucial: if the early adopters are brokers between the two groups overcoming the gap will happen much faster than if the early adopters are at the periphery of the network.

The speed of diffusion processes in varying types of network structures should be an important consideration when designing policies to promote technology adoption—otherwise one cannot realistically estimate peer effects. In this paper, we explicitly model the process in integrated and segregated networks and study how diffusion processes differ with network structure and how the efficacy of incentive programs is conditional on these structures.

3. Theoretical Expectations: Distributional Equity and the Problem of Network Segregation

Governmental goals are mostly set towards reaching certain target percentages of, for instance, renewable energies relative to overall energy production (for the German case, see [41]) or towards the achievement of absolute goals, such as the 100,000 Roof Program for solar PV or the recent example of subsidies for hybrid and electric vehicles in Germany [42]. This means that the success of incentive programs is measured primarily according to their influence on overall adoption rates [43–45]. However, in a world where large gaps between affluent and poorer households are observed, one could argue that an aim of public spending and public policies should lie in minimizing this gap. Over the last decades, public spending towards supporting renewable energies has substantially increased worldwide and is expected to grow further, from an estimated USD 214 billion in 2014 to USD 300 billion by 2020 ([46, p. 5]; [47]). Calls are getting louder that this vast amount of public spending cannot be one-dimensionally directed towards increasing, for example, the share of renewable energies. Instead, "the distribution of the costs and the benefits of these subsidies across socioeconomic groups"—and thus the question of social equity in policy design—must be taken into account ([46, p. 5]; [48, p. 263]; [49, 50]). Therefore, overall adoption rates should not be the only evaluative criterion for policy investment incentives, but the effect of the policy on social equity has to be taken into account when deciding for suitable policies to support renewable energies and other measures towards an energy transition [48, p. 255].

As noted above, one's choice to adopt solar PV is dependent on a given actor's position in a social network. Thus the ability of a given agent to influence the decisions of

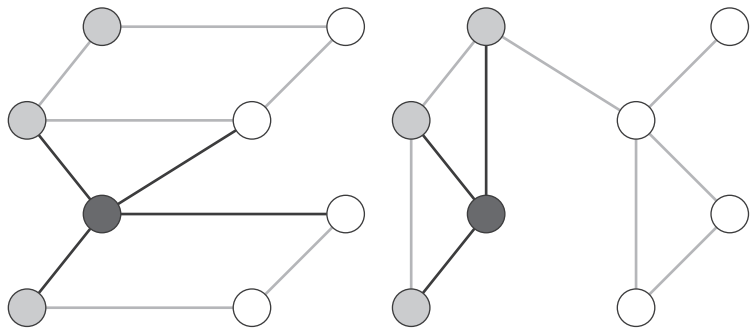

Figure 2: Possible influence relations of an adopter.

others is likely dependent on the level of segregation in the network. Figure 2 illustrates this schematically. In Figure 2(a), a technology adopter (the shaded agent) is embedded in an integrated network, in the sense that the adopter is connected to similar agents (circles) about as often as to dissimilar agents (triangles). Thus, the adopter influences both groups (circles and triangles) equally through the peer effect. In many real-world scenarios, however, we observe that adopters have networks that are segregated in the sense that connections exist primarily among agents with similar attributes [51–53]. Attributes that might be relevant in this context include the level of education, the awareness of environmental problems, the willingness to pay for sustainable technology, and overall financial means [8, p. 344]. This scenario of agents embedded in segregated networks is depicted in Figure 2(b). In this case, peer effects lead to an increased probability of adoption within the group of the first adopters [48, p. 263], while the probability of the members of the other group is not affected at a large scale. In our application, types of actors reflect an actor's individual propensity to adopt solar PV. This propensity may be dependent upon characteristics such as the affluence and environmental beliefs of an actor, among other factors [6].

Figure 1(a) depicts an integrated social network in which links between actors of the same type are as likely as links between actors of different types. Diffusion can flow unhindered from one actor (type) to another. In an integrated network, peer effects can counteract initial differences in adoption propensities if a low-propensity actor is connected to many high-propensity actors who already adopted PV; this will drastically increase its own probability to adopt. In a segregated network, on the other hand, links between actors of the same type are much more likely than links between actors of different types (see Figure 1(b)). Thus, in a segregated network, peer effects cannot enhance the diffusion of positive environmental consumption equally throughout the whole network. Low-propensity actors are mainly influenced by other low-propensity actors, which will hinder diffusion among them. Without any incentives, we thus expect adoption curves of low- and high-propensity actors to be closer together in integrated than in segregated networks–where adoption curves depict the percentage of adopters within a given group over time.

In this way, network segregation can slow the diffusion of positive behaviors in social systems. Segregation limits peer effects between unlike actors, and therefore incentives targeted to affluent actors will not benefit less affluent actors in the long run because sufficient connections between the two groups are missing. A careful evaluation of incentives and their intended and unintended outcomes is needed to set diffusion processes in motion which lead to more, instead of less, energy justice. Our evaluation of equity outcomes of renewable energy subsidies can bring us one step further to answering one of the research questions proposed by Sovacool [10, p. 22]: "Which energy [...] systems help reduce poverty and meet development goals and which ones exacerbate inequality and concentrate wealth?"

3.1. What Incentives Work and When? Various forms of supporting PV installations through incentives are already practiced in numerous contexts; incentives include the feed-in-tariff (e.g., in Germany), leasing programs (e.g., in California) and pilot projects of seeding solar to poorer communities (also in California). While the outcome of increasing overall adoption rates can easily be measured, other effects of incentive programs remain mostly unknown, for example, the questions of who is benefitting from this kind of incentive in the short and the long run. Modelling the processes of solar adoption allows us to analyze the effect of the varying incentives on the adoption dynamics, which include uptake of installations as well as equity between different societal groups. In the following, the three forms of incentives applied in this work will be briefly summarized.

Feed-In Tariff. The feed-in tariff guarantees adopters a long-term fixed rate for every kWh fed into the grid from renewable energies, with solar PV systems being the most feasible option for private households. Through this long-term guarantee, the financial risk of adopting is substantially reduced and the large investment will pay off much faster than without the incentive. This incentive primarily targets actors with the financial means to make the initial investment in solar. This is because the economic benefits of the feed-in tariff are for long term, and the upfront investment is not necessarily made any easier.

The first country to implement a feed-in tariff was USA with its Public Utility Regulatory Policies Act (PURPA) in 1978. (Pub.L. 95–617, 92 Stat. 3117, enacted on November 9, 1978.) In 1991, a feed-in tariff was enacted in Germany, the *Act on the Sale of Electricity to the Grid* [54]. This act had a far-reaching impact on the development of PV installations in Germany. Since then feed-in tariff policies have spread worldwide and are by now world-leading instruments to support renewable energies [55, p. 19]. In the year 2007, 46 jurisdictions worldwide have implemented a feed-in tariff. Beside numerous western countries and jurisdictions such as Switzerland (1991), Italy (1992), Denmark (1993), Spain, and Greece (1994), also quite a number of countries from the global south have implemented a feed-in tariff, such as India (1993), Sri Lanka (1997), and Algeria and Indonesia (2002) to name the first among them [56]. As multiple studies have shown that the implementation of the feed-in tariff in Germany led to a fast uptake of renewable energies in general and solar energy in particular (see, e.g., [57]), this in turn led to decreasing prices for the PV technology making the technology more cost-efficient [58, 59]. By targeting the actors that are most likely to adopt (high-probability agents), we expect that a faster overall uptake of installations will be observable (as compared to no incentives).

However, Welsch and Kühling [6] show that in Germany higher-income households are more likely to invest in solar. This trend is consistent with the feed-in tariff, which makes the adoption of solar a profitable investment for affluent actors. Jenkins et al. [11, 176] thus argue that the German feed-in tariff is an example of a program that promotes energy injustice because it leads to higher energy prices in general in order to refinance the promised fixed feed-in rate for renewable energy producers ([48, p. 263]; [60]). People that are interested in investing, but do not own their home or do not have the initial money to invest, cannot participate in the transition. However, in the long run, they have to bear the burden of rising energy costs due to the guaranteed feed-in, without having had the chance to participate in the beginning ([61, p. 3882]; [11, p. 176]). This phenomenon of feed-in tariffs on energy inequity was analyzed by researchers in a wide variety of contexts, such as in Australia, California, and UK [46], Denmark, Germany, Cyprus, and Spain [62], and Thailand [63]. Based on these observations, we argue in the following that the high and upper middle-income class is disproportionally benefitting from the feed-in tariff, while low-income households are unlikely to benefit from this incentive. Because of missing links to social multipliers, we expect this effect to be more critical in societies with a major income gap and high segregation, having crucial implications for the distributional energy justice of this incentive [11, p. 176]. To evaluate these distributional justice issues, we will examine the adoption dynamics of high- and low-probability actors separately. In integrated networks, we expect that the difference between the dynamics of the two actor groups will not increase significantly through the feed-in tariff (as compared to no incentive in integrated networks). In segregated networks, however, we expect that the difference in adoption dynamics between high- and low-probability actors increases significantly through the feed-in tariff (as compared to no incentive in segregated networks).

Leasing. This form of incentivizing solar adoptions is based on a third-party ownership. Third parties own and operate PV on private households or small industrial buildings. Through the leasing agreement, upfront costs for installing solar are extremely reduced or even eliminated. Economic benefits occur from the first month and not after a long amortization period. Leasing programs are widely present in USA (see, e.g., [37]) and are currently becoming more visible in Europe. Drury et al. [64] as well as Rai and Sigrin [36] are able to show that leasing options are increasing the demand and widening the range of potential adopters through making PV available for less wealthy agents as well. Leasing programs are thus expected to lead to a faster overall uptake of installations (as compared to no incentives). Wealthier agents (particularly those who are risk-averse) will benefit from this type of incentive as well. The leasing program thus targets both high- and low-probability actors. Therefore, we expect the differences in adoption dynamics between high- and low-probability actors to stay stable with leasing programs in integrated as well as in segregated networks (as compared to no incentive in the respective network). These expectations will be tested with the model introduced in the next section. The same dynamic is expected to occur with incentivizing solar adoption through low-interest loans [63, p. 266].

Seeding Less Affluent Communities. Using this strategy, free or low-cost PV systems are given out to a selected number of qualified agents in low-income communities. This has a doubled positive effect on adoption rates: first, strong financial support is especially important for low-income households to support their investment [20, p. 85]; second, it is increasing the visibility of PVs, spurring peer effects within those communities [8, p. 340] (see above on the importance of peer effects in low-income communities). Currently, this form of support is in pilot status only. For example, pilot projects have been implemented in California under the Greenhouse Gas Reduction Fund in collaboration with the Oakland-based nonprofit organization *Grid Alternatives*. The project is partly financed by California's cap and trade program and aims at supporting low-income families through free PVs. The peer effects of this project are not yet monitored. In an agent-based model, Zhang et al. [65] show extremely positive effects of seeding for overall adoption rates. Therefore, seeding programs are expected to lead to a faster overall uptake of installations in our models as well (as compared to no incentives). Since the seeding program is only targeting low-income actors, it drastically increases the probability that these agents will adopt solar. Especially in segregated networks, it will be of major importance to spur peer effects in currently underserved communities. We therefore expect that seeding programs positively affect the adoption dynamics in segregated networks by decreasing the differences between high- and low-probability actors (as compared to no incentive in segregated networks). In integrated networks, however, the difference in adoption dynamics is not expected

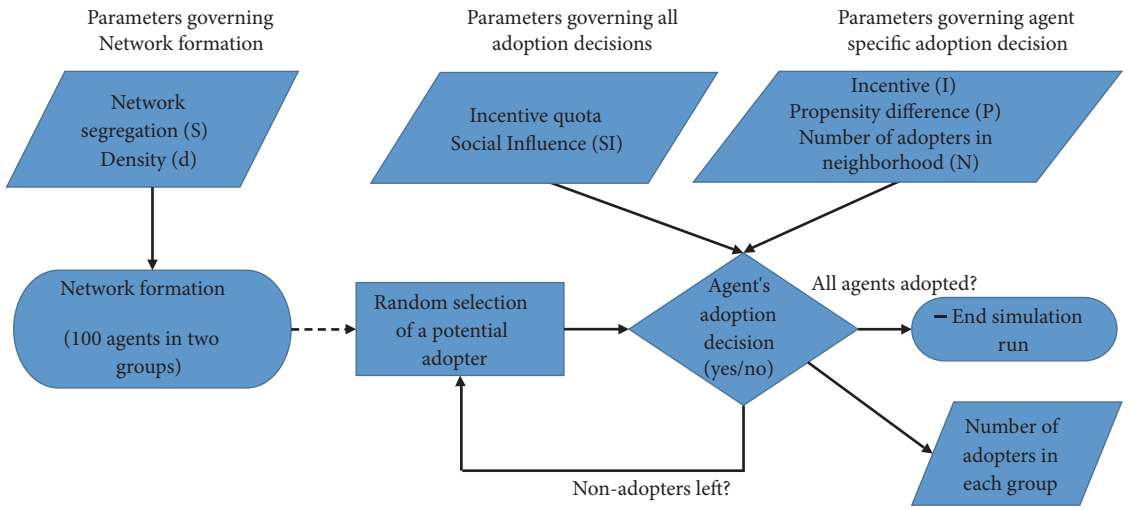

Figure 3: Model overview of one simulation run.

to change significantly with seeding programs (as compared to no incentive in integrated networks).

These adoption dynamics—and the role of governmental interventions in managing the tradeoff between speed and equality of adoption across communities—are the focus of the agent-based model described in the following section.

4. Model Overview

These theoretical expectations are explored through an agent-based model that examines adoption dynamics over time in a hypothetical social system, given variation in the underlying social network structures and incentive in place. This model was coded in R and is an advancement of the model previously developed and explored by Henry and Brugger [66]. The predecessor model included many of the components explained in detail below but laid its focus on the effect that the strategies of firms (when targeting their potential customers) would have on the adoption dynamics, by being a gatekeeper to adoption possibilities without altering the actual adoption decisions. Advancing the previous model, the current version allows explicitly modelling the effect of policy interventions (here through various incentives) on the adoption probabilities of the different types of individual agents and thereby on the overall adoption dynamics.

As noted above, we study peer effects by modelling the social network connecting actors, and that enables and constrains social influence. Figures 1(a) and 1(b) show two illustrative networks in which agents are visualized as circular nodes, with their color representing the fact that they belong to one of two groups, differentiated through socioeconomic attributes that influence the probability of adoption. The links between those nodes represent the relations between them, such as information exchange or proximity, through which peer effects and social influence can unfold. Therefore, agents that are connected to other agents that have already adopted solar are assumed to have a higher probability of adopting solar themselves, compared to agents who are not connected to adopters.

Figure 1(a) shows an integrated network, where links between actors of different types are as likely as links between actors of the same type. This represents a network where actors build their relations entirely independent of their own and of the other agents' group membership. Contrasting this network, Figure 1(b) visualizes a segregated network in which the realization of a relation is highly dependent on whether two agents belong to the same group. In this network structure, agents within one group are much more likely to be influenced by other agents within their own group. How strong this effect is depends on the level of segregation, which is governed by the segregation model parameter (see below). As Henry and Brugger [66] note, this representation of the network may capture various types of social closeness which determine the ability of one agent to influence another, such as spatial proximity, shared participation in social venues, or friendships. Many such real-world networks exhibit segregation.

Figure 3 gives a graphical overview of a model run. In the first step of every model run, a network of 100 agents is formed. The agents are randomly assigned to one of two groups. Links between those agents are built based on the network segregation parameter (S) and the density (d). Following this network formation, in each time step, one potential adopter is selected at random. This agent then makes an adoption decision based on parameters, which are fixed for the whole simulation run (the incentive quota and the social influence parameter, SI) and on parameters that are actor-specific (incentive, I, and propensity difference, P) or even time-step-specific (number of adopters in the neighborhood, N). After each time step, the number of adopters in each group is reported. The random selection of a potential adopter and the following adoption decision is repeated until all agents are adopters. In the following

Table 1: Model scenarios: overview over determining parameters.

	Scenario 1	Scenario 2	Scenario 3	Scenario 4	Scenario 5	Scenario 6	Scenario 7	Scenario 8
Incentive	No incentive	Feed-In	Leasing	Seeding	No incentive	Feed-In	Leasing	Seeding
Segregation	Low (S=0)	Low (S=0)	Low (S=0)	Low (S=0)	High (S=0.75)	High (S=0.75)	High (S=0.75)	High (S=0.75)
Density	**0.05**	**0.05**	**0.05**	**0.05**	**0.05**	**0.05**	**0.05**	**0.05**
Incentive quota	**0.3**	**0.3**	**0.3**	**0.3**	**0.3**	**0.3**	**0.3**	**0.3**
Propensity difference	**0.6**	**0.6**	**0.6**	**0.6**	**0.6**	**0.6**	**0.6**	**0.6**
Social influence	**1**	**1**	**1**	**1**	**1**	**1**	**1**	**1**

With these eight scenarios we can study the diffusion processes under the four possible incentive parameters (no incentive, feed-in, leasing, and seeding) in highly segregated (segregation high, S=0.75) and in integrated (segregation low, S=0) networks. Keeping all other (bold font) parameters constant over all simulations allows us to single out the effects of the different incentives and segregation on the diffusion processes.

section, the model parameters and the decision are explained in greater detail.

4.1. Synopsis of Model Parameters. This model examines the effect of various policy incentives within networks with different structures. The different network structures are governed by the *network segregation* parameter. Three additional key characteristics are defined and controlled for in the model, *incentive quota*, *social influence*, and *propensity difference*, all of which are introduced in the following. All of these characteristics stay constant within one model run but may vary across runs.

Network segregation is captured by parameter S, reflecting the degree to which linkages tend to exist among actors with a similar propensity for technology adoption. For the purpose of this study, the segregation parameter was chosen to be either 0 or 0.75. A value of zero leads to an integrated network (see Figure 1(a)), meaning that agents are as likely to form links with those that are within the same group as to those that are in the other group. In contrast, if S=0.75, the network is highly segregated (see Figure 1(b)) and within-group links are much more likely to be realized than links between agents of different types. In the setup of this model, the link formation is solely governed by this segregation parameter S and the density d of the network. Links between actors of the same type are assumed to occur with probability $d + (S * d)$. On the other hand, links between actors from different groups are assumed to occur with probability $d - (S * d)$. Therefore, with a segregation parameter of 0.75, links between similar agents are seven times as likely to be realized as links between different types of agents (8.75% and 1.25%, resp., displayed in Figure 1(b)). As discussed below, other values might be reasonable as well; however, a clear distinction between the two observed network structures is crucial.

Incentive quota is a model parameter regulating how many incentives are given out. This variable ranges between 0 and 1, where 0 means that no incentives are given out and 1 means that all adoptions are supported by incentives. For the analysis of this paper, we studied an incentive quota of 0.3, which means that adoption decisions are made under the knowledge of the incentives until 30% of the agents have adopted. This quota reflects the governmental course of incentivizing the starting phase of the new technology rather than aiming at supporting all agents to adopt.

Social influence is a parameter determining the strength of the peer effect by which an agent's adoption probability increases as a function of the number of adopters they are connected to. This parameter (SI) takes a value from 0 to 1, inclusive, where 0 indicates that agents are not at all influenced by the adoption of other agents they are connected to, but the strength of this influence increases as SI goes towards 1. In the current model, we simulate a constant strong social influence of $SI = 1$.

Propensity difference is a model parameter (P) that allows differentiating the baseline adoption probability of actors that are part of two different groups. The baseline adoption probability captures an agent's probability to adopt when no neighbors have adopted yet and no incentives are in place. In the current model, we differentiate between two groups, the "high" and "low" propensity agents. We assume a propensity difference parameter of $P = 0.6$, giving a baseline adoption probability for low-propensity agents of 5% and a baseline probability of 8.8% for high-propensity agents.

The model setup consists of three initial steps: (1) the creation of 100 agents, (2) their assignment to one of two groups (either with a high or a low baseline propensity to adopt the technology), and (3) the formation of the network. The segregation parameter and a fixed density of 0.05 govern the network formation. A density of 0.05 means that 5% of all possible relations are realized in the network. The density of the network reflects the overall intensity of social interaction within the network (e.g., how often do people speak about the adoption of solar and how often do they observe that other people have already adopted).

In order to compare a reasonable number of different scenarios, identify only the effect of the parameters that are of major interest within the context of this paper, only the segregation parameter (high versus low), and the type of incentives (no incentive, feed-in, seeding, and leasing) across model runs, leading to eight distinct scenarios as summarized in Table 1.

4.2. Model Dynamics. After the model is set up, an iterative process is started, which consists of two stochastic processes: first, one potential adopter (i.e., any agent that has not yet adopted) is selected at random and, second, the chosen agent makes his adoption decision. In the following, both processes are explained in detail.

Table 2: Incentive parameter values $\boldsymbol{I}(\boldsymbol{r_i}, \boldsymbol{z})$ by incentive program and agent type

	Poorer households ($\boldsymbol{r_i} = 0$)	Richer households ($\boldsymbol{r_i} = 1$)
Feed-In tariff ($\boldsymbol{z} = 1$)	$\boldsymbol{I_{0,1}} = 1$	$\boldsymbol{I_{1,1}} = 1.5$
Leasing ($\boldsymbol{z} = 2$)	$\boldsymbol{I_{0,2}} = 1.25$	$\boldsymbol{I_{1,2}} = 1.25$
Seeding ($\boldsymbol{z} = 3$)	$\boldsymbol{I_{0,3}} = 1.5$	$\boldsymbol{I_{1,3}} = 1$

Random Agent Selection. Each time step starts with the selection of a potential adopter. Therefore, from all current nonadopters, one agent is chosen uniformly at random. This gives every nonadopter the same probability of being selected as all other nonadopters. Mathematically, the probability $Pr_R(i,t)$ that the ith nonadopting agent is selected at time t is therefore given by

$$Pr_R(i,t) = \frac{1}{Q_t}, \tag{1}$$

where Q_t represents the number of agents at time t who have still not adopted the technology. In each time step, exactly one agent is chosen, who will then make an adoption decision.

Agent Adoption Decisions. The agent that has been selected makes a stochastic decision of whether or not they adopt the technology. The probability hereby varies depending on group membership, type of incentive, and importance of social influence. The probability $A(i,t)$ of the potential adopter i to adopt at time step t is therefore governed by the following logistic function:

$$A(i,t) = \frac{\boldsymbol{I_{r_i,s}}}{1 + e^{-(-2.944 + P * r_i + SI * N_{i,t})}}, \tag{2}$$

where r_i indicates the group membership of agent i and is coded as one if the agent is member of the high-propensity group and zero if the agent is a member of the low-propensity group. P and SI are the propensity difference and social influence parameters described above, and $N_{i,t}$ represents the number of adopters the ith agent is connected to at time t. (In some few cases, this can lead to $A(i,t) > 1$; in that case, the probability is redefined to $A(i,t) = 1$.)

Moreover $\boldsymbol{I_{r_i,z}}$ is introduced to model incentive programs. The incentive parameter $\boldsymbol{I_{r_i,z}}$ is contingent on the group that the actor belongs to (r_i) and the incentive (z) in place. If the agent i is profiting from the given incentive, it will increase its probability to adopt ($\boldsymbol{I_{r_i,z}} > 1$). However, if a policy incentive is not targeting the group that i belongs to, the probability function will stay the same as without any incentive ($\boldsymbol{I_{r_i,z}} = 1$); Table 2 shows the respective values for $\boldsymbol{I_{r_i,z}}$. Critical for the idea of the simulation are the relative values of $\boldsymbol{I_{r_i,z}}$ for each incentive—the relationship between the parameter $\boldsymbol{I}_{0,z}$ for the low-propensity and $\boldsymbol{I}_{1,z}$ for the high-propensity agents—rather than their absolute values. This approach is comparable to classical game theoretical models—like the Prisoners Dilemma—in which not the actual payout values matter but rather their relative structure (see, e.g., [67, p. 4f].). However, actual values are necessary for following the decision-making within the game and in our case for simulating decision-making processes.

The feed-in tariff (incentive: $z = 1$), which is most beneficial to the high-propensity group (as explained above), does not alter the probability function of the members of the low-propensity group ($r_i = 0 \implies \boldsymbol{I_{0,1}} = 1$) but does have an impact on the probability function of the high-propensity group ($r_i = 1 \implies \boldsymbol{I_{1,1}} = 1.5$). In this way, the incentive parameter is chosen such that it increases any given probability, which is dependent on propensity difference and the social influence parameter as well as the number of connected agents that have already adopted, for high-propensity actors by 50%.

The seeding incentive (incentive: $z = 3$) targets the low-propensity group by giving out free PVs to poorer households, thus increasing the probability function to adopt. Again the incentive parameter increases any given probability, which is dependent on propensity difference and the social influence parameter as well as the number of connected agents that have already adopted, by 50% ($r_i = 0 \implies \boldsymbol{I_{0,3}} = 1.5$), while keeping the probability function of the high-propensity group unaltered ($r_i = 1 \implies \boldsymbol{I_{1,3}} = 1$).

Under the possibility to lease PVs to private households (incentive $z = 2$), the members of the high- as well as low-propensity groups can benefit, because it gives actors of both groups the chance to avoid high upfront investments and long-term benefits through the installation. However, long-term benefits are not expected to be as high as with the other two incentives (for the targeted group). Thus the incentives through leasing options are expected to have a positive influence on the adoption probability functions of both groups but not as high as when targeted directly. This is reflected in the applied incentive parameter ($r_i = 0 \implies \boldsymbol{I_{0,2}} = 1.25$ & $r_i = 1 \implies \boldsymbol{I_{1,2}} = 1.25$), which increases any given adoption probability for actors of both groups by 25%.

Three additional points about the behavior of this adoption probability function are needed. First, the constant coefficient of -2.944 on the logistic function ensures a minimum probability of adoption of 5% for all agents, no matter their propensity or social connections. The minimum probability that an agent i will adopt is a situation where i has low propensity (i.e., $r_i = 0$) and the agent is not linked to any adopters (i.e., $N_{i,t} = 0$). Thus, a constant coefficient of -2.944 fixes this minimum probability of adoption at approximately 0.05 or 5%. We conjecture that the value of this coefficient will not alter adoption trends other than speeding up or slowing down the overall process. Varying this constant will only speed up or slow down the model and should not fundamentally change the underlying dynamics.

Second, the propensity difference parameter P captures the marginal difference in adoption probability between low- and high-propensity agents. Since P may not be larger than one, a high-propensity agent will be no more than three times as likely to adopt as a low-propensity agent, controlling for other factors. Following the preceding point about minimum adoption probabilities, this means that a low-propensity agent will have a minimum adoption probability of 5%, and

Table 3: Effect of incentive programs on speed of adoption: integrated versus segregated social networks.

	DV = avg. wait time (smaller values signify faster adoption speeds)	
	Model 1: Integrated networks	**Model 2: Segregated networks**
Program dummy variables		
Feed-in tariffs used?	-0.415 ∗ ∗ ∗	-0.394 ∗ ∗ ∗
Leasing program used?	-0.366 ∗ ∗ ∗	-0.413 ∗ ∗ ∗
Seeding program used?	-0.282 ∗ ∗ ∗	-0.362 ∗ ∗ ∗
Constant coefficient	3.328 ∗ ∗ ∗	3.411 ∗ ∗ ∗
N	7,428 simulations	7,408 simulations
R^2	0.029	0.030

Note: the table reports results of OLS regression models with average wait time as the dependent variable. For dummy variable effects, the simulation with no incentive programs is the left-out category. ∗ ∗ ∗ p < 0.001; ∗∗ p < 0.01; ∗ p < 0.05.

if P=1, then a high-propensity agent will have a minimum adoption probability of 15%.

Third, this function assumes that the effect of being connected to an adopter is larger when adoption probability is low. Thus, the connections to adopters have a larger influence on potential adoption for low-propensity agents than for high-propensity agents. This difference increases with larger values of P. This is an artifact of the logistic model being used here and is in line with current findings (see, e.g., [5, 14f.]) that show that peer effects play a more important role for adoption decisions in low-income households.

5. Results

The following results are drawn from running 3,500 simulations with the three incentive programs described above. Approximately 25% of these simulations were run assuming no incentives to establish a baseline for comparison. In another 25% of simulations, the feed-in tariff was modelled, supporting the higher-propensity (wealthier) group, 25% of simulations implemented leasing possibilities favoring both groups equally, and the last 25% of simulations explore the influence of the seeding program to poorer households on the adoption dynamics. The models were not run for a certain amount of time steps but rather until all agents have adopted the technology (i.e., until complete saturation was reached). Since the number of time steps necessary varied between the various model runs, the results are analyzed dependent on the percentage of adopters rather than on time steps. Through this uniform exploration of the results, we are able to analyze how adoption dynamics differ based on the various policy incentives in place and based on the two analyzed network structures.

5.1. Influence of Policy Incentives on Saturation Times. The influence of model parameters, including the existence of certain incentive programs, on adoption dynamics is explored through two regression models summarized in Table 3. Using the individual simulation run as the unit of analysis, these models predict two evaluative criteria—average wait times (Model 1) and differences in average wait times (Model 2)—as a function of model parameters specified at model setup. These evaluative criteria are measures of the speed of adoption and the equity of adoption dynamics between low- and high-propensity groups, respectively.

More specifically, *average wait time* is defined as the number of time steps required for 100% of agents to adopt divided by the number of agents in the system. This measures the average number of time steps that one must wait before any given agent in a system adopts. Average wait time is thus a measure of the overall speed of adoption within a given system but ignores *who* is adopting. Higher values indicate slower adoption speeds (worse outcomes), whereas smaller values indicate faster adoption speeds (better outcomes).

The variable *difference in average wait time* is defined as the average wait time among low-propensity agents minus the average wait time among high-propensity agents. In other words, this is a measure of the degree to which one group lags behind the other in terms of average adoption trends. Large positive values of this variable mean that the high-propensity group becomes saturated much more quickly than the low-propensity group, thus indicating lower equity (i.e., a worse outcome). Values close to zero indicate that high- and low-propensity groups become saturated at approximately the same rate.

These regression models allow us to distill the enormous amount of data generated by our computational simulations into a relatively small set of average trends that emerge across simulations. By integrating the incentive program dummy variables into the model, we are able to examine the degree to which each program influences our evaluative criteria on average, controlling for other stochastic model parameters. In both models, the left-out categories are simulations without any incentive program.

In both models, we see that all programs appear to have a positive effect on overall speed of adoption. This is to be expected because, as noted above, speed of adoption does not account for the distribution of adoption behaviors over space or within a network. In other words, any incentive program yields significantly better outcomes than no incentive program.

By comparing Models 1 and 2, however, we can see that the effectiveness of programs depends on the degree of segregation observed in the networks. While the feed-in tariff seems to generate the fastest saturation times in integrated networks (Model 1), leasing programs appear to

Table 4: Effect of incentive programs on distributional equity: integrated versus segregated social networks.

	DV = difference in avg. wait time (smaller values signify greater equity)	
	Model 1: Integrated networks	**Model 2: Segregated networks**
Program dummy variables		
Feed-in tariffs used?	0.008 ∗	0.024 ∗ ∗ ∗
Leasing program used?	0.007	0.006
Seeding program used?	0.003	-0.011 ∗
Constant coefficient	0.037	0.056 ∗ ∗ ∗
N	7,428 simulations	7,408 simulations
R^2	0.001	0.007

Note: the table reports results of OLS regression model with difference in average wait time (distributional equity) as the dependent variable. For dummy variable effects, the simulation with no incentive programs is the left-out category. ∗ ∗ ∗ p < 0.001; ∗∗ p < 0.01; ∗ p < 0.05.

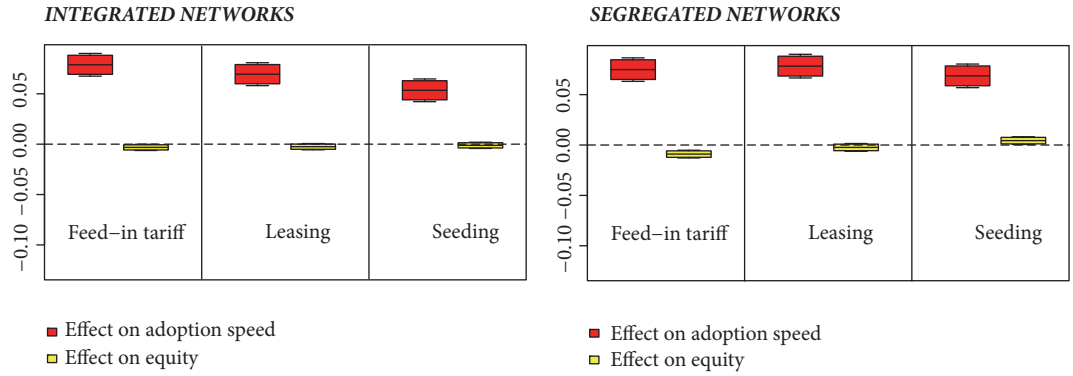

Figure 4: Graphical depiction of program outcomes, speed of adoption versus equity in segregated versus integrated networks.

support faster overall adoption speeds in segregated networks (Model 2).

Evaluating these programs in terms of equity gives yet another picture of program effectiveness. Table 4 summarizes the potential differences in program outcomes in terms of equity of adoption trends. Indeed, seeding programs appear to be the only type of incentive that significantly increases equity in terms of realizing a lower gap in the average number of adopters within high- and low-propensity groups.

Figure 4 offers a graphical depiction of these results. The program effect coefficients were reestimated using a measure of equity and adoption speed that is (1) normalized to fall in a range from 0 to 1, such that the effects of programs are comparable across models and (2) adjusted such that larger values indicate better outcomes and smaller values indicate worse outcomes. Red bars indicate the estimated effect of each program on adoption speeds, while yellow bars indicate the effect on equity. Colored regions indicate a 90% confidence interval for each coefficient estimate, while the outside bars delineate a 95% confidence interval. As seen also in Table 4, only seeding programs have a positive effect on both evaluative criteria when we assume segregated networks. Leasing has a positive effect on adoption speeds and no discernible effect on equity, whereas the feed-in tariff appears to promote *greater* inequalities.

5.2. Characterizing Adoption Dynamics. While these regression models provide useful insights into average trends, they also hide much of the richness of adoption dynamics—that is, the process by which adoption behaviors spread throughout the system over time. Figure 5 provides a descriptive illustration of these dynamics. Each panel of this figure illustrates trends realized across all simulation runs; bars in these figures represent the distribution of the proportion of agents that have adopted at different stages of the process, among high-propensity agents (white bars) and low-propensity agents (green bars). For any given simulation, the "stage" of process is defined as the number of time steps that have elapsed as a proportion of the overall saturation time. Thus, a simulation that takes 1,000 time steps for all agents to adopt is at the 10% mark at 100 time steps; however, a simulation that takes only 500 time steps for all agents to adopt is at the 20% mark at 100 time steps. Viewing adoption trends in this way allows us to focus on the overall shape of adoption curves controlling for the variation in overall saturation times (as seen in Table 3, Model 1).

The trends seen in these figures support the results of the models presented in Table 4. Feed-in tariffs produce much larger inequalities between high- (white) and low- (green) propensity groups, especially later in the process, than we see in any other scenario. Seeding policies tend to

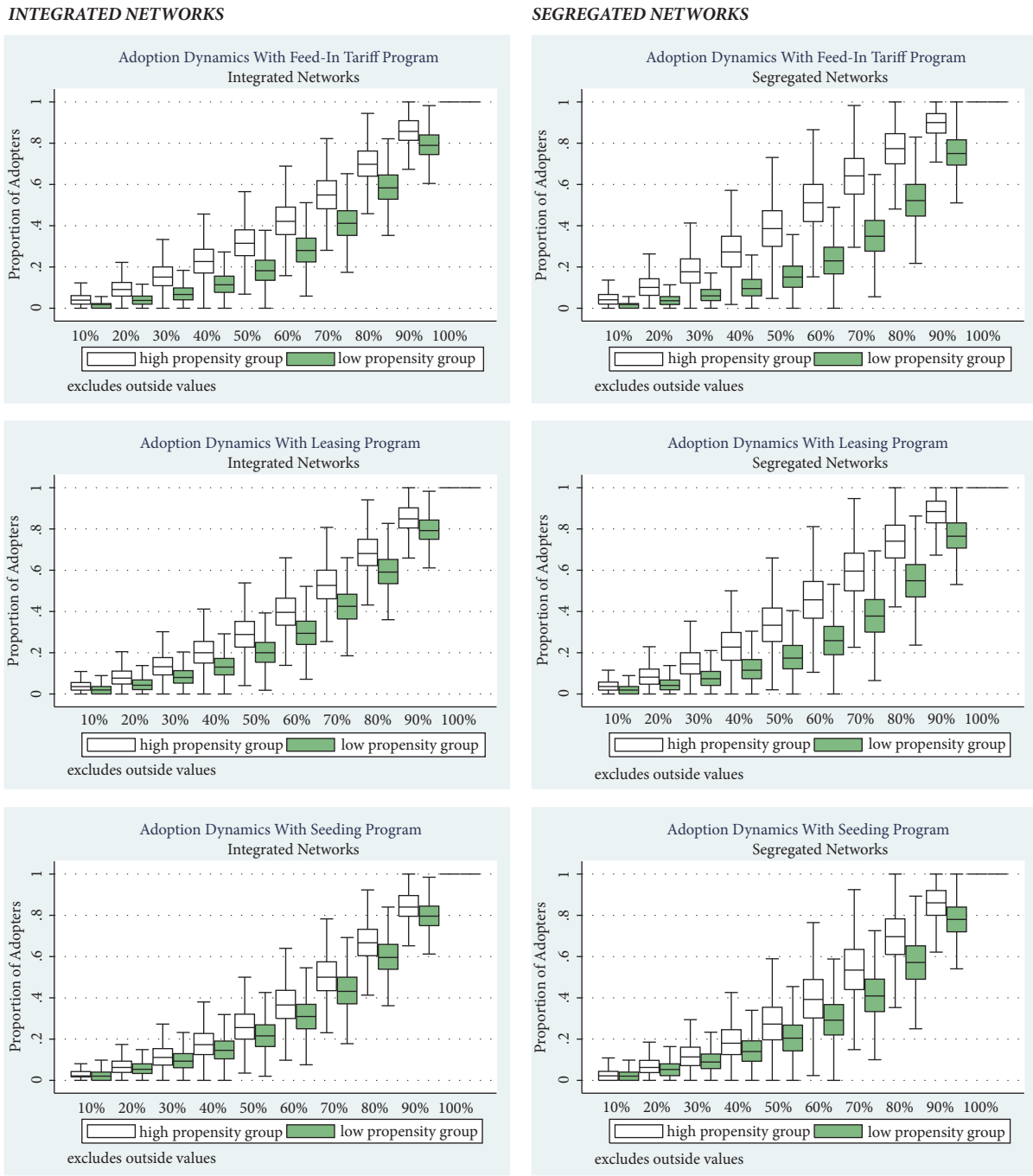

Figure 5: Realized adoption dynamics under various incentive programs.

have very narrow gaps between groups over time, although disparities to tend to increase later in the process as the incentive programs are phased out of more of the simulations. Finally, leasing programs do not appear to alter the shape of adoption curves for either group over and above the no-incentive scenario.

6. Conclusion

This agent-based model allows us to evaluate the effects of various types of (simplified) incentives in a virtual space, accounting for different societal structures. The results demonstrate that underlying network structures of a society have an important effect on the effectiveness of policy incentives.

Our results suggest that policy incentives designed to support primarily high-propensity agents might not be the best or even correct way to induce diffusion throughout a segregated network. In segregated networks, peer effects are dampened by missing societal links between more and less affluent actors. Thus, policy incentives that specifically target actors that are more affluent may further increase energy

inequality. This is an important finding for policy-makers thinking about transferring existing incentives, for example, best practices examples, from other contexts to their own. An incentive that might have worked well in a relatively integrated society can lead to extremely unjust outcomes within segregated societies.

This underscores a need for more reliable measures of the segregation of a society, so that policy programs can be crafted accordingly to enhance peer effects in a way that diffusion spreads throughout the whole social system. Introducing programs that will properly seed underserved communities could be one way to enhance distributional justice. These findings are, of course, not limited to the adoption of solar PV but within any policy domain where governments try to foster diffusion processes through policy interventions. Furthermore, these results can help to inform more complex (agent-based) models, which try to map the effect of policy incentives. They emphasize that peer effects cannot be reduced to simple diffusion models but that models considering social effects need to take more realistic network structures into account.

6.1. Limitations of this Work. The aim of this theoretical model is to study the effect of network structures on diffusion processes and the equity between two groups in this process. Naturally, such a theoretical model comes with a number of limitations. First, for simplification reasons, the model only considers two different types of actors. Those types have to be understood as a compilation of attributes, such as level of income, level of education, or level of environmental concern or geographical proximity, many of which are known to correlate in real life. The important point is that actors with similar attributes are either more likely to be connected to, and thus to influence, each other (in a segregated network) or equally likely to be connected to each other than to actors with different attributes (in an integrated network). Within the scope of this model, no explicit decomposition in the different attributes and their influence on the diffusion of the adoption of solar PV is modelled. Following this level of abstraction, costs of solar PV are also not explicitly modelled but are implicitly taken into account in the baseline propensity to adopt.

Second, it may seem that the results of the model are sensitive to the particular choice of incentive parameters. Two parameters are chosen for each incentive, which determine how the incentive affects the adoption behaviour of actors in the high- and low-propensity group. The key issue is how the assumed parameters influence the direction in which a certain policy will influence the adoption probability in each of the groups. While the magnitude of these parameters influences the speed of adoption, it is not expected to change the adoption patterns. Furthermore, conclusions are not drawn based on findings that directly depend on the setting of these parameters but are drawn from the comparison between adoption dynamics in the two network structures, given the same incentive parameters. Therefore, we do not test the results for varying parameters.

Third, the two types of networks studied here have to be understood as stylized network types, representing the two extremes in which either no barriers or high barriers for relations between two actor types exist. Future work should expand this work by studying diffusion processes in larger networks with underlying real-world network structures, such as networks enxhibiting community structure.

Fourth, in order to reach an analysable number of model parameter combinations, a very limited number of settings for each model parameter had to be selected. Therefore, exemplary settings were chosen, which allowed the contrasting of the process with two distinct network structures while keeping the other conditions (such as density and social influence) constant. However, previous work suggests that the network density plays a crucial role in diffusion (e.g., [68]). Therefore, it would be interesting to explore in future work, whether changing densities and changing social influence parameters have similar effects on the diffusion in integrated and segregated networks.

6.2. Applied Implications of This Work. Despite the theoretical focus of the model, its findings prove to be relevant in actual policy design. Especially, but not only, in segregated societies, public policy-makers are well advised to consider equity effects of the policies they propose. Policies supporting renewable energies can go a long way in empowering poorer households and communities if they are targeted in the right way. The findings in this work show that multiple incentives are suited to realize the targeted outcome of increasing the share of solar PV adopters but that not all incentives have the additional effect of benefiting poorer households and communities. It has to be taken into account that in some contexts it will be most beneficial to aim for a fast diffusion, for example, because this might drive the prices down and would thus allow that a technology could also be adopted by less affluent actors in the long run. However, this kind of long-term positive effects is not always given. This work unveils that equity effects can differ widely for different policies and within different societal structures. It would thus be fruitful if the assessment of how societal structures and social influence could speed up or dampen the diffusion process of the benefits of certain incentives would be part of policy evaluation.

Data Availability

As these are computational simulations, interested readers may run simulations on their own to replicate the findings. All data used will be published at the author's website, and all codes will be made available for replication of models (run in R).

Conflicts of Interest

The authors declare that they have no conflicts of interest.

References

[1] T. Dietz, G. T. Gardner, J. Gilligan, P. C. Stern, and M. P. Vandenbergh, "Household actions can provide a behavioral

wedge to rapidly reduce US carbon emissions," *Proceedings of the National Acadamy of Sciences of the United States of America*, vol. 106, no. 44, pp. 18452–18456, 2009.

[2] Fraunhofer ISE., *Aktuelle Fakten zur Photovoltaik in Deutschland [Current Data on Photovoltaics in Germany]*, Fraunhofer ISE, Freiburg, Germany, 2015.

[3] G. Selby, "Branding at the U.S. census bureau: A case study," *Social Marketing Quarterly*, vol. 6, no. 3, pp. 121–123, 2000.

[4] F. Bass, "A new product growth model for consumer durables," *Management Science*, vol. 15, pp. 215–227, 1969.

[5] B. Bollinger and K. Gillingham, "Peer effects in the diffusion of solar photovoltaic panels," *Marketing Science*, vol. 31, no. 6, pp. 900–912, 2012.

[6] H. Welsch and J. Kühling, "Determinants of pro-environmental consumption: The role of reference groups and routine behavior," *Ecological Economics, The DPSIR framework for Biodiversity Assessment*, vol. 69, no. 1, pp. 166–176, 2009.

[7] M. J. Eppstein, D. K. Grover, J. S. Marshall, and D. M. Rizzo, "An agent-based model to study market penetration of plug-in hybrid electric vehicles," *Energy Policy*, vol. 39, pp. 3789–3802, 2011.

[8] T. Islam, "Household level innovation diffusion model of photovoltaic (PV) solar cells from stated preference data," *Energy Policy*, vol. 65, pp. 340–350, 2014.

[9] D. Noll, C. Dawes, and V. Rai, *Community Organizations and Active Peer Effects in the Adoption of Residential Solar PV (SSRN Scholarly Paper No. ID 2305790)*, Social Science Research Network, Rochester, NY, USA.

[10] B. K. Sovacool, "What are we doing here? Analyzing fifteen years of energy scholarship and proposing a social science research agenda," *Energy Research & Social Science*, vol. 1, pp. 1–29, 2014.

[11] K. Jenkins, D. McCauley, R. Heffron, H. Stephan, and R. Rehner, "Energy justice: A conceptual review," *Energy Research & Social Science*, vol. 11, pp. 174–182, 2016.

[12] R. J. Heffron and D. McCauley, "Achieving sustainable supply chains through energy justice," *Applied Energy*, vol. 123, pp. 435–437, 2014.

[13] J. S. Lansing, "Complex adaptive systems," *Annual Review of Anthropology*, vol. 32, pp. 183–204, 2003.

[14] C. Li, L. Wang, S. Sun, and C. Xia, "Identification of influential spreaders based on classified neighbors in real-world complex networks," *Applied Mathematics and Computation*, vol. 320, pp. 512–523, 2018.

[15] R. Pastor-Satorras, C. Castellano, P. Van Mieghem, and A. Vespignani, "Epidemic processes in complex networks," *Reviews of Modern Physics*, vol. 87, no. 3, pp. 925–979, 2015.

[16] C. Zheng, C. Xia, Q. Guo, and M. Dehmer, "Interplay between SIR-based disease spreading and awareness diffusion on multiplex networks," *Journal of Parallel and Distributed Computing*, vol. 115, pp. 20–28, 2018.

[17] M. Jalili and M. Perc, "Information cascades in complex networks," *Journal of Complex Networks*, vol. 5, no. 5, pp. 665–693, 2017.

[18] R. Axelrod, "Advancing the Art of Simulation in the Social Sciences," in *Simulating Social Phenomena, Lecture Notes in Economics and Mathematical Systems*, D. R. Conte, P. D. R. Hegselmann, and P. D. P. Terna, Eds., pp. 21–40, Springer, Berlin, Heidelberg, Germany, 1997.

[19] V. Rai and A. D. Henry, "Agent-based modelling of consumer energy choices," *Nature Climate Change*, vol. 6, no. 6, pp. 556–562, 2016.

[20] I. Kastner and P. C. Stern, "Examining the decision-making processes behind household energy investments: A review," *Energy Research & Social Science*, vol. 10, pp. 72–89, 2015.

[21] V. Trommsdorff and T. Teichert, *Konsumentenverhalten [Consumer Behavior]*, Kohlhammer, Stuttgart, Germany, 2011.

[22] R Core Team., *R: A Language and Environment for Statistical Computing*, R Foundation for Statistical Computing, Vienna, Austria, 2016.

[23] EuPD Research., *Photovoltaik-Preismonitor Deutschland - German PV ModulePriceMonitor 2013 (No. EX0091- 059-2-3- 01–1)*, vol. No. EX0091, Bundesverband Solarwirtschaft e.V. (BSW-Solar), 2013.

[24] J. Axsen, D. C. Mountain, and M. Jaccard, "Combining stated and revealed choice research to simulate the neighbor effect: The case of hybrid-electric vehicles," *Resource and Energy Economics*, vol. 31, no. 3, pp. 221–238, 2009.

[25] M. C. Claudy, C. Michelsen, and A. O'Driscoll, "The diffusion of microgeneration technologies - assessing the influence of perceived product characteristics on home owners' willingness to pay," *Energy Policy*, vol. 39, no. 3, pp. 1459–1469, 2011.

[26] D. McCoy and S. Lyons, "Consumer preferences and the influence of networks in electric vehicle diffusion: An agent-based microsimulation in Ireland," *Energy Research & Social Science*, vol. 3, pp. 89–101, 2014.

[27] J. Zhao, E. Mazhari, N. Celik, and Y.-J. Son, "Hybrid agent-based simulation for policy evaluation of solar power generation systems," *Simulation Modelling Practice and Theory*, vol. 19, no. 10, pp. 2189–2205, 2011.

[28] M. O. Jackson, *Social and Economic Networks*, Princeton University Press, Princeton, NJ, USA, 2008.

[29] S. Wasserman and K. Faust, *Social Network Analysis: Methods and Applications*, Cambridge University Press, Cambridge, England, 1994.

[30] A. D. Henry and B. Vollan, "Networks and the challenge of sustainable development," *Annual Review of Environment and Resources*, vol. 39, pp. 583–610, 2014.

[31] M. E. J. Newman, "The structure and function of complex networks," *SIAM Review*, vol. 45, no. 2, pp. 167–256, 2003.

[32] M. Altmann, B. C. Wee, K. Willard, D. Peterson, and L. C. Gatewood, "Network analytic methods for epidemiological risk assessment," *Statistics in Medicine*, vol. 13, no. 1, pp. 53–60, 1994.

[33] M. D. Shirley and S. P. Rushton, "The impacts of network topology on disease spread," *Ecological Complexity*, vol. 2, no. 3, pp. 287–299, 2005.

[34] M. H. DeGroot, "Reaching a Consensus," *Journal of the American Statistical Association*, vol. 69, no. 345, pp. 118–121, 1974.

[35] N. E. Friedkin and E. C. Johnsen, *Social Influence Network Theory: A Sociological Examination of Small Group Dynamics*, vol. 33 of *Structural Analysis in the Social Sciences*, Cambridge University Press, Cambridge, UK, 2011.

[36] V. Rai and B. Sigrin, "Diffusion of environmentally-friendly energy technologies: Buy versus lease differences in residential PV markets," *Environmental Research Letters*, vol. 8, article 014022, no. 1, 2013.

[37] L. Strupeit and A. Palm, "Overcoming barriers to renewable energy diffusion: Business models for customer-sited solar photovoltaics in Japan, Germany and the United States," *Journal of Cleaner Production*, vol. 123, pp. 124–136, 2016.

[38] A. Banerjee, A. G. Chandrasekhar, E. Duflo, and M. O. Jackson, "The Diffusion of Microfinance," *Science*, vol. 341, no. 6144, pp. 1236498-1236498, 2013.

[39] P. Erdös and A. Rényi, "On the evolution of random graphs," *Publications of the Mathematical Institute of the Hungarian Academy of Sciences*, vol. 5, pp. 17–61, 1960.

[40] D. J. Watts and S. H. Strogatz, "Collective dynamics of "small-world" networks," *Nature*, vol. 393, no. 6684, pp. 440–442, 1998.

[41] BMWi and BMU., *First Monitoring Report - "Energy of the future."*, Bonifatius GmbH, Paderborn, Germany, 2012.

[42] BMWi., *Rahmenbedingungen und Anreize für Elektrofahrzeuge und Ladeinfrastruktur [WWW Document]*, 2016, http://www.bmwi.de/DE/Themen/Industrie/Elektromobiltaet/rahmenbedingungen-und-anreize-fuer-elektrofahrzeuge.html.

[43] M. Bechberger and D. Reiche, "Renewable energy policy in Germany: Pioneering and exemplary regulations," *Energy for Sustainable Development*, vol. 8, no. 1, pp. 47–57, 2004.

[44] S. Jacobsson and V. Lauber, "The politics and policy of energy system transformation—explaining the German diffusion of renewable energy technology," *Energy Policy, Renewable Energy Policies in the European UnionRenewable Energy Policies in the European Union*, vol. 34, no. 3, pp. 256–276, 2006.

[45] BMWi., *Energie der Zukunft - Vierter Monitoring-Bericht. Bonifatius GmbH*, Bonifatius GmbH, Paderborn, Germany, 2015.

[46] H. Granqvist and D. Grover, "Distributive fairness in paying for clean energy infrastructure," *Ecological Economics*, vol. 126, pp. 87–97, 2016.

[47] IEA and OECD., *World Energy Investment Outlook*, OECD (Organisation for Economic Co-operation and Development), Paris, France, 2014.

[48] D. Grover and B. Daniels, "Social equity issues in the distribution of feed-in tariff policy benefits: A cross sectional analysis from England and Wales using spatial census and policy data," *Energy Policy*, vol. 106, pp. 255–265, 2017.

[49] A. Macintosh, *The Australian Government's solar PV rebate program (Policy Brief No. 21)*, vol. 21, The Australian Institute, 2010.

[50] R. J. Procter, "Fixed-Cost Recovery, Renewables Adoption and Rate Fairness," *The Electricity Journal*, vol. 27, no. 5, pp. 42–53, 2014.

[51] L. C. Freeman, "Segregation in social networks," *Sociological Methods & Research*, vol. 6, no. 4, pp. 411–429, 1978.

[52] A. D. Henry, P. Pralat, and C.-Q. Zhang, "Emergence of segregation in evolving social networks," *Proceedings of the National Acadamy of Sciences of the United States of America*, vol. 108, no. 21, pp. 8605–8610, 2011.

[53] T. C. Shelling, "Dynamic models of segregation," *Journal of Mathematical Sociology*, vol. 1, pp. 143–186, 1971.

[54] BGBl., *Gesetz über die Einspeisung von Strom aus erneuerbaren Energien in das öffentliche Netz (Stromeinspeisungsgesetz)*, 1991.

[55] N. Martin and J. Rice, "Solar Feed-In Tariffs: Examining fair and reasonable retail rates using cost avoidance estimates," *Energy Policy*, vol. 112, pp. 19–28, 2018.

[56] REN21., *Renewables 2007 Global Status Report. REN21, Paris & Washington,DC*, 2008.

[57] S. Chowdhury, U. Sumita, A. Islam, and I. Bedja, "Importance of policy for energy system transformation: Diffusion of PV technology in Japan and Germany," *Energy Policy*, vol. 68, pp. 285–293, 2014.

[58] A. J. Schaffer and S. Brun, "Beyond the sun—Socioeconomic drivers of the adoption of small-scale photovoltaic installations in Germany," *Energy Research & Social Science*, vol. 10, pp. 220–227, 2015.

[59] C. Schelly, "Transitioning to renewable sources of electricity: motivations, policy and potential," in *Controversies in Science and Technology: From Sustainability to Surveillance*, D. L. Kleinman, K. A. Cloud-Hansen, and J. Handelsman, Eds., pp. 62–72, Oxford University Press, New York, NY, USA, 2014.

[60] N. Martin and J. Rice, "The solar photovoltaic feed-in tariff scheme in New South Wales, Australia," *Energy Policy*, vol. 61, pp. 697–706, 2013.

[61] BT- Drs., *Stenografischer Bericht. 40. Sitzung (BT-Plenarprotokoll No. 17/40)*, Deutscher Bundestag, Berlin, Germany, 2010.

[62] A. Pyrgou, A. Kylili, and P. A. Fokaides, "The future of the feed-in Tariff (FiT) scheme in europe: The case of photovoltaics," *Energy Policy*, vol. 95, pp. 94–102, 2016.

[63] T. Tantisattayakul and P. Kanchanapiya, "Financial measures for promoting residential rooftop photovoltaics under a feed-in tariff framework in Thailand," *Energy Policy*, vol. 109, pp. 260–269, 2017.

[64] E. Drury, M. Miller, C. M. Macal et al., "The transformation of southern California's residential photovoltaics market through third-party ownership," *Energy Policy*, vol. 42, pp. 681–690, 2012.

[65] H. Zhang, Y. Vorobeychik, J. Letchford, and K. Lakkaraju, "Predicting rooftop solar adoption using agent-based modeling," in *Proceedings of the 2014 AAAI Fall Symposium Series*, 2014.

[66] A. D. Henry and H. Brugger, "Agent-Based explorations of environmental consumption in segregated networks," in *Social Systems Engineering: The Design of Complexity, Computational and Quantitative Social Science*, C. García-Díaz and C. Olaya, Eds., John Wiley & Sons, 2017.

[67] R. Axelrod, "Effective Choice in the Prisoner's Dilemma," *Journal of Conflict Resolution*, vol. 24, no. 1, pp. 3–25, 1980.

[68] D. J. Watts, "A simple model of global cascades on random networks," *Proceedings of the National Acadamy of Sciences of the United States of America*, vol. 99, no. 9, pp. 5766–5771, 2002.

Hindawi
Complexity
Volume 2019, Article ID 5041681, 11 pages
https://doi.org/10.1155/2019/5041681

Review Article

Policy Modeling and Applications: State-of-the-Art and Perspectives

Bernardo A. Furtado[1,2] **Miguel A. Fuentes**[3,4,5] **and Claudio J. Tessone**[6]

[1] *Department of Innovation and Infrastructure, Institute for Applied Economic Research, Brasília 70076-900, Brazil*
[2] *National Council of Research, Brasília, Brazil*
[3] *Santa Fe Institute, 1399 Hyde Park Road, Santa Fe, NM, 87501, USA*
[4] *Instituto de Investigaciones Filosóficas, Bulnes 642, Buenos Aires 1176, Argentina*
[5] *Facultad de Ingeniería y Tecnología, Universidad San Sebastián, Lota 2465, Santiago 7510157, Chile*
[6] *URPP Social Networks, Universität Zürich, Zürich CH-8050, Switzerland*

Correspondence should be addressed to Bernardo A. Furtado; bernardo.furtado@ipea.gov.br

Received 20 July 2018; Accepted 14 January 2019; Published 3 February 2019

Academic Editor: Qingdu Li

The range of application of methodologies of complexity science, interdisciplinary by nature, has spread even more broadly across disciplines after the dawn of this century. Specifically, applications to public policy and corporate strategies have proliferated in tandem. This paper reviews the most used complex systems methodologies with an emphasis on public policy. We briefly present examples, pros, and cons of agent-based modeling, network models, dynamical systems, data mining, and evolutionary game theory. Further, we illustrate some specific experiences of large applied projects in macroeconomics, urban systems, and infrastructure planning. We argue that agent-based modeling has established itself as a strong tool within scientific realm. However, adoption by policy-makers is still scarce. Considering the huge amount of exemplary, successful applications of complexity science across the most varied disciplines, we believe policy is ready to become an actual field of detailed and useful applications.

1. Introduction

Generally speaking, complex systems are those in which the sum of the parts is insufficient to describe the macroscopic properties of systems' behavior and evolution [1–3]. Interactions among parts of the system, at different scales, in a nonhierarchical [4], nonlinear, and self-organizing manner [5] lead to emerging properties [6, 7] that fail to have a single, certain unfolding in the future.

Social actions, carried out by millions of individuals interacting in a multitude of way and through traditional or digital means, and economic processes, where highly heterogeneous economic actors are interconnected by transactions, ownership relations, competition, and mutualism, are two paradigmatic kinds of complex systems. Policies, as a set of actions to enhance social life and economic processes, are an archetypical example of controlling them. Policies are the product of the interaction of agents and institutions in time and space in which knowledge of current state provides only incomplete views of future states of the system. **Policy modeling**, as an attempt to design the operation of such interactions, presupposes some level of comprehension of the mechanisms, processes, and likely trajectories while maintaining a strict knowledge of the inherent incompleteness of modeling complex systems [8–12].

This view that policies are complex enables the **application** of complex systems' methodologies onto the analysis of public (and private) policy-making. Such application feeds on early contributions and takes many forms that vary from simple construction of indicators and measures of complexity *à la* Shannon [13–15], to cellular automata and artificial intelligence [16], to agent-based modeling [17] and network science [18].

This review provides an overview of contemporary applications of policy modeling that follows the traditional complex systems' methodologies portfolio. Mainly, we focus on

agent-based modeling, network science, and data mining. First, we discuss the methodologies themselves and then we examine three cases in detail. A large consortium for infrastructure analysis applied to the case of Britain, one of the most consolidated families of macroeconomics agent-based models and its applications on fiscal and monetary policies and a land-use model in use by metropolitan governance entities across the USA and abroad. Implications for policy modeling close the paper.

2. Policy Modeling Methodologies

Fuentes [19] describes a landscape of eleven distinct methodologies coming from complex systems' sciences (the complex science referred by Fuentes [19, pp. 55–56] include "nonlinear science, bifurcation theory, pattern formation, network theory, game theory, information theory, super statistics, measures of complexity, cellular automata, agent-based modeling, and data mining"). While that approach is more exhaustive, here, we emphasize applications to public policies, thus focusing more extensively on the discussion of agent-based modeling and cellular automata, data mining, network analysis, and game theory. Other relevant methodologies are considered together in a specific subsection.

2.1. Agent-Based Modeling and Cellular Automata. Agent-based modeling (ABM) is a computational or algorithmic, artificial implementation of agents who interact among themselves and with the environment following a set of rules. As a result of the interaction, the variables that describe the state of the agents may be modified [20–23]. ABM is useful when analytical solutions are too complex or impossible to be calculated. Results are sensitive to initial conditions, although, in many cases, still deterministic, and thus useful interpretation relies on distributions of stochastically repeated simulations of the model and reasonable validation.

The uniqueness of ABM methodology led Epstein [24, 25], probably inspired by Ostrom [26], to suggest a third way of doing science. Verbal or argumentative would be the first one, mathematically quantification a second, and algorithmic simulation the third [27]. Such proposal is in line with the views of philosopher Nicolescu [28] in which social sciences (and therefore, policy-making) have a contained maneuvering space when experimenting with populations and individuals. ABM provides just that liberty of experimenting *in silico* with additional degrees of freedom. Hence, ABM may enhance the capabilities of social sciences to bridge science and policy.

In fact, agent-based modeling as a methodology has a number of attributes that probably make it the method of complex systems most attached to policy-making. It is flexible, adaptable to empirical analysis, cost-effective, and adequate to ever-changing analysis scenarios [29]. ABM is also applied to a number of different disciplines in the realm of policy studies from demography [30], to anthropology [31], and it also gains recognition and scope in economics [27, 32] and international politics [33]. Finally, there is also a profusion of available tools specifically designed for modeling [34].

In economics, Dawid and Delli Gatti [35] categorize seven distinct families of macroeconomic models [36–44]. Dosi, Fagiolo, Roventini, and coauthors [41, 45–47] probably lead the most prolific evolutionary branch of economic modeling whereas Lengnick is a single standalone model proposal which does not include a credit market [42]. Despite these large macroeconomic models, economic studies also emphasize market-specific models: in electricity [48, 49], labor market [47, 50], economic behavior [51, 52] and the problem of commons [53]. Further in economics, ABM is used to criticize current, quantitative, yet perfect (without endogenous crises) economic models [54–56]. Finally, it is worth mentioning the use of ABM to test policies applied to the financial markets, from the early contributions of LeBaron [57, 58] and Westerhoof [59] to the detailing of the effects of transaction taxes and trading halts on assets volatility [60].

Despite all these contributions, institutions and governments are still slow in adopting recommendations. Bank of England [61], OECD [62], the European Union [63] and some academic institutions (such as MITRE, DARPA, and NECSI) have helped fuel the debate. Although Page [64] reminds us with the essence of understanding the mechanism underpinning economic phenomena, policy-makers do not seem ready to accept general results and explanations [65–67], rather sticking to precise (yet probably wrong [54]) numbers.

Cellular automata (CA) also goes back to the infancy of complex studies [3, 6, 68, 69]. Its fundamental design is the related analysis of diffusion by contact processes in a deterministic way when the state of the agents can be described by a finite set of states. Despite a stream of literature by itself, contemporary conceptualization of CA may consider it as a special case of agent-based modeling in which agents are fixed and not mobile and their relationships follow a matrix of adjacency [70, 71]. Even then, CA is much used for spatial analysis, having once been called "space theory based models" [72].

In fact, among geographers and spatial analysts "Land-Use and Transportation" models (LUTs) have yielded results and recommendations for the past two decades. Early models [73, 74] focused on urban development, but those were readily followed by more general land-cover models [75, 76]. Transportation and activities models also intensified their uses in the 2000s [77, 78] and became paradigmatic for actual use in urban planning and transportation [79–81], especially by metropolitan bodies.

Advances in the area have been so intertwining that new models have started to feed from different trends of spatial-modeling literature bridging transportation and land-use models to macroeconomics [82] and actual life-cycle of individuals in order to generate individual demand models [83]. The bridge has also been generous when crossing automated computing techniques and traditional models [84] or when aiding its validation [85].

2.2. Network Science. Network science studies the structure of a given system in general by recourse of tools originated in

graph theory. Here, nodes describe the system constituents and edges conform the interactions between them. One may consider again that networks are generalizations of agent-based models in which not only agents have attributes, but also edges, with varying attributes and lengths. These connections are abstractions, or dimensional relationships of the typical fixed neighborhood found in CA models. These arguments are purely conceptual and only aid the highlighting of the complementarity of complex systems methodologies [86]. In fact, two similar economic models may use either networks [42] or spatial distance [82] as rules towards consumer decision-making.

Despite this inherently attached connection with both ABM and CA, network science has come a long way after its relatively recent birth as an independent yet gregarious discipline, marked by the seminal papers by Watts and Strogatz [87] and Barabási and Albert [88]. In fact, it has developed a large field of literature that has evolved from recent work on network statistics [89] to studies that describe dynamic changes of the network itself [90].

In Finance, applied network analysis has helped illuminate likely policy effects of systemic risk within interbank trading. An early work by Battiston et al. [91, p. 2082] showed that local interactions travelling within networks may function as "an alternative mechanism for the propagation of failures". Subsequent work was able to measure network systemic relevance more precisely [92] and thus apply policy testing, including transparency advocacy [93] and leverage regulation [94]. Together, these analyses have demonstrated with considerable easiness the possibilities of simulating alternative policy scenarios.

A current challenge in network science is "understanding the relationship between structure and function" [95, p. 9]. Scientists are trying to comprehend how the topological structure of a given network—how their nodes are connected–influences their systemic functions and what they do. An example would be to clarify how the connection of proteins determines a resulting phenotype. Conversely, others [96] are trying to find the function or purpose of the network given observed data, having applied examples on migration, congress voting, and the human brain.

2.3. Data Mining. Data mining, or more generally data science, has benefited from continuously decreasing hardware prices, larger software communities, and an abundance of data following generalization of desktops first and mobile devices more recently, which subsumed giving rise to the ongoing digitalization of society. One could date this quantification and empirical emphasis back to around 2001's book by Hastie, Tibshirani, and Friedman [97], deepening the effort in 2009 [98]. Quickly, deep learning [99] and neural networks [100] became standard, maybe due to available software (and accelerators), such as TensorFlow [101].

There is no doubt of the beneficial effects of data science on social life enhancement in fields such as pinpointing fraudulent actions [102, 103] helping in medicine diagnostics [104], training of professionals via simulation [105], or aiding mobility through autonomous systems [106]. However, some concerns are also present [107]. Specifically, there are mentions of results without theory, like the infamous Garbage In, Garbage Out (GIGO) [108].

Such lack of theory is of minor concern for some machine learning scientists who want solely to achieve the best possible prediction, no matter the processes or prejudices. Conversely, there is the argument that complex "description" [109], hitherto unavailable, may provide new theories by induction, which previously seemed as a lackluster source of scientific reasoning.

2.4. Game Theory. Game theory focuses on how a group of agents or elements (which may describe individuals, organizations, economic actors, etc.) interact using strategic decision-making. The two branches that one can visualize in this field are cooperative or noncooperative. A good reference for a discussion on this topic can be seen in [110]. It is usually understood that cooperative game theory is applicable when agreements are enforceable, while noncooperative game theory is applicable otherwise. McCain argue that noncooperative game theory is an effective tool for problem-finding (or diagnostic method). These observations make game theory a useful methodology to be applied in societies that faces continuous decision-making processes. Moreover, recent studies suggest that a combination of game theory with psychology and neuroscience has great potential to understand mechanism involved in social decision-making [111]. It is worth mentioning that the connection between game theory and complexity can be achieved, or it is clearer, when an important number of agents are connected in a network interacting under a game theory dynamics, as in the case of evolutionary game theory [112].

2.5. Other Policy Methodologies. Dynamical systems (DS) is a modeling approach in which there are timed flows among stocks and control of probabilistic input of variables in order to conform a systemic analysis with feedback [113]. On such setting, each stock entity is an abstract construction that allows mathematical simulation of future states of the system. There is not, however, heterogeneity within each entity as in ABM, nor spatial representation, as Batty reminds us [21]. DS was introduced in the 1970s [114] and has accumulated many applications and supporting technologies since then [115]. Even though DS and ABM share some characteristics, they also have important, fundamental, differences [116]. Some of those are the applications on different levels of analyses using ABM on complex networks [117]. In those types of systems, the emergence of new characteristics at higher levels is difficult to analyze using first principles, something that is one of the main characteristics and properties of classical DS [118].

Moreover, numerical simulation, microsimulation, or yet mathematical simulation is also a methodology that solves otherwise intractable analytical equations numerically [119]. It is the simple application of known rules, usually probabilistic ones, to known states so that the researcher can observe the trajectory and results into the future. Numerical simulation is useful, for example, to understand the effects of a given

tax change on specific sectors or taxpayers. Crooks and Heppenstall [120], however, highlight that microsimulation accounts only for direct effects, the effect of taxes on the market, but not the counterreaction, i.e., the indirect effect of having a market that is different from the original one. Numerical simulation has been used in various fields ranging from regional economics [121], to fluids, to pollution.

Before concluding, we highlight that this review is definitely not exhaustive, but covers the methodologies most attached to policy applications. We describe some applications in the following section.

3. Policy Modeling Applications

There has been a wide and spread range of research and output for policy using complex systems' various methodologies. This special issue is, as far as we know, a first effort to put together the main strands of literature specifically on the area of policy. On the same vein, the previous section lists a sample of the most referenced publications that discusses policy modeling and applications in order to help crisscross leading researchers over different fields. In this section, we dwell a bit longer on three cases of larger impact and reverberation, in our opinion.

Specifically towards policy and management, there is significant difference between planning for a known, well-designed trajectory development and planning within a complex system environment. "Complexity theory demonstrates that there are fundamental conceptual difficulties in the concepts of "planning" in any open system which contain a significant level of decentralization of decision-making" [12] [122, p. 320]. In other words, referring to fishery governance, systems are neither predictable nor controllable [123], thus, the need to consider ever-changing environments when doing policy-making.

3.1. System of Systems. A consortium of seven leading universities and other partners in the United Kingdom has formed the Infrastructure Transitions Research Consortium (ITRC). ITRC has put together a National Infrastructure Model (NISMOD) that in turn has evolved into a current program named Multiscale Infrastructure Systems Analytics (MISTRAL). All those acronyms depict a large institutional effort aimed at applying "complexity-based methods" to public policy based on a criticism of reductionist science, systems theory, and mainstream neoclassical economics.

ITRC proposed focusing on four main themes (according to the Report "Final Results from the ITRC" (2015), available at https://www.itrc.org.uk/wp-content/PDFs/ITRC-booklet-final.pdf. For a longer discussion, see [124]):

(a) Develop a capacity to compare quantitative metrics of infrastructure capacity and demand given a varied number of alternative scenarios, which ITRC call **national strategies**, while accounting for **interdependent effects** among infrastructure sectors

(b) Develop a specific model of vulnerabilities and cascading cumulative failures (and resilience) in connected infrastructure systems

(c) Develop an understanding of the dynamics of infrastructure when coupled with evolving socioeconomic (heterogeneous), spatially specific social groups

(d) Develop sound long-term planning of infrastructure systems

MISTRAL proposes going further with four encompassing challenges (see Report [125]): (a) downscale, detail, and emphasize local complexity of infrastructure, (b) focus on its interdependencies and connections, (c) take the experience abroad and change infrastructure decision-making internationally, and (d) maintain its focus on quantifying the relationships between infrastructure and economic growth.

All in all, the best output to follow the production of ITRC's proposal is the book by leading researchers Jim W. Hall, Martino Tran, Adrian J. Hickford, and Robert J. Nicholls [124]. The authors introduce the book motivating the relevance of infrastructure systems, discussing the challenges of handling infrastructure within a contemporary, advanced-economies, interdependent environment, and outlining their "system of systems approach".

Such an approach, the authors claim, would equalize both assumptions and metrics across different infrastructure sectors and make them robust against future uncertainties, all in accordance with strategies developed and scenarios that are outside the control of policy-makers. Further, the system of systems would be able to capture possible risks and vulnerabilities, thus making the infrastructure system more resilient. Hence, better, long-term planning would ensue.

According to their proposed framework, the first methodological step is *scenario generation*. A scenario builds upon a range of possible futures unfolding from demographic, economic, climate change, and environmental alternatives. As a result, "a complete set (times series) of external parameters defining the boundary conditions" [126, p. 15] is produced. The total number of possible scenarios considering all alternatives amounts to 2,112 combinations. However, given that difference, close scenarios provide very similar results and have different probabilities; in practice a set of three most likely scenarios with some variants is actually employed in the analysis.

Next, strategies, defined as the possible ways to tackle infrastructure provision in terms of planning, investment, and projects, are developed. The proposals need to be based on national policy directives and detailed enough so that they can be simulated. At the same time, three approaches per sector are observed: (a) **demand management**, such as regulation of a given sector, which may affect demand; (b) **system efficiency**, including possible gains that come from technology adoption for instance, and (c) **capacity expansion** changes, which actually involves physically altering infrastructure assets.

The third methodological step implies the use of detailed models that are specific for each sector, but that are intertwined with one model's input coming from another model's output. The best description of the system of systems method is that of a "family of models" in which communication and special links are consistent so that policy trade-offs across the full infrastructure system are properly evaluated.

Qualitatively, there are four ways to incorporate changes within the model. When policy-makers propose a change of policy, such a proposal enters the model as a strategy-change, which will end up as a measured change in demand. When incorporating an innovative process, efficiency parameters change. When physical infrastructure changes, the capacity (supply) of the system changes. Finally, when exogenous change happens, scenarios also change. When all the above steps have been implemented, the system is ready to provide evaluation and prognostics. As the authors claim, a "web-based data-viewer (. . .) combines and compares performance across sectors, across time, across regions, and across future conditions" [126, p. 24].

The project has certainly spanned a wide range of results and publications (a full reference guide, divided by nine themes (complex adaptive systems, databases, demographics, digital communications, economic impacts, governance, infrastructure system network risk analysis, and solid waste) can be found at https://www.itrc.org.uk/outputs/research-outputs/). Among the ones with larger reach is a methodological proposal (with 25 authors) [127] and a study on the link between energy and water [128].

3.2. Macroeconomics Agent-Based Model. One of the seven families of macroeconomics models described by Dawid and Delli Gatti [35] and also featured in Dosi and Roventini [129] is coined "Keynes meets Schumpeter" (KS) and was led by Dosi, Fagiolo, Roventini, among other coauthors (we have chosen this family to detail, as it seems to have the larger number of stylized facts reproduced and the more proficuous production). The model baseline was described in [45] and has a recent consolidation in [130]. A new model validation proposal uses KS as case-study [85] and policy applications have been done on climate change [131], labor market [46, 132], and monetary policy [133, 134]. A review on macroeconomics agent-based models policy application is available in [135].

The great contribution of KS is the ability to endogenously reproduce long-term economic cycles [130], while also maintaining short-term results, thus, breaking with the economic paradigm of equilibrium in which crisis is only deviations from a supposedly correct natural path [54]. Crisis in fact may have long-lasting effects on the economy. Further, the KS model seems especially relevant given that it has been shown to be validated [85]. As such, KS refutes the main valid criticism of agent-based modeling which is the lack of validation. Further, it provides actual policy case studies that are concrete and foundational enough to be applied to policy-making.

KS models the attempt of translating conceptual innovation theory into measured, validated output growth, contextually dependent on macroeconomic conjuncture. Such an attempt covers both the short-term (and indicators such as unemployment) and the long run (such as GDP). KS approach is novel, when compared to traditional macroeconomic Dynamic Stochastic General Equilibrium (DSGE) models as traditional ones do not treat technology as an endogenous factor for model explanation [130].

The model is composed of firms from two sectors (capital and consumption-goods), banks, Central Bank, labor force, and government. Capital firms drive innovation when investing in R&D and output more efficient, cheaper machines. Government defines taxes values and unemployment subsidy levels and the Central Bank decides on interest rate levels [130].

The authors list 17 stylized facts, in both macro- and microeconomics, that help ensure the model validity for policy analysis. Those stylized facts go from replicating endogenous economic fluctuations, to recession durations to cross-correlation of macro- and credit-related variables. Further, in microeconomics, the model mimics firms size distribution, firms' productivity heterogeneity, bankruptcies, among others [130]. Despite these resemblances, as previously mentioned, KS model was used as a case-study by [85, p. 138, our emphasis] in which they compared the structures of vector autoregressive models in a five-step process to show that KS "resemble between 65% and 80% of the **causal relation**" in observed macroeconomic time-series.

A bundle of eleven policy analyses derived from KS is available [46, 133, 134]. They include firms' innovation search capabilities, technological opportunities, patents, new firms' productivity, market selection, antitrust, among others. Specifically about income inequality, [133] reports that markup setting influences both the dependence of financial support and the share between profits and wages. Such mechanism affects macroeconomics' stability and growth. Together, the authors agree with inputs by Stiglitz and Piketty that claim that there is a downward trend feedback loop in economics that can be tied to higher levels of inequality. In such a scenario fiscal austerity has more negative effects when coupled with higher markup levels.

Furthermore, recent applications of the KS model on the labor market [47, 136, 137] have helped show that more rigid markets with higher levels of protection and less flexible wage may in fact keep output at increased levels, while maintaining lower inequality. Dosi et al. [137] suggest that coordination failures bring wages down and thus significantly impacting aggregate demand. The authors also suggest [136] that the core reasons of rising unemployment are lower innovation rates, workers' skills deterioration, and reduced firms entry dynamics. This is also relevant because it goes against typical policy recommendations based on DSGE applications hitherto supported by international institutions such as OECD and the IMF, but which is under discussion [138].

In sum, KS model suggests that (a) technological changes and market open for new firms lead to strong positive growth; (b) patent enforcement, however, reduces growth dynamism; and (c) competition is relevant, but producing weaker effects. KS further recommends countercyclical fiscal policy (opposed to fiscal austerity) as a means to convey (a) unemployment and output stability; (b) "higher growth paths", whereas fiscal austerity would be detrimental to the economy and government debt in both the short and long run.

KS is thus a model that clearly exemplifies a new tradition for a given segment of macroeconomics [135]. It seems

to have been able to capture most of the variations of a complex system, the economy, allowing for policy analysis in a validated, fact replicating reasonable model.

3.3. UrbanSim. UrbanSim was first proposed in the mid-1990s [77, 78, 139, 140] as a model that focused on feedback effects from land use into transport and back. Their modeling process include a family of submodels that run independently, feeding on empirical data, while exchanging inputs and outputs among themselves. In practice, a GIS interface with a typical 150-meter grid works as a single unit summing up households and firms. The land price model follows typical neoclassical urban economics [141] and hedonic price regression modeling [142] which is update at each year-step of the model.

Since then, UrbanSim has grown and changed into a 3D platform in 2012 and became proprietary software (urban canvas) in 2014. They have now expanded the simulation to include not only land use and transportation but also the economy and the environment. They claim to account for unfolding effects of infrastructure onto transport, housing affordability, and the environment.

The agents of the model include households, individual citizens, and firms, including land developers, government, and their political constraints [143]. Facing a given environment, agents make choices, such as (a) whether to find a job (and which one) or stay at home, (b) where to locate your own family or your business, and (c) whether a family or business relocation is a sensible move.

The market in the model is asynchronous. Households search for new dwellings facing the short-term needs for a given year. Land developers observe house demand, but augment house supply within a wider, cumulative number of years [143]. Although prices are modeled (calculated) endogenously, the model does not impose equilibrium; i.e., there is no need for markets to "clear" [77].

A first application of the model is available for Eugene-Springfield, Oregon [77]. The interested policy stakeholder, Oregon Department of Transportation, actually financed the project. The model uses data starting in 1994 and runs for 15 years with a resolution grid of 150 square meters. A previous time-frame from 1980 to 1994 was used to validate the model capabilities. A good accuracy (of less than 50 households between simulated and observed results) was achieved for 57% of the sample. A larger error of up to 200 households included 89% of the sample for number of households and 76% for the number of jobs. Although reasonable, the results did not predict isolation and pinpoint change occurrences and have also overpredicted and underpredicted for small areas.

The takeaway from the first UrbanSim implementation is that effective integration of at least land use, transportation, and environmental issues' mechanisms is a must [77]. Such an integration should also be accompanied by considering that, in practice, those areas usually involve different, distinct institutions (responsible for each issue), with conflicting values, epistemologies, and pragmatic policies [143].

Applications of UrbanSim were later developed for Detroit, Michigan [144], Salt Lake City, Utah [139], San Francisco, California [145], Seattle, Washington [146], and Paris, France [147].

The belief for integrated planning shown in the 2011s [143] paper is still present in UrbanSim's most recent output [79]. Once more financed by an interested policy stakeholder, US Department of Energy, the authors propose an integrated "pipeline" among UrbanSim, called a microsimulation platform, along with ActivitySim, an agent-based model platform responsible for the generating traffic demand based on citizens choice of activities and a traffic assignment model (a routing mechanism). The motivation behind the attempt is clear: how to effectively quantify both intended and unintended consequences on urban complex environments, given a specific change in infrastructure or policy. Further, as the authors put it, urban systems are those in which "transportation network, the housing market, the labor market ([via] commuting), and other real estate markets are closely interconnected..." [79, p. 2].

4. Conclusions

In this review, we show some of the impact of the complexity science methodologies has had in public policy. We take special attention to agent-based modeling, network science, data mining, and game theory. We believe that these methodologies are important not only being used extensively nowadays, but also being the ones that are creating the bridge between science (its quantitative and qualitative methods, ways of thinking, etc.) and policy decision-making. We also have presented real cases where the use of such methodologies has been used.

The case analysis suggests that larger efforts are being developed in policy applications of different realms, from macroeconomics (fiscal and monetary policy), to urban planning (mobility and air pollution), to infrastructure (energy, water, and waste). We have selected these examples as they are paradigmatic, while we acknowledge that they are only some of the high-magnitude works currently being developed. The list of references amassed account for other smaller, scattered applications that seem to be wide and spread across disciplines.

Nevertheless, such a growing body of literature does not show that these methodologies have been understood, nor accepted without caveats in academia (in general) and policy-makers. Namely, most macroeconomics policy follows DSGE methods although they have been also heavily criticized [54]. Most infrastructure projects are planned in an isolated manner, following sector guidelines with little or no interface with other sectors. Further, most urban planning carried out observes all of the challenges issues listed by [143] conflicting institutions, values, epistemologies, and policies, but also the inherent communication issues across heterogeneous fields.

All in all, results of the three cases presented in detail reinforce the belief that integrated modeling performed with input originated across disciplines, sectors, and institutions within a complex systems framework deliveries with the added bonus of unveiling large scale effects of policies in an adaptive, evolutionary, nonhierarchical manner.

This work is part of a special issue on Public Policy Modeling and Applications.

Conflicts of Interest

The authors declare that there are no conflicts of interest regarding the publication of this paper.

Acknowledgments

Bernardo A. Furtado would like to acknowledge Grant [306954/2016-8] from the National Council of Research (CNPq). Claudio J. Tessone acknowledges financial support of the University of Zurich through the University Research Priority Program on Social Networks.

References

[1] P. W. Andersen, "More is different," *Science*, vol. 177, no. 4047, pp. 393–396, 1972.

[2] C. G. Langton, "Studying artificial life with cellular automata," *Physica D: Nonlinear Phenomena*, vol. 22, no. 1–3, pp. 120–149, 1986.

[3] J. V. Neumann, "The role of high and of extremely high complication," in *Theory of self-reproducing automata*, pp. 64–87, University of Illinois Press, Urbana, 1966.

[4] H. A. Simon, "The Organisation of Complex Systems," in *Hierarchy Theory - the challenge of complex systems*, H. H. Pattee, Ed., pp. 1–27, New York, NY, USA, 1973.

[5] S. Wolfram, "Universality and complexity in cellular automata," *Physica D: Nonlinear Phenomena*, vol. 10, no. 1-2, pp. 1–35, 1984.

[6] A. M. Turing, "The chemical basis of morphogenesis," *Philosophical Transactions of the Royal Society B: Biological Sciences*, vol. 237, no. 641, pp. 37–72, 1952.

[7] J. J. Hopfield, "Neural networks and physical systems with emergent collective computational abilities," *Proceedings of the National Acadamy of Sciences of the United States of America*, vol. 79, no. 8, pp. 2554–2558, 1982.

[8] R. Geyer and P. Cairney, *Handbook on Complexity and Public Policy*, Edward Elgar Publishing, 2015.

[9] B. Edmonds, "The room around the elephant: tackling context-dependency in the social sciences," in *Non-equilibrium social science and policy*, J. Johnson, P. Ormerod, Y.-C. Zhang, and A. Nowak, Eds., pp. 195–208, Switzerland, 2017.

[10] D. Helbing, *Social Self-Organization: Agent-Based Simulations and Experiments to Study Emergent Social Behavior*, Springer, New York, NY, USA, 2012.

[11] J. Johnson, P. Ormerod, B. Rosewell, A. Nowak, and Y.-C. Zhang, *Non-Equilibrium Social Science and Policy*, Springer, 2017.

[12] B. Mueller, "Complex systems modelling in Brazilian public policies," in *Modeling complex systems for public policies*, pp. 261–278, IPEA, Brasília, 2015.

[13] C. E. Shannon, "A mathematical theory of communication," *Bell System Technical Journal*, vol. 27, no. 4, pp. 623–656, 1948.

[14] A. N. Kolmogorov, "Three approaches to the quantitative definition of information," *Problems of information transmission*, vol. 1, no. 1, pp. 3–11, 1965.

[15] M. Gell-Mann and S. Lloyd, "Effective Complexity," in *Nonextensive Entropy*, pp. 387–398, Murray Gell-Mann and Constantino Tsallis, 2004.

[16] M. Minsky, "Steps Toward Artificial Intelligence," *Proceedings of the IRE*, vol. 49, no. 1, pp. 1–65, 1961.

[17] T. C. Schelling, "A process of residential segregation: neighborhood tipping," in *Racial discrimination in economic life*, vol. 157, p. 174, 1972.

[18] M. E. J. Newman, "The structure and function of complex networks," *SIAM Review*, vol. 45, no. 2, pp. 167–256, 2003.

[19] M. Fuentes, "Methods and methodologies of complex systems," in *Modeling complex systems for public policies*, pp. 55–72, IPEA, Brasília, DF, 2015.

[20] J. M. Epstein and R. L. Axtell, *Growing artificial societies: social science from the bottom up*, Brookings/MIT Press, Cambridge, MA, 1996.

[21] M. Batty, "A generic framework for computational spatial modelling," in *Agent-Based Models of Geographical Systems*, pp. 19–50, Springer, 2012.

[22] L. Tesfatsion, "Agent-Based Computational Economics: A Constructive Approach to Economic Theory," in *Handbook of Computational Economics*, vol. 2, pp. 831–880, Elsevier, 2006.

[23] U. Bilge, "Agent based modelling and the global trade network," in *Handbook on complexity and public policy, Robert Geyer and Paul Cairney*, pp. 414–431, 2015.

[24] J. M. Epstein, "Agent-based computational models and generative social science," *Complexity*, vol. 4, no. 5, pp. 41–60, 1999.

[25] J. M. Epstein, "Remarks on the Foundations of Agent-Based Generative Social Science," in *Handbook of Computational Economics*, vol. 2, pp. 1585–1604, Elsevier, 2006.

[26] T. M. Ostrom, "Computer simulation: The third symbol system," *Journal of Experimental Social Psychology*, vol. 24, no. 5, pp. 381–392, 1988.

[27] P. Terna, "From complexity to agents and their models," in *Agent-based models fo the economy: from theories to applications*, B. Riccardo, M. Matteo, S. Michele, and T. Pietro, Eds., pp. 10–30, 2015.

[28] B. Nicolescu, *Manifesto of transdisciplinarity*, Suny Press, 2002.

[29] B. A. Furtado, P. A. M. Sakowski, and M. H. Tóvolli, *Modeling complex systems for public policies*, Brasíli, IPEA, 2015.

[30] F. C. Billari, F. Ongaro, and A. Prskawetz, "Introduction: Agent-based computational demography," in *Agent-Based Computational Demography*, pp. 1–17, Springer, 2003.

[31] J. S. Dean, G. J. Gumerman, J. M. Epstein et al., "Understanding Anasazi culture change through agent-based modeling," *Dynamics in human and primate societies: Agent-based modeling of social and spatial processes*, pp. 179–205, 2000.

[32] L. Hamill and N. Gilbert, *Agent-based modelling in economics*, John Wiley & Sons, UK, 2016.

[33] R. Geyer and S. Rihani, *Complexity and public policy: a new approach to 21st century politics, policy and society*, Routledge, London, UK, 2010.

[34] S. Abar, G. K. Theodoropoulos, P. Lemarinier, and G. M. P. O'Hare, "Agent Based Modelling and Simulation tools: A review of the state-of-art software," *Computer Science Review*, vol. 24, pp. 13–33, 2017.

[35] H. Dawid and D. D. Gatti, "Agent-Based Macroeconomics," in *Handbook on Computational Economics*, vol. 4, Elsevier, 2018.

[36] D. D. Gatti, C. Di Guilmi, E. Gaffeo, G. Giulioni, M. Gallegati, and A. Palestrini, "A new approach to business fluctuations:

Heterogeneous interacting agents, scaling laws and financial fragility," *Journal of Economic Behavior & Organization*, vol. 56, no. 4, pp. 489–512, 2005.

[37] Q. Ashraf, B. Gershman, and P. Howitt, "Banks, market organization, and macroeconomic performance: An agent-based computational analysis," *Journal of Economic Behavior & Organization*, vol. 135, pp. 143–180, 2017.

[38] H. Dawid, S. Gemkow, P. Harting, S. van der Hoog, and M. Neugart, "An Agent-Based Macroeconomic Model for Economic Policy Analysis: the Eurace@ Unibi model," *Bielefeld Working Papers in Economics and Management*, 2014.

[39] S. Cincotti, M. Raberto, and A. Teglio, "Macroprudential policies in an agent-based artificial economy," *Revue de l'OFCE*, vol. 124, no. 5, pp. 205–234, 2012.

[40] P. Seppecher, "Flexibility of wages and macroeconomic instability in an agent-based computational model with endogenous money," *Macroeconomic Dynamics*, vol. 16, no. 2, pp. 284–297, 2012.

[41] G. Dosi, G. Fagiolo, and A. Roventini, "The microfoundations of business cycles: an evolutionary, multi-agent model," in *Schumpeterian Perspectives on Innovation, Competition and Growth*, U. Cantner, J.-L. Gaffard, and L. Nesta, Eds., pp. 161–180, Springer, Berlin, Heidelberg, 2009.

[42] M. Lengnick, "Agent-based macroeconomics: a baseline model," *Journal of Economic Behavior & Organization*, vol. 86, pp. 102–120, 2013.

[43] A. Haas and C. Jaeger, "Agents, bayes, and climatic risks - A modular modelling approach," *Advances in Geosciences*, vol. 4, pp. 3–7, 2005.

[44] Q. Ashraf, B. Gershman, and P. Howitt, "How inflation affects macroeconomic performance: An agent-based computational investigation," *Macroeconomic Dynamics*, vol. 20, no. 2, pp. 558–581, 2014.

[45] G. Dosi, G. Fagiolo, and A. Roventini, "An evolutionary model of endogenous business cycles," *Computational Economics*, vol. 27, no. 1, pp. 3–34, 2006.

[46] G. Dosi, G. Fagiolo, and A. Roventini, "Schumpeter meeting Keynes: a policy-friendly model of endogenous growth and business cycles," *Journal of Economic Dynamics & Control*, vol. 34, no. 9, pp. 1748–1767, 2010.

[47] G. Dosi, M. C. Pereira, A. Roventini, and M. E. Virgillito, "The Effects of Labour Market Reforms upon Unemployment and Income Inequalities: An Agent Based Model," *Socio-Economic Review*, 2016.

[48] W. Li and L. Tesfatsion, "Market provision of flexible energy/reserve contracts: Optimization formulation," in *Proceedings of the IEEE Power and Energy Society General Meeting (PESGM '16)*, pp. 1–5, Boston, MA, USA, July 2016.

[49] F. Kühnlenz, P. H. J. Nardelli, S. Karhinen, and R. Svento, "Implementing flexible demand: Real-time price vs. market integration," *Energy*, vol. 149, pp. 550–565, 2018.

[50] M. Neugart and M. Richiardi, *Agent-based models of the labor marke*, vol. 125 of *LABORatorio R. Revelli working papers series*, 2012.

[51] W. B. Arthur, "Designing economic agents that act like human agents: A behavioral approach to bounded rationality," *The American Economic Review*, pp. 353–359, 1991.

[52] P. Albin and D. K. Foley, "Decentralized, dispersed exchange without an auctioneer. A simulation study," *Journal of Economic Behavior & Organization*, vol. 18, no. 1, pp. 27–51, 1992.

[53] E. Ostrom, "Beyond markets and states: Polycentric governance of complex economic systems," *American Economic Review*, vol. 100, no. 3, pp. 641–672, 2010.

[54] G. Fagiolo and A. Roventini, "Macroeconomic policy in DSGE and agent-based models redux: New developments and challenges ahead," *Journal of Artificial Societies and Social Simulation*, vol. 20, no. 1, 2017.

[55] P. Krugman, "The profession and the crisis," *Eastern Economic Journal*, vol. 37, no. 3, pp. 307–312, 2011.

[56] J. E. Stiglitz, "Rethinking macroeconomics: What failed, and to how repair it," *Journal of the European Economic Association*, vol. 9, no. 4, pp. 591–645, 2011.

[57] B. LeBaron, "Building the Santa Fe Artificial Stock Market," Working Paper, Brandeis University, 2002.

[58] B. LeBaron, *Agent-based computational finance*, vol. 2, Elsevier, 2006.

[59] F. H. Westerhoff, "The Use of Agent-Based Financial Market Models to Test the Effectiveness of Regulatory Policies," *Jahrbücher für Nationalökonomie und Statistik*, vol. 228, no. 2-3, pp. 195–227, 2008.

[60] S. J. Leal and M. Napoletano, "Market stability vs. market resilience: Regulatory policies experiments in an agent-based model with low- and high-frequency trading," *Journal of Economic Behavior & Organization*, 2016.

[61] S. Burgess, E. Fernandez-Corugedo, C. Groth et al., "The Bank of Englands forecasting platform: COMPASS, MAPS, EASE and the suite of models," Working Paper 471, 2013.

[62] OECD, *Systems Approaches to Public Sector Challenges*, Organisation for Economic Cooperation and Development, Paris, France, 2017.

[63] C. Deissenberg, S. van der Hoog, and H. Dawid, "EURACE: a massively parallel agent-based model of the European economy," *Applied Mathematics and Computation*, vol. 204, no. 2, pp. 541–552, 2008.

[64] S. E. Page, *Diversity and complexity*, Princeton University Press, 2010.

[65] M. Mitchell, *Complexity: A Guided Tour*, Oxford University Press, New York, NY, USA, 2011.

[66] R. Axelrod, *The Complexity of Cooperation: Agent-Based Models of Competition and Collaboration*, Princeton University Press, 1997.

[67] R. Solé and B. Goodwin, *How complexity pervades biology*, Basic, New York, NY, USA, 2000.

[68] S. Wolfram, "Statistical mechanics of cellular automata," *Reviews of Modern Physics*, vol. 55, no. 3, pp. 601–644, 1983.

[69] T. C. Schelling, "Models of segregation," *The American Economic Review*, vol. 59, no. 2, pp. 488–493, 1969.

[70] U. Wilensky and W. Rand, *An introduction to Agent-Based Modeling*, The MIT Press, Cambridge, Massachusetts, 2015.

[71] M. Batty, *Cities and complexity: understanding cities with cellular automata, agent-based models and fractals*, The MIT Press, Cambridge, MASS, USA, 2005.

[72] L. An, "Modeling human decisions in coupled human and natural systems: review of agent-based models," *Ecological Modelling*, vol. 229, pp. 25–36, 2012.

[73] R. White, G. Engelen, and I. Uljee, "The use of constrained cellular automata for high-resolution modelling of urban land-use dynamics," *Environment and Planning B: Planning and Design*, vol. 24, no. 3, pp. 323–343, 1997.

[74] R. White and G. Engelen, "Cellular automata and fractal urban form: a cellular modelling approach to the evolution of urban land-use patterns," *Environment and Planning A*, vol. 25, no. 8, pp. 1175–1199, 1993.

[75] D. C. Parker, S. M. Manson, M. A. Janssen, M. J. Hoffmann, and P. Deadman, "Multi-agent systems for the simulation of land-use and land-cover change: a review," *Annals of the Association of American Geographers*, vol. 93, no. 2, pp. 314–337, 2003.

[76] T. Filatova, D. Parker, and A. van der Veen, "Agent-based urban land markets: Agent's pricing behavior, land prices and urban land use change," *Journal of Artificial Societies & Social Simulation*, vol. 12, no. 1, 2009.

[77] P. Waddell, "Urbansim: Modeling urban development for land use, transportation, and environmental planning," *Journal of the American Planning Association*, vol. 68, no. 3, pp. 297–314, 2002.

[78] P. Waddell and G. F. Ulfarsson, "Dynamic Simulation of real estate development and land prices within an integrated land use and transportation model system," in *Proceedings of the Transportation Research Board 82nd Annual Meeting*, p. 21, Washington, DC, USA, 2003.

[79] P. Waddell, G. Boeing, M. Gardner, and E. Porter, "An Integrated Pipeline Architecture for Modeling Urban Land Use, Travel Demand, and Traffic Assignment," 2018, https://arxiv.org/abs/1802.09335.

[80] H. van Delden, R. Vanhout, M. Te Brommelstroet, and R. White, "Design and development of integrated spatial decision support systems: applying lessons learnt to support new town planning," in *Model Town: using urban simulation in new town planning*, SUN, Amsterdam, Holanda, 2009.

[81] A. Horni, K. Nagel, and K. Axhausen, *The Multi-Agent Transport Simulation MATSim*, Ubiquity Press, London, UK, 2016.

[82] B. A. Furtado, *PolicySpace: agent-based modeling*, IPEA, Brasília, 2018.

[83] E. Galli, L. Cuéllar, S. Eidenbenz, M. Ewers, S. Mniszewski, and C. Teuscher, "ActivitySim: Large-scale agent-based activity generation for infrastructure simulation," in *Proceedings of the Spring Simulation Multiconference, SpringSim '09*, 16:9, 16:1 pages, San Diego, CA, USA, March 2009.

[84] F. Lamperti, A. Roventini, and A. Sani, "Agent-based model calibration using machine learning surrogates," *Journal of Economic Dynamics & Control*, vol. 90, pp. 366–389, 2018.

[85] M. Guerini and A. Moneta, "A method for agent-based models validation," *Journal of Economic Dynamics & Control*, vol. 82, pp. 125–141, 2017.

[86] C. Gräbner, C. S. E. Bale, B. A. Furtado et al., "The best of both worlds: developing complementary Equation-Based and Agent-Based Models," *Computational Economics*, p. 25, 2017.

[87] D. J. Watts and S. H. Strogatz, "Collective dynamics of 'small-world' networks," *Nature*, vol. 393, no. 6684, pp. 440–442, 1998.

[88] A. Barabasi and R. Albert, "Emergence of scaling in random networks," *Science*, vol. 286, no. 5439, pp. 509–512, 1999.

[89] A. Clauset, C. Moore, and M. E. J. Newman, "Hierarchical structure and the prediction of missing links in networks," *Nature*, vol. 453, no. 7191, pp. 98–101, 2008.

[90] A. E. Motter and M. Timme, "Antagonistic Phenomena in Network Dynamics," *Annual Review of Condensed Matter Physics*, vol. 9, pp. 463–484, 2018.

[91] S. Battiston, D. Delli Gatti, M. Gallegati, B. Greenwald, and J. E. Stiglitz, "Credit chains and bankruptcy propagation in production networks," *Journal of Economic Dynamics and Control (JEDC)*, vol. 31, no. 6, pp. 2061–2084, 2007.

[92] S. Battiston, M. Puliga, R. Kaushik, P. Tasca, and G. Caldarelli, "DebtRank: too central to fail? financial networks, the FED and systemic risk," *Scientific Reports*, vol. 2, article 541, 2012.

[93] S. Thurner and S. Poledna, "DebtRank-transparency: Controlling systemic risk in financial networks," *Scientific Reports*, vol. 3, p. 1888, 2013.

[94] S. Poledna, S. Thurner, J. D. Farmer, and J. Geanakoplos, "Leverage-induced systemic risk under Basle II and other credit risk policies," *Journal of Banking & Finance*, vol. 42, no. 1, pp. 199–212, 2014.

[95] K. Gray and A. E. Motter, "Multidisciplinary complex systems research," *Report from an NSF Workshop*, 2017.

[96] T. P. Peixoto, "Nonparametric weighted stochastic block models," *Physical Review E: Statistical, Nonlinear, and Soft Matter Physics*, vol. 97, no. 1, p. 012306, 2018.

[97] J. Friedman, T. Hastie, and R. Tibshirani, *The elements of statistical learning*, vol. 1, Springer series in statistics New York, New York, NY, USA, 2001.

[98] T. Hastie, R. Tibshirani, and J. Friedman, *Elements of Statistical Learning: data mining, inference, and prediction*, Springer, 2nd edition, 2009.

[99] I. Goodfellow, Y. Bengio, and A. Courville, *Deep Learning*, vol. 1, MIT Press, Cambridge, Mass, USA, 2016.

[100] S. Haykin and N. Network, "A comprehensive foundation," *Neural networks*, vol. 2, no. 2004, p. 41, 2004.

[101] M. Abadi, P. Barham, J. Chen et al., "TensorFlow: A system for large-scale machine learning," in *OSDI*, vol. 16, pp. 265–283, 2016.

[102] A. A. Boxwala, K. Jihoon, J. M. Grillo, and L. Ohno-Machado, "Using statistical and machine learning to help institutions detect suspicious access to electronic health records," *Journal of the American Medical Informatics Association*, vol. 18, no. 4, pp. 498–505, 2011.

[103] W. Zhou and G. Kapoor, "Detecting evolutionary financial statement fraud," *Decision Support Systems*, vol. 50, no. 3, pp. 570–575, 2011.

[104] F. Amato, A. López, E. M. Peña-Méndez, P. Vaňhara, A. Hampl, and J. Havel, "Artificial neural networks in medical diagnosis," *Journal of Applied Biomedicine*, vol. 11, no. 2, pp. 47–58, 2013.

[105] R. Aggarwal, J. Ward, I. Balasundaram, P. Sains, T. Athanasiou, and A. Darzi, "Proving the effectiveness of virtual reality simulation for training in laparoscopic surgery," *Annals of Surgery*, vol. 246, no. 5, pp. 771–779, 2007.

[106] J. B. Greenblatt and S. Shaheen, "Automated Vehicles, On-Demand Mobility, and Environmental Impacts," *Current Sustainable/Renewable Energy Reports*, vol. 2, no. 3, pp. 74–81, 2015.

[107] A. D. Thierer, A. Castillo, and R. Russell, *Artificial Intelligence and Public Policy*, George Mason University, VA: Mercatus Research, 2017.

[108] D. T. Brooks, B. Becker, and J. R. Marlatt, "Computer applications in particular industries: securities," in *Computers and the law*, American Bar Association, Section of Science and Technology, 3rd edition, 1981.

[109] J. Grimmer, "We are all social scientists now: How big data, machine learning, and causal inference work together," *PS - Political Science and Politics*, vol. 48, no. 1, pp. 80–83, 2014.

[110] R. A. McCain, *Game theory and public policy*, Edward Elgar Publishing Limited, 2009.

[111] A. G. Sanfey, "Social decision-making: Insights from game theory and neuroscience," *Science*, vol. 318, no. 5850, pp. 598–602, 2007.

[112] E. Lieberman, C. Hauert, and M. A. Howak, "Evolutionary dynamics on graphs," *Nature*, vol. 433, no. 7023, pp. 312–316, 2005.

[113] B. Edmonds and C. Gershenson, "Modelling complexity for policy: opportunities and challenges," in *Handbook on complexity and public policy*, p. 205, 2015.

[114] J. W. Forrester, "Counterintuitive behavior of social systems," *Technological Forecasting & Social Change*, vol. 3, no. C, pp. 1–22, 1971.

[115] R. L. Eberlein and K. J. Chichakly, "XMILE: A new standard for system dynamics," *System Dynamics Review*, vol. 29, no. 3, pp. 188–195, 2013.

[116] H. V. D. Parunak, R. Savit, and R. L. Riolo, "Agent-Based Modeling vs. Equation-Based Modeling: A Case Study and Users' Guide," in *Multi-Agent Systems and Agent-Based Simulation*, vol. 1534 of *Lecture Notes in Computer Science*, pp. 10–25, Springer Berlin Heidelberg, Berlin, Heidelberg, 1998.

[117] M. Niazi and A. Hussain, "Agent-based computing from multi-agent systems to agent-based models: a visual survey," *Scientometrics*, vol. 89, no. 2, pp. 479–499, 2011.

[118] J. Guckenheimer and P. Holmes, *Nonlinear Oscillations, Dynamical Systems, and Bifurcation of Vector Fields*, vol. 42, Springer Science & Business Media, 2013.

[119] N. Gilbert and K. Troitzsch, *Simulation for the social scientist*, McGraw-Hill Education, UK, 2005.

[120] A. T. Crooks and A. J. Heppenstall, "Introduction to agent-based modelling," *Agent-Based Models of Geographical Systems*, pp. 85–105, 2012.

[121] M. Fujita, P. Krugman, and A. J. Venables, *The spatial economy: cities, regions and international trade*, MIT Press, Cambridge, Mass, USA, 1999.

[122] T. Bovaird, "Emergent strategic management and planning mechanisms in complex adaptive system," *Public Management Review*, vol. 10, no. 3, pp. 319–340, 2008.

[123] R. Mahon, P. McConney, and R. N. Roy, "Governing fisheries as complex adaptive systems," *Marine Policy*, vol. 32, no. 1, pp. 104–112, 2008.

[124] J. W. Hall, M. Tran, A. J. Hickford, and R. J. Nicholls, *The future of national infrastructure: A system-of-systems approach*, Cambridge University Press, 2016.

[125] ITRC-MISTRAL, "Multi-scale infrastructure systems analytics," *The UK Infrastructure Transitions Research Consortium*, 2016.

[126] J. Hall, A. Otto, A. J. Hickford, R. J. Nicholls, and M. Tran, "A framework for analysing the long-term performance of interdependent infrastructure systems," *The Future of National Infrastructure: A System-of-Systems Approach*, p. 12, 2016.

[127] J. W. Hall, J. J. Henriques, A. J. Hickford et al., "Assessing the Long-Term Performance of Cross-Sectoral Strategies for National Infrastructure," *Journal of Infrastructure Systems*, vol. 20, no. 3, p. 04014014, 2014.

[128] E. A. Byers, J. W. Hall, and J. M. Amezaga, "Electricity generation and cooling water use: UK pathways to 2050," *Global Environmental Change*, vol. 25, no. 1, pp. 16–30, 2014.

[129] G. Dosi and A. Roventini, "Agent-Based Macroeconomics and Classical Political Economy: Some Italian Roots," *Italian Economic Journal*, vol. 3, no. 3, pp. 261–283, 2017.

[130] G. Dosi, M. Napoletano, A. Roventini, and T. Treibich, "Micro and macro policies in the Keynes+Schumpeter evolutionary models," *Journal of Evolutionary Economics*, vol. 27, no. 1, pp. 63–90, 2017.

[131] F. Lamperti, G. Dosi, M. Napoletano, A. Roventini, and A. Sapio, "Faraway, So Close: Coupled Climate and Economic Dynamics in an Agent-based Integrated Assessment Model," *Ecological Economics*, vol. 150, pp. 315–339, 2018.

[132] M. Napoletano, G. Dosi, G. Fagiolo, and A. Roventini, "Wage formation, investment behavior and growth regimes: An agent-based analysis," *Revue de l'OFCE*, vol. 124, no. 5, pp. 235–261, 2012.

[133] G. Dosi, G. Fagiolo, M. Napoletano, and A. Roventini, "Income distribution, credit and fiscal policies in an agent-based Keynesian model," *Journal of Economic Dynamics & Control*, vol. 37, no. 8, pp. 1598–1625, 2013.

[134] G. Dosi, G. Fagiolo, M. Napoletano, A. Roventini, and T. Treibich, "Fiscal and monetary policies in complex evolving economies," *Journal of Economic Dynamics & Control*, vol. 52, pp. 166–189, 2015.

[135] T. Balint, F. Lamperti, A. Mandel, M. Napoletano, A. Roventini, and A. Sapio, "Complexity and the economics of climate change: a survey and a look forward," *Ecological Economics*, vol. 138, pp. 252–265, 2017.

[136] G. Dosi, M. C. Pereira, A. Roventini, and M. E. Virgillito, "Causes and consequences of hysteresis: aggregate demand, productivity, and employment," *Industrial and Corporate Change*, vol. 27, no. 6, pp. 1015–1044, 2018.

[137] G. Dosi, M. C. Pereira, A. Roventini, and M. E. Virgillito, "When more flexibility yields more fragility: the microfoundations of Keynesian aggregate unemployment," *Journal of Economic Dynamics & Control*, vol. 81, pp. 162–186, 2017.

[138] F. Jaumotte and C. Osorio-Buitron, "Inequality and Labor Market Institutions," *IMF Staff Discussion Note*, p. 31, 2015.

[139] P. Waddell, G. F. Ulfarsson, J. P. Franklin, and J. Lobb, "Incorporating land use in metropolitan transportation planning," *Transportation Research Part A: Policy and Practice*, vol. 41, no. 5, pp. 382–410, 2007.

[140] P. Waddell, "A behavioral simulation model for metropolitan policy analysis and planning: Residential location and housing market components of UrbanSim," *Environment and Planning B: Planning and Design*, vol. 27, no. 2, pp. 247–263, 2000.

[141] J. K. Brueckner, "The structure of urban equilibria: A unified treatment of the muth-mills model," in *Handbook of Regional and Urban Economics*, vol. 2, pp. 821–845, Elsevier Science Publishers B.V., 1987.

[142] S. Rosen, "Hedonic prices and implicit markets: product differentiation in pure competition," *Journal of Political Economy*, vol. 82, no. 1, pp. 34–55, 1974.

[143] P. Waddell, "Integrated land use and transportation planning and modelling: Addressing challenges in research and practice," *Transport Reviews*, vol. 31, no. 2, pp. 209–229, 2011.

[144] P. Waddell, L. Wang, and X. Liu, "UrbanSim: an evolving planning support system for evolving communities," in *Planning support systems for cities and regions*, pp. 103–138, Lincoln Institute for Land Policy, Cambridge, MASS, USA, 2008.

[145] P. Waddell, L. Wang, and B. Charlton, "Integration of a parcel-level land use model and an activity-based travel model," in *Proceedings of the 11th World Conference on Transport Research*, 2007.

[146] P. Waddell, C. R. Bhat, N. Eluru, L. Wang, and R. M. Pendyala, "Modeling interdependence in household residence and workplace choices," *Transportation Research Record*, vol. 2003, no. 1, pp. 84–92, 2007.

[147] A. De Palma, K. Motamedi, N. Picard, and P. Waddell, "Accessibility and environmental quality: inequality in the Paris housing market," *European Transport*, vol. 36, pp. 47–64, 2007.

Hindawi
Complexity
Volume 2019, Article ID 8436505, 16 pages
https://doi.org/10.1155/2019/8436505

Research Article

Liquidity Hoarding in Financial Networks: The Role of Structural Uncertainty

Stojan Davidovic,[1] **Amit Kothiyal**,[1] **Mirta Galesic**,[1,2] **Konstantinos Katsikopoulos**,[1,3] **and Nimalan Arinaminpathy**[4]

[1]*Max Planck Institute for Human Development, Center for Adaptive Behavior and Cognition, Berlin, Germany*
[2]*Santa Fe Institute, Santa Fe, NM, USA*
[3]*Southampton Business School, Southampton, UK*
[4]*Faculty of Medicine, School of Public Health, Imperial College London, London, UK*

Correspondence should be addressed to Stojan Davidovic; stojand@mpib-berlin.mpg.de

Received 15 May 2018; Revised 21 August 2018; Accepted 4 September 2018; Published 8 January 2019

Guest Editor: Bernardo A. Furtado

The dynamics of confidence affect a plethora of financial phenomena including liquidity hoarding. We present a multiagent model of a financial network in which confidence dynamics are shaped by *structural uncertainty*—that is, the lack of knowledge about the network of interbank cross-exposures. During a financial crisis, structural uncertainty makes it difficult for banks to assess the risk of financial contagion and their own health. Under such conditions, banks are more likely to behave conservatively and quickly act on information they receive from their local environment. A sudden financial shock, therefore, can be characterized by high-intensity local impact on confidence. We find that such local impacts quickly spread throughout the network, causing more damage than a shock that evenly affects all localities in the system; for example, a complete breakdown of the system occurs with a higher probability. The results are explained analytically by linking system performance to the speed of decrease in confidence.

1. Introduction

The "freeze" of the interbank market in the recent financial crisis denied financial institutions (banks, for short) access to liquid assets when they needed them most. In late 2007, the U.S. and European markets experienced simultaneous runs on asset-backed commercial papers [1]. The second large shock occurred in the fall of 2008 when failures of AIG and Lehman Brothers set off defaults of money-market funds (e.g., the Reserve Primary Fund), which subsequently triggered runs on the repurchase agreement market. Banks responded with precautionary liquidity hoarding, causing interbank market to dry up [2, 3]. The resulting difficulty of borrowing money and the increase in interest rates produced a series of adverse consequences for financial and real sectors. First, pressure to obtain liquidity through sales of long-term assets led to fire sales that further deteriorated banks' asset positions. Second, facing the growing prospect of illiquidity, banks struggled to maintain their lending activities. Third, given that the price of money in interbank markets is a benchmark for the interest rates in the economy, the real sector experienced difficulty obtaining funding under reasonable conditions. Together, these factors further aggravated already existing symptoms of the crisis.

There are two common explanations for the interbank market collapse: the increase in counterparty risk and liquidity hoarding [4]. The uncertainty about the network of cross-exposures between banks, also known as *structural uncertainty* [5], however, made both of these factors more effective. The fear of counterparty risk—a risk that a business partner cannot meet its obligation—can be linked to the subprime market crash that led a large fraction of banks holding mortgage-backed securities to experience financial difficulties. The resulting increase in liquidity demand and

the reduction in the number of liquidity providers set off basic conditions for banks to withhold liquidity from the market—liquidity hoarding. Furthermore, structural uncertainty made it difficult for liquid banks to assess the risk of events farther in the network and identify risk-free parties. For the same reason, liquid banks could not rule out the possibility of suffering a sudden loss through already existing cross-exposures. In such a context, they were more likely to anticipate increased liquidity needs in the future, as well as the possibility of limited access to the interbank market. The loss of confidence in the interbank market and liquidity hoarding were hence the result of a number of interrelated factors, but it was the structural uncertainty that made each of them more consequential.

In this paper, we explored a model of a banking network in which the confidence of banks is shaped by uncertainty about the network of interbank lending. This is a realistic assumption since the network of interbank cross-exposures is not known due to the over-the-counter character of interbank transactions. We found that when confidence is sensitive to local information only, the probability of systemic failures increases substantially.

We adopted the framework of Arinaminpathy et al. ([6]; hereafter the AKM model) in which a bank's confidence is modeled to reflect the severity of the financial situation in the banking system. A bank's confidence is directly linked to its decision to roll over or withdraw previously established interbank loans—the lower the confidence, the higher the possibility of precautionary withdrawals. The model also includes the effects of fire sales and asset price contagion, as they are in a close relationship with market liquidity. Here, we assumed that banks are responsive to information received from their direct interbank counterparties but not from the banks that are further away in the network. The intuition is that in the face of structural uncertainty, banks rely on actions that take place in their locality. As was done in the AKM model, we also considered a case in which banks receive information from all banks in the system, but we made the information either noisy or delayed relative to the distance information needs to travel in the network to reach the receiver.

The remainder of this paper is organized as follows. We start with the discussion of related literature in Section 2, followed by the model of a banking network in Section 3. Sections 4 and 5 are devoted to our model of uncertainty and the application of initial shock(s) to the system, respectively. In Section 6, we detail our simulation procedure; our main results are presented in Section 7 and additional analysis in Section 8. We end with the discussion in Section 9.

2. Related Literature

Our paper is related to the network models of financial contagion [7]. Network approaches have proven useful for understanding contagion processes in biological, social, and financial systems (e.g., [8–12]). In financial systems in particular, individual institutions are linked to each other through a complex system of interbank lending [13] and holdings in common assets [14, 15]. Such a system lends itself naturally to being modeled with a network approach.

Most models of financial networks have treated contagion as being directly transmitted between institutions (e.g., [16–19]), leaving the mechanism of market panics largely unexplored. One reason may be because the outbreak of herding behavior is not well captured by a cascade that spreads through the network of cross-exposures. Instead, it is predominantly driven by a collective change in expectations, which does not exhibit simple cascade-like spreading patterns. A simultaneous drop in banks' confidence, for instance, can be a mediator of collective withdrawal of liquidity and fire sales. This is because the interbank market relies on the collective confidence in its service as a safe resort in case of unforeseen liquidity needs. Furthermore, the functioning interbank market attenuates banks' liquidity buffers by allowing them to operate with minimal holdings of low-profit liquid assets. Thus, the steady reduction in banks' liquid reserves in the decades prior to the financial crisis reflects the increasing market efficiency and the growing confidence in its reliability (Figure 1). However, the recent crisis demonstrated that such a scheme is not resistant to large financial shocks, which proved to be capable of undermining the collective confidence. Taken together, these all point to the importance of understanding of how confidence decay spreads in the banking system.

Hansen and Sargent [20] studied the sensitivity of beliefs to uncertainty, although they did not look at how such beliefs spread in the financial system. Gai et al. [21] introduced a network model of liquidity hoarding where the propensity for precautionary withdrawals, a proxy of the collective confidence, was exogenously decided. Such a setting left the process of confidence loss out of consideration. By contrast, in the AKM model [6], confidence was endogenously determined as a function of the severity of the financial situation in the interbank market but with the unrealistic assumption that banks have complete information about other banks in the system. This implied that confidence shocks were well distributed among all banks, leaving the impact of structural uncertainty and heterogeneously distributed confidence in the network unexplored.

Our paper is also related to the literature focused on the relationship between liquidity hoarding and asset prices (e.g., [4, 22–24]). For instance, Gale and Yorulmazer [4] and Diamond and Rajan [24] showed that in certain conditions, privately optimal decisions can lead to hoarding behavior and fire sales. These authors also considered speculative hoarding, when a liquidity shortage stimulates liquid buyers to withhold liquidity in expectation of high returns from potential fire sales. Nevertheless, the main difference from our work here is that their studies were not concerned with the complexity of interbank cross-exposures or accompanying structural uncertainty.

There have been several studies connecting different sources of uncertainty to market liquidity. Caballero and Krishnamurthy [25] argued that capital immobility and liquidity hoarding can be explained by the reactions of decision makers to the Knightian uncertainty embedded in

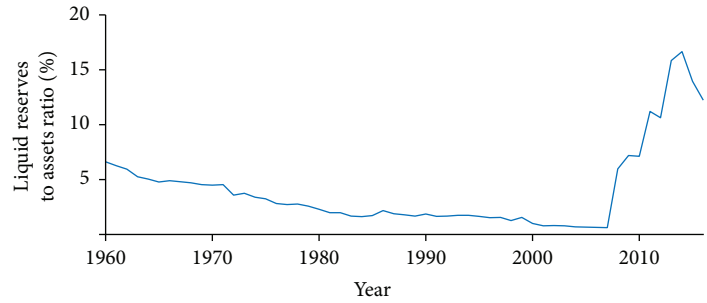

Figure 1: Ratio of bank liquid reserves to bank assets in the United States (1960–2016), that is, the ratio of domestic currency holdings and deposits with the monetary authorities to claims on other governments, nonfinancial public enterprises, the private sector, and other banking institutions. The recent 2007–2008 financial crisis led banks to hoard liquidity. Source: the World Bank, retrieved from http://WorldBank.com and http://NationMaster.com.

the financial environment in the form of sudden events and untested financial innovations. Routledge and Zin [26] showed how derivative pricing under uncertainty produces diverse effects on market liquidity. A link between uncertainty and market complexity was tackled by Zawadowski [27], who found that the layers of financial intermediation amplify uncertainty about the availability of funding, causing a cascade of liquidity withdrawals. However, all banks were familiar with the underlying network of lending.

In a recent paper addressing the same problem as our study, Caballero and Simsek [28] considered structural uncertainty in a model of liquidity hoarding and fire sales. They argued that ignorance about the underlying network of interconnections, a dormant factor in normal times, becomes relevant in a crisis when liquid banks have to consider who will be next affected by the cascade of failures. This shifts their preference toward keeping liquid assets instead of investing long term, causing liquidity shortages and fire sales. While sharing the assumption that banks reliably know only information about their counterparties, the Caballero and Simsek study differs from ours by assuming that banks know the outline of the network of cross-exposures. For simplicity, they also assumed that the banking network forms a circular shape. In our model, the network of interbank lending approximates features of real-world banking networks, and its shape is not known to the banks. Unlike the circular arrangement, the small-world feature of real financial networks makes all banks relatively close to each other [29], which has implications on the spread of information and financial risk in the system.

3. Model of a Banking Network

In the AKM model, banks are connected by lending relationships and holdings in common assets. Our analysis is focused on a short-term horizon in which banks can decide to roll over, shorten loan maturity, or terminate already established lending contracts. Their decisions depend on their confidence, which is expressed as a function of the level of assets and interbank loans in the system. When the system faces financial difficulties and bank defaults, the value of its assets and interbank loans shrinks, lowering confidence. This in turn leads to more preemptive actions of banks, putting pressure on their counterparties and causing more defaults. In this way, the model captures positive feedback between the severity of the financial condition in the system and individual behaviors of banks.

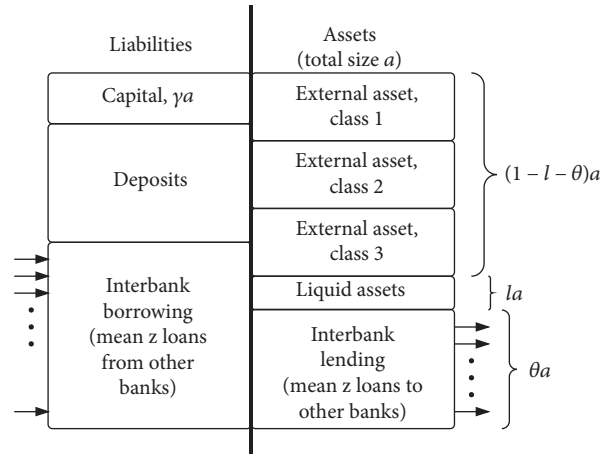

Figure 2: A balance sheet representation of a bank (adapted from [6]). a = total assets; γ = capital ratio; l = liquidity ratio; θ = interbank loans-to-assets ratio; z = average number of incoming and outgoing loans.

In addition to liquidity hoarding, two other contagion mechanisms take place in the model. One relates to the propagation of counterparty credit risk, which affects lenders when borrowers are not able to repay their loans. The other is asset price contagion, which occurs when liquidation of assets of failed banks pushes the corresponding asset prices down. All banks holding the affected assets suffer from the price drop, which is modeled according to Cifuentes et al. [30]. Correlations between assets are not included in our model.

3.1. Nodes and Edges. For simplicity, nodes or banks in the network can only be large or small, where the size disparity is fixed by the size ratio q (q = large bank assets/small bank assets). Banks are represented as simplified balance sheets with properties listed in Figure 2. The liability side contains capital (also known as owner's equity), retail deposits (money in the accounts of banks' customers), and interbank borrowing (assets borrowed from other banks). The level of capital represents the amount of asset loss that a bank can

withstand before becoming insolvent and going bankrupt (insolvency and illiquidity are separately discussed in Section 5). Retail deposits are taken to be external to the system and do not play an active role in the model. Interbank borrowing represents loans received from other banks, and the number of incoming loans represents the in-degree of an individual node. On the asset side, there are n external asset classes (investments in assets that are external to the banking system), liquid assets (e.g., cash), and interbank lending (assets lent to other banks). External asset classes are distributed among banks from a fixed number of distinct asset classes contained in the system (see next section). This means that multiple banks will share the same asset class, which can lead to asset price contagion—the drop in value of one asset class will affect multiple banks. Liquid assets are a small fraction l of the overall assets that banks keep in the most liquid form to meet immediate needs. They are mostly composed of cash or any cash equivalent, such as central bank reserves or high-quality government bonds, which are easily convertible to money. Finally, interbank lending corresponds to outgoing loans to other banks in the system, thus giving rise to a lending network, as described below. Parameters γ and θ (Figure 2) determine the initial proportions of capital and interbank loans in the total assets a, respectively. The balance sheet's parameters reflect the values observed in the banking sector before the crisis [31]: the proportion of total assets initially determined to be held in interbank loans $\theta = 0.2$, the proportion of total assets initially liquid $l = 0.01$, and capital-to-asset ratio $\gamma = 0.04$.

3.2. Network. The network is a directed random graph with $N = 120$ banks (Figure 3). The default value of the size ratio q is 10 (The main pattern of results is insensitive to changes of q and N as long as they are large enough.), which given total number of banks results in a network with $N_b = 11$ large and $N_s = 109$ small banks. The in-degree and out-degree of banks are determined by a Poisson distribution with parameter $z = 5$ for small and $q \times z = 50$ for large banks. That is, small (large) banks on average have five (50) incoming and five (50) outgoing loans. Each edge in the network is a loan with direction from lender to borrower. The default value of each single loan is normalized as 1. The maturity of interbank lending is also simplified: a random half of interbank loans are assigned to be "short-term" and the rest to be "long-term" loans. The short-term loans can be withdrawn immediately by a lender in a single decision, whereas long-term loans have to be shortened first. The banks are also interrelated by sharing the same external asset classes. These relationships are the basis for the asset price contagion. Small banks have 10, and large banks 20 external asset classes $(n_s = 10, n_b = 20)$. Given that on average 10 banks share the same asset class $(g = 10)$, this implies 131 distinctive external asset classes $(G = (N_b n_b + N_s n_s)/g)$.

The difference in the connectivity of large and small banks and the random assignment of their connections result in the core-periphery structure of the network. That is, large banks with many links are densely interconnected—forming the core, and small banks with few links are loosely interconnected—forming the periphery. The resulting structure is

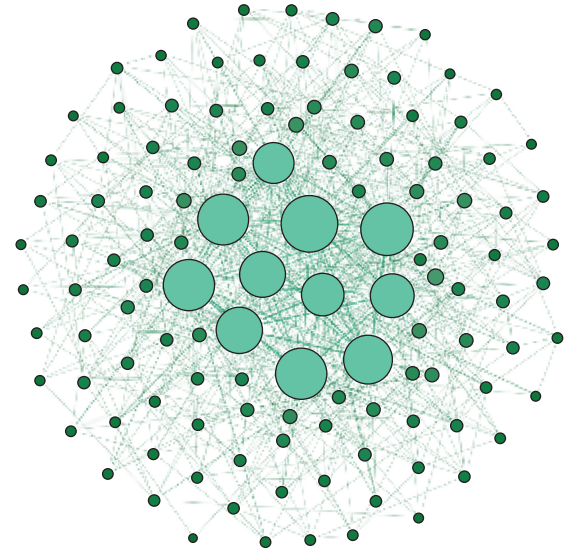

Figure 3: Banking network with 120 banks. The node size is weighted by its degree. Large banks are colored in light green, whereas small banks are colored in dark green. The network is constructed using the default values of the model parameters (Section 3.2) and has a core-periphery structure: large banks with many links are densely interconnected—forming the core, and small banks with few links are loosely interconnected—forming the periphery.

"shallow," (This is in agreement with the core-periphery structure of the global banking network [13]. Roughly speaking, any two banks at the periphery are a few connections away since they are linked via the well-connected core.) meaning that the average path length in the network is relatively short due to the well-connected core.

3.3. Confidence and Individual Health. Confidence C is the first important determinant of a bank's behavior. In the AKM model, confidence is calculated as a function of A and E, which are measures of solvency and liquidity of the system, respectively:

$$\begin{aligned} C &= AE, \\ A &= \sum_{i=1}^{N} A_i, \\ A_i &= \frac{a_i}{\sum_{i=1}^{N} a_i^0}, \\ E &= \sum_{i=1}^{N} E_i, \\ E_i &= \frac{e_i}{\sum_{i=1}^{N} e_i^0}. \end{aligned} \tag{1}$$

At a given point in time, A denotes the total value of all remaining assets in the system as a proportion of its initial value; E is similarly the fraction of interbank loans not withdrawn from the system; A_i and E_i are the remaining assets and interbank loans of bank i as the proportion of initial value of total assets in the system; a_i and e_i are the absolute values of remaining assets and interbank loans of bank i;

and a_i^0 and e_i^0 are the initial absolute values of assets and interbank loans of bank i.

To calculate C as defined in the AKM model, and to take any action, banks have to know the current and initial values of assets and interbank loans of all banks in the system. To explore how the network behaves in a more realistic setting, especially in times of crisis when the system is changing rapidly, we consider several uncertainty scenarios, described in Section 4.

Unlike C, which is a systemic parameter, h_i denotes the individual health of bank i and is calculated as a function of its indicators of solvency c_i and liquidity m_i:

$$\begin{aligned} h_i &= c_i m_i, \quad 0 < h_i < 1, \\ m_i &= \min\left[1, \frac{\left(A_i^{\mathrm{ST}} + l_i\right)}{L_i^{\mathrm{ST}}}\right], \end{aligned} \tag{2}$$

where c_i is the capital of bank i defined as a proportion of its initial value; m_i is the fraction of i's short-term liabilities that the bank can settle immediately, through its liquid and short-term assets; A_i^{ST} is the total value of i's short-term interbank assets; L_i^{ST} is the total value of i's short-term interbank liabilities; and l_i is the amount of liquid assets held by bank i.

3.4. Decision Rules. The dynamics in the model are determined by decisions that banks make in discrete simulation time. For each of its outgoing connections, a loan provider can decide whether to shorten a long-term loan and whether to withdraw a short-term loan. A lender can withdraw short-term loans in a single decision, resulting in the connection between the two banks being removed immediately; long-term loans can only be "shortened" in a single decision, resulting in the connection between the banks becoming a short-term loan. Thus, an eventual withdrawal of a long-term loan requires an additional decision, i.e., time step (see Appendix B). Depending on its maturity, a loan between two banks i and j is, respectively, shortened and withdrawn when

$$\begin{aligned} h_i h_j &< (1 - C), \\ h_i h_j &< (1 - C)^2. \end{aligned} \tag{3}$$

If C is high (1 or close to 1), these conditions are satisfied only under extreme conditions for h_i and h_j. In contrast, a drop in C can cause liquidity hoarding, as both decision conditions are more likely to be satisfied for all banks in the system. In addition, the shortening condition is easier to satisfy than the withdrawing condition, which means that banks resort to withdrawal only in relatively urgent situations.

4. Model of Uncertainty

In interbank markets, business partners trade privately, which often leads to a relationship with preferential treatment and repeated transactions [32, 33]. Accordingly, in our main uncertainty setting—the local information (LI) scenario—we restricted information availability to the nearby, that is, "local" banks in the banking network. This makes banks highly sensitive to local events and insensitive to events that take place further away in the network. Their responsiveness is calibrated so that they do not take action unless they notice signs of trouble in their locality; but when they do, then their reaction is intense. As a reference to models of complete information such as the AKM model, we also consider delayed information (DI) and noisy information (NI) scenarios, in which banks receive information from all banks in the system, but information is either delayed or noisy. For simplicity, details of the DI and NI scenarios are presented in Appendix A. As described in Section 3.3, the assumptions used in the AKM model are equivalent to what we call the complete information (CI) scenario.

To model uncertainty and determine the amount of information that is included in the calculation of confidence C, we rely on the distance between nodes in the network. The distance $d(i, j)$ is the shortest path length between information user i and information source j. If banks are directly connected, the distance between them is 1 and we call them neighbors. All neighbors of a particular bank constitute its neighborhood. The distance between neighbors of neighbors is 2 and so forth. The main principle for modeling uncertainty is that information availability and/or quality deteriorates when the distance from the information source increases. Once uncertainty is introduced, instead of one common estimate of confidence for all banks ($\forall i : C^i = C$ in the AKM model), each bank has its own individual perception of confidence C^i.

We use the following notation template of any model parameter $P : P^{\text{time step (optional)};\text{observer}}_{\text{observed (optional)}}$. For example, a_j^{0i} denotes bank i's judgment of j's initial (0 time step) absolute value of assets. Absence of the time step indicator implies the current value of a parameter. The indicator of an observed bank is omitted in the case of aggregate parameters, such as C, which are not based on information of an individual bank.

In the LI scenario, information is available only up to a certain "interbank" distance. That is, bank i calculates C based on the information about itself and all banks placed within the fixed value of distance $d_{\max}$. This is our general definition of locality where the value of $d_{\max}$ determines whether the locality includes only neighbors or also neighbors of neighbors and so forth. For instance, if $d_{\max} = 1$, then only i and its immediate neighbors contribute information to C. Now we can express the confidence of bank i as

$$\begin{aligned} C^i &= A^i E^i, \\ A^i &= \frac{a_i + \sum_{j \in J_i(d_{\max})} a_j^i}{a^{0i}}, \\ a^{0i} &= a_i^0 + \sum_{j \in J_i(d_{\max})} a_j^{0i}, \\ E^i &= \frac{e_i + \sum_{j \in J_i(d_{\max})} e_j^i}{e^{0i}}, \\ e^{0i} &= e_i^0 + \sum_{j \in J_i(d_{\max})} e_j^{0i}. \end{aligned} \tag{4}$$

A set $J_i(d_{\max})$ contains all banks that i considers for estimation of C, except for i itself, and is a function of $d_{\max}$. It is useful to think of $d_{\max}$ as a parameter that determines the reach of i's perception. To define $J_i(d_{\max})$, we first define the set $J = 1, 2, \ldots, N$, which contains all banks in the network. Then, its subset $J_i(d_{\max})$ is defined as

$$J_i(d_{\max}) = \{j \in J | d(i,j) \leq d_{\max} \& j \neq i\}. \quad (5)$$

We consider two versions of the LI scenario (Figure 4): LI1 in which $d_{\max} = 1$ and LI2 in which $d_{\max} = 2$. Since the network is quite shallow (average path length is barely above 2), LI2 contains almost the full graph, and LI3 is equal to CI. Thus, LI2 will provide a useful sanity check in respect to CI.

5. Model of Shocks and Bank Failures

Under each of the conditions described above, we simulated the response of the system to an initial shock. We explored two types of initial shock: (i) a *concentrated* shock (or a single-bank shock), applied by randomly selecting a large or a small bank and forcing it to fail by setting its capital to zero, and (ii) a *distributed shock* (or a multiple-bank shock), applied by forcing multiple small banks to fail simultaneously. The multiple-bank shock is designed to involve a number of small banks whose aggregate assets are equivalent to the assets of a large bank. Therefore, comparing these two treatments can be informative about how the system responds when the same shock is concentrated in a single bank or distributed among multiple banks.

A bank can go bankrupt for both liquidity and solvency reasons. A bank is *illiquid* if its liquid assets and interbank loans are insufficient to meet the demand of other banks to repay the loans previously taken from them. A bank is *insolvent* once the asset devaluation (from an external asset price decrease or counterparty default, for instance) exceeds its level of capital.

6. Simulation

In our simulation, each replication is a computational experiment with two phases. The first phase is to form the network and apply the initiating shock. The second phase is to simulate the propagation of the shock through the network, which unfolds in several iterations, here called time steps.

To form the network, in- and out-degrees that determine the numbers of banks' incoming and outgoing links were drawn from a Poisson distribution. (To design a network, we first drew out-degrees from a Poisson distribution and used this draw as weights for random sampling of corresponding in-degrees. If both in- and out-degrees were drawn directly from a Poisson distribution, the procedure would require the random draw to be repeated until the sum of all in-degrees is equal to the sum of corresponding out-degrees. As a result, draws with nonmatching degrees would have to be discarded, which is computationally expensive and problematic for the purpose of the analytical analysis.) We used a zero-truncated version of a Poisson distribution to ensure positive values of interbank assets and liabilities, which provided more balanced initial liquidity of banks. Once in- and out-degrees were determined, it was possible to reconstruct the rest of the bank's balance sheets based on the parameters of the model (see Section 3.2).

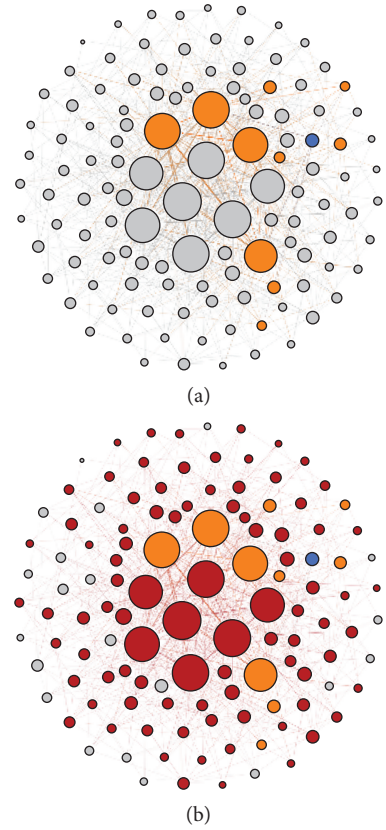

Figure 4: Information availability in the banking network of 120 banks in two local information (LI) scenarios: LI1 and LI2. In the LI1 scenario (a), information is available up to distance 1 in the network. That is, the bank in blue receives information only from the orange banks—its immediate neighbors. In the LI2 scenario (b), information is available up to distance 2. That is, the bank in blue receives information not only from the orange banks but also from the red banks—its neighbors of neighbors. The remaining banks are colored in grey. The node size is weighted by its degree. The network is constructed using the default values of model parameters (Section 3.2).

After the network was formed, a shock was applied. The shock hit one or several randomly chosen banks, depending on the type of shock to be applied. Then, the remaining simulation procedure entailed iteration of actions that take place in discrete time (see Appendix B).

7. Results

The results are based on 1,000 simulation replications per scenario, with each replication lasting until the system came to rest. Figure 5 depicts the probability distribution for the total number of failed banks after a shock is applied to a single small, a single large, and multiple small banks. In the

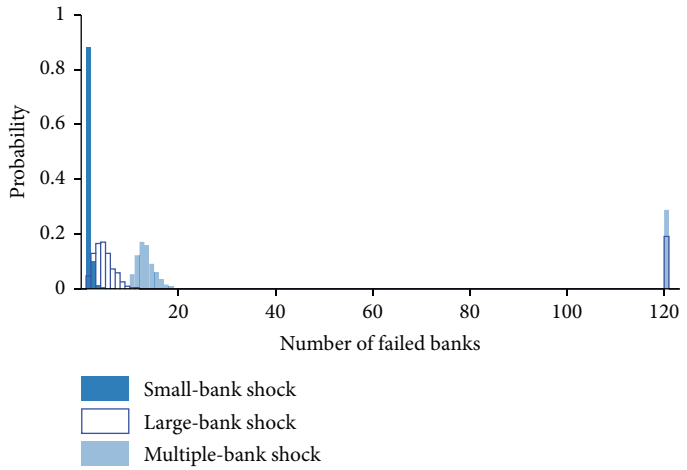

Figure 5: Probability distribution of number of failed banks in the complete information (CI) scenario after a shock is applied to a small bank, a large bank, and multiple small banks. The systemic breakdown occurs with sizable probability of nearly 20% and 30% after a large-bank shock and multiple-bank shock, respectively.

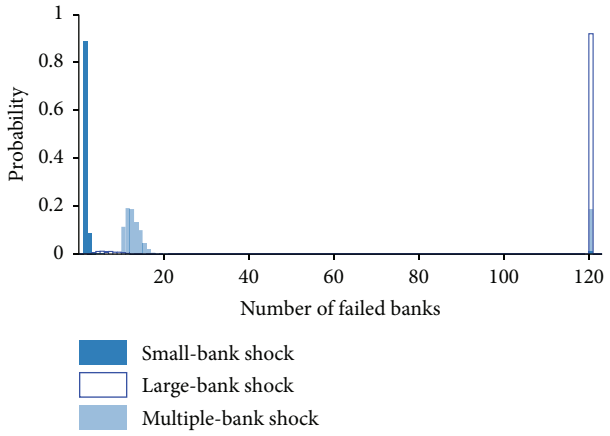

Figure 6: Probability distribution of number of failed banks in the LI1 scenario after a shock is applied to a small bank, a large bank, and multiple small banks. In comparison to the CI scenario, the probability of systemic breakdown increases after both single-bank-shock treatments, whereas it drops after multiple-bank shock. LI1 is a scenario in which a bank has access only to information from its direct neighbors at distance 1. LI = local information; CI = complete information.

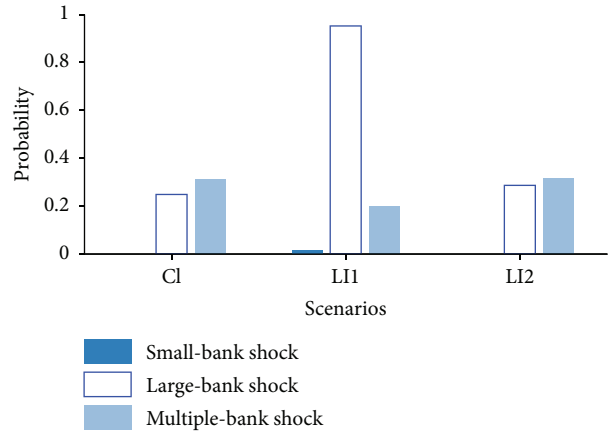

Figure 7: Probability of whole-system breakdown in complete information (CI) and local information (LI) scenarios. The LI1 scenario obtains the highest probability of systemic breakdown in both single-bank shock treatments. LI1 and LI2 = scenarios in which banks have access only to information from banks up to distance 1 and 2, respectively (Figure 15 in Appendix A displays all scenarios).

cases of a large-bank shock and a multiple-bank shock, the fat tail of the distribution indicates that the entire system collapses with a probability of nearly 20% and 30%, respectively.

When uncertainty is introduced, the highest impact on the probability distributions of number of failed banks is realized in the LI1 scenario. Figure 6 shows that the probability of systemic breakdown (i.e., all banks in the system fail) after a large-bank shock is now more than 90% and that even a small-bank shock results in a nontrivial probability of systemic breakdown (In high-resolution data of 10,000 repetitions, the probability of whole-system breakdown after a small-bank shock increases from 0% in the CI scenario to 0.16% in the LI1 scenario. This is easier to see in Figure 7.), whereas the same probability drops to under 20% in the case of a multiple-bank shock.

Figure 7 displays a comparison of probabilities of systemic breakdown across different scenarios in all three shock treatments. The probabilities are consistently higher in the multiple than in the single-shock treatment, except for the LI1 scenario. In fact, the LI1 scenario, which is associated with the largest probability of systemic collapse in the case of a large bank's shock, is at the same time associated with the smallest probability of systemic collapse in the distributed shock condition.

The results of the LI1 scenario are particularly striking as they show that a limited information flow further intensifies the contagion dynamics observed in the AKM model after a

large-bank failure. At the same time, the LI1 scenario mitigates the impact of a multiple-bank shock when compared to the CI scenario, in which this treatment in fact yields the highest probability of systemic failure (Figure 7). While this illustrates that the LI1 scenario does not merely amplify the contagion dynamics, it also shows how an alternative assumption about information availability can flip the conclusion about which event is more likely to trigger catastrophic failures.

In the following section, we mainly focus on explaining the difference between the results obtained in the CI and LI1 scenarios. Given the insignificant change in results produced in the other manipulations (NI and DI scenarios; Appendix A), we discuss those results very briefly.

8. Explaining the Results

In the CI scenario, confidence is assessed over the extent of the whole system: although this captures the notion of a generalized psychological context, it also has the effect of diluting the local impact of a shock. In the LI1 scenario, by contrast, we have introduced the notion of "locally perceived" confidence that can vary with the neighborhood of different banks. The local impact of an initiating shock is therefore more intense than in a CI scenario but limited to the neighborhood, leaving the confidence of the remaining system initially intact. Yet, this local impact is subsequently transmitted through the system (analogous to the dynamics of crack propagation in a solid medium), resulting overall in a higher risk of system collapse than in the CI scenario. The similarity of the results of the LI2 and CI scenarios (Figure 7) provides a useful sanity check, as the portion of the system taken into account for the confidence estimation is minimally different in the two scenarios (Figure 4).

A similar rationale applies to the results of the distributed shock treatment, which involves a failure of multiple small banks. While the impacts of the small-bank failures on confidence "add up" in the CI scenario, irrespective of their placement, in the LI1 scenario, they independently harm confidences of the disparate localities in which they randomly fall. As a result, the probability of whole-system failure after a distributed shock in LI1 is noticeably reduced when compared with the CI scenario (Figure 7). That the "adding-up effect" is less prominent in the LI1 scenario can also be seen by contrasting the results obtained from CI and LI1 after small idiosyncratic and multiple-bank treatments. For this purpose, it is useful to interpret a multiple shock as adding extra instances of small shocks to a small shock. The resulting pattern is somewhat counterintuitive. While a small-bank shock alone leads to a higher probability of systemic failure in the LI1 scenario (than in the CI scenario), after multiple shocks, the system fails with a higher probability in the CI scenario.

To better understand how the dynamics of C affect the discrepancy in the results between the CI and LI1 scenarios, we conducted a further analysis to assess the portion of the system that is initially affected by the shock applied in LI1 scenario, the magnitude of C drop that corresponds to the applied shock, and the sensitivity of the system to different manners in which C can deteriorate. Finally, we compared the time course of C obtained in computational simulations in the two scenarios and designed tests to assess if the observed difference can explain the results.

8.1. Dynamics of Local Confidence. The only distinction between the CI and LI1 scenarios corresponds to the difference in confidence contexts in which banks' decisions are made. Given the complexity of confidence dynamics, we aimed to compare the two scenarios in terms of initial confidence effects caused by the applied shock. Then, we analyzed if the initial difference could account for the results. We focused on the impact of the large-bank shock, which is associated with the most striking contrast between the two scenarios, but the same rationale applies to the small-bank shock. In the CI scenario, to calculate C^1 (the level of C in the immediate aftermath of the shock), one needs to know only the number of small N_s and large N_b banks as well as the size ratio q. Then, from $C = AE$, it follows that

$$C^1 = \left(\frac{qN_s + N_s - q}{qN_b + N_s}\right)^2. \tag{6}$$

For the default values of the model parameters, $C^1 \approx 0.92$, which corresponds to the drop of C for approximately 0.08. Unlike CI scenario where confidence effects are uniformly distributed among all banks, in the LI1 scenario, the shock initially affects only the confidence of banks in the neighborhood of the shock. The assessment of the fraction of banks affected by the shock, therefore, requires the estimation of the size of "average-bank neighborhood"—that is, the expected number of unique large and small banks that are connected to a given bank, including only its borrowers and lenders (Figure 8).

For default values of model parameters, a large bank is on average connected to 40 small and 10 large banks, whereas a small bank is connected to 4 large and 5 small banks (for the proof see Appendix C). This implies that the large-bank shock on average affects approximately three-quarters of the system assets; and among affected banks, large banks experience a decline of confidence to $C_b^1 \approx 0.87$ and small banks to $C_s^1 \approx 0.61$. The faster decline of confidence of small banks is both intuitive because the average-bank neighborhood of a small bank is relatively smaller, and realistic, because it is to be expected that a smaller bank suffers larger confidence loss when faced with a shock of a given size. In what follows, we describe a test designed for the assessment of system sensitivity to the steepness of C decline.

8.2. Test 1—System Sensitivity to the Loss of Confidence. How does the system behave under different C regimes? To investigate this, we externally enforced different time courses of C while keeping the assumption that all banks share the same C. (This means that C is no longer endogenously determined from the fluctuation of asset levels.) The independent manipulation was designed to test the resistance of the system to a variety of hypothetical confidence contexts. The goal was to explore how the system responds if only the perception of decision makers is manipulated, while keeping all remaining

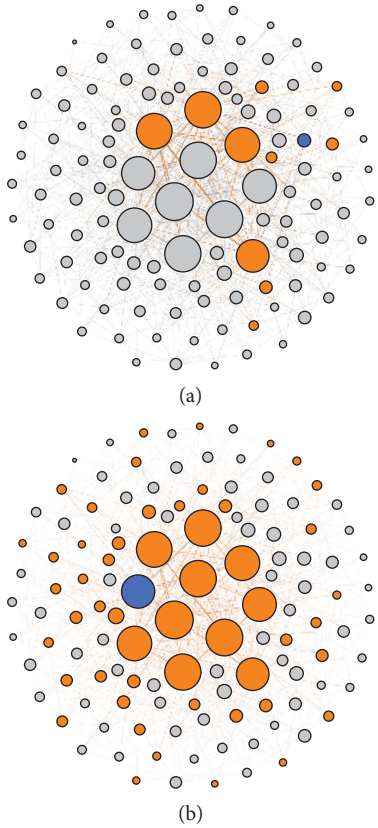

Figure 8: Neighborhood of a small bank (a) and a large bank (b) in the banking network of 120 banks. The small (large) bank is colored in blue, whereas its immediate neighbors are colored in orange. The remaining banks are colored in grey. The node size is weighted by its degree. The network is constructed using the default values of model parameters (Section 3.2).

processes endogenous. We considered different magnitudes of C drop and for each of them we also manipulated the slope of decline. We used the exponential function $f(x) = e^{-rx}$ to model the slope manipulation, where the value of parameter r determines the slope (Figure 9).

Figure 10 shows that the sudden drop of C ($r = 100$) has by far the highest impact on the system. This is a strong indication that the quicker loss of confidence in the LI1 scenario as compared to the CI scenario played a role in the increase in systemic risk. In addition, we compared standard deviations of confidence across the scenarios (Figure 11). The standard deviations of the end-state confidence (when the system is at rest) were calculated across 1000 simulation replications, taking into account only the surviving population of banks. Two results stood out. First, standard deviations of confidence were consistently higher after the large concentrated shock than after the distributed shock. The immediate implication is that the outcome of a large concentrated shock is less predictable. Second, there was a large difference between the standard deviations of confidence in the CI and LI1 scenarios. To determine if this contributed to the difference in the corresponding results, we carried out an analysis of the variance of confidence, described next.

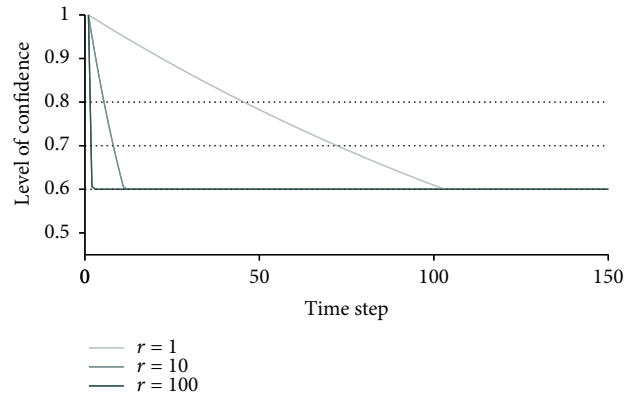

Figure 9: Manipulation of confidence (C) change over time: C drops 20, 30, or 40%, with the slope of decline determined by the parameter r of the exponential function $f(x) = e^{-rx}$; the higher r, the steeper the slope of C decline. Time step refers to discrete simulation time where each step iterates a defined set of actions (see Appendix B). Note: the observed time horizon is extended from 100 to 150 time steps, as additional time steps were needed for the system to reach the steady state when the slope of C decline was low ($r = 1$).

8.3. Test 2—Variance of Confidence. The goal of this test was to assess the sensitivity of total assets A and total interbank loans E to the change in variance of C. A realization of C in a simulation replication is in fact a vector $C(t)$, which contains values of C at different time steps. The manipulation first entailed construction of two vectors $C(t)_{i_{\mathrm{CI}}}$ and $C(t)_{i_{\mathrm{LI1}}}$ based on data from realizations of C in the CI and LI1 scenarios when a large-bank shock is applied. Two newly composed time sequences of C values were generated from a normal distribution with the same mean and two variances: $C(t)_{i_{\mathrm{CI}}} \sim N(C_i^{\mathrm{AV}}, V_i^{\mathrm{CI}})$ and $C(t)_{i_{\mathrm{LI1}}} \sim N(C_i^{\mathrm{AV}}, V_i^{\mathrm{LI1}})$. The mean C_i^{AV} was estimated by averaging the confidence from the realization of the CI scenario over simulation repetitions. The first variance, V_i^{CI}, was calculated from vectors of global confidence realized in the CI scenario and the second, V_i^{LI1}, from vectors of local confidence realized in the LI1 scenario. Finally, the two vectors $C(t)_{i_{\mathrm{CI}}}$ and $C(t)_{i_{\mathrm{LI1}}}$ were exogenously applied to the CI setting of the simulation (Figure 12). The exogenous application of confidence implies that the calculation of confidence is decoupled from assets and interbank loans in the actual simulation and taken as given. The sequences of realized networks were controlled to be the same in both conditions by setting the same seeding of the random number generator in the simulation $C(t)_{i_{\mathrm{CI}}} \sim N(C_i^{\mathrm{AV}}, V_i^{\mathrm{CI}})$.

Even when the mean of C over simulation replications is kept constant, as Figure 12 illustrates, a higher variance of C yields a faster drop of total assets A. Given that assets determine the level of C by definition, we designed an additional test to assess the impact of the time course of C on the results.

8.4. Test 3—Time Course of Confidence. For this purpose, the mean of individual confidences of all banks in the LI1

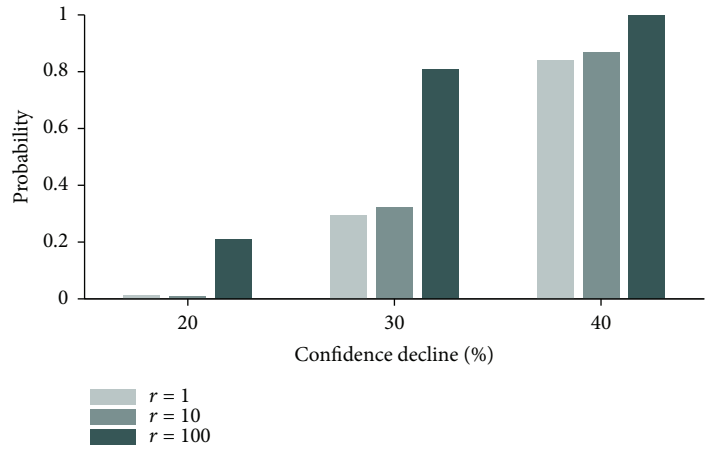

Figure 10: Probability of systemic breakdown for various magnitudes and speeds of confidence (C) decline. The magnitude of decline refers to the percentage of the initial value of C that is lost. The speed of decline is determined by the parameter r of the exponential function $f(x) = e^{-rx}$; the greater the value of r, the greater the speed of C decline. The sudden decline of C ($r = 100$) is associated with a sharp increase in the probability of systemic breakdown, especially in the cases of 20% and 30% of C decline.

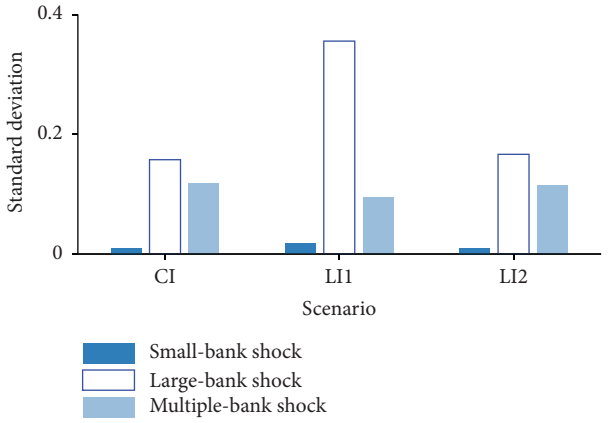

Figure 11: Standard deviation of confidence across complete information (CI) and local information (LI) scenarios and three shock treatments: to a small bank, a large bank, and multiple small banks. The LI1 scenario inflates standard deviations of confidence in both single-bank-shock treatments. The multiple-bank treatment involves a number of small banks whose total assets amount to the assets of a single large bank. LI1 and LI2 = scenarios in which a bank has access only to information from banks up to distance 1 and 2, respectively (Figure 16 in Appendix A displays all scenarios).

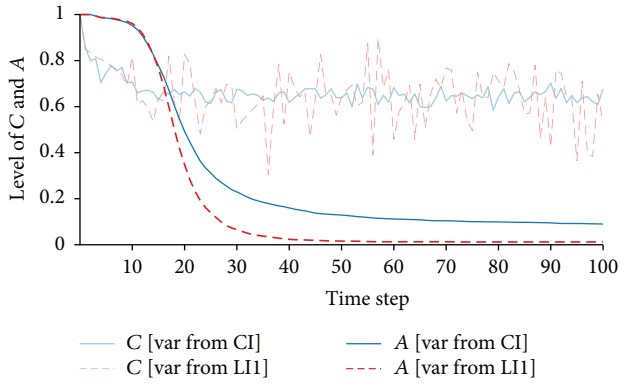

Figure 12: The impact of exogenous manipulation of confidence (C) on the level of total assets (A) in the system. Two applied manipulations of C follow normal distribution with the same mean and different variances: V_i^{CI} [derived from the complete information (CI) scenario] and V_i^{LI1} [derived from the local information (LI) LI1 scenario]. The higher variance corresponds to the faster decline of total assets in the system. CI is a scenario in which a bank has access to information from all other banks in the network. LI1 is a scenario in which a bank has access only to information from banks at distance 1.

scenario was calculated and denoted as local confidence. Confidence calculated according to the standard procedure, as in the CI scenario, was denoted global confidence. Figure 13 indicates a steeper decline of local as compared to global confidence when corresponding simulations were performed in an identical simulation setting, that is, when the identically placed large-bank shock was applied to an identical set of networks by controlling the seeding of the random number generator in the simulation.

In the next step, we estimated the impact of the observed slope difference between the two C curves by exogenous application of the local confidence to a hypothetical CI scenario together with the large-bank shock treatment. In the hypothetical scenario, as in the standard CI scenario, all banks in the system perceive confidence equally, but their perception is no longer endogenously determined. Instead, we forced their global confidence to be equal to previously determined local confidence taken from the realization of the LI1 scenario depicted in Figure 13. This procedure yielded a probability of over 90% of the whole system failing, a result similar to that in the LI1 scenario (Figure 14). The decline of confidence is therefore capable of explaining the difference in the results between the scenarios.

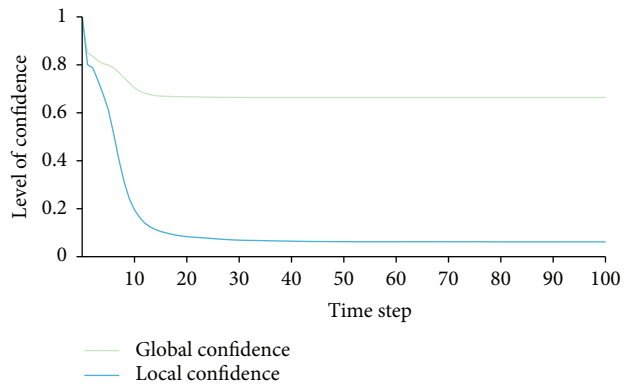

Figure 13: Time course of global and local confidence. Global confidence is calculated in a standard way as in the complete information (CI) scenario. Local confidence is an average of individual confidences of all banks in the local information (LI) LI1 scenario. CI is a scenario in which a bank has access to information from all other banks in the network. LI1 is a scenario in which a bank has access only to information from banks at distance 1.

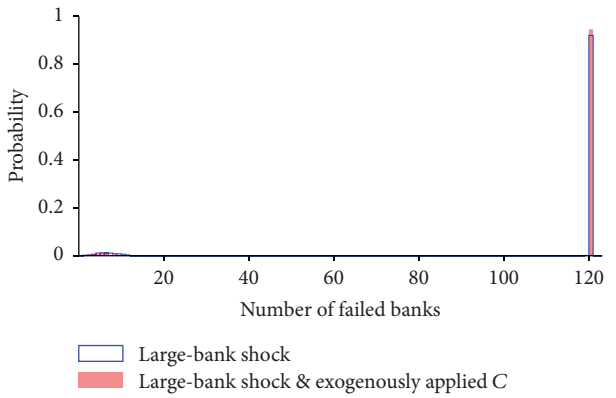

Figure 14: A comparison of probability distributions of number of failed banks after a large-bank shock in the LI1 scenario, and scenario in which confidence from the LI1 scenario was exogenously applied to the CI scenario. The probability of systemic breakdown is nearly the same in both scenarios. CI is a scenario in which a bank has access to information from all other banks in the network. LI1 is a scenario in which a bank has access only to information from its direct neighbors at distance 1.

9. Discussion

The increasing interconnectedness of the global financial network has introduced an enormous amount of structural uncertainty in the financial system. Yet, its implications went unnoticed until the recent financial crisis when the interdependencies in the network made it nearly impossible to disentangle low- from high-risk investments and partnerships. In this paper, we presented a model where structural uncertainty shapes patterns of confidence loss in a financial network. We found that a severe confidence loss in a limited part of the network carries a higher systemic risk than a moderate confidence loss in the entire network.

Our use of a multiagent model allowed us to analyze more specific aspects of confidence decline and to consider different types of shocks that can affect the system. We found that while the magnitude of decline was important, as was expected, a sudden decline of confidence was also a major factor in the increase in systemic risk; when the average level of confidence was controlled for, higher variance of confidence corresponded to higher systemic risk. We also found that under uncertainty, a shock affecting one large bank was by far more impactful than the same shock distributed among multiple smaller banks; when complete information was assumed, the opposite was true. This suggests that it is the failure of a large bank that poses a major threat to the system.

One caveat of our work is that there is a lack of understanding of how banks react to structural uncertainty during a financial crisis. Here we assumed that in a crisis, when it is infeasible to assess relevant risks, banks emphasize the information that they observe in their local environment. An alternative view explored in the literature assumes that banks maintain the practices developed prior to the crisis and rely on their own assessment of relevant risks (e.g., [28]). However, such an assessment would require the knowledge of the underlying structure of the financial network, which is exactly unavailable under structural uncertainty. Moreover, a possible extension of our work would be to explore how structural uncertainly interacts with other sources of uncertainty, such as uncertainty about the value of assets [34], in hoarding behavior.

From the view of policymaking, our observed sensitivity of the system to sudden loss of confidence suggests that interventions, such as bailouts of distressed banks or liquidity injections, should be done without delay. Our results also confirm previous findings that large banks carry disproportionate amount of systemic risk and hence are more likely to require stricter regulations than what was previously assumed. More generally, our results indicate the need for regulation designed to improve overall transparency in the financial system. For instance, policies that aim at reducing and eventually eliminating over-the-counter markets or constraining the complexity of financial contracts would be highly desirable. Only a transparent financial system would allow banks to make sound decisions from the perspective of systemic risk.

Appendix

A. Delayed Information and Noisy Information Scenarios

Unlike in the LI scenarios, in the DI scenarios banks receive information from all other banks in the system ($d_{\max}$ is no longer exogenously set), but some of the information is outdated. We modeled information delay as a function of distance—the further the information source, the longer the delay. If k denotes the time step when information originated,

Table 1: The size of delay in time steps assigned to banks at different distance in different scenarios.

Scenario	Size of delay		
	0	1	2
DI1	i + neighbors	All remaining banks	
DI2	i + neighbors		All remaining banks
DI3	i	All remaining banks	
DI4	i		All remaining banks

Note: DI = Delayed information; i = information user.

t the time step in which it is received, d_s the distance at which delay starts, and s the size of applied delay, then

$$a_i^j = a_i^{kj}, \quad e_i^j = e_i^{kj}$$
$$k = \begin{cases} t & \text{if } d < d_s \\ \max(0, t - s) & \text{if } d < d_s \end{cases}, \quad d(i,j) \in \{1, 2 \dots d_{\max}\}, \quad d_s \in \{1, 2\}, \quad s \in \{1, 2\}. \tag{A.1}$$

We designed four variants of the DI scenario by manipulating s and d_s (Table 1). For instance, in the DI1 and DI3 scenarios, the size of the delay is 1 time step ($s = 1$), and in the DI2 and DI4 it is 2 time steps ($s = 2$). In the DI1 and DI2 scenarios, delay starts from neighbors of neighbors ($d_s = 2$), whereas in the DI3 and DI4 scenarios, it starts immediately from neighbors ($d_s = 1$). We set the minimum value of k to 0 since negative values of time do not make sense in this context.

In the NI scenario, noise in information increases with distance. If $\in$ denotes a random error with normal distribution $\in \sim N(0, \sigma^2)$, v the size of variance in the noise term, and $d_{\max}$ maximal distance in the network, then

$$a_j^i = a_j^j + d \in, \quad d(i,j) = 1, 2, \dots, d_{\max}, \quad \sigma^2 = v a_j^j$$
$$e_j^i = e_j^j + d \in, \quad d(i,j) = 1, 2, \dots, d_{\max}, \quad \sigma^2 = v e_j^j \tag{A.2}$$

We considered two variants of the NI scenario: NI5 and NI30. In the former, $v = 5\%$ and in the latter, $v = 30\%$.

Regardless of the amount of noise, the NI scenarios yield similar results to those of the CI scenario. In the case of the DI scenarios, although the impact is very small the probabilities of systemic failure increase with delay. This is particularly noticeable in the nonzero probabilities of systemic failure after a small-bank shock. In the NI scenarios, normally distributed noise averaged out across banks, producing no difference in results compared to the CI scenario (Figures 15 and 16). Assuming an alternative distribution of noise would potentially produce more interesting results. On the other hand, the DI scenarios indicate that the delay matters. The result can be accounted for as the effect of overconfidence. Namely, in the DI scenarios, confidence at a particular moment in time was higher than what actual information would imply. This narrows the time window for the preemptive action that would enable shortening of long-term loans, which otherwise could not be used to meet the upcoming liquidity needs.

B. Simulation Procedure over Time Steps

After the application of the shock, the simulation procedure entailed five actions taking place in each time step:

(1) Recalculate health h_i of all banks. The health is used for stipulating liquidation of banks. Zero health implies that a bank needs to be liquidated.

(2) Liquidate banks that failed in the previous time step (or those that failed because of the initial shock). If bank i is to be liquidated then the procedure is as follows:

(a) Withdraw all short-term loans $A^{ST}{}_i$ that can be collected from the borrowers of i. Triggering the collection procedure means that i's borrowers will ask their own borrowers for money, and so forth. Record banks that consequently satisfy the condition of illiquidity and are to be liquidated in the next time step.

(b) Settle all short-term borrowings $L^{ST}{}_i$ of bank i that can be paid from its initial liquid assets l_i and collected short-term loans $A^{ST}{}_i$. Record the resulting shortage or surplus.

(c) Calculate the total long-term assets of i by adding long-term loans to the capital c_i. To this sum add the result from substep b. If there is a shortage of assets when the sum is compared to

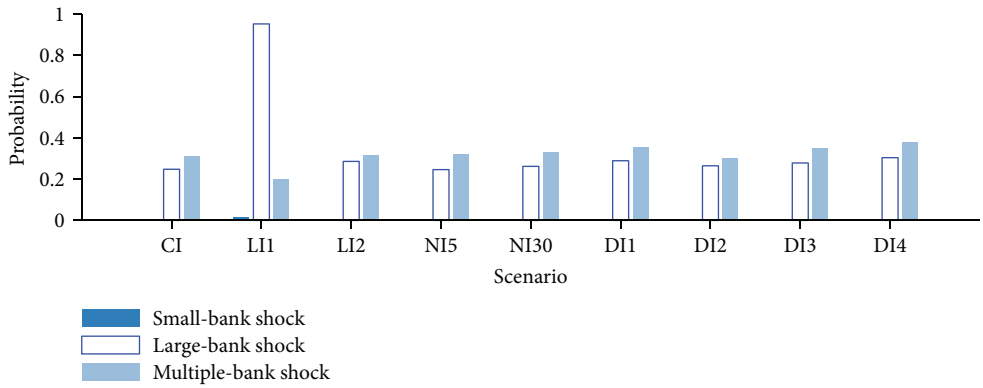

Figure 15: Probability of systemic failure across all scenarios. CI = Complete information; LI = local information; NI = noisy information; DI = delayed information; LI1 and LI2 = scenarios in which banks have access only to information at distance 1 and 2, respectively; NI5 and NI30 = scenarios in which noise parameter v is 5% and 30%, respectively; the delay scenarios are defined in Table 1.

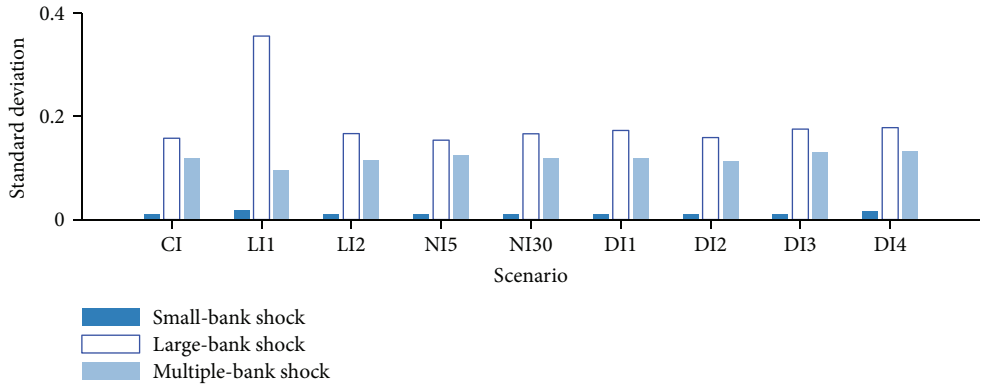

Figure 16: Standard deviations of confidence across all scenarios and three shock treatments: to a small bank, a large bank, and multiple banks. CI = Complete information; LI = local information; NI = noisy information; DI = delayed information; LI1 and LI2 = scenarios in which a bank has access only to information at distance 1 and 2, respectively. NI5 and NI30 = scenarios in which noise parameter v is 5% and 30%, respectively. The delay scenarios are defined in Table 1.

long-term liabilities of i, then i's long-term lenders suffer from this amount of shock u applied to their capital. The shock is evenly distributed among the lenders, but only up to the level of individual exposures. This ensures that the shock cannot exceed the level of individual lending amount.

(d) Sell external assets of i, applying the shock to all holders of the same asset classes that i had in its portfolio. The external assets are sold at a market that is taken to be external to the model. The price of asset w is assumed to be decreasing to a fraction $exp(-\alpha x_w)$ of its initial value (modeled as in Arinaminpathy et al., 2012), in which x_w is a proportion of the asset w that is sold by i, and α is an indicator of market liquidity that is directly related to confidence C, $\alpha = 1 - C$. If any bank suffers from the capital default based on the shocks from substeps c and d, its health once it is recalculated will be 0. This automatically qualifies such banks for liquidation in the next time step.

(3) Apply decision rule 2 (see Section 3.4) and withdraw short-term loans if condition is satisfied. It is assumed that loans are perfectly divisible and partial withdrawals are possible. Then, record all banks that become illiquid during the withdrawal in order to be liquidated in the next time step. Note that the second decision rule is applied first as otherwise it would be possible to withdraw long-term loans in a single time step.

(4) Apply decision rule 1 (see Section 3.4) and administer shortening of long-term loans if the condition is satisfied.

(5) Recalculate the network and other parameters and go back to step 1 for the next time step.

C. Calculation of the Size of an Average–Bank Neighborhood

In the main text, we stated that the size of a particular bank neighborhood is probabilistic. Here, we provide a simple

calculation of the size of an average-bank neighborhood for a small and a large bank.

Let us consider a network of N banks, of which N_s are small and N_b are large. Let L be the out-degree of a small bank and q be the ratio of average degree of a large bank over average degree of a small bank. In the main text we assumed that in- and out-degrees of all banks are drawn independently from a Poisson distribution with mean z for small and qz for large banks. Here, we make a simplifying assumption that out-degrees of all small (large) banks are equal. When tested in a simulation this assumption did not change our previously reported results. To determine the size of an average-bank neighborhood of a bank i, which includes i's borrowers and lenders, we have to calculate the expected number of unique small and large banks connected to i. For this purpose, let us define random variables:

$$X_{\overrightarrow{ij}} = \begin{cases} 1 & \text{if there is a directed connection from } i \text{ to } j \\ 0 & \text{otherwise} \end{cases}$$
$$X_{ij} = \begin{cases} 1 & \text{if there is a connection between } i \text{ to } j \\ 0 & \text{otherwise} \end{cases} \tag{C.1}$$

with the correspondence $X_{ij} = \max\{X_{\overrightarrow{ij}}, X_{\overrightarrow{ji}}\}$. From here it follows that

$$\begin{aligned} E[X_{ij}] &= 1P(X_{ij} = 1) + 0P(X_{ij} = 0) \\ &= P(X_{ij} = 1) = 1 - P(X_{ij} = 0). \end{aligned} \tag{C.2}$$

Given there are small and large banks in the system, there are three cases: one bank is small and another is large, both banks are small, and both banks are large.

Case 1: both banks (i and j) are small.

The probability that a connection originating from i goes to j is a fraction of the in-degree of j and the total in-degree of all banks in the network except for i:

$$w_{ij}^{ss} = \frac{L}{(N_s - 1)L + qN_bL} = \frac{1}{(N_s - 1) + qN_b}. \tag{C.3}$$

From Equations C.4 and C.13 it follows that the probability that there is at least one connection from i to j is

$$P\left(X_{\overrightarrow{ij}} = 1\right) = 1 - P\left(X_{\overrightarrow{ij}} = 0\right) = 1 - \left(1 - w_{ij}^{ss}\right)^L, \tag{C.4}$$

where $(1 - w_{ij}^{ss})^L$ is the probability that none of L outgoing links of i connect to j (note that the probabilities of connections are independent).

Then, the probability that there is at least one connection between i and j irrespective of the direction is

$$\begin{aligned} P(X_{ij} = 1) &= P\left(X_{\overrightarrow{ij}} = 1 \cup X_{\overrightarrow{ji}} = 1\right) \\ &= P\left(X_{\overrightarrow{ij}} = 1\right) + P\left(X_{\overrightarrow{ji}} = 1\right) \\ &\quad - P\left(X_{\overrightarrow{ij}} = 1 \cap X_{\overrightarrow{ji}} = 1\right) \\ &= 2P\left(X_{\overrightarrow{ij}} = 1\right) - P^2\left(X_{\overrightarrow{ij}} = 1\right) \\ &\quad \cdot \left(\because P\left(X_{\overrightarrow{ij}}\right) = P\left(X_{\overrightarrow{ji}}\right) \& X_{\overrightarrow{ij}} \coprod X_{\overrightarrow{ji}}\right) \\ &= P\left(X_{\overrightarrow{ij}} = 1\right)\left(2 - P\left(X_{\overrightarrow{ij}} = 1\right)\right) \\ &= \left(1 - \left(1 - w_{ij}^{ss}\right)^L\right)\left(1 + \left(1 - w_{ij}^{ss}\right)^L\right) \\ &= 1 - \left(1 - w_{ij}^{ss}\right)^{2L}. \end{aligned} \tag{C.5}$$

We can now express the expectation of Y_i^s, which is the number of unique small banks connected to i, as:

$$E(Y_i^s|L) = \sum_{i=1}^{N_s - 1} P(X_{ij} = 1|L) = (N_s - 1)\left(1 - \left(1 - w_{ij}^{ss}\right)^{2L}\right). \tag{C.6}$$

Case 2: one bank is small and another is large.

Case 2a: i is a small and j is a large bank.

The probability that a connection originating from i goes to j is

$$w_{ij}^{sb} = qw_{ij}^{ss} = \frac{q}{(N_s - 1) + qN_b}. \tag{C.7}$$

The probability that there is at least one connection from i to j is

$$P\left(X_{\overrightarrow{ij}} = 1\right) = 1 - P\left(X_{\overrightarrow{ij}} = 0\right) = 1 - \left(1 - w_{ij}^{sb}\right)^L. \tag{C.8}$$

Case 2b: i is a large and j is a small bank.

The probability that a connection originating from i goes to j is

$$w_{ij}^{bs} = \frac{L}{N_sL + q(N_b - 1)L} = \frac{1}{N_s + q(N_b - 1)}. \tag{C.9}$$

Similarly to Case 2a, it follows that

$$P\left(X_{\overrightarrow{ij}} = 1\right) = 1 - P\left(X_{\overrightarrow{ij}} = 0\right) = 1 - \left(1 - w_{ij}^{bs}\right)^{qL}. \tag{C.10}$$

From Case 2a and Case 2b we derive the probability that there is at least one connection between i and j irrespective of the direction:

$$\begin{aligned} P\left(X_{ij}=1\right) &= P\left(X_{\overrightarrow{ij}}=1 \cup X_{\overrightarrow{ji}}=1\right) \\ &= P\left(X_{\overrightarrow{ij}}=1\right)+P\left(X_{\overrightarrow{ji}}=1\right) \\ &\quad - P\left(X_{\overrightarrow{ij}}=1\right)P\left(X_{\overrightarrow{ji}}=1\right) \\ &= 2-\left(1-w_{ij}^{sb}\right)^{L}-\left(1-w_{ij}^{bs}\right)^{qL} \\ &\quad - \left[\left(1-\left(1-w_{ij}^{sb}\right)^{L}\right)\left(1-\left(1-w_{ij}^{bs}\right)^{qL}\right)\right]. \end{aligned} \tag{C.11}$$

Then, the expectations for the number of unique large banks connected to a small bank i (Case 2a) and the number of unique small banks connected to a large bank i (Case 2b) are

$$\begin{aligned} E\left(Y_i^b|L\right) &= \sum_{i=1}^{N_b} P\left(X_{ij}=1|L\right) \\ &= N_b\left\{2-\left(1-w_{ij}^{sb}\right)^{L}-\left(1-w_{ij}^{bs}\right)^{qL}\right. \\ &\quad \left. - \left[\left(1-\left(1-w_{ij}^{sb}\right)^{L}\right)\left(1-\left(1-w_{ij}^{bs}\right)^{qL}\right)\right]\right\}, \\ E\left(Y_i^s|L\right) &= \sum_{i=1}^{N_s} P\left(X_{ij}=1|L\right) \\ &= N_s\left\{2-\left(1-w_{ij}^{sb}\right)^{L}-\left(1-w_{ij}^{bs}\right)^{qL}\right. \\ &\quad \left. - \left[\left(1-\left(1-w_{ij}^{sb}\right)^{L}\right)\left(1-\left(1-w_{ij}^{bs}\right)^{qL}\right)\right]\right\}. \end{aligned} \tag{C.12}$$

Case 3: both banks (i and j) are large.

The probability that a connection originating from i goes to j is

$$w_{ij}^{bb} = q w_{ij}^{bs} = \frac{q}{N_s + q\left(N_b-1\right)}. \tag{C.13}$$

The probability that there is at least one connection from i to j is

$$P\left(X_{\overrightarrow{ij}}=1\right) = 1-P\left(X_{\overrightarrow{ij}}=0\right) = 1-\left(1-w_{ij}^{bb}\right)^{qL}. \tag{C.14}$$

Similarly to the previous cases, it follows that

$$\begin{aligned} P\left(X_{ij}=1\right) &= P\left(X_{\overrightarrow{ij}}=1 \cup X_{\overrightarrow{ji}}=1\right) \\ &= P\left(X_{\overrightarrow{ij}}=1\right)\left(2-P\left(X_{\overrightarrow{ij}}=1\right)\right) \\ &= 1-\left(1-w_{ij}^{bb}\right)^{2qL}. \end{aligned} \tag{C.15}$$

The expectation of the number of unique large banks connected to a large bank i is

$$E\left(Y_i^b|L\right) = \sum_{i=1}^{N_b-1} P\left(X_{ij}=1|L\right) = \left(N_b-1\right)\left(1-\left(1-w_{ij}^{bb}\right)^{2qL}\right). \tag{C.16}$$

Data Availability

We do not use any data that are not publicly available.

Disclosure

Part of this work is based on the first author's dissertation [35].

Conflicts of Interest

The authors declare that they have no conflicts of interest.

Acknowledgments

This research was funded by a pre-doctoral fellowship from the Max Planck Institute for Human Development to the first author. We thank Sujit Kapadia, Jolene Tan, members of the ABC group, the IMPRS Uncertainty School for their helpful comments on an earlier draft; and Anita Todd for editing the manuscript. This paper is dedicated to the memory of Professor Alfred Hübler who inspired our exploration of complexity.

References

[1] D. Covitz, N. Liang, and G. A. Suarez, "The evolution of a financial crisis: collapse of the asset-backed commercial paper market," *Journal of Finance*, vol. 68, no. 3, pp. 815–848, 2013.

[2] V. V. Acharya and O. Merrouche, "Precautionary hoarding of liquidity and interbank markets: evidence from the subprime crisis," *Review of Finance*, vol. 17, no. 1, pp. 107–160, 2013.

[3] J. Berrospide, *Liquidity Hoarding and the Financial Crisis: An Empirical Evaluation (FEDS Working Paper no. 2013–3)*, Washington, DC, 2012 http://www.bis.org/bcbs/events/bhbibe/berrospide.pdf.

[4] D. Gale and T. Yorulmazer, "Liquidity hoarding," *Theoretical Economics*, vol. 8, no. 2, pp. 291–324, 2013.

[5] M. Pritsker, "Knightian uncertainty and interbank lending," *Journal of Financial Intermediation*, vol. 22, no. 1, pp. 85–105, 2013.

[6] N. Arinaminpathy, S. Kapadia, and R. M. May, "Size and complexity in model financial systems," *Proceedings of the National Academy of Sciences of the United States of America*, vol. 109, no. 45, pp. 18338–18343, 2012.

[7] P. Glasserman and H. P. Young, "Contagion in financial networks," *Journal of Economic Literature*, vol. 54, no. 3, pp. 779–831, 2016.

[8] S. Battiston, D. Delli Gatti, M. Gallegati, B. Greenwald, and J. E. Stiglitz, "Liaisons dangereuses: increasing connectivity, risk sharing, and systemic risk," *Journal of Economic Dynamics and Control*, vol. 36, no. 8, pp. 1121–1141, 2012.

[9] D. Brockmann and D. Helbing, "The hidden geometry of complex, network-driven contagion phenomena," *Science*, vol. 342, no. 6164, pp. 1337–1342, 2013.

[10] S. Martinez-Jaramillo, B. Alexandrova-Kabadjova, B. Bravo-Benitez, and J. P. Solórzano-Margain, "An empirical study of the Mexican banking system's network and its implications for systemic risk," *Journal of Economic Dynamics and Control*, vol. 40, pp. 242–265, 2014.

[11] E. Nier, J. Yang, T. Yorulmazer, and A. Alentorn, "Network models and financial stability," *Journal of Economic Dynamics and Control*, vol. 31, no. 6, pp. 2033–2060, 2007.

[12] S. Thurner and S. Poledna, "DebtRank-transparency: controlling systemic risk in financial networks," *Scientific Reports*, vol. 3, no. 1, p. 1888, 2013.

[13] C. Minoiu and J. A. Reyes, "A network analysis of global banking: 1978–2010," *Journal of Financial Stability*, vol. 9, no. 2, pp. 168–184, 2013.

[14] F. Caccioli, J. D. Farmer, N. Foti, and D. Rockmore, "Overlapping portfolios, contagion, and financial stability," *Journal of Economic Dynamics and Control*, vol. 51, pp. 50–63, 2015.

[15] F. Caccioli, M. Shrestha, C. Moore, and J. D. Farmer, "Stability analysis of financial contagion due to overlapping portfolios," *Journal of Banking & Finance*, vol. 46, pp. 233–245, 2014.

[16] D. Acemoglu, A. Ozdaglar, and A. Tahbaz-Salehi, "Systemic risk and stability in financial networks," *American Economic Review*, vol. 105, no. 2, pp. 564–608, 2015.

[17] F. Allen and D. Gale, "Financial contagion," *Journal of Political Economy*, vol. 108, no. 1, pp. 1–33, 2000.

[18] L. Eisenberg and T. H. Noe, "Systemic risk in financial systems," *Management Science*, vol. 47, no. 2, pp. 236–249, 2001.

[19] M. Elliott, B. Golub, and M. O. Jackson, "Financial networks and contagion," *American Economic Review*, vol. 104, no. 10, pp. 3115–3153, 2014.

[20] L. P. Hansen and T. J. Sargent, "Fragile beliefs and the price of uncertainty," *Quantitative Economics*, vol. 1, no. 1, pp. 129–162, 2010.

[21] P. Gai, A. Haldane, and S. Kapadia, "Complexity, concentration and contagion," *Journal of Monetary Economics*, vol. 58, no. 5, pp. 453–470, 2011.

[22] V. V. Acharya and D. Skeie, "A model of liquidity hoarding and term premia in inter-bank markets," *Journal of Monetary Economics*, vol. 58, no. 5, pp. 436–447, 2011.

[23] M. K. Brunnermeier and L. H. Pedersen, "Predatory trading," *Journal of Finance*, vol. 60, no. 4, pp. 1825–1863, 2005.

[24] D. W. Diamond and R. G. Rajan, "Fear of fire sales, illiquidity seeking, and credit freezes," *The Quarterly Journal of Economics*, vol. 126, no. 2, pp. 557–591, 2011.

[25] R. J. Caballero and A. Krishnamurthy, "Collective risk management in a flight to quality episode," *Journal of Finance*, vol. 63, no. 5, pp. 2195–2230, 2008.

[26] B. R. Routledge and S. E. Zin, "Model uncertainty and liquidity," *Review of Economic Dynamics*, vol. 12, no. 4, pp. 543–566, 2009.

[27] A. Zawadowski, "Interwoven lending, uncertainty, and liquidity hoarding: Boston University School of Management Research Paper No. 2011–13," *SSRN Electronic Journal*, 2011.

[28] R. J. Caballero and A. Simsek, "Fire sales in a model of complexity," *Journal of Finance*, vol. 68, no. 6, pp. 2549–2587, 2013.

[29] M. Boss, H. Elsinger, M. Summer, and S. Thurner, "Network topology of the interbank market," *Quantitative Finance*, vol. 4, no. 6, pp. 677–684, 2004.

[30] R. Cifuentes, G. Ferrucci, and H. S. Shin, "Liquidity risk and contagion," *Journal of the European Economic Association*, vol. 3, no. 2-3, pp. 556–566, 2005.

[31] Bank of England, *Instruments of Macroprudential Policy (Bank of England Discussion Paper)*, London, England, 2011 http://scholar.google.com/scholar?hl=en&btnG=Search&q=intitle:Instruments+of+macroprudential+policy#3.

[32] F. Bräuning and F. Fecht, "Relationship lending in the interbank market and the price of liquidity," *Review of Finance*, vol. 21, no. 1, pp. 33–75, 2016.

[33] A. Temizsoy, G. Iori, and G. Montes-Rojas, "The role of bank relationships in the interbank market," *Journal of Economic Dynamics and Control*, vol. 59, pp. 118–141, 2015.

[34] A. W. Lo, "Complexity, concentration and contagion: a comment," *Journal of Monetary Economics*, vol. 58, no. 5, pp. 471–479, 2011.

[35] S. Davidovic, *The ecology of financial markets: from analogy to application, [Ph.D. thesis]*, Humboldt University of Berlin, 2016.

Hindawi
Complexity
Volume 2019, Article ID 7643685, 23 pages
https://doi.org/10.1155/2019/7643685

Research Article

A Case Study of Complex Policy Design: The Systems Engineering Approach

Shqipe Buzuku,[1] **Javier Farfan**,[2] **Kari Harmaa**,[3] **Andrzej Kraslawski**,[1,4] **and Tuomo Kässi**[1]

[1]*School of Engineering Science, Industrial Engineering and Management, Lappeenranta University of Technology, P.O. Box 20, FI-53851, Lappeenranta, Finland*
[2]*School of Energy Systems, Lappeenranta University of Technology, P.O. Box 20, FI-53851, Lappeenranta, Finland*
[3]*Pöyry Finland Oy, P.O. Box 4, FI-01621, Vantaa, Finland*
[4]*Faculty of Process and Environmental Engineering, Lodz University of Technology, Poland*

Correspondence should be addressed to Shqipe Buzuku; shqipe.buzuku@lut.fi

Received 19 April 2018; Revised 8 August 2018; Accepted 13 September 2018; Published 3 January 2019

Guest Editor: Bernardo A. Furtado

Design, structure, modelling, and analysis of complex systems can significantly benefit from a systematic approach. One way to address a complex system using a systematic approach is to combine creative and analytical methods, such as general morphological analysis and design structure matrix. The aim is to propose a framework to address complex systems in two stages: first, formulation and generation of alternatives through general morphological analysis, and second, improvement and integration with design structure matrix for sequence optimization and cluster analysis. Moreover, general morphological analysis is further optimized through a novel sensitivity analysis approach reducing up to 80% the iteration time. The proposed approach is showcased in a case study of sustainable policy formulation for a wastewater treatment plant at a pulp and paper industry in Brazil. The results show that it is possible to generate a solution space that highlights the best possible combinations of the given alternatives while also providing an optimal sequence and grouping for an optimized implementation. The paper contributes to the field of conceptual modelling by offering a systematic approach to integrate sustainability.

1. Introduction

1.1. Problem Definition. In recent years, tackling problems regarding water management policies has received considerable attention. Water management has embedded within complex issues such as industrial wastewater treatment, water protection and conservation, and rational water use. The growing complexity of water management systems generates increasingly difficult policy design problems [1]. Policy design is rather complex due to the increasing amount of policy measures available for addressing the problems of a system. Consequently, policy problems are often defined as "messy" [2] or "wicked" problems [3–5]. Rittel and Webber [5] stated that "Wicket Problems do not have an enumerable set of potential solutions." (Rittel and Weber [5] coin the term wicked problems, assigned ten characteristics to wicked problems, which have been further generalized by Conklin [4], to the following six characteristics: (1) Wicked problems cannot be understood until a solution has been developed. (2) Wicked problems have no stopping rules. (3) Solutions to wicked problems are not right or wrong they are better or worse. (4) Every wicked problem is essentially unique and novel. (5) Every solution to a wicked problem is a one-shot operation. (6) Wicked problems have no given alternative solutions.)

The term wicked problems is used to describe social complex problems that are multidimensional and possess nonquantifiable aspects, where causal modelling and simulation are not appropriate [6]. For example, in the industry sector, decision-making commonly includes complex problems associated with conflicting performance objectives and contradictory requirements, for which the application of traditional multiobjective decision-making approaches shows evident limitations [7]. In addition, there is a growing need to create a systematic approach to facilitate the definition

and structuring of relevant problems and the decision-making process among stakeholders for transparent decision support systems (DSS). A major challenge facing industrial organizations is "green policy" design and upgrading of policy measures [8]. This problem involves, for instance, knowledge management specialists, planners, and decision-makers, who all work with rather complex issues [9]. The task thus requires the creation of new tools to improve the understanding of the complexities embedded in tackling problems and reaching optimal solutions. Engineers frequently use analytical modelling methods to aid understanding the operation of complex systems, to gauge to what extent systems achieve overall their goals and targets, and how the systems in question can be improved [10].

Many traditional quantitative methods have been explored for dealing with multiobjective decision-making in the public policy realm. For example, Philips et al. [11] presented his work by applying quality function deployment (QFD) techniques to product design procedures, which are used to formulate annual policy, leading to designs that better reflect customer's requirements. Yeomans [12] applied the coevolutionary simulation-optimization modelling-to-generate-alternatives approach in order to generate effectively multiple solutions for environmental policy formulation to municipal solid waste management. Taeihagh et al. [13] proposed a network-centric policy design approach based on network analysis and ranking of alternatives [14], often done using multicriteria decision analysis (MCDA) methods, to select and analyse the internal properties of proposed measures and their interactions in the transport policy domain.

Moreover, Taeihagh et al. [15] argued that agent-based modelling could be used for the analysis of different combinations of policy measures, aiming at generating policy packages to advance sustainable transportation. However, traditional multiobjective optimization and simulation are not sufficient to tackle complex multidimensional and non-quantifiable problems. Besides, in the case of physical sciences and economics, research in the policy domain mostly focuses on the simulation and optimization of policy alternatives, instead of their synthesis and generation. Therefore, there is still a need for further research to enhance the capacity of policy generation and evaluation of this approach. Consequently, a systematic approach is imperative, particularly when addressing complex problems, such as socio-technical systems.

The analysis of complex sociotechnical systems, like a set of policies, is a challenging problem [16]. The first reason is that the elements contained in the systems are often non-quantifiable, as they are of social, political, or cognitive nature. The second reason is that uncertainties characteristic for such complex problems are hard to be represented. The emerging need of specific tools, techniques, and systems to aid the generation, management, and enforcement of effective policies requires research on the suitability of various approaches in the context of policy instruments' choice [17].

Various problem-structuring methods (PSMs) have been presented in the literature. Among them, general morphological analysis (GMA) [6, 18, 19] is presented as a promising method for the generation of new concepts and finding the best solution. In principle, GMA is based on the "divide and conquer technique" [20], which tackles a problem using two basic approaches: "analysis" and "synthesis"—referred to as "the basic method for developing scientific models" by Ritchey [21]. In addition, some authors propose different creative methods to be used in early conceptual design to support new concept of business model creation [22] and new concept of selection [23, 24]. GMA, as a creative method, has been used widely and tested in various domains such as policy planning and scenario development [25], strategic foresight [26], technology forecasting [27–29], and idea creation [30–32]. The core objective of GMA is to structure and investigate the behaviour and solutions among stakeholders.

From the engineering design perspective, different matrix-based tools and techniques have been developed also to aid the design process. An example of this is design structure matrix (DSM), typically used to map, visualize, and analyse the dependences and relationships among properties of a product or activities in the design process. In other words, by applying the DSM, these dependencies can be reorganized so the process can be optimized.

However, no work has been done before on combining GMA with DSM. Furthermore, to the authors' best knowledge, GMA and cross-consistency assessment- (CCA-) based optimization techniques have not yet considered optimization of the iteration process through sensitivity analysis, nor have DSM-based simulation techniques been considered for reworking of policy improvements in areas such as policy design and policy measures. Therefore, the presented research fills this specific gap in the policy design literature.

In this paper, a case study example of the Brazilian pulp and paper mill industry related to wastewater treatment plant (WWTP) is shown in order to display the empirical use of the presented model for policy formulation. Brazil is an upper middle-income country with a fast-rising economy [33], which may eventually develop into the world's leading producer of pulp and paper. The pulp and paper industry is tackling a wide array of implementation of sustainability trends, such as (but not limited to) conservation and rational water use; development of sustainability measures for industrial wastewater treatment and water systems management becomes necessary. It is evident that there is a large potential for the adoption of sustainable practices in the pulp and paper industry in a developing country's environment.

1.2. Motivation and Purpose of the Study. This research is motivated by an attempt to assess the potential of integrating modelling methods in such a way that the integrated approach supports complex problem solving for policy design in water management systems, while supporting sustainable development in the organization.

The aim of this paper is to develop a systematic approach for generating, designing, and improving policy alternatives using a computational methodology that integrates the diverse modelling techniques of GMA, sensitivity analysis, and DSM. The specific goal is to interlink GMA and DSM as potential problem structuring methods to tackle wicked problems and to support the decision-making of policy formulation in complex systems.

By developing a systematic approach, it is possible to (a) better understand the problem structure and to decompose it into subproblems, (b) improve analysis and optimization of the environmental policy formulation process through sensitivity analysis, and (c) decrease the time required for problem analysis and problem solving. The proposed methodology will enable decision-makers and managers to generate and explore various alternatives and to promote combination of alternatives, their optimization, and improvement of the policy development process. The proposed approach includes sensitivity analysis for optimization of the iteration process of GMA, clustering analysis through DSM, and development of the configurations of policy measures included in the policy package so that they match the objectives of the organization.

This study focuses on specific objectives as the following: the first objective is to generate policy measures or alternatives using GMA for policy design. While policy measures can be extracted from literature or derived from an expert's opinions, different organizations can have different perceptions of policy measures to create a coherent policy. Therefore, the same policy measures may have different effects for different companies, industries, or countries. Hence, the reduced set of viable policy measures is then the subject of analysis by the stakeholders involved in policy formulation in various organizations. The second objective is to evaluate and improve the policy measures or alternatives. In light of this, a DSM approach is used for identifying the relationships of the policy measures in a qualitative manner [34].

The significance of this work, and how it differs from the other works, is that decision-makers can utilize the full potential of the proposed systematic approach to tackle wicked problems in the context of policy design and meet the companies' objective for increasing their sustainability scores.

The results are expected to further promote the use of modelling methods for policy formulation in sectors such as energy, environment, healthcare, food, water, and e-waste, in which modelling can be systematically employed as part of a DSS. Consequently, the work facilitates greater use of modelling procedures to address complex problems such as those found in environmental policy management.

1.3. Structure of the Paper. The remainder of this paper is organized as follows: first, key considerations in policy design, particularly sustainable policy design and problems of policy formulation, are briefly described. Then, the main features of the design modelling approaches used, GMA and DSM, are presented. The following section discusses the proposed approach integrating GMA, optimized through sensitivity analysis, with DSM. To illustrate the approach considered in this work, an illustrative case study is described. The findings are then revealed, and the paper concludes with the main results, discussion of contributions, limitations, and suggestions for future work.

2. Literature Review

When attempting to improve policy in areas such as water management and to mitigate problems arising from the complexity of modern sociotechnical systems, adoption of a systematic approach has become an essential part of policy design. Further consideration is given to the selection of appropriate methods, software, and tools to support understanding of the complexities embedded. For instance, Taeihagh et al. [32] developed a novel framework and design support system to ease and accelerate the design of polices to meet the CO_2 emission targets for the transport sector in the UK. The proposed method and computer implementation constituted the first general approach towards the development of a branch of computer-based systems that support environmental policy. Moreover, policy design research can be divided into several categories dealing with different types of objectives and criteria in public environmental policy formulation [13, 35].

In recent years, the topic of policy portfolios [36] and policy mix formulation has evolved from definition of problems via exploration of basic concepts, to development of policy measures and classification of policy measures into categories, and further to analysis of descriptive and normative scenarios. In addition, Howlett [17] defined that the nature of the criteria for effective policy design is a significant aspect in order to ensure the portfolio's effectiveness to policy formulation and its implementation. Current research trends focus on advanced and practical levels of design policies, which involve greater integration of the related concepts and methodologies [13, 15, 35, 37]. The perception of policy design has evolved from a "single-target/single-tool" approach towards a "multitarget/multitool" approach in order to tackle complex policy design [13, 37, 38].

Earlier work on policy design and policy formulation methodology was based on dynamic modelling approaches such as network analysis [13], agent-based modelling (ABM) [39], and multiple criteria decision analysis (MCDA) [40]. Taeihagh et al. [15] introduced ABM to formulation of transport policies and proposed a systematic approach for use of a virtual environment for the exploration and analysis of different configurations of policy measures. Furthermore, Wollmann and Steiner [41] proposed a model for strategic decision processes that takes into account the influence of limited rationality and organizational policy. The proposed model combines strategic decision-making, complex adaptive system (CAS), and the mathematical techniques analytic network process (ANP) and linear programming (LP) [41]. Also, complexity theory has been proposed as a complexity-driven approach to assist project management in decision-making, while defining complexity-based criteria [42].

2.1. Sustainable Policy Design. A policy is generally described using natural language, which makes it difficult to understand, especially when they occasionally compete and conflict with each other. According to Pohl [43], a "policy" is a "principle or guideline for action in a specific context" and "policy design" is "the task of selecting policy components and formulating overall policy." Policy formulation is defined as "the development of effective and acceptable courses of action to address items on the policy agenda" [8, 44]. Policy design involves the deliberate and conscious attempt to define policy goals and connect them to instruments or tools

expected to realise those objectives, and to formulate a policy, there is a need to follow a policy agenda that meets the standards and regulations [44]. It can be considered one of the most difficult parts of the policy design process [35], and it underlies the explicit actions of policy design [8, 44]. The development of successful and acceptable policy is usually a manual task involving various activities and several teams with different objectives and criteria for policy success [32].

Within environmental management studies, environmental policies have traditionally been defined as policies that assist successful decision-making to meet the requirements of sustainable development [45, 46]. To meet the criteria of sustainable development, policies have to address the legal, technological, social, economic, and environmental aspects.

Policy formulation and policy implementation are two very different activities. Policy formulation is an important phase devoted to "generating options about what to do about a public problem" ([47], p. 29) and is inherent to most, if not all, forms of policymaking [48]. The agenda-setting step in the policy cycle focuses on identifying *where* to go, while the policy formulation step focuses on *how* to get there [49]. Considering policy formulation as "a process of identifying and addressing possible solutions to policy problems or, to put it another way, exploring the various options or alternatives available for addressing a problem," then the development or use of *policy formulation tools* becomes a vital part of the policy formulation process ([47], p. 30). It is difficult to conceive, or properly study, policy formulation without thinking in terms of tools. According to Dunn [50], these are tools for forecasting and exploring future problems, tools for identifying and recommending policy options, and tools for exploring problem structuring.

Some of the most traditionally used approaches are cost-benefit analysis (CBA) and MCDA in the environmental policy domain [13, 51]. However, CBA has significant drawbacks such as difficulty to measure social costs and benefits, conflict between wellbeing and financial benefits, and assigning controversial monetary value to human displacement and human life [52]. Likewise, the methods that fall under the MCDA umbrella struggle to manage decisions with inherent uncertainty, are unable to address dependencies, are prone to manipulation, and face difficulties with problem structuring [51].

Currently, decisions on what to include in policies (their synthesis) is done manually, and considering the size of the space of alternative policies, a large portion of the design space is left unexplored [32]. Moreover, Howlett and Mukherjee [53] and Chindarkar et al. [54] conducted research on comparative policy analysis, making an emphasis on effectiveness and impact of managing the policy processes [55]. Furthermore, the knowledge and objectives of the different stakeholders involved (e.g., central authority, local authority, employees, company/industry, NGOs, local residents, and researchers from academia) may differ greatly and bring dissimilar attitudes to proposed solutions, which influences the decision-making process [56].

Therefore, traditional approaches to policymaking are not well suited for solving today's complex problems. A comprehensive methodology that supports the identification, design, modelling, and evaluation of policies to tackle complex problems is still missing, and existing methodologies and frameworks to tackle the complexity of sustainable policy formulation in organizations are not fully developed. Therefore, alternative approaches and tools are required in order to overcome the limitations of traditional approaches. One possibility is to integrate multiple methods based on policy design concepts. For example, GMA and DSM are both modelling methods that may be systematically employed in a DSS [57], and this paper proposes combining GMA and DSM to facilitate modelling procedures in problem solving of complex problems such as those found in sustainable policy design.

2.2. The Complex Problem of Policy Formulation. For policy design in general, and water management in particular, decisions regarding measures for inclusion in policy require exploration of a large pool of policy options as part of the problem space [32, 53, 54]. Furthermore, designing a sustainable policy is rather complex because of the influence of different factors—technical, legal, and ethical—an example of this is management of industrial wastewaters. These factors require the adoption of a large number of different policy measures. In addition, the multiple tasks to be carried out require input from multidisciplinary teams [58]; hence, policymakers still struggle with evaluating and improving the outcome of the policy design process.

To date, a single universal approach for sustainable policy design in wastewater treatment does not exist, and suitable policy measures need to be identified based on the organization's strategy and environmental aims. Utilization of a systematic approach to generate alternative policies by using GMA [18] and DSM [34] will help decision-makers to accelerate and improve policymaking. Furthermore, incorporating and adopting the diverse preferences from various interest groups and stakeholders will improve the policy's performance and acceptance.

While identification of feasible policy measures for complex industrial wastewater treatments can be obtained from literature review and expert inputs, it is worth noting that different companies might have different views regarding suitable policy measures. This paper considers well-defined policy measurement criteria such as legal, technical, financial, social, and environmental measures taking into consideration sustainability development goals (SDGs) [59].

The selection of policy measures to be considered is complex for several reasons. Under a simplified setting, a local company requiring an environmental permit for the installation of a WWTP would require a local permit, following regulations familiar to local experts. However, in this case study, the complexity is largely increased because it is an international company with headquarters in Finland, seeking an environmental permit for a WWTP in Brazil; thus, it requires following protocols from the company and from the location. Moreover, the specific location of the case study WWTP is next to a river separating two states, so both the regional regulation (Instituto Ambiental do Pantanal/Secretaria do Empresas y Meio Ambiente) IMAP/SEMA

Table 1: List of policy measures designed for an industrial WWTP in Brazil.

Parameters	Values
Implementation of legislation (legal aspects)	Requirements in Brazilian Environmental Law, Conama 20 EU-BAT Bref (2001) sectorial Best Available Technology listing and associated limit values
	World Bank/IFC EHS sectorial (pulp and paper industry) environmental performance limit values
	Parana river water quality requirements (Class II) local limit values for river water
	Saving water target to diminish water footprint of the mill
	Storm water control to prevent accidental impacts to the river water
Water/effluent quality (technical aspects)	Determination of the appropriate treated effluent quality for physical and chemical parameters
	Determination of the concentrations of organic compounds, nutrients, and absorbable organic halogens in treated effluent
	Determination of the organic compounds, nutrient, and absorbable organic halogens in treated effluent and temperature increase no more than 3°C at mixing zone in the river
	Determination of dissolved oxygen and turbidity in the river water
	Separation of uncontaminated and contaminated storm water to keep hydraulic design of the effluent treatment plant reasonable
Effluent treatment plant (financial aspects)	Implement specific process equipment (cooling towers) to achieve legal requirements
	Choose those pulping processes (oxygen delignification, ECF bleaching) to give lower emissions
	Choose an effluent treatment process (extended aeration) to give good treated effluent quality and less sludge production
	Create water management system for clean used process water (collecting, controlling, and recycling used clean waters)
	Storm water management by sectorial storage lagoons
Capacity building (social aspects)	Training courses for all at the site for safety measures
	Environmental training events for workers of production departments
	Detailed training of operators of effluent treatment plant concerning process, incomes and outcomes, and equipment and their control and maintenance
Monitoring (environmental aspects)	Preparation and implementation of an integrated program for monitoring river water
	Preparation and implementation of an internal program for monitoring untreated effluent for process upsets
	Preparation and implementation of an integrated program for monitoring treated effluent
	Preparation and implementation of an integrated program for monitoring groundwater at the production area
	Preparation and implementation of an integrated program for monitoring groundwater as a part of monitoring system of the landfill
	Preparation and implementation of an internal program for monitoring outlet of storm water lagoons

WWTP: wastewater treatment plant; BAT: best available technology; EFC: elemental chlorine free; Conama: Conselho Nacional do Meio Ambiente.

and the federal regulation (Conselho Nacional do Meio Ambiente) Conama 20 apply in this case. The selected 25 policy measures were thus extracted by the experts from the aforementioned regulations. This selection and the first stages of GMA analysis happened during the first day of the workshop.

The policy measures were divided into five categories based on sustainability criteria (law-related policy measures, technical-related measures, financial-related measures, social-related measures, and environmental measures) using expert evaluation (data collection and data analysis details are given in Sections 4.3.1 and 4.3.2). The specific policy measures identified are provided in Table 1.

2.3. GMA for Generating Alternatives. GMA was originally introduced by Zwicky [19] and Zwicky and Wilson [60] as a "non-quantified modelling method for identifying, structuring and studying complex problems." The GMA approach has been widely used for identification of possible combinations of problem variables in many different disciplines [29]. The GMA technique is a decomposition method that splits a system into subsystems with their parameters and selects the most valuable alternatives [61].

GMA enables problem representations using a group of parameters, which can take any of several values [62]. The identified conditions in each dimension can be combined to derive all the possible alternatives that can solve the problem. Yoon and Park [29] recommend a group of 5–7 experienced experts representing different aspects of the problem to be resolved. The specific way of application of GMA for this study is described further in Section 3.3.

The basic procedure of GMA is described by Wissema [63] as follows. First, in the morphological field, the system is decomposed into multiple parameters [29]. In the next step, the possible alternatives or values in each parameter are identified. The values for each parameter should be defined in a mutually exclusive manner [62]. A morphology matrix is then built with the obtained parameters and values. The whole system should be described in the morphology matrix as comprehensively as possible [23]. Finally, solutions are obtained by combining the values of each parameter. The number of possible solutions can be calculated by multiplying the number of values in each parameter [24].

GMA has been applied to a wide variety of fields and contexts like jet and rocket propulsion systems [19] and

computer-aided design modelling [64]. The research reported by Belaziz et al. [65] was aimed at simplifying computer-aided design model modification by integrating GMA into the design process. In addition, Ölvander et al. [66] proposed a computerized optimization framework for the morphological matrix applied to aircraft conceptual design. In the field of scenario space modelling and development, the research conducted by Coyle and McGlone [67], Coyle and Yong [68], Voros [69], and Johansen [25] confirmed that GMA has been extensively applied. Also, as reported by Haydo [70], GMA has been successfully applied to optimize complex industrial operation scenarios.

According to Ritchey [71], GMA is a "basic, conceptual (non-quantified) modelling method that can be compared with a wide range of other scientific modelling methods, including System Dynamics Modelling (SDM), Bayesian Networks (BN) and various forms of 'influence diagrams.'" Furthermore, Duczynski [72] developed general morphological analysis for application in organizational design and transformation, while Zeiler [73] used the morphology in conceptual building design. In addition, Buzuku and Kraslawski [74] proposed applying GMA to policy formulation for wastewater treatment. In particular, GMA provides a possibility for generating unexpected combinations of policy measures [18].

The morphological approach has several advantages, including discovery of the total set of new configurations and its suitability for utilization with work groups. The use of work groups increases scientific communication and enables integration of state-of-the-art knowledge from practitioners of different fields. However, the main advantage of this method lies in its ability to structure models for complex problems in a nonquantitative manner through systematic procedures [75]. Another significant advantage is the method's ability to provide an auditable trail [76].

Drawbacks of the method include issues with vague formulation, static analysis modelling of the values, nontreatment of variable interdependencies, and insufficient screening and selection of satisfactory combinations. Thus, the approach demonstrates limitations in defining and evaluating different parameters against each other and generating conditions within the problem space. Therefore, GMA requires support from other processes.

The most promising method in this context is DSM [34], which can describe different methods and enables visualization, analysis, and improvement of partial solutions. In this study, GMA is integrated with DSM as a screening, visualizing, and development tool [57].

2.4. DSM for Analysing and Improving Alternatives. DSM is an often-used efficient method for analysing complex systems by enabling the overview of the system and the interdependencies of the system's elements, developed by [77, 78]. DSM provides the representation of a complex system and the dependencies, relationships, and interactions of the system's elements [34]. In addition, DSM breaks down a complex problem into smaller problems and enables deconstruction of the organizational and functional components of a system by eliciting the relationship between components in ways that make trade-off analyses more understandable and manageable [10].

DSM generates a directed graph that describes relationships between elements or parameters for the design, management, and optimization of a complex system, organization member assignments, and activity scheduling, concentrated in an n by n adjacency matrix. A system of n number of parameters is represented by DSM in an n by n matrix, in which the elements are listed in the exact same order from 1 to n both in rows and in columns, where the dependencies between the parameters can be marked. When parameter a depends on parameter b, then the cell a, b (where both a and $b < n$) is marked in a binary manner with any symbol, e.g., with a "●." In case of no dependency, the cell a, b is left empty [79]. When the parameters are listed in the DSM in their execution order, if cell a, b is marked under the diagonal of the DSM matrix, it represents an output (or "outwards" relationship) from parameter a to b. However, if a cell a, b is marked over the diagonal of the matrix, it means that cell a receives feedback from b (a depends on b).

DSM has been used in the past to solve complex decision-making problems and to improve organizational performance [77]. Therefore, DSM is considered a consolidated approach to manage complexity [9, 80–82]. DSM is known as a contemporary method that has been used for modelling and managing complex systems in engineering [83, 84], design planning [85], and operation management [86]. According to Eppinger and Browning [34], DSM can be applied to public policy because public policy and social systems are multidimensional and uncertain complex problems. Environmental policy design and its implementation is a complex problem comprising a mix of numerous types of policy instruments or measures [87, 88] adopted by a range of organizations and stakeholder participation [89].

DSM visualization provides the advantage of compactness and clear representation of essential patterns. On the other hand, as the graph becomes larger with nodes and edges, it can become difficult to understand the overall network representation. Moreover, DSM further provides the option to improve the system's structure using matrix-based analysis techniques. Although the policy measures are listed as sequential steps in the DSM, the modelling process requires attention to their dependencies, interdependencies, and relations. The main advantage of DSM lies in combining elements/components in a novel and creative integrative framework, displaying, analysing, and improving satisfactory combinations. It is thus suitable for evaluating policy measures extracted from GMA ([90], 2015; [34]).

3. Methodology

In this section, the overall process mechanics of the two-part approach for generating and improving policy measures with experts' evaluation feedback is described. The experts interact with the stakeholders outside the frame of this study. The methodology proposes an integrative framework for designing a sustainable policy that helps to improve policy

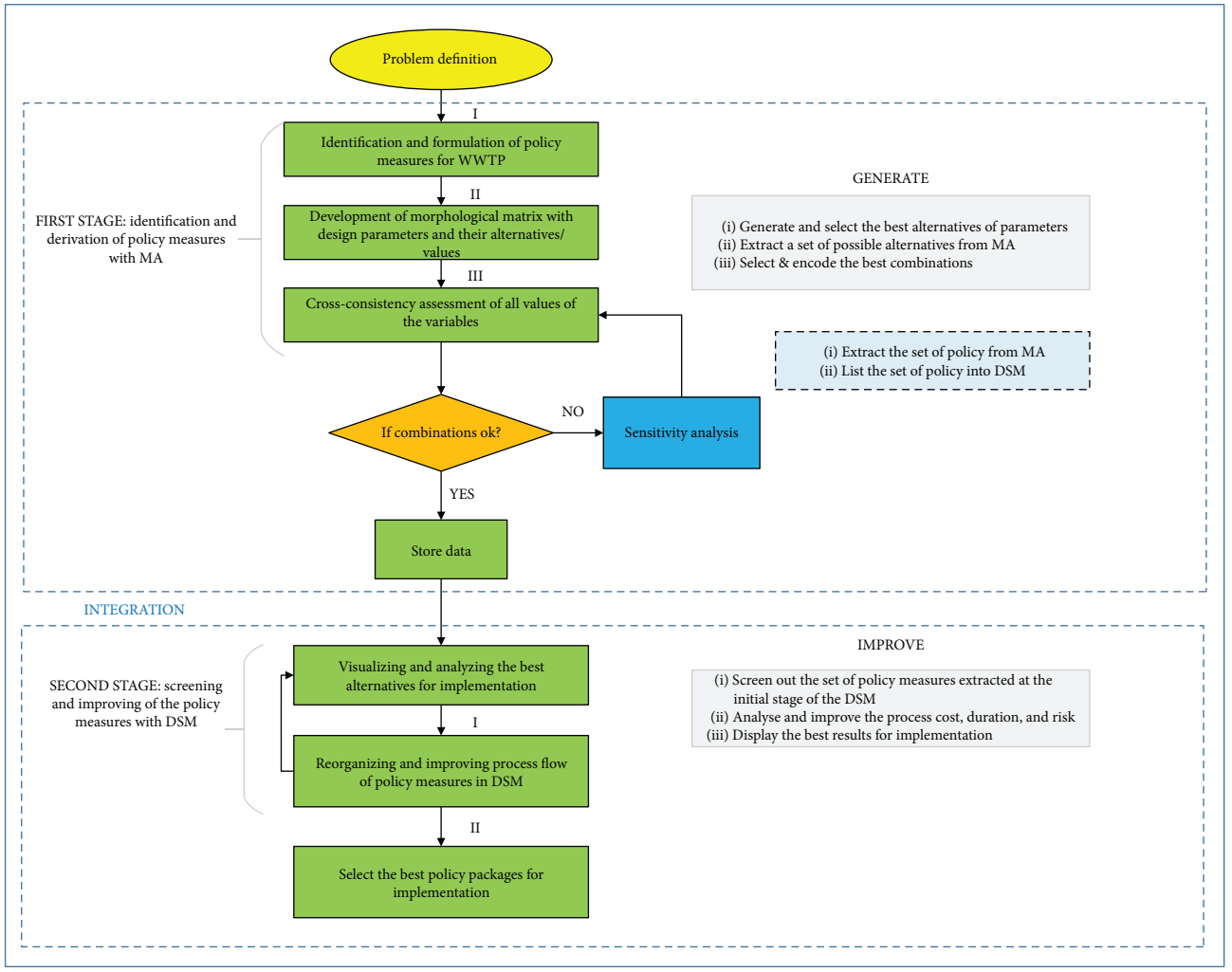

Figure 1: Process overview of the integrated general morphological analysis (GMA) and design structure matrix (DSM) method.

effectiveness, as well as a comprehensive system structure for sustainable management in organizations.

The proposed methodology is aimed at improving the impact of the different policy measures generated during policy formulation in the early stages of conceptual project design, when decision-makers start to set up and embed design solutions into problem-solving systems. During policy formulation, decision-makers and designers often model a functional net using a graph structure [91, 92], and they may produce a set of partial solutions (or alternatives) for a specific type of problem. Each set of partial solutions is interpreted and strengthened by a DSM in order to better manage the complexity and, subsequently, to aid reasoning about the sustainability of environmental policy formulation concepts.

Among alternative approaches, the choice had to be made between a matrix representation or a network representation. Network representations are often simple and easier to read; however, they are not as flexible for increasing or decreasing in size and can become almost impossible to follow if the number of inputs is very large. Ultimately, a matrix representation was chosen because a matrix can easily be rearranged, it is able to show parameters for a rather large number of inputs, it can always be expanded [93], and it can be mathematically analysed (in this case with sensitivity analysis), among other advantages.

The experts are quite familiar with the sustainability assessment of relevant environmental policy measure concepts, a very relevant factor for the evaluation of policy measures. The policy concepts themselves belong to either corporate, regional, or federal environmental regulations, and they were designed and assessed by their corresponding institutions. Moreover, the experts made it a specific goal to include or consider the most relevant policy measures that tackle the social, environmental, and technoeconomic requirements of a sustainable endeavour. Therefore, the sustainability assessment of the policy measures is not addressed in this paper.

3.1. Proposed Approach. This section examines the overall process and gives a brief explanation of each stage. The proposed new approach is divided into two stages (Figure 1):

(1) Generation: identification and derivation of policy measures with GMA, and optimization of GMA through sensitivity analysis

(2) Improvement: screening and improving the policy measures with DSM

The first stage comprises generation of sustainable policy measures or alternatives using GMA for policy design. The identification and derivation of policy measures with GMA entails the following steps: (a) identification and formulation of a library of policy measures, (b) development of a morphological matrix by building dimensions (parameters) and generating policy measures as named alternatives (values), (c) assessment of the consistency of all possible combinations of parameter values, and (d) optimization through sensitivity analysis.

The second stage consists of searching for improvements to the policy measures or alternatives using DSM clustering. Since GMA is not able to investigate and explore the dependence and interdependence relationships between policy measures or alternatives, the DSM approach is employed to analyse and better manage the policy design structure, thereby supporting the identification of the interdependencies and improving the overall process flow. The obtained results and the reduced sets of policy measures are analysed by the experts involved in policy formulation.

3.2. Problem Definition. The full complexity of water management systems and policy structure is difficult for managers and designers to understand using traditional modes of analysis. Hence, this study develops a systematic approach for exploring, generating, and improving the policy alternatives using GMA, sensitivity analysis, and DSM to identify, optimize, and improve the policy measure interactions of the system. The approach will enable managers and designers of water management systems and WWTPs to tackle the system's complexity more wisely, a topic increasingly relevant in developing regions like China and Brazil [94, 95].

The environmental policies, provided in Table 1, are virtually represented in the GMA matrix so that it is possible to analyse their effectiveness in the specific project. The main target of the resulting designed policies is the improvement of the quality of measures and their performance. In an optimal scenario, all stakeholders are involved.

3.3. First Stage: Generation of Policy Measures with GMA. The first stage of GMA comprises the identification and formulation of a set of specific policy measures related to the problem, in the illustrative case in this work, an industrial WWTP. The policy measures identified were categorized by experts into economic, environmental, social, and technical sustainability criteria, using the GMA tool to build the morphological box during the workshop.

There are multiple ways to conduct GMA. Zec and Matthes [96] elaborated in four possible ways the application of the method: (1) alone, (2) in a relaxed manner with like-minded individuals, (3) in a workshop with experts and stakeholders, and (4) in a distributed manner through remote online workshops. The third option, a workshop with experts and stakeholders further detailed by [97], is the approach chosen for this study. The exercise for evaluation of policy measures and classification into the categories they belong was performed with preprinted forms, white paper, and pen from a groupthink of experts in a workshop, described in Section 4.3.1.

The identification and derivation of policy measures with GMA comprise the following steps: (a) identification and formulation of a library of policy measures and classification by the experts, (b) development of a morphological matrix by building dimensions (parameters) and generating policy measures as named alternatives (values), (c) assessment of the consistency of all possible combinations of parameter values, and (d) optimization through sensitivity analysis for subsequent iterations.

The experience and knowledge of experts from a wide range of disciplines is required to develop the morphological matrix. A methodology to gather and organize this knowledge through a participatory dialogue process, such as a structured workshop, is also required. Approaches like CCA, invented by Ritchey [18], allow the number of alternatives and iterations to be reduced significantly. The reduced set is then the subject of process analysis by the experts involved in the policy formulation. The role of expert opinion and experts' participation in decision-making is crucial for environmental policy management [98].

The set of combinations of alternatives obtained from the morphological matrix is analysed, screened, and improved with DSM. The consistency of combinations is evaluated by exploring all possible combinations of the morphology matrix via CCA. The sensitivity analysis step proposed in this work can further optimize the CCA process and highlight the most relevant parameters.

3.4. Second Stage: Improvement of Policy Measures with DSM. The use of DSM enables visualization of the dependencies and interdependencies of combinations of variables and values. Once optimal combinations of policy measures have been derived using GMA (described in detail in Section 4.1.3), it is necessary to integrate them into the DSM for screening and improvement of the policy measures and to select the most suitable set of policy measures for implementation. More specifically, the proposed approach (shown in Figure 1) can be used to observe the complex interactions and improve the understanding of underlying relationships between the policy measures. To perform the analysis of the policy correlations, this study suggests visualizing and identifying of the best alternatives for implementation, and reorganizing and improving the process flow of policy measures with DSM. Since results extracted from GMA are used as input to DSM, the DSM process can be applied from the analysis step.

4. Illustrative Case Example

The proposed approach is illustrated with a case study for the construction, operation, and maintenance of a large industrial WWTP. This case study was conducted with an

international engineering and consultant firm, hereafter, called "company A." Due to increasing pressure for sustainable wastewater treatment globally, particularly in the pulp and paper industry [95], there is a significant need to design and formulate sustainable policies that promise sustainable solutions for wastewater treatment facilities. The new plant was planned to become an integrated facility in the wastewater sector through collaboration with the local community, potential stakeholders, and enhanced engagement with the company in the region. Industrial water systems management, including wastewater treatment systems, is a complex problem that requires expert's knowledge and years of experience in a wide range of disciplines. The decision-making can be classified as a complex problem, the activity is situated on a federal river forming a border area between the states of Mato Grosso do Sul and Sao Paulo, Brazil, and there are large capital and operational costs involved, as well as involvements of multistakeholders. A relevant factor in the development of sustainability measures for industrial wastewater treatment is the participation of stakeholders from various levels and functional areas of society [99] involved in the process.

Some policy measures are of interest to both internal and external stakeholders. This interest generates a "policy measure-stakeholder" relationship. In the case in progress, stakeholders are

(i) *Central Authority*. The central authority commonly is responsible of taking care for the issues that could destabilise the relationships between the present stakeholders and any other possible conflict on stage.

(ii) *Local Authority*. The local authorities have interest in the issues related to the legal aspects of operation of the plant on their territory.

(iii) *Employees*. The main interest of the employees is in environmental aspects, health and safety (EHS) issues including training programs, and workshops aiming for the better quality of the working conditions.

(iv) *Company/Industry*. For the company or industry, and more specifically its top management level authority, the key interests are the health and safety conditions for the staff, aiming for the high quality of the work environment and other social aspects that are directly linked to the plant operation and its maintenance, and of course to profit from the activity.

(v) *NGOs*. The civil society and NGOs have interest in the topics that are related to broader perspectives, which target environmental, advocatory, and other social issues, e.g., human work rights.

(vi) *Local Residents*. Local residents and the community around usually have interest in the public services provided by WWTP, and having impact on their healthy lifestyle.

(vii) *Researchers from Academia*. The researchers from the academia typically have high interests in providing conditions for collecting data and sampling analysis for scientific research purposes.

The stakeholders provide feedback to the experts. Afterwards, with the acquired knowledge, the experts participated in the workshop. In this way, stakeholders remotely influence the decision-making in this case study. Nor were the experts or the stakeholders previously familiar with the methods used for this research.

4.1. Identification and Derivation of Policy Measures with GMA. The empirical knowledge of experts, stakeholders, and members of society is required to compile available environmental measures [99]. The compiled set of environmental policy measures has been generated as described in Section 2.2, and the selection is depicted in Section 3. Measures may be regulatory (e.g., legislation on emission limits), economic (e.g., taxation of wastewater discharge), technical (e.g., investment in best available technology), social (e.g., increase in social awareness), and environmental (e.g., decrease in pollutant concentrations in effluents). The measures can be quantitative or qualitative and affect all aspects of sustainability. The policy measures can be ranked by effectiveness, time of deployment, cost, risk, uncertainty, technical complexity, social acceptability, and organizational complexity, depending on whether the policy is meant to adapt or mitigate, or whether it is designed to reward improvements or punish noncompliance.

4.1.1. Development of the Morphological Matrix with Design Parameters or Dimensions and Alternatives or Values. After problem definition, the main task in GMA is generation of a morphological field comprising the most relevant dimensions (parameters) and production of design alternatives (values) for each parameter. Therefore, policy measures must be identified and formulated in accordance with sustainability criteria to achieve the environmental targets. These sustainability criteria are considered the constituents of the WWTP and can be used as the morphological field's parameters. The parameters of the morphological field are set in the header in the spreadsheet table, and their generated values are placed under each parameter. Figure 2 shows the development of a morphological field with five parameters—legal, financial, technical, social, and environmental dimensions—and their values. The specific WWTP parameters in the case study are written in bold. For each parameter, possible values are defined in their respective column.

Table 2 illustrates the combination of different design parameters and values obtained using the principles proposed by Zwicky [19] and Ritchey [18], and Table 1 shows the list of policy measures designed for the industrial WWTP in Brazil considered in the case study. The combination of policy measures of one partial solution from every column leads to the overall principle solution or policy formulation concept. Since GMA has many iterative steps [100], modifications in the morphological matrix can occur throughout the process [62]; thus, the proposed GMA optimization

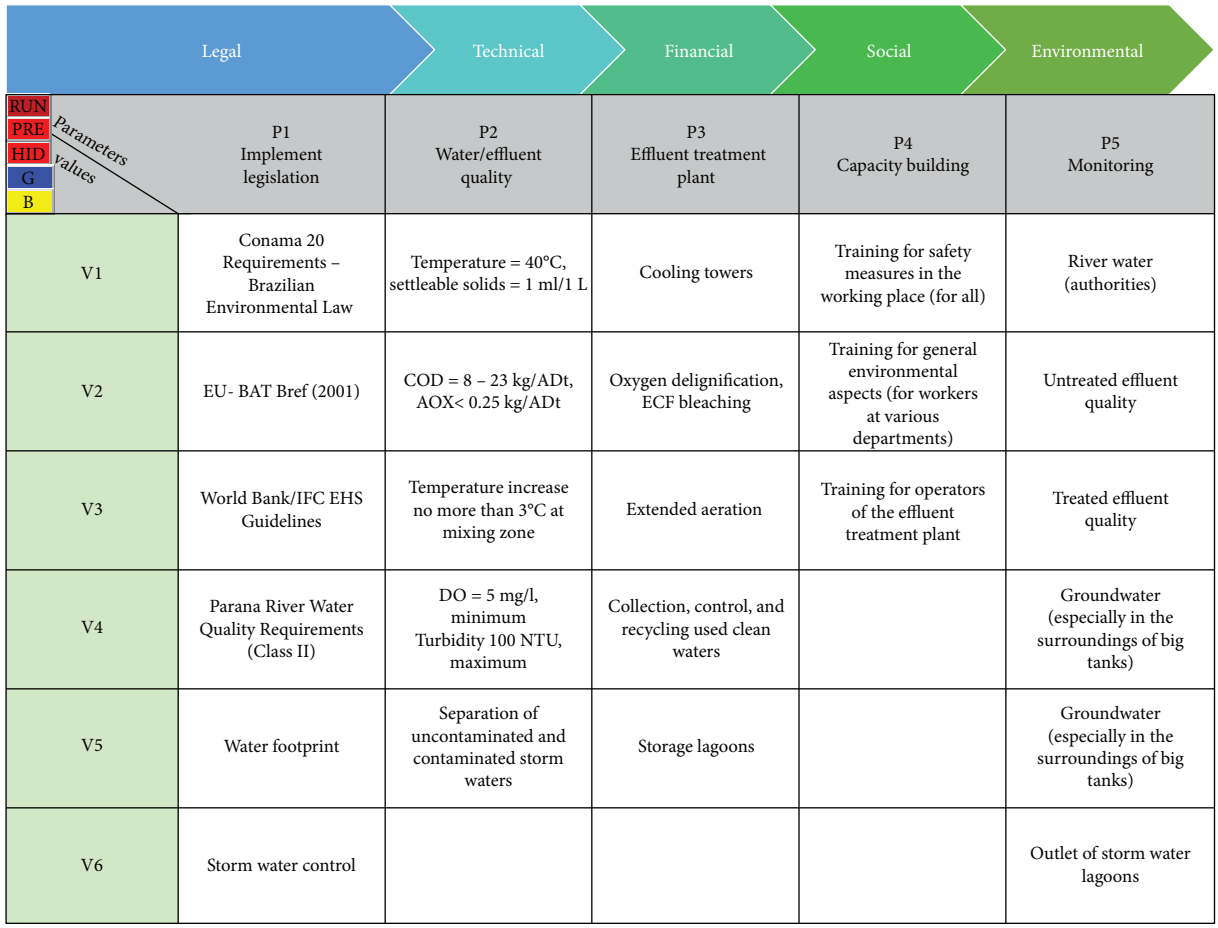

Figure 2: Development of the morphological field with five parameters and their values. BAT: Best Available Technology; IFC EHS: International Finance Corporation Environmental Health and Safety; COD: chemical oxygen demand; ADt: air dry tons; AOX: absorbable halogen compounds; DO: dissolved oxygen concentration; NTU: nephelometric turbidity unit; ECF: elemental chlorine free; Conama: Conselho Nacional do Meio Ambiente.

Table 2: Combinations of parameters/values.

Values	Parameters				
	*P*1	*P*2	*P*3	*P*4	*P*5
*V*1	*P*1*V*1	*P*2*V*1	*P*3*V*1	*P*4*V*1	*P*5*V*1
*V*2	*P*1*V*2	*P*2*V*2	*P*3*V*2	*P*4*V*2	*P*5*V*2
*V*3	*P*1*V*3	*P*2*V*3	*P*3*V*3	*P*4*V*3	*P*5*V*3
*V*4	*P*1*V*4	*P*2*V*4	*P*3*V*4		*P*5*V*4
*V*5	*P*1*V*5	*P*2*V*5	*P*3*V*5		*P*5*V*5
*V*6	*P*1*V*6				*P*5*V*6

through sensitivity analysis described in Section 5.2 is thus justified.

The GMA approach outlined in this study may take practitioners and researchers up to several weeks to execute. The actual time and effort required for any GMA application depends on several factors, including familiarity with the process being modelled and the degree of difficulty of information gathering and defining and evaluating parameters and values. In the case of parameter building, Geum and Park [30] and Geum et al. [101] suggest that an expert-based qualitative approach provides more powerful results. Although some GMA models can be extracted automatically from project management models, most entail the direct involvement of experts.

4.1.2. Assessment of Consistent Combinations of All Parameter Values. CCA, proposed by Ritchey [18], can be used to evaluate all the feasible combinations of parameter values. CCA assesses compatibility for each value via pairwise comparison (one pairwise value from one column or morphological class with another pairwise value from another morphological class). To reduce the problem space, decision elements are compared pairwise by experts (further detailed in Section 4.3.1) in terms of their control criteria. Each condition is compared with another condition and evaluated for internal consistency, which is noted as their assigned values in a matrix called the CCA matrix.

Figure 3 presents the CCA matrix for this study. The assessment of the conditions, done by the experts, is carried out by evaluating the level of compatibility of two parameters during a workshop described in Section 4.3.1. For example, the question is asked to the experts: is P_1, V_4 "Parana River

	Temperature = 40°C, settleable solids = 1 ml/1 l	COD = 8 – 23 kg/ADt, AOX< 0.25 kg/ADt	Temperature increase no more than 3°C at mixing zone	DO = 5 mg/l, minimum turbidity 100 NTU, maximum	Separation of uncontaminated and contaminated storm waters	Cooling towers	Oxygen delignification, ECF bleaching	Extended aeration	Collecting, control, recycling used clean waters	Storage lagoons	Training for safety measures in the working place (for all)	Training for general environmental aspects (for workers at various departments)	Training for operators of the effluent treatment plant	River water (authorities)	Untreated effluent quality	Treated effluent quality	Groundwater (especially in the surroundings of big tanks)	Groundwater (especially in the surroundings of big tanks)	Outlet of storm water lagoons
Conama 20 Requirements Brazilian Environmental Law	3	1	2	3	1	3	1	1	2	3	1	3	3	3	2	3	3	3	3
EU- BAT Bref (2001)	1	3	1	2	1	1	3	3	2	1	1	1	3	1	3	3	1	1	3
World Bank/IFC EHS Guidelines	3	3	3	2	1	3	3	3	1	1	3	3	3	1	3	3	1	1	3
Parana River Water Quality Requirements (Class II)	1	2	3	3	3	2	1	2	3	3	1	3	3	3	2	3	3	3	3
Water footprint	1	2	1	1	3	3	1	1	3	3	1	2	2	1	3	1	1	1	1
Storm water control	1	2	1	1	3	1	1	1	3	3	1	2	2	3	1	1	1	1	3
Temperature = 40°C, Settleable solids = 1 ml/1 l						3	1	1	2	2	1	1	3	3	2	3	1	3	3
COD = 8 – 23 kg/ADt, AOX< 0.25 kg/ADt						1	3	3	2	2	1	2	3	2	2	3	1	1	3
Temperature increase no more than 3°C at mixing zone						3	1	1	1	3	3	3	3	3	1	3	1	1	1
DO = 5 mg/l, minimum turbidity 100 NTU, maximum						2	2	3	1	2	2	2	2	3	2	3	1	2	3
Separation of uncontaminated and contaminated storm waters						1	1	1	3	3	2	3	3	3	1	1	3	3	3
Cooling towers											3	3	3	3	3	3	1	1	1
Oxygen delignification, ECF bleaching											3	2	1	1	3	3	1	1	1
Extended aeration											1	2	3	1	1	3	1	1	1
Collection, control, recycling used clean waters											1	3	3	3	2	2	2	2	3
Storage lagoons											1	3	3	3	2	2	2	2	3
Training for safety measures in the working place (for all)														2	1	2	3	2	1
Training for general environmental aspects (for workers at various departments)														2	2	2	3	3	2
Training for operators of the Effluent treatment														3	3	3	2	2	3

Figure 3: Cross-consistency assessment matrix.

water quality requirements (Class II)" compatible, neutral, or incompatible with P_3, V_1 "Cooling towers"? When compatible, the interaction is evaluated as optimal (marked with a 3 in the CCA matrix). When neutral, the interaction is evaluated as acceptable (marked with 2). Finally, if the interaction is incompatible, it is evaluated as nonacceptable (marked with a 1). The values assigned in the example shown in Figure 3 are 122 (49.4% of the total) optimal combinations, 27 (11%) acceptable, and 98 (39.6%) nonacceptable.

The CCA matrix reduces the total problem space to an internally consistent solution space. Furthermore, the CCA in a multidimensional matrix is then reduced to find an approximation for an optimal solution. A "parameter-block" is the two-dimensional block of cross-referenced values between two parameters and their values, and it is shown as alternate white and shaded blocks in Figure 3. In some cases, all the cells in the blocks will have optimal combinations, meaning that these two blocks do not constrain each other. If more than half of the block contains optimal values, the solution space will not reduce significantly. On the other hand, if more than half of the values are nonacceptable (or even fewer if distributed in large consecutive arrays), then it will risk choking the model, and no solution will be possible. Poorly and nonadequately defined parameters make the process difficult to manage, and parameters and values must be reformulated in such cases. This process can prove rather time-consuming, and consequently, it is very important to optimize the iteration. This work proposes the use of sensitivity analysis to address this issue.

Table 3: Detailed description of the parameters that combine optimally pairwise in policy 1.

Compared parameter		Combines optimally pairwise with values	
Parameter	Description	Values	Description
$P1V1$	Requirements in Brazilian Environmental Law, Conama 20	$P2V1$	Determination of the appropriate treated effluent quality for physical and chemical parameters
		$P2V4$	Determination of dissolved oxygen and turbidity in the river water
		$P3V1$	Implement specific process equipment (cooling towers) to achieve legal requirements
		$P3V5$	Storm water management by sectorial storage lagoons
		$P4V2$	Environmental training events for workers of production departments
		$P4V3$	Detailed training of operators of effluent treatment plant concerning process, incomes and outcomes, and equipment and their control and maintenance
		$P5V1$	Preparation and implementation of an integrated program for monitoring river water
		$P5V3$	Preparation and implementation of an integrated program for monitoring treated effluent
		$P5V4$	Preparation and implementation of an integrated program for monitoring groundwater at the production area
		$P5V5$	Preparation and implementation of an integrated program for monitoring groundwater as a part of monitoring system of the landfill
		$P5V6$	Preparation and implementation of an internal program for monitoring outlet of storm water lagoons

4.1.3. Generation of New Sets of Policy Concepts. As seen in Figure 3, some parameter values have more optimal combinations than others do. The parameters with the highest amount of optimal combinations share between each other nineteen satisfactory sets of policy concepts. These identified parameters are grouped into three clusters or packages as a final result of GMA. The mentioned clusters are the following.

The parameter value $P1, V1$ "requirements in Brazilian environmental law, Conama 20," seen in the first row of Figure 3, has eleven optimal pairwise combinations with other values. The parameter values $P2V1$, $P2V4$, $P3V1$, $P3V5$, $P4V2$, $P4V3$, $P5V1$, $P5V3$, $P5V4$, $P5V5$, and $P5V6$, described in detail in Table 3, optimally combine pairwise with $P1, V1$. For simplicity purposes, $P1, V1$ and its optimal combinations will be referred from this point onwards as policy 1. The high level of compatibility of policy 1 makes it relevant for WWTP and therefore is selected for further analysis in the next stages.

Likewise, the parameter value $P1, V3$ "World Bank/IFC EHS Guidelines" (third row in Figure 3) combines optimally pairwise with twelve parameter values. The parameters combining in an optimal manner with $P1, V3$ are $P2V1$, $P2V2$, $P2V3$, $P3V1$, $P3V2$, $P3V3$, $P4V1$, $P4V2$, $P4V3$, $P5V2$, $P5V3$, and $P5V6$, and from now on will be referred to as policy 2. Just as in the case of policy 1, the high compatibility of this cluster makes it relevant for further analysis and thus is selected to be taken to the next stages.

In the same manner, the parameter value $P1, V4$ "Parana River Water Quality Requirements (Class II)" (fourth row of Figure 3) combines optimally pairwise with twelve parameter values. The parameter values mentioned are $P2V3$, $P2V4$, $P2V5$, $P3V4$, $P3V5$, $P4V2$, $P4V3$, $P5V1$, $P5V3$, $P5V4$, $P5V5$, and $P5V6$ and henceforth constitute policy 3. Just like in the previous two cases, the high compatibility of policy 3 is enough to be taken for further analysis in the following steps. A list of the parameter values and the amount of optimal pairwise combinations is shown in Figure 4, where policies 1, 2, and 3 are highlighted in yellow.

After defining and identifying the packages or clusters (policies 1, 2, and 3), these clusters are presented back to the experts for their judgment and approval according to their experience. Figures 5 and 6 show the selection of the parameter values that generate optimal combinations of polices 1, 2, and 3 for new WWTP according to environmental experts' judgments. All the parameter values that present optimal combinations to either/or policies 1, 2, and 3 seen in Figure 4 are listed in Figure 5.

To facilitate visualization of the correlation between the policies and their optimal parameter values, a colour code was created and assigned to each policy, further improving understanding of the interactions of the parameter values contained within policies 1, 2, and 3. Red, blue, and green were assigned to the parameter values that combine optimally with policies 1, 2, and 3, respectively. When policies 1 and 2 share a common optimal parameter value combination, it is marked as magenta. Similarly, when policies 2 and 3 share optimal parameter values, it is marked as cyan, and for policies 1 and 3, yellow is used. When policies 1, 2, and 3 share a common parameter value, it is marked as purple.

Figure 6 shows the constitution of the policy packages and the parameter values they have in common. For example, policy package 1 is constituted by 11 parameter values, all of which appear common to either or both policy packages 2 and 3 as indicated in Figure 6. Likewise, it can be seen also for policy packages 2 and 3.

4.2. Optimization through Sensitivity Analysis. In order to establish a relationship between parameters to evaluate

P1,V1	P2,V1	P2,V4	P3,V1	P3,V5	P4,V2	P4,V3	P5,V1	P5,V3	P5,V4	P5,V5	P5,V6	
P1,V2	P2,V2	P3,V2	P3,V3	P4,V3	P5,V2	P5,V3	P5,V6					
P1,V3	P2,V1	P2,V2	P2,V3	P3,V1	P3,V2	P3,V3	P4,V1	P4,V2	P4,V3	P5,V2	P5,V3	P5,V6
P1,V4	P2,V3	P2,V4	P2,V5	P3,V4	P3,V5	P4,V2	P4,V3	P5,V1	P5,V3	P5,V4	P5,V5	P5,V6
P1,V5	P2,V5	P3,V1	P3,V4	P3,V5	P5,V2							
P1,V6	P2,V5	P3,V4	P3,V5	P5,V1	P5,V6							
P2,V1	P3,V1	P4,V3	P5,V1	P5,V3	P5,V5	P5,V6						
P2,V2	P3,V2	P3,V3	P4,V3	P5,V3	P5,V6							
P2,V3	P3,V1	P3,V5	P4,V1	P4,V2	P4,V3	P5,V1	P5,V3					
P2,V4	P3,V3	P5,V1	P5,V3	P5,V6								
P2,V5	P3,V4	P3,V5	P4,V2	P4,V3	P5,V1	P5,V4	P5,V5	P5,V6				
P3,V1	P4,V1	P4,V2	P4,V3	P5,V1	P5,V2	P5,V3						
P3,V2	P4,V1	P5,V2	P5,V3									
P3,V3	P4,V3	P5,V3										
P3,V4	P4,V2	P4,V3	P5,V1	P5,V6								
P3,V5	P4,V2	P4,V3	P5,V1	P5,V6								
P4,V1	P5,V4											
P4,V2	P5,V4	P5,V5										
P4,V3	P5,V1	P5,V2	P5,V3	P5,V6								

Figure 4: Results of cross-consistency assessment, highlighting the parameter values that generate optimal pairwise combinations.

P2,V1	Physical and chemical parameters	Policy 1
P2,V2	Organic compounds and nutrients	Policy 2
P2,V3	Temperature in the mixing zone	Policy 3
P2,V4	Dissolved oxygen and turbidity in the river	Policy 1 + 2
P2,V5	Separation of uncontaminated storm water	Policy 2 + 3
P3,V1	Implement specific equipement cooling tower	Policy 1 + 3
P3,V2	Oxygen delignification, EFC bleaching	Policy 1 + 2 + 3
P3,V3	Extended aeration for effluent quality	
P3,V4	Create water management system for clean used process water	
P3,V5	Storm water control to prevent accidents	
P4,V1	Training for safety measures	
P4,V2	Environmental training for production department	
P4,V3	Detailed training of operators of effluent treatment plant	
P5,V1	Integrated program for monitoring river water	
P5,V2	Integrated program for monitoring untreated effluent	
P5,V3	Integrated program for monitoring treated effluent	
P5,V4	Integrated program for monitoring groundwater	
P5,V5	Integrated program for monitoring system of the landfill	
P5,V6	Program for monitoring outlet of storm water lagoons	

Figure 5: Colour-coded selection of the parameter values that generate optimal combinations for policies 1, 2, and 3, for a new WWTP.

the compatibility of different combinations, meetings and workshops must be organized with experts and iterations must be repeatedly executed to achieve a desirable solution. A desirable solution requires that the number of optimal combinations is big enough to provide options for the decision-makers to analyse, but not so big that the decision-making within the optimal solutions becomes complex again. According to [102], there are no strictly defined higher or lower limits to how extensive the share of optimal combinations from the total possible combinations should be, as it is very case-specific. Nevertheless, the share of optimal combinations typically lies between 1% and 10% of total possible combinations.

However, gathering the required experts for the amount of time required to go through several iterations may be a difficult starting point for the project. In order to optimize the iteration process, a sensitivity analysis can be executed across the CCA matrix (Figure 3) to reduce the number of relationships to evaluate, thus reducing the time required for evaluative iteration.

Figure 7 shows the proportional distribution for pairwise combinations of the values shown in Figure 3. The ratio of combinations of Figure 7 is calculated by obtaining the amount of combinations of value exclusivity and in each cell (containing a parameter value) of the CCA matrix, then aggregating them row-wise. Value exclusivity in this case

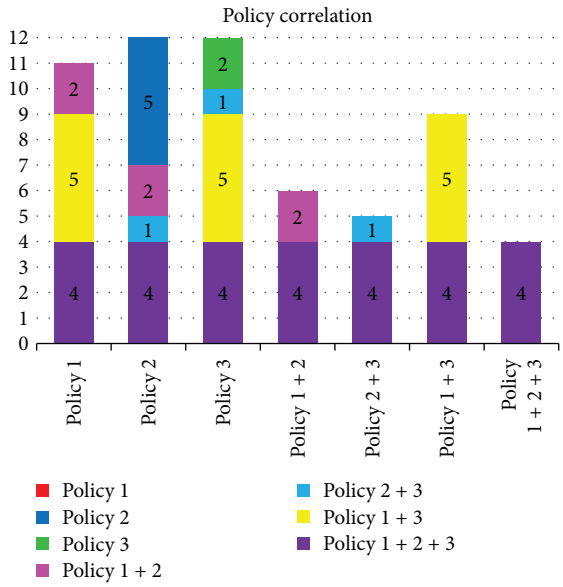

Figure 6: Overall view of the parameter value combinations and their correlations among policies 1, 2, and 3.

means that cells of value 3 are combined exclusively with other cells of value 3 in the matrix. While in theory the method can combine parameters of all values, an optimal solution in principle (and for this case) is considered to be constituted by a combination of optimal parameter values.

For the CCA matrix presented in Figure 3, the optimal combinations of parameter values of the cell $P1, V3$–$P2, V1$ presented in Figure 8(b) is larger than $P1, V1$–$P2V1$ shown in Figure 8(a) and $P1, V4$–$P2, V3$ in Figure 8(c). Simultaneously, the aforementioned cells have more optimal correlations than, for example, $P1, V4$–$P2, V1$. Based on this premise, by analysing the CCA matrix (Figure 3), it is possible to extract the number of correlations of every combination pair (cell) and then compare the number of correlations to the total number of combinations of a selected value, which is done taking into account each parameter value (optimal, acceptable, or nonacceptable) separately.

All cells in a row are then aggregated according to their parameter value, as shown in Figure 7. For example, the row $P1V1$ adds up to 286 unique combinations when only cells of the same value are combined, out of which 226 are of optimal value, 30 are acceptable, and 30 are nonacceptable (or 79.2% optimal, 10.4% acceptable, and 10.4% nonacceptable).

Figure 7 also shows the total distribution of optimal, acceptable, and nonacceptable combinations (right-hand column). The high number of optimal combinations (49.1%) means further iterations can be considered to revaluate the combinations if considered necessary, in order to reduce the number of optimal combinations. The proposed sensitivity analysis is aimed at identifying the effect of modifying the dependence value between two specific elements in the total number of solutions. As expected, some combinations are strongly correlated to more parameters than others.

Figure 8 shows all the unique optimal combinations (value 3) present for the cells: (a) $P1V1$–$P2V1$ (20 combinations), (b) $P1V3$–$P2V1$ (27 combinations), and (c) $P1V4$–$P2V3$ (20 combinations). The rows containing these cells ($P1, V1$, $P1V3$, and $P1, V4$, respectively) contain the largest number of optimal correlations, both in relative numbers (columns 1, 3, and 4 of Figure 7) and in absolute numbers. Therefore, these rows, and the elements contained within them, are thus selected to be the policy packages *policy 1*, *policy 2*, and *policy 3*, chosen for analysis in DSM. The large number of optimal combinations present in these specific cells highlights the potential impact of modifying the values in such cells whilst, for example, changing the value of cell $P1V5$–$P2V5$ could only reduce 4 optimal combinations from the solution space.

Figure 8 shows also something that is not so clear at first glance. For every additional parameter block, the amount of combinations increases in an exponential manner, at a ratio proportional to the number of parameter values of that parameter block. Likewise, the larger number of parameter values within a parameter block would increase significantly the amount of combinations. For example, if an additional parameter block of the size of $P4$ (the smallest parameter block from the example as visible in Figure 2) is added, the total possible amount of combinations would triple. This can potentially become rather problematic, as the evaluation time and computational time can eventually increment beyond the capabilities of a workshop. Hence, decreasing the amount of parameter pairs to be evaluated becomes paramount, opening a gap for sensitivity analysis to select only the most influential values to evaluate, based on their relative weight, thus decreasing dramatically the array of evaluations to be made by experts in one iteration.

Equation 1 shows the method used to calculate the relative weight (RW). The RW of an element pair in respect to the total combinations "K" (subsequent combinations calculated as indicated by Ritchey [18] and exemplified in Figure 8) of value "x" (1, 2, or 3 in the example) in position (a, b) (where "a" is the row and "b" is the column of the CCA matrix). In the equation, "R" stands for the total number of rows; "C" stands for the total number of columns. For example, if the number of combinations of value "3" of the element pair (3,4) is seven $(K_{3(3,4)} = 7)$ and the total of subsequent combinations of all element pairs is one thousand, $\Sigma^R\Sigma^C K_{3(i,j)} = 1000$ = then the $\mathrm{RW}_{3(3,4)}$ would be 0.7%

$$\mathrm{RW}x_{(a,b)} = \frac{Kx_{(a,b)}}{\sum_{i=1}^{R}\sum_{j=1}^{C} Kx_{(i,j)}}. \quad (1)$$

Figure 9 shows the relative weight of all element pairs, colour-coded to facilitate the evaluation; the colour coding and sensitivity limits assigned for this case are also shown.

Once the RW of all element pairs has been analysed and classified, it is possible to focus on reiteration of the combinations with higher RW value. By revaluating only the combinations with higher RW, shown in red and yellow in Figure 9, up to 54.4% of the total combinations can be shifted from one value to another. This means reducing the optimal solution space by revaluating and possibly changing a combination value from optimal to acceptable, for example, while reiterating only 45 out of the 247 element pairs that

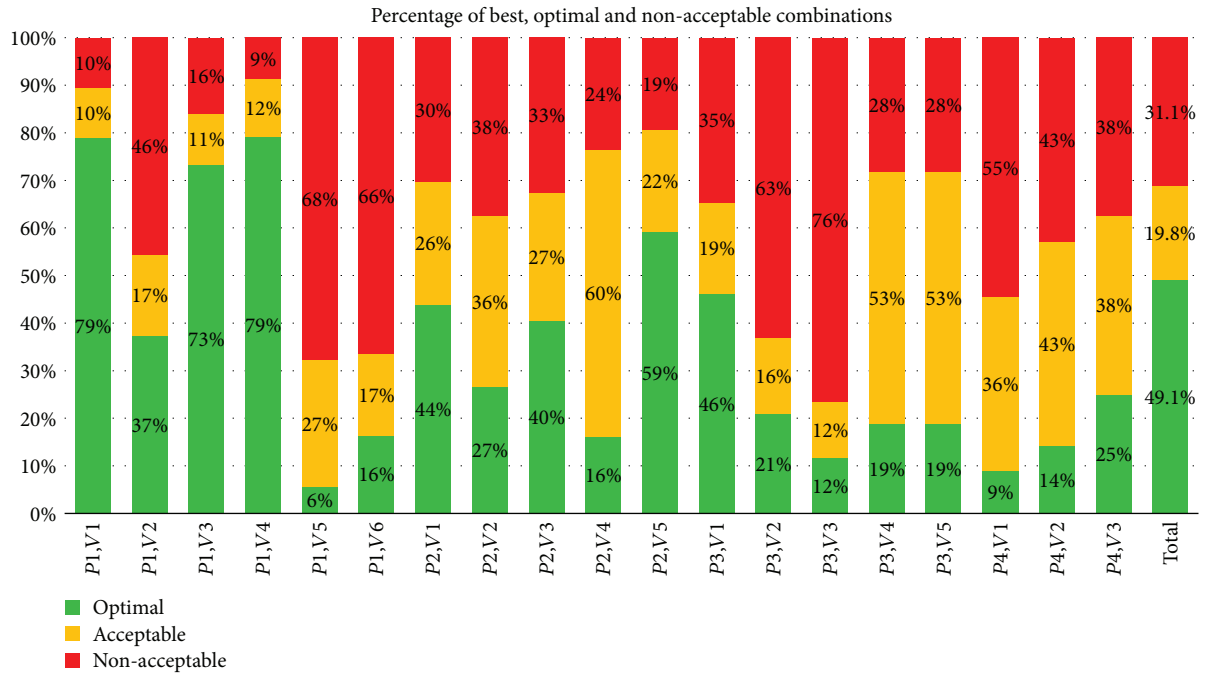

Figure 7: Percentage of optimal, acceptable, and non-acceptable pairwise combinations of parameter values.

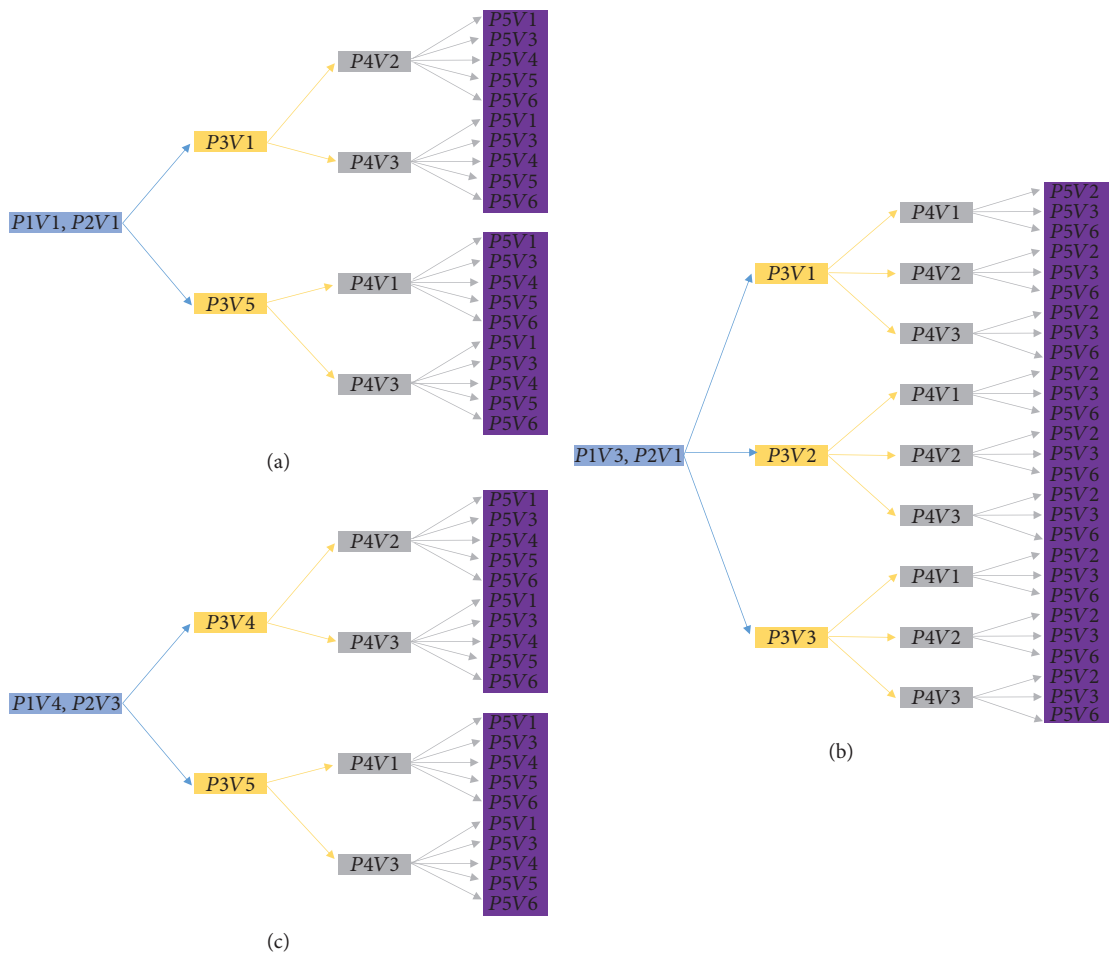

Figure 8: Example of unique optimal combinations for the cells associated with policies 1, 2, and 3 (a, b, and c, respectively).

	P2,V1	P2,V2	P2,V3	P2,V4	P2,V5	P3,V1	P3,V2	P3,V3	P3,V4	P3,V5	P4,V1	P4,V2	P4,V3	P5,V1	P5,V2	P5,V3	P5,V4	P5,V5	P5,V6
P1,V1	0.8%	0.0%	0.0%	0.8%	0.0%	1.0%	0.0%	0.0%	0.0%	1.1%	0.0%	1.3%	1.5%	1.3%	0.0%	1.3%	0.8%	0.8%	1.3%
P1,V2	0.0%	0.6%	0.0%	0.0%	0.0%	0.0%	0.6%	0.7%	0.0%	0.0%	0.0%	0.0%	1.3%	0.0%	0.7%	1.2%	0.0%	0.0%	1.2%
P1,V3	0.8%	0.8%	0.8%	0.0%	0.0%	1.0%	0.9%	1.0%	0.0%	0.0%	1.0%	1.3%	1.5%	0.0%	1.1%	1.5%	0.0%	0.0%	1.5%
P1,V4	0.0%	0.0%	0.8%	0.8%	0.9%	0.0%	0.0%	0.0%	1.0%	1.2%	0.0%	1.3%	1.6%	1.3%	0.0%	1.4%	0.9%	0.9%	1.4%
P1,V5	0.0%	0.0%	0.0%	0.0%	0.5%	0.5%	0.0%	0.0%	0.4%	0.6%	0.0%	0.0%	0.0%	0.0%	0.7%	0.0%	0.0%	0.0%	0.0%
P1,V6	0.0%	0.0%	0.0%	0.0%	0.5%	0.0%	0.0%	0.0%	0.5%	0.7%	0.0%	0.0%	0.0%	1.0%	0.0%	0.0%	0.0%	0.0%	1.1%
P2,V1						0.7%	0.0%	0.0%	0.0%	0.0%	0.0%	0.0%	1.3%	1.0%	0.0%	1.0%	0.0%	0.5%	1.0%
P2,V2						0.0%	0.4%	0.5%	0.0%	0.0%	0.0%	0.0%	1.2%	0.0%	0.0%	1.1%	0.0%	0.0%	1.1%
P2,V3						0.7%	0.0%	0.0%	0.0%	0.8%	0.6%	0.9%	1.2%	1.2%	0.0%	1.3%	0.0%	0.0%	0.0%
P2,V4						0.0%	0.0%	0.5%	0.0%	0.0%	0.0%	0.0%	0.0%	0.9%	0.0%	1.0%	0.0%	0.0%	1.0%
P2,V5						0.0%	0.0%	0.0%	0.7%	0.9%	0.0%	1.0%	1.3%	1.1%	0.0%	0.0%	0.7%	0.7%	1.2%
P3,V1											0.5%	0.8%	1.1%	1.0%	0.7%	1.1%	0.0%	0.0%	0.0%
P3,V2											0.4%	0.0%	0.0%	0.0%	0.5%	1.0%	0.0%	0.0%	0.0%
P3,V3											0.0%	0.0%	1.0%	0.0%	0.0%	1.0%	0.0%	0.0%	0.0%
P3,V4											0.0%	0.7%	1.0%	1.0%	0.0%	0.0%	0.0%	0.0%	1.0%
P3,V5											0.0%	0.7%	1.0%	1.0%	0.0%	0.0%	0.0%	0.0%	1.0%
P4,V1														0.0%	0.0%	0.0%	0.4%	0.0%	0.0%
P4,V2														0.0%	0.0%	0.0%	0.4%	0.4%	0.0%
P4,V3														0.8%	0.4%	0.9%	0.0%	0.0%	0.9%

Red = RW > 1.5%
Yellow = 1% < RW < 1.5%
Blue = 0.5% < RW < 1%
Green = RW < 0.5%

Figure 9: Colour-coded relative weight (RW) of element pairs.

would otherwise be reiterated. Assuming that experts would require roughly the same amount of time to evaluate every combination, conducting a sensitivity analysis in the iteration presented reduced the iteration evaluation time by 81.8% in this example. To put it into numbers, the evaluation of 247 combinations was done in this case during a two-day workshop described in general by Ritchey [97] and in detail for the case study in Section 4.3.1. Considering 9 hours of work (9 hours of the second long day of the workshop) to evaluate 247 combinations, the time required breaks down into an average of one combination evaluated every 2.2 minutes, a rather fast pace due to the high level of experience from the experts. If only 45 element pairs are evaluated instead (as in the example), the whole iteration process would take approximately one hour and forty minutes.

Using the same method, a reduction of over 80% was achieved in all iteration experiments carried out with different variants of the values obtained from the case study. Moreover, through a 1000 loop of randomly generated values for a matrix of the same dimensions (done in Matlab R 2014), it was found that by revaluating an average of 12.2% of total cells, the solution space can be reduced by an average of 73.9%. Even considering that the revaluation of certain combinations would require a different amount of time from others, still by the amount of revaluations avoided the potential for optimization is clear.

Furthermore, sensitivity analysis can be done automatically and directly from the CCA matrix with a spreadsheet to further optimize the iteration process, since the RW of different combinations would change after every iteration and single-cell evaluation.

4.3. Screening and Improving Policy Measures with DSM

4.3.1. Data Collection. The data gathering was conducted through a workshop preceded by interviews and feedback with design practitioners at the industry. In the case under study, a two-day workshop was organized with the participation of 10 experts. Among them were designers and engineers, planners, and managers of different backgrounds and specializations, to rate the sets of policy measures and derive suggestions for reorganization and improvements. Their opinions serve as the directional driver for policy design improvements towards sustainability. The formed group of experts consisted of one general manager, one financial manager, one environmental manager, two heads of manufacturing plants, two designers, two senior planning analysts, and one IT manager with more than 10 years' experience. None of the workshop participants had any experience with GMA or CCA. One of the advantages of carrying out the evaluations of the pairwise combinations in a group of 10 experts is that the individual bias factor is greatly mitigated, as the ultimate chosen value is the result of a consensus between all 10 experts.

The workshop held had a duration of two full days in March 2016 at the facilities of the engineering and consulting company. The experts in the workshop participated on a voluntary basis. A meeting face-face with the experts for a detailed interview preceded the workshop. The abovementioned participants selected and evaluated 25 policy measures for the WWTP during the workshop. The first author was personally involved in the workshop as a facilitator and direct observer and responsible for data collecting. The interviews and the workshop were not recorded due to confidentiality, but detailed notes of answers and their feedback were taken from each interview and the workshop. The members of the multidisciplinary group validated the policy measures for further procedures of the DSM model.

4.3.2. Data Analysis. When building a DSM model, the main objectives are to highlight the information in the system's elements, to design parameters or elements that can be represented in a DSM graph, and to identify the intensity of

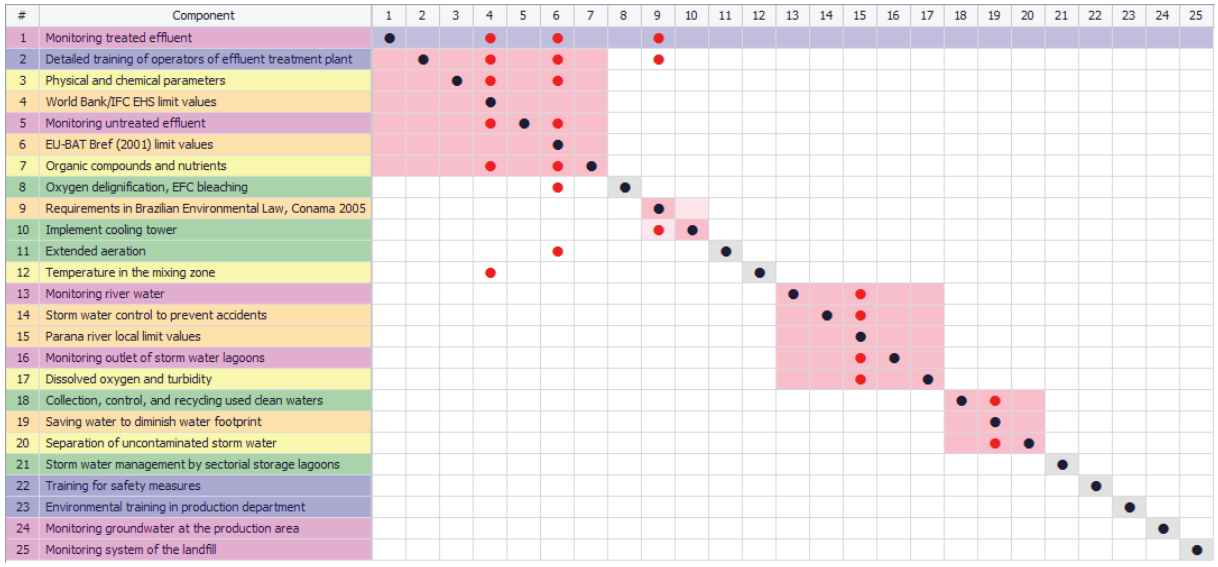

Figure 10: WWTP policy formulation process DSM after partitioning.

dependencies among those elements. A dataset involving policies 1, 2, and 3 with their 19 attributes obtained from GMA (see Figures 4 and 6) was used to build the elements of the DSM matrix. The data was used to examine options for chunking components into subsystems. The analysis was conducted for each dimension of dependency and for the overall DSM.

First, the policies and their elements or policy measures were mapped on a 25×25 square DSM (that includes all policy measure of the system for consistency), where these policy measures are listed vertically in the "Component" column. Second, the dependencies of the elements to be analysed are defined. Based on the dependencies, a DSM graph structure was built and analysed using the ProjectDSM v2.0 (http://www.projectdsm.com) software, which provides an automated DSM optimization step for triangulation. By running the software, the input data is analysed using an algorithm for optimization that consists of two steps: sequencing and clustering. The sequencing step rearranges the order of the parameters to improve the flow based on their dependencies, while the clustering step groups the elements that are strongly interconnected.

The total interactions for each of the 19 elements were assessed, resulting in 22 entries (red dots in Figure 10) in the dataset. The screening mechanism was conducted and implemented using the ProjectDSMv2.0 project planning software. This is extremely helpful for users to optimize the policy sequence within coupled blocks. Therefore, analysing and optimizing the interactions and sequence of policy measures can significantly improve the performance of the policy formulation process [90].

4.3.3. Model Analysis and Visualization of the Policy Measures for Implementation. The policy measures obtained from GMA are listed in the DSM as rows and columns symmetrically. All policy measures' dependencies used for the DSM were obtained during the first day of the workshop for the identified policy measures. The corresponding interaction levels are identified and evaluated in joint collaboration with the experts, chosen, based on their familiarity with the system.

The DSM results are formulated through clustering and partitioning, which, in turn, are used for future work on development of business process diagrams. The second stage of the proposed approach consists of visualization and analysis of the optimal clustering alternatives in order to estimate and reduce the process costs' required time and evaluate risk (high, medium, and low) and effort (days). The visual representation of the policy measures' dependencies provides further insight into the relationships within a complex system, sometimes highlighting information that otherwise could have been missed. This type of evaluation is a fundamental characteristic of design-science research.

The improved sequence of policy in the DSM is shown in Figure 10, indicating the elements and their interdependencies after clustering of the original matrix. This DSM analysis resulted in four clusters, each of which was then defined as a development sequence of policies. The four coupled blocks (in sequence) are (1, 2, 3, 4, 5, 6, 7), (9, 10), (13, 14, 15, 16, 17), and (18, 19, 20). Each block is visualized separately and independently, and this places the most connected elements in the matrix. It can clearly be seen that four shaded blocks along the diagonal were defined based on interdependencies that generally require reorganizing policies with stakeholders.

From the elements' interactions shown in Figure 10, the elements in the lower part of the matrix require inputs from the elements of the upper part of the matrix. Because of this, the elements in the upper part of the matrix should be given higher priority, in order to improve the flow of the policy by executing first the elements that are input to others.

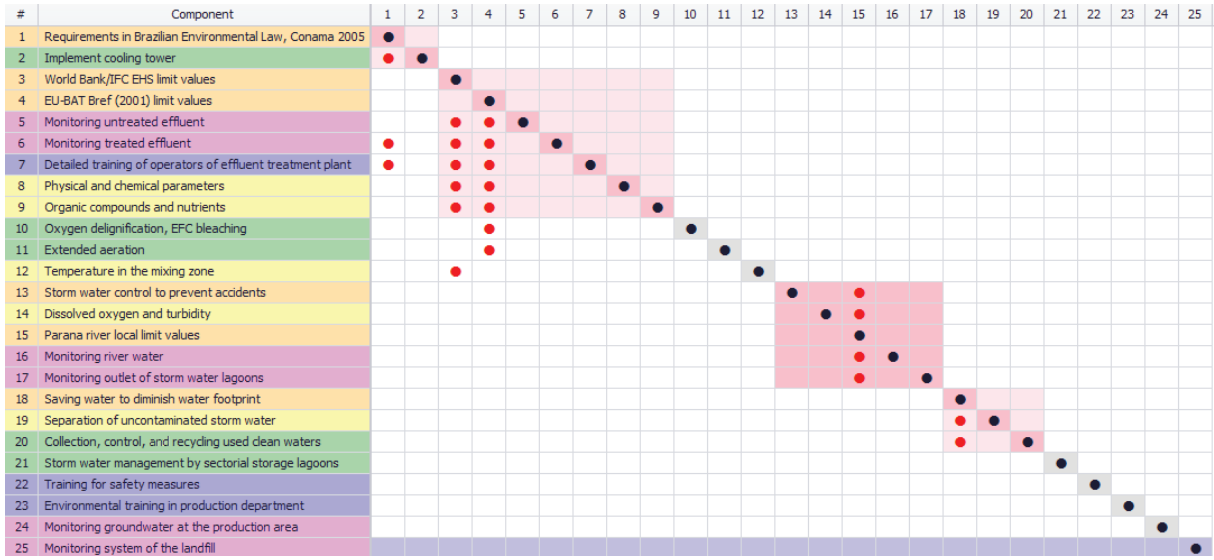

Figure 11: Partitioned DSM.

4.3.4. Reorganization and Improvement of the Process Flow of Policy Measures in DSM. The last stage consists of the reorganization, screening, and improvement of policy process flow understanding via DSM sequence optimization. In the proposed framework, different interaction types in DSM clustering (given in Figure 10) document the original structure of the policy design system in the case study. Next, the DSM partitioning function reveals the most interdependent elements in the matrix. Last, the policy design structure is reorganized and optimized by splitting the larger interdependent clusters into smaller subgroups (shown in Figure 11) that are more manageable.

Although various criteria have been proposed to evaluate policy measures and packages [37, 103], details for a policy package have rarely been revealed with DSM. In this study, interdependent elements were identified and analysed for improvements in the presence of domain specialists and experts involved in the project, who found the process and its resulting sequence of policy measures quite valuable.

The reorganized structure of the DSM matrix through partitioning in Figure 11 proposes an improved organizational structure for the policy measures in the system, thus minimizing the instances of rework. For instance, Figure 11 shows that the element in row 2 "Implement cooling tower" is related to the element "Requirements in Brazilian Environmental Law, Conama 20" under subsystem "Implement legislation," which makes perfect sense. This element in row 2 "Implement cooling tower" originally belonged to the effluent treatment plant (financial aspects in GMA matrix). As a result, managers and designers should consider to restructure their policy design system by reassigning row 2 to "Implement legislation," for better coordination. Through several computational clustering iterations, optimal solutions are reached while considering internal and external block dependencies under certain assumptions. The results were approved by the panel of environmental experts, engineers, and managers who participated in the workshop.

5. Discussion and Managerial Implications

5.1. Policy Measure Development vs. Policy Formulation. GMA and DSM were conducted with the participation of a panel of domain experts in a two-day workshop that resulted in a policy measure reduction model. The concept of policy measures is very complex, since the policies are generally described using natural language, making them difficult to be interpreted, especially when they are competing and conflicting with each other. Another important characteristic of policy measures is that they are intangible, and due to this, it is very hard to systematically break down, analyse, and improve. This is especially difficult considering integration of the sustainability aspects in the early stage of conceptual design. Hence, DSM allows the mentioned analysis and improvement.

5.2. Development of Parameters and Development of Values in GMA. The two morphology constituents, parameters and values, are very different in nature. The definition of parameters requires comparatively more consideration of an expert in comparison to a value, because the interaction of parameters should comprehensively represent the policy concept. To achieve the development of innovative solutions of policy concepts, parameters must be mutually exclusive and collectively exhaustive. Furthermore, the iterative process of GMA and CCA receives a significant improvement through the use of sensitivity analysis [104]. Sensitivity analysis as an optimization tool can be performed with any set of values, in every iteration, and target any type of combination (optimal, acceptable, and nonacceptable). It is a powerful and adaptable tool capable of obtaining desirable solutions in a fraction of the time required otherwise. The analysis can also be automated in a spreadsheet. In addition, the sensitivity limits can be tailored to adapt the method to CCA matrixes of any dimensions, adding another layer of flexibility.

5.3. Defining Information Flow, Dependencies, and Interdependencies in DSM. The most important constituents of DSM—system elements, defining the strength of these element dependencies and interdependencies, and cluster analysis—set the foundation for the advantages of DSM usage. The approach itself helps to illustrate the power of the process architecture, provides a clustering and reorganizing method, and shows all possible information hidden in the policy design and its measures or alternatives. A key insight from the model is the difference between planned and unplanned iterations. With this tool, it is possible to increase the overall understanding of environmental sustainability policy design of wastewater treatment system management among different experts and decision-makers.

5.4. Involvement of Field Experts. The proposed approach of combining GMA and DSM can effectively and efficiently be used for managing complexity of environmental policy formulation. Both GMA and DSM approaches are qualitative methods, and the involvement of the expert's judgment has high impact in the evaluation of solutions, elimination of contradictions in the GMA, building of the elements, and analysis and evaluation of DSM dependencies. In addition, close collaboration between academic or research institutions and companies could facilitate the work of domain experts in order to make optimal decisions.

5.5. Managerial and Practical Implications. The current manuscript has multiple implications for policy design science and society. The main contribution is facilitation of the decision-making process for decision-makers and industry experts. It allows designers and managers to become aware of the complexity of policy measures' generation, policy improvement, and policy implementation in a DSS context. Once the basic understanding of these policy measures and issues is acquired, the relevant authorities have further insights for addressing and tackling counterproductive measures implemented in the industry. The authorities also become more capable of recognising the most important policy measures in order to coordinate efforts to create effective strategies. This work finally aids decision-makers to prepare and practice the implementation of DSS. The proposed approach may assist decision-makers to identify and assess the environmental policy measures, while enabling them to enhance the sustainability of the companies implementing the measures.

The results show the potential of applying DSM to significantly improve the development of policy alternatives, accelerate the design of policies, and improve the entire system's policy structure towards sustainable management. The findings obtained in this work are aimed at further promoting the use of modelling methods in policy formulation with the purpose of performance and effectiveness improvement of policies.

In this sense, the proposed approach targets to support decision-making and to address specific problems in a systematic manner.

6. Conclusions

Environmental policy formulation is a rather complex process that is affected by several uncertain factors, nonquantifiable problems, and unspecified targets. In this paper, a new systematic integrative approach to environmental policy formulation based on structural modelling techniques was presented. The goal of the proposed approach is to support the design of policy, management, and planning in the early stages of conceptual design. The aim was to integrate GMA and DSM, using a case study for generation and improvement of policy measures. The approach consisted of two stages:

(1) First stage: generation, identification, and derivation of policy measures with GMA

(2) Second stage: improvement and screening of the policy measures with DSM

Furthermore, GMA optimization was achieved by reducing iteration time using sensitivity analysis. The methodology for combination of GMA with DSM and avenues for their integration was discussed in detail.

The effectiveness of this integrated approach was illustrated with a real case study of industrial WWTP management planning. The results show the potential of applying GMA and DSM to significantly generate and improve the development of policy alternatives, hasten the design of policies, and improve the whole system's policy structure for sustainable management in WWTP for pulp and paper companies.

The main results of this paper are as follows:

(i) The integration of DSM with GMA improves the overall process from conception and design to integration for improvement and management of complex systems

(ii) The combination of DSM with GMA significantly reduces the policy design process time

(iii) GMA optimization using sensitivity analysis reduces the iteration time

(iv) Combined GMA and DSM methods can define absolute priority importance in a DSS

6.1. Contributions

6.1.1. Theoretical Contribution. This study has several contributions to the field of the sustainable policy design literature. First, from the fundamental research perspective, this work opens the door for further studies of theoretical aspects of the integration of system modelling methods beyond GMA and DSM.

Second, from a methodological point of view, this work expands to the utilization in policy formulation area, by applying systematic modelling methods to sustainable policy design. The presented approach contributes to and promotes research in the domain of multicriteria analysis

and multiobjective optimization using the complex and challenging example of industrial water systems management. Third, the proposed optimization method of CCA through sensitivity analysis is showcased.

6.1.2. Empirical Contribution. From the practical perspective, the suggested approach will help decision-makers and managers in dividing a complex problem into subproblems in the process of policy design. Using creative and analytical modelling methods and decision tools can further improve environmental decision-making performance of policy formulation. Finally this study is, to the authors' best knowledge, the first attempt to develop a systematic integrative approach for environmental policy formulation. Therefore, the suggested approach may be used for future policy design in the current and potentially other fields.

6.2. Limitations. Along with these contributions, however, there are some limitations. First, the GMA-based structural model was not an easy task to implement by the participants in the workshop. All participants needed several iterations of the exercise and guidelines from the facilitator on how to develop the parameters and generate the values in order to familiarize them with the methods. The proposed approach, particularly development of parameters and values in morphological space, is rather significant and strongly dependent on the expert's judgment. Second, the suggested optimization of GMA and CCA through sensitivity analysis should be tailored by the user to matrixes of varied dimensions, as well as decide specific sensitivity limits for each case. Since a large number of combinations are generated in a solution space, appropriate optimization methods and tools can be considered and procedures should be prepared to facilitate the process.

Third, the DSM visualization and clustering method is required to validate the relationships of the policy measures. However, it is still unclear how to prioritize the implementation of policy measures within the clusters. Currently, the scope of this study is limited to the sustainable policy design for water management system and WWTP. Further research and application of the proposed approach to other contexts is still required and will be addressed in future work.

Data Availability

The data used to support the findings of this study have not been made available because of privacy agreements with the interviewees and their respective companies. However, the form used to gather information from the interviewees is available and attached in Appendices A, B, and C.

Additional Points

Highlights. (i) Proposes an integrated framework for generation and improvement of policy measures. (ii) Shows the benefits of combining general morphological analysis and design structure matrix. (iii) Proposes optimization of general morphological analysis through sensitivity analysis. (iv) Presents a case study to show strengths and weaknesses of methods in policy design.

Conflicts of Interest

The authors declare that there is no conflict of interests regarding the publication of this paper.

Acknowledgments

This work was supported by the Foundation for Economic Education (grant number 160039) and partly funded by the Research Foundation of Lappeenranta University of Technology (grant number 122/16). The authors extend heartfelt gratitude to Mark Irving for the DSM software and license (support@projectdsm.com). The main author would also like to extend gratitude to Peter Jones for his professional English proofreading and reviewing of the article.

Supplementary Materials

Appendix A: the list of questions used in the first day of the workshop for building the MA matrix. Appendix B: a blank morphological matrix used to build and analyse the parameters and values in GMA in the first day of the workshop with participation of stakeholders. Appendix C: cross-consistency assessment (CCA) matrix used in the second day of the workshop with experts for assessment of parameters and their values. *(Supplementary Materials)*

References

[1] T. Flüeler, "Decision making for complex socio-technical systems: robustness from lessons learned in long-term radioactive waste governance," in *Environment & Policy*, Springer, Netherlands, 2006.

[2] S. Ney, "Resolving messy policy problems: handling conflict in environmental, transport, health and ageing policy," in *The Earthscan Science in Society Series*, Routledge, 2012.

[3] B. R. Bakshi, "The path to a sustainable chemical industry: progress and problems," *Current Opinion in Chemical Engineering*, vol. 1, no. 1, pp. 64–68, 2011.

[4] J. Conklin, *Dialogue Mapping: Building Shared Understanding of Wicked Problems*, John Wiley & Sons, 2005.

[5] H. W. J. Rittel and M. M. Webber, "Dilemmas in a general theory of planning," *Policy Sciences*, vol. 4, no. 2, pp. 155–169, 1973.

[6] T. Ritchey, "Problem structuring using computer-aided morphological analysis," *Journal of the Operational Research Society*, vol. 57, no. 7, pp. 792–801, 2006.

[7] N. H. Zardari, K. Ahmed, S. M. Shirazi, and Z. B. Yusop, "Literature review," in *Weighting Methods and Their Effects on Multi-Criteria Decision Making Model Outcomes in Water Resources Management*, Springer International Publishing, 2015.

[8] T. A. Birkland, *An Introduction to the Policy Process: Theories, Concepts, and Models of Public Policy Making*, Routledge, 2015.

[9] T. R. Browning, "Applying the design structure matrix to system decomposition and integration problems: a review

and new directions," *IEEE Transactions on Engineering Management*, vol. 48, no. 3, pp. 292–306, 2001.

[10] W. B. Rouse and N. Serban, "Understanding and managing the complexity of healthcare," in *Book collections on Project MUSE*, MIT Press, 2014.

[11] M. Philips, P. Sander, and C. Govers, "Policy formulation by use of QFD techniques: a case study," *International Journal of Quality & Reliability Management*, vol. 11, no. 5, pp. 46–58, 1994.

[12] J. S. Yeomans, "Efficient generation of alternative perspectives in public environmental policy formulation: applying co-evolutionary simulation-optimization to municipal solid waste management," *Central European Journal of Operations Research*, vol. 19, no. 4, pp. 391–413, 2011.

[13] A. Taeihagh, M. Givoni, and R. Bañares-Alcántara, "Which policy first? A network-centric approach for the analysis and ranking of policy measures," *Environment and Planning B: Planning and Design*, vol. 40, no. 4, pp. 595–616, 2013.

[14] A. Taeihagh, "Network-centric policy design," *Policy Sciences*, vol. 50, no. 2, pp. 317–338, 2017.

[15] A. Taeihagh, R. Bañares-Alcántara, and M. Givoni, "A virtual environment for the formulation of policy packages," *Transportation Research Part A: Policy and Practice*, vol. 60, pp. 53–68, 2014.

[16] B. A. Furtado, P. A. M. Sakowski, and M. H. Tóvolli, *Modeling Complex Systems for Public Policies*, Institute for Applied Economic Research-IPEA, Brasília, Brasil, 2015.

[17] M. Howlett, "The criteria for effective policy design: character and context in policy instrument choice," *Journal of Asian Public Policy*, vol. 11, no. 3, pp. 245–266, 2017.

[18] T. Ritchey, "Wicked problems–social messes: decision support modelling with morphological analysis," in *Risk, Governance and Society*, Springer, Berlin, Heidelberg, 2011.

[19] F. Zwicky, *Discovery, Invention*, Research-Through the Morphological Approach, Macmillan, 1969.

[20] M. S. Levin, "Morphological methods for design of modular systems (a survey)," 2012, http://arxiv.org/abs/1201.1712.

[21] T. Ritchey, "Analysis and synthesis on scientific method-based on a study by Bernhard Riemann," *Systems Research*, vol. 8, no. 4, pp. 21–41, 1991.

[22] K. Im and H. Cho, "A systematic approach for developing a new business model using morphological analysis and integrated fuzzy approach," *Expert Systems with Applications*, vol. 40, no. 11, pp. 4463–4477, 2013.

[23] C. Kim, S. Choe, C. Choi, and Y. Park, "A systematic approach to new mobile service creation," *Expert Systems with Applications*, vol. 35, no. 3, pp. 762–771, 2008.

[24] C. Lee, B. Song, and Y. Park, "Generation of new service concepts: a morphology analysis and genetic algorithm approach," *Expert Systems with Applications*, vol. 36, no. 10, pp. 12454–12460, 2009.

[25] I. Johansen, "Scenario modelling with morphological analysis," *Technological Forecasting and Social Change*, vol. 126, pp. 116–125, 2018.

[26] M. de Fátima Teles and J. F. de Sousa, "A general morphological analysis to support strategic management decisions in public transport companies," *Transportation Research Procedia*, vol. 22, pp. 509–518, 2017.

[27] B. Yoon, "On the development of a technology intelligence tool for identifying technology opportunity," *Expert Systems with Applications*, vol. 35, no. 1-2, pp. 124–135, 2008.

[28] B. Yoon, I. Park, and B. Coh, "Exploring technological opportunities by linking technology and products: application of morphology analysis and text mining," *Technological Forecasting and Social Change*, vol. 86, pp. 287–303, 2014.

[29] B. Yoon and Y. Park, "A systematic approach for identifying technology opportunities: keyword-based morphology analysis," *Technological Forecasting and Social Change*, vol. 72, no. 2, pp. 145–160, 2005.

[30] Y. Geum and Y. Park, "How to generate creative ideas for innovation: a hybrid approach of WordNet and morphological analysis," *Technological Forecasting and Social Change*, vol. 111, pp. 176–187, 2016.

[31] S. Jeong, Y. Jeong, K. Lee, S. Lee, and B. Yoon, "Technology-based new service idea generation for smart spaces: application of 5G mobile communication technology," *Sustainability*, vol. 8, no. 11, 2016.

[32] A. Taeihagh, R. Bañares-Alcántara, and C. Millican, "Development of a novel framework for the design of transport policies to achieve environmental targets," *Computers and Chemical Engineering*, vol. 33, no. 10, pp. 1531–1545, 2009.

[33] OECD, *OECD Economic Outlook, Volume 2015 Issue 2*, OECD Publishing, Paris, 2015.

[34] S. D. Eppinger and T. R. Browning, *Design Structure Matrix Methods and Applications, Engineering Systems*, MIT Press Cambridge, Massachusetts, London, England, 2012.

[35] M. Howlett and I. Mukherjee, *Routledge Handbook of Policy Design*, Taylor & Francis, 2018.

[36] M. Howlett and P. del Rio, "The parameters of policy portfolios: verticality and horizontality in design spaces and their consequences for policy mix formulation," *Environment and Planning C: Government and Policy*, vol. 33, no. 5, pp. 1233–1245, 2015.

[37] M. Givoni, "Addressing transport policy challenges through policy-packaging," *Transportation Research Part A: Policy and Practice*, vol. 60, pp. 1–8, 2014.

[38] M. Howlett, J. Vince, and P. Del Río, "Policy integration and multi-level governance: dealing with the vertical dimension of policy mix designs," *Politics and Governance*, vol. 5, no. 2, p. 69, 2017.

[39] A. Taeihagh and R. Bañares-Alcántara, "Towards proactive and flexible agent-based generation of policy packages for active transportation," in *2014 47th Hawaii International Conference on System Sciences*, pp. 895–904, Waikoloa, HI, USA, January 2014.

[40] N. Fenton and M. Neil, "Making decisions: using Bayesian nets and MCDA," *Knowledge-Based Systems*, vol. 14, no. 7, pp. 307–325, 2001.

[41] D. Wollmann and M. T. A. Steiner, "The strategic decision-making as a complex adaptive system: a conceptual scientific model," *Complexity*, vol. 2017, Article ID 7954289, 13 pages, 2017.

[42] R. Poveda-Bautista, J.-A. Diego-Mas, and D. Leon-Medina, "Measuring the project management complexity: the case of information technology projects," *Complexity*, vol. 2018, Article ID 6058480, 19 pages, 2018.

[43] C. Pohl, "From science to policy through transdisciplinary research," *Environmental Science & Policy*, vol. 11, no. 1, pp. 46–53, 2008.

[44] M. Howlett and I. Mukherjee, "Handbook of policy formulation," in *Bandbooks of Research on Public Policy Series*, Edward Elgar Publishing, 2017.

[45] A. Clark, R. Grünig, C. O'Dea, and R. Kühn, "Successful decision-making: a systematic approach to complex problems," in *Business and Economics*, Springer, Berlin, Heidelberg, 2009.

[46] J. Loomis and G. Helfand, "Environmental policy analysis for decision making," in *The Economics of Non-Market Goods and Resources*, Springer, Netherlands, 2006.

[47] M. Howlett, *Designing Public Policies: Principles and Instruments*, Routledge textbooks in policy studies, Routledge, 2011.

[48] J. R. Turnpenny, A. J. Jordan, D. Benson, and T. Rayner, "The tools of policy formulation: an introduction," in *The Tools of Policy Formulation*, A. J. Jordan and J. R. Turnpenny, Eds., pp. 3–30, Edward Elgar Publishing Ltd, Cheltenham, United Kingdom, 2015.

[49] M. Hill and F. Varone, *The Public Policy Process*, Taylor & Francis, 2014.

[50] W. N. Dunn, "Public Policy Analysis: an Introduction," in *Pearson/Prentice Hall*, Upper Saddle River, New Jersey, 2004.

[51] F. Tscheikner-Gratl, P. Egger, W. Rauch, and M. Kleidorfer, "Comparison of multi-criteria decision support methods for integrated rehabilitation prioritization," *Water*, vol. 9, no. 2, p. 68, 2017.

[52] J. A. Annema, N. Mouter, and J. Razaei, "Cost-benefit analysis (CBA), or multi-criteria decision-making (MCDM) or both: politicians' perspective in transport policy appraisal," *Transportation Research Procedia*, vol. 10, pp. 788–797, 2015.

[53] M. Howlett and I. Mukherjee, "The contribution of comparative policy analysis to policy design: articulating principles of effectiveness and clarifying design spaces," *Journal of Comparative Policy Analysis: Research and Practice*, vol. 20, no. 1, pp. 72–87, 2018.

[54] N. Chindarkar, M. Howlett, and M. Ramesh, "Introduction to the special issue: "conceptualizing effective social policy design: design spaces and capacity challenges"," *Public Administration and Development*, vol. 37, no. 1, pp. 3–14, 2017.

[55] X. Wu, M. Ramesh, M. Howlett, and S. A. Fritzen, *The Public Policy Primer: Managing the Policy Process*, Edi, Ed., Routledge, London and New York, 2nd edition, 2018.

[56] A. Stirling, "Renewables, sustainability and precaution: beyond environmental cost-benefit and risk analysis," *Sustainability and Environmental Impact of Renewable Energy Sources*, vol. 19, pp. 113–134, 2003.

[57] S. Buzuku, A. Kraslawski, and K. Harmaa, "Supplementing morphological analysis with a design structure matrix for policy formulation in a wastewater treatment plant," in *Modeling and Managing Complex Systems*, pp. 9–18, Carl Hanser Verlag GmbH & Co. KG, Fort Worth (Texas, USA), 2015.

[58] M. G. Moehrle, "MorphoTRIZ - solving technical problems with a demand for multi-smart solutions," *Creativity and Innovation Management*, vol. 19, no. 4, pp. 373–384, 2010.

[59] World Commission on Environment and Development, *Our Common Future (The Brundtland Report)*, vol. 4, no. 1, 1987, Oxford Univeristy Press, Oxford, 1987.

[60] F. Zwicky and a. G. Wilson, "New methods of thought and procedure," in *Symposium on Methodologies*, Springer, Berlin, Heidelberg, 1967.

[61] B. Yoon and Y. Park, "Development of new technology forecasting algorithm: hybrid approach for morphology analysis and conjoint analysis of patent information," *IEEE Transactions on Engineering Management*, vol. 54, no. 3, pp. 588–599, 2007.

[62] T. Eriksson and T. Ritchey, "Scenario development using computerised morphological analysis. Papers presented at the Cornwallis and Winchester international OR conference, England," 2002, June 2017, http://citeseerx.ist.psu.edu/viewdoc/download?doi=10.1.1.469.9096&rep=rep1&type=pdf.

[63] J. G. Wissema, "Morphological analysis: its application to a company TF investigation," *Futures*, vol. 8, no. 2, pp. 146–153, 1976.

[64] R. G. Weber and S. S. Condoor, "Conceptual design using a synergistically compatible morphological matrix," *FIE '98. 28th Annual Frontiers in Education Conference. Moving from 'Teacher-Centered' to 'Learner-Centered' Education. Conference Proceedings (Cat. No.98CH36214)*, 1998, pp. 171–176, Tempe, AZ, USA, November 1998.

[65] M. Belaziz, A. Bouras, and J. M. Brun, "Morphological analysis for product design," *Computer-Aided Design*, vol. 32, no. 5-6, pp. 377–388, 2000.

[66] J. Ölvander, B. Lundén, and H. Gavel, "A computerized optimization framework for the morphological matrix applied to aircraft conceptual design," *Computer Design*, vol. 41, no. 3, pp. 187–196, 2009.

[67] R. G. Coyle and G. R. McGlone, "Projecting scenarios for south-east Asia and the south-West Pacific," *Futures*, vol. 27, no. 1, pp. 65–79, 1995.

[68] R. G. Coyle and Y. C. Yong, "A scenario projection for the South China Sea," *Futures*, vol. 28, no. 3, pp. 269–283, 1996.

[69] J. Voros, "On a morphology of contact scenario space," *Technological Forecasting and Social Change*, vol. 126, pp. 126–137, 2018.

[70] P. A. Haydo, "From morphological analysis to optimizing complex industrial operation scenarios," *Technological Forecasting and Social Change*, vol. 126, pp. 147–160, 2018.

[71] T. Ritchey, "General morphological analysis as a basic scientific modelling method," *Technological Forecasting and Social Change*, vol. 126, pp. 81–91, 2018.

[72] G. Duczynski, "Morphological analysis as an aid to organisational design and transformation," *Futures*, vol. 86, pp. 36–43, 2017.

[73] W. Zeiler, "Morphology in conceptual building design," *Technological Forecasting and Social Change*, vol. 126, pp. 102–115, 2018.

[74] S. Buzuku and A. Kraslawski, "Application of morphological analysis to policy formulation for wastewater treatment," *Journal of Mining Institute*, vol. 214, pp. 102–108, 2015.

[75] M. Pidd, *Tools for Thinking: Modelling in Management Science*, Wiley, 2009.

[76] A. De Waal and T. Ritchey, "Combining morphological analysis and Bayesian networks for strategic decision support," *ORiON*, vol. 23, no. 2, 2007.

[77] D. V. Steward, "The design structure system: a method for managing the design of complex systems," *IEEE Transactions on Engineering Management*, vol. EM-28, no. 3, pp. 71–74, 1981.

[78] D. V. Steward, "Systems analysis and management: structure, strategy, and design," in *A Petrocelli Book*, Petrocelli Books, 1981.

[79] A. Yassine, "An introduction to modeling and analyzing complex product development processes using the design

structure matrix (DSM) method," *Urbana*, vol. 51, no. 9, pp. 1–17, 2004.

[80] J. E. Bartolomei, "Qualitative knowledge construction for engineering systems: extending the design structure matrix methodology in scope and procedure by Jason," in *Massachusetts Institute of Technology*, Engineering Systems Division, 2007.

[81] M. Danilovic and T. R. Browning, "Managing complex product development projects with design structure matrices and domain mapping matrices," *International Journal of Project Management*, vol. 25, no. 3, pp. 300–314, 2007.

[82] S. D. Eppinger, "Innovation at the speed of information," *Harvard Business Review*, vol. 79, pp. 149–158, 2001.

[83] T. R. Browning, "Managing complex project process models with a process architecture framework," *International Journal of Project Management*, vol. 32, no. 2, pp. 229–241, 2014.

[84] T. R. Browning, S. D. Eppinger, D. M. Schmidt, and U. Lindemann, "Modeling and managing complex systems," in *Proceedings of the 17th International Dependency and Structure Modeling Conference, DSM 2015*, Fort Worth, TX, USA, November 2015.

[85] S. Austin, A. Baldwin, B. Li, and P. Waskett, "Application of the analytical design planning technique to construction project management," *Project Management Journal*, vol. 31, no. 2, pp. 48–59, 2000.

[86] T. R. Browning and S. D. Eppinger, "Modeling impacts of process architecture on cost and schedule risk in product development," *IEEE Transactions on Engineering Management*, vol. 49, no. 4, pp. 428–442, 2002.

[87] M. P. Howlett and J. S. Cuenca, "The use of indicators in environmental policy appraisal: lessons from the design and evolution of water security policy measures," *Journal of Environmental Policy and Planning*, vol. 19, no. 2, pp. 229–243, 2016.

[88] OECD, *Instrument Mixes for Environmental Policy*, Instrument Mixes for Environmental Policy, Paris, 2007.

[89] E. Challies, J. Newig, E. Kochskämper, and N. W. Jager, "Governance change and governance learning in Europe: stakeholder participation in environmental policy implementation," *Policy and Society*, vol. 36, no. 2, pp. 288–303, 2017.

[90] S. Buzuku, A. Kraslawski, and T. Kässi, "A case study in the application of design structure matrix for improvements of policy formulation in complex industrial wastewater treatment," in *DSM 2016: Sustainability in Modern Project Management-Proceedings of the 18th International DSM Conference*, pp. 91–101, Sao-Paulo, Brazil, August 2016.

[91] L. al-Hakim, A. Kusiak, and J. Mathew, "A graph-theoretic approach to conceptual design with functional perspectives," *Computer Design*, vol. 32, no. 14, pp. 867–875, 2000.

[92] S. Rizzuti, L. de Napoli, and C. Rocco, "A graph-based approach to check a product functional net," in *Theory and Research Methods in Design, International Design Conference - Design 2006*, pp. 111–118, Dubrovnik, Croatia, May 2006.

[93] N. Henry and J. D. Fekete, "MatrixExplorer: a dual-representation system to explore social networks," *IEEE Transactions on Visualization and Computer Graphics*, vol. 12, no. 5, pp. 677–684, 2006.

[94] B. Lu, X. Du, and S. Huang, "The economic and environmental implications of wastewater management policy in China: from the LCA perspective," *Journal of Cleaner Production*, vol. 142, pp. 3544–3557, 2017.

[95] A. Patel, N. Arora, V. Pruthi, and P. A. Pruthi, "Biological treatment of pulp and paper industry effluent by oleaginous yeast integrated with production of biodiesel as sustainable transportation fuel," *Journal of Cleaner Production*, vol. 142, pp. 2858–2864, 2017.

[96] M. Zec and F. Matthes, "Web-based software-support for collaborative morphological analysis in real-time," *Technological Forecasting and Social Change*, vol. 126, pp. 168–181, 2018.

[97] T. Ritchey, "Facilitating GMA workshops for modelling wicked problems facilitating GMA workshops for modelling wicked problems," *Acta Morphologica Generalis*, vol. 6, no. 2, pp. 1–14, 2017.

[98] T. Krueger, T. Page, K. Hubacek, L. Smith, and K. Hiscock, "The role of expert opinion in environmental modelling," *Environmental Modelling & Software*, vol. 36, pp. 4–18, 2012.

[99] P. Glasbergen and R. Smits, "The policy laboratory for sustainable development: a new learning context for environmental scientists," *International Journal of Sustainability in Higher Education*, vol. 4, no. 1, pp. 57–74, 2003.

[100] T. Ritchey, M. Stenström, and H. Eriksson, "Using morphological analysis to evaluate preparedness for accidents involving hazardous materials," in *4th International Conference for Local Authorities*, pp. 1–6, Shanghai, 2002.

[101] Y. Geum, H. Jeon, and H. Lee, "Developing new smart services using integrated morphological analysis: integration of the market-pull and technology-push approach," *Service Business*, vol. 10, no. 3, pp. 531–555, 2016.

[102] T. Ritchey, "Principles of cross-consistency assessment in general morphological modelling," *Acta Morphologica Generalis*, vol. 4, pp. 1–20, 2015.

[103] A. Justen, N. Fearnley, M. Givoni, and J. Macmillen, "A process for designing policy packaging: ideals and realities," *Transportation Research Part A: Policy and Practice*, vol. 60, pp. 9–18, 2014.

[104] S. Buzuku and A. Kraslawski, "Optimized morphological analysis in decision-making," in *Advances in Systematic Creativity*, L. Chechurin and M. Collan, Eds., pp. 225–244, Palgrave Macmillan, Cham, 2019.

Hindawi
Complexity
Volume 2018, Article ID 3493492, 18 pages
https://doi.org/10.1155/2018/3493492

Research Article

The Political Complexity of Regional Electricity Policy Formation

Kyungjin Yoo [1] **and Seth Blumsack** [1,2]

[1] *John and Willie Leone Family Department of Energy and Mineral Engineering, Pennsylvania State University, USA*
[2] *Santa Fe Institute, Santa Fe, New Mexico, USA*

Correspondence should be addressed to Seth Blumsack; sab51@psu.edu

Received 18 May 2018; Revised 9 October 2018; Accepted 8 November 2018; Published 5 December 2018

Guest Editor: Miguel Fuentes

The integration of renewable power supplies into existing electrical grids, or other major technology transitions in electric power, is a complex sociotechnical process. While the technical challenges are well-understood, the process of adapting electricity policy and market rules to these new technologies is understudied. Planning and market rules are a critical determinant of the technical success of renewable energy integration efforts and the financial viability of renewable energy investments. Organizational adaptation can be particularly complex in electric power, where transmission grids cross multiple political boundaries and decisions are made not by central authorities or governments, but in cooperative regional frameworks that must accommodate many divergent interests. We add to a recently emerging literature on the governance of regional organizations that plan and operate electric power grids by developing and illustrating a novel approach to the study of political power in multistakeholder electricity organizations. We use semistructured interviews with participants in a specific regional electric grid authority, the PJM Regional Transmission Operator in the Mid-Atlantic United States, to elicit perceptions of where tensions arise in stakeholder-driven processes for changing PJM's rules and perceptions of those groups of stakeholders that possess political power. We treat these perceptions as hypotheses that can be evaluated empirically using five years of data from PJM on how stakeholders voted on a wide variety of regional electricity policy issues. Representing voting behavior as a network, we use a community detection method to identify strong coalitions of stakeholders in PJM that provide support for some stakeholder perceptions of political power and refute other perceptions. The degree distribution of the voting network exhibits a fat tail relative to those in other canonical graph models. We show, using relatively simple network metrics including degree, betweenness, and the mixing parameter, that the reason for this fat tail in the degree distribution is the existence of "swing" voters in RTO stakeholder networks. These voters are identifiable in the tail of the degree distribution of the voting network and are influential in pushing highly contentious rule change proposals towards passage or failure. The method we develop is generalizable to other contexts and provides a new framework for the study of regional electricity policy formation.

1. Introduction

As large-scale electric power systems undergo various types of technological transition, including the integration of large amounts of renewable power generation and an increase in adoption of distributed power generation and electrification of transportation, the rules that govern markets, planning, and operations of the power grid need to adapt along with technology [1–6]. These rules are important for determining the value of technology options that explicitly or implicitly compete to provide electric generation and transmission services [7]. The challenges in integrating weather-dependent wind and solar power into regional electric grids have provided some recent examples of how grid operators have needed to adapt their rules, especially when those grid operators span multiple political jurisdictions (e.g., regional grid operators covering all or parts of several states in the United States or coalitions of national grid operators in Europe). In the United States, grid operators have adapted to rapid growth in wind energy by changing market and

generator dispatch rules to minimize the frequency with which wind energy output must be curtailed [5] and have adopted new power transmission planning procedures aimed at finding synergies between wind energy development and other electric transmission needs [8]. In California, growth in solar energy has challenged that state's power grid to be able to balance the rapid decline in solar output that occurs at the end of the daytime period with a coincident increase in demand [4]. The response of the California grid operator has been to establish a new market construct for "imbalance energy" services that are able to increase and decrease output quickly in response to changes in state electricity demand or solar power production. The Irish electric grid operator has responded to increased wind penetration by adjusting market rules to require other generation resources to provide a certain level of system support.

The necessity of power grid operators to adapt planning and operational rules to handle the increased penetration of renewable energy or other technologies on the electric power system is clear, but an underappreciated aspect of this adaptation is that in many jurisdictions the market, planning, and operational rules are made in a collective decision process requiring coordination and negotiation among multiple parties rather than by a government or other central authority [7]. The process of integration of renewable energy or distributed energy resources into large-scale power grids is thus not simply a problem of engineering and technology but is a complex sociotechnical process in which the process for enacting changes in the rules governing power grid planning and operations can have a measurable impact on grid performance after the rule changes have been made [4, 7, 9].

In contrast to the large literature that has used models of distributed decision-making or multiagent models to analyze the impacts of consumer or distributed energy decisions on power grid operations (examples from this voluminous literature include [7, 10–14]), the analysis of how regional power grid operators make decisions has emerged only recently. This literature has largely focused on the governance of regional power grid operators and the relationship between these grid operators and their regulators [2, 4, 15, 16]. Particularly in the United States, however, the rules governing the operation and planning of regional power grids are made in a stakeholder-driven setting that resembles a negotiated political process more than a regulatory process (although the stakeholder-driven proceedings will typically end with the regulatory approving or disapproving of the rule changes supported by the stakeholder group) [17, 18].

Some very recent analyses of these stakeholder processes in regional power grids in the United States have suggested that the decisions emerging from these processes are highly influenced by the structure of the process itself [16–19]. Which parties have standing to participate formally in the stakeholder process, the way that stakeholders are segmented into coalitions, and the voting mechanisms can all shift political power in ways that can be consequential for the performance of the electric power system. Political power within the stakeholder process has been identified in the literature as particularly problematic when stakeholders are asked to make collective decisions on highly contentious issues such as the rules governing incentives for new power plant construction [18]. This literature, however, is not in agreement as to which interests may or may not wield political power in different circumstances.

We provide and illustrate a network-based method for identifying political power structures in the stakeholder-driven organizations (Regional Transmission Organizations or RTOs) that govern the electric power grid in many jurisdictions that have adopted some form of electricity restructuring and deregulation. We illustrate this method using a detailed case study of one particular jurisdiction in North America but the method itself is portable to other contexts. The issue of how RTOs engage in stakeholder-driven self-governance has been raised as an important energy policy issue in the academic literature and by policymakers [15–19], and the approach that we develop and implement opens up the study of restructured electricity market processes to the use of network-based tools. Our paper makes three distinct contributions addressing RTO governance and the development of network tools for electricity policy analysis. First, we synthesize qualitative information from semistructured interviews with participants in RTO stakeholder processes to formulate hypotheses about the distribution of political power in these processes. Second, we use quantitative information from RTO voting histories in the PJM Interconnection to evaluate these hypotheses. We find empirical support for some perceptions of the distribution of political power but not others. Third, we show how relatively simple network metrics contain information that can identify "swing" voters in RTO stakeholder networks. These swing voters have previously been shown to play an important role in enabling or thwarting the ability of the RTO to make changes to its market rules and procedures [17, 18].

We apply this analysis framework to the PJM Regional Transmission Organization in the United States. PJM Interconnect operates the electric grid in all or parts of thirteen states plus the District of Columbia in the Mid-Atlantic region of the United States. In addition to being one of the largest regional power grid operators, PJM makes public highly detailed data on the proceedings of its stakeholder process. The special role and decision structure of the Regional Transmission Organization is described in the remainder of this section. In Section 2, we describe our analysis framework and the process for conducting the semistructured interviews. In Section 3, we provide qualitative evidence from our stakeholder interviews for multiple perceptions of political power; these perceptions serve as hypotheses that we evaluate with our voting network data in Section 4. Based on our analysis of voting data, we find some evidence in support of some of these stakeholder perceptions and evidence that refutes some stakeholder perceptions. We are also able to refute some of these perceptions based on the voting network data. Finally, we show that some simple properties of the voting network are sufficient to identify participants who may possess pivotal voting power in highly contentious issues. Section 5 provides some concluding thoughts and future directions for integrated qualitative and

quantitative research into the governance of large energy organizations.

1.1. The Role of Regional Transmission Organizations in North American Electric Power Planning and Operations. The electric power system integrates a highly diverse set of technologies and organizations by means of regional high-voltage transmission grids that can span multiple political jurisdictions. Most of North America, for example, is served through three large-scale power grids that cross state and national boundaries. Many parts of the electric power industry have undergone a process of restructuring and deregulation over the past two decades, involving the unbundling of electric utilities into separate companies for power generation, transmission, and distribution; the creation of competitive markets for power generation (effectively replacing the function of the electric utility or state-owned electricity authority with competitive market signals for power system planning and investment); and, in North America specifically, the increased regionalization of power grid operations through the creation of Regional Transmission Organizations (RTOs). Currently, approximately 70% of all electricity demand in the United States, along with some Canadian provinces and portions of Mexico, is served through Regional Transmission Organizations. A map of those areas in North America that lie within RTO footprints is shown in Figure 1.

The RTO was originally created in the United States to meet regulatory standards for regional coordination in power system planning [21] and broadening of electricity markets to enable generation resources from multiple utilities to compete with one another using the regional transmission grid as a kind of market platform. The formation of RTOs in the United States has been voluntary. Utilities are not required to form or join one of the RTOs but are encouraged to do so by the Federal Energy Regulatory Commission (FERC), which regulates RTO practices. Broadly, the role of the RTO in North America can be described in a few distinct functions:

(i) The RTO is responsible for determining investment needs for power generation and transmission to meet standards for reliable power system operations, but it does not own any physical assets and must provide financial incentives for generation and transmission firms to make needed investments. Many of these incentives come through market signals.

(ii) The RTO is responsible for real-time operations within its footprint (dispatching power generation to meet electricity demand) but the command-and-control capabilities of the RTO are very limited. Most RTOs use market mechanisms to provide financial incentives for power plants to offer electricity production services.

(iii) RTOs are intended to be technology-neutral (they cannot favor one technology or fuel over any other, including renewable and distributed power generation) and the FERC has asked RTOs to operate in a very stakeholder-driven way.

1.2. The Decision Structure of RTOs. With relatively few exceptions, changes to market rules or operational and planning protocols within RTOs happen through a stakeholder-driven process that reflects the many different organizations and interests that make up the electric power sector. Organizations that are typically recognized as stakeholders within the process include power generation and transmission owners (including renewable energy and distributed energy), electric distribution utilities, large electricity consumers (such as manufacturing facilities), and firms that engage in the wholesale trade of electric power. RTOs typically have a large number of formally recognized stakeholders: PJM, the focus of the illustrative analysis in this paper, had 525 recognized stakeholders at the time that we conducted our analysis. These stakeholders are stratified according to one of five defined industry sectors, as shown in Table 1. These industry sectors include End Use Customers (EUC), which primarily represent large industrial electricity users; Electric Distributors (ED), which primarily includes utilities that deliver electricity to retail consumers; Generation Owners (GO), which own and operate power plants; Transmission Owners (TO), which own the high-voltage transmission wires; and Other Suppliers (OS), a diverse group of financial players in electricity markets and firms who offer services like demand curtailment to electricity markets but do not fit easily into any of the other four sector categories.

While the structure of these stakeholder processes varies somewhat by RTO, the movement of a rule change generally involves a few different steps [2, 22]. Proposed RTO rule changes are first debated and discussed in one of a number of thematic working groups or task forces, where there may be more limited participation. Rule changes that are approved by the working group or task force are elevated to a vote by a central committee consisting of all stakeholders. Successful issues are then passed to the RTO Governing Board and then on to the FERC for regulatory approval. It is important to remember that the scope of stakeholder involvement in the RTO is limited to rule changes and not real-time operational decisions or planning outcomes. For example, the stakeholders in an RTO might determine the specific reliability criteria that are used in a transmission planning study or they might determine the level of the price cap for offers into an RTO's electricity market, but the stakeholders would not have any direct involvement in the conduct of planning studies or the clearing of markets.

The analysis in this paper uses the PJM stakeholder process and voting data from that process as an illustrative case study. The central committee in PJM, which votes on all proposed rule changes, is referred to as the Members Committee (MC). All stakeholders are eligible to vote on any issue that is brought before the MC. The MC in PJM is interesting not only because of how much detailed voting data

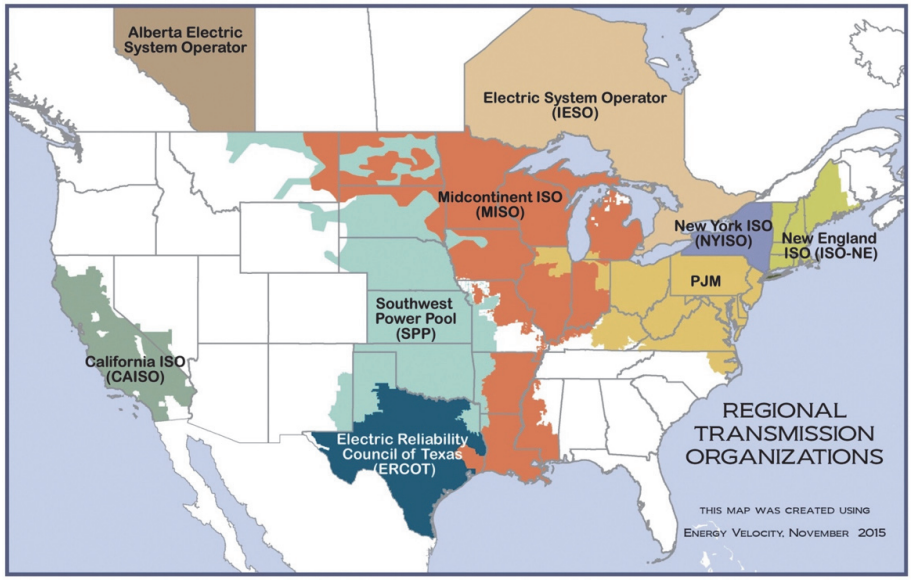

Figure 1: RTOs in North America. The PJM RTO, which is the focus of our case study, covers the Mid-Atlantic United States. *Source: Federal Energy Regulatory Commission.*

Table 1: Composition of voters in the PJM Members Committee (MC). Source: [18], based on data from [20].

Sector	Number of Firms (%)	Example Firms
End Use Customers (EUC)	21 (4%)	Air Products, Proctor & Gamble
Electric Distributors (ED)	43 (8%)	Old Dominion Electric Cooperative, Northern Virginia Electric Cooperative
Generation Owners (GO)	95 (18%)	Calpine, NRG
Transmission Owners (TO)	14 (3%)	Duquesne Light, PSEG
Other Suppliers (OS)	354 (67%)	Direct Energy (Curtailment Service Provider), Citigroup Energy (Financial), EDF Trading (Marketer)

is available from the proceedings of this committee, but also because the PJM MC has perhaps the greatest degree of rule-making authority of any North American RTO. They make decisions on behalf of all the others who could not participate on operating rules and policies. The MC uses a system of *sector-weighted voting* in which all five industry sectors (as outlined in Table 1) are equally weighted and the vote of each individual member carries identical weight within a sector. When voting, all participants vote yes or no or abstain on a single issue, producing a sector-specific voting score that measures the proportion of voting stakeholders in that sector supporting the rule change. The final voting score $\boldsymbol{V}$ is the sum of all sector-level scores, defined as

$$\boldsymbol{V} = \sum_{k} \sum_{j=1}^{(n_k - a_k)} w_{jk} = \sum_{k} \sum_{j=1}^{(n_k - a_k)} \frac{\delta_{jk}}{n_k - a_k} \quad (1)$$

where δ_{jk} is an indicator variable equal to one for a yes vote of voter j in sector k and zero for a no vote. n_k is the total number of voters in sector k, and a_k is the number of abstention votes in sector k. Abstention votes are excluded when counting the total number of votes and thus have the same effect as a smaller number of sector voters; i.e., abstentions increase the weight of an individual voter. Note that as the number of voters in a sector increases, the weight of an individual voter in that sector $(1/(n_k - a_k))$ declines. In the PJM stakeholder process, an issue passes if the final voting score $\boldsymbol{V}$ exceeds 3.335, roughly equivalent to a two-thirds majority among the five sectors. This implies that any two sectors could jointly prevent passage regardless of the number of voters in those sectors.

Table 2 illustrates a *hypothetical* voting result, taken from [18], that results in passage, with a total voting score of 3.457. The column showing the percentage of votes in favor is

Table 2: Sector-weighted voting example. Source: [18].

Sector	For	Against	Abstain	Total	Total - Abstain	% in favor
Transmission Owner (TO)	8	2	4	14	10	0.8
Generation Owner (GO)	15	0	1	16	15	1
Other Supplier (OS)	10	10	5	25	20	0.5
Electric Distributor (ED)	3	7	15	25	10	0.3
End Use Customer (EUC)	12	2	0	14	14	0.857
					Final voting score $\boldsymbol{V}$	3.457

calculated by taking the proportion of *For* votes relative to the total of *For* plus *Against* votes. Abstentions are not counted at all in the voting process.

The decisions made by the PJM MC are highly consequential to the functioning of PJM's electricity markets and the economic incentives faced by different power generation technologies: these rules and incentives effectively emerge from the many individual voters in the stakeholder process, which have their own commercial interests. The relative power of various coalitions (groups of stakeholders whose interests are aligned across one or more issues) and the behavior of voters that do not neatly align with identifiable coalitions play an important role in determining which power grid rules are adopted and which rules are not adopted. The performance of the physical power grid is thus inextricably tied to the behaviors in the stakeholder process. Some recent work has questioned the effectiveness and of PJM's stakeholder process [16, 19], pointing out that rule changes have become so contentious as to make the passage of any rule change very difficult, and also questioning the degree to which the sector definitions themselves may concentrate political power and influence voting outcomes.

Our work addresses a number of important RTO governance issues raised by this body of literature by describing and illustrating a novel approach that uses mixed methods of qualitative interview data with voting network analysis to identify strong voter coalitions that could act in a coordinated fashion and screen for the existence of pivotal voters who may be able to swing voting outcomes in certain directions.

2. Methods

In this section we provide a high-level overview of the analytical approach that we use to identify political power in RTO stakeholder processes. This method integrates qualitative information gleaned from semistructured interviews with a network analysis of RTO stakeholder voting data to develop quantitative measures and draw conclusions about political power. The method that we employ draws from two distinct research philosophies, the theory of engaged scholarship as described by van de Ven [23] and the grounded theory approach from Strauss et al. [24–26]. The engaged scholarship approach to developing organizational knowledge emphasizes the need for repeated practitioner interaction to define and refine relevant research questions and ensure that research results are relevant to the organizational frameworks being studied. Our analysis has some common threads with grounded theory in that we allowed our interactions with practitioners, through semistructured interviews, to assist in defining the problem and identifying relevant analytical hypotheses.

A schematic of our overall approach is shown in Figure 2. Semistructured interviews were conducted with several dozen stakeholders in multiple RTOs, and the qualitative information from these interviews was used to identify perceptions of the stakeholder process by those who were participants in that process (panel A in Figure 2). These perceptions will be discussed in more detail in Section 3. Taking some of those perceptions as hypotheses provided a framework through which we could build voting networks and examine properties of those networks (panel B of Figure 2). These network properties then gave us metrics or other information that could be used to determine which stakeholder perceptions were consistent with the voting data and which were not (panel C of Figure 2). Specific voting issues could be analyzed using the voting network data or other models to generate predictions about the outcome of similar voting issues (as was done in prior work on "capacity markets" in RTOs, which are forward markets for electric generation capacity), and computational experiments can be run to examine possible voting outcomes under different stakeholder process structures or voting rules and how those voting outcomes manifest themselves in the performance of the power grid or of electricity markets (panel D). The whole research process can eventually circle back to the stakeholders themselves (moving from panel D to panel A).

The analysis in the present paper is focused primarily on showing how qualitative information can be used to build quantitative theories in electricity policy formation through RTO stakeholder processes. It thus effectively covers panels A through C in Figure 2.

3. Using Semistructured Interview Data to Generate Perceptions of Political Power in RTO Stakeholder Processes

During the summer and fall of 2014, approximately 70 individual interviews were performed with stakeholders and RTO staff at three RTOs in the United States: PJM, the Midcontinent ISO, and the California ISO. Figure 3 shows a breakdown of the types of respondents in our interviews. A group of initial interviewees spanning the industry sectors identified in Table 1 was initially selected, and additional

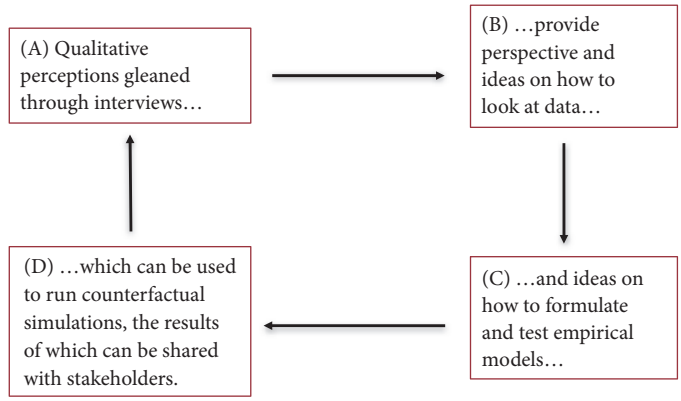

Figure 2: A model of integrating qualitative and quantitative data on electricity policy formation.

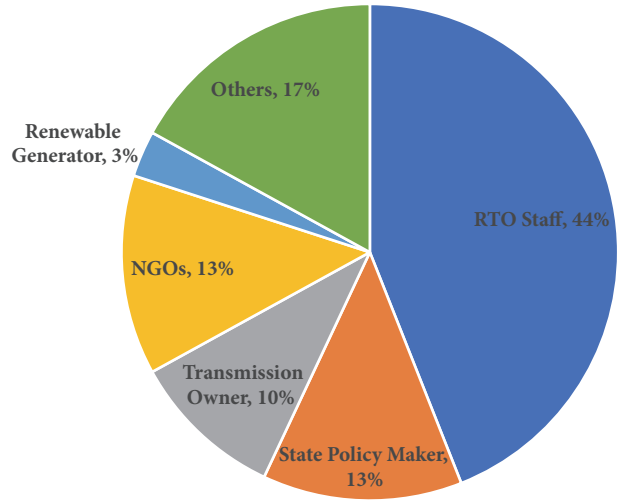

Figure 3: Distribution of respondents to semistructured interviews.

respondents were identified via the snowballing method. One-third of these interviews were with stakeholders and RTO staff in PJM, which is the focus of our illustrative case study. The interviews were conducted in-person as well as over the telephone and ranged from 45 to 90 minutes in length. In addition to interviewing stakeholders, we reviewed a number of public documents related to the stakeholder process and attended several working group meetings as well as meetings of the full Members Committee in PJM.

Respondents were chosen based on a review of PJM documents and identifying individuals and organizations that were active and experienced, particularly in issues related to the integration of renewable energy into large-scale power grids. Our initial group of respondents also spanned the industry sectors identified in Table 1. We engaged in some snowballing to identify additional interview respondents beyond those identified in our original document search. Each interview was professionally transcribed and then coded in the NVIVO environment by the research team. Second-level coding within NVIVO focused on categories such as political power, shifts in the dynamics of the stakeholder process, and the complexities involved in seeing a proposed rule change through to completion. Quotes used in this paper are representative of perceptions shared with the research team by multiple respondents, and respondents are identified only as [PJM-XX]. We describe the context of these observations here and summarize the quotes in Table 3.

The semistructured interview format, along with the set of questions for respondents, is described in more detail in the Appendix. We note that because of the semistructured nature of the interviews few constraints were placed on the path of the conversation with each respondent other than to focus the conversation on the stakeholder process.

In our interviews with PJM stakeholder participants, we observed that many perceived the stakeholder process as becoming more complex and time-consuming, in part because the total number of stakeholders has grown as more participants have joined PJM's markets. One of our stakeholder participants observed, "You needed significantly smaller rooms to have the meetings. The intensity of disagreements was just as great as today. There were things they never reached agreement on but there was definitely more of a spirit of, 'We're all in this together and we need to make it work,' than there is today" (PJM-01). This perception was shared

Table 3: Summary of PJM Stakeholder Perceptions.

Perception in the PJM Stakeholder Process	Illustrative Stakeholder Quote
Growth in the number of stakeholders, and increasing conflicts in commercial interests among stakeholders, are creating challenges in moving rule changes forward.	You needed significantly smaller rooms to have the meetings. The intensity of disagreements was just as great as today. There were things they never reached agreement on but there was definitely more of a spirit of, 'We're all in this together and we need to make it work,' than there is today" (PJM-01).
The stakeholder process has become factionalized into consumer-side interests and supply-side interests. (Note that "load" is electricity-industry parlance for consumers.)	"The problem that some people find is that one side can stymy the other. You have generation, transmission, load, and so on. Generation's always worried that load can stop them from doing things. Load is worried about generation." (PJM-02).
Perceptions that consumer-side interests have more political power.	"There is a lot of leverage on the load side." (PJM-03); What you actually find now is the load interest, where it used to be they had about 50 percent of the vote, they now have 65 percent of the vote." (PJM-04.)
Perceptions that supplier-side interests have more political power.	"[The stakeholder process is] tilted towards the supplier side" (PJM-05); "There have certainly been complaints by load that. . .PJM pushed through a whole bunch of changes through the capacity market without really knowing how they were going to interact with each other." (PJM-03)

by a number of our stakeholder respondents across multiple sectors of the PJM market.

Along with the perceptions of increased tension within the stakeholder process and a greater level of effort required for the process to culminate in a passable rule change when rule changes were needed, we also observed different perceptions of which stakeholder groups were more or less influential, either in pushing rule changes through the Members Committee or in stopping rule changes from being approved. One observer of the stakeholder process noted that "The problem that some people find is that one side can stymy the other. You have generation, transmission, load, and so on. Generation's always worried that load can stop them from doing things. Load is worried about generation." (PJM-02).

We observed multiple stakeholder respondents suggesting that since consumer-side (or "load") interests dominated two of the five sectors in the PJM stakeholder process that these consumer-side interests were able to exercise substantial political power. According to one such respondent describing the voting process in the Members Committee, "There is a lot of leverage on the load side." (PJM-03). An observer of the stakeholder process reported, "What you actually find now is the load interest, where it used to be they had about 50 percent of the vote, they now have 65 percent of the vote." (PJM-04).

We also observed multiple stakeholder respondents suggesting the opposite: that supply-side (or "generation") interests were able to exercise substantial political power in the PJM Members Committee. One consumer-side respondent expressed the belief that the process was "tilted towards the supplier side" (PJM-05), while another observer noted that "There have certainly been complaints by load that. . .PJM pushed through a whole bunch of changes through the capacity market without really knowing how they were going to interact with each other." (PJM-03).

4. Finding Evidence of the Perceptions on Political Power via Voting Network Analysis

Multiple organizational and political processes have been represented using network-based tools [27–33]. The present analysis is the first to do so in the context of regional electricity markets and is motivated by the use of voting data to support or refute the stakeholder perceptions identified in Section 3. The perceptions about the PJM stakeholder process elicited as part of our semistructured interviews suggest two possible hypotheses about the balance of political power.

Hypothesis 1. Supplier-side perceptions are correct, and consumer-side interests possess substantial political power in the Members Committee.

Hypothesis 2. Consumer-side perceptions are correct, and supplier-side interests possess substantial political power in the Members Committee.

If the perceptions of supply-side interests are correct and consumer-side interests jointly possess a substantial amount of political power, we should observe a strong voting bloc among the two consumer-side sectors in the PJM stakeholder process (the ED and EUC voters). If the perceptions of consumer-side interests are correct, we should observe a strong voting bloc among generation firms in the PJM stakeholder process (principally those stakeholders in the GO and TO sectors). We represent several years' worth of stakeholder voting data from PJM as a network (Section 4.1) and use a community detection method [34] to identify coalitions from the voting data (Section 4.2).

Prior analysis of some specific issues in the PJM stakeholder process [19] has found circumstances in which a few voters can sway a voting result. While this prior work showed the importance of such "swing voters" in determining the outcomes of highly contentious voting issues, in the

present paper we use the structure of the voting network to specifically identify these swing voters. We compare the structure of the PJM voting network with several canonical graph models of similar size to the PJM voting network. We observe similar properties in the PJM voting network as would emerge from a model of preferential attachment (we would expect such homophily if stakeholders' perceptions of a strong voting bloc are correct), but we also observe a small number of stakeholders exhibiting a higher node degree than would be expected from a preferential attachment network.

We argue in Section 4.3 that these high-degree voters are effectively swing voters who tend not to vote with any of the identified voting blocs on a consistent basis. Since betweenness centrality has been identified in the literature as an indicator of power within a social network [29, 35–38] we also examine this measure as a potential way to identify swing voters. Finally, we also use the detected community structure to calculate the mixing parameter for each voter and evaluate that as an identifier for a swing voter. We then examine the actual voting behavior for each stakeholder identified as a swing voter by each network structure measure and calculate a false-positive rate for each measure.

This section of our analysis utilizes firm-level voting data from the PJM Members Committee since detailed voting data is only available for that specific stakeholder body. We are not able to quantitatively describe political power in any of the lower-level working groups or task forces, since data from those proceedings are not made public. We gathered data from PJM that contains information on 26 voting items from 2011 to 2015, including the outcome of each vote and the way that each stakeholder voted (we note that by aggregating data across a five-year period we are ignoring any dynamic changes to the structure of the voting network. While this structure may change from year to year depending on the kinds of voting issues presented to the PJM MC, we note that over this period there were very few changes in the composition of the stakeholder group in PJM). Our dataset also includes stakeholder information such as name, sector, subsector, and other asset-related information about specific stakeholders.

4.1. Construction of the Voting Network for the PJM Members Committee. We gathered data from PJM that contains information on 26 voting items from 2011 to 2015. The dataset includes a brief description of the issue being voted on, the outcome of each vote, and that way that each stakeholder voted. Our dataset also includes stakeholder information such as name, sector, and other information about specific stakeholders. Unlike many social networks there is thus little semantic information that we can use to identify ideological preferences or alignment among voters [39]. We use this voting data to construct an undirected voting network [30, 33, 40], in which a vertex represents a single voter in the MC and is connected to another vertex when the two vertices (voters) vote on the same side, yes, no, or abstain, on the same issue. A connection in our voting network thus represents ideological alignment between two voters on a specific issue. In this way our voting network has some commonalties with the similar-view networks constructed on social media platforms [41]. The connections, or edges, are weighted by the frequency of the two connected voters voting together. Figure 4 shows the voting network in the PJM MC when connections represent two stakeholders voting "no" on a specific issue (the no network), while Figure 5 shows the voting network in the PJM MC when connections represent two stakeholders voting "yes" on a specific issue (the yes network). We did construct a network for abstentions, but this network turns out to be quite sparse so it is not shown here.

In Figures 4 and 5, vertices are located on one of the five axes representing each industry sector in an order of degree and the size of vertices is proportional to the weighted degree. Edge colors represent different detected communities, as described further in Section 4.2. Among 147 nodes in the network, there are 21 GOs, 18 TOs, 61 OS's, 30 EDs, and 17 EUCs. The no network has 8,173 edges and an average degree of 111.2 as well as an average weighted degree of 284.83; the yes network has 8,853 links with an average degree of 119.63 and average weighted degree of 505.54.

4.2. Detection of Strong Coalitions. We apply the Louvain method [34, 40] to discover the community structure of the PJM voting network. A number of different community detection algorithms exist [42–46]; we chose the Louvain method because our network has a relatively small number of nodes and relatively large average mixing parameters [45]. The algorithm maximizes modularity through iterative process of clustering nodes and altering community assignments. The modularity is a function that measures the difference between the number of edges within communities and the expected number of randomly placed edges; it has been used in a number of studies of community structure [33, 40, 47–51]. Thus, high modularity is desirable for searching community structure since it implies that there are more edges than expected within communities, or nodes in the same community are more connected than expected [34, 40, 47, 52]. Hence, the scheme optimizes the modularity measure over the possible segmentation of a network and finds a division that produces the largest modularity value. Equation (2) is a mathematical representation of the modularity measure [34] where Aij is the edge weight between vertices i and j, k_i represents the sum of edge weight of vertex i, and ci is the assigned community of vertex i. $m = (1/2m) \sum_{i,j} A_{ij}$ and the delta function $\delta(a, b)$ is 1 if $a = b$ and 0 otherwise.

$$Q = \frac{1}{2m} \sum_{i,j} \left[A_{ij} - \frac{k_i k_j}{2m} \right] \delta \left(c_i, c_j \right) \tag{2}$$

The community detection algorithm identifies three distinct communities in the no network, indicated by the green, yellow, and orange colors in Figure 4. It identifies two distinct communities in the yes network, indicated by the red and blue colors in Figure 5. In the context of voting, we interpret an identified community as a *coalition*, meaning voters in the same community voted more frequently together than voters of the other communities.

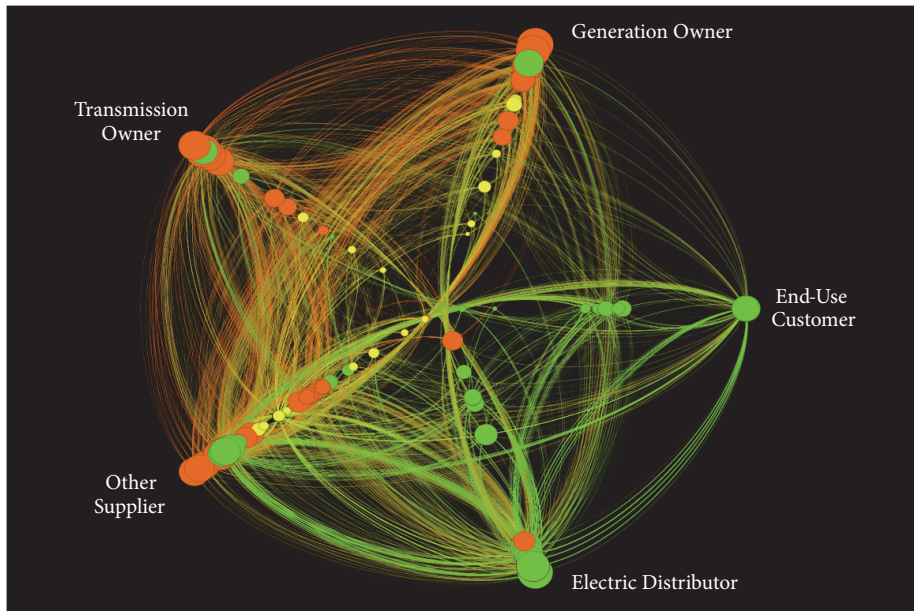

Figure 4: The no voting network in the PJM Members Committee from 2011 to 2015. The node and edge colors correspond to the three different communities detected within the no network.

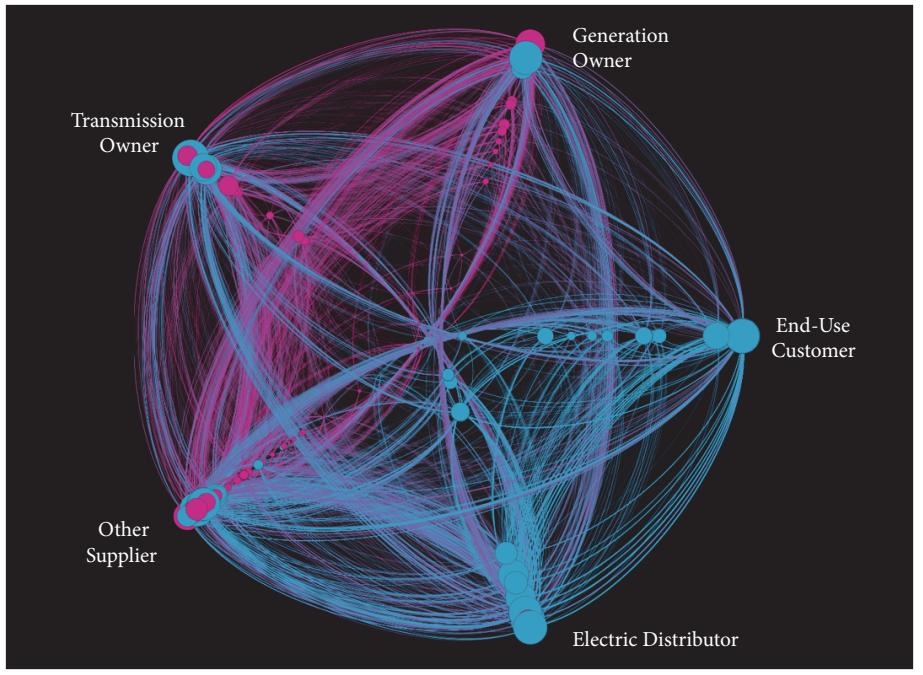

Figure 5: The yes voting network in the PJM Members Committee from 2011 to 2015. The node and edge colors correspond to the two different communities detected within the yes network.

Table 4 shows the number of voters in the communities by sectors in the no network, while Table 5 shows the yes network. Voters in the ED and EUC sectors tend to be entirely contained within the ED-EUC community, while voters in the GO and TO sectors are distributed more evenly among the identified communities.

We acknowledge that modularity may show a *resolution limit* that suggests failure to detect small size communities and there are potential improvements to this limitation [46, 53]. Although this could remain as a future work, this study focuses on identifying sizable coalitions that could exercise political power (e.g., veto power). Still, to address a concern

Table 4: The number of voters in the detected communities by industry sectors (no network).

	Community 1 (orange)	Community 2 (yellow)	Community 3 (green)	Total
Generation Owners (GO)	13 (62%)	5 (24%)	3 (14%)	21
Transmission Owners (TO)	11 (61%)	3 (17%)	4 (22%)	18
Other Suppliers (OS)	25 (41%)	21 (34%)	15 (25%)	61
Electric Distributors (ED)	2 (7%)	0 (0%)	28 (93%)	30
End-Use Customers (EUC)	0 (0%)	0 (0%)	17 (100%)	17

Numbers in parenthesis are percentages of voters in each community within a sector.

Table 5: The number of voters in the detected communities by industry sectors (yes network).

	Community 1 (red)	Community 2 (blue)	Total
Generation Owners (GO)	18 (86%)	3 (14%)	21
Transmission Owners (TO)	13 (76%)	4 (24%)	17
Other Suppliers (OS)	41 (65%)	22 (35%)	63
Electric Distributors (ED)	1 (3%)	29 (97%)	30
End-Use Customers (EUC)	0 (0%)	17 (100%)	17

Numbers in parenthesis are percentages of voters in each community within a sector.

of the quality of detected communities, we adopt a measure called *mixing parameter* [42, 54]. This parameter is defined as

$$\mu = \frac{k_i^{out}}{k_i^{in} + k_i^{out}}, \tag{3}$$

where k_i^{out} is the external degree of node i, meaning the number of edges connecting node i outside its community (or, intercommunity edges), and k_i^{in} is the internal degree of the node or the number of intracommunity edges. If μ is high, the communities are not well defined. In other words, a high value of the mixing parameter indicates that vertices are more connected to vertices of different communities than within the community. The threshold for a "high" value of μ varies in the literature. Reference [55] suggests that any value of μ greater than 0.5 is considered large, while [42] suggests a criterion for μ to be smaller than $(N - n_c)/N$, where N is the total number of nodes and n_c is the number of nodes of the community c. Tables 6 and 7 show the mixing parameters by identified communities in the no and yes networks, respectively. All communities identified in the PJM voting network satisfy the condition suggested by [42], having lower average μ than $(N - n_c)/N$. Only community 2 in the no network (made up largely of voters from the ED and EUC sectors and thus representative of a consumer coalition) has average μ lower than 0.5, which would satisfy the mixing-parameter threshold suggested in [55]. The consumer coalition in the both the no and yes networks has the lowest average mixing parameter, suggesting that voters in the consumer coalition tend to have the same position with the coalition more frequently compared to voters in the supplier coalition.

The strong consumer-side coalition that we identify is consistent with the perception of some of our interview respondents that consumer-side interests wield a greater amount of political power than supplier-side interests. Recall that because of the structure of the voting system in the PJM Members Committee; two sectors that vote in the same way can effectively prevent any potential rule change from passing. The strong ED-EUC coalition suggests that consumer-side interests do possess structural voting power. We do see evidence in the voting data set of four instances in which a proposed rule change failed to pass because the ED-EUC coalition. We do not, however, see evidence in our voting data of a strong supplier-side coalition that is able to ensure or prevent passage of any proposed rule change. Information from our interviews does shed some light on why consumer-side interests are able to form a stronger coalition than supplier-side interests. As one of our stakeholder respondents put it, "Therefore, when there's a load interest or industrial interest vote, you . . . get Generators voting yes, and the reason is because they're actually industrial customers disguised as Generators." (PJM-04). The implication from this quote is that stakeholders in the GO and TO sectors have a more heterogeneous set of interests than voters in the ED or EUC sectors.

4.3. Topological Structure of the Voting Network. Although there have been numerous studies of identification of communities, to the best of our knowledge, topological structure of a voting network is not well-explored, especially given the lack of studies on RTO governance. In this section, we compare degree distribution of PJM MC's voting network to those of common abstract network models: Erdős-Rényi (ER), small-world (SW), and preferential attachment (PA). By doing so, we would be able to check whether the voting network has similar properties of abstract network models and to put the PJM's voting network in the context of existing social network literature.

Table 6: Mixing parameters in detected communities in the no network.

	Community 0 (Supplier coalition)	Community 1 (Supplier coalition)	Community 2 (Consumer coalition)
Number of nodes in the community	51	29	67
Range of mixing coefficient μ within a community	[0, 0.667]	[0.48, 0.769]	[0.147, 0.514]
Average mixing coefficient μ of a community	0.556	0.682	0.449
$(N - n_c)/N$	0.653	0.803	0.544

Table 7: Mixing parameters in detected communities in the yes network.

	Community 0 (Consumer coalition)	Community 1 (Supplier coalition)
Number of nodes in the community	75	73
Range of mixing coefficient μ within a community	[0.049, 0.485]	[0.088, 0.61]
Average mixing coefficient μ of a community	0.417	0.464
$(N - n_c)/N$	0.493	0.507

A summary of our synthetic networks is shown in Table 8. The synthetic networks that we generate are designed to have the same number of nodes and a similar number of edges as the PJM voting network. Our structural analysis uses a version of the PJM voting network with near-unanimous votes removed, since these votes will tend to inflate the node degree distribution. After producing synthetic networks, we tested whether they have a power-law degree distribution by Kolmogorov-Smirnov (KS) goodness-of-fit test (based on 1,000 simulations) [48, 56–58]. Parameters for generating an ER random network [59] are the number of nodes and the probability for drawing an edge between two arbitrary nodes, which in our case is the total number of edges divided by all the possible number of edges with 147 nodes. The parameters for generating small-world networks [60] are dimension of the lattice, number of nodes, number of neighbors, and rewiring probability. We use one dimension, 147 nodes, 28 neighbors, and a rewiring probability of 0.3. The number of neighbors, 28, is set to yield a similar number of edges as the actual PJM voting network (4,116 edges). We generate three small-world networks by three different rewiring probabilities (0.2, 0.3, and 0.5) [60–62]. Finally, we created a scale-free network with 147 nodes and 4,290 edges. To have similar number of edges to the PJM voting network, we specified 33 edges to be added in each time step of the network growth.

Even though the average degrees are similar, the degree distributions show different shape: Figure 6 shows cumulative degree distributions (in log-scale) of all three synthetic networks and the PJM no voting network. The degree distributions of the ER random and the small-world networks are more concentrated around their average degrees than commonly observed synthetic networks, which is due to a small number of nodes (n = 147) with high probability of drawing edges (p = 0.408). The degree distribution of the PJM MC voting network exhibits similar shape to that of the preferential attachment network but the longer tail is more pronounced.

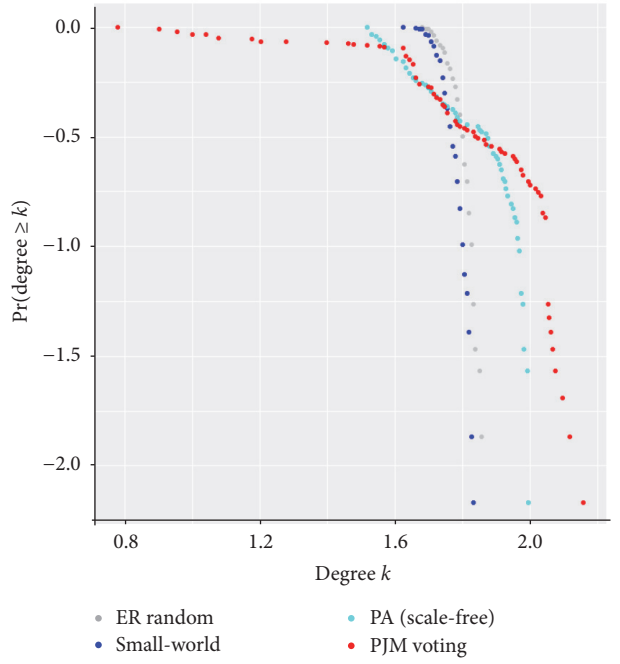

Figure 6: Cumulative degree distribution of the ER random (grey), the small-world (blue), the scale-free (cyan), and the PJM voting (red) networks.

Kolmogorov-Smirnov (KS) tests, also shown in Table 8, reject the null hypothesis that the tested sample is drawn from the power-law distribution. While this is surprising (particularly for our synthetic preferential attachment graphs), examination of the tails of the degree distributions shows why. Figure 7 shows the power-law fit for both the synthetic preferential attachment graph and the PJM voting network. Both have fast-decaying tails but have a small number of nodes with a larger than expected degree.

Based on the structure of the PJM stakeholder process, we argue that these tail voters are likely swing voters, who

Table 8: Comparison between the PJM voting network and synthetic networks.

	PJM voting network	Erdős-Rényi	Small world			Preferential attachment
			p = 0.2	p = 0.3	p = 0.5	
Number of nodes	147	147	147	147	147	147
Number of links	4381	4380	4116	4116	4116	4290
Average degree	59.67	59.59	56	56	56	58.37
Range of degrees	[6, 144]	[48, 72]	[43, 70]	[46, 69]	[42, 68]	[33, 99]
Range of betweenness centrality	[0, 0.06157]	[0.00258, 0.00595]	[0.00226, 0.00667]	[0.00224, 0.00633]	[0.00231, 0.00653]	[0.00067, 0.01134]
Power-law exponent	3.205	8.637	8.285	8.127	8.038	2.93
KS t-test result	0	0.011	0	0	0	0

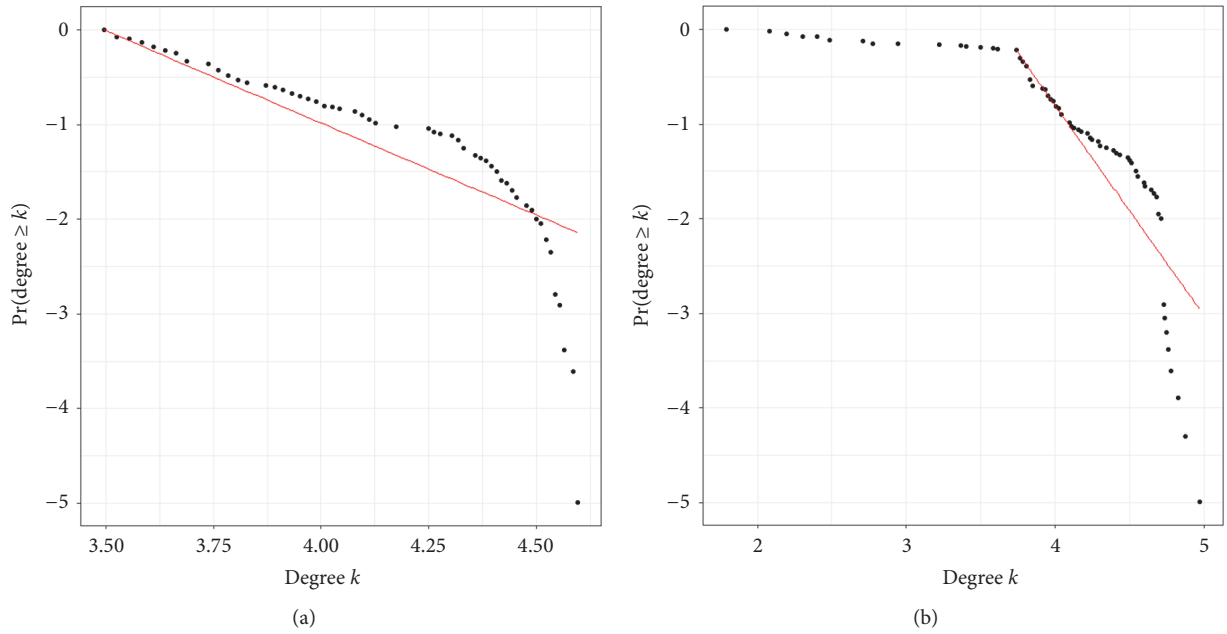

Figure 7: Power-law fitting of (a) the scale-free network and (b) the PJM voting network.

may be able to sway the final voting outcome by switching their positions. Our reasoning behind this argument is that if a voter is connected by a degree to which one can explain with homophily, then the voter is just following a common behavior: voting with others who have shared interests. If, however, a voter is connected to more voters than we can explain with homophily, then it means that the voter has voted with diverse groups of voters who might have opposite interests. In other words, given the community structure that we have detected in the PJM MC the voters in the tail of the degree distribution in Figures 6 and 7 are those who have voted with all of the coalitions at various points.

We thus have a more nuanced view of how to capture whether the tail voters are, in fact, swing voters. We have already seen how we expect swing voters to have high degree. Because our voting network covers a number of different voting issues over a period of five years, a swing voter would also be one that connected two voters that otherwise are unconnected. Thus, we would also expect swing voters to have high betweenness centrality. Finally, we would also expect swing voters to be connected to multiple detected communities (i.e., sometimes voting with consumer interests and sometimes voting with supplier interests), implying a high mixing parameter for these voters. Figure 8 shows the betweenness centrality distribution and the mixing-parameter distribution of the PJM voting network. Most voters in the network have low betweenness centrality value, between 0 and 0.01, but there are a few that have extremely higher betweenness centrality than the other nodes; four voters have the centrality over 0.03 including one voter with the centrality value over 0.06. The mixing-parameter distribution is more symmetric than the betweenness distribution, though it is somewhat left-skewed.

To examine whether our network structure measures (node degree, betweenness centrality, and mixing parameter) are sufficient to identify swing voters, we correlate these measures for potential swing voters (those in the tail of the degree distribution) with the proportion of time that these voters voted with the consumer coalition on issues that we identified as contentious: based on issue's clear divisiveness between consumers and suppliers and existence of strong coalition formation (an example of such a contentious issue was a set of proposed pricing changes in PJM's market for generation capacity, further described in [19]. Some of these proposed pricing changes would have clearly benefited suppliers and harmed consumers, while others would have had the opposite effect. We identified twelve such contentious issues for this analysis). Voting with the consumer coalition very frequently or very infrequently would suggest that the voter in question was not actually a swing voter. Thus, network structure measures can detect potential swing voters, while a review of the frequency of voting with the consumer coalition acts as a kind of false-positive test.

Table 9 shows the frequency of a false positive when we attempt to identify swing voters using each of our three structural measures. Each column of Table 9 shows the top fifteen voters (identified by name) based on node degree, betweenness centrality, and mixing parameter. The percentage figure next to each voter's name is the frequency with which that voter voted with the consumer coalition on contentious issues.

We note a few important observations about Table 9. First, there are relatively few voters that are identified as potential swing voters based on all three network metrics. Direct Energy and Enerwise are example of voters that are identified as potential swing voters regardless of the network metric used. Second, the false-positive rate for

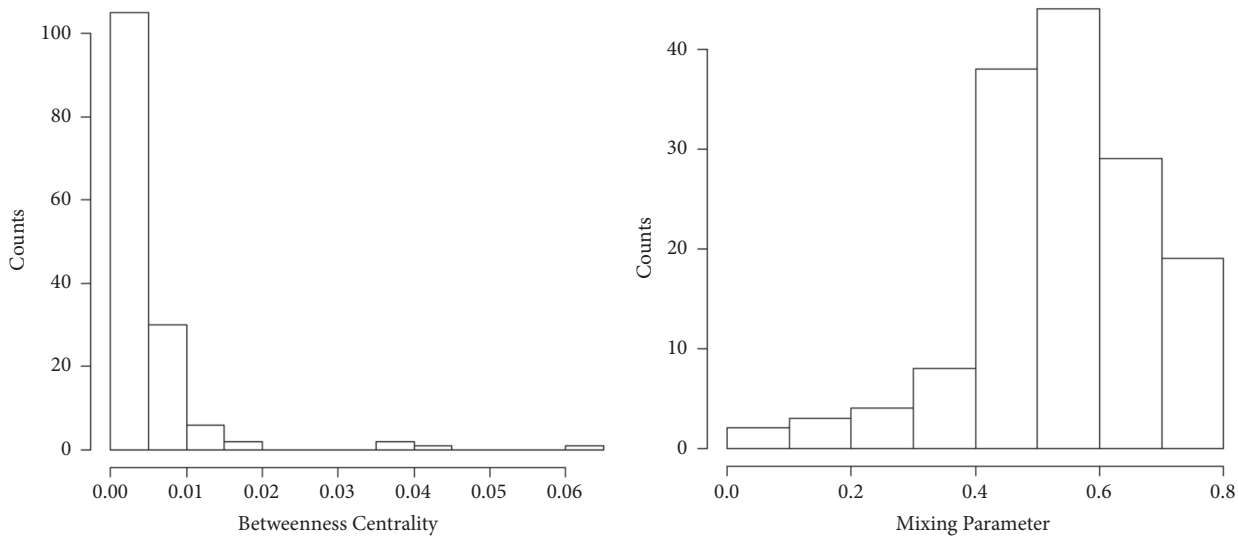

Figure 8: Histogram of (a) (normalized) Betweenness centrality and (b) mixing-parameter distribution of the PJM voting network.

Table 9: Top fifteen voters in the PJM voting network based on node degree, betweenness centrality, and mixing parameter. The figures in the % column represent the frequency with which each voter voted with the consumer coalition on contentious rule changes in PJM.

Degree	**%**	**Betweenness Centrality**	**%**	**Mixing parameter**	**%**
Brookfield Energy Marketing LP	38%	Brookfield Energy Marketing LP	38%	Direct Energy Business, LLC	50%
Potomac Electric Power Company	40%	Potomac Electric Power Company	40%	Enerwise Global Technologies, Inc	33%
PBF Power Marketing LLC	40%	PBF Power Marketing LLC	40%	MidAtlantic Power Partners, LLC	50%
Enerwise Global Technologies, Inc	33%	TransCanada Power Marketing Ltd	25%	Iron Mountain Generation LLC	33%
Direct Energy Business, LLC	50%	Central Virginia Electric Cooperative	100%	West Deptford Energy, LLC	33%
Iron Mountain Generation LLC	33%	Virginia Electric & Power Company	0%	Black Oak Energy, LLC	50%
Central Virginia Electric Cooperative	100%	Energy Consulting Services, LLC	100%	Apple Group, LLC	33%
West Deptford Energy, LLC	33%	Invenergy LLC	0%	Dyon, LLC	33%
Apple Group, LLC	33%	Enerwise Global Technologies, Inc	33%	E Minus LLC	33%
Dyon, LLC	33%	Direct Energy Business, LLC	50%	Great Bay Energy I, LLC	33%
E Minus LLC	33%	Galt Power Inc	100%	Hexis Energy Trading, LLC	33%
Great Bay Energy I, LLC	33%	Borough of Lavallette, New Jersey	100%	Mac Trading, Inc	33%
Hexis Energy Trading, LLC	33%	The Trustees of the University of Pennsylvania	100%	Monterey MA, LLC	33%
Mac Trading, Inc	33%	Borough of Madison, New Jersey	100%	Pure Energy, Inc	33%
Monterey MA, LLC	33%	Borough of Milltown, New Jersey	100%	BJ Energy, LLC	33%

betweenness centrality as a swing voter identification metric is quite high. Two-thirds of those identified as swing voters using betweenness centrality either voted with the consumer coalition 100% of the time on contentious issues or never voted with the consumer coalition on contentious issues. By this criterion, the false-positive rate for node degree is one out of fifteen, and the false-positive rate for the mixing parameter is zero. The betweenness centrality may in this case be capturing voters that make connections between the nonconsumer coalitions. Finally, we note a high degree of overlap between those voters identified as potential swing voters using node degree and those identified using the mixing parameter. Eleven of the voters identified as potential swing voters using node degree were also identified using the mixing parameter.

5. Conclusion

Technological change in electric power systems requires not only that physical systems adapt to integrate new technologies and market players, but also that policies and rules adapt to support that technological integration. The process of policy and rule adaptation in many areas of the world is not driven by the decisions of governments or other central decision-making authorities but emerges as the output of a political process involving stakeholders representing many divergent interests. These stakeholder-driven decision processes can be modeled theoretically, but the literature on governance of regional electricity organizations has only recently attempted to do so.

This work adds to an emerging body of literature on stakeholder decision processes and electricity policy formation by developing and illustrating a novel method for integrating qualitative information elicited from stakeholder perceptions with quantitative voting data; using community detection methods to identify political coalitions among stakeholders in Regional Transmission Organizations; and leveraging voting network structure to identify potential swing voters in the stakeholder group. Using the PJM Regional Transmission Organization in the United States as a case study, we elicited perceptions of the stakeholder process from process participants via semistructured interviews. We treated those perceptions as hypotheses regarding the presence and possession of political power and used a network representation of voting data in PJM to evaluate these hypotheses. We find some evidence in support of the perception that customer-side interests form a strong coalition that is able to exercise some power in defeating proposed rule changes in the PJM market. We find less evidence in support of the perception that supplier-side interests are able to exercise a similar amount of political power in the PJM Members Committee. The structure of the voting network and detected communities, particularly as embodied in the node degree and mixing parameter, also allow us to identify a number of stakeholder participants that act as swing voters on highly contentious rule changes. These swing voters tend not to vote with any one of the identified coalitions on a consistent basis and may thus be engaged in vote trading or other strategic activity.

The framework illustrated for the PJM Regional Transmission Organization in the United States is portable to other contexts and represents an approach to defining questions and hypotheses about stakeholder-driven governance, using data from these processes to build models and evaluate hypotheses and (as part of future work) using these models to evaluate alternative structures or voting rules for stakeholder processes.

Appendix

Interview Protocol and Questions

There were three versions of the interview protocol used. Shown here is the second and main version. The first version used for early interviews was modified in language, especially in the probing questions, to better reflect a natural flow of conversation. The content remained essentially the same. A customized protocol was used for the final interview to target the respondent's specific employment background. All interviews were semistructured.

Opening Script. The primary goal of our research project is to understand how the decision making process works at RTOs. We've been trying to understand the formal process; we need to understand better the experiences of those who participate in the actual process. Our questions are really a conversational guide to help us understand your experience at/with ___ [RTO].

Demographics/History

How have you been involved with ____ [RTO]?

Probe: How long have you been involved with _____ [RTO]?

Understanding the Process for Decision Making

How would you characterize the stakeholder process at ____ [RTO]?

Probe: What is a typical meeting like?

Probe: Are there any other elements in the process that I wouldn't understand from information on the website?

Probe:

It sounds like you've had a *positive experience*; can you tell me more about what works well in the process? Is there anything that you would change?

It sounds like you've had a *negative experience*; what were some of the challenges or what would you change in the process?

How would I know when a decision has been made?

Probe: Who is involved in deciding what items are put on the agenda or how quickly issues move through the process?

Probe: Could you provide an example?

Do stakeholders or staff work on issues outside of the formal meetings?

[UNDERSTAND EXPERIENCE / SENSE OF RTOs]

Probe: How does that work?

Probe: Is it important to have certain stakeholders or staff involved in an issue?

Understanding the Stakeholder Groups

Who are the stakeholder groups involved [in the issues you are working on?

Probe: Who are the stakeholders frequently involved in stakeholder processes?

How would you characterize the stakeholders?

How would you describe the influence of certain stakeholder groups?

How would I recognize different stakeholder groups in a meeting?

What is it like for newcomers to participate in the stakeholder process?

Probe: What have ____ [names of new stakeholder groups] had to do to be part of the process?

Probe: How would you know if a newcomer is doing something wrong or how would you help a newcomer figure out the process?

Understanding Influences

Are issues regarding transmission, markets and reliability related?

Are these coordinated in the decision making process?

What are some common disagreements you see in the process?

How do people enter into leadership positions?

I'm trying to understand leadership. Do stakeholder groups identify formal or informal leaders?

Can you describe the board/advisory committee nomination process?

Conclusion

That's all for my questions. What else should I know or be asking in order to understand the _____ [RTO]'s processes, stakeholder groups and participation?

Is there anything you would like to ask me?

Would you mind recommending anyone else who you think I should speak with that would be interested in participating?

Thank you for your time. We really appreciate it!

Data Availability

The data used to construct the PJM voting network are freely available from the PJM Members Committee website at http://www.pjm.com/committees-and-groups/committees/mc.aspx. Information from the semistructured interviews is restricted by the Office of Research Protections at the Pennsylvania State University in order to protect the privacy of interview respondents. Data are available from the corresponding author for researchers who meet the criteria for access to confidential data.

Conflicts of Interest

The authors declare no conflicts of interest.

Acknowledgments

The authors acknowledge support from the US National Science Foundation under award SES-1261867 as well as the Alfred P. Sloan Foundation for their support of the workshop "The Nature of Technological, Social and Industrial Transition in the Electric Power Industry," held at the Santa Fe Institute in March 2016. We thank participants at the Santa Fe Workshop and the CRRI Eastern Workshop on Regulation and Competition for helpful comments and suggestions. Additional helpful feedback was provided by Stephanie Lenhart, Natalie Nelson-Marsh, Christina Simeone, David Solan, Benjamin Stafford, and Elizabeth Wilson. The authors would like to extend particular thanks to David Anders at PJM for his assistance in understanding the PJM stakeholder process and for locating data related to voting outcomes from the PJM Members Committee.

References

[1] J. C. Stephens, E. J. Wilson, and T. R. Peterson, "Socio-Political Evaluation of Energy Deployment (SPEED): An integrated research framework analyzing energy technology deployment," *Technological Forecasting & Social Change*, vol. 75, no. 8, pp. 1224–1246, 2008.

[2] S. Blumsack, N. Johnson, and E. Wilson, "Cross-Organizational Learning in Regional Planning for Electric Transmission," in *In Association of Public Policy Analysis and Management Annual Research Meeting*, Albuquerque, New Mexico, 2014.

[3] N. Nelson-Marsh, D. Solan, S. Lenhart, and J. Kopczynski, "Power Innovation in Regional Transmission Organizations: Understanding the Complexity of Interorganizational Planning," in *In Association of Public Policy Analysis and Management Annual Research Meeting*, Albuquerque, New Mexico, 2014.

[4] S. Lenhart, N. Nelson-Marsh, E. J. Wilson, and D. Solan, "Electricity governance and the Western energy imbalance market in the United States: The necessity of interorganizational collaboration," *Energy Research and Social Science*, vol. 19, pp. 94–107, 2016.

[5] B. A. Stafford and E. J. Wilson, "Winds of change in energy systems: Policy implementation, technology deployment, and regional transmission organizations," *Energy Research and Social Science*, vol. 21, pp. 222–236, 2016.

[6] M. Deissenroth, M. Klein, K. Nienhaus, and M. Reeg, "Assessing the Plurality of Actors and Policy Interactions: Agent-Based Modelling of Renewable Energy Market Integration," *Complexity*, vol. 2017, Article ID 7494313, 24 pages, 2017.

[7] N. Paine, F. R. Homans, M. Pollak, J. M. Bielicki, and E. J. Wilson, "Why market rules matter: Optimizing pumped hydroelectric storage when compensation rules differ," *Energy Economics*, vol. 46, pp. 10–19, 2014.

[8] A. J. Prabhakar, L. Rauch, L. Hecker, and J. Lawhorn, "Business case justification for multi-value projects in the MISO Midwest region," in *Proceedings of the 2013 IEEE Power and Energy Society General Meeting, PES 2013*, pp. 1–5, IEEE, Canada, July 2013.

[9] J. C. Stephens, E. J. Wilson, and T. R. Peterson, *Smart grid (R) evolution*, Cambridge University Press, 2015.

[10] F. Xue, Y. Xu, H. Zhu, S. Lu, T. Huang, and J. Zhang, "Structural evaluation for distribution networks with distributed generation based on complex network," *Complexity*, vol. 2017, Article ID 7539089, 10 pages, 2017.

[11] J. Jackson, "Improving energy efficiency and smart grid program analysis with agent-based end-use forecasting models," *Energy Policy*, vol. 38, no. 7, pp. 3771–3780, 2010.

[12] D. M. Jiménez-Bravo, J. F. De Paz, G. Villarrubia, J. Bajo, and D. M. Jiménez-Bravo, "Dealing with Demand in Electric Grids with an Adaptive Consumption Management Platform," *Complexity*, vol. 2018, Article ID 4012740, 14 pages, 2018.

[13] M. Alizadeh, A. Scaglione, J. Davies, and K. S. Kurani, "A scalable stochastic model for the electricity demand of electric and plug-in hybrid vehicles," *IEEE Transactions on Smart Grid*, vol. 5, no. 2, pp. 848–860, 2014.

[14] D. P. Chassin, J. C. Fuller, and N. Djilali, "GridLAB-D: An agent-based simulation framework for smart grids," *Journal of Applied Mathematics*, vol. 2014, Article ID 492320, 2014.

[15] M. H. Dworkin and R. A. Goldwasser, "Ensuring consideration of the public interest in the governance and accountability of regional transmission organizations," *Energy LJ*, vol. 28, p. 543, 2007.

[16] C. Simeone, *Can reforms improve outcomes*, Kleinman Center for Energy Policy, 2018, http://kleinmanenergy.upenn.edu/sites/default/files/PJM%2020Governance%20Reforms.pdf.

[17] K. Yoo and S. Blumsack, "Can Capacity Markets be Designed by Democracy?" in *Proceedings of the 50th Hawaii International Conference on System Sciences*, Waikoloa HI, 2017.

[18] K. Yoo and S. Blumsack, "Can capacity markets be designed by democracy?" *Journal of Regulatory Economics*, vol. 53, no. 2, pp. 127–151, 2018.

[19] M. James, K. B. Jones, A. H. Krick, and R. R. Greane, "How the RTO Stakeholder Process Affects Market Efficiency," *R Street Policy Study*, vol. 112, p. 19, 2017.

[20] PJM. (2015c). Rosters of the Members Committee. http://www.pjm.com/committees-and-groups/committees/mc.aspx.

[21] A. N. Kleit, *Electric Choices*, Rowman & Littlefield, Lanham, MD, USA, 2007.

[22] PJM. (2016). Committees & Groups FAQs. https://learn.pjm.com/pjm-structure/member-org/committees-groups-faqs/sector-weighted-voting.aspx.

[23] A. Van de Ven, *Engaged Scholarship A Guide for Organizational and Social Research*, Oxford University Press, Oxford, New York, USA, 2007.

[24] J. M. Corbin and A. Strauss, "Grounded theory research: procedures, canons, and evaluative criteria," *Qualitative Sociology*, vol. 13, no. 1, pp. 3–21, 1990.

[25] B. Glaser and A. Strauss, *The Discovery of Grounded Theory: Strategies for Qualitative Research*, Aldine, Chicago, Ill, USA, 1967.

[26] A. Strauss, "Grounded Theory Methodology," in *Handbook of Qualitative Research*, Y. S Denzin and N. K. Lincoln, Eds., pp. 217–285, Sage Publications, Thousand Oaks, Calif, USA, 1994.

[27] D. E. Campbell, "Social Networks and Political Participation," *Annual Review of Political Science*, vol. 16, no. 1, pp. 33–48, 2013.

[28] J. H. Fowler, "Connecting the congress: A study of cosponsorship networks," *Political Analysis*, vol. 14, no. 4, pp. 456–487, 2006.

[29] K. Ingold, "Network structures within policy processes: Coalitions, power, and brokerage in swiss climate policy," *Policy Studies Journal*, vol. 39, no. 3, pp. 435–459, 2011.

[30] D. Lazer, "Networks in Political Science: Back to the Future," in *PS: Political Science & Politics*, vol. 44, pp. 61–68, Cambridge University Press, 1 edition, 2011.

[31] P. J. Mucha, T. Richardson, K. Macon, M. A. Porter, and J.-P. Onnela, "Community structure in time-dependent, multiscale, and multiplex networks," *Science*, vol. 328, no. 5980, pp. 876–878, 2010.

[32] M. D. Ward, K. Stovel, and A. Sacks, "Network analysis and political science," *Annual Review of Political Science*, vol. 14, pp. 245–264, 2011.

[33] W. Andrew Scott, P. Liuyi, H. James, J. Peter, and M. Alexander Porter, *Party Polarization in Congress: A Network Science Approach*, Porter, 2009, https://papers.ssrn.com/sol3/papers.cfm?abstract_id=1437055.

[34] V. D. Blondel, J. Guillaume, R. Lambiotte, and E. Lefebvre, "Fast unfolding of communities in large networks," *Journal of Statistical Mechanics: Theory and Experiment*, vol. 2008, no. 10, Article ID P10008, 2008.

[35] C. Ansell, S. Reckhow, and A. Kelly, "How to reform a reform coalition: Outreach, agenda expansion, and brokerage in Urban school reform," *Policy Studies Journal*, vol. 37, no. 4, pp. 717–743, 2009.

[36] L. C. Freeman, "Centrality in social networks conceptual clarification," *Social Networks*, vol. 1, no. 3, pp. 215–239, 1978-1979.

[37] J. Lienert, F. Schnetzer, and K. Ingold, "Stakeholder analysis combined with social network analysis provides fine-grained insights into water infrastructure planning processes," *Journal of Environmental Management*, vol. 125, pp. 134–148, 2013.

[38] Y. Erjia and Y. Ding, "Applying Centrality Measures to Impact Analysis: A Coauthorship Network Analysis," *Journal of the American Society for Information Science and Technology*, vol. 60, no. 10, pp. 2107-18, 2009.

[39] Z. Xia and Z. Bu, "Community detection based on a semantic network," *Knowledge-Based Systems*, vol. 26, pp. 30–39, 2012.

[40] M. E. J. Newman and M. Girvan, "Finding and evaluating community structure in networks," *Physical Review E: Statistical, Nonlinear, and Soft Matter Physics*, vol. 69, no. 2, Article ID 026113, 2004.

[41] Z. Bu, Z. Xia, and J. Wang, "A sock puppet detection algorithm on virtual spaces," *Knowledge-Based Systems*, vol. 37, pp. 366–377, 2013.

[42] A. Lancichinetti and S. Fortunato, "Community Detection Algorithms: A Comparative Analysis," *Physical Review E*, vol. 80, no. 5, Article ID 056117, p. 10, 2009.

[43] A. Lancichinetti, S. Fortunato, and F. Radicchi, "Benchmark graphs for testing community detection algorithms," *Physical Review E: Statistical, Nonlinear, and Soft Matter Physics*, vol. 78, no. 4, Article ID 046110, 2008.

[44] G. K. Orman, V. Labatut, and H. Cherifi, "Towards realistic artificial benchmark for community detection algorithms evaluation," *International Journal of Web Based Communities*, vol. 9, no. 3, pp. 349–370, 2013.

[45] Z. Yang, R. Algesheimer, and C. J. Tessone, "A Comparative Analysis of Community Detection Algorithms on Artificial Networks," *Scientific Reports*, vol. 6, no. 1, 2016.

[46] P. Ronhovde and Z. Nussinov, "Multiresolution community detection for megascale networks by information-based replica correlations," *Physical Review E: Statistical, Nonlinear, and Soft Matter Physics*, vol. 80, no. 1, Article ID 016109, 2009.

[47] M. E. J. Newman, "Modularity and community structure in networks," *Proceedings of the National Acadamy of Sciences of the United States of America*, vol. 103, no. 23, pp. 8577–8582, 2006.

[48] A. Clauset, M. E. J. Newman, and C. Moore, "Finding community structure in very large networks," *Physical Review E: Statistical, Nonlinear, and Soft Matter Physics*, vol. 70, no. 6, Article ID 066111, 2004.

[49] M. A. Porter, P. J. Mucha, M. E. J. Newman, and A. J. Friend, "Community structure in the United States House of Representatives," *Physica A: Statistical Mechanics and its Applications*, vol. 386, no. 1, pp. 414–438, 2007.

[50] K. Wakita and T. Tsurumi, "Finding community structure in mega-scale social networks: [extended abstract]," in *Proceedings of the 16th International World Wide Web Conference (WWW '07)*, pp. 1275-1276, Banff, Canada, May 2007.

[51] Y. Zhang, A. J. Friend, A. L. Traud, M. A. Porter, J. H. Fowler, and P. J. Mucha, "Community structure in Congressional cosponsorship networks," *Physica A: Statistical Mechanics and its Applications*, vol. 387, no. 7, pp. 1705–1712, 2008.

[52] M. E. Newman, "Fast algorithm for detecting community structure in networks," *Physical Review E*, vol. 69, no. 6, Article ID 066133, 2004.

[53] S. Fortunato and M. Barthélemy, "Resolution limit in community detection," *Proceedings of the National Academy of Sciences of the United States of America* , vol. 104, no. 1, pp. 36–41, 2006.

[54] G. K. Orman, V. Labatut, and H. Cherifi, "Qualitative Comparison of Community Detection Algorithms," in *Digital Information and Communication Technology and Its Applications*, vol. 167 of *Communications in Computer and Information Science*, pp. 265–279, Springer, Berlin, Germany, 2011.

[55] F. Radicchi, C. Castellano, F. Cecconi, V. Loreto, and D. Paris, "Defining and identifying communities in networks," *Proceedings of the National Acadamy of Sciences of the United States of America*, vol. 101, no. 9, pp. 2658–2663, 2004.

[56] A. Clauset, C. R. Shalizi, and M. E. . Newman, "Power-law distributions in empirical data," *SIAM Review*, vol. 51, no. 4, pp. 661–703, 2009.

[57] A. N. Kolmogorov, "Sulla determinazione empirica di una legge di distribuzione," *Giornale dell'Instituto Italiano degli Attuari*, vol. 4, pp. 83–91, 1933.

[58] V. Smirnov Nikolai, "Estimate of Deviation between Empirical Distribution Functions in Two Independent Samples," *Bulletin Moscow University*, vol. 2, no. 2, p. 16, 1939.

[59] P. Erdös and A. Rényi, "On random graphs," *Publicationes Mathematicae*, vol. 6, pp. 290–297, 1959.

[60] D. J. Watts and S. H. Strogatz, "Collective dynamics of "small-world" networks," *Nature*, vol. 393, no. 6684, pp. 440–442, 1998.

[61] H. Hong, B. J. Kim, M. Y. Choi, and H. Park, "Factors that predict better synchronizability on complex networks," *Physical Review E: Statistical, Nonlinear, and Soft Matter Physics*, vol. 69, no. 6, 2004.

[62] Q. Wang, M. Perc, Z. Duan, and G. Chen, "Impact of delays and rewiring on the dynamics of small-world neuronal networks with two types of coupling," *Physica A: Statistical Mechanics and its Applications*, vol. 389, no. 16, pp. 3299–3306, 2010.

Hindawi
Complexity
Volume 2018, Article ID 3568085, 16 pages
https://doi.org/10.1155/2018/3568085

Research Article

Countering Protection Rackets Using Legal and Social Approaches: An Agent-Based Test

Áron Székely[1,2] **Luis G. Nardin**[3] **and Giulia Andrighetto**[1,2,4]

[1]*Institute of Cognitive Sciences and Technologies, Italian National Research Council, Rome, Italy*
[2]*Institute for Futures Studies, Stockholm, Sweden*
[3]*Dept. of Informatics, Brandenburg University of Technology, Cottbus, Germany*
[4]*Mälardalen University, Vasteras, Sweden*

Correspondence should be addressed to Áron Székely; aron.szekely@iffs.se

Received 18 May 2018; Revised 20 August 2018; Accepted 16 September 2018; Published 2 December 2018

Guest Editor: Bernardo A. Furtado

Protection rackets cause economic and social damage across the world. States typically combat protection rackets using legal strategies that target the racketeers with legislation, strong sentencing, and increasing the presence and involvement of police officers. Nongovernmental organizations, conversely, focus on the rest of the population and counter protection rackets using a social approach. These organisations attempt to change the actions and social norms of community members with education, promotional campaigns, and discussions. We use an agent-based model, which draws on established theories of protection rackets and combines features of sociological and economic perspectives to modelling social interactions, to test the effects of legal and social approaches. We find that a legal approach is a necessary component of a policy approach, that social only approaches should not be used because they lead to large increases in violence, and that a combination of the two works best, although even this must be used carefully.

1. Introduction

Protection rackets are widespread and can be found in many countries in the world. Although they vary in multiple ways, mafias can be defined as groups that specialise in the production and sale of protection to people and businesses [1, 2]. Put another way, mafias run protection rackets. The Sicilian Mafia [1]—as well as other mafias in Italy [3], the Russian Mafia [2, 4, 5], and the Yakuza [6] may all be considered to be mafias. The protection they provide includes the supply of real, but often illegal, services, whereby the racketeers protect businesses from criminals and legal competition, as well as pure extortion, in which the only "protection" that racketeers provide is from themselves [1]. Ultimately, mafias harm the societies in which they operate. Among the many costs are those that they impose on businesses for maintaining security, the direct costs of crime, the state-level costs to combatting and countering protection rackets, and the help that they provide to criminals and businesses to conduct illegal transactions [7–13]. While estimates of the costs vary greatly, all agree upon the basic point: the costs of protection rackets are substantial [9–15]. One study, for instance, estimates that the presence of mafias has lowered GDP growth per capita by 16% in Apulia and Basilicata (regions of Italy) relative to "synthetic controls" [9], while a much more inclusive estimate by the United Nations Office on Drugs and Crime calculates the crime proceeds of transnational organised crime at $0.9 trillion [16]. Despite the damage caused by protection rackets, they have proven to be resilient. A core difficulty around combatting them is that they comprise a complex system with multiple relevant actors including a state, a mafia (of which there may be multiple competing against each other), shopkeepers and business-people, consumers, nongovernmental organisations, and the rest of society, as well as nonlinear feedback loops between the actions of these actors. Another problem is that it is extremely difficult to conduct experiments on different policies to test their causal effects. Yet, doing so would allow knowledge about effective counter-mafia techniques to accumulate. To understand this usually hidden phenomenon of protection

rackets, and test policy approaches to countering them, we use computational tools. This is different from the tools traditionally used in criminology although there are some recent exceptions [17, 18].

Specifically, our contribution here is to use our agent-based model (ABM) of protection rackets, configured to represent a single neighbourhood in the city of Palermo, to conduct experiments that are relevant to policy, with a focus on the dynamics of social norm change, and discuss the implications of these results for countering protection rackets. We also describe the theoretical grounding of the model. We have presented our model before from a technical perspective in [19], and the simulator underlying the model has been described in [20]. The model, the normative architecture, and some of the results are described in the deliverables of the FP7 EU project GLODERS (deliverables 3.1, 3.3, and 3.4). Some preliminary results are published in a conference proceedings [21] and the model as a book chapter [22]. We use our ABM to ask how effective are laws alone at countering protection rackets? How resilient are any effects that emerge? Are laws sufficient to change social norms and promote a "culture of legality?". Is a social approach capable of countering protection rackets? Our experimental tests yield insights into the policies that may be effective, the policies that are unlikely to be effective, and the policies that have troubling side effects. They also allow us to consider the resiliency and long-term effects of these approaches.

ABMs allow researchers to observe the social system under study at multiple levels. They can observe agents' cognitive processes, their individual behaviours, and the patterns of behaviour that emerge from their interactions. As an example of the first level, we could inspect the "minds" of individuals and investigate the dynamics of the expectations and beliefs that support certain behaviours and their change. Such a multilevel investigation is crucial for enriching our understanding of this social phenomenon. ABMs also allow researchers to manipulate variables and run experiments that could not be conducted in real settings. We cannot run field experiments on the different counter-racket approaches, so we test them in our virtual world [17].

The entities in our model are the *state*, the *mafia*, business-people (*entrepreneurs*), the broader population (*consumers*), and a nongovernmental (*NGO*) antimafia organisation. We gave these entities rules on how to behave based on the literature in criminology, discussions with organised crime experts (see Validation for details), and information extracted from specialised databases. We then use our ABM to test two common approaches of combatting mafias. To counter protection rackets, governments typically use a top-down *legal approach*. They enact and enforce legislation, and increase policing and sentencing, in an attempt to imprison mafiosi. Nongovernmental organisations use alternative means. They use a bottom-up *social approach* to change peoples' actions through nonlegal means. Often this is aimed to shape the expectations and beliefs of the population about the socially appropriate action to take—"reporting protection racketeers to the police" for instance. In other words, they work on the social norms of a population. Educational and promotional campaigns, communal discussions, and commitment devices—asking to consumers to sign declarations stating that they commit to not buying from pizzo-paying shops, are all tools in the NGO toolkit [23, 24].

In guiding our ABM development, we draw on two, out of many, theoretical approaches [25]. One approach, which can be found predominantly in the early works on the Sicilian Mafia, *emphasises the role of culture* in shaping protection rackets and determining behaviour [26–31]. Schneider and Schneider [30], for instance, argue that cultural codes celebrating honour, cleverness, and friendship are especially important for understanding the organisation and success of the mafia (p. x). When characterising the mafia too, many of these scholars focus on culture. For them "mafiosi personified a series of attitudes and values, a 'subculture' widespread throughout the whole of Sicilian society" [32]. Santoro describes another example of this approach: Pitré "famously argued against the identification of Mafia as a criminal social organization, insisting on its being a diffuse cultural attitude instead" [25]. When these authors make their substantive claims, among them that the Sicilian Mafia is not a united organisation, they employ a cultural focus to elucidate their arguments.

Another, more recent but now-widespread, approach relies on the theoretical framework of economics to explain the features and success of organised crime and mafias. It draws on, among others, "game theory, transaction costs analysis, economic neo-institutionalism" [25] and uses *beliefs*, *preferences*, *and constraints* as the core components of its explanations. It provides explanations at the individual level and in terms of people's decisions. Exemplified in the foundational works of Thomas Schelling [33] and Diego Gambetta [1, 34], this approach draws parallels between protection rackets and businesses. Gambetta, for instance, characterises the Sicilian Mafia as being involved in the industry of private protection and that low levels of trust (the belief that people will cheat other when possible) leads to a demand for protection that is fulfilled by those who are both willing to provide it (based on certain preferences) and are able to do so given their resources.

A fundamental distinction between these two theoretical approaches is in their conception of human nature. The cultural perspective relies on *Homo Sociologicus* as its model: an "oversocialised conception of man" that presumes people unthinkingly follow the social norms that they have internalised, blindly shifting their actions according to others' expectations [35, 36]. Conversely, the economic perspective employs a *Homo Economicus* view of human nature in which people follow their incentives, often self-interested ones, irrespective of social norms or others disapproval, when deciding what to do [35].

Extensive research now shows that both contain insights. Incentives are fundamental drivers of human behaviour [37–40], yet people consider also social factors when deciding how to act (e.g., [35, 41–43]). Social norms are one of the most important of these social factors [40]. In addition to the decades of observational studies (e.g., [44]), extensive experimental evidence demonstrates the important influence of social norms on behaviour [45–55].

Social norms can be defined as shared behavioural rules proscribing or prescribing certain actions that are followed because of reciprocal expectations and, in some cases, social punishment [51, 56–58]. Norms may, in their simplest incarnations, take the forms "do *X*" or "do not do *Y*" [37], but they can be more complex and take conditional forms. The expectations motivating norm compliance can be separated into empirical and normative expectations [56]. The former are people's beliefs about how prevalent a behaviour is, while the latter are people's beliefs about what others expect them to do. From another perspective, social norms can also be considered as particular components of institutions [59].

Social norms influence many aspects of our lives: shaping how we interact with our family, friends, and strangers [60]. Given that social norms permeate social life, it seems highly likely that they also operate in the domain of protection rackets. There are empirical hints to back up this supposition. Norms of fairness, reciprocity, in-group favouritism, and omertà—a code of silence—are all plausibly important in affecting paying pizzo, money paid by businesses and individuals to mafias in exchange for protection, and reporting pizzo requests to the police (see [61]).

Our model integrates Homo Economicus and Homo Sociologicus. Key agents in our model, entrepreneurs, who represent business people, and consumers, who represent the broader population of citizens, consider both their incentives and social norms when deciding how to act. These decision makers' utility is based on the economic rewards that they obtain and on the degree to which their actions comply with social norms, in the form of taking actions considered as socially appropriate and avoiding those viewed as socially inappropriate. Ultimately, they weigh up both individual and normative reasons to determine what they do (see also [46, 54, 62]).

In the past, the empirical basis for social norms, what they are and how they affect behaviour, was weak. In particular, both the measurement of expectations—the drivers of norm-following behaviour, and experimental manipulations to test the causal effects of social norms were lacking. With the advent of more precise measurement and experimental techniques, we are now better able to provide an empirical grounding for social norms [49, 50, 54, 56]. Another critique of social norms was that they are vague, ignore cognitive mechanisms, and that they are used as a catch-all term. Using a computer simulation forces us to be explicit and precise about what social norms are and the effects they may have in our model. Our model uses prior work done by scholars who have developed a normative agent architecture, "EMIL-A," that allows norms to be realistically implemented in a model [57]. It is a cognitively grounded normative agent architecture that provides a measure that indicates how active and prominent, or inactive and inconspicuous, a norm is, the "salience of a norm," which facilitates the incorporation of normative considerations into the agents' decision-making processes.

There is a large literature on modelling social norms in the complex systems field as well as in the social sciences. Much of this addresses how cooperation can be promoted with social norms [63]. Schlüter and colleagues [64] consider a common pool resource problem and test how resource abundance and variability influences norm-driven cooperation, while Tessone and coauthors [65] focus on how the distribution of individuals' sensitivities towards social norms within a population affects norm-following. The latter find that heterogeneity in sensitivity can increase norm-following. Others examine the roots of social norms and test how they emerge [66–69]. Some work tests how social structure and access to information about the behaviour of other agents, only those close by or also those more distant, influences norm-following [70]. ABMs of institutions are also related to our work here [71].

The closest existing ABM that specifically addresses protection rackets comes from the work of Troitzsch [72–74]. Troitzsch presents an ABM of a protection racket in which he integrates instrumental and normative considerations in the decision-making of agents. Different to ours, Troitzsch's model is more complex, containing more parameters and processes, and he does not use a calibrated version of it to run policy-relevant experiments. Other related ABMs look at instrumental factors [75], how a team-reasoning approach changes entrepreneurs' willingness to resist [76], and whether presence of fakers, who pose as mafiosi but are unwilling to use violence towards nonpaying shopkeepers, changes the protection racket dynamic [77].

2. Materials and Methods

2.1. Model Overview. Our event-based agent-based model is configured to represent a single neighbourhood of Palermo in which a mafia runs a protection racket and hence we call it the Palermo Scenario. We built our agent-based model as part of the FP7 EU funded project GLODERS. This project included more than twenty domain experts from multiple European countries allowing us to use an iterative participatory modelling approach to construct the model, identify the main actors, and validate the model's assumptions, dynamics, and outcomes. We identified entrepreneurs, the state, the Sicilian Mafia, consumers, and nongovernmental organisations as key players in the dynamics of protection rackets and implemented these as the agents (Figure 1). This was based on the iterative participatory modelling process with the domain experts and evidence that we extracted from a range of sources including judicial and confiscated mafia documents, academic studies, and newspapers and television interviews. We draw on the model description we previously used in [19] for this section; see also the same paper for technical details of the model. We present an ODD+D (Overview, Design Concepts, and Details + Decision) document [78] concerning our model in Table S1 of the Supplementary Information.

Entrepreneurs represent businessmen and the self-employed. They sell products to consumers and receive an income periodically. They face the decisions to pay pizzo, or not, if approached by mafiosi (*pay*); report pizzo requests to the state if they decide not to pay pizzo (*report*); report any damages to the state that they sustained from mafiosi attacks (*report*); collaborate with the state against specific mafiosi following a request by the state (*collaborate*); and join the

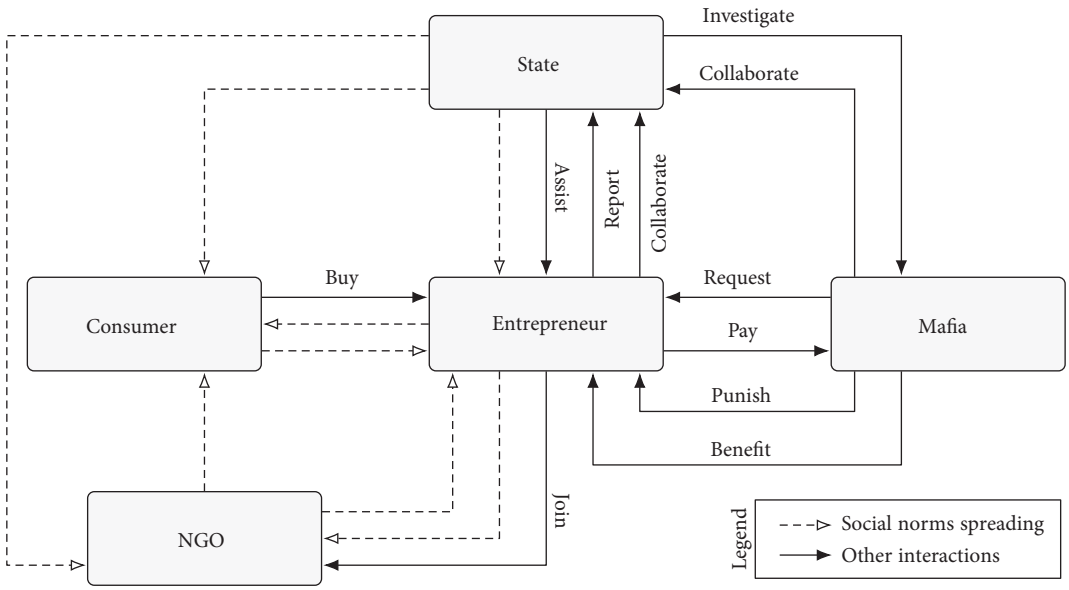

Figure 1: Schematic of the agents in the Palermo Scenario and their dynamics. Boxes represent agent types and arrows represent actions.

NGO to signal that they are unwilling to pay pizzo and likely to report pizzo requests and punishments (*join*). Entrepreneurs and consumers are connected to each other in a static scale-free network [79] that is defined at the start of the simulation. This network defines their range of perceptions regarding others' actions and it is used to update their normative behaviour.

Consumers represent people buying goods from shops. Consumers have a single decision regarding which entrepreneur to buy a product from (*buy*), restricted to their neighbour entrepreneurs in the defined scale-free network. Consumers also spread information through this network that can influence other consumers and entrepreneurs and serve as reservoirs of normative behaviours (*social norm spreading*).

The state represents the government and its institutions that are responsible for enforcing antiracket laws. It is composed of police officers who try to detect pizzo requests and imprison mafiosi based on general or specific investigations (*investigate*). General and specific investigations differ in how they are initiated, their duration, and the probability of success. General investigations, which may be thought of as a patrol, occur on an ongoing basis without specific evidence. As such, they have a short duration—allowing police officers to explore more space—but have a low probability of success. In contrast, specific investigations are initiated based on evidence and reports by entrepreneurs, thus justifying the use of resources for a longer period as they have a higher probability of success. Imprisoned mafiosi are removed from the simulation for a set amount of time. After the police capture a mafioso, they may find information about the entrepreneurs who paid pizzo to that mafioso—some mafiosi keep accounting books to record information about pizzo payers. The state can then use this evidence to elicit collaboration from those entrepreneurs (*collaborate*). If collaboration is obtained, the state uses the collected information to prosecute that mafioso. If collaboration is not obtained, the state may, with a small probability, fine entrepreneurs. The state can also support entrepreneurs who have suffered damages at the hands of mafiosi (*assist*). Entrepreneurs may apply for monetary support from a fund that periodically recharges and is specifically set up for this purpose. In Italy, this fund is known as the "*Fondo di Solidarietà*." The state also spreads information about successful actions that it has carried out against the mafia: consider this as the state providing information to journalists who report and propagate the news in newspapers and television programs (*social norm spreading*), and it can work to change people's social norms regarding the mafia by sponsoring and supporting antiracket festivals (*social norm spreading*). The *Festival della Legalità* is one example of the state supporting antiracket festivals.

The mafia represents a "family" covering a neighbourhood and is composed of mafiosi who request pizzo from entrepreneurs (*request*) and provide benefits, which we intend as a simple representation of protection, to pizzo-paying entrepreneurs (*benefit*). Mafiosi can also punish non-paying and reporting entrepreneurs. Since they are part of the same family, mafiosi coordinate their actions—whom they target, how often they request pizzo, how much they request, and how severely they punish (*punish*). Mafiosi can, with a small probability, turn informant and help the state capture other mafiosi that they know (*collaborate*).

The model mafia in our setup is intended to represent the post-1990s Sicilian Mafia. Following a change in leadership from Totò Riina to Bernardo Provenzano, and protests by parts of the Sicilian population over their public execution of government officials, the mafia undertook a "hidden" strategy in which they limit obvious violent retaliations and request modest pizzo from a greater proportion of the population (see Table S2 for the parameters used).

The NGO represents an antiracket nongovernmental organisation. We primarily draw on Addiopizzo ("goodbye pizzo") for our model NGO and we go into more detail about this organisation in Section 3.1. It promotes lawful behaviour

among consumers and entrepreneurs through events such as talks in schools or the organisation of and participation in festivals (*social norm spreading*). The civil society organisation Libera is the main organiser of the aforementioned *Festival della Legalità*. The NGO spreads information depending on the number of actions the state takes against the mafia and the number of extortive actions shared by the affiliated entrepreneurs. It serves as an organisation that entrepreneurs can join if they are not paying pizzo.

2.2. Decision-Making. Agents can be separated into two groups based on their decision-making complexity. The state, the mafia, and the NGO are represented as agents whose decisions are based on fixed probabilities initialised at the start of the simulation. In contrast, entrepreneurs and consumers use more sophisticated reasoning abilities. They base their choices on a combination of instrumental and social considerations.

Instrumental considerations approximate instrumental rationality. They involve strict cost-benefit calculations that motivate agents to take decisions that maximise their own material pay-offs, independently of what a certain norm dictates. Exactly what factors are considered depends on the agent and on the decision being made. For instance, when deciding whether to pay pizzo or not, entrepreneurs consider the cost of paying pizzo, the potential benefit received from paying, the anticipated violence from the mafia to not paying, and the ability of the state to identify pizzo-paying entrepreneurs and the resulting fine.

Social considerations represent the agents' motivations to comply with a norm. The parameter considered is the "salience of a norm." It refers to a measure that indicates how active and prominent, or inactive and inconspicuous, a norm is within a group in a given context. It is a function of how important agents believe norms to be and it approximates in a single value the combined empirical and normative expectations that agents have about a norm. Norm salience is updated by each agent based on its own behaviour (whether it followed the norm or not), the information gathered by observing the behaviour of and actions inflicted on neighbouring agents (whether others followed the norm or not) and normative information spread by the state and NGO (see also [46, 62]).

2.3. Social and Legal Norms. Social norms in our model are implemented using the agent architecture EMIL-A [57], an architecture specifically designed to capture the complex dynamics of social norms. Agents that possess normative reasoning modules (entrepreneurs and consumers) in our model can *recognise* social norms and decide to *comply* with the social norm.

Recognition entails that agents discriminate between whether others' behaviour is driven by, at least in part, the existence of a social norm and if this is the case, to subsequently form a belief concerning that norm. This belief may simply state that the norm exists or it may be more complex and include the further specifications that the norm is applicable to the belief-holding agent who recognised it, and potentially, that the norm is supported by rewards or punishments.

Following recognition, agents adopt a norm and decide whether to comply with it. Compliance means here that the goals of agents are potentially turned into action. Turning a goal into an action however depends on both the normative goal and instrumental considerations. A key part of the decision-making process that determines the influence of social norms on behaviour is *social norm salience*. This represents the importance that agents place on a social norm and is determined by multiple factors including observed compliance, observed violation, and observed and applied punishments. For details, (see [19], Section 5.4).

The specific social norms we include for entrepreneurs are pay pizzo requests, do not pay pizzo requests, report pizzo requests, and do not report pizzo request. We explicitly represent both a norm and its opposite norm for entrepreneurs, such as pay pizzo and do not pay pizzo, because this allows us to model a greater space of normative situations than if we were to make them complementary. We can represent situations in which the norm of pay pizzo and do not pay pizzo are both low in salience, in which case there are weak or no social norms associated with paying pizzo, or that they are both high in which case there is internal normative conflict within agents. Although these social norms are aimed to capture the mafia-relevant features of the reciprocity, fairness, in-group favouritism, and omertà, they are not meant to relate in a one-to-one way with the norms that occur in reality. Rather, they summarise and capture the effects of those norms that are relevant to the protection racket. The effects of norms of fairness, for instance, are summarised in the salience the four social norms of entrepreneurs.

Consumers also have one social norm: to avoid pizzo-paying entrepreneurs. This is a norm that is not yet widespread nor established in Sicily, but there is some suggestion that it is growing. We do not include the opposite norm, to choose pizzo-paying entrepreneurs, because we could not find evidence that this exists in Sicily or Palermo. We also include legislation in the model that primarily works by targeting mafiosi. All these norms are summarised below (Table 1).

It is worth mentioning that our implementation captures an important feature of real social norms. It allows social norms to simultaneously exist, contained within agents' minds, yet remain latent in a population without being manifested as behaviour [51, 56–59]. It may be that everybody within a population abandons a norm; however, since agents know about this, they keep monitoring how salient it is within their community. Consequently, it is possible that social norm consistent behaviour emerges or reemerges.

2.4. Validation. We built the model using an iterative participatory modelling process. This means that we presented the model to people with antimafia expertise, they gave us feedback, we updated the model, and then at a later stage, we presented them the model again. This process gives the agents and model dynamics *prima facie* validity. In addition, we used participatory modelling as a "powerful tool that can (a) enhance the stakeholders' knowledge and

Table 1: Social and legal norms in the Palermo Scenario.

Legal norms	Social norms
Criminalise mafia-style organisations	Pay pizzo request
Confiscate mafiosi resources	Do not pay pizzo request
Reimburse victims of mafia crimes	Report pizzo request
	Do not report pizzo request
	Avoid pizzo-paying entrepreneurs

understanding of a system and its dynamics under various conditions, as in collaborative learning and (b) identify and clarify the impacts of solutions to a given problem, usually related to supporting decision-making, policy, regulation, or management" ([80], see also [81]). Ultimately, an iterative participatory modelling approach increases the benefits that can be derived from the model to both policymakers and researchers.

Although the iterative participatory validation approach is an important piece of specifying a general protection racket simulation model—as well as increasing the relevance of the model, it does not validate the model for a specific protection racket, e.g., the Sicilian Mafia. To do this, we compare whether the model's outputs match data already acquired from the real system (known as replicative validity or retrodiction) [82]. Zeigler [82] distinguishes between three types (or levels) of validity for this purpose: *replicative validity* means that the model matches data already acquired from the real system (also known as retrodiction); *predictive validity* means that the model matches data before the data are acquired from the real system; and *structural validity* means that the model is not only capable of replicating the observed real system behaviour but reflects exactly the sequence of steps the real system operates to produce this behaviour. Structural validity can almost never be accomplished, especially in models that represent individuals who are reluctant to communicate about their motivations and behaviour propensities. In these circumstances, one will never uncover how real individuals operate to produce their behaviour in sufficient detail. Predictive validity is also difficult to accomplish due to this same issue in which one would not have enough detail about the behaviours to consistently reproduce them in yet unknown future circumstances. However, if we succeed in finding simulation output which is in line with relevant statistics, we can claim that our model is replicatively valid—but this has no direct consequences for its predictive and, more so, for its structural validity. We undertake replicative validation by comparing the model's outputs to historical trends in Sicily and to contemporary empirical data collected from police records and judicial trials as well as surveys. By applying this approach, we validate our model in two further ways.

Our first approach is to compare the qualitative patterns observed in the model to historical trends reported from Sicily (for further details of this validation, see [19]). To do this, we group the relevant historical periods into five categories: pre-1980s, 1980 to early 1990s, early 1990s to mid 1990s, mid 1990s to 2000, and post-2000. We draw on historical information to qualitatively set up the model's parameters and then we run the model for 50,000 time units. At every 10,000 time units, we shift the parameter setup to match that drawn from the historical literature and carry over the information from the prior time units. This provides a continuity to the simulation. Each 10,000 time units thus corresponds to a historical time period (time units are not intended to correspond on a 1 : 1 basis with real time. Instead, the 10,000 time units per historical period were chosen to allow changes to stabilise before the model's parameters are changed). We repeated the simulation, for the purposes of validation, 10 times to ensure that the results are robust.

We find results that are broadly consistent with the trends from these periods in Sicily. Pre-1980s, the governmental authorities did not have effective laws to fight the Sicilian Mafia. So, the mafia could proliferate and use violence against entrepreneurs without fear of strong reactions from the authorities, resulting in a high number of pizzo requests and pizzo paid [83]. During the 1980 to early 1990s, several antimafia laws were implemented enabling the state to effectively fight against mafia (Rognoni-La Torre law; law n. 646, 1982; law n. 8, 1991; law n. 82, 1991; law n. 44, 1999; law n. 512, 1999). This reduced the absolute number of pizzo payments, but increased the amount of damage and violence against entrepreneurs who did not pay [84]. From the early 1990s to mid-1990s, however, the Sicilian Mafia changed its strategy by reducing violence and the amount of pizzo requested, thus being less visible and avoiding imprisonment [84–86]. However, the level of pizzo reporting did not increase in these periods because the population's social norms were not changed. In the mid-1990s to 2000, the improvement in legislation has been highly effective at imprisoning mafiosi (see law n. 356, 1992), seizing their properties (see law n. 109, 1996; law n. 296, 2006; law n. 92, 2008; law n. 40, 2010), and creating the conditions for the emergence and thriving of civil society organisations. In this period, several nongovernmental organisations began to operate and to raise awareness of the importance of reporting extortion to the authorities. This change on the population mind-set increased the number of reports helping the authorities to fight the mafia. Later, the state also started to raise awareness on the population helping to increase even further the proportion of reports and investigations successes.

The second validation approach we take is to compare the output pattern of our model to contemporary empirical data extracted from police reports and court trials that indirectly gives us information on the Sicilian Mafia. This empirical data is a database of more than 600 cases of extortion in Sicily and Calabria during the past decade (database available at https://doi.org/10.7802/1116). For this validation, the percentages of unreported cases (i.e., cases where the police got to know about an extortion without the help of the victim) and the percentages of completed extortions (i.e., not only attempted, but also unsuccessful) that took place in Palermo were calculated.

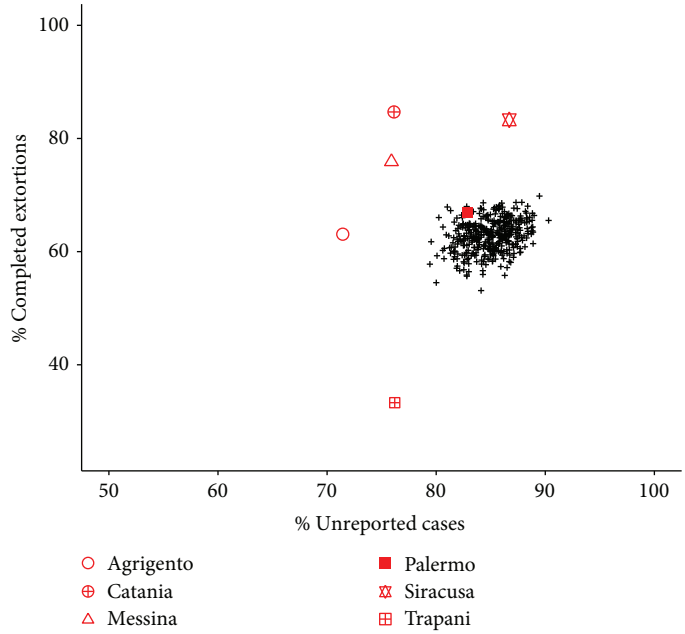

Figure 2: Comparison between empirical data of different cities in Sicily and simulated data. Simulated data shown in black while survey data shown in red.

We calibrate some of the input parameters using data concerning Southern Italy and the surrounding islands that are extracted from surveys such as the European Values Study (European Values Study data is available at https://europeanvaluesstudy.eu). Using this survey data, Troitzsch [87] estimates that the population in Southern Italy has individual weight of 0.41 and normative weight of 0.59, which implies that people in this region are highly sensitive to norms—even more so than individual factors. We use the ordering, a greater weight on normative than individual factors, reported by Troitzsch, but fine-tune the weights by comparing the outputs of our model with data observed in Palermo. We find that the weights of 0.2 and 0.8, respectively, for the individual and normative weight, replicate the data observed in Palermo well and thus use these. However, to check whether our results depend on these weights, we also run our model with an individual weight of 0.41 and a normative weight of 0.59 and find that the substantive results remain the same (see Figures S1–4 in the Supplementary Information).

Given the fact that the empirical data do not cover all parameters of the model due to the secretive nature of protection rackets, we cannot use traditional validation methods in which empirical data is extensively used. Instead, we let input parameters randomly vary, run our simulation model multiple times varying these parameter values at each run, and we then compare the outcomes of the simulation with the trends of empirical data. If they match, we can claim that our model is replicatively valid and calibrated.

Therefore, we run our model 400 times varying multiple input parameter values (i.e., the state's frequency and duration of general investigations, probability of accepting to conduct and duration of specific investigations, probability to capture and convict mafiosi, and duration of imprisonment and the mafia's pizzo amount request, probability, and severity of punishment or benefit) and compare the outcomes with the empirical data collected in several cities in Sicily concerning the percentages of unreported cases (i.e., the number of extortions that were identified by the police through independent investigations, so never reported, divided by the total number of extortions) and the percentages of completed extortions (i.e., the number of extortions paid to the mafia divided by the number of extortion requests). Figure 2 shows that the percentage of unreported cases and completed extortions generated with our model (black plus "+" signs) closely reproducing the outcomes observed in Palermo as the Palermo empirical data (red square) lies within the cloud formed by the simulation outcomes. These results indicate that our model is calibrated to represent the protection racket characteristics observed in Palermo more than in other city in Sicily.

3. Results and Discussion

3.1. Treatments and Research Questions. We test three treatments in the Palermo Scenario and compare them against a *baseline* setup (B). The treatments are a *legal approach* (LA), a *social approach* (SA), and a *combined approach* (CA). For the specific parameters used in our treatments, see Table S2. Our core research question is *what are the independent and combined effects of legal and social approaches on the mafia and the rest of the population?*

States typically use legal approaches to combat organised crime (this is represented by our LA treatment). These rely on the institutions of the state to identify, prosecute, and incarcerate people running protection rackets. Their targets, in an ideal system, are only criminals. In Italy, the government introduced specific laws that allow mafiosi to

be prosecuted and help victims and increased police presence and sent special investigators to direct the antimafia efforts, for instance, General Carlo Alberto Della Chiesa during the Second Mafia War (see [89]) into Sicily. The crime of mafia association was introduced by the Rognoni-La Torre law n. 646 of 13/9/1982 along with the possibility of confiscating mafia properties with their consequent social reuse. In addition, law n. 8 of 15/01/1991 and law n. 82 of 15/03/1991 aim at providing denouncing incentives and protecting victims who report extortion activities. Finally, law n. 44 of 23/02/1999 and law n. 512 of 22/12/1999, respectively, introduced economic support to victims of extortions and the solidarity fund for victims of mafia crimes and intimidation (see [88] for details). Here, we test if this approach works to imprison mafiosi and reduce the activity of mafia, as expected, and whether it has any effects on the behaviour and social norms of the population. Moreover, we explore whether a LA has resilient effects (see below for an explanation of how we test the resilience of the treatments).

While a social strategy is typically used by NGOs, in recent years, the Italian state also supports these social initiatives through festivals (e.g., *Festival della Legalità*), education campaigns, and strongly publicized successful antimafia operations. We include this pathway in our model. In Italy, a number of NGOs use such an approach, among them, Addiopizzo, Fondazione Rocco Chinnici, Libera, and Professionisti Liberi. Consider the approaches used by Addiopizzo to combat the mafia [23, 24]. They (*i*) certify shops as pizzo-free and provide them with a visible indicator of their certification allowing shopkeepers to reliably signal their opposition to the paying pizzo, (*ii*) condemn mafia activity in the media, (*iii*) educate schoolchildren in various campaigns, and (*iv*) collect signatures from consumers in which they declare that they will avoid pizzo-paying shops. The expectation is that these activities will change the social norms and behaviours of the population thereby indirectly undermining the mafia. Will this be borne out in our model? And is this approach resilient to exogenous shocks?

Combined approaches use both legal and social strategies to counter protection rackets. They employ the traditional institutional tools of the state to capture and imprison mafiosi, and, they add a bottom-up norm-change strategy that targets citizens. This two-pronged approach to targeting mafias, with both legal and cultural sides, is an approach that is advocated for among scholars by Godson and coauthors [90, 91] and by Orlando, the current, and previous, mayor of Palermo [89]. They argue that the development of a "culture of lawfulness" is a crucial factor in fighting organised crime.

"Bolstered by a sympathetic culture 'culture of lawfulness' law enforcement and regulatory systems function more effectively in myriad ways. Those who transgress the rules find themselves targeted not only by law enforcement but also by many sectors of society. Community support and involvement can also focus on preventing and on rooting out criminal and corrupt practices without the need for expenditures for a massive law enforcement and punitive establishment. This involvement also reduces the risk and expense of intrusive government surveillance and regulatory practices harmful to individual liberties and creative economic, social, and political initiatives" [90].

We put this idea to the test: will a combined approach perform best?

We compare these three approaches to a baseline setup. This setup represents a state of affairs in which the state almost entirely lacks a legal approach and there is no social approach at all. It is used as an experimental control.

Almost all systems, states and NGOs, use some combination of social and legal approaches to reduce crime, and, where applicable protection rackets. So, this is an important approach to test. The reason we also explore social and legal approaches in isolation is to see the causal effect that these "extreme" strategies would lead to and to contrast it with that of the combined approach. Because of this reasoning, we test a pure legal approach in which there is no campaigning or information promotion by the state or NGO. When testing the social approach, we leave a weak legal backing in place: this is because it is never the case that a state has no legal approach entirely. Were this to be the case, the "state" would cease to be a state in that area.

To test the causal effect and robustness of each treatment, we run the Palermo Scenario for 10,000 time units and then revert the parameters of the simulation to the B setup and continue to run the simulation for a further 10,000 time units. With this approach, we test the average treatment effect with the initial 10,000 time units and the stability of the results that arise from each of the different approaches by comparing the second 10,000 time units. We then repeat the simulation 30 times for each treatment to give us a robust average of the results. The simulation has 100 entrepreneurs, 200 consumers, 20 mafiosi, 1 NGO, and 1 state agent. The state has 20 police officers. For simplicity, the number of each type of agents remains fixed throughout the simulation (e.g., there are always 20 mafiosi in the simulation).

3.2. Findings. To understand what happens in the different treatments, we consider the following outcomes: the imprisonment of mafiosi, the efficiency of the state at imprisoning mafiosi, pizzo requests and punishments meted out by the mafia, pizzo paying and reporting by entrepreneurs, and the social norm saliences of entrepreneurs. The model outcomes we refer to are always averages of the 30 repetitions aggregated by 1000 time units because our model is based on an event-based rather than a time-step approach.

Consider the ability of the state to imprison mafiosi. In both the B and the SA, very few mafiosi are incarcerated (3/20 and 5/20 on average, respectively), while in the LA and the CA, around 65% (13/20) are incarcerated (Figure 3(a)). None of the effects on increased imprisonment are really robust. After the change in parameters, LA and SA tend to converge with the B treatment, although the CA retains some capacity to imprison over the baseline.

While the LA and CA end up imprisoning a similar number of mafiosi, they do so in very different ways (Figure 3(b)). The LA achieves this solely through general investigations—the police conducting their routine antimafia activity.

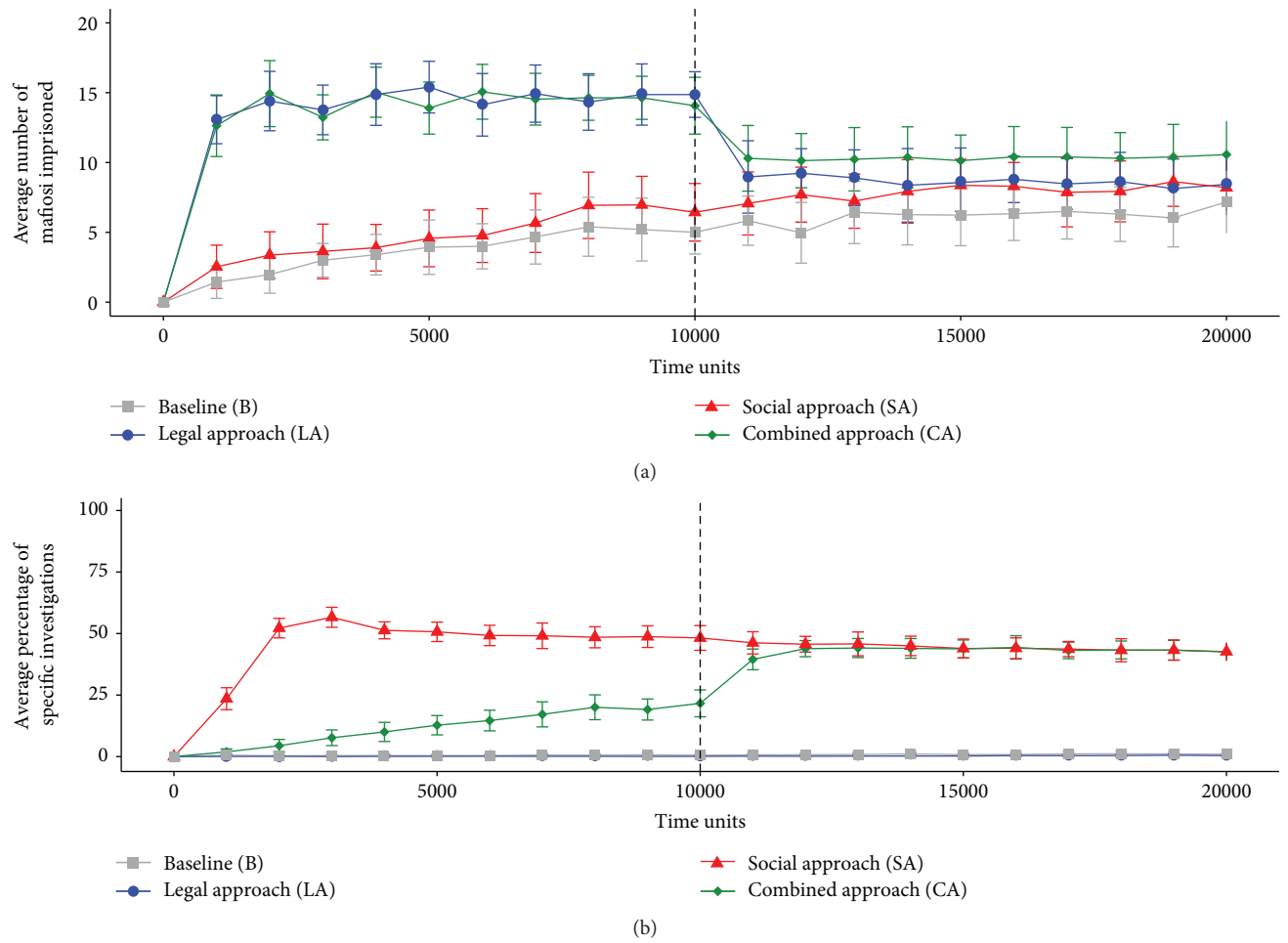

Figure 3: Mafia imprisonment. Means plotted and error bars indicate ±1 standard deviation. (a) The number of mafiosi (out of 20) imprisoned in each treatment and (b) proportion of investigations that are specific investigations. The dashed line indicates the change to baseline parameters.

While the CA attains a substantial percentage of its imprisonments through specific investigations. This suggests that the CA is more efficient at imprisoning mafiosi since it can target them based on information it receives from entrepreneurs. The BA, similar to the LA, uses no specific investigation and there are very few mafiosi whom it imprisons, while the SA, even though the state pursues specific investigations, leads to little imprisonment.

Pizzo requests are substantively affected by the different policies (Figure 4(a)). The LA and the CA hugely decrease the number of pizzo requests that entrepreneurs are approached with relative to the B. However, there is little resilience to the LA but some resilience to the CA following a change to B parameters. The SA has a small effect on reducing the number of pizzo requests.

Particularly interesting is the treatments' effects on punishment (Figure 4(b)). The SA, in the first 10,000 time units, strongly increases the number of punishments that entrepreneurs receive. Employing only a SA leads to increased violence relative to the B treatment. This is because Entrepreneurs increase their refusal to pay pizzo, yet because they lack state support, in the form of strong counter-mafia measures, they are punished for their resistance. Conversely, the LA and the CA both reduce violence to a lower level even than in the B.

Following the change in parameters back to the baseline setup, violence returns to baseline levels in the LA treatment, but in the SA, the harmful effects are maintained, while in the CA, harmful effects emerge. Punishment in the CA becomes higher than in the B and worst of all, in terms of punishment is the SA. Two factors drive this: entrepreneurs not paying and reporting pizzo requests in the SA and CA combined with the inability of the state to imprison mafiosi (Figures 5(a) and 5(b)). As mafiosi are released from prison in the CA, punishment rapidly rise.

Given the persistence with which our model citizens report mafiosi and refuse to pay pizzo despite the punishments that they receive in the SA, one may wonder whether the high punishment finding would extend to the real world. As mentioned before, we consider this, as well as the LA, to be extreme tests. Yet, we think that the core finding, a higher level of punishment than in the other treatments, would be found also in reality. Even if the extent to which it occurs is lower, the lack of state support, coupled with some reporting and refusal to pay pizzo would increase punishment.

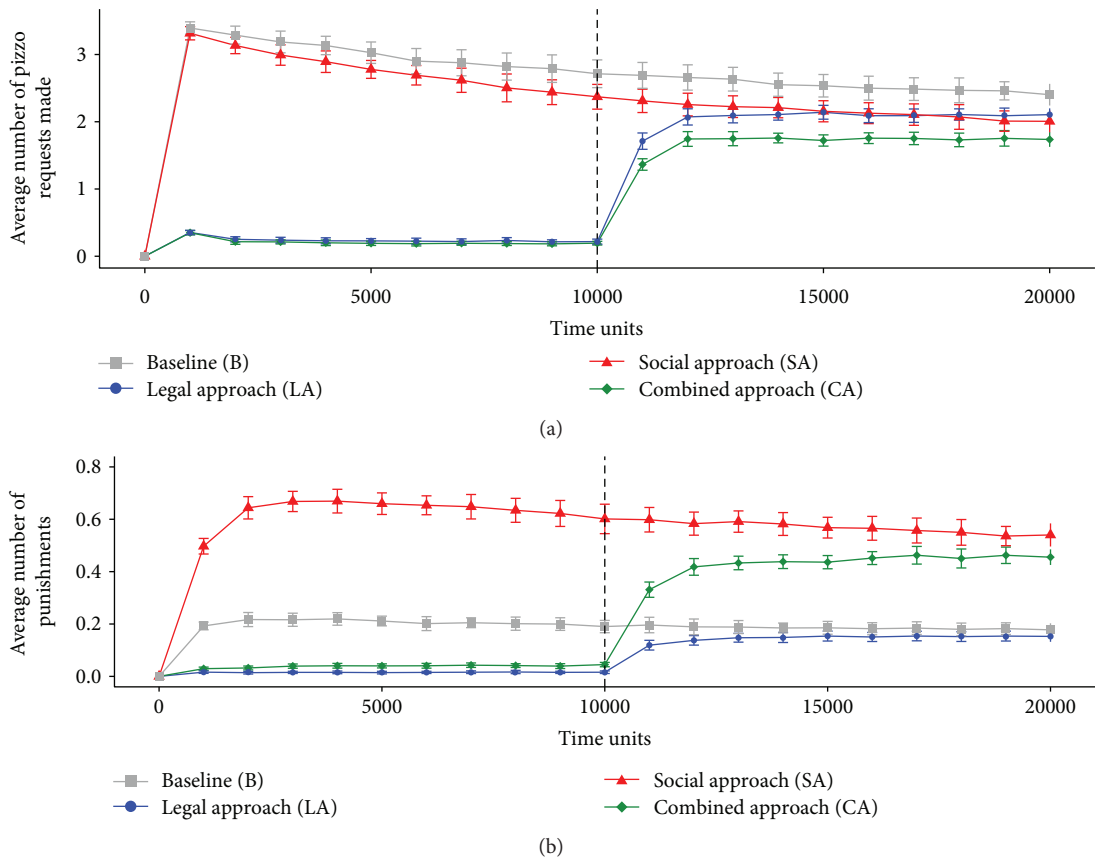

Figure 4: Actions of the mafia. Means plotted and error bars indicate ±1 standard deviation. The number of (a) pizzo requests made by mafiosi and (b) punishments inflicted upon entrepreneurs. The dashed line indicates the change to baseline parameters.

Entrepreneurs in the B treatment pay pizzo the greatest percentage of the time (Figure 5(a)). The LA has no effect on reducing pizzo payment relative to B (79% are paid in both), while the SA and the CA reduce pizzo payment substantially to 49% and 54%, respectively (it is unclear whether the difference in pizzo paying between SA and CA is meaningful. There are reasons to be sceptical: it is small, likely to decrease in longer simulations—much of it arises in the first 5000 time units, and it essentially disappears with different individual and normative weights (see Figure S3A). Moreover, the effects of the treatments are largely resilient to the change to the baseline parameters. This implies that the changes brought about in pizzo payment by the SA and CA are robust. Later, we show that this is down to changes in social norms (see Figure 6).

A greater proportion of pizzo requests are reported in the CA (10.7% on average) and the SA (10.9%) than in the LA (0.2%) and the B (0.2%) (Figure 5(b)). So, the CA and the SA are the most effective at eliciting cooperation from citizens. And the LA is entirely ineffective. Interestingly, the SA is comparable to the CA in increasing reporting also in its resilience: after 10,000 time units reporting in the SA increases to 12.8%, while in the CA, it increases to 16.3%. The effects of the SA and CA treatments are maintained, and even increased, after the parameters return to the B levels.

Consider now the social norms for paying and not paying pizzo. In the B, the social norm salience for paying pizzo decreases slightly from the starting level and stabilises (average of 89.2%; Figure 6(a)), while the salience of not paying pizzo remains stable at an average of 6.8% (Figure 6(b)). The norm saliences for both norms in the LA follow the same pattern. In contrast, the salience of the norm for paying pizzo decreases strongly (average of 53.7% in the SA and 60.2% in the CA) and the salience of the norm do not pay pizzo increases strongly (average of 51.2% in the SA and 44.4% in the CA) in the SA and the CA (Figures 6(a) and 6(b)). All these effects are resilient to the change in parameters that occurs after 10,000 time units.

Following closely the pattern observed for pay pizzo and do not pay pizzo, we find that the saliences for the norms report pizzo and do not report pizzo in the B and the LA are very similar (Figures 6(c) and 6(d)). The norm salience for reporting pizzo remains stable at the low level of 2.3% in the B and 4.2% in the LA and the norm salience remains high at 97.2% in the B and 96.4% in the LA. The SA and the CA are able to change the norms to make them less mafia supporting (Figures 6(c) and 6(d)). In both treatments, the norm salience of report pizzo increases to around 40% (average of 39.6% in the SA and 37.5% in the CA) and the do not report pizzo goes below the 50% level for the SA and approaches that level in the CA (average of 44.6% in the SA and 58.2% in the CA). The treatment effects are unaffected by the change in parameters at 10,000 time units.

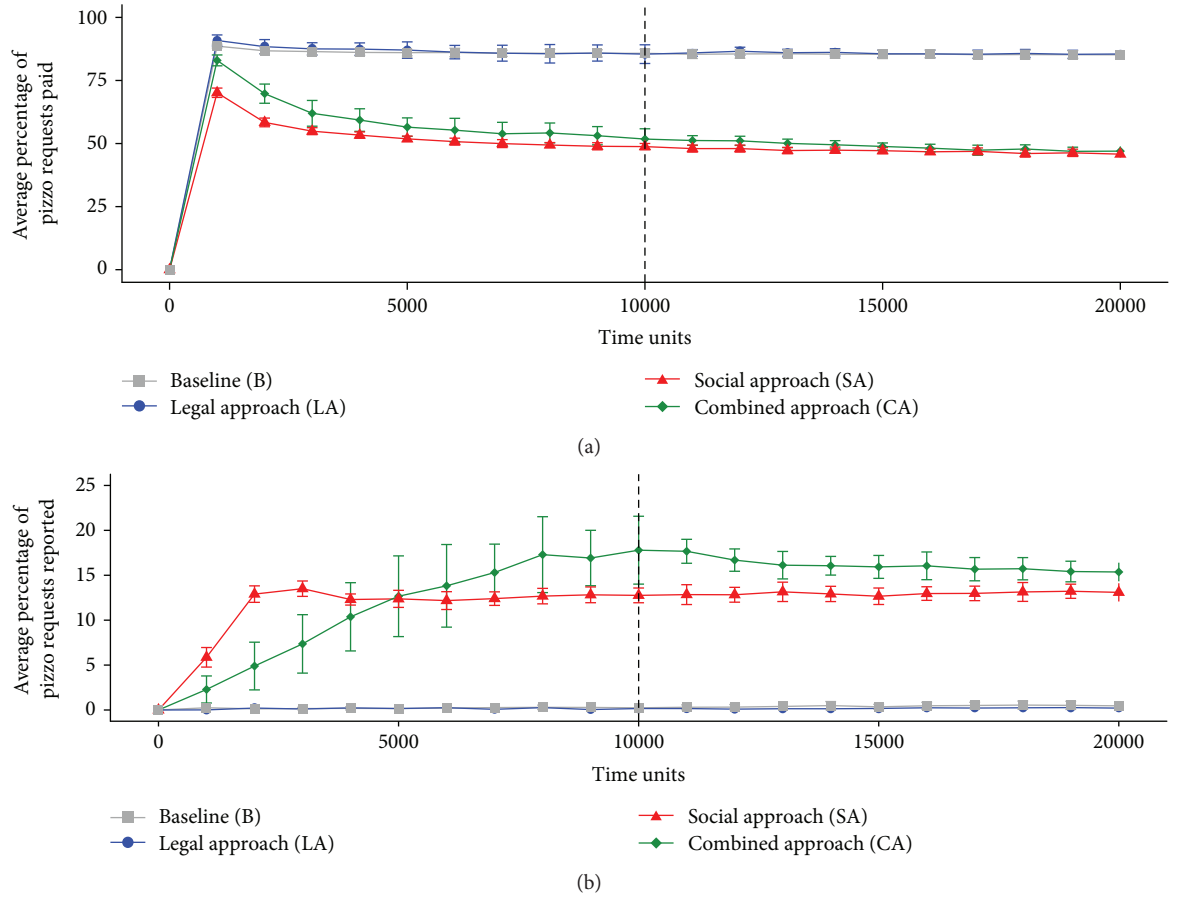

Figure 5: Entrepreneurs' actions. Means plotted and error bars indicate ±1 standard deviation. The (a) proportion of pizzo requests paid and (b) reported in each treatment. The dashed line indicates the change to baseline parameters.

Social norms remain stable even after the change in parameters at 10,000 time units because once they have been built up, they are difficult to change. It is particularly difficult to change them through punishment by mafiosi since this has a low weight in the norm salience calculation relative to the observation of other entrepreneurs' actions. Additionally, the actions of entrepreneurs influence norm salience in the opposite direction to the punishment of mafiosi making their net effect on social norm salience small.

Concerning norm diffusion and change, we ultimately find that norms, whether good or bad, are unaffected by a B or LA approach. Instead, social norms are strongly changed with a SA or CA approach. Interestingly, a social only approach, SA, diffuses and changes norms faster than a combined approach. This counterintuitive result is a consequence of an increase on extortion-related actions—pizzo requests and punishments due to more free mafiosi—which causes the NGO to increase the promotion of lawful behaviour among the population. It is also a finding that holds when we use individual and normative weights of 0.41 and 0.59 (see Figure S4).

4. Conclusion

Our agent-based model combines elements of both cultural and economic approaches to understanding protection rackets, in part, by modelling agents that combine core features of Homo Sociologicus and Homo Economicus. This implementation allows us to represent realistic aspects of cultural and normative transmission and influence. Agents are capable of enacting cultural change by affecting each other's behaviour through changes in the strength of social norms and agent's actions shape culture and culture simultaneously shapes agent's decisions.

Using the model, we then test widespread approaches that policymakers and law-enforcement agencies employ to counter protection rackets. Simulations of social, legal, and combined approaches in our model world have uncovered a range of relevant findings.

Start with the legal approach: the standard tool in the antimafia toolkit of agencies and governments. We find that the LA approach dramatically increases the state's capability to imprison mafiosi (although not its efficiency in achieving this). Consequently, requests for pizzo and punishment received by citizens are greatly reduced. Thus, such antimafia efforts lead to strong and direct results.

The LA, however, fails to change how compliant citizens are to the mafia: the proportion of entrepreneurs paying pizzo and reporting remain the same as in the baseline. Additionally, the LA does not change social norm and the benefits that it produces lack resilience. These findings imply that if a state reduces its antimafia efforts, say, due to a decrease in

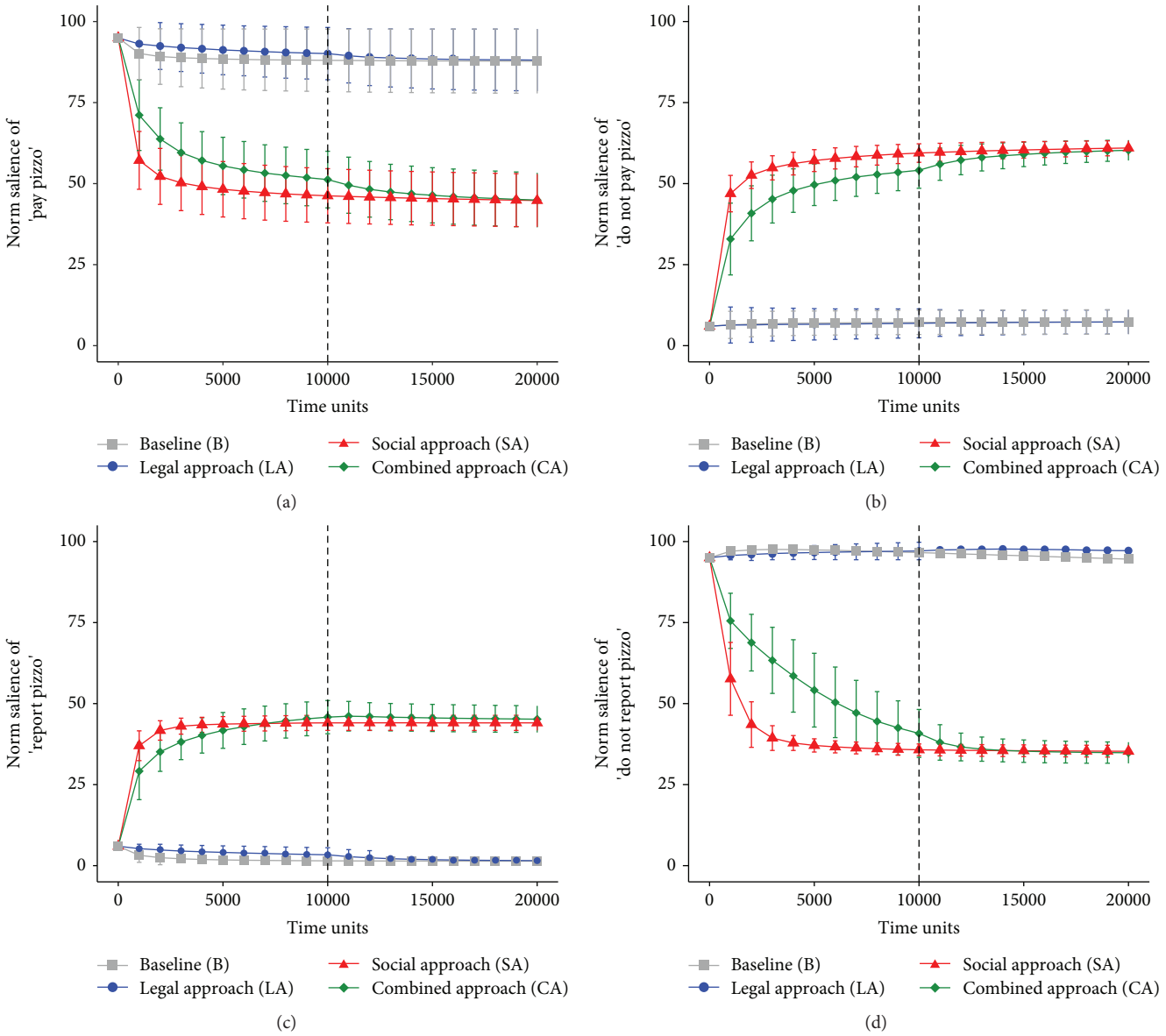

Figure 6: Social norm importance in the population. Means plotted and error bars indicate ±1 standard deviation. Saliences of the social norm (a) pay pizzo, (b) do not pay pizzo, (c) report pizzo, and (d) do not report pizzo. The dashed line indicates the change to baseline parameters.

resources or a change in political agenda, then the gains that it previously made are lost. For these reasons, a legal only approach is not an ideal, nor a long-lasting, anti-mafia tool.

Next, consider the strategy utilised by NGOs: the social approach. This approach changes citizens' behaviours and social norms for the better. Entrepreneurs decrease the proportion of pizzo that they pay, increase their reporting of mafiosi to the tate, and their social norms become less supportive of the mafia. These positive changes are robust and remain even after the SA is abandoned.

Yet the SA has flaws. The approach barely increases the number of mafiosi in prison and the efficiency with which the state puts them there. Because of the former, the number of pizzo requests made to entrepreneurs decreases only a little. Although one could expect that decreased support and increased reporting among citizens leads to distributed enforcement, thereby imprisoning mafiosi and reducing pizzo requests, this is not the case. The lesson to draw is that without state support, reporting by citizens is largely ineffective.

Worst of all, the lack of support from the state leads to large increases in violence. This is the fatal problem of the SA approach: it substantially increases the number of punishments that mafiosi inflict on citizens. It does this to a higher level than in all the other treatments. And, even after the SA approach is stopped, the increase in violence remains. In other words, initiating the policy increases violence straightaway and stopping the policy does not revert punishments to baseline levels. For this reason, a pure SA is dangerous and not a viable antimafia policy.

The final approach we look at combines the legal and social approaches simultaneously. The CA also leads to a

higher number of mafiosi being imprisoned and it increases the efficiency with which the state imprisons mafiosi. Although the number of mafiosi that the state imprisons in the CA is similar to the number that it imprisons in the LA, the former approach is more efficient at achieving the same outcome since it relies on targeted investigations for the job. This means that a state operating with a CA, in real-world terms, spends fewer resources to achieve the same level of imprisonment as a state using only a LA.

Other benefits created by the CA are that it reduces pizzo requests, punishments, and pizzo payment and increases reporting to the state. The CA also changes the social norms of entrepreneurs to make them less mafia supporting.

Some of the effects of the CA are robust: the increase in specific investigations, the reduction in pizzo payment, the increase in reporting, and the change in social norms are all resilient. These changes last even after the approach is reverted back to the baseline. To a much smaller degree, the increase in mafia in prison and the reduction in pizzo requests all retain some resilience.

There is however a drawback of the CA. Surprisingly, once the CA is removed, and the parameters are reverted to the baseline, punishments against Entrepreneurs increase. This increase is nearly as high as that which occurs in the SA following a reversion to the baseline. Using the CA and then abandoning it lead to high levels of violence.

Overall, the CA has many benefits. It imprisons mafiosi the most efficiently, and it changes citizens' behaviours and social norms for the better. Moreover, some of these beneficial changes are resilient. Yet, it has one important failing: preemptively stopping the CA leads to high levels of violence against entrepreneurs. If a state starts a combined approach, it needs to fundamentally undermine a mafia before it decreases its counter-mafia efforts.

We can summarise the main findings from our model as follows:

(1) Legal approaches are necessary components of an effective antimafia strategy. Without legal backing, antimafia efforts fail

(2) Purely social approaches should be avoided. Small advantages are more than offset by the increase in punishment and violence towards citizens

(3) Combined approaches are the most powerful antimafia tools

(4) Combined approaches should not be stopped prematurely, before the mafia is essentially defeated, because this leads to high levels of violence

It is worth reiterating an unexpected but troubling finding. The most violent situations are those in which entrepreneurs are convinced to change their behaviour by the state and the NGO but are not supported by legal power. This is because in these configurations, entrepreneurs partially change their behaviour but, since they are not supported by the state, are subject to high levels of punishments and retaliation by the mafia. This occurs directly in the SA and in the CA after the policy is stopped. A clear policy recommendation can be drawn from this: states should ensure that any social change initiatives are sufficiently supported by legal backing and that such combined approaches should be used until mafias are overcome. The crucial part of this recommendation is the last one: *combined approaches should not be prematurely stopped* as this could lead to large outbreaks of violence.

From the perspective of nonstate actors, a possible policy implication is that NGOs should only work carefully and to a limited extent and avoid directly challenging protection rackets when governments are weak. Conversely, when governments are strong, NGOs can be bolder in their counter-mafia steps and change the population norms.

Our findings need to be accompanied with a number of caveats. First, although our model is complex, it still is only a model of reality. Empirical tests are essential to check whether its predictions hold in the real world. Second, the mafia in our setup is configured as a marginally exploitative organisation. Entrepreneurs pay slightly more to the mafia than the benefits that they receive in return. This setup captures important cases in which the state is providing effective protection and the protection from a genuine protection-providing mafia is unnecessary and somewhat costly. Alternatively, it may be that the mafia is somewhat parasitic, irrespective of the state's protection provisioning. What it does not capture is the situation in which the mafia provide genuine protection that is useful to many entrepreneurs, which, as Gambetta [1] and Varese [92] write, is undoubtedly true in some cases. Thus, our results may not apply to a mafia type organisation that entrepreneurs prefer to pay. Third, even in the best-case configurations, the majority of entrepreneurs pay pizzo, and only minority of them ever choose to report. Moreover, entrepreneurs' social norms are only just reversed regarding pizzo paying and not reporting, from mafia supporting to antimafia, and their social norms for reporting are never reversed. Putting these caveats to one side, our results are fairly encouraging regarding the possibility of overcoming protection rackets using a combination of top-down legal and bottom-up social approaches.

Our simulation demonstrates how complex and hard-to-study social problems such as protection rackets can be fruitfully addressed using an ABM. Simulations may have substantial untapped benefits in studying hidden and dangerous phenomena and have relevance to policy development in constantly changing environments. Our model has allowed us to understand the relative benefits that different counter-mafia public policies may yield as well as their longer-term resilience. We have also been able to explore the dynamics of norm change within a population and identify policies that may be effective, ineffective, and harmful.

Data Availability

The simulation code and data are available on the OSF at https://osf.io/f34mh/. The model implementation is also available at https://github.com/LABSS/gloderss.

Conflicts of Interest

The authors declare that there is no conflict of interest regarding the publication of this paper.

Acknowledgments

We wish to thank Francesco Calderoni, Nicolas Payette, and Mario Paolucci for their insightful comments and suggestions. This work was partially supported by the FP7-ICT Science of Global Systems program (no.: 315874), the Knut and Wallenberg Grant "How do human norms form and change?" (2016.0167), and the Horizon 2020 Framework Programme Project PROTON "Modelling the Processes leading to Organised crime and Terrorist Networks" (No.: 699824).

Supplementary Materials

Additional tables are provided in the Supplementary Information. Table S1 is an ODD + D protocol for the Palermo Scenario. Table S2 contains a full list of the initial parameter values of the model and indicates the parameter values that are changed for the different treatments. *(Supplementary Materials)*

References

[1] D. Gambetta, *The Sicilian Mafia: The Business of Private Protection, New Edition*, Harvard University Press, Cambridge, MA, USA, 1993.

[2] F. Varese, *The Russian Mafia: Private Protection in a New Market Economy*, Oxford University Press, Oxford, 2001.

[3] E. U. Savona, "Italian mafias' asymmetries," in *Traditional Organized Crime in the Modern World*, D. Siegel and H. Bunt, Eds., vol. 11 of Studies of Organized Crime, pp. 3–25, Springer, Boston, MA, USA, 2012.

[4] F. Varese, "Is Sicily the future of Russia? Private protection and the rise of the Russian mafia," *European Journal of Sociology/ Archives Européennes de Sociologie*, vol. 35, no. 2, pp. 224–258, 1994.

[5] F. Varese, "What is the Russian mafia?," *Low Intensity Conflict and Law Enforcement*, vol. 5, pp. 129–138, 1996.

[6] P. B. E. Hill, *The Japanese Mafia: Yakuza, Law, and the State*, Oxford University Press, Oxford, 2006.

[7] V. Daniele, "Organized crime and regional development. A review of the Italian case," *Trends in Organized Crime*, vol. 12, no. 3-4, pp. 211–234, 2009.

[8] A. M. Lavezzi, "Economic structure and vulnerability to organised crime: evidence from Sicily," *Global Crime*, vol. 9, no. 3, pp. 198–220, 2008.

[9] P. Pinotti, "The economic costs of organised crime: evidence from southern Italy," *The Econometrics Journal*, vol. 125, no. 586, pp. F203–F232, 2015.

[10] P. Pinotti, "The causes and consequences of organised crime: preliminary evidence across countries," *The Econometrics Journal*, vol. 125, no. 586, pp. F158–F174, 2015.

[11] G. Frazzica, M. Lisciandra, V. Punzo, and A. Scaglione, "The Camorra and protection rackets: the cost to business," *Global Crime*, vol. 17, no. 1, pp. 48–59, 2016.

[12] G. D. Gennaro and A. L. Spina, "The costs of illegality: a research programme," *Global Crime*, vol. 17, no. 1, pp. 1–20, 2016.

[13] M. Lisciandra, "Proceeds from extortions: the case of Italian organised crime groups," *Global Crime*, vol. 15, no. 1-2, pp. 93–107, 2014.

[14] A. Asmundo and M. Lisciandra, "The cost of protection racket in Sicily," *Global Crime*, vol. 9, no. 3, pp. 221–240, 2008.

[15] G. D. Gennaro, "Racketeering in Campania: how clans have adapted and how the extortion phenomenon is perceived," *Global Crime*, vol. 17, no. 1, pp. 21–47, 2016.

[16] UNODC, *Estimating Illicit Financial Flows Resulting from Drug Trafficking and Other Transnational Organized Crimes*, 2011.

[17] E. Groff and L. Mazerolle, "Simulated experiments and their potential role in criminology and criminal justice," *Journal of Experimental Criminology*, vol. 4, no. 3, pp. 187–193, 2008.

[18] D. Weisburd, A. A. Braga, E. R. Groff, and A. Wooditch, "Can hot spots policing reduce crime in urban areas? An agent-based simulation," *Criminology*, vol. 55, no. 1, pp. 137–173, 2017.

[19] L. G. Nardin, G. Andrighetto, R. Conte et al., "Simulating protection rackets: a case study of the Sicilian mafia," *Autonomous Agents and Multi-Agent Systems*, vol. 30, no. 6, pp. 1117–1147, 2016.

[20] L. G. Nardin, Á. Székely, and G. Andrighetto, "GLODERS-S: a simulator for agent-based models of criminal organisations," *Trends in Organized Crime*, vol. 20, no. 1-2, pp. 85–99, 2017.

[21] L. G. Nardin, G. Andrighetto, Á. Székely, and R. Conte, "Modelling extortion racket systems: Preliminary results," in *New Frontiers in the Study of Social Phenomena*, F. Cecconi, Ed., pp. 65–80, Springer, Cham, 2016.

[22] L. G. Nardin, G. Andrighetto, Á. Székely, V. Punzo, and R. Conte, "An agent-based model of extortion racketeering," in *Social Dimensions of Organised Crime*, Computational Social Sciences, C. Elsenbroich, D. Anzola, and N. Gilbert, Eds., pp. 105–116, Springer, Cham, 2016.

[23] C. Superti, "Addiopizzo: can a label defeat the mafia?," *The Journal of International Policy Solutions.*, vol. 11, 2009.

[24] A. Vaccaro, "To pay or not to pay? Dynamic transparency and the fight against the Mafia's extortionists," *Journal of Business Ethics*, vol. 106, no. 1, pp. 23–35, 2012.

[25] M. Santoro, "Introduction," *The Mafia and the Sociological Imagination, Sociologica*, vol. 2, 2011.

[26] P. Arlacchi, *Mafia Business: The Mafia Ethic and the Spirit of Capitalism*, Oxford University Press, Oxford, 1988.

[27] A. Blok, *The Mafia of a Sicilian Village, 1860–1960: A Study of Violent Peasant Entrepreneurs*, Harper and Row, New York, 1974.

[28] H. Hess, *Mafia & Mafiosi: The Structure of Power*, Saxon House, 1973.

[29] L. Paoli, *Mafia Brotherhoods: Organized Crime, Italian Style*, Oxford University Press, New York, NY, USA, 2003.

[30] J. Schneider and P. Schneider, *Culture and Political Economy in Western Sicily*, Academic Press Inc, New York, NY, USA, 1976.

[31] J. Schneider and P. Schneider, "Mafia, antimafia, and the plural cultures of Sicily," *Current Anthropology*, vol. 46, no. 4, pp. 501–520, 2005.

[32] G. Fulvetti, "The mafia and the 'problem of the mafia': organised crime in Italy, 1820–1970," in *Organised Crime in Europe*, C. Fijnaut and L. Paoli, Eds., vol. 4 of Studies Of Organized Crime, pp. 47–75, Springer, Dordrecht, 2004.

[33] T. C. Schelling, "What is the business of organized crime?," *The American Scholar*, vol. 20, pp. 71–84, 1971.

[34] D. Gambetta, "Fragments of an economic theory of the mafia," *European Journal of Sociology/Archives Européennes de Sociologie*, vol. 29, no. 01, pp. 127–145, 1988.

[35] E. Fehr and H. Gintis, "Human motivation and social cooperation: experimental and analytical foundations," *Annual Review of Sociology.*, vol. 33, no. 1, pp. 43–64, 2007.

[36] D. H. Wrong, "The oversocialized conception of man in modern sociology," *American Sociological Review.*, vol. 26, no. 2, pp. 183–193, 1961.

[37] J. Elster, *Explaining Social Behavior: More Nuts and Bolts for the Social Sciences*, Cambridge University Press, Cambridge, 2007.

[38] H. Gintis, "A framework for the unification of the behavioral sciences," *Behavioral and Brain Sciences*, vol. 30, no. 01, pp. 1–61, 2007.

[39] S. Lindenberg and L. Steg, "Normative, gain and hedonic goal frames guiding environmental behavior," *Journal of Social Issues.*, vol. 63, no. 1, pp. 117–137, 2007.

[40] S. Lindenberg and L. Steg, "Goal-framing theory and norm-guided environmental behavior," in *Encouraging Sustainable Behavior*, H. Trijp, Ed., pp. 37–54, Psychology Press, New York, NY, USA, 2013.

[41] S. Bowles and S. Polania-Reyes, "Economic incentives and social preferences: substitutes or complements?," *Journal of Economic Literature*, vol. 50, no. 2, pp. 368–425, 2012.

[42] E. Fehr and U. Fischbacher, "Social norms and human cooperation," *Trends in Cognitive Sciences*, vol. 8, no. 4, pp. 185–190, 2004.

[43] T. R. Tyler, "Psychological perspectives on legitimacy and legitimation," *Annual Review of Psychology*, vol. 57, no. 1, pp. 375–400, 2006.

[44] R. C. Ellickson, *Order without Law: How Neighbors Settle Disputes*, Harvard University Press, Cambridge, MA, USA, 1991.

[45] H. Aarts and A. Dijksterhuis, "The silence of the library: environment, situational norm, and social behavior," *Journal of Personality and Social Psychology*, vol. 84, no. 1, pp. 18–28, 2003.

[46] G. Andrighetto, J. Brandts, R. Conte, J. Sabater-Mir, H. Solaz, and D. Villatoro, "Punish and voice: punishment enhances cooperation when combined with norm-signalling," *PLoS One*, vol. 8, no. 6, article e64941, 2013.

[47] C. Bicchieri, "The fragility of fairness: an experimental investigation on the conditional status of pro-social norms 1," *Philosophical Issues*, vol. 18, no. 1, pp. 229–248, 2008.

[48] C. Bicchieri and A. Chavez, "Behaving as expected: public information and fairness norms," *Journal of Behavioral Decision Making*, vol. 23, no. 2, pp. 161–178, 2010.

[49] C. Bicchieri, J. W. Lindemans, and T. Jiang, "A structured approach to a diagnostic of collective practices," *Frontiers in Psychology*, vol. 5, article 1418, 2014.

[50] C. Bicchieri and E. Xiao, "Do the right thing: but only if others do so," *Journal of Behavioral Decision Making*, vol. 22, no. 2, pp. 191–208, 2009.

[51] R. Cialdini, R. R. Reno, and C. A. Kallgren, "A focus theory of normative conduct: recycling the concept of norms to reduce littering in public places," *Journal of Personality and Social Psychology*, vol. 58, no. 6, pp. 1015–1026, 1990.

[52] K. Keizer, S. Lindenberg, and L. Steg, "The spreading of disorder," *Science*, vol. 322, no. 5908, pp. 1681–1685, 2008.

[53] E. L. Krupka and R. A. Weber, "The focusing and informational effects of norms on pro-social behavior," *Journal of Economic Psychology*, vol. 30, no. 3, pp. 307–320, 2009.

[54] E. L. Krupka and R. A. Weber, "Identifying social norms using coordination games: why does dictator game sharing vary?," *Journal of the European Economic Association.*, vol. 11, no. 3, pp. 495–524, 2013.

[55] A. Schram and G. Charness, "Inducing social norms in laboratory allocation choices," *Management Science*, vol. 61, no. 7, pp. 1531–1546, 2015.

[56] C. Bicchieri, *The Grammar of Society: The Nature and Dynamics of Social Norms*, Cambridge University Press, Cambridge, 2006.

[57] R. Conte, G. Andrighetto, and M. Campennì, Eds., *Minding Norms: Mechanisms and Dynamics of Social Order in Agent Societies*, Oxford University Press USA, New York, NY, USA, 2013.

[58] J. Elster, "Social norms and economic theory," *The Journal of Economic Perspectives*, vol. 3, no. 4, pp. 99–117, 1989.

[59] G. M. Hodgson, "What Are Institutions?," *Journal of Economic Issues*, vol. 40, no. 1, 2006.

[60] J. E. Anderson and D. Dunning, "Behavioral norms: variants and their identification," *Social and Personality Psychology Compass.*, vol. 8, no. 12, pp. 721–738, 2014.

[61] Á. Székely, G. Andrighetto, and L. G. Nardin, "Social norms and extortion rackets," in *Social Dimensions of Organised Crime*, Computational Social Sciences, C. Elsenbroich, D. Anzola, and N. Gilbert, Eds., Springer, Cham, 2016.

[62] J. Realpe-Gómez, G. Andrighetto, L. G. Nardin, and J. A. Montoya, "Balancing selfishness and norm conformity can explain human behavior in large-scale prisoner's dilemma games and can poise human groups near criticality," *Physical Review E*, vol. 97, no. 4, article 042321, 2018.

[63] D. Helbing and A. Johansson, "Cooperation, norms, and revolutions: a unified game-theoretical approach," *PLoS One*, vol. 5, no. 10, article e12530, 2010.

[64] M. Schlüter, A. Tavoni, and S. Levin, "Robustness of norm-driven cooperation in the commons," *Proceedings of the Biological Sciences*, vol. 283, no. 1822, p. 20152431, 2016.

[65] C. J. Tessone, A. Sánchez, and F. Schweitzer, "Diversity-induced resonance in the response to social norms," *Physical Review E*, vol. 87, no. 2, article 022803, 2013.

[66] S. Gavrilets and P. J. Richerson, "Collective action and the evolution of social norm internalization," *Proceedings of the National Academy of Sciences of the United States of America*, vol. 114, no. 23, pp. 6068–6073, 2017.

[67] T. Fent, P. Groeber, and F. Schweitzer, "Coexistence of social norms based on in- and out-group interactions," 2007, May 2018 http://arxiv.org/abs/0708.4155.

[68] F. C. Santos, F. A. C. C. Chalub, J. M. Pacheco et al.F. Almeida e Costa, L. M. Rocha, E. Costa et al., "A multi-level selection model for the emergence of social norms," in *Advances in Artificial Life. ECAL 2007*, vol. 4648 of Lecture Notes in Computer Science, pp. 525–534, Springer, Berlin, Heidelberg, 2007.

[69] F. P. Santos, F. C. Santos, and J. M. Pacheco, "Social norm complexity and past reputations in the evolution of cooperation," *Nature*, vol. 555, no. 7695, pp. 242–245, 2018.

[70] D. Centola, R. Willer, and M. W. Macy, "The emperor's dilemma: a computational model of self-enforcing norms," *American Journal of Sociology*, vol. 110, no. 4, pp. 1009–1040, 2005.

[71] C. Gräbner, "Agent-based computational models– a formal heuristic for institutionalist pattern modelling?," *Journal of Institutional Economics.*, vol. 12, no. 01, pp. 241–261, 2016.

[72] K. G. Troitzsch, "Distribution effects of extortion racket systems," in *Advances in Artificial Economics*, F. Amblard, F. J. Miguel, A. Blanchet, and B. Gaudou, Eds., vol. 676 of Lecture Notes in Economics and Mathematical Systems, pp. 181–193, Springer, Cham, 2015.

[73] K. G. Troitzsch, "Extortion racket systems as targets for agent-based simulation models. Comparing competing simulation models and emprical data," *Advances in Complex Systems*, vol. 18, no. 05n06, article 1550014, 2015.

[74] K. G. Troitzsch, "Extortion rackets: an event-oriented model of interventions," in *Social Dimensions of Organised Crime*, Computational Social Sciences, C. Elsenbroich, D. Anzola, and N. Gilbert, Eds., pp. 117–131, Springer, Cham, 2016.

[75] B. Sonzogni, F. Cecconi, and R. Conte, "On the interplay between extortion and punishment. An agent based model of "*Camorra*"," *Sociologia e Ricerca Sociale*, vol. 33, no. 99, pp. 65–77, 2012.

[76] C. Elsenbroich, "The Addio Pizzo movement: exploring social change using agent-based modelling," *Trends in Organized Crime*, vol. 20, no. 1-2, pp. 120–138, 2016.

[77] C. Elsenbroich and J. Badham, "The extortion relationship: a computational analysis," *Journal of Artificial Societies and Social Simulation*, vol. 19, no. 4, p. 8, 2016.

[78] B. Müller, F. Bohn, G. Dreßler et al., "Describing human decisions in agent-based models – ODD + D, an extension of the ODD protocol," *Environmental Modelling & Software*, vol. 48, pp. 37–48, 2013.

[79] R. Albert and A.-L. Barabási, "Statistical mechanics of complex networks," *Reviews of Modern Physics*, vol. 74, no. 1, pp. 47–97, 2002.

[80] A. Voinov and F. Bousquet, "Modelling with stakeholders," *Environmental Modelling and Software.*, vol. 25, no. 11, pp. 1268–1281, 2010.

[81] A. M. Ramanath and N. Gilbert, "The design of participatory agent-based social simulations," *Journal of Artificial Societies and Social Simulation*, vol. 7, no. 4, 2004.

[82] B. P. Zeigler, *Theory of Modeling and Simulation*, John Wiley, New York, NY, US, 1976.

[83] A. Scaglione and R. mafiose, *Cosa Nostra e Camorra: organizzazioni criminali a confronto*, Franco Angeli, Milano, Italy, 2011.

[84] G. D. Cagno and G. Natoli, *Cosa nostra ieri, oggi, domani: la mafia siciliana nelle parole di chi la combatte e di chi l'ha abbandonata*, Edizioni Dedalo, 2004.

[85] A. Dino, *Gli ultimi padrini*, Indagine sul governo di Cosa Nostra, Laterza, Roma, 2011.

[86] S. Palazzolo and M. Prestipino, *Il codice Provenzano*, Laterza, Roma, 2007.

[87] K. G. Troitzsch, "Survey data and computational qualitative analysis," in *Social Dimensions of Organised Crime*, Computational Social Sciences, C. Elsenbroich, N. Gilbert, and D. Anzola, Eds., Springer, Cham, 2016.

[88] V. Militello, "Legal norms against the Italian mafia," in *Dimensions of Organised Crime*, Computational Social Sciences, C. Elsenbroich, N. Gilbert, and D. Anzola, Eds., Springer, Cham, 2016.

[89] L. Orlando, *Fighting the Mafia and Renewing Sicilian Culture*, Encounter Books, San Francisco, CA, USA, 2001.

[90] R. Godson, "Guide to developing a culture of lawfulness," *Trends in Organized Crime*, vol. 5, no. 3, pp. 91–102, 2000.

[91] R. Godson, D. J. Kenney, M. Litvin, and G. Tevzadze, "Building societal support for the rule of law in Georgia," *Trends in Organized Crime*, vol. 8, no. 2, pp. 5–27, 2004.

[92] F. Varese, "Protection and extortion," in *The Oxford Handbook of Organized Crime*, L. Paoli, Ed., Oxford University Press, 2014.

Hindawi
Complexity
Volume 2018, Article ID 6348413, 14 pages
https://doi.org/10.1155/2018/6348413

Research Article

Minimization of Drug Shortages in Pharmaceutical Supply Chains: A Simulation-Based Analysis of Drug Recall Patterns and Inventory Policies

Rana Azghandi,[1] **Jacqueline Griffin**,[1] **and Mohammad S. Jalali**[2]

[1]*Department of Mechanical and Industrial Engineering, Northeastern University, Boston, MA, USA*
[2]*Sloan School of Management, Massachusetts Institute of Technology, Cambridge, MA, USA*

Correspondence should be addressed to Jacqueline Griffin; ja.griffin@northeastern.edu

Received 21 May 2018; Revised 12 September 2018; Accepted 28 October 2018; Published 2 December 2018

Guest Editor: Miguel Fuentes

The drug shortage crisis in the last decade not only increased health care costs but also jeopardized patients' health across the United States. Ensuring that any drug is available to patients at health care centers is a problem that official health care administrators and other stakeholders of supply chains continue to face. Furthermore, managing pharmaceutical supply chains is very complex, as inevitable disruptions occur in these supply chains (exogenous factors), which are then followed by decisions members make after such disruptions (internal factors). Disruptions may occur due to increased demand, a product recall, or a manufacturer disruption, among which product recalls—which happens frequently in pharmaceutical supply chains—are least studied. We employ a mathematical simulation model to examine the effects of product recalls considering different disruption profiles, e.g., the propagation in time and space, and the interactions of decision makers on drug shortages to ascertain how these shortages can be mitigated by changing inventory policy decisions. We also measure the effects of different policy approaches on supply chain disruptions, using two performance measures: inventory levels and shortages of products at health care centers. We then analyze the results using an approach similar to data envelopment analysis to characterize the efficient frontier (best inventory policies) for varying cost ratios of the two performance measures as they correspond to the different disruption patterns. This analysis provides insights into the consequences of choosing an inappropriate inventory policy when disruptions take place.

1. Introduction

1.1. Background. Between 2006 and 2016, drug shortages in the United States increased a whopping 120%, with the highest peak of 280% in 2011 [1]. In 2017, 146 new shortages were added to the list of nonresolved shortages from prior years, and by the end of 2017, there were 183 active shortages [1]. Drug shortages not only bring the cost of health care above $400 million annually [2] but can also be considered a public health threat since patient lives are put at risk. Despite all the efforts undertaken by health care administrators to ensure product availability, there are still drugs that have experienced shortages for several years [3].

One drug that consistently creates challenges for health care providers is saline (sodium carbonate 9%) which has experienced shortages since 2013. In the United States, saline has been widely used (more than 40 million bags per month [4]) for treating dehydration and for patients undergoing dialysis, surgery, and chemotherapy. In the past decade, shortages of saline have raised questions about the ability to manage the pharmaceutical supply chain. What makes saline interesting to study is its low price (approximately US $4 for a 250ml bag of saline [5]), simple ingredients (only salt and water), high demand, exclusive production by certain manufacturers, and in some cases nonsubstitutability [6]. The US Food and Drug Administration (FDA) announced an ongoing national shortage of saline in early 2014. Several disruptions occurred around this time in the saline supply chain, e.g., multiple recalls and spikes in demand due to flu seasons [7], and the FDA attempted to mitigate these shortages by advising manufacturers to collaborate with each other and importing saline from other countries such as

Norway and Germany. Despite these efforts, shortages in the United States persisted for several months [7]. The failure of these two approaches can be explained by the fact that: (1) the FDA cannot dictate the production changes by manufacturers, and (2) the import of saline from new sources requires several months of regulatory processing. Compounding the latter challenge, outsourcing was limited since manufacturers in other countries have limited capacities to expand their production.

The saline shortage is getting worse, and its supply chain was not fully recovered when a sudden severe disruption in the production of saline occurred after Hurricane Maria, in Puerto Rico in 2017 [8]. The hurricane shut down two of the United States' main manufacturers of saline for several months and created a major disruption in the supply chain. A combination of this disruption with the other preexisting shortages amplified the shortages even more. Following that, the shortage increased as another producer interrupted its production for maintenance purposes. Interestingly, this was announced several months in advance, yet there remained no clear plan to stockpile the inventories to bolster the supply chain. Additionally, due to high rates of influenza during the 2017 flu season, demand for saline increased and drove further shortages of saline in most of the United States [8]. Despite the direct effect of these shortages on patients, health care providers faced the challenge of deciding who should receive the limited supply of saline and how to procure more units of saline, if any were available.

Commonly identified causes of drug shortages include complex manufacturing processes, supply or demand uncertainties, regulatory actions, and the discontinuation of products [9]. Furthermore, quality issues or a lack of incentives for manufacturers to produce high-quality products are other known reasons for drug shortages [9]. However, 53% of the reasons behind the shortages of drugs in 2017 designated by the American Society of Health-System Pharmacists (ASHP) database are labeled as unknown [1]. In fact, these shortages may be explained by a combination of these reasons in conjunction with the effects of decision making by supply chain stakeholders.

In general, pharmaceutical supply chains mirror other supply chains that are exposed to the risk of disruptions. Previous research has indicated that because drug shortages are caused by one or multiple disruptions in the pharmaceutical supply chain, preventing these disruptions can be nearly impossible [6]. The reasons for recalls can vary including mislabeling, defective products, or defects in the container. When product recalls occur in a pharmaceutical supply chain, the inventory of some or all of the supply chain members is removed. While product recalls are common for pharmaceutical products, the characteristics and patterns of recalls can differ between products both in terms of the frequency of shortages and the size of each recall, or the total number of units affected. Beyond recalls, pharmaceutical supply chains can also experience temporary shutdowns of manufacturing plants for multiple months on end. Designing a supply chain that remains resilient to different types of disruptions is among the major challenges researchers in supply chain risk management must tackle.

One common solution for mitigating shortages is to keep more inventory [10], as this will ensure that more inventories are available to treat patients in the event that products are recalled. However, retaining more inventory results in added costs in the supply chain and may not be feasible for many health care centers due to storage and budget limitations. With the need to balance the advantages and costs of holding inventory, strategic decisions about inventory policies throughout the supply chain become critical.

1.2. Research Problem and Contribution. The importance and complexity of supply chain management in the pharmaceutical industry raises critical questions that are not addressed in the literature. In this paper, we focus on answering the following questions. What is the effect of altering inventory policies on the ability to withstand product recalls? How should inventory policies be chosen to address a variety of disruption patterns? Is there any inventory policy that is robust to all disruption patterns?

In order to address these questions, we evaluate the performance of inventory policies such that the policies defining order quantities and target inventory levels do not change over time. Further, we evaluate the performance under various disruption patterns. We model product recall disruptions in pharmaceutical supply chains under deterministic and stochastic settings which are more realistic for pharmaceutical supply chains. To demonstrate the complexity of the pharmaceutical supply chains under disruptions including interactions among key decision makers, we employ a mathematical simulation model accounting for the dynamic features of the system. Different inventory policies are implemented as decision rules in the simulation. As the most critical consequences of drug shortages are experienced at the health care centers with unmet patient demand, the performance metric used to distinguish between policies is the total cost of the health care center. We also employ an approach similar to data envelopment analysis to prune inefficient policies corresponding to different disruption patterns and the ratio of costs. Finally, we aim to demonstrate the effects of making unsuitable inventory policy decisions under different types of disruptions and explore if an inventory policy exists that is efficient for all types of disruptions.

While the present study focuses on saline shortages, it should be noted that the findings are applicable to a wider range of drugs that frequently experience shortages, such as chemotherapy drugs and antibiotics, among others. The results of the presented research reveal that an inventory policy that is optimal for one disruption pattern may be inefficient when an alternate disruption pattern occurs. Therefore, preparing for one intense disruption will not render a system robust if multiple small disruptions happen instead.

The remainder of this paper is organized as follows. In the next section, we provide a review of the literature. Our model formulations and assumptions are then presented in Section 3, followed by numerical analyses in Section 4. Finally, Section 5 presents the conclusion and future research directions.

2. Literature Review

In order to address our research questions, we divide the literature areas into three sections: pharmaceutical supply chain modeling, supply chain disruption mitigation, and simulation modeling for supply chains.

Pharmaceutical Supply Chain Modeling. In recent years there has been a noticeable focus on researching pharmaceutical supply chain management. A study by Lücker and Seifert [10], focuses on operational strategies for managing pharmaceutical supply chains under disruption. They model disruptions with features defining the probability of the occurrence and intensity in length. They analyze three operational risk mitigation strategies for pharmaceutical supply chains experiencing disruption risks, namely (i) Risk Mitigation Inventory (RMI), (ii) Dual Sourcing and (iii) Agility Capacity, with a focus on minimizing the total cost, as a function of product stock-outs and fulfilled demand, over only one cycle [10]. While Lücker and Seifert's [10] study considers one type of drug, Uthayakumar and Priyan [11] model an inventory decision tool for a two-echelon pharmaceutical supply chain with multiple products without considering disruptions in the system. They use continuous ordering policies to optimize and define the lot size, lead-time, and the number of deliveries for a hospital to minimize the total cost for the supply chain with respect to the target cycle service level for the hospital or pharmaceutical companies.

Overall, research in pharmaceutical supply chain disruptions has neglected to examine the role of product recalls, a critical type of disruption in this domain [10–15]. We develop a model to capture the role of various recall disruptions in the pharmaceutical supply chain.

Supply Chain Disruption Mitigation. While the focus on disruption mitigation in pharmaceutical supply chain management research is limited in the scope of the types of disruptions examined, research on modeling supply chain disruptions and response strategies has been conducted for other industries. There are many different approaches for mitigation of disruption risks that have been examined. Common tactics for alleviating the effects of disruptions are financial mitigation, operation mitigation, and operational contingencies [16]. Mitigation tactics are those in which the firm takes an action in advance of a disruption and correspondingly incurs the cost of the action regardless of a disruption's occurrence. Operational tactics, such as inventory management, multiple sourcing, and flexibility in production are also studied in the literature of supply chain disruptions [16].

Researchers in the supply chain disruption area, demonstrate that an optimal strategy to implement when coping with a disruption varies based on the characteristics of the disruption. Tomlin [16] suggests inventory, dual sourcing, and acceptance strategies for dealing with disruptions, and demonstrates that the optimal strategy changes as disruptions become longer or more frequent. In this research, disruptions are modeled as an uncertainty in supply or demand. Tomlin and Snyder [17] demonstrate how strategies change when a firm has advanced warning of an impending disruption. Chopra et al. [18] evaluate the errors resulting from "bundling" disruptions and yield uncertainty for making inventory decisions. Atan et al. [19] present hybrid strategies for dealing with supply uncertainty or demand uncertainty in multiechelon supply chains. They consider disruptions which occur at a specific location and demonstrate that an optimal policy for addressing a supply uncertainty disruption is not the same as the optimal policy for addressing a demand uncertainty disruption.

A variety of different features have been used by researchers for characterizing and modeling supply chain disruptions. The majority of disruptions are modeled as follows: (i) all-or-nothing events (also known as on and off disruptions, in which a disruption at a node will deplete the entire capacity) or (ii) random yield disruptions [20–24]. Most studies focus on large disruptions that happen for a short time duration. Some studies look at the different ordering policies and frequency of the disruptions, e.g., frequent but short disruptions versus rare but long disruptions [16]. To the best of our knowledge, there are no studies that examine the sequence of the disruptions.

In this study, we examine operational mitigation tactics which characterize the role of inventory policies in the prevention of shortages by studying the relationship between the performance of these policies and the disruption pattern exhibited. Rather than all-or-nothing disruptions or random yield disruptions, this research is unique in the focus on removing a fraction of inventory from nodes throughout the network.

Simulation Modeling for Supply Chains. In pharmaceutical supply chain disruptions, and particularly in cases of product recalls, inventory management behaviors are believed to be key to the behavior of the entire system. Often theoretical models in Operations Research misrepresent the 'behavioral' aspects of supply chain stakeholders and focus solely on the supply chain mechanisms. Unlike many of these models, system dynamics (SD) simulation modeling is able to represent interactions, nonlinearities, time delays, and feedback among the members of the supply chain [25–27]. Sterman [28] develops a simulated inventory distribution system for the beer game distribution supply chain which contains multiple actors. He examines the interaction of individual decision makers who make irrational decisions with the objective of minimizing the total supply chain costs and demonstrates the resulting bullwhip effect in the system. Lee et al. [29] demonstrate that even if each agent acts rationally and uses optimal ordering policies, the supply chain is still at the risk of experiencing the bullwhip effect.

Some studies using SD as a tool to model food or drug supply chains include Minegishi and Thiel [30], Georgiadis, Vlachos, and Iakovou [31], and Strohhecker and Größler [14, 15]. Minegishi and Thiel [30] study the complexities of the behavior of poultry supply chains. They examine different simulations to reveal the role of changes in the demand on the behavior of the supply chain. Georgiadis, Vlachos, and Iakovou [31] develop an SD model for a multiechelon food supply chain. In this study, they try to identify effective long-run policies for managing a food supply chain under

uncertainty of demand and transportation capacity using a periodic order-up-to-level policy (R,S,s) when demand has a normal distribution. Strohhecker and Größler [14] study the effects of severe production shutdowns on the performance of pharmaceutical products. In separate work, Strohhecker and Größler study the effect of severe but infrequent quality breakdowns, as disruptions, on the conditions for preventing stock-outs by adapting safety stock levels using a SD simulation [15]. Among the SD-based studies, there is only one study which examines the performance of the system when there are transportation disruptions at two different locations in the supply chain and it compares the results for a traditional supply chain with a vendor managed inventory supply chain [32].

Prior research on supply chain disruptions, including those focused on pharmaceutical supply chains, reveals the importance of distinguishing the disruption features and identifying operational mitigation policies that address these characteristics. Despite this, minimal research examines supply chain performance as it pertains to (i) pharmaceutical product recalls and the unique features of recalls, (ii) patterns of disruptions that account for disruptions affecting multiple nodes and multiple disruptions occurring over time, and (iii) the inventory management policies and behaviors that drive the dynamics of the system.

To address these features, we employ a mathematical simulation model that accounts for the dynamics underlying the system. While there are a limited number of models which analyze the complexities of supply chains with disruptions, this is the first simulation model that focuses on product recalls and the role of disruption patterns in pharmaceutical supply chain.

3. Mathematical Modeling

We integrate two analytical methods to examine the performance of inventory policies in pharmaceutical supply chains experiencing disruptions: simulation modeling and data envelopment analysis (DEA) approaches. To identify the optimal performance—which is a function of the inventory policy corresponding to the safety stock level, inventory holding costs, and shortage costs—for varying disruption patterns, we populate data points from the simulation results. Using the simulation results, an approach derived from DEA is used to identify the optimal inventory policy for various types of disruptions and relative values of shortage and inventory holding costs.

3.1. Model Structure. The pharmaceutical supply chain that is presented in this paper has a serial network structure consisting of four echelons: manufacturer, distributor, wholesaler, and health care center with a single pharmaceutical product being distributed across the system over a finite time horizon. The assumption of considering the pharmaceutical supply chain as including four echelons is in alignment with the main players identified by the FDA [32]. Additionally, this is similar to the assumptions made in other models of these supply chains [33, 34]. The formulation of this model is adapted from the beer distribution game simulated by Sterman [28] and Croson and Donohue [33].

The supply chain members, each corresponding to one echelon, are denoted as $i = 1, \ldots, 4$ for the health care center, wholesaler, distributor, and manufacturer, respectively. In each time period t ($t = 1, 2, 3, \ldots, 260$) representing a week during a 5-year period, each supply chain member will receive product shipments from the supply chain member immediately upstream, resulting in increased inventories, and will receive orders for products from supply chain members immediately downstream. Since there is no upstream echelon for the manufacturer, the inventory of the manufacturer is increased by the quantity that is produced in the previous period. Moreover, there is no downstream node for the health care center. Hence the health care center should satisfy the patients' demand in each period.

After satisfying orders, if there are not enough inventories available, the remaining orders are added to the backlog of each member, except for the health care center, and must be satisfied in the next period. The unsatisfied demand for the health care center is lost, resulting in a shortage. At the end of each period, each supply chain member, other than the manufacturer, will place an order for more products with the supply chain member immediately upstream. The manufacturer will determine how much to produce in the next period, similar to an order. In this model, we assume all members use a periodic review inventory model with zero fixed costs when determining how much to order in each period. This order quantity is dependent on two features: *cycle stock* (for satisfying the expected demand) and *safety stock* (as extra inventory to buffer against uncertainty). Cycle stock is calculated as the mean of lead-time demand, and safety stock is a function of the standard deviation of lead-time demand and the target cycle service level (CSL). The cycle service level can be defined as the expected percentage of order cycles in which no shortage occurs. Each member wants to keep safety stock to address the uncertainty related to demand fluctuations during the lead-time.

Additionally, information about disruptions in the supply chain due to product recalls may become available to the affected member during any time period. If there is a product recall, some products will be removed from the inventory of the health care center, wholesaler, and distributor (in Section 3.2.2 we discuss why we do not consider removals from the manufacturer). Each member's remaining inventory which was not recalled can be used to satisfy orders or patient demand.

We assume that the members of the supply chain make their ordering decisions based on a forecast of uncertain, but stationary, demand in each period. Lee et al. [29] indicate that even a rational ordering decision—which is changed dynamically—can lead to the bullwhip effect or the phenomena in which orders placed by downstream nodes to upstream nodes are variable over time and variability is amplified at members further upstream from the customer. There are four elements considered for the bullwhip effect in a supply chain: demand signal processing, rationing game, order batching, and price variations. Due to the lack of fixed ordering costs, price variability, and rationing ability in the presented model of these elements, only demand signal processing would be expected to cause the bullwhip effect phenomena.

3.2. Model Formulation

3.2.1. Ordering Decisions. The model used in this paper assumes that members place orders based on a periodic review policy with zero fixed costs. We follow the same notation as presented by Sterman [28]. The indicated order rate for echelon i (IO_{it}) is based on the anchoring and adjustment heuristic. In our model, we assume that each member is a rational decision maker and uses an approximately optimal local policy to place orders. Therefore, the indicated order rate is a function of demand, lead-time, service level, inventory level, and the order amount that has ordered but has not been received (on-order). The anchoring corresponds to the base stock (S_{it}) over time which is locally optimal for a periodic review policy under certain assumptions. Furthermore, adjustments can be equivalent to the inventory position (IP_{it}), which is a function of on-hand inventory, on-orders (orders that have been placed but not yet received), backlog (health care center does not have backlog), and disruptions (as recalls).

$$IO_{it} = S_{it} + IP_{it}, \tag{1}$$

As mentioned earlier each member is assumed to be a rational optimizer and uses a periodic review policy with zero fixed costs to place orders. The periodic inventory policy with base stock (order-up-to-level) is optimal under these assumptions:

(1) demands are stationary,

(2) the lead-time is fixed and there is no limitation on production,

(3) there is no fixed ordering cost and there are no changes in the purchase cost of the product over time.

When using a periodic review policy, the base stock level at time t is given by

$$S_{it} = \mu_{it}^{L} + z_{\alpha}\sigma_{it}^{L}, \tag{2}$$

where μ_{it}^{L}, and σ_{it}^{L}, are the mean and standard deviation of the stationary demand for echelon i over the fixed lead-time, respectively. Furthermore, z_{α} is denoted as the α^{th} fractal of a standard normal distribution, known as the cycle service level (CSL). Also, it can be interpreted as the likelihood of being able to satisfy demand assuming no disruptions. In return, this drives the level of safety stock that is held to buffer against uncertainties in demand.

Since the distribution of the demand is unknown and may change in each period, we use the moving average forecasting technique to estimate the mean and standard deviation of the lead-time demand. This estimation may change periodically and adjust based on the demand for the previous n time periods. This process of updating demand forecasts is known as demand signal processing and can result in the bullwhip effect [34, Ch. 10]. Assuming that the demand is independent of previous periods, then, as demonstrated by Snyder and Shen [34], the estimator for the mean lead-time demand ($\widehat{\mu}_{it}^{L}$) is

$$\widehat{\mu}_{it}^{L} = L\left(\frac{\sum_{j=1}^{n} D_{it-j}}{n}\right), \tag{3}$$

where L is lead-time and D_{it-j} is demand at time t.

The forecast error for the lead-time demand is

$$\widehat{\sigma}_{iet}^{L} = k\sqrt{\frac{\sum_{j=1}^{n}\left(e_{it-j}\right)^{2}}{n}}, \tag{4}$$

where k is a constant and assumed to be $\sqrt{L}$. And the forecast error in time t is assumed to be the one-period forecast error as

$$e_{it} = D_{it} - \widehat{\mu}_{it}^{1}. \tag{5}$$

Following from the definition above, the base stock level at each period is defined as

$$S_{it} = \widehat{\mu}_{it}^{L} + z_{\alpha}\widehat{\sigma}_{iet}^{L}, \tag{6}$$

where it is approximately optimal by using the defined estimators to forecast demand.

The other element necessary to calculate for the indicated order is the inventory position of member i in time t (IP_{it}), which is defined as follows:

$$IP_{it} = IP_{it-1} + a_{it-1} - D_{it-1} - R_{it-1} - B_{it-1} + OnO_{it}, \tag{7}$$

where $a_{i,t-1}$ is the acquisition amount in time $t-1$, $D_{i,t-1}$ is the demand in time $t-1$, $R_{i,t-1}$ is the quantity of recalled products that is removed from the inventory of member i in time $t-1$, $B_{i,t-1}$ is the quantity of back ordered units in time $t-1$, and OnO_{it} is the quantity of on-order products expected to arrive in time period t.

If the health care center does not have enough inventories to satisfy all patient demand, then the unmet demand is lost and not transferred to the next period, and a shortage will result. Shortage is defined as

$$Shortage_{1t} = D_{1t} - \left(D_{1t} * Fullfillment\ ratio_{1t}\right), \tag{8}$$

where the fulfillment ratio is the percentage of demand at the health care center which is satisfied. However, for the rest of the supply chain members, the excess amount is added to the backorder quantity and must be satisfied in the subsequent periods.

Finally, the order amount should be nonnegative such that

$$O_{it} = \max\left(0, IO_{it}\right). \tag{9}$$

3.2.2. Disruption Modeling. In the model, we examine supply chain disruptions due to product recalls, which are modeled as exogenous shocks that can affect the availability of inventory at all echelons of the system. As discussed earlier, a product recall happens when there are concerns related to the safety of products produced in the past. Consequently, the manufacturer enforces a voluntary recall of the affected product that has been already distributed within the supply chain. Because this process usually begins after some time has passed, we only consider recalls from three echelons, the distributor, the wholesaler and the health care center. It is possible to have multiple disruptions, or product recalls,

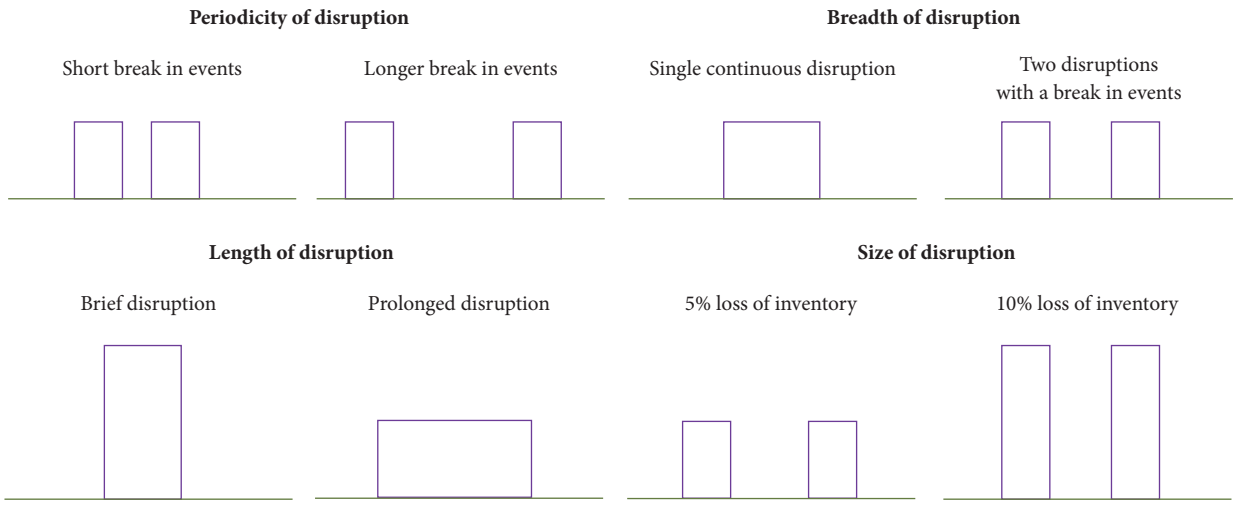

Figure 1: Graphical description of elements characterizing disruptions including the periodicity, breadth, length, and size.

occurring over a period of time. Additionally, the size of the disruption, as defined by the amount of product recalled, can vary significantly based on the driving forces.

Disruptions as external interruptions have been studied in supply chain risk management as deterministic and stochastic events [16, 24, 35, 36]. However, to the best of our knowledge, there are no studies which model the effects of product recalls. To address the lack of modeling of pharmaceutical shortages, we develop deterministic and stochastic models of these types of disruptions which account for the possibility of multiple events over time and varying sizes of the disruptive events.

In deterministic scenarios, the hypothetical disruptions are defined in advance. There are multiple different elements that are considered for characterizing disruption patterns. Adapted from [37], the elements that are considered for characterizing a disruption are disruption periodicity, disruption breadth, disruption length, and disruption size. Figure 1 demonstrates each element. The periodicity of disruptions refers to the duration of time between disruption events. Disruption breadth refers to whether the disruption happens once or if there are multiple distinct disruptions. In this paper, we examine the effect of a single disruption versus multiple disruptions. Additionally, the length of the disruption refers to the duration of the time period during which the disruption occurs. In our model, we assume this element is either brief but severe in intensity or prolonged but moderately sized. The disruption quantity lost or the size of disruption refers to the total loss of the system due to disruption occurrence.

In addition to the deterministic set of disruptions, we model disruptions as exogenous stochastic events that happen during the simulation time horizon. We assume that the time between disruptions is variable and uncertain, but the occurrence of disruptions is modeled as a Poisson distribution with an average arrival rate lambda (λ). For the Poisson process with a mean of λ events occurring in a specified time period, the time between events are independent and identically distributed with a continuous exponential distribution of mean $1/\lambda$. In order to generate the random interarrival times with the rate of arrival as λ in a Poisson distribution, we use the algorithm presented in Algorithm 1.

$T_0 \longleftarrow 0$
$i \longleftarrow 0$
while $(T_0 < runningTime)$
$\quad i \longleftarrow i + 1$
$\quad$ generate $U_i \sim U(0, 1)$
$\quad T_i \longleftarrow T_{i-1} - (1/\lambda)\ln(1 - U_i)$
Return $T_1, T_2, \ldots, T_{i-1}$

Algorithm 1: Algorithm for simulating a Poisson Process with Exponential interarrival times between disruption events.

In our model, we assume that the duration of recalls is greater than or equal to the lead-time to make sure that no defective product remains in the transshipment. The current simulation model is employed over multiple random scenarios which facilitates the comparison of the effects of recall periodicity and the size of disruptions on the shortages and inventory costs with varying inventory policies. Furthermore, in order to compare the different patterns of disruptions, the expected total amount recalled for all scenarios is assumed to be fixed. Another challenge for modeling recalls in both deterministic and stochastic settings is the need to ensure that there are enough defective products in the inventory compared to the recall amount which is removed, such that the inventory cannot be negative. Correspondingly, we assume that the amount that we recall from each echelon is proportional to the available inventory of that echelon.

The objective is to minimize the total costs of the health care center, as presented in (10), which consists of the summation of the total cost of shortages and the total cost for

Table 1: Model parameters.

Parameter	Definition	Value
T (Time to review inventory and place an order at Hc, Ws, Ds, Mn)	Review period length	1 week
L (Lead-time from the upstream node to a downstream node)	Time required to transport/ship products between upstream nodes and downstream nodes	2 weeks
Manufacturing cycle time	Time between the production decision point and the first shipment point	3 weeks
n (Forecast demand time period Hc, Ws, Ds, Mn)	Number of previous time periods used in the estimation and the forecast of demand	12 weeks
CSL (Cycle service level)	The CSL parameter defines the inventory policy and level of safety stock held by Hc, Ws, Ds, and Mn	0.95 (initial value)

holding inventory at the health care center where h is the per unit holding cost and p is the per unit shortage cost. The total cost varies based on the product recall disruption pattern and the inventory policy, as defined by the target cycle service level (CSL).

$$\text{minimize} \quad hIL_{1t} + p\,Shortage_{1t}. \tag{10}$$

3.3. Data Envelopment Analysis. Accessing the true value of the inventory costs and the shortage costs is challenging because health care centers are unlikely to share this information with the public. Moreover, if these costs are available for a particular drug, it may vary substantially in comparison to other pharmaceutical products. In order to assess the performance of the system, without knowledge of the true underlying costs of the system, we employ an approach derived from the concepts of the data envelopment analysis (DEA) approach. DEA is a data-driven approach which seeks to assess the relative performance of multiple systems, referred to as decision-making units (DMUs), accounting for multiple inputs and outputs without exact information about the relative costs and values associated with the inputs and outputs, respectively. Thus, a system, or DMU, is defined as efficient, in comparison to the others under consideration, if there is some set of costs of inputs and values of outputs that leads it to have the best, or most efficient, performance. A set of optimization problems are solved in order to determine which DMUs are denoted as efficient under some combination of costs and values. These DMUs are defined as making up the 'efficient frontier' [38, 39].

We employ an approach similar to DEA to evaluate which policies, as defined by a CSL, are efficient for some set of inventory costs and shortage costs, under different disruption patterns. The data created from the simulation is used as input into this approach. Using an approach similar to DEA with constant-returns to scale [38], we identify which policies, defined by the CSL value, are efficient, or perform best for some relative value of inventory and shortage costs. Correspondingly, we also identify which CSL values never perform best for any set of inventory and shortage costs, and therefore are denoted as inefficient. When plotting the outcomes of the policies, with respect to both the level of shortage and inventory, the efficient frontier can be estimated by connecting the efficient policies with isoquant lines. This efficient frontier can be interpreted as the set of inventory and shortage levels that are efficient for some pair of inventory and shortage costs.

4. Analysis

4.1. Data. Using the saline demand patterns as a basis for the model, we assume that demand follows a normal distribution with a mean of 10,000 bags per week and a standard deviation of 100 bags per week. In all experiments, we use a common random number seed to generate demand data. This allows for the isolation of variations due to ordering behavior and inventory policies rather than variations due to different demand streams in the comparison of the results.

As mentioned in Section 3.1, the simulated supply chain has a serial structure with four echelons (manufacturer, distributors, wholesalers, and health care centers). We assume that there is no limit on the capacity of the manufacturer to meet the demand. The simulated model is defined by several parameters. These parameters are assumed to be consistent across the duration of the entire simulation run, or 5 years. However, in order to capture the effect of inventory policies on the ultimate goal of minimizing shortages and limiting inventory costs as the health center, the CSL value which defines the inventory policy may change. While the CSL may vary among simulation runs, we assume that all echelons will have the same CSL. Table 1 provides a summary of the parameters and their values.

4.2. Disruption Pattern Comparison. As the characteristics defining product recalls can vary based on multiple characteristics, the goal of this section is to provide insights into the behavior of the supply chain defined in Section 4.1 under different disruption patterns while assuming that the inventory policies, as defined by the CSL, remain the same. For this purpose, we create five disruption scenarios (A-E) to examine the effects of disruption characteristics, presented in Figure 1, on the health care center behavior and the performance metrics.

Table 2 summarizes the characteristics of each scenario. To allow for easy comparison of these scenarios, we assume that all disruptions start at the same time (week 50), and that the total recall quantity remains the same for all of the scenarios, except Scenario C, which has a greater recall size.

Table 2: Disruption scenarios.

Scenarios	Definition	Total Recall	Breadth (λ)	Time Between∗	Duration (γ)∗	Intensity (θ)	% Lost	Start Time∗
A	1% loss of inventory, brief disruption, single continuous disruption	26,200	1	-	12	2,183	1%	50
B	1% loss of inventory, prolonged disruption, single continuous disruption	26,200	1	-	24	1,092	1%	50
C	5% loss of inventory, prolonged disruption, single continuous disruption	131,000	1	-	24	5,458	5%	50
D	1% loss of inventory, two disruptions, short break in events	26,200	2	3	12	1,092	1%	50
E	1% loss of inventory, two disruptions, long break in events	26,200	2	24	12	1,092	1%	50

∗The unit of measure for time is weeks.

The total recall amount corresponds to the area under the rectangles in Figure 1. Therefore, we define the variable λ as the number of disruptions (breadth), γ as the duration of each disruption, and θ as the intensity of the disruption. The intensity of the disruption corresponds to the quantity of product effected, or recalled, during each period of time during the disruption. Equation (11) shows the relationship among these factors. In all scenarios, we assume that the total recall amount is equal to a percentage of the total demand during the simulation duration, or the percentage lost. The total recall amount is defined as

$$\text{Total recall} = \lambda\gamma\theta. \tag{11}$$

Length of Disruption. To examine the effect of the length of the disruption, Scenarios A and B are compared. While both scenarios have the same amount of total recalls, corresponding to 1% of the total demand, Scenario A represents a disruption that has a higher quantity of product recalled per week which lasts for fewer weeks than Scenario B. All other features of the scenarios are the same. Graphical depictions of the disruption pattern and behavior at the health center including inventory levels, shortage levels, and order amounts for Scenarios A and B are presented in Figure 2. While both systems quickly recover to a state of no shortages within one week after the disruption occurs, the ultimate effects of the disruption scenarios are different. For example, as presented in Table 3, the total shortage is 19% greater in Scenario A than in Scenario B when demand is modeled stochastically. When demand is modeled deterministically, the shortage in Scenario A is 13% greater than in Scenario B. While the shortage amounts differ, the total inventory does not vary significantly between the scenarios. These results demonstrate that the effects of recalls are driven by more than just the total amount recalled. Instead, the rate of products recalled per week and the duration of time over which recalls occur will affect the total number of individuals that are unable to receive the needed product, referred to as the shortage amount.

Breadth of Disruption. To examine the effect of the number of disruptions, or the disruption breadth, we compare Scenarios B and D. While in Scenario B there is one disruption that lasts for a total of 24 weeks, in Scenario D there are two disruptions each with a length of 12 weeks and with 3 weeks passing between the disruptions. Both scenarios have the same intensity (θ), defined as the number of products recalled each week during the disruption. The results for these scenarios with deterministic demand are shown in Figure 2. Scenario B and D have slightly different behavior. It takes one week more for Scenario D to return to steady state than Scenario B. Also, the total order amount in Scenario D is greater than in Scenario B. As presented in Table 3, the total shortage is 2% greater in Scenario D than in Scenario B when the system is modeled with stochastic demand and 1% greater when the demand is modeled deterministically. This implies that the system performs slightly better when there is a continuous disruption as opposed to having a short break between the shortages. This is further examined by studying the effects of periodicity of the disruptions.

Periodicity of Disruption. Scenarios D and E are compared in order to examine the effect of periodicity of the disruptions. All disruption parameters except for the time between the disruptions are the same. Unlike the 3-week duration that occurs in Scenario D, in Scenario E there is a 24-week break between the disruptions. Similar to the results seen through the comparison of Scenarios B and D, as the time between the recall disruptions increase, so does the level of shortage in the system. As presented in Table 3, the shortage in Scenario E is

Figure 2: Inventory levels, shortage rates, and orders at health centers over time for disruption Scenarios A-E when demand is modeled deterministically.

10% greater than that in Scenario D for both deterministic and stochastic demand patterns. We hypothesize that the reason for this behavior is that when another disruption has recently occurred the system is already working to recover, with greater production and shipping levels. Thus it is more prepared for a subsequent disruption. As the time between disruptions increases the system is more likely to revert to a steady state which is not prepared to accommodate an additional disruption.

Size of Disruption. Finally, we examine the effect of the size of the disruption on the system by comparing Scenario B and Scenario C. In Scenario C, the number of products recalled per week is five times that found in Scenario B. From examining Figure 2, it is shown that the pattern is the same for the two disruption scenarios, but the intensity differs. Similarly, the temporal patterns pertaining to the inventory, orders, and shortage at the health center are similar for the two scenarios, although the scale of the effects are different. As shown in Table 3, the total shortage in Scenario C is 470% of that in Scenario B when demand is modeled deterministically. Similarly, when demand is modeled stochastically, the total shortage in Scenario C is five times that found in Scenario B.

The higher rate of shortage in proportion to the increase in the recall rate is expected since it is assumed that the inventory policy, as defined by the CSL, is the same regardless of the recall pattern. In practice, it would be natural for a supply chain stakeholder to choose a higher CSL if it was expected that substantially greater recalls were likely. Similarly, if a particular product is more likely to exhibit short and intense disruptions rather than long and more mild disruptions this should inform the management decisions

Table 3: Performance metrics for the recall scenarios with deterministic demand and stochastic demand.

Recall Scenarios	Total Recall	Demand constant 10000 bags/week		Demand Normal (10000,100) bags/week	
		Average Health Center's Inventory	Total Shortage	Average Health Center's Inventory	Total Shortage
0/ No Recall	0	10,000	0	10,203	281
A	26,200	9,941	18,501	10,131	18,262
B	26,200	9,943	16,317	10,127	15,293
C	131,000	9,728	77,214	9,909	76,720
D	26,200	9,942	16,504	10,125	15,574
E	26,200	9,942	18,235	10,122	17,125

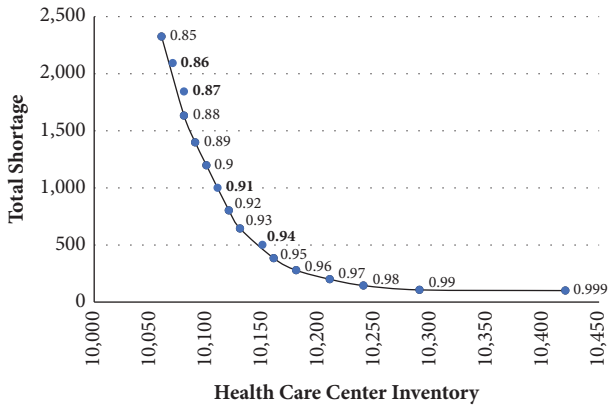

Figure 3: Effects of inventory policies, defined by CSL, on the total shortage and health center inventory and an estimate of the efficient frontier defining nondominated inventory policies. The CSLs equal to .86, .87, .91, and .94 are inefficient and not included on the efficient frontier.

made by supply chain members. As demonstrated in the comparison of scenarios here, even with just one change in the features of the disruption and no changes in the inventory strategy or the total amount recalled, the performance of the system can vary significantly. Thus, it is important to consider potential disruption features when choosing an inventory strategy.

The results for the defined scenarios show that the system acts very differently based on the differing disruption characteristics. In the next section, we examine how different policies affect the performance of the underlying system.

4.3. Effect of Inventory Policies on the Performance. The driving parameter that defines the inventory management policy, and correspondingly the safety stock, at each echelon of the supply chain, is the cycle service level. In the previous section, it was seen that for different recall disruption scenarios (A-E) and a constant CSL the performance of the system varied significantly. Next, we examine the effects of changes to the inventory policies as they correspond to changing the CSL for the different recall scenarios. While we allow for the policies to change, it is assumed that all echelons will have the same CSL value. Further, we examine the effects of these changes in inventory policies and disruption patterns jointly on two performance metrics, (i) total shortage and (ii) inventory at the health center.

To provide a baseline performance level for the inventory policies, Scenario 0 is defined which represents the system when no disruptions occur.

Figure 3 demonstrates the effects of different CSL values on the two performance metrics in Scenario 0. As this figure shows, by increasing the CSL, the total inventory level increases and the total shortage level decreases.

Identifying the optimal CSL among the policy options is dependent on the relative costs associated with the two performance measures of total shortage and health care center inventory. We evaluate the performance of the policy options for different relative costs using the approach discussed in Section 3.3. The efficient frontier in Figure 3 depicts the estimated levels of both shortages and health care center inventory that can be achieved, and would be optimal, for some relative value of shortage and inventory costs. Thus, all CSL values that do not fall precisely on this efficient frontier are classified as inefficient by the DEA approach. An alternate interpretation of inefficiency is provided by noting that there is a point on this efficient frontier that achieves fewer shortages or fewer inventories while keeping the same level with respect to the second measure. Thus, the outcomes estimated by the efficient frontier are strictly better than those achieved with the inefficient CSL value. As shown in Figure 3, and determined by applying the DEA approach, the policies corresponding to the CSLs of 0.86, 0.87. 0.91, and 0.94 are not on the corresponding efficient frontiers and therefore are never efficient when no shortages occur, regardless of the relative values of the inventory holding cost and the shortage cost. All efficient inventory policies among those simulated are on the efficient frontier in the graph in Figure 3.

To identify efficient inventory policies when the system is experiencing disruptions, we introduce a stochastic model of recalls to present a more realistic setting in which the number of disruptions and the time between disruptions vary. To ensure that the total expected number of products recalled is consistent across scenarios, we model the disruptions with a Poisson distribution with the parameter lambda (λ) corresponding to the expected number of disruptions, or the disruption breadth. Additionally, with the assumption that the duration of each recall disruption (γ) is the same, the average recall quantity per week (θ) is scaled to ensure that the total expected quantity recalled is the same. Due to the stochastic nature of the modeling, it is possible that simulation instances experience different numbers of disruptions, and therefore different quantities are recalled, but the expected number recalled remains the same.

In order to study the effect of different inventory policies on the performance metrics of the health center, we simulate each recall pattern for 16 different CSLs. Furthermore, we run the simulation for multiple disruption patterns defined by the value of λ, for λ = (5, 10, 15, 20), for a 5% of loss inventory, to examine the relationship between policies and recall patterns. For smaller values of λ there are fewer disruptions with higher intensity. More frequent disruptions with fewer recalls per week results from higher values of λ. Figure 4 shows the performance of these policies, defined by the CSL, for different recall patterns, defined by the λ value. From the results, it is clear that different inventory policies perform significantly different depending on the disruption pattern. Additionally, the incremental difference in inventory and shortage between policies varies for different disruption patterns. Thus, the choice of policy should vary with respect to the expected disruption characteristics and with the relative costs of one unit of shortage and one unit of inventory.

Similar to the identification of efficient inventory policies for the scenario with no recalls, we can identify inventory policies that are inefficient regardless of the relative valuation of the two performance measures. This can be achieved

Table 4: Optimal CSL for varying ratios of shortage and inventory costs under different disruption patterns as defined by the expected number of recall disruptions (λ).

	Relative value of cost (unit cost of shortage/ unit cost of inventory)						
λ	**0.8**	**1**	**1.2**	**1.4**	**1.6**	**1.8**	**2**
5	0.9	0.94	0.95	0.96	0.98	0.98	0.99
10	0.9	0.94	0.97	0.98	0.99	0.999	0.999
15	0.93	0.98	0.98	0.99	0.999	0.999	0.999
20	0.96	0.98	0.98	0.999	0.999	0.999	0.999

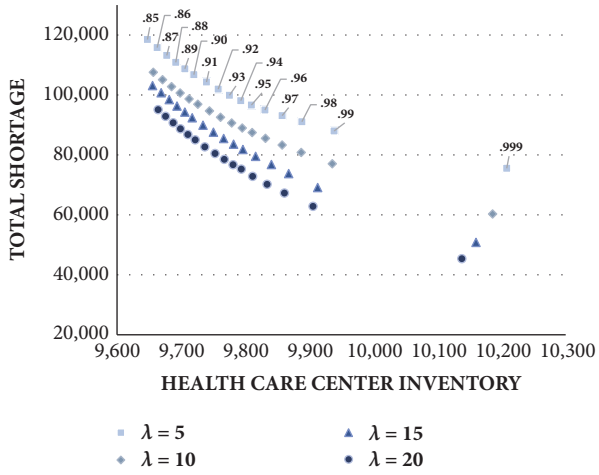

Figure 4: For different recall patterns, defined by λ, the resulting total shortage and health care center inventory for various inventory policies, defined by the CSL.

by using an approach similar to DEA. For example, when λ equals 5, 15 and 20, inventory policies with CSL equal to 0.91, 0.86 and 0.96, and 0.95, respectively, are found to be inefficient using the mathematical models in the DEA approach. While an inventory policy may be identified as efficient it will not be optimal for all relative values of per unit shortage costs and per unit inventory costs. The optimal CSLs for a selection of relative costs and for different disruption patterns, defined by λ, are provided in Table 4.

For different ratios of the unit cost of shortage and the unit cost of inventory, we can identify the optimal CSL for the inventory policy. Table 4 illustrates the result of this analysis. This analysis reveals that increasing the CSL, which is equivalent to choosing to hold more safety stock in inventory, is not always best and it varies based on the ratio of costs and the type of disruption that is expected to occur. For example, if the ratio of the costs is 1, a CSL equal to 0.98 is optimal only if there are frequent recalls, of approximately more than 15 over 5 years, or low intensity in this model. However, if it is expected that there will only be one recall per year ($\lambda = 5$) of a high intensity, then choosing a CSL of 0.98 is no longer optimal and we should instead choose a CSL of 0.94.

Finally, the results in Table 4 demonstrate the sensitivity of the choice of inventory policy for a disruption pattern. For example, if the ratio of costs is 1.4, choosing an inventory policy with the assumption of five recalls over the five-year duration will leave the supply chain stakeholder very far from the optimal policy if in fact there are fifteen recalls and the same total quantity is recalled. This demonstrates the criticality of choosing a policy that correctly matches the expected recall disruption pattern. Further, this supports the value of stakeholders gathering information about historical patterns in recalls and forecasting future recalls. By achieving a better understanding of the likely recall scenarios, supply chain decision makers can adjust and ultimately reduce costs from inventory and shortages. These results support the consideration of the use of adaptive policies such that inventory decisions change over time either in anticipation of or in response to recalls. This ultimately may lead to reduced drug shortages and reduced supply chain costs. As discussed below, we suggest expanding the model to integrate adaptive inventory policies in future work.

5. Conclusion

We present a mathematical simulation model of the pharmaceutical supply chain to understand the behavior of the drug shortages under different disruption patterns. There are currently few models that study the entire pharmaceutical supply chain, and none that focus on recalls and disruption patterns. To provide insights into this critical relationship we examine (i) the role of the disruption characteristics and (ii) the role of the inventory management policies within a simulation model inspired by the saline supply chain. Sterile solutions, such as saline, constitute a large portion of the pharmaceutical recalls and shortages that occur each year.

Through analysis of this supply chain, we find that small differences in the disruption patterns lead to very different system performance when the inventory management policies are held consistent. Further, this relationship holds for changes to either the (i) length, (ii) breadth, (iii) periodicity, or (iv) size of the disruptions. Additionally, we demonstrate the sensitivity of the optimal inventory policy to these features of the disruptions. Thus, rather than a traditional approach of using a consistent cycle service level (i.e., holding more safety stock in inventory), our results support the need for evolving inventory management strategies that account for the features of the disruption.

In the case of saline, frequent small recalls occurred in the system prior to 2017. If the inventory policies were designed to instead be resilient against major disruptions or large recalls, the inventory management policy and levels

of safety stock would not be efficient. Thus, choosing a policy that best responds to the likely disruptions is critical. Further, with an understanding of the effects of frequent small disruptions, one option for stakeholders in the saline supply chain would be to invest in manufacturing equipment and institute practices that would decrease the likelihood of this disruption pattern. Additionally, instituting policies that allow for inventory policies to agilely adapt based on current and expected future circumstances would improve the overall system performance.

A key challenge to implementing policies that adapt to disruptions is the critical unknown features of disruptions that will occur in the future. But while full knowledge of future events is not possible, the results of this work support the need for supply chain managers to examine and identify the best inventory management policies for a variety of types of disruptions that are probable. In return, understanding this relationship between the best policies and the disruption characteristics can inform implementation of policies that are robust to a variety of types of disruptions. Further, as disruptions occur and estimates of their features, such as length, breadth, size, and periodicity, are updated supply chain stakeholders can modify their inventory policies accordingly. Lastly, these results support the importance of supply chain stakeholder investing in gaining information about these disruption characteristics both in anticipation of or during a disruption. This additional information will be valuable as it allows the decision makers to adapt policies in real-time.

There are several limitations and extensions which require further investigation. First, this paper considers that there is no limitation on the manufacturing capacity. A more realistic model with inclusion of limited capacities and a sensitivity analysis examining the role of manufacturing capacity may be informative for future consideration as the capacity is expected to significantly influence the shortage size and the time for the system to return to a steady state. Second, we assume that all the echelons use the same inventory policy and have the same CSL. This representation may be violated for pharmaceutical supply chains in which downstream nodes tend to hold more safety stock to reduce the likelihood of unmet patient demand. Third, defining the total cost of the system as the inventory holding cost and shortage cost of the health care center is a limiting feature. While we only consider the inventory of health care centers, this can be considered to serve as a proxy that represents the total inventory in the supply chain. Additionally, with a focus on addressing the critical societal problem of drug shortages, we focus on developing an understanding of the elements driving shortages. Future extensions of this model can account for additional system elements in the objective function.

We propose to address these limitations in future research. Additionally, since, in the real world, planners are often unsure of the type of disruption that will occur, in future research we aim to construct and examine the performance of adaptive inventory policies by building on the findings from this work. There are also opportunities to expand this study to investigate other types of pharmaceutical supply chain disruptions, including manufacturing shutdowns and surges in demand to compare and contrast with the effects of recall disruptions. Also, consideration of the cooccurrence of manufacturing shutdowns and product recalls can further inform operational policies for supply chain stakeholders seeking to prevent future drug shortages.

Data Availability

The data used to support the findings of this study are available from the corresponding author upon request.

Conflicts of Interest

The authors declare that they have no conflicts of interest.

Acknowledgments

This research was funded in part by the National Science Foundation (Grant CMMI #1638302).

References

[1] E. Fox, *Drug Shortages Statistics - ASHP*, University of Utah Drug Information Service, Drug Shortage Statistics, 2018, http://www.webcitation.org/6zJN2q9LR.

[2] P. Loftus, "Shortages of simple drugs thwart treatments," *Wall Street Journal*, p. 01, 2017.

[3] U. S. Government Accountability Office, "Drug Shortages: Certain Factors Are Strongly Associated with This Persistent Public Health Challenge," no. GAO-16-595, 2016.

[4] M. Mazer-Amirshahi and E. R. Fox, "Saline Shortages — Many Causes, No Simple Solution," *The New England Journal of Medicine*, vol. 378, no. 16, pp. 1472–1474, 2018.

[5] D. Crow, "Saline investigation highlights the cost of American healthcare," *Financial Times*, 2018, https://www.ft.com/content/4593b93e-1887-11e8-9376-4a6390addb44.

[6] U.S. Department of Health and Human Services, *A Review of FDA's Approach to Medical Product Shortages*, U.S. Food and Drug Administration, 2011.

[7] E. FRY, "There's a national shortage of saline solution. Yeah, we're talking salt water. Huh?" *Fortune*, 2015, http://fortune.com/2015/02/05/theres-a-national-shortage-of-saline/.

[8] U.S. Food and Drug Administration, "Press Announcements - FDA Commissioner Scott Gottlieb, M.D., updates on some ongoing shortages related to IV fluids," https://www.fda.gov/NewsEvents/Newsroom/PressAnnouncements/ucm592617.htm, 2018.

[9] E. R. Fox, A. Birt, K. B. James et al., "ASHP guidelines on managing drug product shortages in hospitals and health systems," *American Journal of Health-System Pharmacy*, vol. 66, no. 15, pp. 1399–1406, 2009.

[10] F. Lücker and R. W. Seifert, "Building up Resilience in a Pharmaceutical Supply Chain through Inventory, Dual Sourcing and Agility Capacity," *OMEGA - The International Journal of Management Science*, vol. 73, pp. 114–124, 2017.

[11] R. Uthayakumar and S. Priyan, "Pharmaceutical supply chain and inventory management strategies: optimization for a pharmaceutical company and a hospital," *Operations Research for Health Care*, vol. 2, no. 3, pp. 52–64, 2013.

[12] J. Jia and H. Zhao, "Mitigating the U.S. drug shortages through pareto-improving contracts," *Production Engineering Research and Development*, vol. 26, no. 8, pp. 1463–1480, 2017.

[13] S. Saedi, O. E. Kundakcioglu, and A. C. Henry, "Mitigating the impact of drug shortages for a healthcare facility: an inventory management approach," *European Journal of Operational Research*, vol. 251, no. 1, pp. 107–123, 2016.

[14] J. Strohhecker and A. Größler, "Lead-weighted jacket or life vest? Inventories in the presence of major production disruptions," in *Proceedings of the presented at the 21st EurOMA Conference*, p. 51, Palermo, 2014.

[15] J. Strohhecker and A. Größler, "Dynamic Life cycle inventory policies for consumer goods with severe production disruptions," in *Proceedings of the presented at the 22nd EurOMA Conference*, p. 78, 2015.

[16] B. Tomlin, "On the value of mitigation and contingency strategies for managing supply chain disruption risks," *Management Science*, vol. 52, no. 5, pp. 639–657, 2006.

[17] B. Tomlin and L. V. Snyder, "On the value of a threat advisory system for managing supply chain disruptions," in *Working Paper*, Kenan-Flagler Business School, University of North Carolina-Chapel Hill USA, 2006.

[18] S. Chopra, G. Reinhardt, and U. Mohan, "The importance of decoupling recurrent and disruption risks in a supply chain," *Naval Research Logistics (NRL)*, vol. 54, no. 5, pp. 544–555, 2007.

[19] Z. Atan, L. V. Snyder, and G. R. Wilson, "Lateral Transshipment and Rationing Policies for Multi-Retailer Systems," in *Social Science Research Network*, SSRN Scholarly, Rochester, NY, USA, 2013.

[20] S. Saghafian and M. P. Van Oyen, "The value of flexible backup suppliers and disruption risk information: Newsvendor analysis with recourse," *Institute of Industrial Engineers (IIE). IIE Transactions*, vol. 44, no. 10, pp. 834–867, 2012.

[21] S. Demirel, R. Kapuscinski, and M. Yu, "Strategic behavior of suppliers in the face of production disruptions," *Management Science*, vol. 64, no. 2, pp. 533–551, 2018.

[22] C. A. Yano and H. L. Lee, "Lot sizing with random yields: a review," *Operations Research*, vol. 43, no. 2, pp. 311–334, 1995.

[23] T. Sawik, "On the fair optimization of cost and customer service level in a supply chain under disruption risks," *Omega*, vol. 53, pp. 58–66, 2015.

[24] L. V. Snyder, Z. Atan, P. Peng, Y. Rong, A. J. Schmitt, and B. Sinsoysal, "OR/MS models for supply chain disruptions: a review," *IIE Transactions*, vol. 48, no. 2, pp. 89–109, 2016.

[25] A. Größler, J.-H. Thun, and P. M. Milling, "System dynamics as a structural theory in operations management," *Production Engineering Research and Development*, vol. 17, no. 3, pp. 373–384, 2008.

[26] J. B. Morrison and R. Oliva, "Integration of behavioral and operational elements through system dynamics," in *Social Science Research Network*, SSRN Scholarly, Rochester, NY, USA, 2017.

[27] J. Sterman, R. Oliva, K. Linderman, and E. Bendoly, "System dynamics perspectives and modeling opportunities for research in operations management," *Journal of Operations Management*, vol. 39-40, pp. 1–5, 2015.

[28] J. D. Sterman, "Modeling managerial behavior: misperceptions of feedback in a dynamic decision making experiment," *Management Science*, vol. 35, no. 3, pp. 321–339, 1989.

[29] H. L. Lee, V. Padmanabhan, and S. Whang, "Information distortion in a supply chain: the bullwhip effect," *Management Science*, vol. 43, no. 4, pp. 546–558, 1997.

[30] S. Minegishi and D. Thiel, "System dynamics modeling and simulation of a particular food supply chain," *Simulation Modelling Practice and Theory*, vol. 8, no. 5, pp. 321–339, 2000.

[31] P. Georgiadis, D. Vlachos, and E. Iakovou, "A system dynamics modeling framework for the strategic supply chain management of food chains," *Journal of Food Engineering*, vol. 70, no. 3, pp. 351–364, 2005.

[32] M. C. Wilson, "The impact of transportation disruptions on supply chain performance," *Transportation Research Part E: Logistics and Transportation Review*, vol. 43, no. 4, pp. 295–320, 2007.

[33] R. Croson and K. Donohue, "Behavioral causes of the bullwhip effect and the observed value of inventory information," *Management Science*, vol. 52, no. 3, pp. 323–336, 2006.

[34] L. V. Snyder and Z.-J. M. Shen, *Fundamentals of Supply Chain Theory*, John Wiley Sons, 2011.

[35] S. Chopra and M. S. Sodhi, "Managing risk to avoid: supply-chain breakdown," *MIT Sloan Management Review*, vol. 46, no. 1, pp. 53–61, 2004.

[36] L. V. Snyder and Z.-J. M. Shen, *Supply and Demand Uncertainty in Multi-Echelon Supply Chains*, vol. 15, Lehigh University Press, 2006.

[37] S. A. Melnyk, A. Rodrigues, and G. L. Ragatz, "Using Simulation to Investigate Supply Chain Disruptions," in *Supply Chain Risk*, vol. 124 of *International Series in Operations Research & Management Science*, pp. 103–122, Springer US, Boston, MA, 2009.

[38] A. Charnes, W. W. Cooper, and E. Rhodes, "Measuring the efficiency of decision making units," *European Journal of Operational Research*, vol. 2, no. 6, pp. 429–444, 1978.

[39] W. W. Cooper, L. M. Seiford, and J. Zhu, "Data envelopment analysis: history, models, and interpretations," in *Handbook on Data Envelopment Analysis*, vol. 164 of *39*, p. 1, Springer US, Boston, MA, USA, 2011.

Hindawi
Complexity
Volume 2018, Article ID 5738135, 10 pages
https://doi.org/10.1155/2018/5738135

Research Article

Quantifying the Robustness of Countries' Competitiveness by Network-Based Methods

Ming-Yang Zhou, Xiao-Yu Li, Wen-Man Xiong, and Hao Liao

Guangdong Province Key Laboratory of Popular High Performance Computers, College of Computer Science and Software Engineering, Shenzhen University, Shenzhen 518060, China

Correspondence should be addressed to Hao Liao; jamesliao520@gmail.com

Received 17 May 2018; Accepted 1 November 2018; Published 2 December 2018

Guest Editor: Claudio Tessone

In economic researches, much effort was devoted to the problem of how to increase the economics of countries. However, the development of a country may fluctuate a lot due to international and domestic problems. Thus, we should also evaluate the robustness of countries against unexpected economic recessions. In this paper, we use perturbation to quantify the robustness of countries using two renowned algorithms: method of reflections (MR) and fitness-complexity method (FCM). The robustness characterizes the stability of countries' competitiveness against economic recessions. The experiments in the international trade networks show that FCM could characterize the robustness better than MR. High fitness countries of FCM have strong robustness against economic crises, which enlarges the application fields of FCM. Additionally, we simulate the trade conflict between USA and China. The simulation results show that China suffers much in the trade conflict, while USA loses very little and has strong robustness in this conflict.

1. Introduction

In network science, the development of a country is assessed by the amount of its imported and exported products. Recent works developed methods to unveil the underlying factors that drive the economic growth of countries based solely on the international trade network [1–4]. As nowadays the economic relationship between countries is strong, an economic depression that starts from one country may largely influence other countries, which may lead to economic crisis and recessions in the whole world. Thus, apart from the assessment of the economic growth of countries, an important feature of countries to consider is their robustness against various economic recessions. However, a new problem arises: would the increase of robustness lead to a decrease of economic growth? Studies show that developed countries should focus on some high-tech and profitable products [3, 5], since the high-tech products help maintain and improve their competitiveness. However, unexpected tariff protectionism and natural disasters may deeply influence the exports of some targeted products [6, 7]. Then, in order to protect against this, a country should diversify its production [1, 8]. This is against the classical specialization theory [3, 5]. Consequently, the relationship between robustness and the competitiveness of countries should be investigated.

Measuring the competitiveness of countries usually requires the detailed industrial data [9, 10]. However, in recent years, network-based methods provide a simplification of this [8, 11]. In network-based methods, the only required information is the amount of exports for each country-product pair. If a country is competitive enough in the export of a product, a link is created in the network between the country and the product. The resulting network is the country-product bipartite network. There are two main network-based methods to investigate the countries performance: (1) the method of reflections (MR), which uses a linear iterative process to compute the scores of countries and products; this method share similarities with the famous algorithm PageRank [12–14]; (2) the fitness-complexity method (FCM), which uses a nonlinear iterative method to compute the fitness of countries and the complexity of products [1]. MR was shown to outperform previous indices based on governance, education, and other economic competitiveness factors [15, 16]. However, MR

fails in precisely evaluating the competitiveness of some special countries, such as India and China [17, 18]. The fitness-complexity method is based on the fact that only competitive countries can produce high-quality products, while less competitive countries can only produce low-quality products. If a product is only produced by competitive countries, it is a high-quality product; otherwise it is a low-complexity product. FCM outperforms MR both in accuracy and efficiency [8, 19]. The previous works mainly focused on how to accurately evaluate and predict the economic growth of countries. In this work, we use both methods to study how a country is influenced by the international and domestic economic recessions.

Based on state of the art MR and FCM methods, our paper explores the robustness of countries' competitiveness. Using the matrix perturbation theory, we propose a convenient analytical method to test the stability of the competitiveness of countries and complexity of products. Then the proposed method is applied to the international trade networks, and we show that FCM can not only evaluate the fitness of countries, but also precisely characterize the robustness of their competitiveness. On the other hand, the MR scores fail to assess the robustness of countries' competitiveness compared to FCM. According to the results, only a very small number of countries possess strong robustness against economic recessions. In order to increase its robustness, a country should improve its fitness, which is also equivalent to diversifying its products according to refs. [1, 3, 8]. Moreover, we also use our method to simulate the trade conflict between USA and China and predict that the trade conflict sharply decreases the fitness of China, whereas it seldom influences USA, revealing strong robustness of USA.

The paper is organized as follows. In Section 2, we briefly describe the method of reflection and the fitness-complexity method, and then we introduce our way to use perturbation method. In Section 3, we apply the proposed method to the international trade networks. Finally, the conclusion is given.

2. Materials and Methods

In the section, we first describe the country-product networks in Section 2.1 and then introduce the classical method of reflections and fitness-complexity method in Section 2.2. Finally we describe our method to test the robustness of countries' competitiveness in Section 2.3.

2.1. Dataset Description of the Country-Product Networks. The dataset we use ranges from 1962 to 2014 [2, 20–23]. We use a network representation, in which one kind of nodes is countries and the other kind is products. Edges can only connect country and a product, meaning that the network is bipartite. The products are indeed not considered individually: each exported product was assigned to a predefined category. The dataset has 263 countries (or zones) and 988 product categories. Besides, we neglect a very small fraction of categories that are ambiguous (aggregate categories). Note that in the rest of the work we use the word product for category of product.

For each country-product pair, we know the total export in US$ of products of a country. In practice, a country may produce more or less of a product. In order to characterize whether a country is a competitive exporter of a product or not, we use the "Revealed Comparative Advantage" (RCA) to renormalize the weight of the country-product relations and only edges with weight greater than 1 are kept. The RCA is defined as

$$RCA_{i\alpha} = \frac{e_{i\alpha}/\sum_j e_{j\alpha}}{\sum_\beta e_{i\beta}/\sum_{j\beta} e_{j\beta}}, \tag{1}$$

where $e_{i\alpha}$ is the export in US$ of country i for product α. After processing the data, we obtain the weighted matrix of the country-product network, denoted by $M = (M_{ij})_{N_c \times N_p}$, where N_c and N_p represent the number of countries and products, respectively, and $M_{i\alpha} = RCA_{i\alpha}$. $RCA_{i\alpha}$ determines the relative importance of an export for a country and compares it with its relative importance for other countries. In network, we defined the number of products exported by country i as its degree d_i, and the number of times a product α is exported as d_α. Note that in general only the adjacency matrix of the network is considered, but for perturbation theory it is indeed more suitable to use the weighted matrix.

2.2. Methods of Reflections (MR) and Fitness-Complexity (FCM). **Method of reflections** is a classical economic complexity index by Hidalgo and Hausmann [3, 24]. This method defines a score or each country $\{d_i^{(n)}\}$ and a score for each product $\{u_\alpha^{(n)}\}$ in an iterative way,

$$\begin{aligned} d_i^{(n)} &= \frac{1}{d_i}\sum_\alpha M_{i\alpha} u_\alpha^{(n-1)}, \\ u_\alpha^{(n)} &= \frac{1}{u_\alpha}\sum_i M_{i\alpha} d_i^{(n-1)}, \end{aligned} \tag{2}$$

where d_i and u_α are the country degree and product degree, respectively. According to (2), with the increase of iterations, $\{d_i^{(n)}\}$ and $\{u_\alpha^{(n)}\}$ will asymptotically converge to a trivial fixed point for arbitrary initial $\{d_i^{(0)}\}$ and $\{u_\alpha^{(0)}\}$ [25, 26]. However, this problem is solved by defining the final country score as $\widetilde{d_i^c} = (d_i^c - \langle d_i^c \rangle)/\sigma_{d_i^c}$, where $\langle d_i^c \rangle$ and $\sigma_{d_i^c}$ represent the average and the standard deviation of the final score d_i^c. When $n \longrightarrow +\infty$, the fixed point solution is equivalent to an approach using the eigenvectors of the matrix M [26]. In practice, we use $n = 2$, as different iterations have different interpretation. The initial conditions for $\{d_i^{(0)}\}$ and $\{u_\alpha^{(0)}\}$ are set as $\{d_i^{(0)}\} = d_i$ and $\{u_\alpha^{(0)}\} = u_\alpha$. The results of (2) agree with the assumption that complex products (or high-quality products) have high scores and tend to be produced by developed countries, while developing countries only produce some low-quality products. This can be used to evaluate the competitiveness and the economic growth of a country. The index of (2) outperforms the degree-based index [8].

Fitness-complexity method defines the country fitness $\{F_i\}$ and product complexity $\{Q_\alpha\}$ as the stationary point of the following nonlinear recursive process [1]:

$$\widetilde{F}_i^{(n)} = \sum_\alpha M_{i\alpha} Q_\alpha^{(n-1)},$$
$$\widetilde{Q}_\alpha^{(n)} = \frac{1}{\sum_i M_{i\alpha}\left(1/F_i^{(n-1)}\right)}. \tag{3}$$

The scores are normalized after each step:

$$F_i^{(n)} = \frac{\widetilde{F}_i^{(n)}}{\left\langle \widetilde{F}_i^{(n)} \right\rangle},$$
$$Q_\alpha^{(n)} = \frac{\widetilde{Q}_\alpha^{(n)}}{\left\langle \widetilde{Q}_\alpha^{(n)} \right\rangle}, \tag{4}$$

where $\langle \ldots \rangle$ is the average operation. The initial values of $F_i^{(0)}$ and $Q_\alpha^{(0)}$ do not influence the final stationary state except some particular singular points. Without loss of generality, the initial condition are set as $F_i^{(0)} = 1$ and $Q_\alpha^{(0)} = 1$. When we apply (3) to the country-product bipartite networks, developed countries and high-quality products are inclined to have high fitness, while developing countries and low-quality products tend to have small complexity. Therefore, FCM can evaluate the competitiveness of countries and the complexity of products [1, 25] and predict the future economic development [19, 27]. This method has been successfully applied to other fields, such as ecological networks [28] and scientific competitiveness of nations [29].

Note that we use both MR and FCM to describe the "Economic Complexity Index" of countries or "Product Complexity Index" of products in the paper. In the following, we define the competitiveness as the "Economic Complexity Index" of both MR and FCM method. For MR method, the competitiveness is represented by d_i in (2), while, for FCM method, the competitiveness is represented by the fitness $F_i^{(n)}$ in (4).

2.3. Robustness of the Countries' Competitiveness. In order to stimulate the economy, countries design various tariffs and other policies to promote or reduce the exports/imports of certain products. In theory, it would be possible to infer these changes based on an analysis of the matrix M. However, analyzing the detailed reason of the fluctuation of M is prohibitive in practice. In the work, we investigate how the competitiveness of countries changes with perturbations of matrix M. Smaller fluctuations of the metrics mean higher robustness. This can reflect how resilient a country is to a change of policy. For the precise relationship between the exports and policies, please refer to [30–32].

In order to study the perturbation, we introduce a small number ε and a perturbation matrix B. The resulting perturbed matrix is $M(\varepsilon) = M + \varepsilon B$, $\Delta M = \varepsilon B$. After the perturbation, the stationary points of (2) become $\overline{d}_i(\varepsilon)$ and $\overline{u}_\alpha(\varepsilon)$. A straightforward approach to obtain $\overline{d}_i(\varepsilon)$ and $\overline{u}_\alpha(\varepsilon)$ is recalculating (2) based on $M(\varepsilon)$. Here, we introduce a perturbation method to compute $\overline{d}_i(\varepsilon)$ and $\overline{u}_\alpha(\varepsilon)$, as well as the FCM scores. If you are not interested in the complex derivation procedure, please skip the following part, which does not influence the global comprehension of the paper.

We use Taylor's formalism [33, 34] to represent the perturbed quantities $\overline{d}_i(\varepsilon)$ and $\overline{u}_\alpha(\varepsilon)$; i.e., $\overline{d}_i(\varepsilon) = \overline{d}_i + \sum_{k=1}^{+\infty} g_i^{(k)} \varepsilon^k$ and $\overline{u}_\alpha(\varepsilon) = \overline{u}_\alpha + \sum_{k=1}^{+\infty} h_\alpha^{(k)} \varepsilon^k$. When $\varepsilon = 0$, $\overline{d}_i(\varepsilon)$ and $\overline{u}_\alpha(\varepsilon)$ reduce to $\overline{d}_i$ and $\overline{u}_\alpha$. Moreover, the degree d_i and u_α change to $d_i(\varepsilon) = d_i + \varepsilon d_{B,i}$ and $u_\alpha(\varepsilon) = u_\alpha + \varepsilon u_{B,\alpha}$, where $d_{B,i} = \sum_\alpha B_{i\alpha}$ and $u_{B,\alpha} = \sum_i B_{i\alpha}$.

According to the perturbation theory [34, 35], by substituting the Taylor's formalism of each variable into (2) and keeping only the first order of ε, we obtain Taylor's decomposition of (2),

$$g_i^{(1)}\varepsilon = -\frac{\varepsilon d_{B,i}}{\overline{d}_i^2}\sum_\alpha M_{i\alpha}\overline{u}_\alpha + \frac{\varepsilon}{d_i}\sum_\alpha \left(B_{i\alpha}\overline{u}_\alpha + M_{i\alpha}h_\alpha^{(1)}\right),$$
$$h_\alpha^{(1)}\varepsilon = -\frac{\varepsilon u_{B,\alpha}}{\overline{u}_\alpha^2}\sum_i M_{i\alpha}\overline{d}_\alpha + \frac{\varepsilon}{u_\alpha}\sum_i \left(B_{i\alpha}\overline{d}_i + M_{i\alpha}g_i^{(1)}\right). \tag{5}$$

We denote $\mathbf{g}^{(1)} = [g_i^{(1)}]_{N_c\times 1}$, $\mathbf{h}^{(1)} = [h_\alpha^{(1)}]_{N_p\times 1}$, $\mathbf{C}_1(B) = [c_i(B)]_{N_c\times 1}$,$\mathbf{C}_2(B) = [c_\alpha(B)]_{N_p\times 1}$, where $c_i(B) = -(d_{B,i}/\overline{d}_i^2)\sum_\alpha M_{i\alpha}\overline{u}_\alpha + (1/d_i)\sum_\alpha B_{i\alpha}\overline{u}_\alpha$ and $c_\alpha(B) = -(u_{B,\alpha}/\overline{u}_\alpha^2)\sum_i M_{i\alpha}\overline{d}_\alpha + (1/u_\alpha)\sum_i B_{i\alpha}\overline{d}_i$.

Equation (5) can be written in matrix formalism as

$$\begin{bmatrix}\mathbf{g}^{(1)}\\ \mathbf{h}^{(1)}\end{bmatrix} = \begin{bmatrix}\mathbf{C}_1(B)\\ \mathbf{C}_2(B)\end{bmatrix} + \begin{bmatrix}0, D_1^{-1}M\\ D_2^{-1}M^T, 0\end{bmatrix}\begin{bmatrix}\mathbf{g}^{(1)}\\ \mathbf{h}^{(1)}\end{bmatrix}, \tag{6}$$

where $D_1 = \mathrm{diag}\{d_1, d_2, \ldots, d_{N_c}\}$ and $D_2 = \mathrm{diag}\{u_1, u_2, \ldots, u_{N_c}\}$. $\mathbf{g}^{(1)}$ and $\mathbf{h}^{(1)}$ could be solved as

$$\begin{bmatrix}\mathbf{g}^{(1)}\\ \mathbf{h}^{(1)}\end{bmatrix} = \left(I - \begin{bmatrix}0, D_1^{-1}M\\ D_2^{-1}M^T, 0\end{bmatrix}\right)^{-1}\begin{bmatrix}\mathbf{C}_1(B)\\ \mathbf{C}_2(B)\end{bmatrix}. \tag{7}$$

Equation (7) is used to compute the influence of the perturbation ΔM on the MR. Next we analyze the influence of $\Delta M = \varepsilon B$ on FCM. Supposing that $\overline{F}_i(\varepsilon)$ and $\overline{Q}_\alpha(\varepsilon)$ are the stable point of the matrix $M' = M + \Delta M$ and could be represented by Taylor's formalism; i.e., $\overline{F}_i(\varepsilon) = \overline{F}_i + \sum_{k=1}^{+\infty} f_i^{(k)}\varepsilon^k$ and $\overline{Q}_\alpha(\varepsilon) = \overline{Q}_\alpha + \sum_{k=1}^{+\infty} q_\alpha^{(k)}\varepsilon^k$. Following the procedure introduced above, we substitute Taylor's formalism of each variable into (3) and (4) and keep only the first order of ε,

$$f_i^{(1)}\varepsilon = c_1\sum_\alpha \left(M_{i\alpha}q_\alpha^{(1)} + B_{i\alpha}\overline{Q}_\alpha\right)\varepsilon + c_2\varepsilon,$$
$$q_\alpha^{(1)}\varepsilon = c_3\sum_i \left(-M_{i\alpha}\frac{1}{\overline{F}_i^2}f_i^{(1)} + B_{i\alpha}\frac{1}{\overline{F}_i}\right)\varepsilon + c_4\varepsilon, \tag{8}$$

where $c_1 = 1/\langle\widetilde{F}_i\rangle$ and $c_3 = -\widetilde{Q}_i^2/\langle\widetilde{Q}_i\rangle$. $c_2 = -(\widetilde{F}_i/\langle\widetilde{F}_i\rangle^2)\langle\sum_\alpha(M_{i\alpha}q_\alpha^{(1)} + B_{i\alpha}\overline{Q}_\alpha)\rangle$ and $c_4 = (\widetilde{Q}_i/\langle\widetilde{Q}_i\rangle^2)\langle\sum_i[(-M_{i\alpha}(1/\overline{F}_i^2)f_i^{(1)} + B_{i\alpha}(1/\overline{F}_i))\widetilde{Q}_i^2]\rangle$ are two parameters relevant to i and α, respectively, which

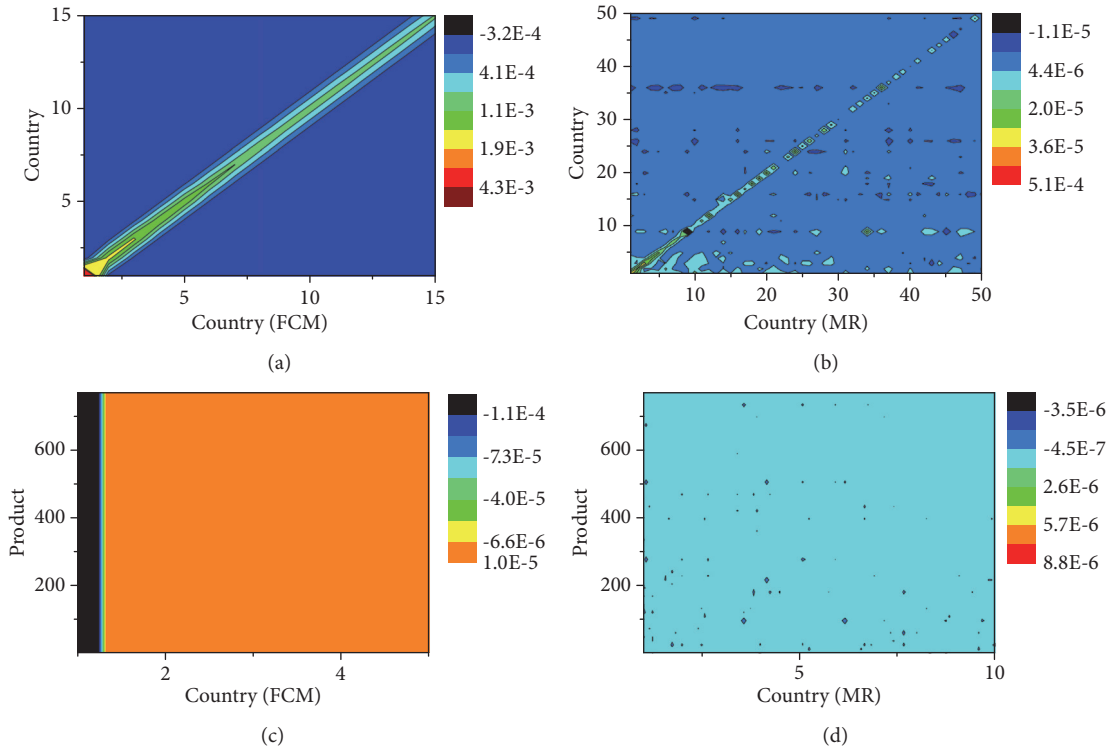

FIGURE 1: (Color online) The decrease of the counties and products scores induced by individually reducing the exports of countries by 5% for FCM and MR, as a function of the countries as rank in their respective method. (a) Change of the fitness scores (in FCM) of countries. (b) Change of the countries scores (in MR). (c) Change of the complexity (FCM) of products. (d) Change of the products scores (MR). Note that in the dataset, we have 263 countries (or zones) and 988 product categories. However, in the four panels, we only show the snapshot results of some competitive countries and complex product because the influence of other countries and products is much small.

guarantee the normalization of $\overline{F}_i(\varepsilon)$ and $\overline{Q}_\alpha(\varepsilon)$. Though c_2 and c_4 are function of $q_\alpha^{(1)}$ and $f_i^{(1)}$, we treat them as constants since they have average operations of the two variables when calculating $q_\alpha^{(1)}$ and $f_i^{(1)}$. Denote $\mathbf{f}^{(1)} = (f_i^{(1)})_{N_c\times 1}$ and $\mathbf{q}^{(1)} = (q_\alpha^{(1)})_{N_p\times 1}$. Similar to (7), the perturbation of FCM is

$$\begin{bmatrix}\mathbf{f}^{(1)}\\ \mathbf{q}^{(1)}\end{bmatrix} = \left(I - \begin{bmatrix}0, c_1 M\\ -c_3 M^T D_3, 0\end{bmatrix}\right)^{-1}\begin{bmatrix}\mathbf{C}_3(B)\\ \mathbf{C}_4(B)\end{bmatrix}. \quad (9)$$

where $D_3 = \mathrm{diag}\{1/\overline{F}_1^2, \ldots, 1/\overline{F}_i^2, \ldots, 1/\overline{F}_{N_c}^2\}$, $\mathbf{C}_3(B) = (c_1 \sum_\alpha B_{i\alpha}\overline{Q}_\alpha + c_2)_{N_c\times 1}$, and $\mathbf{C}_4(B) = (c_3 \sum_i B_{i\alpha}(1/\overline{F}_i) + c_4)_{N_p\times 1}$. Note that c_2 and c_4 seldom influence the analysis of $\mathbf{f}^{(1)}$ and $\mathbf{q}^{(1)}$, since the eigenvector corresponding to the largest eigenvalue of matrix $(I - \left[\begin{smallmatrix}0, c_1 M\\ -c_3 M^T D_3, 0\end{smallmatrix}\right])^{-1}$ actually represents the stationary point of the FCM. When analyzing the perturbation of the stationary point of FCM, we can ignore c_2 and c_4 for convenience.

$\mathbf{f}^{(1)}$ and $\mathbf{q}^{(1)}$ represent the fluctuation induced by a small perturbation in FCM. In the experiments, based on the proposed method, we will show how the competitiveness (d_i and $F_i^{(n)}$) of a country changes with different perturbations. Note that without (7) and (9), we can still obtain the results by recalculating (2) and (3) every time when M changes.

3. Results

The exports of countries are influenced by a wide range of factors, and obtaining the precise influence of each factor is prohibitive. Instead, we perturb the country-product matrix M following two different scenarios: (1) National recession: a country suffers from natural disasters (e.g., volcanic eruptions, tsunamis), unexpected crisis, or inner industrial problems. All its product exports are reduced by a fixed quantity. (2) Product reduction: the exports of a certain product are reduced for all exporting countries. For example, adverse weather happens, or the products (e.g., mobile phone, clothes) may be out of fashion and people change their tastes, which leads to the export decrease of a certain product. At last, we utilize the method to simulate the trade conflict between USA and China.

We first consider the case of national recession. Suppose that country i is the targeted country and that the export of its products is reduced by 5%. Then the elements of ΔM are $\Delta M_{kj} = -M_{kj} \times 5\%(k = i)$ and $\Delta M_{kj} = 0$ otherwise. The other changes (e.g., 1%, 4%) of the edge weights do not influence the analysis. By substituting $B = \Delta M$ and $\varepsilon = 1$ into (7) and (9), we obtain the changes of competitiveness of the country and the country's influence on other countries. Figure 1 shows the influence of the national recession case as a function of FCM and MR scores. In Figure 1(a), the decrease of fitness mainly occurs on the diagonal elements, implying

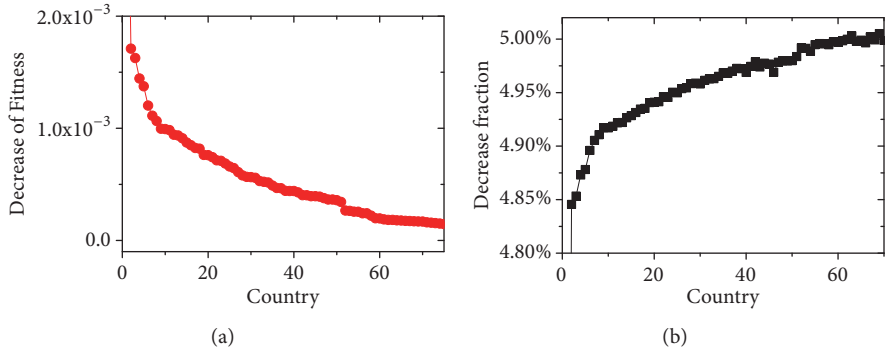

FIGURE 2: (Color online) The decrease of countries' fitness as a function of their rank for FCM. (a) Absolute decrease of countries' fitness. (b) Relative decrease of countries' fitness.

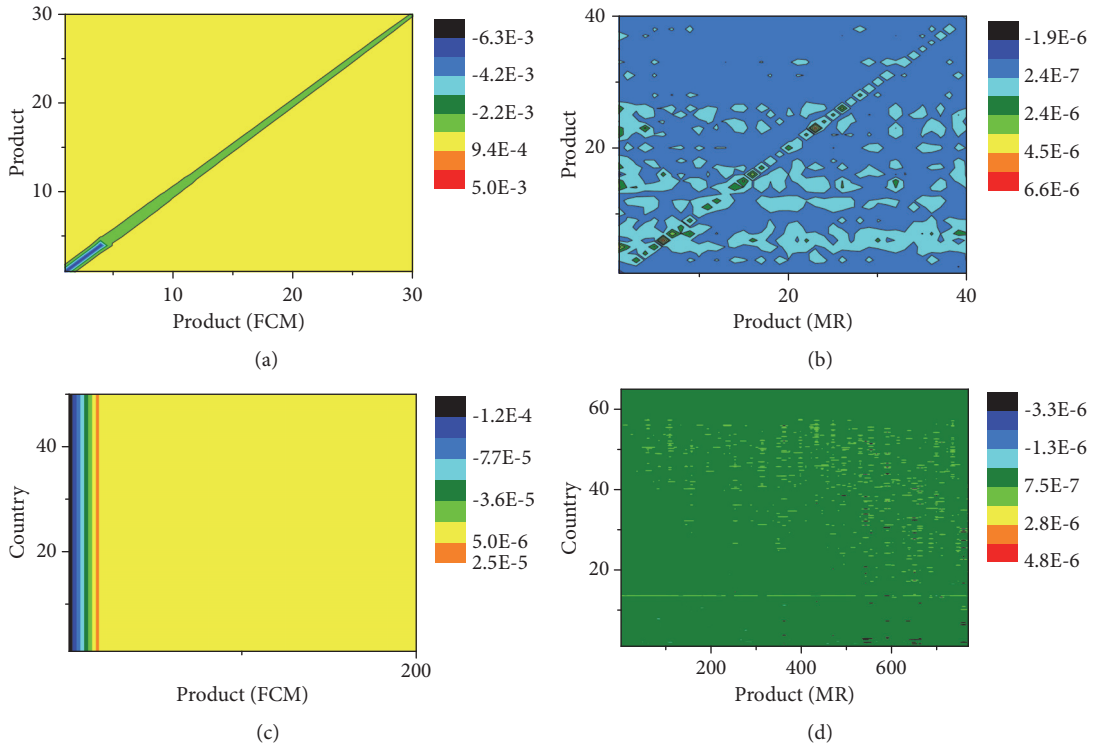

FIGURE 3: (Color online) The decrease of the counties and products scores induced by individually reducing the exports of products by 5% for FCM and MR, as a function of the countries and products rank in their respective method. (a) Change of the fitness scores (in FCM) of countries. (b) Change of the countries scores (in MR). (c) Change of the complexity (FCM) of products. (d) Change of the products scores (MR).

that the targeted countries influence other countries a little. Note that high fitness countries are well linked together and influence each other more that low fitness countries, whereas low high fitness countries seldom influence the other countries. Consequently, FCM index could be used to evaluate the robustness of countries; higher fitness means stronger robustness and is better. In Figure 1(b), the influence ordered by MR is chaotic, and, thus, the MR index cannot characterize the country robustness. Further, Figure 1(c) shows the influence of country recession on product complexity, where competitive countries exert big influence on the complexity of products, which is in accord with reality that the prices of various products are largely determined by the markets of developed countries. However, in Figure 1(d), the influence of MR is chaotic.

According to Figure 1, FCM is a perfect index to characterize the robustness of countries. Figure 2 shows the decrease of the countries' fitness when reducing the exports of themselves. We see that high fitness countries are sensitive to the decrease of their exports. Moreover, in Figure 2(b), the fitness decreases of countries have a positive correlation with their fitness, which further illustrates the effectiveness of FCM in characterizing the robustness of countries. Additionally, we also investigate the robustness based on MR. Similar to

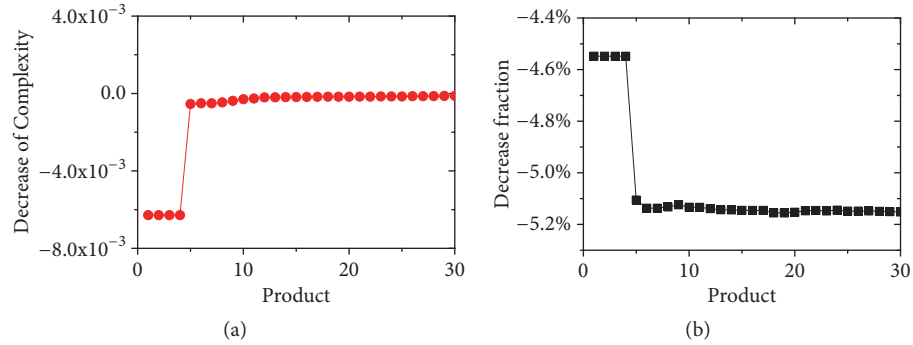

Figure 4: (Color online) The decrease of products' complexity as a function of their rank for FCM. (a) Absolute decrease of products' complexity. (b) Relative decrease of products' complexity.

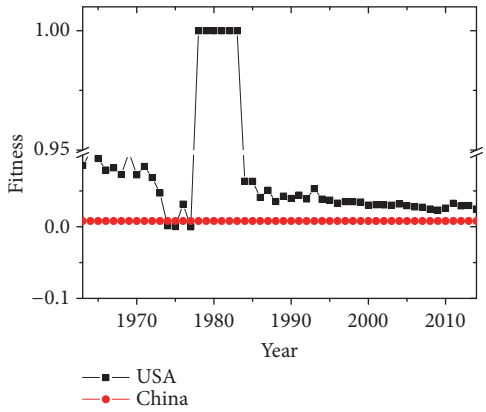

Figure 5: (Color online) The evolving paths of the fitness of USA and China range from 1962 to 2000. The fitness of the two countries is calculated every year.

Figures 2(a) and 2(b), the average decrease of country score is about 4.9%.

Following the same method, we also analyze the influence of reduced products in Figure 3. Suppose that the targeted product reduces 5% weight of its connected edges, which means that all countries reduce 5% exports of the particular product. In Figure 3, FCM outperforms MR in characterizing the relationship between product score and the robustness, since the change of products' complexity mainly occurs on the diagonal elements. Note that decreasing the export volume of a certain product would increase its complexity, which agrees with the phenomenon "thing with rare be expensive". In order to better understand the complexity fluctuation, Figure 4 shows the decrease of the complexity as a function of the product perturbation. We see that the reduced exports of some high-quality products lead to a sharp increase of their complexity, while the complexity of low-quality products fluctuate a little (see Figure 4(a)). However, the relative fluctuations of high-quality products are very small in Figure 4(b), revealing that high-quality products have stronger robustness against the reduction of themselves than low-quality products. Note that the results of Figure 4 are in contrast with Figure 2. The recession of countries (products) will reduce (increase) their scores more than any other countries (products).

Next, we investigate which countries and which products have high scores and how the connection is between high fitness countries and high-quality products. Since MR cannot describe the robustness of the countries' competitiveness, we focus on the FCM case. In Table 1, we can see that the developed countries, such as USA, UK, and Germany, export not only high-quality products, but also some low-quality products including fish and accessories. China also exports some high-quality products and ranks high in fitness. The reason is that China exports some consumer electronics, such as electric cookers and washing machines, which are categorized into the same classes. Note that though Russia is considered as a developed country, its exports are mainly low-quality products and should be a developing country based on FCM. Moreover, we also show the export countries of products with different qualities in Table 2. In Table 2, competitive countries export products of diverse qualities, while less competitive countries only export low-quality products. Note that the robustness is positively correlated with the fitness in Figure 2. Though some developed countries have small product diversity, they have strong robustness against different economic failures.

At last, based on the robust theory of the paper, we simulate the current trade conflict between USA and China. Recently, the president Donald Trump of USA imposes high tariff on Chinese exports to force China renegotiating its trade balance with USA, while China opposes the policy and proposes the tit-for-tat tariff on American products. How to quantify the win and loss of the two countries is an open problem. Here, we simulate the fitness dynamics of the two countries. We first show the evolving paths of the fitness of USA and China range from 1962 to 2014, respectively, in Figure 5. In Figure 5, the fitness of China grows slowly, meaning the economic increase of China, whereas USA has large fluctuation between 1979 and 1986. This can be explained by several factors (e.g., political problems, cold war between the Soviet Union and USA) influencing the trades.

According to the public news, USA imposes high tariff on Chinese high-tech products that include aircraft, iron, and medical instruments [36]. China plans to improve the tariff on products such as soya beans or cars [37]. Until now, we

Table 1: The main export products of some high fitness countries. The first column is the descending order of the countries by the fitness of countries in FCM. In the table, only the top-10 influential export products are listed here, where the products are ranked according to the product scores by FCM.

Fitness Ranking	Country	Top-10 influential export products
1	USA	(1) Fuel oils. (2) Construction and mining machinery. (3) Non-ferrous base metal waste and scrap. (4) Gasoline and other light oils. (5) Machinery for specialized industries. (6) Parts and accessories of some special instruments. (7) Special transactions and commodities. (8) Crude petroleum and oils from bituminous materials. (9) Petroleum bitumen, petroleum coke and bituminous mixtures. (10) Petroleum gases and other gaseous hydrocarbons.
2	UK	(1) Crustaceans and molluscs, fresh, chilled, frozen, salted, etc. (2) Non-ferrous base metal waste and scrap. (3) Petroleum bitumen, petroleum coke and bituminous mixtures. (4) Fish, dried, salted or in brine. (5) Crustaceans and molluscs, prepared or unprepared. (6) Coffee green, roasted. (7) Sheep and lamb skin without the wool. (8) Building and monumental (dimension) stone. (9) Fuel oils. (10) Petroleum gases and other gaseous hydrocarbons.
3	Germany	(1) Crude petroleum and oils from bituminous materials. (2) Parts and accessories of some special instruments. (3) Surveying, navigational, compasses, etc, instruments. (4) Crustaceans and molluscs, fresh, chilled, frozen, salted, etc. (5) Coffee green, roasted. (6) Non-ferrous metal waste and scrap. (7) Fuel oils. (8) Petroleum gases and other gaseous hydrocarbons. (9) Fuel oils. (10) Diamonds (non-industrial).
9	Italy	(1) Castor oil seeds. (2) True hemp, raw or processed but not spun. (3) Coal gas, water gas and similar gases. (4) Potassium salts, natural, crude. (5) Iron pyrites, unroasted. (6) Roasted iron pyrites. (7) Ores and concentrates of uranium and thorium. (8) Vegetable textile fibres and waste. (9) Rye, unmilled. (10) Mate.
7	China	(1) Non-ferrous base metal waste and scrap. (2) Crude petroleum and oils from bituminous materials. (3) Fuel oils. (4) Construction and mining machinery. (5) Parts of some special machinery and equipment. (6) Machinery for specialized industries. (7) Passenger motor vehicles. (8) Trailers and transports containers. (9) Surveying, navigational, compasses, etc, instruments. (10) Special transactions and commodities.
10	Russia	(1) Coffee green, roasted. (2) Petroleum gases. (3) Building and monumental (dimension) stone. (4) Crude petroleum and oils from bituminous materials. (5) Fish, frozen, excluding fillets. (6) Fish fillets, frozen. (7) Fish, dried, salted or in brine. (8) Crustaceans and molluscs. (9) Non-ferrous metal waste and scrap. (10) Fuel oils.

cannot obtain the data to compute the volumes of the reduced exports induced by the trade conflict. However, we can simulate the influence based on historical dataset. Figure 6 shows the increases of different products for USA and China covering from the year 1962 to 2014. The original dataset only gives the product categories, not the export details of each product. In the simulation, we treat all categories that contain the key words, such as "iron" and "medical", as the corresponding products. In Figure 6, most of the exports increase on the whole except the soya beans. Due to enormous inner demands and restricted natural resource, China reduces its export of soya beans from 1989. Integrating Figures 5 and 6, we find that the exports of the two countries increase on the whole.

Next, we artificially introduce some perturbation into the exports of the two countries. Following the tariff policies of the two countries, we suppose that the soya bean export of USA reduces 5% and the iron export of China reduces 5% for every year between 1975 and 2014. Here, we do not start from the year 1962, because that USA and China established diplomatic relations in the year 1972. Before 1972, China did not integrate into the global economics completely and the two countries had little trade connection. Thus, we start the simulation from 1975 to avoid noisy fluctuations. According to our proposed method (9), we obtain the fluctuation of the fitness of the two countries in Figure 7. If we reduce 5% of the American soya beans and of the Chinese Iron steels, China will suffer more decrease of the fitness in Figure 7(a).

Next, we simulate another case. The aim of American policy is to reduce the growth of China, especially high-tech products. If USA does not start the conflict, supposing that the high-tech aircraft of China increases by 5%, Figure 7(b) shows the increase of the fitness of the two countries. We find that the export increase of aircraft would improve the fitness of China much, whereas the fitness of USA would decrease only a little. Besides, we also simulate the perturbation of other high-tech products, such as industrial equipment and medical instruments, and the results are similar with Figure 7. Thus, we can predict that the trade conflict between the two countries would hurt China severely. However, USA

Table 2: The main export countries of some products. The first column is the descending order of the products by the score Q_i of FCM. In the table, the countries are ranked according to the country scores of FCM.

Product Ranking	Product	Top-10 influential export countries
1	Wood-based panels	(1) China. (2) USA. (3) Spain. (4) France. (5) India. (6) UK. (7) Venezuela. (8) Brazil. (9) Canada. (10) Germany.
2	Castor oil seeds	(1) China. (2) USA. (3) Spain. (4) France. (5) India. (6) UK. (7) Venezuela. (8) Brazil. (9) Canada. (10) Germany.
3	Coal gas, water gas and similar gases	(1) USA. (2) Oman. (3) UK. (4) Brazil. (5) China. (6) Ecuador. (7) Dominican Rp. (8) Algeria. (9) France. (10)Germany.
4	Copra	(1) China. (2) France. (3) Morocco. (4) Tunisia. (5) USA. (6) Iran. (7) Italy. (8) Kazakhstan. (9) Pakistan. (10)Venezuela.
5	Manila hemp, raw or processed but not spun	(1) China. (2) Canada. (3) Germany. (4) Belgium-Lux. (5) France. (6) Netherlands. (7) USA. (8) Austria. (9) Spain. (10)Australia.
766	Parts of and accessories for apparatus electrical instruments	(1) USA. (2) UK. (3) France. (4) Germany. (5) Spain. (6) Belgium-Lux. (7) Netherlands. (8) China. (9) Italy. (10)Brazil.
767	Non-ferrous base metal waste and scrap	(1) China. (2) France. (3) USA. (4) Brazil. (5) Australia. (6) Austria. (7) Belgium-Lux. (8) Germany. (9) India. (10)Morocco.
768	Machinery for specialized industries	(1) China. (2) France. (3) USA. (4) Brazil. (5) Australia. (6) Austria. (7) Belgium-Lux. (8) Germany. (9) India. (10)Morocco.
769	Special transactions and commodities	(1) China. (2) France. (3) USA. (4) Brazil. (5) Australia. (6) Austria. (7) Belgium-Lux. (8) Germany. (9) India. (10)Morocco.
770	Postal packages not classified into other classes	(1) Algeria. (2) Angola. (3) Argentina. (4) Australia. (5) Austria. (6) Belgium-Lux. (7) Brazil. (8) Bulgaria. (9) Canada. (10)Chile.

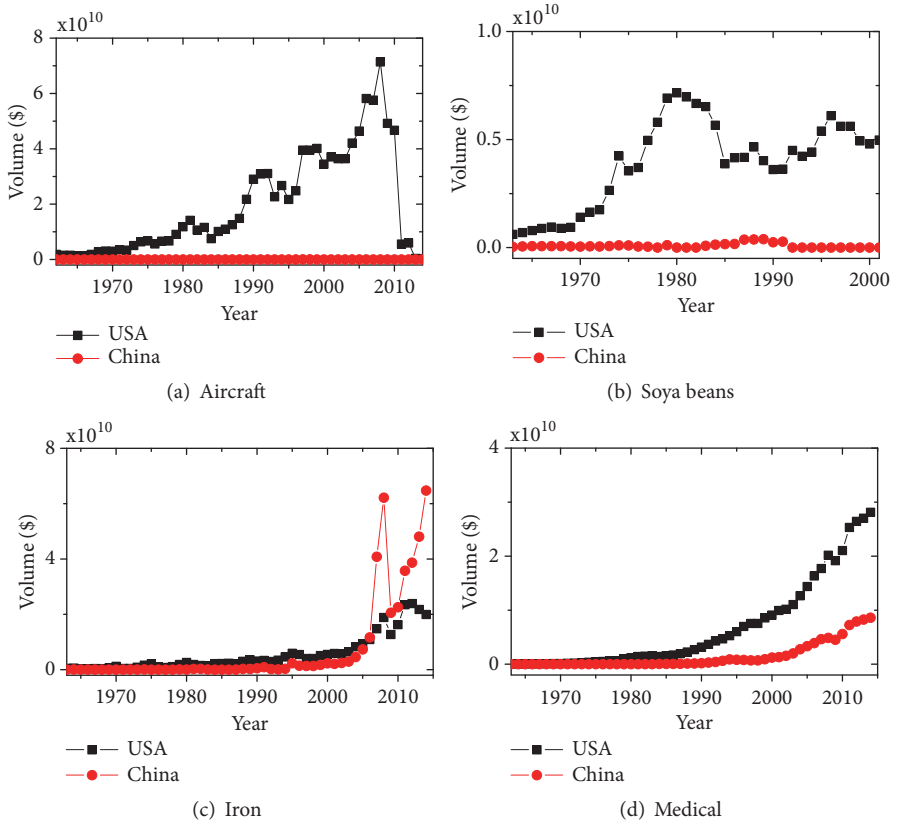

Figure 6: (Color online) The increase of different product exports (in US dollars) for USA and China from 1962 to 2000. (a) Aircraft. (b) Soya beans. (c) Iron steels. (d) Medical instruments.

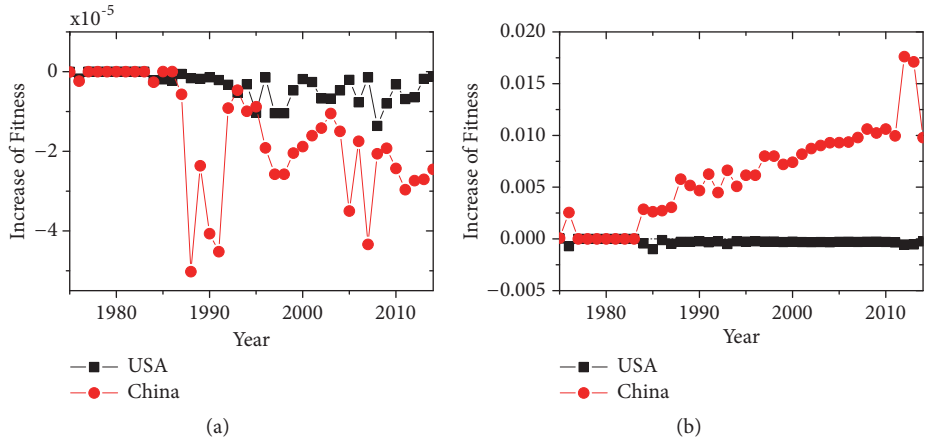

FIGURE 7: (Color online) Fluctuation of the fitness scores of USA and China. (a) The decrease of the fitness of USA and China by reducing 5% of the American soya beans and of the Chinese Iron steels. (b) The increase of the fitness by increasing 5% of the export of Chinese aircraft. Note that we do not simulate the performance before the year 1975, because that USA and China established diplomatic relations in the year 1972. After 1972, China built diplomatic relations with many western countries and started to integrate into the global economics. Thus, we start the experiments from 1975 to avoid noisy fluctuations.

benefits only a little from the conflict. Note that, in the analysis, we do not consider the decrease of the American exports induced by the increase of the Chinese corresponding exports. China may take away some market shares of some high-tech products, which is beyond the scope of the paper.

4. Conclusion

In summary, we propose an analytical approach to calculate the robustness of the MR and FCM. The robustness of both methods is tested using perturbation theory. This analysis shows that the FCM is more resilient to perturbation, as the propagation between countries is less important than in MR. Moreover, we use our method to simulate the trade conflict between USA and China using FCM. The simulation results show that China will lose much competitiveness, whereas USA will get a small benefit from the conflict. Therefore, our work could supply additional information that organizations could benefit by taking the competitiveness robustness of countries into accounts. Since the robustness analysis is based on the artificial simulation, the inner relationships between countries (products) are not considered in the analysis. Consequently, the fluctuation of real economics may be different from the results in the paper. Detailed perturbation of real economic data could be integrated into the method to enhance the accuracy in the future.

Data Availability

The data used to support the findings of this study are available in the dataset collection of [20].

Conflicts of Interest

The authors declare no competing financial interests.

Acknowledgments

This work was jointly supported by the National Natural Science Foundation of China (nos. 61703281, 11547040, 61803266, and 61873171), the Ph.D. Start-Up Fund of Natural Science Foundation of Guangdong Province, China (nos. 2017A030310374 and 2016A030313036), the Science and Technology Innovation Commission of Shenzhen (no. JCYJ20160520162743717), Shenzhen Science and Technology Foundation (nos. JCYJ20150529164656096 and JCYJ20170302153955969), Guangdong Pre-National Project (2014GKXM054), Guangdong Province Key Laboratory of Popular High Performance Computers (2017B030314073), Foundation for Distinguished Young Talents in Higher Education of Guangdong (2015KONCX143), and the Young Teachers Start-Up Fund of Natural Science Foundation of Shenzhen University.

References

[1] A. Tacchella, M. Cristelli, G. Caldarelli, A. Gabrielli, and L. Pietronero, "A new metrics for countries' fitness and products' complexity," *Scientific Reports*, vol. 2, article 723, 2012.

[2] C. A. Hidalgo, B. Winger, A.-L. Barabási, and R. Hausmann, "The product space conditions the development of nations," *Science*, vol. 317, no. 5837, pp. 482–487, 2007.

[3] C. A. Hidalgo and R. Hausmann, "The building blocks of economic complexity," *Proceedings of the National Acadamy of Sciences of the United States of America*, vol. 106, no. 26, pp. 10570–10575, 2009.

[4] H. Liao, M. S. Mariani, M. Medo, Y.-C. Zhang, and M.-Y. Zhou, "Ranking in evolving complex networks," *Physics Reports*, vol. 689, pp. 1–54, 2017.

[5] G. M. Grossman and E. Helpman, "Quality Ladders in the Theory of Growth," *The Review of Economic Studies*, vol. 58, no. 1, p. 43, 1991.

[6] D. Greenaway, *International trade policy: From tariffs to the new protectionism*, Macmillan, London, UK, 1983.

[7] H. Liepmann, *Tariff Levels and The Economic Unity of Europe: An Examination of Tariff Policy, Export Movements and The Economic Integration of Europe*, vol. 25, Routledge, 2017.

[8] M. S. Mariani, A. Vidmer, M. Medo, and Y.-C. Zhang, "Measuring economic complexity of countries and products: which metric to use?" *The European Physical Journal B*, vol. 88, no. 11, article 293, pp. 1–9, 2015.

[9] C. Kao, W.-Y. Wu, W.-J. Hsieh, T.-Y. Wang, C. Lin, and L.-H. Chen, "Measuring the national competitiveness of Southeast Asian countries," *European Journal of Operational Research*, vol. 187, no. 2, pp. 613–628, 2008.

[10] E. Siggel, "International competitiveness and comparative advantage: A survey and a proposal for measurement," *Journal of Industry, Competition and Trade*, vol. 6, no. 2, pp. 137–159, 2006.

[11] C. Antonelli, *Handbook on the Economic Complexity of Technological Change*, Edward Elgar Publishing, 2011.

[12] S. Brin, "The anatomy of a large-scale hypertextual Web search engine," *Computer Networks*, vol. 30, no. 1, pp. 107–117, 1998.

[13] L. Page, S. Brin, R. Motwani, and T. Winograd, "The pagerank citation ranking: Bringing order to the web," Tech. Rep., Stanford InfoLab, 1999.

[14] S. Albeaik, M. Kaltenberg, M. Alsaleh, and C. A. Hidalgo, "729 new measures of economic complexity (addendum to improving the economic complexity index)," 2017, https://arxiv.org/abs/1708.04107.

[15] J. Felipe, U. Kumar, A. Abdon, and M. Bacate, "Product complexity and economic development," *Structural Change and Economic Dynamics*, vol. 23, no. 1, pp. 36–68, 2012.

[16] S. Poncet and F. Starosta de Waldemar, "Export upgrading and growth: The prerequisite of domestic embeddedness," *World Development*, vol. 51, pp. 1–15, 2013.

[17] A. Tacchella, M. Cristelli, G. Caldarelli, A. Gabrielli, and L. Pietronero, "Economic complexity: conceptual grounding of a new metrics for global competitiveness," *Journal of Economic Dynamics & Control*, vol. 37, no. 8, pp. 1683–1691, 2013.

[18] F. Battiston, M. Cristelli, A. Tacchella, and L. Pietronero, "How metrics for economic complexity are affected by noise," *Complexity Economics*, vol. 3, no. 1, pp. 1–22, 2014.

[19] H. Liao and A. Vidmer, "A comparative analysis of the predictive abilities of economic complexity metrics using international trade network," *Complexity*, vol. 2018, Article ID 2825948, 12 pages, 2018.

[20] A. Simoes et al., "Country-Product Dataset," https://atlas.media.mit.edu/en/resources/data/.

[21] R. Feenstra, R. Lipsey, H. Deng, A. Ma, and H. Mo, "World Trade Flows: 1962-2000," National Bureau of Economic Research, 2005.

[22] R. Hausmann, J. Hwang, and D. Rodrik, "What you export matters," *Journal of Economic Growth*, vol. 12, no. 1, pp. 1–25, 2007.

[23] G. Gaulier and S. Zignago, *Baci: International Trade Database at The Product-Level (The 1994-2007 Version)*, 2010.

[24] R. Hausmann, C. A. Hidalgo, S. Bustos, M. Coscia, A. Simoes, and M. A. Yildirim, *The Atlas of Economic Complexity: Mapping Paths to Prosperity*, Mit Press, 2014.

[25] M. Cristelli, A. Gabrielli, A. Tacchella, G. Caldarelli, and L. Pietronero, "Measuring the intangibles: A metrics for the economic complexity of countries and products," *PloS One*, vol. 8, no. 8, Article ID e70726, 2013.

[26] G. Caldarelli, M. Cristelli, A. Gabrielli, L. Pietronero, A. Scala, and A. Tacchella, "A network analysis of countries' export flows: firm grounds for the building blocks of the economy," *PLoS ONE*, vol. 7, no. 10, Article ID e47278, 2012.

[27] M. Cristelli, A. Tacchella, and L. Pietronero, "The heterogeneous dynamics of economic complexity," *PLoS ONE*, vol. 10, no. 2, Article ID e0117174, 2015.

[28] V. Domínguez-García and M. A. Muñoz, "Ranking species in mutualistic networks," *Scientific Reports*, vol. 5, article 8182, 2015.

[29] G. Cimini, A. Gabrielli, and F. S. Labini, "The scientific competitiveness of nations," *PLoS ONE*, vol. 9, no. 12, 2014.

[30] D. Hausman, M. McPherson, and D. Satz, *Economic analysis, moral philosophy, and public policy*, Cambridge University Press, 2018.

[31] R. G. Ehrenberg, R. S. Smith et al., *Modern labor economics: Theory and public policy*, Routledge, 2016.

[32] S. A. Marglin, *Public Investment Criteria (Routledge Revivals): Benefit-Cost Analysis for Planned Economic Growth*, Routledge, 2014.

[33] M. Nørgaard, N. K. Poulsen, and O. Ravn, "New developments in state estimation for nonlinear systems," *Automatica*, vol. 36, no. 11, pp. 1627–1638, 2000.

[34] T. Kato, *Perturbation Theory for Linear Operators*, vol. 132, Springer Science & Business Media, 2013.

[35] W. G. Stewart, *Matrix Perturbation Theory*, 1990.

[36] https://zh.scribd.com/document/375467984/Trump-China-trade-targets#from_embed.

[37] https://www.usatoday.com/story/money/business/2018/04/04/full-list-us-products-china-planning-hittariffs/485071002/.

Hindawi
Complexity
Volume 2018, Article ID 9253846, 13 pages
https://doi.org/10.1155/2018/9253846

Research Article

Analyzing Policymaking for Tuberculosis Control in Nigeria

Nura M. R. Ahmad,[1,2] **Cristina Montañola-Sales**,[2,3] **Clara Prats**,[1] **Mustapha Musa**,[4] **Daniel López**,[1] **and Josep Casanovas-Garcia**[1,2]

[1] *Universitat Politècnica de Catalunya, Barcelona, Spain*
[2] *Barcelona Supercomputing Center (BSC), Barcelona, Spain*
[3] *IQS Barcelona, Ramon Llull University, Barcelona, Spain*
[4] *Gombe State Primary Health Care Development Agency, Gombe, Nigeria*

Correspondence should be addressed to Cristina Montañola-Sales; cristina.montanola@iqs.edu

Received 18 May 2018; Revised 25 September 2018; Accepted 11 October 2018; Published 7 November 2018

Guest Editor: Bernardo A. Furtado

Today, tuberculosis (TB) is still one of the major threats to humankind, being the first cause of death by an infectious disease worldwide. TB is a communicable chronic disease that every year affects 10 million people and kills almost 2 million people in the world. The main key factors fueling the disease are the progressive urbanization of the population and poverty-related socioeconomic factors. Moreover, the lack of effective tools for TB diagnosis, prevention, and treatment has decisively contributed to the lack of an effective model to predict TB spread. In Nigeria, the rapid urbanization along with unprecedented population growth is causing TB to be endemic. This paper proposes a mathematical model to evaluate TB burden in Nigeria by using data obtained from the local TB control program in the community. This research aims to point out effective strategies that could be used to effectively reduce TB burden and death due to TB in this country at different levels. The study shows that efforts should be oriented to more active case finding rather than increasing the treatment effectiveness only. It also reveals that the persistence of the disease is related to a large number of latently infected individuals and quantifies the lives that could be saved by increasing the notification rate using active case finding strategy. We conclude that undiagnosis is the bottleneck that needs to be overcome in addition to the incorporation, improvement, and/or strengthening of treatment management and other essential TB control measures in Nigeria.

1. Introduction

Tuberculosis (TB) is the most challenging infectious disease that humankind faces. It is estimated that in the last 200 years TB has killed one billion (1.000.000.000) people [1]. Currently, TB is still among the main worldwide causes of death by an infectious disease [2]. In 2017, there were 10.4 million new TB cases and 1.7 million related deaths worldwide [3]. It is a very silent disease that has eluded mankind for a very long time. It affects people of all social statuses, although most TB cases occur in resource-limited countries.

TB is caused by *Mycobacterium tuberculosis* (*Mtb*). This bacillus is transmitted by the inhalation of infected aerosols generated by active TB patients. The inhalation of the bacilli will usually lead to the trigger of an immune response that can have one of the three different clinical outcomes: (1) complete clearance of the pathogen, (2) latent TB infection (LTBI), or (3) progression to primary active disease [4, 5]. LTBI occurs when the host's immune response manages the initial containment of the *Mtb* by developing and encapsulating granulomas. More often than not, the bacilli remain physically contained and immunologically constrained by these encapsulated granulomas throughout the lifetimes of the hosts [6, 7]. During this process, an endogenous reinfection can produce new infection spotlights that will presumably undergo the same control dynamics [4]. However, even decades after infection especially in the case of immunocompromised hosts (like HIV patients), the control process can fail and the host can develop an active disease. On average, about 10% of the LTBI people develop active TB during their lives [8]. A latent infected host can be reinfected several times, thereby increasing the load of *Mtb* in its body and

hence increasing the chance of progressing to active disease. According to the World Health Organization (WHO), there were an estimated number of 2 to 3 billion people with LTBI in 2015 [9], thus at risk of developing an active disease.

Overcrowding and time in contact with patients are key factors of TB infection. Paradoxically, TB is often seen as a XIX century disease, mainly associated with the poor living conditions of workers in crowded cities. Today, TB is reaching the highest number of cases in absolute numbers in the history [9] precisely because of the massive urbanization of populations. This fact is especially painful in Nigeria, a country that is undergoing rapid urbanization with a rapidly growing population. At the current growth rate of about 2.8% to 3.5% a year, it is estimated that Nigeria's urban population will double in the next two decades [10]. As a consequence, TB is endemic in Nigeria. The control of the disease is coordinated by the *National Tuberculosis and Leprosy Control Program (NTBLCP)*, in line with the *End TB Partnership* initiatives whose ultimate target is to eliminate TB as a public health problem by the year 2050 (meaning reaching less than 1 case per million-person population) [11]. Despite current global control efforts to reduce TB, Nigeria's TB incidence is refusing to show any significant decline [9]. On March 14th, 2017, a wide circulated paper announced that Nigeria ranks 4th in TB infection worldwide [12]. This was followed by the press release by the NTBLCP national coordinator. The statistics show that over 80% of TB cases in Nigeria are still undetected while the disease has been claiming millions of lives over the years in the country [9, 13].

Many studies show that more intensified case finding is needed especially in areas with higher prevalence of TB [14–16]. For instance, Brewer et al. [17] indicated that active case finding of TB in homeless individuals in the USA is the most effective strategy that leads to a decrease in the death of the TB patients. Moreover, a study by Dodd et al. [18] indicates that policymakers need to alternate between active case finding and passive case detection strategy from period to period in order to have effective TB control. This paper aims to use mathematical modeling in order to evaluate the effect of an increase in diagnosis rate and treatment success on TB dynamics in Nigeria.

Assessing TB Policymaking: Mathematical Models for TB Transmission. Several mathematical models have been used to estimate long-term dynamics of TB to help to assess the development of strategies to control it. The literature on compartment models to describe complex systems is extensive [19–21]. Following a top-down approach, the population is divided into different compartments (e.g., susceptible, exposed, infected, and recovered in the case of an SEIR model) and specific fluxes are set between these compartments. The dynamics of the disease is therefore defined with ordinary nonlinear differential equations through rigorous mathematical analysis [22].

Many different studies have been able to draw important conclusions on TB dynamics by means of models and other methods [23–33]. Okuonghae and Ikhimwin [16], for example, developed a model which classified the population by their TB awareness level, a key factor which could affect the case detection rate. Another factor which could contribute to better adjust TB models is the HIV dynamics, especially in the sub-Saharan African region [34]. HIV patients have a higher risk of becoming infected and also of progressing to active disease once infected than non-HIV infected people. According to WHO [35], nearly all HIV-positive people with active TB will die.

By means of mathematical models, Wallis [36] was able to identify individuals with an innate resistance to *Mtb*. He concluded that understanding the mechanisms of resistance may lead to therapeutic strategies to counter immune evasion by *Mtb*. Moreover, models were also used by Wallis [36] to assess the affinity of LTBI reactivation when patients are administered with drugs with TNF blockers. Similarly, another research project by Moualeu-Ngangue et al. [37] worked with a model simulating the global TB dynamics. The study showed that TB spreading crucially depends on the basic reproduction number (number of new cases one case generates during its sick period, which is estimated to be between 10 and 15 [36, 38]). The research was done in Cameroon where the roles of TB diagnosis, treatment, TB awareness level, and traditional medicine in the dynamics of TB were assessed. Song et al. [39] investigated the epidemiological time scales of TB and they evaluated the risk of infection from both close contacts (clusters) and casual contacts (random). They concluded that the risk of infection depends on the source of infection as well as on different environmental characteristics.

Lastly, Guzzeta et al. [40] presented three different ways to model TB dynamics: (1) an ODE model with no age structure and constant population size, (2) an age-structured, stochastic version of the ODE model, and (3) a sociodemographic Individual-Based Model (IBM). An IBM is a model formed by autonomous agents which interact among them, including their environment, to follow their objectives. The models were fitted to epidemiological data from Arkansas, USA. The authors concluded that different modeling techniques have their advantages and drawbacks and they should be chosen carefully. For example, an ODE model is best suited to describe the evolution of prevalence, incidence, and mortality. On the other hand, an IBM would be best to estimate the fraction of reactivated cases or to fit age-specific incidence of active TB.

Although there are many studies into TB epidemic, cause, spread, and suggestive measures for therapy and control, none of the aforementioned studies uses a mathematical model to evaluate the actual epidemic of TB in Nigeria using data obtained from the local TB control program in the community. This paper proposes a mathematical model that will be used to evaluate TB burden in this country. We aim to point out effective strategies that could be used to effectively reduce TB burden and death due to TB in Nigeria.

Specifically, we present a mathematical model that aims to investigate if more TB active case finding is needed in Nigeria, in order to help policymakers to make sound decisions in implementing effective TB control measures in the country. Section 2 shows the developed methodology and explains the proposed model. Sections 3 and 4 present and discuss the results obtained as well as their limitations and

other possibilities for further research. Finally, the last section highlights the main conclusions drawn from this study.

2. Materials and Methods

Our goal is to develop a close-enough-to-reality mathematical model of the TB epidemic that can allow us to investigate effects of demographics and notification of TB epidemics in a population of Nigeria, as well as to estimate the actual burden of the disease including death toll and case fertility ratio in some of the regions in the country.

2.1. Model Description. Figure 1 represents the model diagram, which we briefly outline. Birth occurs at a constant rate Π into the susceptible class S with the assumption that all newborns are susceptible to *Mtb*. $E_1, E_2, \ldots, E_7, E_{>7}$ represent the noninfectious population infected with tuberculosis without any clinical symptoms (LTBI) in their various years of infection; i.e., an individual who was infected recently (less than one year ago) will be assigned to E_1, while an individual who was infected last year would be assigned to the E_2 population. The last LTBI compartment, $E_{>7}$, consists of the whole latently infected population with more than 7 years of infection. I_1 and I_2 represent the population that is sick; i.e., they have an active disease with clinical symptoms and they can infect the general population; T is the sick population that was diagnosed and is receiving effective chemoprophylaxis, thus unable to infect anyone. As shown in the diagram, only people in the I_2 compartment will be diagnosed and will move towards the T compartment, while the I_1 compartment accounts for the missed TB cases. Death rates in the model depend on disease status; they are fixed into μ_S for susceptible population, ν_1 for exposed classes, and μ_{I_1}, μ_{I_2}, and μ_T for sick individuals of I_1, I_2, and T, respectively. Based on the disparate time scale of natural death versus death due to TB disease, we assume that $\mu_S \leq \nu_1 \leq \mu_T \leq \mu_{I_2} \leq \mu_{I_1}$.

Transmission of *Mtb* TB occurs following adequate contact between the sick infectious individuals (I_1 and I_2) and the susceptible population. We assume that the latently infected (E_i) are not infectious and thus not capable of transmitting the bacteria. We use the incidence expression $\alpha(\theta I_1 + I_2)/N$ to indicate successful transmission of *Mtb* due to nonlinear contact dynamics in a large population [41]. α is the transmission rate that represents possible interactions that may occur among the susceptible population and the sick infectious population, which is defined as the average contact per unit time. Infectivity of I_1 is assumed to be lower ($0 \leq \theta \leq 1$), as the undiagnosed long-term sick individuals probably reduce their activity due to their poor health conditions.

Newly infected individuals progress directly to the infected class E_1 and stay there for a period of one year, where the probability of developing active disease is p_1. If they do not become sick, they progress to E_2 (at a *per capita* rate k_1) the subsequent year, where the probability of developing the active disease is p_2. The progression through the latently infected compartment will continue yearly at a constant *per capita* rate k_1. Finally, all latently infected patients with more than seven years of infection will remain in the compartment $E_{>7}$ for a very long period of time, where the probability of becoming sick (p_8) is very low and later would be integrated back into the susceptible society at a constant *per capita* rate of k_4.

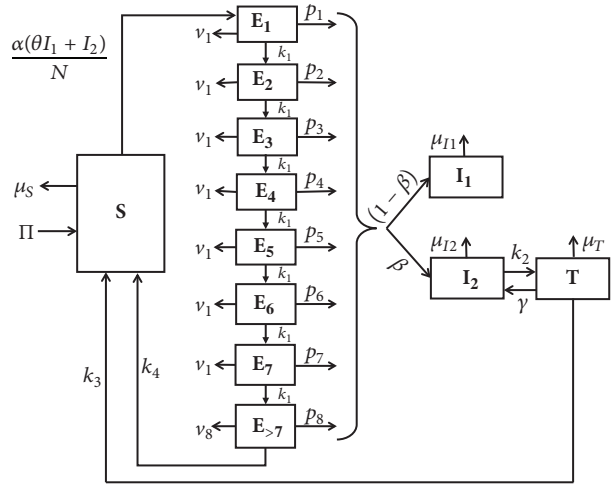

Figure 1: *The model: a compartment model for tuberculosis transmission in Nigeria.* The model shows the dynamic flow of tuberculosis (TB) including susceptible population *S*; the latently infected population are discerned based on the time since they were infected; therefore E_1 stands for people latently infected for a period of one year, E_2 stands for people infected for 2 years, etc.; $E_{>7}$ stands for people that have been infected for more than 7 years; two types of the nondiagnosed sick population are considered, I_1 and I_2, and the sick under treatment is shown as T. Birth occurs at constant rate Π. Transmission of *Mtb* depends on $\alpha(\theta I_1 + I_2)/N$ and probability leading to active TB is given as $p_i = ai^2 + bi + c$, where i is the i^{th} year of infection. k_1 indicate succession from one infected compartment to the next. A fraction of the sick, β, will be detected and notified; k_2 is related to diagnosis time delay before starting treatment and γ indicates a fraction of relapse for the sick under treatment. Recovery rate is given as k_3 while k_4 represents the fraction of the infected population that gets rid of the disease spontaneously. We account for all courses of death, μ_s, ν_i, μ_{I_2}, and μ_T, and death due to active TB, μ_{I_1}.

The probability of developing an active disease decreases across the latently infected compartment, p_i, which is assumed to be an autonomous decreasing quadratic function, given as $p_i = ai^2 + bi + c$, where i is the i^{th} year of infection. The sum ($\sum p_i E_i$) represents the 10–13% of the latently infected population that will become sick in seven years or more, and $p_1 E_1 + p_2 E_2$ is about 5-6% of the latently infected population that will become sick in the first two years of infection.

We define T as the fraction of the sick infectious population that were notified and are receiving effective chemoprophylaxis, k_2 as the rate of effective *per capita* notification, and k_3 as the *per capita* rate of successful therapy completion. We assume that starting a treatment removes an individual from infectious class I_2 and places them into T. We also assume that individuals receiving chemoprophylaxis can abandon therapy, thus showing a relapse at a *per capita* rate γ.

2.1.1. Model Formulation. We used a system of nonlinear differential equations to model the dynamics of individuals within the population settings. Setting $N(t) = S(t) + E_1(t) + E_2(t) + E_3(t) + E_4(t) + E_5(t) + E_6(t) + E_7(t) + E_{>7}(t) + I_1(t) + I_2(t) + T(t)$ and suppressing time dependence, t, for each variable, $N(t)$ represent the total population size at time t. The twelve model equations are

$$\frac{dS}{dt} = \Pi + k_4 E_{>7} + k_3 T - \left(\frac{\alpha (\theta I_1 + I_2)}{N} + \mu_s \right) S, \tag{1}$$

$$\frac{dE_1}{dt} = \left(\frac{\alpha (\theta I_1 + I_2)}{N} \right) S - (\nu_1 + k_1) E_1 + p_1 E_1, \tag{2}$$

$$\frac{dE_2}{dt} = k_1 E_1 - (\nu_1 + k_1) E_2 + p_2 E_2, \tag{3}$$

$$\frac{dE_3}{dt} = k_1 E_2 - (\nu_1 + k_1) E_3 + p_3 E_3, \tag{4}$$

$$\frac{dE_4}{dt} = k_1 E_3 - (\nu_1 + k_1) E_4 + p_4 E_4, \tag{5}$$

$$\frac{dE_5}{dt} = k_1 E_4 - (\nu_1 + k_1) E_5 + p_5 E_5, \tag{6}$$

$$\frac{dE_6}{dt} = k_1 E_5 - (\nu_1 + k_1) E_6 + p_6 E_6, \tag{7}$$

$$\frac{dE_7}{dt} = k_1 E_6 - (\nu_1 + k_1) E_7 + p_7 E_7, \tag{8}$$

$$\frac{dE_{>7}}{dt} = k_1 E_7 - (\nu_1 + k_1) E_{>7} + p_8 E_{>7}, \tag{9}$$

$$\frac{dI_1}{dt} = \sum (1 - \beta) (p_i E_i) + (1 - \beta) p_8 E_{>7} - \mu_{I_1} I_1, \quad i = 1, 2, 3 \ldots, 7. \tag{10}$$

$$\frac{dI_2}{dt} = \sum \beta (p_i E_i) + \beta p_8 E_{>7} + \gamma T - \left(\mu_{I_2} + k_2 \right) I_2, \quad i = 1, 2, 3 \ldots, 7. \tag{11}$$

$$\frac{dT}{dt} = k_2 I_2 - (\gamma + k_3 + \mu_T) T. \tag{12}$$

Equation (1) describes the rate of change of the susceptible population S. There is a gain into this population through constant birth rate Π. A loss in this population occurs as a result of infection with *Mtb* with transmission rate $\alpha(\theta I_1 + I_2)S/N$ and constant death rate μ_s. Equations (2) through (9) represent the rate of change of the latently infected population over time. The rate of change of E_1 increases as a result of *Mtb* infection that results in latent infection at a rate $\alpha(\theta I_1 + I_2)S/N$ and decreases by developing active TB at a rate $p_1 E_1$, natural death ν_1, and movement to the second year of latent infection class at a rate $k_1 E_1$. $E_2(t), E_3(t), \ldots, E_{>7}(t)$ increase by successive movement of latently infected individuals from one class to the next and decrease by progressive movement to the next infected class, natural death ν_1, and developing of active TB at the rate $p_i E_i$ in each $i^t h$ latently infected class. A fraction $(1 - \beta)$ of the *Mtb* infection which progress to active TB and were undetected decrease by death due to TB and other causes at the rate μ_{I1}, and the detected fraction are increased by relapse at a rate γT and decrease by diagnosis at a rate $k_2 I_2$ and by death at a rate μ_{I2}. The rate of change of sick individuals under treatment is increased at a rate $k_2 I_2$ and reduced at a rate γT, recovery rate $k_3 T$, and natural death at the rate μ_T.

2.1.2. Model Calibration and Validation. In order to determine the effects of various parameters on the dynamics of TB in Nigeria, (1) to (12) are integrated by a Runge–Kutta method of order 4, using Matlab software (Ode45). We started by fitting our model to the 2000–2010 prevalence data on Nigeria from the official WHO reports and Nigerian epidemiological fact sheets [42]. The reason why this period was chosen is because of reliability of available data together with the fact that all parameters can be approximately considered constant for that period, which would not be applicable if the period was longer. We used the least squares curve fitting in Matlab, by specifying the lower and upper bounds of specific parameters to be estimated. The recruitment rate of the susceptible was chosen and calculated such that the population of the country remains constant during the simulation. The treatment efficacy $(1 - \gamma)$ is considered to be 80% with probability of relapse taken as 20%. The parameter values that gave the best fit are given in Table 1 and were obtained with $R^2 = 0.9992$.

The initial conditions were chosen in accord with available data when possible (i.e., for the total population, estimates of global LTBI population, the population in sick compartments, and the ratio I_1/I_2). The distribution of LTBI among time-since-infection compartments was also fitted in this process. We finally obtained these initial conditions (considering a population of 100,000):

$$\begin{aligned} &\left(S(0), E_1(0), E_2(0), E_3(0), E_4(0), E_5(0), E_6(0), E_7(0), E_{>7}(0), I_1(0), I_2(0), T(0)\right) \\ &= (58303, 6100, 5000, 4438, 4020, 3550, 3140, 2860, 12250, 284, 55, 0). \end{aligned} \tag{13}$$

This corresponds to initial prevalence of 339 and a notification rate of 16%. Figure 2 shows the epidemiological data together with the best fit of the model.

As a validation of the previous calibration, we took data from a wider period (1990–2015) and confronted it with the model. Keeping all the parameters constant but with a small change in the force of infection value, as well as in the initial conditions, the new R^2 was 0.9706. Therefore, we assumed the calibration for the 2000–2010 period to be the baseline for our subsequent virtual experiments.

Table 1: Summary description of parameters of the model fitted to Nigeria data (2000-2015).

Parameter	Parameter description	Values ($month^{-1}$)	Source
Π	Birth rate in S class	Constant	NA
μ_s	Death rate in S	0.012	calibrated
μ_{i_1}	Death rate in I_1	0.146	calibrated
μ_{i_2}	Death rate in I_2	0.146	calibrated
μ_T	Death rate in T	0.01	calibrated
ν_1	Death rate in LTBI	0.0108	calibrated
α	Contact rate of sick population	3.54	calibrated
k_1	Movement rate in LTBI population	$\frac{1}{12}$	calibrated
p_i	Probability of developing active TB	$ai^2 + bi + c$	derived
β	Notification rate	0.16	[35]
θ	Reduced probability for sick individuals in I_1	0.78	calibrated
k_3	Recovery rate	$\frac{1}{6}$	[35]
k_4	Inverse TB clearance rate	$\frac{1}{120}$	calibrated
γ	Relapse rate	0.20	[35]
ν_8	Death rate in $E_{>7}$	0.008	calibrated
k_2	Inverse of diagnosis delay time	$\frac{1}{3}$	[11]
a	Probability component for active TB	0.001035	calibrated
b	Probability component for active TB	-0.0152	calibrated
c	Probability component for active TB	0.06	calibrated
$(1-\gamma)$	Effective TB treatment rate	0.80	[35]

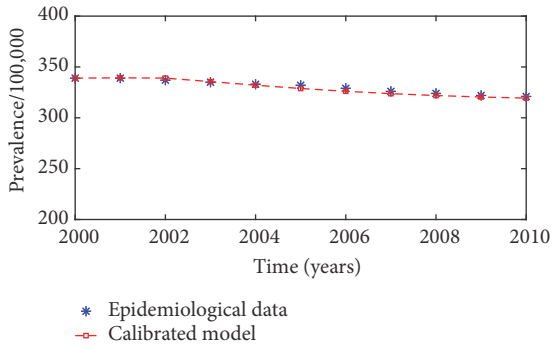

Figure 2: *Model simulation calibrated against tuberculosis prevalence data in Nigeria:* The figure shows the tuberculosis prevalence curve of the model, calibrated with 2000–2010 data, compared with the data estimates from WHO in that period. The model prevalence curve is obtained by solving (1) to (12), using the initial conditions in (13) and parameter values in Table 1. The goodness-of-fit measure (R^2) for simulation trajectories was evaluated and found to be 0.9992.

2.2. Facts and Hypotheses. For the purpose of this paper, we assume a constant birth rate Π. All newborns into the model susceptible class are uninfected, and TB/HIV coinfection is not explicitly modeled. These assumptions are simplifications that are not relevant to the current purpose, which is the identification of significant damage caused by poor case detection in the TB control program. They will be modified in a subsequent study in order to account for the effects of changes in the birth rate over time and to evaluate the significance of TB/HIV coinfection.

We propose to use the model in the exploration of different situations in Nigeria as a virtual experiments platform. The situations evaluated have been selected to start working on four wide hypotheses, although the final confirmation of all of them would require further research including on-field projects and incorporating experts from other involved disciplines. The four starting hypotheses are the following:

(1) TB prevalence still remains a major health challenge in Nigeria due to poor case detection

(2) Increase in effective treatment may not necessarily cause a significant decrease in the prevalence of TB in the country if active case finding is not implemented. In other words, increasing the notification rate is necessary for decreasing TB transmission in Nigeria

(3) The persistence and nondecreasing dynamics of TB in Nigeria are also related to a large number of latently infected individuals

(4) Poor notification rate has resulted in a large number (hundreds of thousands) of deaths of TB patients

3. Results

Numerical simulations of the model allowed us to estimate some important parameters associated with TB in Nigeria. In addition, we were able to observe and quantify the effect

of the infected population on the prevalence of TB in the country. They also allowed us to make a distinct connection between the notification parameter and the death toll on the sick population (infectious) population, the relationship between the death and the prevalence of the disease in the country. To illustrate these effects, we divide this section into 3 subsections. Hypotheses 1 and 2 were used to explain the case detection and how effective treatment affects TB dynamics in Nigeria; we made a prediction of new TB cases and provide an alternative strategy for TB control. Hypothesis 3 was used to explain the relationship between LTBI and the dynamics of TB prevalence. Finally, by means of Hypothesis 4 we quantified the death due to TB and estimate the death toll due to TB for the next decade in Nigeria, and we also estimate lives that could be saved with the alternative strategy proposed.

3.1. Hypotheses 1 and 2: Case Detection and Effective Treatment. The model was successfully fitted into WHO data of TB prevalence in Nigeria. Then, we compared the fitted tendency with predictions regarding an increase in notification parameter. The parameter values obtained after fitting the model into data of Nigeria are briefly summarized and discussed in Table 1. As shown in Figure 2, the obtained baseline simulation represents the epidemic TB situation in Nigeria successfully. Values for many parameters were determined from vital statistics: TB data from NTBLCP in Gombe State, official TB data from the World Health Organization (WHO), and other recent literatures mentioned in Table 1. When the values could not be estimated from data or literature, as in the case of the parameters associated with the contact rate, they were obtained with the model's fitting into epidemiological data ($R^2 = 0.9992$).

Recall, WHO estimates that about 30% of the world population is infected with LTBI [43]. However, the model revealed that about 34–37%(depending on the choice of contact rate for the sick population and some other parameters that where calibrated) of Nigeria's population is latently infected with TB. This population is distributed across the various infected classes ranging from E_1 to $E_{>7}$, and the time since infection in this population was also fitted.

We then used our model to investigate how the notification of new TB cases affects the dynamics of TB in Nigeria. We tested the hypothesis that the nonimprovement in notification observed in the situation of Nigeria may partially explain why the prevalence of TB in this country is very persistent and not declining as compared to others, showing an incidence rate between 400 and 500/100,000 (more than 130 times the incidence rate in the USA) [44–46]. The notification rate of TB in Nigeria is about 16% [35]. Therefore, initial conditions for new TB cases were calculated by assigning 16% of new cases to I_2 (i.e., the compartment that gathers the sick population that goes to hospital and receives care at some point), and 84% were assigned to I_1 (i.e., the population that remain sick throughout their life cycle until death).

Figure 3 shows the fitting of the model into the prevalence of TB in Nigeria, namely, baseline, together with some simulations where an increase in the notification rate was explored. The mean prevalence for the epidemiological data is 330.64 with a standard deviation of 6.7, while the mean for the model is 330.39 with a standard deviation of 6.6 and an R^2 coefficient of 0.9992 (Table 2). The model is pretty consistent with the epidemiological data. The mean resultant prevalence for each simulated notification rate is recorded in Table 2 as well. These results show a clear decrease in the prevalence of TB when the notification of the new TB cases increases.

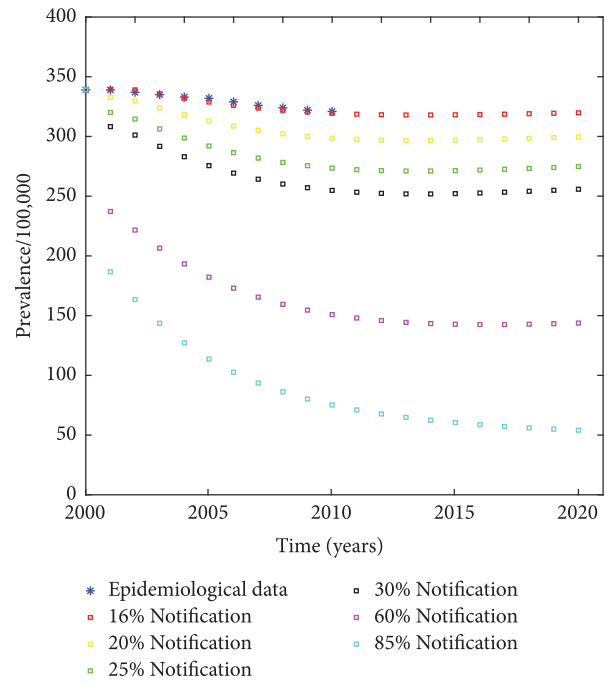

FIGURE 3: *Hypothesis 1: baseline simulation and effect of the notification rate.* Model fitted to the prevalence of tuberculosis in Nigeria. The blue star represents the epidemiological data of tuberculosis prevalence while the red line-circle represents the model simulation. The fitting was done with 16% of the sick population being notified. The experiment was repeated with 20% (yellow curve), 25% (green curve), 30% (black curve), 60% (magenta curve), and 85% (cyan curve) notification, respectively.

In the baseline simulation, the model predicted 62,000 deaths due to TB in the year 1990, 72,000 deaths in the year 1995, and 118,000 in the year 2014. These results are within the range of annual TB deaths estimated by WHO [35]. Figure 4 shows the predicted decline in prevalence after 10 years for each of the notification rates tested. In fact, a simply 10% relative increase in case notification of people with active TB reduces the TB prevalence by 15% when compared with the current situation. Predicted TB deaths also would decline by more than 15% when compared with the baseline simulation that fitted the epidemiological data.

A new simulation series was designed in order to explore the effect of an improvement of effective treatment, i.e., a decrease in γ. The results showed that a 10% improvement of effective treatment among active TB individuals produces a decline of only 5% in the prevalence of TB and related deaths compared with the baseline fitting, as shown in Figure 5(a).

Table 2: Summary of the mean prevalence of data and model simulations, as well as R^2 of the fitting.

Case detection rate	Mean prevalence	Standard deviation	References
Epidemiological data	330.64	6.7	[35]
Model 16% Notification	330.40	6.8, $R^2 = 0.9992$	Model
Model 20% Notification	311	NA	Model
Model 25% Notification	288	NA	Model
Model 30% Notification	266	NA	Model
Model 60% Notification	156	NA	Model
Model 85% Notification	105	NA	Model

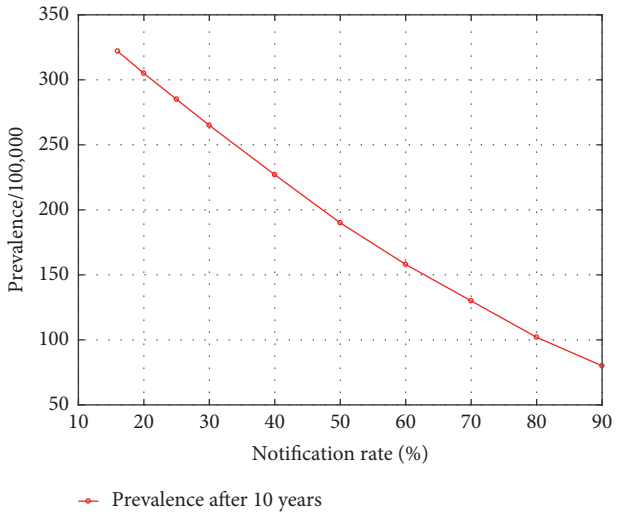

Figure 4: *Hypothesis 1:* evolution of tuberculosis prevalence in Nigeria after 10 years of simulation with different notification rate. Each point on the curve shows the prevalence of tuberculosis in Nigeria when simulated with the corresponding notification value on the x-axis for 10 years.

Given these results, the most effective intervention for reducing future TB cases and related deaths in Nigeria as predicted by the model is active case finding.

A final virtual experiment was designed in order to explore the effect of an improvement of effective treatment in a context with a high case detection rate. In this simulation series, the detection rate was fixed at 80% and different treatment success rates were explored. The results showed that, in this case, the improvement in treatment effectiveness would provide a significant decrease in TB prevalence (Figure 5(b)). With a notification rate of 80%, the increase in effective treatment by 10% will lead to a decline in the prevalence of 23% and associated deaths by almost 30%. In the case of a poor case detection rate, increase in 10% of effective treatment is associated with only 5% decrease in prevalence and related deaths. Therefore, an increase in the treatment effectiveness is only relevant if it is combined with active case finding or in a scenario where the notification rate is significantly high. Nevertheless, with the growing problem multidrug-resistant TB, investment in treatment becomes more relevant and needs to be maintained.

3.1.1. TB Prediction in Nigeria. Looking at the current TB situation in Nigeria, one can wonder what the situation will be if all parameters are left unchanged especially in terms of passive case finding. We envisioned this scenario and with the help of the baseline simulation results, the following results are presented. Figure 6(a) shows the predicted evolution of TB when the notification rate is gradually increased, while Figure 6(b) shows the effect of a sudden increase in this parameter. The simulation starts with the baseline that represents the current situation (16% notification, red-dashed line). Keeping the notification at this rate without any changes may keep the prevalence of TB in the country between 350 and 320/100,000 even after 40 years from the present day. This is precisely the present situation of TB in Nigeria, where there have not been any significant changes or decline in TB prevalence for the past 25 years (323/100,000 in 1990 and 332/100,000 in 2015 [35]). Increasing the notification rate up to 20% in 10 years could keep the prevalence between 300 and 290/100,000 people. If no more effort is made to increase the notification further, the prevalence would remain in this range even after a period of 50 years. Increasing the notification further to 25% in another 10 years would reduce the prevalence to between 290 and 260/100,000 people, and a further increase in notification to 30% would bring down the prevalence to between 220 and 240/100,000. We repeated the experiment with a sudden increase in the notification from 16% to 30% as seen in Figure 6(b) when the prevalence would remain in the range of 270/100,000 to 280/100,000.

For a successful and reasonable decline in TB cases in Nigeria to be achieved, case finding needs to be active and increased from period of time to time. Although a 30% notification rate is viable, a real TB prevalence decrease in Nigeria can only be achieved with a notification rate around 80%. Both strategies presented in Figures 3 and 6 produce the same results in the long run in terms of TB prevalence decline. However, in terms of public health, a progressive decreasing strategy would be more feasible due to the economic resources that need to be allocated by health authorities. In contrast, increasing the notification rate by a large percentage could be very ambitious and resource demanding. At this junction, the most important point is to be able to make interventions as soon as possible given the long time required to actually see changes in TB prevalence.

3.2. Hypothesis 3: Latently Infected Population. Although it is known that latently infected individuals are connected

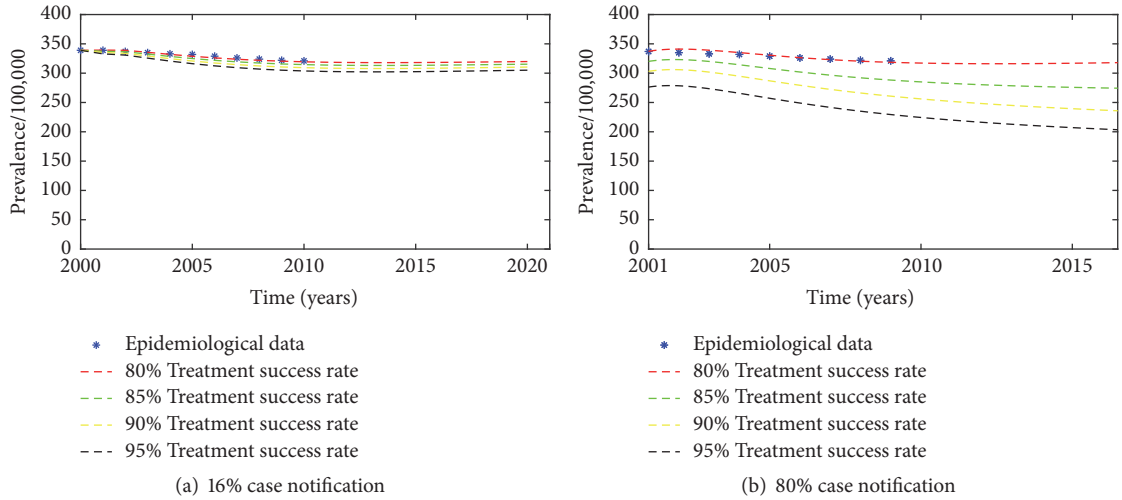

Figure 5: *Hypothesis 2: effective treatment in the population with good surveillance and poor surveillance.* (a) The figure depicts a relative increase in effective treatment from 80%, 85%, and 90% to 95% in a population with poor case detection, where the notification rate is only 16%. (b) The figure shows a significant decrease in prevalence due to increase in effective treatment from 80%, 85%, and 90% to 95%, in a population with very good case detection, where the notification rate is 80%.

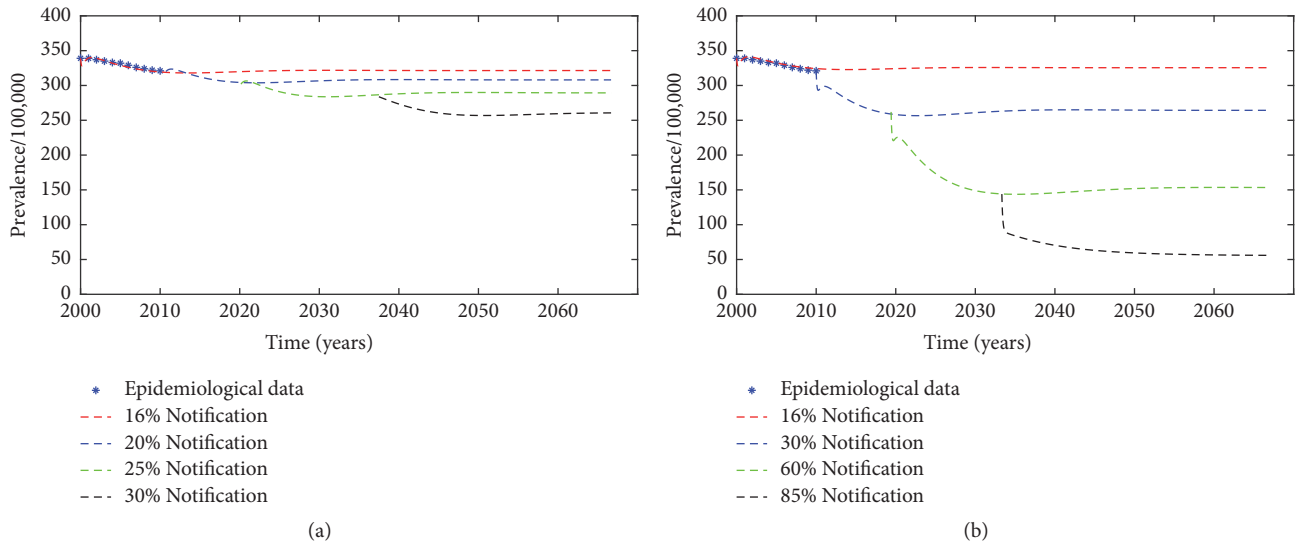

Figure 6: *Hypothesis 1: effective strategies in a gradual increase in tuberculosis notification in the case of poor tuberculosis surveillance.* (a) Result of the prediction made by the model when the notification of new tuberculosis cases is gradually increased. The red curve shows the poor notification rate situation, which represents the present situation of tuberculosis in Nigeria (the blue stars). The rest of the curves represent a change in case detection and increasing in the notification of new cases by some percentages over a period of time. (b) Result of the prediction made when the notification of new tuberculosis cases is suddenly increased.

with the incidence of TB, it is not completely clear how this connection can influence the dynamics of the disease in a population. Our first hypothesis implied that poor case detection leads to a higher number of unnotified TB cases, which leads to a high number of latently infected individuals that are at risk of developing active TB, thus resulting in persistent high TB prevalence. Our model was also used as a virtual experimental device to test the effect of the latently infected population in Nigeria, which can provide significant information that can be very difficult or impossible to guess otherwise. We are going to show why the prevalence of TB in Nigeria is substantially high and nondecreasing for a very long period of time.

We explored the effect of increasing the notification rate or the treatment success on the LTBI population (Figure 7). Figure 7(a) shows the result of various simulations of the latently infected population carried out with different notification parameters. The latently infected population consistently declines with each increase in notification rate. This result explains why a population with a poor case detection program can fail to achieve significant progress in reducing new TB cases, because the latently infected population remains the same for a very long period of time due to what is called the replacement principle, where each sick TB patient produces at least one sick patient before death or progress to receiving treatment (the number of new cases

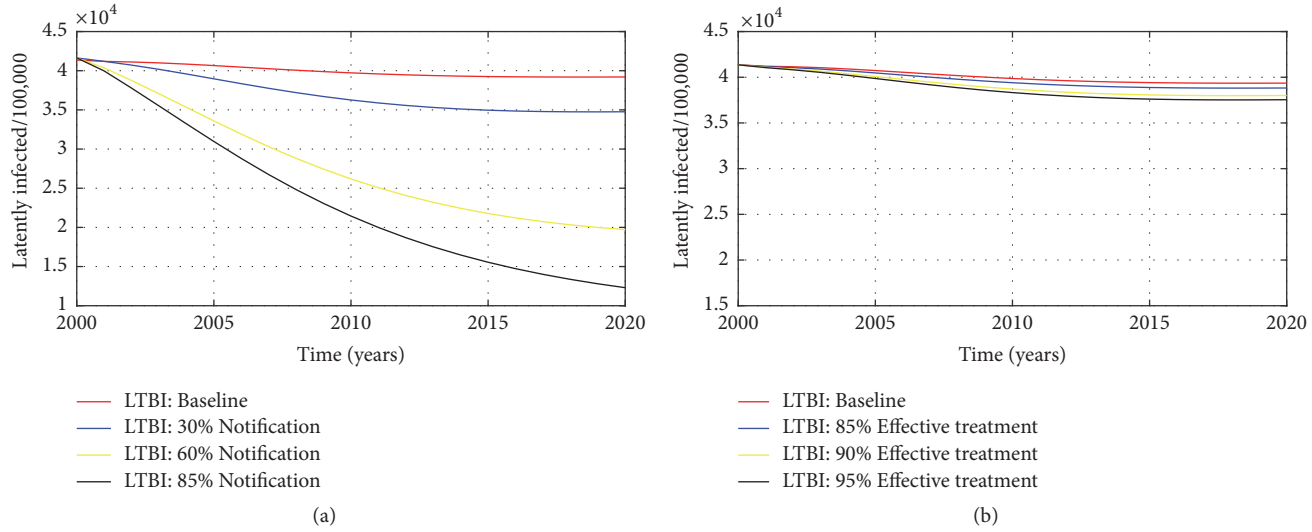

Figure 7: *Hypothesis 3: changes in latent tuberculosis with respect to an increase in notification rate or in effective treatment.* (a) Simulated dynamics of the latently infected population (LTBI) with different notification levels, with all other parameters kept constant in the population of Nigeria. The red curve shows the LTBI population that remained constant for more than 20 years, thereby producing new sick people constantly. With an increase in notification up to 30%, the pool of the LTBI starts decreasing (blue curve), and a further increase in notification shows a much higher decrease in the pool of LTBI (black curve, 85% notification rate). (b) Simulation of the LTBI population with improvement in effective treatment, with all other parameters kept constant in the population of Nigeria. There is little or no change in the number of LTBI cases before and after increasing the effective treatment.

that receive treatment is very low). This type of situation guaranteed the consistent production of newer TB cases if active case finding is not implemented.

The increase in notification rate affects not only the active new TB cases but also the latently infected population. A 10% increase in notification was associated with a 38% decline in latent infected TB (Figures 7(a) and 8), while a 10% increase in effective treatment showed only a 2.9% decline in the latently infected population (Figure 7(b)).

3.3. Hypothesis 4: Poor Notification and Mortality in Sick Population. We finally tested the hypothesis that low notification rate has resulted in massive deaths in the sick population. This phenomenon might be a mystery in Nigeria as not every death is reported to the authorities. Only the deaths that occur in a notified case of TB are recorded as a death due to this disease. As the notification rate of TB in Nigeria is just 16%, one can wonder how many death cases due to TB went unnoticed. As mentioned earlier, we used the notification of 16% to fit the data to the model.

Figure 9 shows the estimated TB-related mortality per a hundred thousand individuals in the population of Nigeria obtained from the model. The present-day mortality rate in Nigeria is shown by the red curve, which shows that mortality due to TB in Nigeria is between 70 and 65 individuals per 100,000 individuals. This result is very consistent with the report from WHO [35]. The model shows that an increase in the notification by 10% would lead to the decrease in mortality by 20%. Actually, we see from Figure 9 that if the notification is increased from 16% to 25%, the mortality declines to less than 60/100,000 individuals, which implies hundreds of thousands of lives that would be saved. In

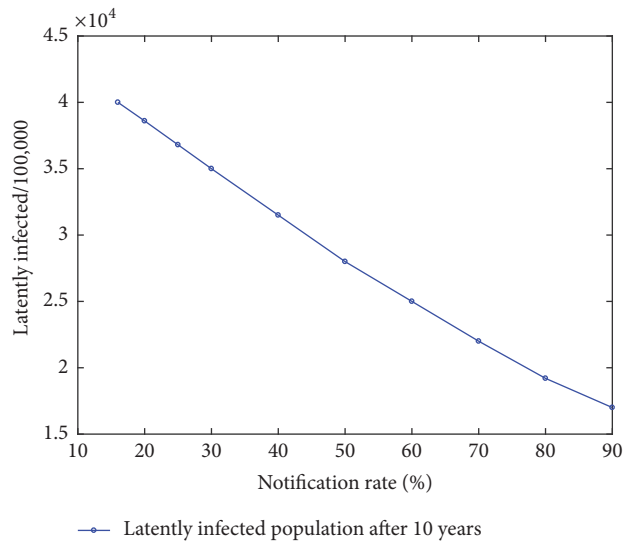

Figure 8: *Hypothesis 3:* latently infected population after 10 years of simulation of the model with different notification levels. Each point of the curve represents the corresponding population of the latently infected compartments, when the model is simulated with the corresponding notification rate on the x-axis.

order to better understand these dynamics, we estimated the mortality rate in Nigeria after 10 years of simulation with the model by using different notification parameters, starting from the current situation in Nigeria (notification rate of 16%). The result of this experiment is shown in Figure 10.

The expected cumulative number of deaths due to TB with the 16% notification after 10 years of simulation is

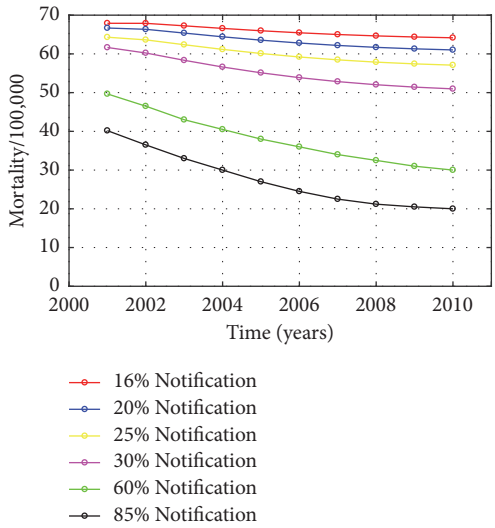

Figure 9: *Hypothesis 4:* The figure shows the decrease in mortality due to tuberculosis in the sick population for a period of 10 years with different notification levels. The red curve represents the current mortality due to tuberculosis in Nigeria (baseline), and the rest of the curves show what the situation would look like if the notification were to be different.

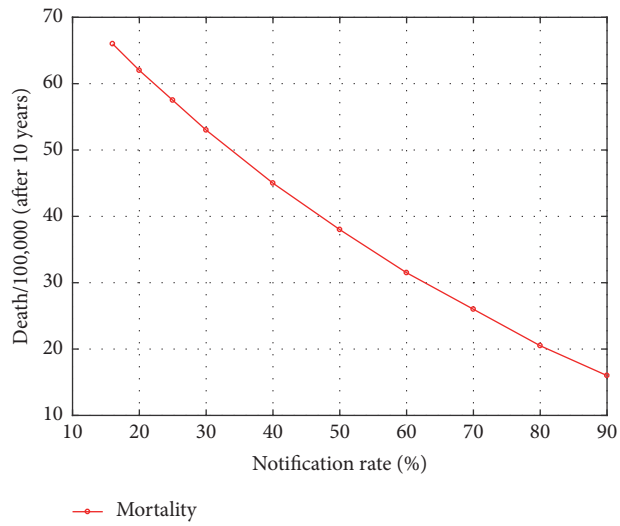

Figure 10: *Hypothesis 4:* the result of 10-year simulation of the model using different notification rates. Each point on the curve represents the mortality in the sick population after the model is simulated for 10 years with the corresponding notification rate on the x-axis.

4,748,971. An increase in notification to a rate of 20% could save up to 292,244 lives within this period. If the notification rate was increased to 25%, up to 584,489 lives could be saved within this period.

Although the estimated TB prevalence in Nigeria from 1990 to the year 2016 remains the same, the estimated number of new cases increases annually. These are attributed to the increase in the population of the country, but, at the same time, it shows a massive increase in the number of deaths due to TB in the population as estimated by the model. The estimated new TB cases rise from 310,000 in 1990 to more than 600,000 in 2015, and the estimated number of TB-related deaths by the model rises from 62,000 in 1990 to more than 120,000 in 2015. If the population of Nigeria continues to grow at the rate of 3.2% annually [47] and the case finding remains passive at 16% notification, then TB-related deaths will reach up to 3,456,640 in the year 2030; this is twice the current number of deaths due to TB in the world reported by WHO in 2017 [3]. Depending on availability of funds, political willingness to implement active case finding in Nigeria, and the strategy implemented, millions of lives could be saved from 2018 to 2030. Globally, the model predicted a total death number of 11,872,530 individuals from 2017 to 2030. An increase in case detection by 15% within this period could save up to 2,557,160 lives and would reduce the incidence by more than 30%.

4. Discussion

Epidemiological data from Nigeria shows that the TB situation in this country is very persistent over time, in spite of the efforts made by all the stakeholders battling the disease. While TB prevalence in Nigeria in 1990 was 323/100,000 individuals, today it is around the same number (330/100,000) according to WHO. The same situation is observed in the number of deaths due to the disease (70/100,000 today compared to 65/100,000 in 1990). The reason for this steady state of the TB epidemic in the country is still unclear. Many associate it with poverty and population growth. Nigeria recently overtook India as the world's poverty capital [48] with about 87 million people in abject poverty [48]. Its unprecedented demographic growth (from 95,62 million people in 1990 to 206,20 in 2018) is mainly due to a very high fertility rate (5.526 according to the World Bank in 2016). Others presume that there is a need for a better strategy in order to fight the disease towards a significant decline in the near future [11].

Nigeria is a particular setting where several healthcare options (medical pluralism) including orthodox medicine (public, private, or drugstores), traditional medicine, and spiritual healers operate freely [11]. The public health facilities where the TB control program operates are distanced from the citizens. More often than not, these health facilities are not the first choice during health seeking decisions. Unlike the theory of Dim and Dim [11] and Zwerling et al. [49], we believe that high TB prevalence in Nigeria has a lot to do with policies of its TB control program, as stated in other studies [18, 45, 50, 51]. Today, Nigeria is ranked as number 3 in the world in terms of TB burden [52] just behind China and India. The country has adopted passive case finding as recommended by WHO [42], based on a study conducted in India [53, 54]. Nevertheless, the Indian context has completely different demographic, cultural, and literacy settings from Nigeria. However, successful TB control only happens when social and cultural factors are taken into consideration [55]. It is therefore imperative to revise and consider the means of extending the NTBLCP strategy.

In this study, we applied epidemic models to real populations to draw conclusions about one of the leading health challenges in Nigeria. We numerically showed that an increase in the diagnosis rate together with a treatment's success of TB patients is an essential step towards TB control in Nigeria. In order to increase notification rate of TB in Nigeria using the current passive case detection strategy, the people at the community level should be empowered with adequate knowledge of the growing burden of the disease and accessible potentials for a cure. Alternatively, active case finding strategies could be explored and implemented, although the existence of many remote communities in some Nigerian areas would dramatically make this task difficult. In any case, the analysis reveals that, with current strategies, it will be impossible to actualize the aims of the End TB strategy, with targets to reduce TB deaths by 95% and to cut new TB cases by 90% between 2015 and 2035 [56].

Even with a high increase in the notification and without considering HIV/TB coinfection and the problem of multidrug-resistant (MDR) strains, mortality from TB in Nigeria will still be dramatic for the next few decades to come. Two main facts will contribute to this increase in mortality: first, Nigeria's population growth of more than 3.2% annually [47, 57] and, second, the resulting deaths due to TB which are expected to drastically increase by 2030 unless effective TB control is implemented in the country. The results we obtained in our study confirm this situation. This issue poses a great threat not only to Nigeria but also to the entire world's TB program and to the ambitious *End TB Partnership* [56] by 2030.

The increase of TB diagnosis by applying active case finding along with specific actions to guarantee TB treatment's adherence and success could be used to achieve the goals set by WHO in Nigeria by reducing TB mortality significantly, TB prevalence, and LTBI population. Perhaps the time has come for a critical reexamination of the costs, risks, and benefits of active case finding in this country. Indeed, the strategies evaluated in this paper would require substantial resources and extraordinary mobilization of international attention, since the greater part of TB control program funding comes from external sources [42]. We have not attempted to estimate the cost difference of the control strategies proposed. Initiating and sustaining such a large-scale effort of active case finding would be very challenging. However, the first step needs to include both a realistic assessment of implementing these ambitious initiatives and the identification of an optimal way to implement them. For that, the socioeconomic context of the different Nigerian territories and the social inequalities within and between them should be taken into account, so that they can be transformed into feasible policy recommendations. Furthermore, success could not be guaranteed without both realistic evaluation of the costs of pursuing active case finding and the treatment of new diagnosed TB sick individuals.

Our results exploring different scenarios show the high relevance of increasing the notification rate in contrast to the modest effects of an improvement of treatment efficacy only. Nevertheless, the treatment efficacy would probably turn out to be crucial if we included the problem of MDR, which would be addressed in further studies. Despite contemplating the absence of MDR as a limitation of the model, our conclusions cannot be questioned, since the main problem is still the pool of nondiagnosed TB sick individuals. Future studies could also include the study of the reinfection effect in the model. This new setting would allow a detailed study of the LTBI population and its distribution between old and recent infections. Nonetheless, the reinfection effect would not change the main dynamics given by the current model and the recommendations that arose from it.

5. Conclusions

The model shows that WHO targets stated by the End TB strategy [56] would not be achieved with the current public management of TB in Nigeria. In fact, its forecasted situation for 2030 suggests being far away from ending the TB epidemics as aimed in the United Nations Sustainable Development Goals under Goal 3. The high percentage of undiagnosed TB sick individuals in this country is a huge obstacle for the target incidence's disease. It is essential to increase the number of the diagnosed and successfully treated, thus requiring not only a significant economic effort but also a boost in social work in the community. This result is valid not only for Nigeria, but also for such countries where nondiagnosis is a serious problem. In all cases, a significant TB incidence's decrease can only be achieved by both increasing the notification rate to the 80%-90% range and providing appropriate management of diagnosed patients. With both measures, new infections can be prevented and the treatment's success can be guaranteed. This situation is the bottleneck that needs to be overcome in addition to the incorporation, improvement, and/or strengthening of other essential TB control measures such as directly observed treatment or contact tracing.

Data Availability

The epidemiological data supporting this study are from previously reported studies and datasets, which have been cited. The processed data are available from the corresponding author upon request.

Conflicts of Interest

The authors declare that they have no conflicts of interest.

References

[1] T. Paulson, "A mortal foe," *Nature*, vol. 502, pp. S2–S3, 2013.

[2] R. M. Houben, P. J. Dodd, and J. Z. Metcalfe, "The Global Burden of Latent Tuberculosis Infection: A Re-estimation Using Mathematical Modelling," *PLoS Medicine*, vol. 13, no. 10, p. e1002152, 2016.

[3] World Health Organization, "Global Tuberculosis Report," 2017.

[4] P.-J. Cardona, "Patogénesis de la tuberculosis y otras micobacteriosis," *Formación médica continuada: infecciones por micobacterias*, vol. 36, no. 1, pp. 38–46, 2018.

[5] K. Bhatt and P. Salgame, "Host innate immune response to *Mycobacterium tuberculosis*," *Journal of Clinical Immunology*, vol. 27, no. 4, pp. 347–362, 2007.

[6] P. Peyron, J. Vaubourgeix, Y. Poquet et al., "Foamy macrophages from tuberculous patients' granulomas constitute a nutrient-rich reservoir for M. tuberculosis persistence," *PLoS Pathogens*, vol. 4, no. 11, 2008.

[7] R. L. Hunter, "Pathology of post primary tuberculosis of the lung: an illustrated critical review," *Tuberculosis*, vol. 91, no. 6, pp. 497–509, 2011.

[8] W. W. Stead, J. P. Lofgren, E. Warren, and C. Thomas, "Tuberculosis as an Endemic and Nosocomial Infection among the Elderly in Nursing Homes," *The New England Journal of Medicine*, vol. 312, no. 23, pp. 1483–1487, 1985.

[9] World Health Organization and Others, "Global tuberculosis report 2016," 2016.

[10] A. Aliyu and L. Amadu, "Urbanization, cities, and health: The challenges to Nigeria - A review," *Annals of African Medicine*, vol. 16, no. 4, pp. 149–158, 2017.

[11] C. Dim and N. Dim, "Trends of tuberculosis prevalence and treatment outcome in an under-resourced setting: The case of Enugu state, South East Nigeria," *Nigerian Medical Journal*, vol. 54, no. 6, p. 392, 2013.

[12] Punch, "Nigeria ranked 4th in TB infection worldwide – Report," http://www.punchng.com/nigeria-has-4th-tb-infection-rate-worldwide-report/.

[13] "Nigeria Development Data," http://www.demographic-dividend.org/country_highlights/nigeria/.

[14] R. Yaesoubi and T. Cohen, "Identifying dynamic tuberculosis case-finding policies for HIV/TB coepidemics," *Proceedings of the National Acadamy of Sciences of the United States of America*, vol. 110, no. 23, pp. 9457–9462, 2013.

[15] J. V. Lazarus, M. Olsen, L. Ditiu, and S. Matic, "Tuberculosis-HIV co-infection: Policy and epidemiology in 25 countries in the WHO European region," *HIV Medicine*, vol. 9, no. 6, pp. 406–414, 2008.

[16] D. Okuonghae and B. O. Ikhimwin, "Dynamics of a mathematical model for tuberculosis with variability in susceptibility and disease progressions due to difference in awareness level," *Frontiers in Microbiology*, vol. 6, 2016.

[17] T. F. Brewer, G. A. Colditz, S. M. Krumplitsch, S. J. Heymann, M. E. Wilson, and H. V. Fineberg, "Strategies to decrease tuberculosis in US homeless populations: A computer simulation model," *Journal of the American Medical Association*, vol. 286, no. 7, pp. 834–842, 2001.

[18] P. J. Dodd, R. G. White, E. L. Corbett, and S. P. Tripathy, "Periodic Active Case Finding for TB: When to Look?" *PLoS ONE*, vol. 6, no. 12, p. e29130, 2011.

[19] P. Kim and C. H. Lee, "Epidemic Spreading in Complex Networks with Resilient Nodes: Applications to FMD," *Complexity*, vol. 2018, Article ID 5024327, 9 pages, 2018.

[20] A. Corberán-Vallet, F. J. Santonja, M. Jornet-Sanz, and R.-J. Villanueva, "Modeling Chickenpox Dynamics with a Discrete Time Bayesian Stochastic Compartmental Model," *Complexity*, vol. 2018, Article ID 3060368, 9 pages, 2018.

[21] S. I. Bala and N. M. Ahmad, "Bistability analysis in mathematical model of M-phase control in Xenopus oocyte extracts," *Computational and Applied Mathematics*, vol. 37, no. 3, pp. 2667–2692, 2018.

[22] C. Ozcaglar, A. Shabbeer, S. L. Vandenberg, B. Yener, and K. P. Bennett, "Epidemiological models of Mycobacterium tuberculosis complex infections," *Mathematical Biosciences*, vol. 236, no. 2, pp. 77–96, 2012.

[23] M. R. Nyendak, B. Park, M. D. Null et al., "Mycobacterium tuberculosis Specific CD8+ T Cells Rapidly Decline with Anti-tuberculosis Treatment," *PLoS ONE*, vol. 8, no. 12, p. e81564, 2013.

[24] H. J. Na, J. S. Eom, G. Lee et al., "Exposure to Mycobacterium tuberculosis during flexible bronchoscopy in patients with unexpected pulmonary tuberculosis," *PLoS ONE*, vol. 11, no. 5, 2016.

[25] L. Telisinghe, K. L. Fielding, J. L. Malden et al., "High tuberculosis prevalence in a South African prison: The need for routine tuberculosis screening," *PLoS ONE*, vol. 9, no. 1, Article ID e87262, 2014.

[26] P. Nahid, E. E. Bliven, E. Y. Kim et al., "Influence of M. tuberculosis lineage variability within a clinical trial for pulmonary tuberculosis," *PLoS ONE*, vol. 5, no. 5, 2010.

[27] A. Parhar, Z. Gao, C. Heffernan, R. Ahmed, M. L. Egedahl, and R. Long, "Is early tuberculosis death associated with increased tuberculosis transmission?" *PLoS ONE*, vol. 10, no. 1, 2015.

[28] J.-M. García-García, R. Blanquer, T. Rodrigo et al., "Social, clinical and microbiological differential characteristics of tuberculosis among immigrants in Spain," *PLoS ONE*, vol. 6, no. 1, 2011.

[29] J. Millet, A. Orcau, C. Rius et al., "Predictors of Death among Patients Who Completed Tuberculosis Treatment: A Population-Based Cohort Study," *PLoS ONE*, vol. 6, no. 9, p. e25315, 2011.

[30] Shaip Krasniqi, Arianit Jakupi, Armond Daci et al., "Tuberculosis Treatment Adherence of Patients in Kosovo," *Tuberculosis Research and Treatment*, vol. 2017, Article ID 4850324, 8 pages, 2017.

[31] S. W. Asgedom, M. Teweldemedhin, and H. Gebreyesus, "Prevalence of Multidrug-Resistant Tuberculosis and Associated Factors in Ethiopia: A Systematic Review," *Journal of Pathogens*, vol. 2018, Article ID 7104921, 8 pages, 2018.

[32] L. Liu and Y. Wang, "A mathematical study of a TB model with treatment interruptions and two latent periods," *Computational and Mathematical Methods in Medicine*, vol. 2014, Article ID 932186, 15 pages, 2014.

[33] S. Liu, A. Li, X. Feng, X. Zhang, and K. Wang, "A Dynamic Model of Human and Livestock Tuberculosis Spread and Control in Urumqi, Xinjiang, China," *Computational and Mathematical Methods in Medicine*, vol. 2016, 2016.

[34] F. A. Krsulovic, M. Lima, and P. Cardona, "Tuberculosis Epidemiology at the Country Scale: Self-Limiting Process and the HIV Effects," *PLoS ONE*, vol. 11, no. 4, p. e0153710, 2016.

[35] World Health Organization, "Media Centre: Tuberculosis, Fact sheet," 2016.

[36] R. S. Wallis, "Mathematical Models of Tuberculosis Reactivation and Relapse," *Frontiers in Microbiology*, vol. 7, 2016.

[37] D. P. Moualeu-Ngangue, S. Röblitz, R. Ehrig, and P. Deuflhard, "Parameter identification in a tuberculosis model for Cameroon," *PLoS ONE*, vol. 10, no. 4, 2015.

[38] S. Ohno, *Evolution by Gene Duplication*, Springer Berlin Heidelberg, 1970.

[39] B. Song, C. Castillo-Chavez, and J. P. Aparicio, "Tuberculosis models with fast and slow dynamics: the role of close and casual contacts," *Mathematical Biosciences*, vol. 180, no. 1-2, pp. 187–205, 2002.

[40] G. Guzzetta, M. Ajelli, Z. Yang, S. Merler, C. Furlanello, and D. Kirschner, "Modeling socio-demography to capture tuberculosis transmission dynamics in a low burden setting," *Journal of Theoretical Biology*, vol. 289, no. 1, pp. 197–205, 2011.

[41] B. M. Murphy, B. H. Singer, and D. Kirschner, "On treatment of tuberculosis in heterogeneous populations," *Journal of Theoretical Biology*, vol. 223, no. 4, pp. 391–404, 2003.

[42] "Nigeria Tuberculosis Fact Sheet, United States Embassy in Nigeria," 2012.

[43] A. Zumla, A. George, V. Sharma, R. H. N. Herbert, A. Oxley, and M. Oliver, "The WHO 2014 global tuberculosis report—further to go," *The Lancet Global Health*, vol. 3, no. 1, pp. e10–e12, 2015.

[44] H. H. Kyu, E. R. Maddison, N. J. Henry et al., "The global burden of tuberculosis: results from the Global Burden of Disease Study 2015," in *The Lancet Infectious Diseases*, vol. 18, pp. 261–284, 2018.

[45] C. Lienhardt, P. Glaziou, M. Uplekar, K. Lönnroth, H. Getahun, and M. Raviglione, "Global tuberculosis control: Lessons learnt and future prospects," *Nature Reviews Microbiology*, vol. 10, no. 6, pp. 407–416, 2012.

[46] "Centers for Disease Control and Prevention (US) and National Center for Prevention Services (US). Division of Tuberculosis Elimination and National Center for HIV and STD and TB Prevention (US). Division of Tuberculosis Elimination, *Reported tuberculosis in the United States*; US Department of Health and Human Services, Public Health Service, Centers for Disease Control and Prevention, National Center for Prevention Services, Division of Tuberculosis Elimination," 1999.

[47] USAID, "Health fact sheet," https://www.usaid.gov/sites/default/files/documents//USAID-Nigeria-Health-Fact-Sheet.pdf.

[48] Vanguard News paper, "Nigeria overtakes India as world's poverty capital — Report," https://www.vanguardngr.com//06/nigeria-overtakes-india-as-worlds-poverty-capital-report/ Vanguard News paper.

[49] A. Zwerling, S. Shrestha, and D. W. Dowdy, "Mathematical Modelling and Tuberculosis: Advances in Diagnostics and Novel Therapies," *Advances in Medicine*, vol. 2015, Article ID 907267, 10 pages, 2015.

[50] N. A. Menzies, T. Cohen, H.-H. Lin, M. Murray, and J. A. Salomon, "Population health impact and cost-effectiveness of tuberculosis diagnosis with Xpert MTB/RIF: a dynamic simulation and economic evaluation," *PLoS Medicine*, vol. 9, no. 11, Article ID e1001347, 2012.

[51] C. J. L. Murray and J. A. Salomon, "Modeling the impact of global tuberculosis control strategies," *Proceedings of the National Acadamy of Sciences of the United States of America*, vol. 95, no. 23, pp. 13881–13886, 1998.

[52] "Nigeria Tuberculosis profile," http://www.who.int/tb/country/data/profiles/en/profile.

[53] D. R. Nagpaul, M. K. Vishwanath, and G. Dwarakanath, "A socio-epidemiological study of out-patients attending a city tuberculosis clinic in India to judge the place of specialized centres in a tuberculosis control programme.," *Bulletin of the World Health Organization*, vol. 43, no. 1, pp. 17–34, 1970.

[54] D. Banerji and S. Andersen, "A sociological study of awareness of symptoms among persons with pulmonary tuberculosis," *Bulletin of the World Health Organization*, vol. 29, pp. 665–683, 1963.

[55] A. J. Rubel and L. C. Garro, "Social and cultural factors in the successful control of tuberculosis," *Public Health Reports*, vol. 107, no. 6, pp. 626–635, 1992.

[56] World Health Organization, "The End TB Strategy," http://www.who.int/tb/End_TB_brochure.pdfStrategy.

[57] M. W. Rosegrant, M. C. Agcaoili-Sombilla, and N. D. Perez, *Global Food Projections to 2020: Implications for Investment*, Diane Publishing, 1995.

Hindawi
Complexity
Volume 2018, Article ID 3427826, 11 pages
https://doi.org/10.1155/2018/3427826

Research Article

Infrastructure as a Complex Adaptive System

Edward J. Oughton,[1] **Will Usher**,[1] **Peter Tyler**,[2] **and Jim W. Hall**[1]

[1]*Environmental Change Institute, University of Oxford, South Parks Road, Oxford, OX1 3QY, UK*
[2]*Department of Land Economy, University of Cambridge, 19 Silver Street, Cambridge, CB3 9EP, UK*

Correspondence should be addressed to Edward J. Oughton; edward.oughton@ouce.ox.ac.uk

Received 18 May 2018; Revised 6 October 2018; Accepted 25 October 2018; Published 4 November 2018

Guest Editor: Claudio Tessone

National infrastructure systems spanning energy, transport, digital, waste, and water are well recognised as complex and interdependent. While some policy makers have been keen to adopt the narrative of complexity, the *application* of complexity-based methods in public policy decision-making has been restricted by the lack of innovation in associated methodologies and tools. In this paper we firstly evaluate the application of complex adaptive systems theory to infrastructure systems, comparing and contrasting this approach with traditional systems theory. We secondly identify five key theoretical properties of complex adaptive systems including adaptive agents, diverse agents, dynamics, irreversibility, and emergence, which are exhibited across three hierarchical levels ranging from agents, to networks, to systems. With these properties in mind, we then present a case study on the development of a system-of-systems modelling approach based on complex adaptive systems theory capable of modelling an emergent national infrastructure system, driven by agent-level decisions with explicitly modelled interdependencies between energy, transport, digital, waste, and water. Indeed, the novel contribution of the paper is the articulation of the case study describing a decade of research which applies complex adaptive systems properties to the development of a national infrastructure system-of-systems model. This approach has been used by the UK National Infrastructure Commission to produce a National Infrastructure Assessment which is capable of coordinating infrastructure policy across a historically fragmented governance landscape spanning eight government departments. The application will continue to be pertinent moving forward due to the continuing complexity of interdependent infrastructure systems, particularly the challenges of increased electrification and the proliferation of the Internet of Things.

1. Introduction

Infrastructure systems across the world are becoming increasingly challenged as a result of growing demand and the fact that many assets are coming to the end of their lifespan. One technological solution to these problems is the use of Information Communication Technology (ICT) to provide smart management in both the supply of and demand for infrastructure. However, the pervasive use of ICT means we have transitioned to a position where infrastructure sectors are becoming more and more interdependent [1–4]. Because of this interconnectivity, individual infrastructure sectors can no longer be assessed in isolation, motivating the increased use of decision support methods which utilise systems-based approaches.

When contrasted against the level of intellectual enquiry focusing on complexity, there has hitherto been relatively limited *application* of complexity-based methods to support public policy decision-making. This is despite the dissatisfaction shown regarding the rigid application of the assumptions associated with general systems theory, neoclassical economics, and rational decision-making, in favour of more evolutionary, complexity-based approaches [5–10]. There needs to be greater understanding of how national infrastructure systems and their agents adapt and change across time and space. One approach that may prove promising in this endeavour is the application of complex adaptive system (CAS) theory, as it can help to generate new knowledge on how to model infrastructure systems. In this article we investigate the application of CAS to infrastructure systems by building on the work of others who have examined this problem [1, 11–14].

We first consider the characteristics of a national infrastructure system and secondly outline the basis of an approach

based on complex adaptive systems, including how it can be distinguished conceptually from general systems theory. We then examine how the properties of a CAS approach can be used to understand more about national infrastructure, before providing a case study of how this has been utilised by the UK's National Infrastructure Commission to model national infrastructure strategies.

2. The Key Characteristics of a National Infrastructure System

High-quality national infrastructure systems comprised of the energy, transport, ICT, water, and waste are essential for economic prosperity and a fully functioning society [17]. However, defining infrastructure is difficult as the term is used to refer to a variety of objects and technological artefacts and the human systems that enable their effective functioning. We synthesise a working definition within this context, whereby infrastructure is an enabling system that provides a range of different *services* to intermediate and end users.

Increasingly, infrastructure assets require inputs from other sectors to function, for example, as smart infrastructure systems increasingly rely on digital connectivity to operate. These assets are coordinated to undertake a variety of processes which provide business-to-business or business-to-consumer *infrastructure services*. Often this takes place in a hierarchical manner, with networks operating across multiple spatial layers [18, 19], resulting in nested processes. Two of the main processes which infrastructure assets can undertake are the *transformation* or *preservation* of different material and immaterial entities. These processes can be carried out to a range of materials and objects or to intangible forms of capital such as information. In addition, infrastructure assets are also able to *transmit* and distribute these material or intangible forms of capital across space. We therefore define infrastructure as *the coordinated operation and management of a group of physical assets to perform a range of processes, thereby providing infrastructure services to users* [20].

Given that infrastructure services having low substitutability [21], poor infrastructure decision-making can have severe economic and societal effects, with infrastructure assets being durable commodities which can last decades. These systems are frequently very large in scale and consequently, particularly with regard to the aforementioned factors, can become susceptible to path dependent "lock-in" effects [22]. Infrastructure investments, particularly once reinforced by increasing returns, can lock infrastructure systems on path dependent economic or environmental trajectories which are incredibly hard to break away from due to the substantial financial hurdles involved with path divergence.

Infrastructure is deeply intertwined in all economic and societal systems. It mediates the way we create new value, how we move across space, and the way we interact and communicate, as well as bringing a driver of technological uncertainty [23]. Transport, energy, and ICT are good examples as they can have the most dramatic economic effects on productivity, location, and innovation, by enabling agglomeration benefits including increasing trade specialisation, labour market efficiency, and helping the spread of new ideas. Recent analysis indicates that infrastructure stocks can positively affect long-run economic output by somewhere between the range of 0.07 and 0.10 [24]. Although a variety of papers use different infrastructure stock definitions and econometric techniques, recent studies indicate that there are generally positive economic effects from infrastructure investment (although they can vary by infrastructure sector), even if they are relatively humble [25–30].

National infrastructure systems often have mixed planning, delivery, operation, ownership, and regulatory frameworks, where governance frequently extends across private firms and individuals, public institutions, and third-sector organisations [31]. This reflects the historical legacy of many infrastructure systems, which were once publicly owned and centralised systems. Past governance arrangements significantly shape the current character, structure, and operation of national infrastructure systems and continue to have profound hysteretic impacts in the future. As an example, Table 1 details the diverse attributes of the UK national infrastructure system.

Like all national infrastructure systems, the actors involved in Table 1 operate over a multitude of spatial scales including the local, regional, national, and international levels, with a wide range of motivations and constraints. This makes it a very challenging task for those trying to manoeuvre each system to provide economically efficient, spatially equitable, and environmentally sustainable outcomes [32].

In the next section we consider the key properties of a CAS and assess how it might assist in understanding national infrastructure. In making this assessment we draw upon the growing literature of CAS theory.

3. The Properties of a Complex Adaptive System

A complex system has a multitude of individual components and agents that are highly connected and interdependent, to the extent that "emergent" behavioural phenomena occur which cannot be explained using other reductionist approaches. Complexity theory is used as a form of guiding metatheory to understand a range of evolving natural and social systems, frequently applying computational simulation methodologies as the method of enquiry [33–37].

Many authors make the distinction between systems that are simple or complicated, but not *complex* [13, 38, 39]. This is because many find it easier to begin by defining what complexity *is not*, before attempting to define what *it is*. Table 2 draws upon the work of Arthur [10], Delorme [16], and Lei et al. [12] to compare the properties of general systems theory and a CAS approach.

In a complex system functionality arises not only from the multitude of (often nonlinear) interactions between the physical components and incumbent agents of the system, but also from interactions with the surrounding environment. Complex systems are seen to undergo a variety of possible

Table 1: Characteristics of the UK National Infrastructure System (adapted from Hall et al. [15]).

	Energy	Transport	Water	Waste		Digital Communications
				Wastewater	Solid Waste	
Scale	National International	Regional National International	Regional	Regional	Regional	National International
Ownership	Private	Mixed (by mode)	Mixed (by region)	Mixed (by region)	Mixed (public responsibility with private operation	Private
Governance and Regulation	Varies e.g. electricity has unregulated market prices but regulated network charges	Varies e.g. rail has regulated efficiency targets; roads and government planned with some private provision	For England and Wales, price and investment regulated by Ofwat, drinking water quality regulation by DWI, environmental regulation by EA.		Local Authority run. Environmental regulation by EA/DEFRA in England and Wales, SEPA in Scotland	Competition regulation by Ofcom; universal service obligations; spectrum licences and coverage obligations
Issues	Security of supply; GHG emissions	Congestion; high speed rail; airport capacity	Demand management; climate change; environmental regulation	Energy costs; environmental regulation	Waste minimisation and recycling targets; resource management	Technological innovation; rural coverage

Table 2: Properties of general systems and complex adaptive systems [10, 12, 16].

General Systems Theory	Complex Adaptive Systems Theory		
Key Properties	***Key Properties***	***Property Category***	***Hierarchical Level***
Complicated	Complex	Emergent behaviour and self-organisation	System level
Aggregable with functional decomposition	Emergent with limited functional decomposition		
Centralised control	Distributed control		
Determinate and Linear	Non-determinate and Non-linear	Instability and robustness	
Static	Perpetual Dynamics	Dynamics and evolution	Network level
Equilibrium	A Far-from-equilibrium State		
Closed	Open		
Reversible	Irreversible		
Rational, deductive behaviour	Adaptive, evolutionary behaviour	Adaptiveness	Agent level
Simplified assumptions and homogenous agents	Diversity among agents and more realistic assumptions	Agent diversity	

states. They are in a state of flux which, often resulting from self-organising tendencies, changes the configuration of the system. It is important to make the distinction between a complex system and the subsequent concept of a complex *adaptive* system. The word adaptive comes from the Latin "adaptation" which relates to the modification required to suit new conditions. Thus, to adapt is to improve over time in relation to one's environment (whether natural, economic, social, technical, institutional, or some other variant). But the key to the definition is the verb to *improve*.

Winder et al. [40] state that not all complex systems display evolutionary dynamics as some can exhibit mechanistic dynamics. The dynamic quantitative change which results from a complex system responding to an external stimulus may display only mechanistic, responsive change. The evolutionary dynamics evident in complex adaptive

systems only take place if the relationships between the parts of the system components *are modified*, in order to gain some form of advantageous position. Hence, the ability for a group of entities to generate a variety of responses to a changing selection environment is a defining feature of an evolutionary system. The absence of this changing, evolving behaviour may indicate that a system is only dynamically mechanistic, rather than evolutionary. Consequently, a CAS can be defined as containing a large number of agents which interact, learn, and, most crucially, *adapt* to changes in their selection environment in order to improve their future survival chances [41].

The main properties of a CAS can be identified as evolution, aggregate behaviour, and anticipation (Holland, 1992). Evolution is a key feature; while adaptation can be described as the improvements made by entities in response to external environmental stimuli, evolution is different as it is the algorithmic process that produces these improvements [42]. Yet the use of this metaphor as a transformational process is often ill-defined [43]. For a process to be described as evolutionary it must exhibit certain properties, specifically the generation of novelty endogenously, from within the system. A system is not evolutionary if change is only incorporated as some form of exogenous shock which momentarily changes the system's "equilibrium" position. Moreover, evolutionary systems are also dynamic and undergoing perpetual change, with the relationships between the key components in continual flux. Indeed, the process of evolution is discontinuous and irreversible.

4. Applying the Key Concepts to an Infrastructure System

Chaudet at al. [44] state that after considering key properties, infrastructures "can be considered excellent metaphors of complex systems". But to gain a true understanding of a specific system one must undertake an in-depth investigation. This section considers the extent to which the key features of a CAS appear to characterise the workings of a national infrastructure system. Following the structure presented in Table 2, the analysis is undertaken at the agent, network, and the system levels.

4.1. Agent-Level Properties

4.1.1. Adaptive, Evolutionary Behaviour. Although dynamic behaviour is a feature of many types of general systems, this property is especially prominent in complex adaptive systems and linked to perpetual dynamics at the network level. For example, individuals, households, and firms exhibit *adaptive behaviour* change driven by changing supply and demand conditions. This is particularly true for infrastructure service providers operating in market contexts. These behavioural changes can result from new technologies, new infrastructure assets, and flows of financial investment on the supply side. On the demand side, new technology drives change in how infrastructure services are used and where they are required. An example of this change is evident in the adoption of smartphones, 4G LTE services, and the subsequent explosion in data demand associated with video streaming. Changes in user behaviour, coupled with the proliferation of new technologies, dramatically changed the supply and demand characteristics of mobile telecommunications infrastructure systems from 2008 onwards, following the release of the Apple iPhone and the proliferation of smartphones.

4.1.2. Diversity among Agents and More Realistic Assumptions. The heterogeneous attributes of individuals, households, and firms, incumbent to the supply and demand of infrastructure services are visibly evident. A general characteristic that defines the demand side is the demographic group of particular consumers. For example, trends in broadband adoption associated with Internet Protocol Television (IPTV) (e.g., Netflix) are correlated with particular demographic groups, where older households generally have a lower propensity to adopt these services.

4.2. Network-Level Properties

4.2.1. Perpetual Dynamics. We witness *perpetual dynamic change* in the national infrastructure system in both the supply and demand for infrastructure. For example, the development of infrastructure is incremental, so the physical network according to current and expected demand undergoes a perpetual process of expansion, modification, and contraction at different points in space. Moreover, the flows across the physical network are also altered in accordance with these processes. Innovation has a particular impact on driving change in technological and institutional regimes in infrastructure systems [45]. Disruptive technologies and new forms of organisation combine with and result from the adaptive, self-organising behaviour of the firms, households, and individuals that produce and consume infrastructure services on a daily basis. The economy and society are thus seen to perpetually *coevolve* with changes in infrastructure networks, advancements in infrastructure technology and organisation, and the new trajectories of economic growth and development.

4.2.2. A Far-from-Equilibrium State. The factors that influence the demand for and supply of infrastructure are subject to continuous dynamic change and thus it would appear naive to adopt a theoretical perspective that assumes it is at an optimal equilibrium at some point in time. A CAS approach would appear more appropriate, as it pays more attention to the imperfections of the system.

4.2.3. Openness. National infrastructure systems are *open* entities characterised by inward and outward flows of goods, services, and capital. They have no precise, fixed boundary between the system under investigation, other nested systems in the hierarchy, and the wider environment. While we define "the national infrastructure system" purely for practical purposes in research, it is not an isolated, "closed" system. Instead it undergoes constant interaction and exchange with its economic, social, and natural environment. We have historically been quite poor at integrating long-term behavioural change into models of infrastructure systems.

The system requires a wide range of inputs to flow into different infrastructure sectors to enable functionality, such as energy, raw and intermediate materials, labour, information, and financial capital. This openness can result in the system behaving differently to ostensibly similar shocks from its environment, at different points in time. This is because national infrastructure systems can change their network structure over temporal periods, changing the system's complexity. Homogenous responses to perturbations are highly unlikely.

4.2.4. Irreversibility. The notion of irreversibility in infrastructure systems refers to the fact that time-independent decisions are rare. In fact, infrastructure providers are almost certainly taking decisions within a set of constrained capabilities, because they must work with durable, long-lived infrastructure assets and networks operating in market contexts. "Lock-in" effects with infrastructure assets often prevent viable transitions to other forms of organisation and operation. For example, in the energy sector many countries have addressed emissions controls by introducing regulatory mechanisms combined with energy demand management and renewable energy generation policies. These have inevitably affected the cost of energy because they attempt to move the system away from the existing "locked-in" state. Moreover, there are also microeconomic irreversibilities resulting from the adaptive behaviours of firms, households, individuals, regulators, and other institutions that inevitably explore, learn, and retain information relating to their activities.

4.3. System-Level Properties

4.3.1. Complexity. The system is complex because it is comprised of diverse adaptive agents, there is distributed control throughout the system, and infrastructure networks are joined by a range of different physical and cyber-interdependencies. Moreover, the functionality of the system arises not only from the multitude of (often nonlinear) interactions between the physical components and incumbent agents of the system, but also from how the system *per se* interacts with its *surrounding environment*.

4.3.2. Emergence and Limited Functional Decomposition. The highly dynamic structure of the national infrastructure system results from the high level of interconnection between incumbent networks. When the national infrastructure is driven by a set of exogenous drivers (demographic change, economic growth, climate scenarios, etc.), interdependencies between different sectors lead to second-order, indirect demands for infrastructure services. Hence, it is not straightforward to *functionally decompose the national infrastructure into individual stable parts*.

Moreover, unlike in the natural sciences where individual natural processes can often be isolated for experimentation, the sociotechnical processes pertaining to the economic, technological, spatial, demographic, institutional, and environmental aspects of national infrastructure systems need to be considered and examined in the widest sense, because they are not readily decomposable [46].

4.3.3. Distributed Control. National infrastructure systems in developed, free market economies do not have one individual entity in control of the system. This can be problematic for coordination. Often top-down management approaches can yield undesirable outcomes as a result. This has increasingly been the case over the past three decades where nationalised industries have been opened to market-based competition between different actors. Whereas the state previously had a centralised command-and-control structure, now it only has limited regulatory control. Complexity approaches naturally lend themselves to being utilised to investigate the implications of different game-theoretic behaviours that play out in a decentralised market context, although there has been relatively limited application to infrastructure hitherto.

4.3.4. Indeterminateness and Nonlinearity. A consequence of increasing interdependency in national infrastructure means these systems become indeterminate and nonlinear. Additionally, feedback mechanisms arise when externalities in the system alter the costs and benefits which accrue from an individual's decisions, therefore causing behavioural change. Positive feedback often has a destabilising effect on a system, while negative feedback can create an effect which is homeostatic. Nonlinear feedback mechanisms can cause the system to undergo transitions to other organisational states. Moreover, endogenously created technologies can be responsible for this type of transition, inducing qualitative change in the relationships of key system components. For example, the evolution of energy and transportation systems over the past century has instigated organisational and operational transitions in the national infrastructure, encouraging coevolutionary change in tandem with the demand patterns.

The nonlinearities and the degree of technological innovation inherent in the system make *unpredictable outcomes* occur. These emergent outcomes might not have seemed logical or possible from close examination of the actions of individuals. Complex adaptive properties mean that the system can shift to a very wide variety of possible future states. Indeed, the path dependent properties of certain components often play a part in this. There is thus a need to move away from the past "predict and provide" planning approaches used for large technical systems and recognise the importance of greater understanding of the plethora of interacting technical and social processes which can push the system into states that arise unexpectedly. Rather than focusing solely on technology and infrastructure, we should shift our thinking to also include *sociotechnical regimes*, including the users and their behaviours in infrastructure analysis.

5. A System-of-Systems Approach to Infrastructure: A Case Study of the UK

We now present a case study which uses CAS properties to develop a system-of-systems (SoS) approach to infrastructure, as an example of a complexity-based method applied to

support public policy decision-making. As already identified, there has been growing recognition in recent decades of the importance that national infrastructure systems are interconnected. While infrastructure (especially energy) has underpinned many vital systems for over a century, the increasing proliferation of ICT has been a key driver and will continue to be, considering those technologies on the horizon such as the Internet of Things or Connected and Autonomous Vehicles. Past analytical approaches prevent thorough analysis of this complexity by ignoring interdependencies; therefore we need new tools and methodologies that position us to quantify these systems. This has the potential to revolutionise both the quality and quantity of infrastructure analytics available to public policy decision-makers, leading to the development of more effective infrastructure planning and resilience policies. This case study begins by detailing the main decision-makers and their goals and information requirements. Subsequently, a novel approach to infrastructure assessment is detailed before being critically reviewed.

5.1. Key Decision-Makers. An important issue with infrastructure policy is that responsibility has traditionally been fragmented and spread out across the UK Government. For example, energy, transport, ICT, water, and waste policy has included up to eight government departments, namely, (i) Business, Energy and Industrial Strategy, (ii) the Department for Transport, (iii) the Department for Digital, Culture, Media and Sport, (iv) the Department for the Environment, Farming and Rural Affairs, (v) HM Treasury, (vi) the Cabinet Office, (vii) the Ministry of Housing, Communities and Local Government, and (viii) the Department for International Trade.

Over the past decade the UK has attempted to take a far more strategic approach to infrastructure, as promoted by the release of the UK Council of Science and Technology (2009) report entitled *Infrastructure for the 21st Century*. Subsequently, under the labour government a white paper was published titled *Building Britain's Future*, promoting the infrastructure agenda as a way of dealing with the damage caused by the Global Financial Crisis. This led to a new body being created called Infrastructure UK (known as "IUK"), within HM Treasury, with the key responsibility of developing a National Infrastructure Plan.

In light of this fragmented governance landscape, the creation of a strategic high-level planning body within HM Treasury called the National Infrastructure Commission (NIC) was tasked with coordinating infrastructure policy across government. This body is like those that have been established in Australia (Infrastructure Australia) and New Zealand (National Infrastructure Advisory Board). The NIC operates via a set of infrastructure commissioners who have responsibility to develop a long-term strategy for the delivery of national infrastructure. There is a requirement to undertake a National Infrastructure Assessment at least once every parliament (5 years) as well as responding to emerging issues at the direction of the Chancellor, which have recently included smart power systems, 5G communications, the East-West transport corridor, and coordinating the development of a digital twin of the UK's national infrastructure system. The NIC is the key decision-making body focused on within this analysis, given its need to coordinate across all areas of infrastructure policy.

The overall goal of the UK's infrastructure policy is to deliver efficient and effective infrastructure systems which are sustainable, enhance productivity, and provide economic opportunity for everyone in society. However, long-term infrastructure planning is a classic decision-making under uncertainty problem which needs to navigate changes in demography, economy, society, and environment. Infrastructure policy can also be highly political and subject to radical technological change.

5.2. Information Used for Decision-Making. Each infrastructure sector may have its own specific set of metrics required to assess the state of the current and future system. However, a general approach is to consider (i) system capacity, (ii) service coverage, (iii) investment costs, and (iv) potential emissions. The traditional approach to infrastructure analytics for public policy decision-making constitutes fragmented sector modelling, often taking place in individual government departments who derive information from a niche set of models pertinent to each infrastructure sector, including the UK TIMES energy model, DECC energy demand model, the National Transport Model, and the LTIS flood model. This is problematic because transport modellers may use completely different epistemological approaches, assumptions, and forward-looking scenarios when compared to energy, digital, water, or waste management. This firstly introduces additional uncertainty when comparing the potential results between these models and, secondly, completely ignores the feedback between infrastructure sectors. Hence, this leads to the treatment of infrastructure existing in a closed system, with centralised command and control which is considerably detached from reality and may lead to unintended outcomes. For example, new electrification strategies in one sector may work from the assumption that enough electricity is available to support this approach, which may not be true. Hence, by capturing the key characteristics of national infrastructure, by representing the interdependencies between the systems, more accurate information can be provided to decision-makers. This accuracy is achieved by reducing the level of uncertainty inherent in the data, models, and results.

5.3. The Infrastructure Transitions Research Consortium (ITRC) Approach. One example of where this methodology has been applied is by the ITRC (see Hall et al. [47]). Taking inspiration from the Council of Science and Technology (2009) report, the ITRC project was formed based on the proposition that modelling and simulation techniques can be highly important to understand and effectively manipulate complex systems. Moreover, the design and planning of infrastructure can be improved using powerful systems models as these techniques can help to optimise across a wide range of policy constraints. The ITRC subsequently collaborated with the newly created IUK to analyse the National Infrastructure Pipeline and undertake a "hotspots"

analysis of critical risks to infrastructure across the UK (see Thacker et al. [18, 19]). Following this the ITRC undertook the analysis for the UK's first National Needs Assessment (NNA) led by Sir John Armitt, the then President of the Institution of Civil Engineers. Consequently, the modelling capability was utilised to inform the UK's first National Infrastructure Assessment published in 2018. Had the modelling approach not been available to undertake a holistic evaluation, these activities either would not have taken place or would have relied on fragmented modelling approaches for each individual sector used in the past, ignoring the interconnected and interdependent nature of national infrastructure. This would likely have led to an underestimation in total demand for future infrastructure services.

The framework developed by ITRC for conducting a National Infrastructure Assessment is based on an initial step which defines a set of "what if" questions pertinent to the current needs of policy makers. Four stages follow: firstly, collecting scenarios that represent future uncertainties such as demography, economic growth, and climate; secondly, developing both plausible and experimental infrastructure strategies for testing [48]; thirdly, applying a national infrastructure system-of-systems model to simulate the performance of infrastructure under various exogenous scenarios; finally, evaluating the performance of different strategies and identifying robust options.

ITRC and NIC have been working together to produce an original evidence base that underpins the NIC's strategic work. This evidence base has been augmented by utilising a national infrastructure system-of-systems model (NISMOD) consisting of a family of models. The NISMOD suite includes a model for long-term planning (-LP) and for the analysis of risk and vulnerability (-RV) of critical national infrastructure. NISMOD-LP implements the National Infrastructure Assessment approach developed by ITRC (see Hall et al. [47] for a more complete description). NISMOD-LP is an infrastructure system-of-systems model that enables users to explore strategic planning of multiple infrastructure sectors, while simulating the operation of the individual sectors and their key interdependencies under a range of unified scenarios of future developments spanning natural sciences, demography, and economics. Demands for infrastructure services are derived from these scenarios of key demand drivers [49]. For example, demand for transport services, such as car passenger travel, is derived from future scenarios of population, GVA, and endogenously computed travel time and cost (an example of adaptive dynamic behaviour). Long-term dynamics are explored through narratives of technological change and consumer acceptance that affect the attributes of infrastructure assets and demand for infrastructure services. The infrastructure sectors are represented by detailed engineering simulation models that are linked with one another, and while a comprehensive description of each model is beyond the theoretical focus of this paper, they are available for energy [50], transport [51], digital communications [52, 53], solid waste [54, 55], and water [56, 57]. The linkages between these models represent the critical dependencies between sectors (see Figure 1) including flows ranging from resources to information.

For example, the energy supply model simulates the operation of the UK's portfolio of current and potential future electric power stations, the electricity transmission and distribution networks, gas pipeline, pumps, and storage facilities. Electricity and gas are thus supplied to meet demand for energy-related infrastructure services. The simulation models enable analysts to test the implications of *strategies* within the infrastructure system. Crucially, the simulation models produce quantitative performance metrics which allow analysts to evaluate the performance of the infrastructure system under different conditions. By comparing the performance metrics of multiple model runs across a wide range of scenarios and combinations of planning strategies, analysts can explore robust policy options across the infrastructure system-of-systems.

5.4. Critically Reviewing a System-of-Systems Approach to Infrastructure Public Policy Decision-Making. In this section we evaluate the added-value provided by utilising a system-of-systems approach for infrastructure decision-making. We discuss the existing limitations, as seen from the perspective of complex adaptive systems theory, and whether new insights can be provided into the properties of the national infrastructure system.

We illustrate a mapping in Figure 2, from the distinct properties of infrastructure as a complex adaptive system to the implemented methodology, with infrastructure being modelled as a system-of-systems using NISMOD. This firstly includes adaptive agents, whereby operators of critical national infrastructure deploy different long-term planning strategies to meet future demand under a range of exogenous scenarios and conditions. Secondly, diverse agents are represented by different infrastructure decision-makers across the various sectors in the system-of-systems simulation framework. Diverse agents are also represented on the demand side, where demands for infrastructure services are segmented by socioeconomic attributes using a set of spatially disaggregated household demographic profiles and commercial and industrial productivity statistics. Thirdly, the modelling approach captures short-term dynamics of interdependencies between systems; as decisions are made by each individual sector, this changes the system-level conditions, with ramifications for investment and operational decisions elsewhere in national infrastructure. By simulating the operation of the system, we capture the supply dynamics to meet the diverse demands for infrastructure services. Fourthly, as in reality, the decision to invest in a sequence of irreversible interventions locks the system structure into a long-term trajectory. Finally, because of these properties, a spatially explicit national infrastructure system structure emerges, which is assessed using a set of performance criteria metrics, such as capacity, coverage, cost, and emissions.

However, while developing and applying new theories can be a useful intellectual academic exercise, there is still the question as to whether this *improves* the existing understanding of infrastructure. This case study demonstrates that complex adaptive systems theory and system-of-systems methodologies can be combined predicated on the

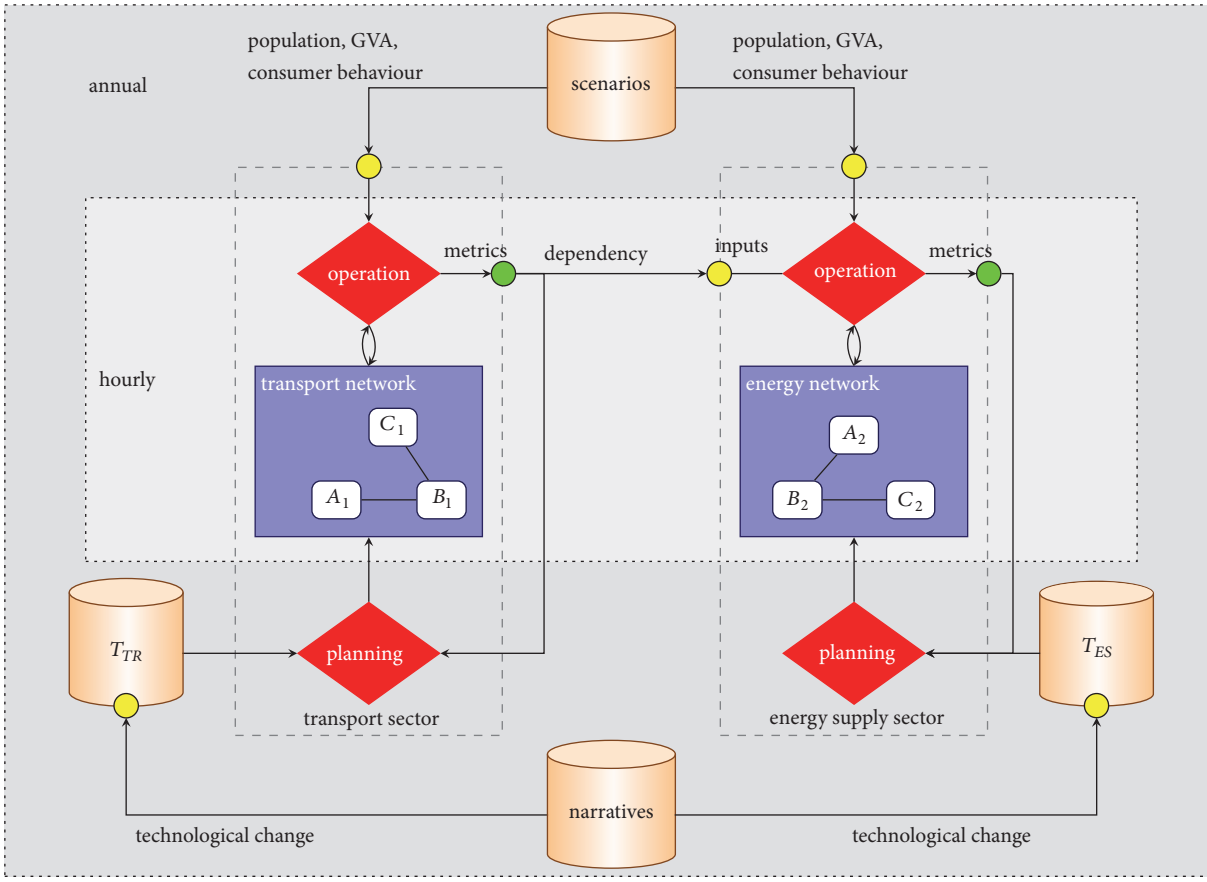

Figure 1: A dependency shown between just two infrastructure sectors contained in the ITRC's National Infrastructure System Model. The cylinders labelled T_{tr} and T_{es} represent the stock of available technologies for the transport and energy sectors. Narratives hold the collection of assumptions exogenous to the modelled system about long-term technological changes and modify the attributes of available technologies. Scenarios capture changes in socioeconomic drivers of infrastructure service demands. The network structure that underpins the hourly operation of the sector is altered over annual planning timescales as technology changes, and long-term planning investments result in the turnover of the infrastructure stock. Performance metrics produced from the operation of the system simulation feed back into the planning strategies governing future investments and provide the results of a model run.

properties outlined in Table 2, enabling developments beyond traditional systems-based analysis. Given there is growing dissatisfaction assuming that reality can be modelled as static, deterministic, and containing homogenous, rational agents, this is to be welcomed.

While there have been relatively few examples of complexity-based approaches supporting public policy, in this application to long-term infrastructure decision-making we have detailed a methodology addressing five properties of complex adaptive systems (adaptive agents, diverse agents, dynamics, irreversibility, and emergence), across three hierarchical levels ranging from agents, to networks, to systems. The main contribution of this application of the national infrastructure system model is that we capture the emergence of a whole national infrastructure system, driven by agent-level decisions and explicitly modelled interdependencies across the sectors of energy, transport, digital, water, and waste. The breaching of individual infrastructure sector system boundaries creates new opportunities for understanding trade-offs and synergies across sectors, not only within individual systems, with cumulative potential to make more effective policy decisions, while reducing the likelihood of unintended consequences. Adopting these methods will require a change in mindset by both model developers and policy decision-makers, as it requires increased use of system-of-systems-based thinking and associated modelling methodologies. In doing so, this could further unshackle approaches that view reality as something that is predictable and linear, towards increased recognition that the world is highly dynamic, diverse, and evolving: in essence, *complex*.

6. Conclusion

In this article we have sought to build on the core properties identified by Arthur [10], Delorme [16], and Lei et al. [12], to assess whether a CAS approach might help to provide a better understanding of the forces underpinning change in national infrastructure systems. We find that properties of a complex adaptive system characterise the workings of infrastructure systems well and subsequently articulate a system-of-systems

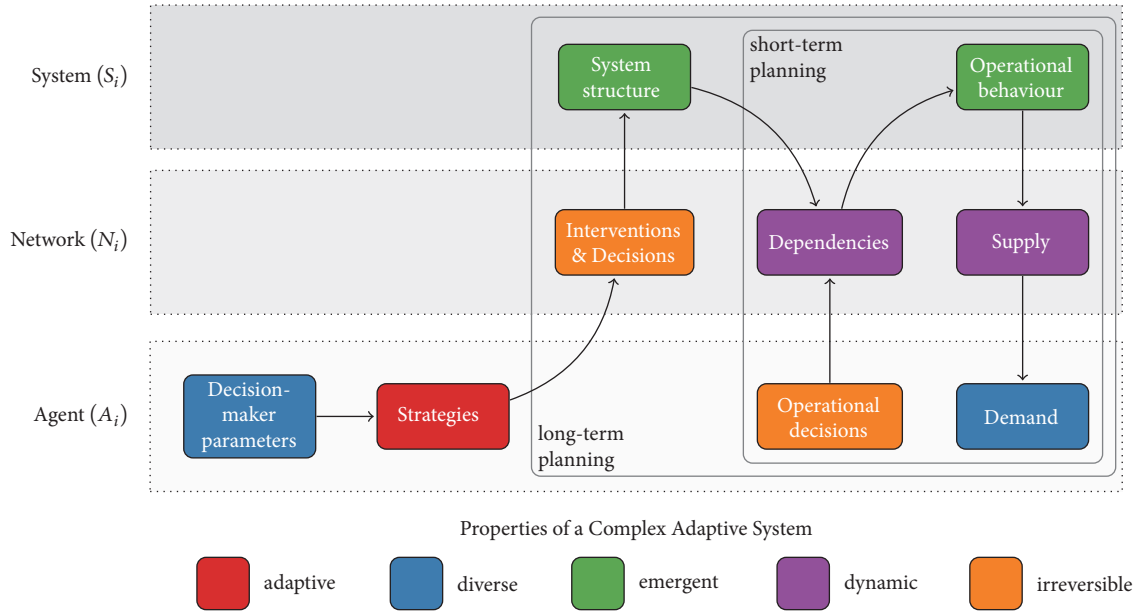

Figure 2: Mapping the properties of a complex adaptive system to a system-of-systems approach.

method grounded in this theory. The novel contribution of the paper is the articulation of the case study describing a decade of research which applies complex adaptive systems properties to the development of a national infrastructure system-of-systems model. This enables decision-makers to explore the trade-offs and properties of an emergent national infrastructure system, driven by agent-level decisions and explicitly modelled interdependencies between energy, transport, digital communications, waste, and water. Subsequently, the approach has been used by the UK National Infrastructure Commission to produce a National Infrastructure Assessment which is capable of coordinating infrastructure policy across a historically fragmented governance landscape spanning eight government departments. The application will continue to be pertinent moving forward due to the continuing complexity of interdependent infrastructure systems, particularly from increased electrification and the proliferation of the Internet of Things.

Data Availability

In this article we theoretically review the use of complexity methods and provide a case study based on a particular application. We reference the models developed and used for this process but do not report results from them. Data used by these models can be traced via the references provided in the paper.

Conflicts of Interest

The authors declare that they have no conflicts of interest.

Acknowledgments

The authors would like to thank the UK Engineering and Physical Science Research Council for support via programme grant http://gow.epsrc.ac.uk/NGBOViewGrant.aspx?GrantRef=EP/N017064/1 (Multi-scale InfraSTRucture systems AnaLytics).

References

[1] S. M. Rinaldi, J. P. Peerenboom, and T. K. Kelly, "Identifying, understanding, and analyzing critical infrastructure interdependencies," *IEEE Control Systems Magazine*, vol. 21, no. 6, pp. 11–25, 2001.

[2] H.-S. J. Min, W. Beyeler, T. Brown, Y. J. Son, and A. T. Jones, "Toward modeling and simulation of critical national infrastructure interdependencies," *Institute of Industrial Engineers (IIE). IIE Transactions*, vol. 39, no. 1, pp. 57–71, 2007.

[3] S. V. Buldyrev, R. Parshani, G. Paul, H. E. Stanley, and S. Havlin, "Catastrophic cascade of failures in interdependent networks," *Nature*, vol. 464, no. 7291, pp. 1025–1028, 2010.

[4] J. Gao, S. V. Buldyrev, H. E. Stanley, and S. Havlin, "Networks formed from interdependent networks," *Nature Physics*, vol. 8, no. 1, pp. 40–48, 2012.

[5] R. R. Nelson and S. G. Winter, *An Evolutionary Theory of Economic Change*, Harvard University Press, Cambridge, MA, 1982.

[6] D. Giovanni, C. Freeman, N. Richard, G. Silverberg, and L. Soete, *Technical Change and Economic Theory*, IFIAS Research Series, Pinter, London, 1988.

[7] P. Saviotti and J. S. Metcalfe, *Evolutionary Theories of Economic and Technological Change: Present Status and Future Prospects*, Harwood Academic Publishers, Chur, New York, USA, 1990.

[8] R. R. Nelson, "Recent Evolutionary Theorizing about Economic Change," *Journal of Economic Literature*, vol. 33, no. 1, pp. 48–90, 1995.

[9] K. Dopfer and J. Potts, *The General Theory of Economic Evolution*, Routledge, 2008.

[10] W. B. Arthur, *Complexity and the Economy*, Oxford University Press, Oxford; NY, USA, 1 edition, 2014.

[11] I. Nikolic and G. P. J. Dijkema, "On the development of Agent-Based Models for infrastructure evolution," *International Journal of Critical Infrastructures*, vol. 6, no. 2, pp. 148–167, 2010.

[12] T. E. Van Der Lei, G. Bekebrede, and I. Nikolic, "Critical infrastructures: A review from a complex adaptive systems perspective," *International Journal of Critical Infrastructures*, vol. 6, no. 4, pp. 380–401, 2010.

[13] K. H. Dam, I. Nikolic, and Z. Lukszo, *Agent-Based Modelling of Socio-Technical Systems*, Springer Netherlands, Dordrecht, 2013.

[14] C. S. Bale, L. Varga, and T. J. Foxon, "Energy and complexity: New ways forward," *Applied Energy*, vol. 138, pp. 150–159, 2015.

[15] J. W. Hall, J. J. Henriques, and A. J. Hickford, "A Fast Track Analysis of Strategies for Infrastructure Provision in Great Britain: Technical Report," Tech. Rep., Environmental Change Institute, University of Oxford, 2012.

[16] R. Delorme, *Deep Complexity and the Social Sciences: Experience, Modelling and Operationality*, Edward Elgar Publishing, 2010.

[17] World Economic Forum, *The Global Competitiveness Report 2016-2017*, World Economic Forum, Geneva, Switzerland, 2016, http://www3.weforum.org/docs/GCR2016-2017/05FullReport/TheGlobalCompetitivenessReport2016-2017_FINAL.pdf.

[18] S. Thacker, R. Pant, and J. W. Hall, "System-of-Systems Formulation and Disruption Analysis for Multi-Scale Critical National Infrastructures," *Reliability Engineering System Safety, Special Section: Applications of Probabilistic Graphical Models in Dependability, Diagnosis and Prognosis*, vol. 167, C, pp. 30–41, 2017, https://doi.org/10.1016/j.ress.2017.04.023.

[19] S. Thacker, S. Barr, R. Pant, J. W. Hall, and D. Alderson, "Geographic Hotspots of Critical National Infrastructure," *Risk Analysis*, vol. 37, no. 12, pp. 2490–2505, 2017.

[20] A. Otto, J. W. Hall, A. J. Hickford et al., "A Quantified System-of-Systems Modeling Framework for Robust National Infrastructure Planning," *IEEE Systems Journal*, vol. 10, no. 2, pp. 385–396, 2016.

[21] J. R. Baldwin and J. Dixon, "Infrastructure Capital: What is it? Where is it? How Much of it is There?" SSRN Electronic Journal, Social Science Research Network, Rochester, NY, 2008.

[22] W. Usher and N. Strachan, "Critical mid-term uncertainties in long-term decarbonisation pathways," *Energy Policy*, vol. 41, pp. 433–444, 2012.

[23] P. M. Allen, L. Varga, and M. Strathern, "The evolutionary complexity of social and economic systems: The inevitability of uncertainty and surprise," *Risk Management*, vol. 12, no. 1, pp. 9–30, 2010.

[24] C. A. Calderon, E. Moral-Benito, and L. Servén, "Is Infrastructure Capital Productive? A Dynamic Heterogeneous Approach," *SSRN Electronic Journal*, 2011, http://papers.ssrn.com/sol3/papers.cfm?abstract_id=1871578.

[25] S. Démurger, "Infrastructure Development and Economic Growth: An Explanation for Regional Disparities in China?" *Journal of Comparative Economics*, vol. 29, no. 1, pp. 95–117, 2001.

[26] R. Crescenzi and A. Rodríguez-Pose, "Infrastructure Endowment and Investment as Determinants of Regional Growth in the European Union," EIB Paper 8/2008, European Investment Bank, Economics Department, 2008, http://ideas.repec.org/p/ris/eibpap/2008_008.html.

[27] H. S. Esfahani and M. T. Ramírez, "Institutions, infrastructure, and economic growth," *Journal of Development Economics*, vol. 70, no. 2, pp. 443–477, 2003.

[28] É. Balázs, T. Kozluk, and D. Sutherland, *Infrastructure and Growth: Empirical Evidence*, SSRN ELibrary, 2009, http://papers.ssrn.com/sol3/papers.cfm.

[29] C. F. Del Bo and M. Florio, "Infrastructure and growth in a spatial framework: evidence from the EU regions," *European Planning Studies*, vol. 20, no. 8, pp. 1393–1414, 2012.

[30] R. P. Pradhan, M. B. Arvin, N. R. Norman, and S. K. Bele, "Economic growth and the development of telecommunications infrastructure in the G-20 countries: A panel-VAR approach," *Telecommunications Policy*, vol. 38, no. 7, pp. 634–649, 2014.

[31] N. Carhart and G. Rosenberg, "A framework for characterising infrastructure interdependencies," *International Journal of Complexity in Applied Science and Technology*, vol. 1, no. 1, pp. 35–60, 2016.

[32] T. Dolan, C. L. Walsh, C. Bouch, and N. J. Carhart, "A conceptual approach to strategic performance indicators," *Infrastructure Asset Management*, vol. 3, no. 4, pp. 132–142, 2016.

[33] M. M. Waldrop, *Complexity: The Emerging Science at the Edge of Order and Chaos*, Viking, London, uk, 1993.

[34] J. S. Lansing, "Complex adaptive systems," *Annual Review of Anthropology*, vol. 32, pp. 183–204, 2003.

[35] A. Bennet and D. Bennet, *Organizational Survival in the New World: The Intelligent Complex Adaptive System: A New Theory of the Firm*, Butterworth-Heinemann, Amsterdam, 2004.

[36] M. Batty, *Cities and Complexity: Understanding Cities with Cellular Automata, Agent-Based Models, and Fractals*, The MIT Press, London, 2007.

[37] B. Edmonds and R. Meyer, *Simulating Social Complexity: A Handbook*, Springer, 2017.

[38] P. Cilliers, *Complexity and Postmodernism: Understanding Complex Systems*, Routledge, 2002.

[39] E. Garnsey and J. McGlade, "Preface," *Complexity and Co-Evolution: Continuity and Change in Socio-Economic Systems*, pp. viii–ix, 2006.

[40] N. Winder, B. S. McIntosh, and P. Jeffrey, "The origin, diagnostic attributes and practical application of co-evolutionary theory," *Ecological Economics*, vol. 54, no. 4, pp. 347–361, 2005.

[41] J. H. Holland, "Studying complex adaptive systems," *Journal of Systems Science & Complexity*, vol. 19, no. 1, pp. 1–8, 2006.

[42] I. Nikolic and J. Kasmire, "Theory and Practice," in *Agent-Based Modelling of Socio-Technical Systems*, K. Dam, I. Nikolic, and Z. Lukszo, Eds., UK, Springer, 2013.

[43] R. A. Boschma and R. L. Martin, Eds., *The Handbook of Evolutionary Economic Geography*, Edward Elgar Publishing, Cheltenham, UK, 2010.

[44] C. Claude, G. Le Grand, and V. Rosato, "Critical Infrastructures as Complex Systems," *International Journal of Critical Infrastructures*, vol. 5, pp. 1–4, 2009.

[45] M. P. C. Weijnen and I. Bouwmans, "Innovation in networked infrastructures: Coping with complexity," *International Journal of Critical Infrastructures*, vol. 2, no. 2-3, pp. 121–132, 2006.

[46] J. M. Epstein and R. Axtell, *Growing Artificial Societies: Social Science from the Bottom Up*, Mit Press, 1996.

[47] J. W. Hall, M. Tran, A. J. Hickford, and R. J. Nicholls, *The Future of National Infrastructure*, Cambridge University Press, 2016.

[48] A. J. Hickford, R. J. Nicholls, A. Otto et al., "Creating an ensemble of future strategies for national infrastructure provision," *Futures*, vol. 66, pp. 13–24, 2015.

[49] C. Thoung, R. Beaven, C. Zuo et al., "Future Demand for Infrastructure Services," in *The Future of National Infrastructure: A*

System-of-Systems Approach, J. Hall, R. Nicholls, M. Tran, and A. Hickford, Eds., Cambridge University Press, UK, 2016.

[50] B. Pranab, C. Modassar, M. Qadrdan, N. Eyre, and N. Jenkins, "Energy Systems Assessment," in *The Future of National Infrastructure: A System-of-Systems Approach*, Cambridge, Cambridge University Press, 2016, https://doi.org/10.1017/CBO9781107588745.005.

[51] S. P. Blainey and J. M. Preston, "Transport Systems Assessment," in *The Future of National Infrastructure: A System-of-Systems Approach*, Cambridge, Cambridge University Press, 2016, https://doi.org/10.1017/CBO9781107588745.006.

[52] E. J. Oughton, M. Tran, B. Cliff, and R. Ebrahimy, "Digital Communications and Information Systems," in *The Future of National Infrastructure: A System-of-Systems Approach*, Cambridge University Press, 2016, https://doi.org/10.1017/CBO9781107588745.010.

[53] E. Oughton, Z. Frias, T. Russell, D. Sicker, and D. D. Cleevely, "Towards 5G: Scenario-based assessment of the future supply and demand for mobile telecommunications infrastructure," *Technological Forecasting & Social Change*, vol. 133, pp. 141–155, 2018.

[54] V. R. Watson Geoff, M. Anne, P. William, D. A. Turner, and J. Coello, "Solid Waste Systems Assessment," in *The Future of National Infrastructure: A System-of-Systems Approach*, Cambridge, Cambridge University Press, 2016, https://doi.org/10.1017/CBO9781107588745.009.

[55] K. P. Roberts, D. A. Turner, J. Coello et al., "SWIMS: A dynamic life cycle-based optimisation and decision support tool for solid waste management," *Journal of Cleaner Production*, vol. 196, pp. 547–563, 2018.

[56] S. Mike, M. C. Ives, J. W. Hall, and C. G. Kilsby, "Water Supply Systems Assessment," in *The Future of National Infrastructure: A System-of-Systems Approach*, Cambridge, Cambridge University Press, 2016, https://doi.org/10.1017/CBO9781107588745.007.

[57] L. J. Manning, D. W. Graham, and J. W. Hall, "Wastewater Systems Assessment," in *The Future of National Infrastructure: A System-of-Systems Approach*, Cambridge, Cambridge University Press, 2016, https://doi.org/10.1017/CBO9781107588745.008.

Hindawi
Complexity
Volume 2018, Article ID 4092056, 7 pages
https://doi.org/10.1155/2018/4092056

Research Article

Competition May Increase Social Utility in Bipartite Matching Problem

Yi-Xiu Kong,[1,2] **Guang-Hui Yuan**,[3] **Lei Zhou**,[1] **Rui-Jie Wu**,[2] **and Gui-Yuan Shi**[1,2]

[1]*Faculty of Computer and Software Engineering, Huaiyin Institute of Technology, Huaian 233003, China*
[2]*Department of Physics, University of Fribourg, Fribourg 1700, Switzerland*
[3]*Fintech Research Institute, Shanghai University of Finance and Economics, Shanghai 200433, China*

Correspondence should be addressed to Gui-Yuan Shi; guiyuan.shi@unifr.ch

Received 12 June 2018; Revised 19 September 2018; Accepted 23 October 2018; Published 1 November 2018

Guest Editor: Claudio Tessone

Bipartite matching problem is to study two disjoint groups of agents who need to be matched pairwise. It can be applied to many real-world scenarios and explain many social phenomena. In this article, we study the effect of competition on bipartite matching problem by introducing conformity into the preference structure. The results show that a certain amount of competition can improve the overall utility of society and also eliminate the giant shift of social utility when matching unequal numbers of men and women.

1. Introduction

Bipartite matching problem is to study how the two disjoint groups of agents can be matched pairwise for their personal preferences, such as the matching between men and women, students and colleges, workers and jobs, consumers and products [1–3], and many other scenarios [4–7]. For convenience we use the paradigm of marriage problem, where N men and N women need to be matched. In this problem, each participant is selfish, everyone tries to optimize their own choices, and the competition is inevitable. A key question is how to find a stable solution in which there is no such a pair of man and woman who prefer themselves more than the assigned partner [8]. The number of stable solutions is very large [9]; the most famous one among them is obtained by the Gale-Shapley algorithm, which was awarded the Nobel Prize in Economics in 2012.

In 1962, Gale and Shapley proved that for the same number of men and women, a stable solution can always be obtained through Gale-Shapley algorithm [1]. In this algorithm, every agent has a preference list, which is a ranking list of all members from the opposite sex. Men act as suitors and send proposals to women according to their preference lists. When a woman has multiple candidate partners, she always retains her favorite one. The algorithm will continue until all agents find their spouses. This matching result can easily prove to be stable, because the only way for men to improve their current situation is to send proposals to women who have already rejected them, but the spouse of these women must be in front of this man in the women's lists. Besides, it also proved to be the men-optimal solution among all stable solutions.

Statistical physicists also find areas of interest in the bipartite matching problem because the model is very similar to a system in which two different particles interact [10, 11]. We assume that the utility of an agent is corresponding to the ranking of her/his spouse in her/his preference list [12]. It can be generally regarded as a cost function, or 'energy' in physics terminology. In the following text, the term 'energy' of an agent is used to express the utility of an agent. If a person just happens to match the person at the top of her/his preference list as a spouse, then she/he will be the happiest and have an 'energy' of 1. In the worst case, one had to choose the person at the bottom of the list and the 'energy' would be N. In most of the previous researches [9, 12, 13], for simplicity, the preference lists are always established randomly and independently.

Physicists are constantly interested in finding a solution with the lowest 'energy', which is called the ground state [13–16]. This is equivalent to the commonly used term 'minimal cost solution'. The replica method in spin glass is used to compute the minimal cost solution in the bipartite matching problem [14], and the result gives that the average 'energy' of each individual in the minimal cost solution is $0.808\sqrt{N}$ [12]. However, 24.2% of men can find one or more women [13], so that both of them prefer each other to their current spouses. Therefore, this minimal cost solution is a very unstable matching. Moreover, the Mean Field Theory is utilized to calculate the average 'energy' of the stable solution obtained by Gale-Shapley algorithm [12]. In this case, the average 'energy' of men is $\log(N)$, and the average 'energy' of women is $N/\log(N)$. Further, with the aid of the 'energy' distribution function, it is proved that for all stable solutions, there exists a relationship $\epsilon_m * \epsilon_w = N$. The average 'energy' is $\epsilon_g = (\epsilon_m + \epsilon_w)/2 = 0.5(\epsilon_m + N/\epsilon_m)$. It is easy to see that the global optimal stable solution corresponds to the same 'energy' $\sqrt{N}$ for both men and women, which is a little worse than the global optimal solution. In addition, it is worthwhile to mention that the men-optimal solution has the highest total 'energy' among all stable solutions. After that, various issues were investigated, such as the matching problem under partial choice [17, 18], which means the lists of men only contain a fraction of all women, or people have a spatial distribution and tend to match people who are geometrically closer [19], etc.

One of the interesting questions is, if people's preference lists are not strictly random, i.e., if we induce a conformity term into the preference structure, i.e., the agents have similar preferences, which makes some of the agents become more popular than others for all agents, how will the popularity of agents affect the matching results? Later we will show that the weight of popularity in the preference structure is directly related to the competition intensity. In previous studies [19], numerical simulation showed that the exerting of competition will lead to higher 'energy' and lower utility. Here we thoroughly study the impact of competition on bipartite matching, and instead of intuitive result that competition may reduce the utility of the society, our result shows that a certain amount of competition can increase the social utility. On the other hand, a recent research [20] shows that random bipartite matching is very sensitive to the symmetry of the sizes of the two sides; even reducing the number of women by only one will lead to a dramatic change of the 'energy' in the matching result. However, this dramatic change in social utility is rarely observed in real life, even though the numbers of matching parties in reality are often different. Our research shows that introducing competition into the preference list can effectively decrease the symmetry sensitivity of the matching result and explain the absence of the dramatic change in daily observation.

2. Method

The Gale-Shapley algorithm [1] is described below: suppose we have two disjoint sets of N men and N women who need to be matched pairwise. Each person has her/his preference list which stores the ranking of all members from the opposite sex. At the beginning, everyone is unengaged. In each step, each unengaged man issues a proposal to his favorite woman among those he has not proposed to. The courted woman will choose her favorite from all the suitors and her provisional partner. The process iteratively runs until everyone is matched and it is easy to realize that a final matching will be achieved eventually.

3. Results and Discussions

3.1. Matching between N Men and N Women. Let us firstly consider the matching problem when the two groups have equal size. For simplicity, it is usually assumed that everyone's preference list is completely random. Considering the process of Gale-Shapley algorithm, men make proposals to women. If the courted woman is unengaged, then the total number of matched pairs will increase by one. If this woman is engaged, no matter the suitor or her current partner is retained, the number of partners will not change.

It is proved that on average [12], a total number of $N(\log(N)+0.522)$ proposals need to be sent to make everyone engaged. Every proposal leads to a man's 'energy' increasing by one; the average 'energy' of men is the same as the average number of proposals that he needs to make; i.e., the average 'energy' of men is $\log(N) + 0.522$. On the other hand, for women, each of them receives on average $\log(N) + 0.522$ proposals. Each time they receive a proposal, they can make a choice and decide the man whom they prefer. Obviously, the more proposals they receive, the lower 'energy' women have. Since each suitor is randomly distributed in the preference list, the optimal one among many choices is equivalent to the first order statistic of multiple random sampling from uniform distribution. It is easy to obtain the woman's average 'energy' as $N/(\log(N) + 0.522 + 1)$. When N is large, the average male 'energy' is approximately equal to $\log(N)$, and the average female 'energy' is approximately equal to $N/\log(N)$. This conclusion is consistent with the results of the 'energy' distribution function method used in previous study [12].

However, in reality the preference lists are seldom purely random. Some intrinsic properties, such as beauty, intelligence, and wealth, will affect the ranking order of the preference lists and then a certain level of conformity can be observed in the structure of their preference lists. People with those widely accepted attributes are easier to rank in front of the preference lists of all agents. Let us consider the extreme case, when the preferences of all agents are strictly based on popularity term; then everyone should have an identical preference list. At the first step, all men will make proposals to the woman they all prefer. The man ranked at the top of women's preference list will be accepted and the other men are refused. After that, the remaining men make proposals to the woman who is their second favorite, the man ranked second in the women's preference lists will be accepted and the others will be rejected. The process continues, it is easy to know that the men's 'energy' from low to high are $1, 2, 3 \ldots N$

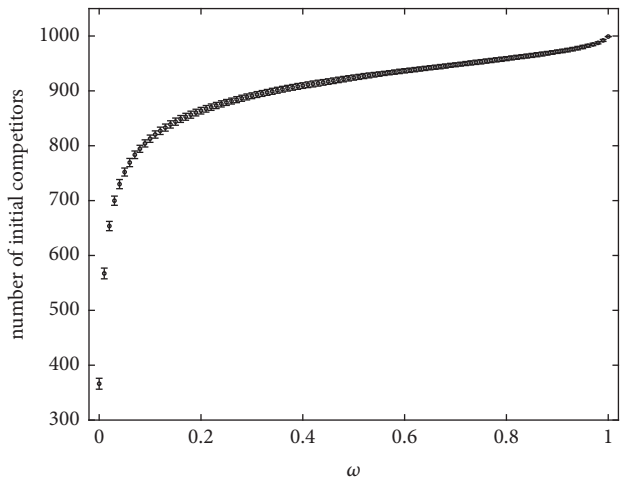

Figure 1: The number of initial competitors versus the weight of popularity, $N = 1000$; the result is averaged over 100 realizations.

and the average 'energy' $(N + 1)/2$. The average 'energy' of women is the same.

We define the men who have been rejected after the first round of proposing as the initial competitors. Thus, the total number of initial competitors can be regarded as a measure of the competition intensity of the matching. In the extreme case above (preference lists are completely the same), following the Gale-Shapley algorithm, all men will propose to the same woman so that the number of initial competitors is $N - 1$. Now consider the other extreme case when the preference lists are purely random; theoretically the probability that a woman does not receive any proposal is $(1 - 1/N)^N$; when N is large, this probability is close to $1/e$. Since the number of men who have been rejected is equal to the number of women who have not received any proposals, the number of initial competitors is $N/e \simeq 0.368N$.

In general, we propose a model to characterize the realistic situation that some of the agents are ranked high in the preference lists of all the opposite sex agents. In this model the scores of each agent rating the agents of the opposite sex consist of two parts: the popularity term that reveals the conformity of the preference lists and a random term that brings diversification of the personal preferences.

We assume that woman i rates man α with a score $S_{\alpha,i}$.

$$S_{\alpha,i} = \omega \times F_\alpha + (1 - \omega) \times N_{\alpha,i} \quad (1)$$

Here F_α is popularity of man α and $N_{\alpha,i}$ is a random term. For simplicity, we assume that F and N are uniformly distributed on [0,1] and that weight of popularity ω is universal for all men and women. One can choose other distributions for the popularity, but it does not change the main conclusion. For any intermediate situations the number of initial competitors lies in [0.368N, N] because of the monotonous relationship of $S_{\alpha,i}$ and the weight ω by definition.

Below we present a numerical simulation result (Figure 1) which shows how the number of initial competitors changes with the weight of popularity in our model. The simulation is done on a system containing N=1000 agents on each side, and the result is averaged over 100 realizations. As shown in Figure 1, the number of initial competitors gets increasingly higher as the weight of conformity grows.

The preference list of woman i is generated according to the order of her ratings of all men. Similarly, we can obtain the preference list of everyone. With these preference lists, implementing Gale-Shapley algorithm, we will obtain the final stable matching.

Now we start to analyze this matching result. As shown in Figure 2(a), the average 'energy' of men increases monotonically with the weight of popularity, ω. This is because when the weight of popularity increases, more proposals are required for everyone to be engaged. However, a slight competition will significantly reduce the women's 'energy'. This increase of women's average 'energy' grows with N (Figure 2(b)), and the competition intensity required for the women to reach optimal 'energy' decreases as the population grows (Figure 2(c)). As competition further intensifies, the women's 'energy' will also increase. On the one hand, due to the increase of the number of proposals, the number of choices of woman increases. It can be known from the nature of the order statistics that the minimum number of multiple random sampling decreases as the number of sampling increases. The increase in competition between men is beneficial to the women. On the other hand, the increase in the weight of popularity also leads women to tend to favor the men with high popularity and thus increases the intensity of competition among women. Many women have to be matched with the men positioned further down on their preference lists. This will lead to an increase in the average 'energy' of women and all people.

Due to the increase of ω in the beginning, the reduction of women's 'energy' is more significant than the increase of men's 'energy'. As shown in Figure 3(a), there exists a ω_g^* that can make average 'energy' of all people reaches the optimal value. In other words, it is a certain degree of social popularity that increases the total social utility.

In order to study the relationship between a person's intrinsic popularity and her/his level of utility, we cluster

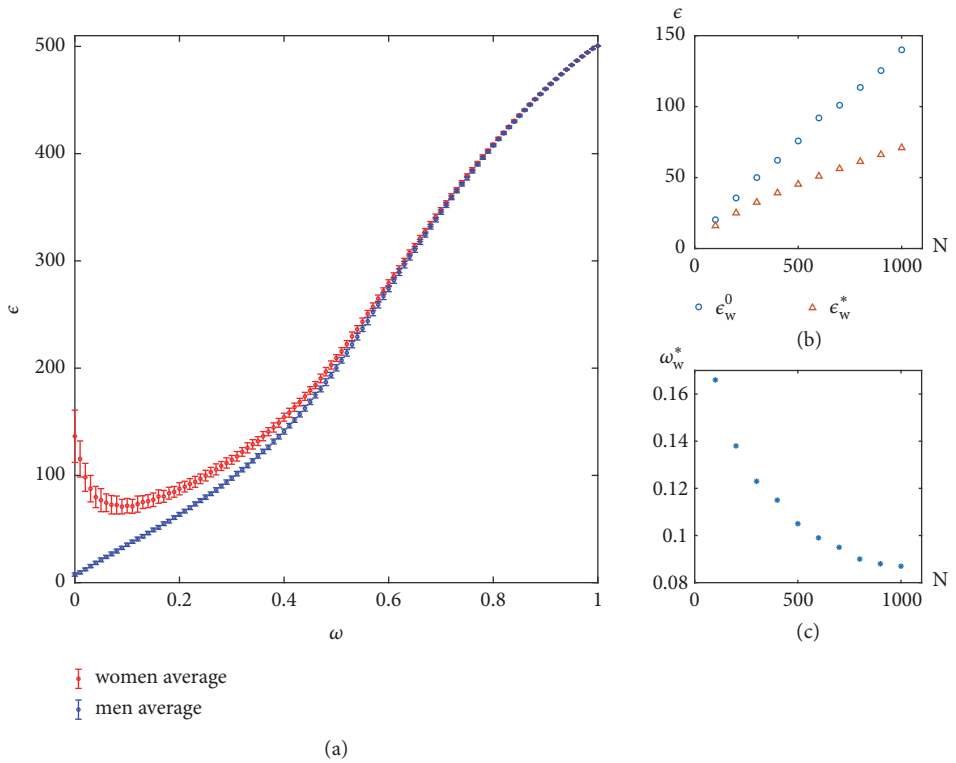

FIGURE 2: The numerical simulation of average 'energy' of men and women, $N = 1000$; the result is averaged over 100 realizations. (a) The average 'energy' of men and women, as a function of ω; (b) for $N = 100, 200, 300, \ldots, 1000$, the average 'energy' of women at $\omega = 0$ is denoted by ϵ_w^0 and at $\omega = \omega_w^*$ is denoted by ϵ_w^*. Here ω_w^* is the women-optimal value of conformity weight; (c) the optimal weight ω_w^* versus N.

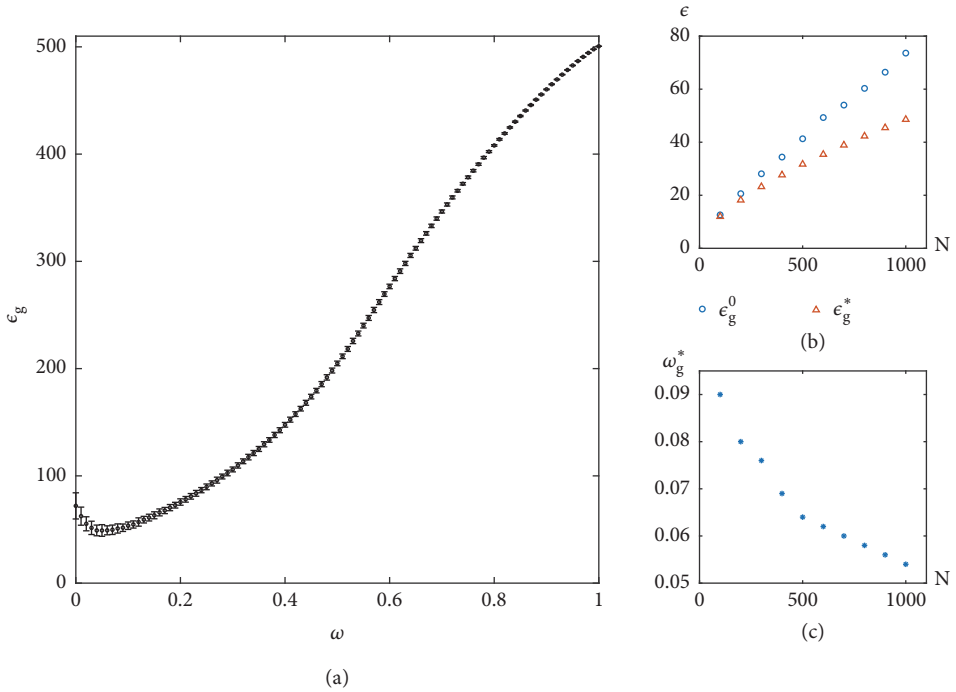

FIGURE 3: The numerical simulation of average 'energy' of all agents, $N = 1000$; the result is averaged over 100 realizations. (a) The average 'energy' of all agents, as a function of ω; (b) for $N = 100, 200, 300, \ldots, 1000$, the average 'energy' at $\omega = 0$ is denoted by ϵ_g^0 and at the global optimal popularity weight ω_g^* is denoted by ϵ_g^*; (c) the optimal weight ω_g^* versus N.

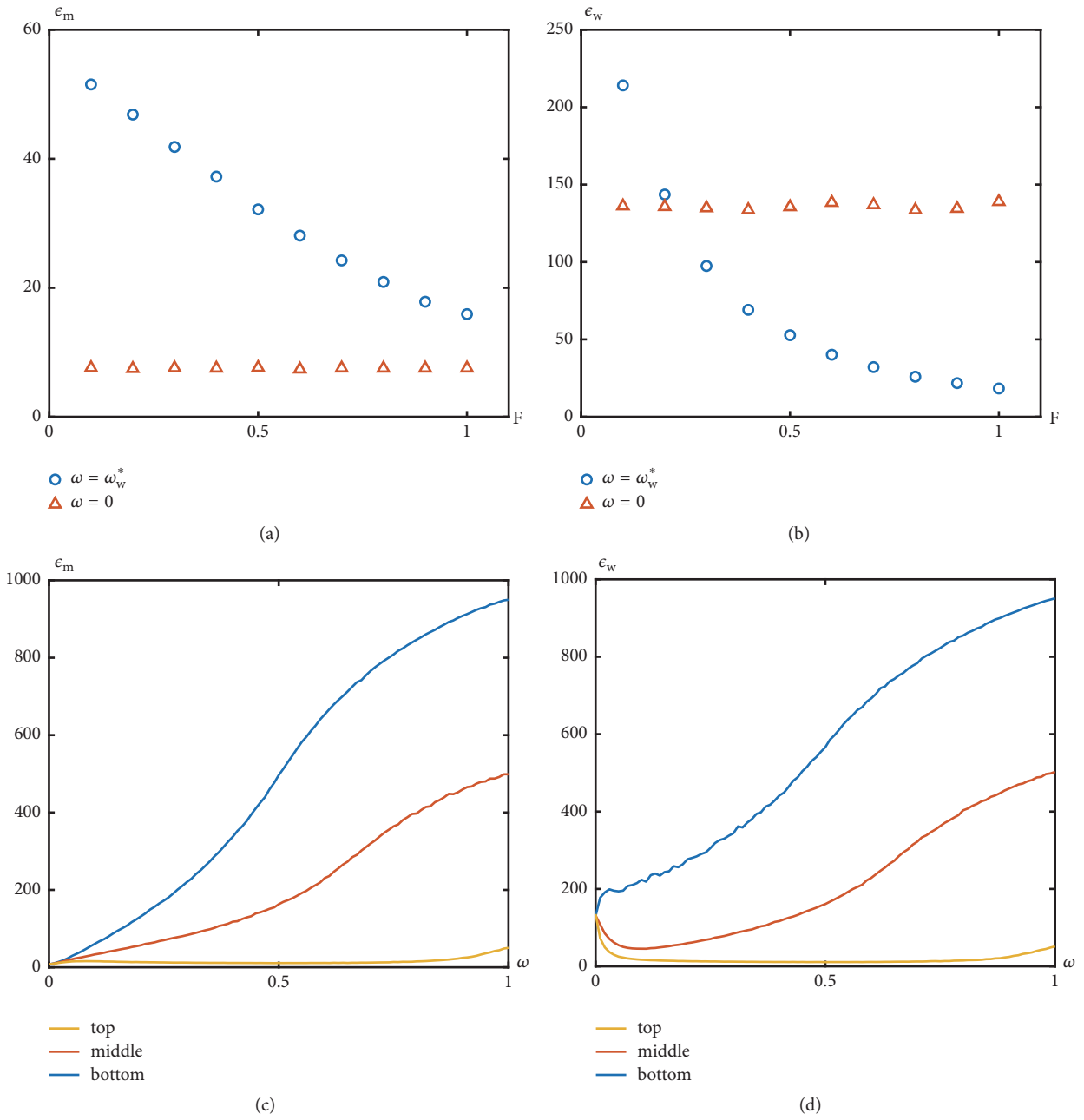

FIGURE 4: The average 'energy' of different popularity groups; the horizontal axis shows the different values of popularity. $N = 1000$; the result is averaged over 100 realizations. (a) The average 'energy' of men at $\omega = 0$ and $\omega = \omega_w^*$; (b) the average 'energy' of women at $\omega = 0$ and $\omega = \omega_w^*$; (c) the average 'energy' of three representative popularity groups of men, bottom(0,0.1), middle(0.45,0.55), and top(0.9,1), versus ω; (d) the average 'energy' of three representative popularity groups of women, bottom(0,0.1), middle(0.45,0.55), and top(0.9,1), versus ω. Note that when $\omega = 0$ (triangles) the average 'energy' of men or women stays the same as the value shown in Figure 2(a); the small deviations are the random fluctuations which are irrelevant to the popularity.

the 'energy' of men and women to 10 groups according to the range of popularity [0, 0.1), [0.1, 0.2), . . . , [0.9, 1] (data binning) and compare their utility in two cases: $\omega = 0$ and $\omega = \omega_w^*$ (women's optimal). As shown by Figure 4(a), the competition causes 'energy' of men to rise in all popularity groups. As shown in Figure 4(b), at the women's optimal weight of popularity, the 'energy' of women in lowest 20% conformity groups increases, and the 'energy' of the remaining 80% women decreases. In general, women will have lower 'energy' with a certain level of competition, as we have known above.

In addition, we take three representative agent groups and label them as bottom (popularity ranges [0,0.1]), middle (conformity ranges [0.45,0.55]), and top (popularity ranges [0.9,1]), respectively. With the increase of competition, i.e., the increase of ω, the 'energy' of the three groups of men

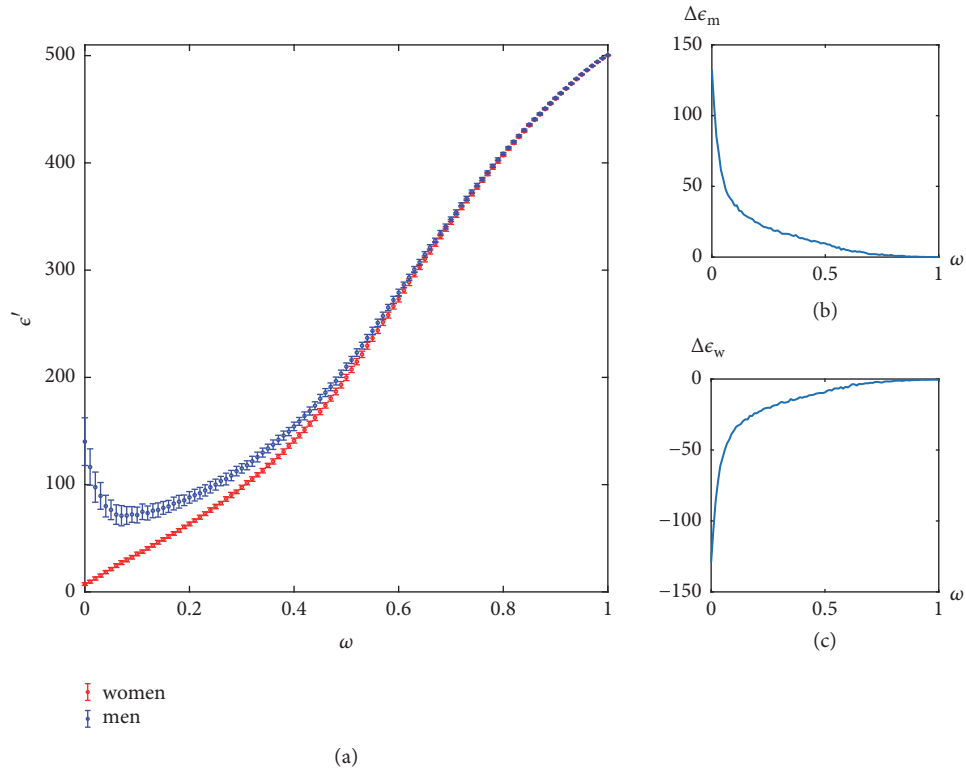

FIGURE 5: The matching between 1000 men and 999 women, as a function of ω. The result is averaged over 100 realizations. (a) The average 'energy' of men and women; (b) $\Delta\epsilon_m$ versus ω; (c) $\Delta\epsilon_w$ versus ω.

will increase, while the top women will have lower 'energy' and the bottom women will have higher 'energy' (as shown in Figures 4(c) and 4(d)). This change is very sensitive to ω; even if ω is very small (0.01), the 'energy' difference between the top group and bottom group has an obvious gap. For the middle group women, a slight competition improves their utility, but as the competition intensifies, their 'energy' becomes even higher.

3.2. Matching between N Men and N − 1 Women. For a long time, the G-S algorithm has been considered to produce a men-optimal stable matching. In particular, for a completely random preference list, that is, when $\omega = 0$, the average 'energy' of men is $\log(N) + 0.522$, which is far less than the average 'energy' of women, which is $N/[\log(N) + 0.522]$, so the active side takes a huge advantage in the matching. However, a recent research [20] shows that in a random bipartite matching, if one woman is removed from the matching, the average 'energy' of men will become $N/\log(N)$, and the average 'energy' of women will become $\log(N)$. The 'energies' of the positive and passive sides are completely reversed.

In our daily life, the sizes of matching parties are rarely equal. Imagine removing one agent of passive party in the bipartite matching, for example, reducing a woman in the marriage problem, downsizing one job position in the labor market, or cutting one offer in the college admission; under the assumption of random bipartite matching, the pairing result will change drastically with the smallest change of the size of passive side. In particular in the marriage problem, due to the natural inequality of birth rates of different sex as well as some other cultural or political impact, the sex ratio (boys versus girls) is larger than 1. It makes the matching of unequal numbers of men and women have even more practical meaning. However, in reality, one of the possible reasons for the phenomenon that such a large difference in social utility is rarely seen, is that the low-popularity agents will be quickly eliminated and other people's pairing results are almost unaffected.

We analyze the matching results in the case of 1000 men and 999 women with different ω. As shown in Figure 5(a), the curves are extremely similar to that of Figure 2(a), despite the fact that the gender has reversed. The women become the dominant side of the matching. We compare this asymmetric case with the symmetric case above and examine the changes of the average 'energy' of men and women, $\Delta\epsilon_m = \epsilon'_m - \epsilon_m$ and $\Delta\epsilon_w = \epsilon'_m - \epsilon_w$. The results are shown in Figures 5(b) and 5(c), respectively. It is found that this difference sharply decreases with the increase of ω, which explains why the slight change in the number of people in reality does not obviously affect overall utility society.

4. Conclusion

In this article we introduce competition in bipartite matching problem by bringing the conformity in the preference lists

of agents. While in the traditional Gale-Shapley model, the preference lists of agents are randomly generated, the active agents can easily acquire the results they want and stop sending proposals so that the agents from the passive side are left with little freedom of choice. We show that if a certain amount of competition is introduced, the active agents have to make more efforts and send more proposals, which will slightly decrease their utility. However, at the same time, the utility of the passive side will be obviously increased, and society as a whole will have a higher total utility than the original matching result. To summarize, a certain amount of competition increases the total utility of the society. This not only is true for the bipartite matching problem, but also enlightens our understanding of many other social phenomena. Besides, when matching two parties of different sizes, the utility of the two parties can be dramatically changed compared to the symmetric case. The introduction of conformity in the preference lists can also eliminate this potential significant utility change, which provides a possible explanation why this significant utility change is rarely seen in human society.

Data Availability

No data were used to support this study.

Conflicts of Interest

The authors declare no conflicts of interest.

Acknowledgments

We would like to thank Prof. Yi-Cheng Zhang and Wen-Yao Zhang for helpful discussions. This research is supported in part by the Chinese National Natural Science Foundation under grant No. 61602202 and Natural Science Foundation of Jiangsu Province under grants No. BK20160428, BK20161302. Gui-Yuan Shia and Yi-Xiu Kong acknowledge the support from China Scholarship Council (CSC).

References

[1] D. Gale and L. S. Shapley, "College admissions and the stability of marriage," *The American Mathematical Monthly*, vol. 69, no. 1, pp. 9–15, 1962.

[2] A. E. Roth, "The Evolution of the Labor Market for Medical Interns and Residents: A Case Study in Game Theory," *Journal of Political Economy*, vol. 92, no. 6, pp. 991–1016, 1984.

[3] A. E. Roth and M. A. Sotomayor, *Two-sided matching*, vol. 18 of *Econometric Society Monographs*, Cambridge University Press, Cambridge, 1990.

[4] B. M. Maggs and R. K. Sitaraman, "Algorithmic nuggets in content delivery," *Computer Communication Review*, vol. 45, no. 3, pp. 52–66, 2015.

[5] D. Lebedev, F. Mathieu, and L. Viennot, "On using matching theory to understand P2P network design," in *In INOC 2007, International Network Optimization Conference*, 2007.

[6] M. Hasan and E. Hossain, "Distributed resource allocation in 5G cellular networks," in *Towards 5G: Applications, requirements and candidate technologies*, pp. 245–269, Wiley, 2015.

[7] G. J. Hitsch, A. Hortaçsu, and D. Ariely, "Matching and sorting in online dating," *American Economic Review*, vol. 100, no. 1, pp. 130–163, 2010.

[8] A. E. Roth, "The economics of matching: stability and incentives," *Mathematics of Operations Research*, vol. 7, no. 4, pp. 617–628, 1982.

[9] M. Dzierzawa and M.-J. Oméro, "Statistics of stable marriages," *Physica A: Statistical Mechanics and its Applications*, vol. 287, no. 1-2, pp. 321–333, 2000.

[10] Y. Zhang, "The Information Economy," in *Non-Equilibrium Social Science and Policy*, Understanding Complex Systems, pp. 149–158, Springer International Publishing, Cham, 2017.

[11] A. Chakraborti, D. Challet, A. Chatterjee, M. Marsili, Y.-C. Zhang, and B. . Chakrabarti, "Statistical mechanics of competitive resource allocation using agent-based models," *Physics Reports*, vol. 552, pp. 1–25, 2015.

[12] M.-J. Oméro, M. Dzierzawa, M. Marsili, and Y.-C. Zhang, "Scaling behavior in the stable marriage problem," *Journal de Physique II*, vol. 7, no. 12, pp. 1723–1732, 1997.

[13] G.-Y. Shi, Y.-X. Kong, H. Liao, and Y.-C. Zhang, "Analysis of ground state in random bipartite matching," *Physica A: Statistical Mechanics and its Applications*, vol. 444, pp. 397–402, 2016.

[14] M. Mézard and G. Parisi, "Replicas and optimization," *Journal de Physique Lettres*, vol. 46, no. 17, pp. 771–778, 1985.

[15] M. Mézard and G. Parisi, "The Euclidean matching problem," *Le Journal de Physique*, vol. 49, no. 12, pp. 2019–2025, 1988.

[16] V. S. Dotsenko, "Exact solution of the random bipartite matching model," *Journal of Physics A: Mathematical and General*, vol. 33, no. 10, pp. 2015–2030, 2000.

[17] Y.-C. Zhang, "Happier world with more information," *Physica A: Statistical Mechanics and its Applications*, vol. 299, no. 1-2, pp. 104–120, 2001.

[18] P. Laureti and Y.-C. Zhang, "Matching games with partial information," *Physica A: Statistical Mechanics and its Applications*, vol. 324, no. 1-2, pp. 49–65, 2003.

[19] G. Caldarelli and A. Capocci, "Beauty and distance in the stable marriage problem," *Physica A: Statistical Mechanics and its Applications*, vol. 300, no. 1-2, pp. 325–331, 2001.

[20] G. Shi, Y. Kong, B. Chen, G. Yuan, and R. Wu, "Instability in Stable Marriage Problem: Matching Unequally Numbered Men and Women," *Complexity*, vol. 2018, 5 pages, 2018.

Hindawi
Complexity
Volume 2018, Article ID 1589016, 10 pages
https://doi.org/10.1155/2018/1589016

Research Article

Congenital and Blood Transfusion Transmission of Chagas Disease: A Framework Using Mathematical Modeling

Edneide Ramalho,[1] **Jones Albuquerque**,[1,2] **Cláudio Cristino**,[1] **Virginia Lorena**,[3] **Jordi Gómez i Prat**,[4] **Clara Prats**,[5] **and Daniel López**[5]

[1] *Universidade Federal Rural de Pernambuco, Departamento de Estatística e Informática, Recife, PE, Brazil*
[2] *LIKA –Laboratório de Imunopatologia Keizo Assami, UFPE, Recife, PE, Brazil*
[3] *FIOCRUZ – Fundação Oswaldo Cruz - Pernambuco, Recife, Brazil*
[4] *Unitat de Salut Internacional, PROSICS, Programa Especial de Malalties Infeccioses Vall d'Hebron-Drassanes, Barcelona, Spain*
[5] *Universitat Politècnica de Catalunya BarcelonaTech, Departament de Física, Escola Superior d'Agricultura de Barcelona, Castelldefels, Spain*

Correspondence should be addressed to Clara Prats; clara.prats@upc.edu

Received 21 May 2018; Accepted 4 October 2018; Published 1 November 2018

Guest Editor: Miguel Fuentes

Chagas disease or American trypanosomiasis is an important health problem in Latin America. Due to the mobility of Latin American population around the world, countries without vector presence started to report disease cases. We developed a deterministic compartmental model in order to gain insights into the disease dynamics in a scenario without vector presence, considering congenital transmission and transmission by blood transfusion. The model was used to evaluate the epidemiological effect of control measures. It was applied to demographic data from Spain and sensitivity analysis was performed on model parameters associated with control strategies.

1. Introduction

Chagas disease or American trypanosomiasis is caused by the protozoan parasite *Trypanosoma cruzi*, and it is an important health problem in Latin America. The most effective transmission route is through contact with triatomines bug (the disease vector) feces. Other transmission routes can occur by blood transfusion, organ transplantation, and congenital transmission [1]. Some cases of oral transmission have been reported in Brazil, Venezuela, Colombia, Mexico, Argentina, and Bolivia [2].

The disease presents an initial acute phase, generally asymptomatic, and a subsequent chronic phase, which can present clinical manifestations (cardiac, digestive, and/or neurological) [1]. Since the 1960s the only drugs used in Chagas disease treatment are benznidazole and nifurtimox, which have a great efficiency if the treatment starts early and can control disease progression in chronic cases [1, 3].

Although some Latin American countries, as Argentina, Bolivia, Brazil, Chile, Paraguay, Uruguay, and Peru, have received from the Pan American Health Organization (PAHO) the International Certification of Disease Elimination by the main vector *Triatoma infestans*, the disease is still a challenge [4]. According to the World Health Organization, around 8 million people are infected worldwide and 10,000 people die every year due to disease clinical manifestation [1]. Moreover, it estimates that 25 million people are at risk of acquiring the disease. Around 30-40% of infected people develop cardiomyopathy, digestive megasyndromes, or both [5].

Since 2000, cases of the disease started to be reported in nonendemic countries such as European countries, Canada, USA, Japan, and Australia, due to the large flow of Latin American immigrants [6]. In 2010, the World Health Assembly approved a resolution, WHA 63.20 [7], recognizing the increase in the number of cases and established a way to track

all of the transmission routes. The global cost of the disease is similar to rotavirus or cervical cancer [8].

By 2009, 4,290 cases had been diagnosed in Europe, compared with an estimated incidence ranging from 68,000 to 122,000 cases, hence 95% of cases are nondiagnosed, reflecting the difficulty in tracking infected people [9, 10]. Due to uncertainty about the real number of cases in each country, estimates are based on PAHO [11] and Schmunis et al. 2014 [12].

Spain is the European country with most Latin American immigrants, ranking the second on the world list, after the United States of America [13]. In 2008, there were approximately 4 million immigrants in Spain. 1.5 million of them were born in a country endemic for Chagas disease and, therefore, they are potential carriers of the disease [14]. The first case of the disease by blood transfusion in Spain was detected in 1984, with two more cases in 1995 and 2004 [15]. Cases of congenital transmission were also reported [16, 17].

Due to its silent evolution after infection and the resulting underdiagnoses, there is no complete and reliable data about the disease. Therefore, mathematical models can be a particularly useful tool on the study of disease spread and control.

Several mathematical modeling studies have been done in order to assess different aspects of Chagas disease and control strategies. For instance, Velasco-Hernandez et al. [18] considered a compartmental model with humans, vectors, and transmission by blood transfusion. Inaba and Sekine [19] also considered humans, vectors, and blood transfusion but with infection age dependent infectivity. Congenital transmission was considered by Massad [4], Raimundo et al. [20], and Coffield et al. [21]. Fabrizio et al. [22] explored an interhuman model, considering congenital transmission and blood transfusion transmission.

In this work, we present a novel deterministic compartmental model considering congenital and blood transfusion as the main mode of transmission using demographic data from Spain. The aim is to gain insight into the dynamics of the disease in a scenario without the vector and to evaluate the epidemiological impact through the implementation of control strategies like an improvement on surveillance in blood transfusion and treatment of infected newborns. We also introduced a cure rate for infected individuals to verify how it affects disease dynamics. This cure rate means decrease in the number of parasites inside host, and consequently decreasing the risk of developing clinical manifestation.

2. Materials and Methods

2.1. Model Description. We introduce a deterministic compartmental model for Chagas transmission without the vector presence. The model distinguishes Latin American people from countries with active vector transmission and natives and immigrants from countries without vector transmission. It also splits men and women in different compartments in order to take vertical transmission into account. Therefore, the population is classified into eight compartments:

(1) M_{vh}: healthy men from country with active vector transmission;

(2) M_{vi}: infected men from country with active vector transmission;

(3) M_h: healthy men from country without vector transmission;

(4) M_i: infected men from country without vector transmission;

(5) W_{vh}: healthy women from country with active vector transmission;

(6) W_{vi}: infected women from country with active vector transmission;

(7) W_h: healthy women from country without vector transmission;

(8) W_i: infected women from country without vector transmission.

In the model simulations we analyze the number of individuals over time in each of the compartments. The processes considered for driving their dynamics are the simplest as possible, keeping in mind the essence of the system's structure, the objectives of the model and the questions to be answered. The reasons for looking for such simplicity are various. From a theoretical perspective, a strictly gradual increase in complexity is essential in any model development in order to elucidate the different drivers of the overall dynamics. From a social perspective, this simplicity facilitates the necessary interaction with nonmodelers like community health workers, social scientists, and patients' associations in order to seek real and feasible applications.

The processes considered by the current model are birth, mortality, and flows among compartments. Infections flows are associated with two possible causes: blood transfusion and congenital transmission. Figure 1 shows a flowchart of the model. The assumptions for the dynamics of transmission are the following:

(i) It is assumed that vertical transmission is proportional to the number of infected women. People who are born in Spain will be considered in the without vector compartment, that is, W_i or M_i, even though their family origin is Latin American.

(ii) We considered that the birth rate α is the same for women from countries with and without the vector presence. We also assumed that 50% of the descendants are women and 50% are men, for simplicity.

(iii) If a woman is infected, she has a probability β to infect her son or daughter.

(iv) The parameter γ stands for mortality rate for healthy people. For infected individuals we assumed a mortality rate induced by the disease δ, where $\delta > \gamma$.

(v) Flow among health and infected classes due to blood transfusion is considered as the result of interaction between susceptible and infected people. We considered that there is no difference in the blood and organ donation rate for populations from countries without the vector and for countries with the vector. The parameter τ stands for the yearly blood donation rate.

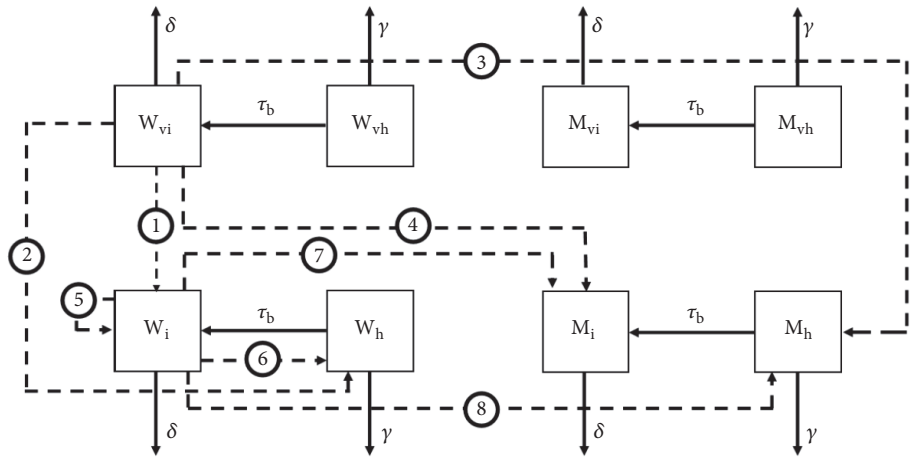

Figure 1: Flow chart for the dynamics of proposed model. Letters inside box indicate the number of individuals in each compartment: infected women from country with vector (W_{vi}), healthy women from country with active vector transmission (W_{vh}), infected men from country with active vector transmission (M_{vi}), healthy men from country with active vector transmission (M_{vh}), infected women from country without vector transmission (W_i), healthy women from country without vector transmission (W_h), infected men from country without vector transmission(M_i), and healthy men from country without vector transmission (M_h). γ is the death rate for healthy people and δ is the death rate for infected people. τ_b is the rate of infection due to blood transfusion. Dashed lines indicate the births. Newborns from W_{vi} can be an infected female (1), healthy female (2), healthy male (3), or infected male (4). The same occur for newborns from W_i that can be infected female (5), healthy female (6), infected male (7), or healthy male (8). Healthy women W_{vh} and W_h only gave birth to healthy newborns (flows not shown).

(vi) We also considered that a proportion p_i of donated blood is potentially contaminated with *T. cruzi*. Once donation has been made, health services carry out controls screening. We considered ξ as the probability of an effective surveillance in screening donated blood samples, thus $1 - \xi$ is the probability that an infected sample will not be detected, reach a receptor, and infect him or her. In this way, the rate at which a healthy person becomes infected with a parasite from an infected person will be proportional to the product $\tau_b = \tau p_i(1 - \xi)$. We also considered that all transfusions are made with the same rate for all individuals.

(vii) We supposed that infected individuals can be cured with a rate C due to treatment. This cure rate means a reduction in the number of parasites inside host, reducing the chances of clinical manifestation. We consider that a yearly percentage d of infected individuals will be diagnosed and receive treatment. Considering e as the treatment effectiveness, we can write $C = e \cdot d$. The detected patients that do not receive any treatment due to different reasons (e.g., reported difficulties in accessing it [29]) are not distinguished from nondiagnosed individuals by the model.

(viii) No migration flows (neither immigration nor emigration) were considered by the model, since they are not relevant for its current purpose.

According to the assumptions above, the model is represented by the following system of ordinary differential equations (1)-(8):

$$\frac{dM_h}{dt} = 0.5\alpha\left(W_h + W_{vh}\right) + 0.5\alpha\left(1 - \beta + \rho\right)\left(W_i + W_{vi}\right) + CM_i - \gamma M_h - \tau_b\left(1 - \xi\right)M_h\left(\frac{I}{N}\right) \quad (1)$$

$$\frac{dW_h}{dt} = 0.5\alpha\left(W_h + W_{vh}\right) + 0.5\alpha\left(1 - \beta + \rho\right)\left(W_i + W_{vi}\right) + CW_i - \gamma W_h - \tau_b\left(1 - \xi\right)W_h\left(\frac{I}{N}\right) \quad (2)$$

$$\frac{dM_{vh}}{dt} = CM_{vi} - \gamma M_{vh} - \tau_b\left(1 - \xi\right)M_{vh}\left(\frac{I}{N}\right) \quad (3)$$

$$\frac{dW_{vh}}{dt} = CW_{vi} - \gamma W_{vh} - \tau_b\left(1 - \xi\right)W_{vh}\left(\frac{I}{N}\right) \quad (4)$$

$$\frac{dM_i}{dt} = 0.5\alpha\beta\left(W_i + W_{vi}\right)\left(1 - \rho\right) - \left(\delta + C\right)M_i + \tau_b\left(1 - \xi\right)M_h\left(\frac{I}{N}\right) \quad (5)$$

$$\frac{dW_i}{dt} = 0.5\alpha\beta\left(W_i + W_{vi}\right)\left(1 - \rho\right) - \left(\delta + C\right)W_i + \tau_b\left(1 - \xi\right)W_h\left(\frac{I}{N}\right) \quad (6)$$

$$\frac{dM_{vi}}{dt} = \tau_b\left(1 - \xi\right)M_{vh}\left(\frac{I}{N}\right) - \left(\delta + C\right)M_{vi} \quad (7)$$

$$\frac{dW_{vi}}{dt} = \tau_b (1 - \xi) W_{vh} \left(\frac{I}{N} \right) - (\delta + C) W_{vi} \quad (8)$$

where $I = W_i + M_i + W_{vi} + M_{vi}$ is the number of all infected individuals and N is the total population.

Formulating and evaluating the model behavior will help us to find out what information is known and what is unknown, to analyze the relative importance of each one of the parameters, and to understand the system's dynamics, observing the long-term dynamics based on the control actions that are carried out.

3. Results

3.1. Parameter Estimation. In order to evaluate the trends and the important factors on the dynamic system, it is necessary to attribute parameters values used by the model. Thus, the model was fed with available data from Spain. The diversity of model parameters to be fixed required the use of different data sources. After exploring data availability, we chose 2007 as the starting point of the simulation because it guaranteed the access to all necessary information. The sources and obtained values are described below.

3.1.1. Birth Rate and Vertical Transmission. By 2007 birth rate in Spain was 10.9 per 1,000 inhabitants [23]. In a study performed in two maternity clinics in Barcelona, Muñoz et al. [24] reported a prevalence of 3.4% among pregnant Latin American and 7.3% of newborns were infected. Then, we set the birth rate as $\alpha = 0.0109\ \text{year}^{-1}$ and the probability of vertical transmission as $\beta = 0.073$.

3.1.2. Mortality Rates. By 2007 mortality rate in Spain was 8.5 per 1,000 inhabitants [25]. Cunubá et al. [26] published a systematic review about mortality attributed to Chagas disease. The authors found that the annually mortality rate for Chagas patients was twice higher than non-Chagas patients in a moderate clinical group (0.16 (Chagas) *vs.* 0.08 (non-Chagas) with RR = 2.10, 95% CI: 1.52-2.91). Therefore, we set $\gamma = 0.0085$ per year and $\delta = 2\gamma = 0.017$.

3.1.3. Transmission by Blood Transfusion. We defined the rate of transmission by blood transfusion as $\tau_b = \tau p_i$, where τ is the donation rate per year and p_i is the proportion of potentially infected blood samples. The proportion of potentially infected blood samples was reported as 0.67 per 1,000 [27]. The rate of blood donation in Spain in 2007 was 33.4 per 1,000 inhabitants [28]. Then, the rate of infection by blood transfusion τ_b was calculated as 0.00022378 per year.

3.1.4. Control Strategies. Actions to control the increase in new cases of Chagas disease are incorporated into the model ((1)-(8)) by assuming some control parameters. We considered two kinds of control strategies:

(i) Increasing the proportion of infected newborn treated, by means of increasing the parameter ρ on the model simulation.

(ii) Increasing surveillance in blood transfusion, by means of increasing the parameter ξ in the model simulation.

Moreover, we also assumed a cure rate by diagnosing and treating infected individuals. In the model simulation, it was done by increasing the parameter d.

A summary of parameters used in the simulations is listed in Table 1.

3.2. Numerical Simulations. Population in Spain in 2007 was 45,226,803 [30] of which 1,638,694 were immigrants from countries with the vector presence and potential Chagas disease carriers. The estimated number of infected individuals was 53,134. Besides, taking into account the demographic characteristics of the population, the estimated number of infected women in the childbearing age in Spain was 24,000 [24, 27].

Based on that, the initial conditions were set as $M_h(0) = 21,791,055$, $M_i(0) = 0$, $M_{vh}(0) = 792,780$, $M_{vi}(0) = 29,134$, $W_h(0) = 21,792,055$, $W_i(0) = 0$, $W_{vh}(0) = 792,780$, $W_{vi}(0) = 24,000$.

By use of model (1)-(8), we simulated the cumulative number of infected people over time. Numerical simulations were performed using the software R 3.5.0, integrating the system ((1)-(8)) by Runge–Kutta fourth-order method, using the parameters shown in Table 1 and the initial conditions set above. Time step used was one year and time range for simulation was 40 years.

3.3. Total Infected Population. The dynamics of the total number of infected individuals ($I = M_i + W_i + M_{vi} + W_{vi}$) was simulated for 40 years in order to observe the epidemiological behavior given by the model. We observe a decreasing behavior on the total number of infected people along time as shown in Figure 2. This result is due to the higher death rate attributed to infected people and to the fact that migration flows are not considered, thus resulting in a decreasing rate of change in the total number of the infected. At the end of 40 years simulation, there was a 48% reduction in the number of the total infected when compared with the initial value.

3.4. Comparing the Effect of Transmission Routes. Beyond the number of infected people immigrating to the country without vector presence, another quantity of interest is the number of new cases of the disease, i. e., the cumulative number of new infected arising due blood transfusion and congenital transmission, represented by the sum of individuals in the compartments W_i and M_i.

We can compare the difference in the disease dynamics when only one route of infection is considered, as displayed in Figure 3. The results show that congenital transmission has a higher impact than the transmission by blood transfusion, causing 38% more new infections.

3.5. Control Strategies. Two control strategies were considered, as above mentioned, treatment of infected newborns

Table 1: Parameters used in numerical simulation of proposed model (1)-(8).

Parameter	Meaning	Value	Source
α	Birth rate (year^{-1})	0.0109	[23]
β	Probability of vertical transmission	0.073	[24]
γ	Mortality rate (year^{-1})	0.0085	[25]
δ	Mortality rate due disease (year^{-1})	0.0017	[26]
τ_b	Rate of infection by infected blood (year^{-1})	0.00022378	[27, 28]
C	Cure rate (year^{-1})	Various	
ρ	Proportion of new born treated	Various	
ξ	Probability of a efficient surveillance	Various	

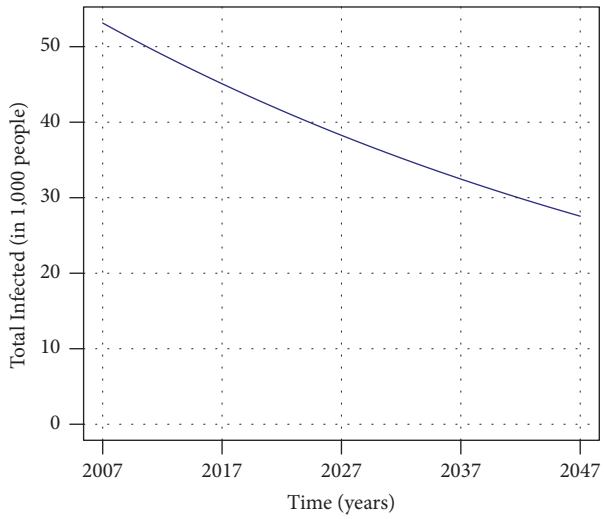

Figure 2: Dynamics on the number of total infected people along 40 years simulation considering death rate due to disease as twice the natural death rate and no migration flows.

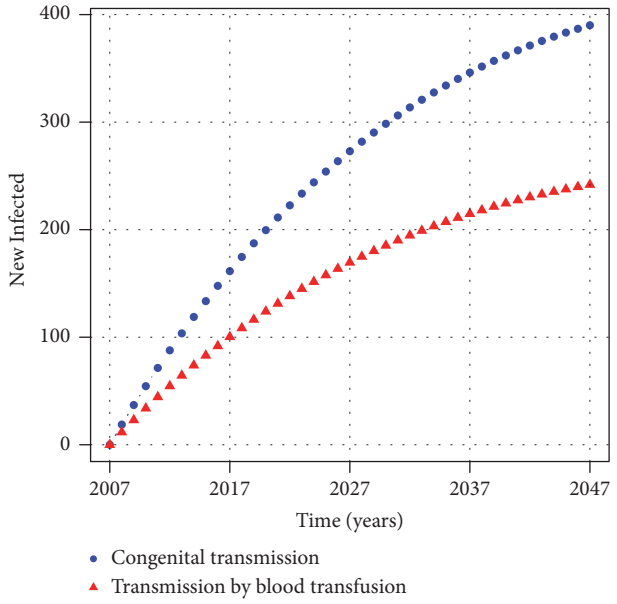

Figure 3: Comparison of the number of cumulative new infections along time when a single transmission route is considered.

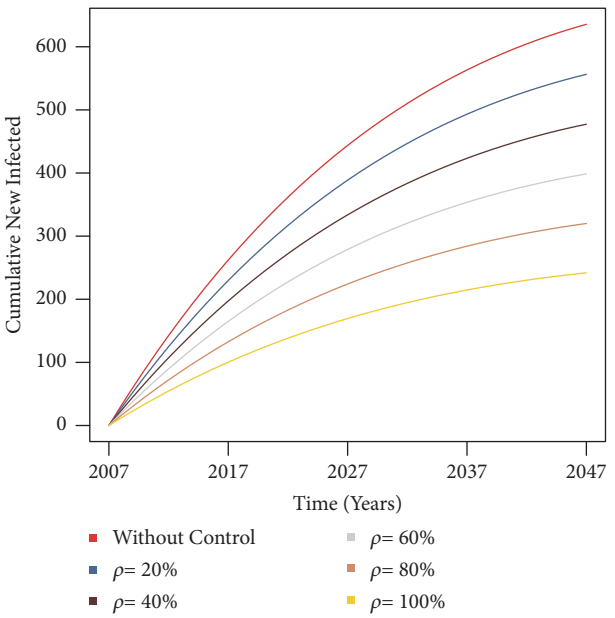

Figure 4: Sensitivity analysis on the cumulative number of newly infected individuals by varying ρ, i.e., the proportion of treatment of infected newborn.

(ρ) and surveillance in blood transfusion (ξ). These strategies were simulated, isolated, and combined.

3.5.1. Considering Only Treatment of Infected Newborns. In this simulation, we evaluated the effect of performing a control strategy only on newborns. The parameter associated with this control strategy is ρ, which represents the proportion of successfully treated infected newborns. This parameter was varied by 20%. The other parameters of the model remained constant as in Table 1, while the parameter ξ representing the control in blood transmission was set to zero. Figure 4 displays the result of this sensitivity analysis in the cumulative number of newly infected individuals.

When comparing these tendencies with the scenario without control (Figure 2), the obtained percentage reductions on the cumulative number of new infected after 40 years are shown in Table 2. Treating 100% of infected newborn means that the cumulative number of newly infected individuals will arise only due to transmission by blood transfusion.

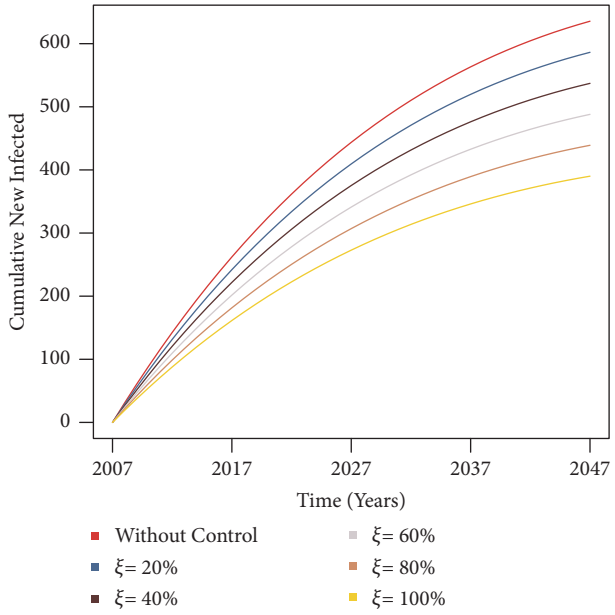

Figure 5: Sensitivity analysis on the cumulative number of newly infected individuals by varying ξ, i.e., the probability of effective surveillance in blood transfusions.

Table 2: Percentage reductions due to variation only in parameter ρ – the proportion of treatment in infected newborn.

ρ values	Reduction (%)
20%	12.5
40%	24.9
60%	37.29
80%	49.64
100%	61.95

Table 3: Percentage reductions in the number of new cases due to variation in parameter ξ – the probability of an effective surveillance in blood transfusion.

ξ values	Reduction (%)
20%	7.75
40%	15.49
60%	23.22
80%	30.93
100%	38.63

3.5.2. Control Only in Blood Transfusion. In this simulation, we evaluated the effect of performing a control strategy only on blood transfusion. Figure 5 displays the result of sensitivity analysis on the cumulative number of newly infected individuals by varying the probability of an effective surveillance ξ on blood transfusions, while the other parameters remain constant and the parameter associated with the control of infected newborn ρ is set to zero.

The obtained percentage reductions in the cumulative number of the newly infected after a 40 years simulation, when compared with the without control scenario (Figure 2), are shown in Table 3. When a probability of an effective surveillance reaches 100%, new cases are only due to congenital transmission.

Table 4: Percentage reductions in the number of new cases due to variation in both parameters associated with control strategies – ρ (percent of infected newborn treated) and ξ (probability of an effective surveillance in blood transfusion).

Parameters values	Reduction (%)
ρ = 20%, ξ = 20%	20.2
ρ = 40%, ξ = 20%	32.6
ρ = 60%, ξ = 40%	52.6
ρ = 80%, ξ = 60%	72.6
ρ = 100%, ξ = 80%	92.4.

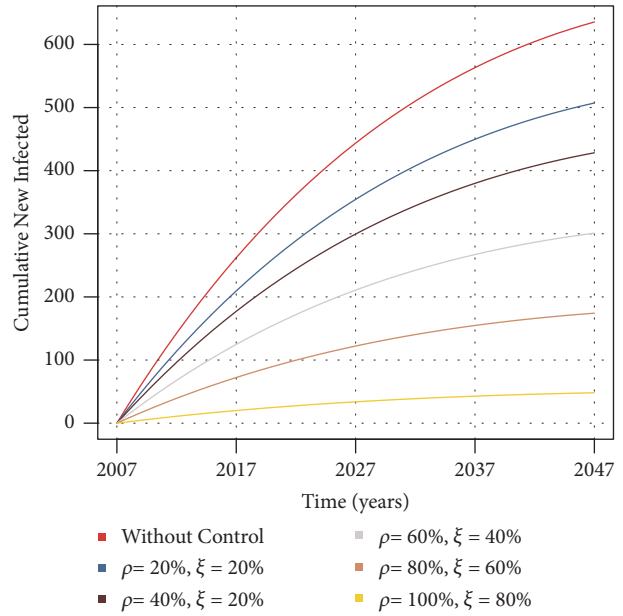

Figure 6: Sensitivity analysis on the cumulative number of newly infected by applying combined control: increasing proportion of treatment in infected newborns (parameter ρ) and on the surveillance in blood transfusion transmission (parameter ξ).

3.5.3. Combined Control. Sensitivity analysis can also be performed by varying the two parameters associated to control strategies at the same time. Figure 6 shows the results of combined control, by varying ρ and ξ simultaneously. Resulting percentage reductions on the cumulative number of newly infected when compared with a without control scenario at the end of 40 years simulation are shown in Table 4.

We also explored the effect of a certain cure rate on the dynamics of infected individuals. The effectiveness due to treatment with nifurtimox and/or benznidazole in patients in the chronic indeterminate phase of Chagas disease is about 7-8% [3].

According to [10], the index of underdiagnosis in Spain is in the range 92.0-95.6%. It justifies the low values considered for the percent of detected individuals in model simulation,

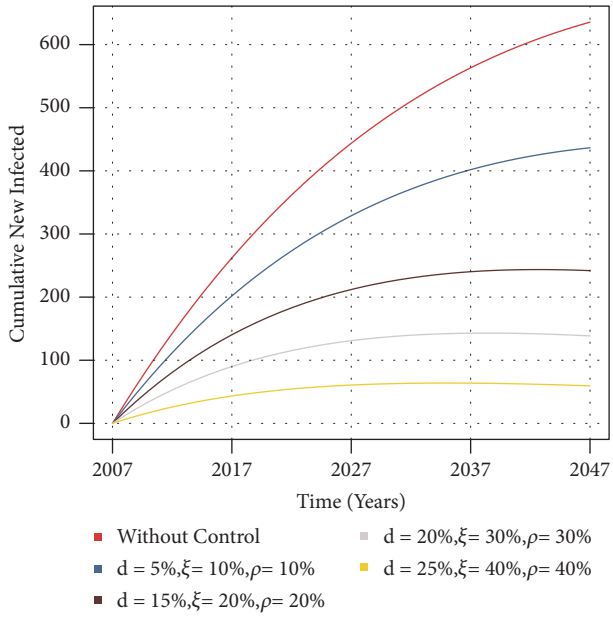

Figure 7: Sensitivity analysis considering detection and treatment of infected individuals d, treatment of infected newborns ρ, and surveillance in blood transfusion transmission ξ.

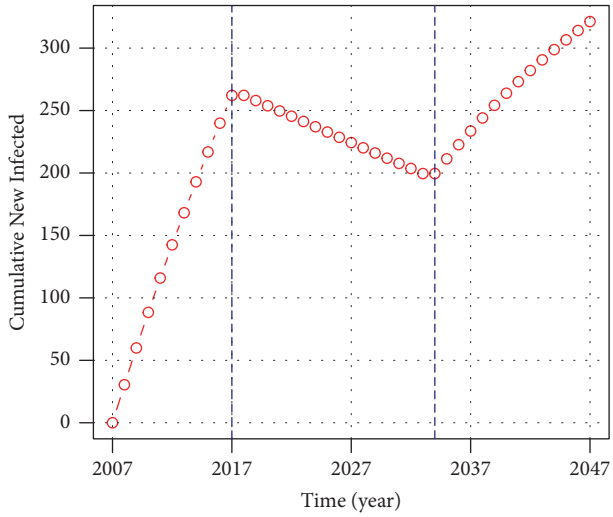

Figure 8: The result of simulation of interrupted control. Parameters associated with control strategies were $d = 25\%$ (detection of infected people), $\rho = 80\%$ (treatment of infected newborn), and $\xi = 80\%$ (effectiveness on surveillance in blood transfusion). The control strategies were applied after 10 years of simulation. After 15 years of application, the control strategies were stopped.

included in the parameter d. Based on that, we set the treatment effectiveness as $e = 7.5\%$ and varied the detection and treatment of infected individuals d. The cure rate is assessed as $C = 7.5\% \cdot d$.

The detection and treatment of infected patients are difficult, mainly due to the asymptomatic characteristics of the disease [10] but also because of other barriers such as health care access limitations or the own misperception of the disease [29]. Therefore, we varied the parameter d between 0 and 25%.

Table 5: Percentage reductions on the total number of infected individuals by varying the proportion of detection and treatment of infected individuals d.

d values	Reduction (%)
$d = 5\%$	13.93
$d = 15\%$	36.23
$d = 20\%$	45.11
$d = 25\%$	52.76

Table 6: Percentage reductions for each parameter variation.

Parameters	Reduction (%)
d = 5%, ξ= 10%, ρ= 10%	22.63
d = 15%, ξ= 20%, ρ= 20%	48.78
d = 20%, ξ= 30%, ρ= 30%	60.51
d = 25%, ξ= 40%, ρ= 40%	69.75

Percentage reductions in the total number of infected individuals from the initial year simulation to 40 years are shown in Table 5.

The cumulative number of new infected is strongly affected by the introduction of the cure rate. Figure 7 displays the sensitivity analysis by varying the parameters ρ, ξ, and d. The corresponding percentage reductions when compared with the scenario without control at the end of 40 years simulation for each parameter combination are displayed in Table 6.

3.5.4. Interrupted Control. Another interesting scenario explored by our model was the simulation of interrupted control. We simulated the cumulative number of new cases by applying control strategies after ten years without control, followed by a control period of 15 years, and interrupted again after this period. We used a detection proportion of 25%, a treatment success of 80% of infected newborns, and surveillance in blood transfusion 80% effective. Figure 8 displays the result. In the first ten years, the number of new cases increases because there are more infected people in the population. When control strategies are performed, the number of new cases decreases because infected people are treated avoiding transmission by congenital and blood transfusion routes. When the control strategies are stopped, the number of new cases start increasing again, since there will be more infected newborns and people infected by blood transfusions over time.

4. Discussion

In this work, we used a compartmental mathematical model to evaluate the dynamics of Chagas disease in a scenario with vector absence, where the transmission can only occur through congenital or blood transfusion routes.

Our results show that, although the total number of infected individuals presents a decreasing behavior (Figure 2), in 40 years its reduction reaches less than half of its initial value, even assuming a death rate for infected individuals as twice the rate for healthy people and no immigration. It means that if the disease is not taken seriously, it can be present in the population for a long period of time [31], even with the vector absence, generating a burden to the public health system which should be prepared to provide patient care and conduct an adequate treatment in order to prevent the long-term disease manifestations.

According to the model, transmission exclusively due to blood transfusion has a smaller impact on the number of new cases when compared with the transmission exclusively due to congenital route (Figure 3). Low prevalence in blood banks in countries with vector absence, oftentimes by self-exclusion of Latin American immigrants in transfusion services, can explain this fact [9]. Nevertheless, blood screening should be sustained and it is vital to prevent infection through transfusion and organ transplantation also in nonendemic countries. Optimizing blood transfusion safety and screening is one of the resolutions of the World Health Assembly for the control and elimination of Chagas disease (WHA 63.20) [7]. In Spain, the control strategy is based on selective donor screening from a questionnaire and it has been implemented since 2005. Donations from at-risk individuals are accepted and the blood is tested [15]. It can prevent a transfusion by a contaminated blood sample beyond identifying infected people. Simulation results plotted in Figures 4 and 5 display the application of isolated control strategies. They show that, even if all infected newborns are treated or if a totally effective surveillance in blood banks is reached, the reduction on the number of new cases when compared with a scenario without control is not 100% achieved.

The model simulation also shows that application of combined control strategies (i.e., treatment of infected newborns and effective surveillance in blood transfusion) can lead to a more significant reduction in the number of new cases when compared with a scenario without control (Figure 6). For instance, treating 80% of infected newborns and having 60% of effectiveness on surveillance in blood banks entails 72.6% less new infections when compared with a scenario without control. It is important to highlight that, although there are standard protocols to deal with the disease control, the quality of the service is very important and sometimes difficult to be measured. In this sense, the study of patients' perceptions and experiences should be included in such protocols in order to increase the quality assessment of services. This fact justifies the values used on our parameters associated with control strategies, varying from 20% to 100% on the effectiveness.

Regarding congenital transmission, an important fact to mention is that the majority of Latin American immigrants in Italy, Japan, Switzerland, Australia, and New Zealand are women in childbearing age, highlighting the importance of programs to screen pregnant women. These programs lead to an early detection of congenital transmission, as stated in World Health Assembly [7]. By 2014 only the Tuscany region in Italy had legislation to screen pregnant women from areas considered endemic [8]. In Spain, only Catalonia, Valencia, and Galicia regions had protocols in screening pregnant women from Latin America up to 2014 [8]. The other countries do not have national programs for disease prevention [32, 33]. The adoption of screening protocols is extremely important since the identification and treatment of infected newborns have good therapeutic results [24].

Although the detection of infected people is difficult due to the asymptomatic characteristic of the disease leading to an underestimation on the number of current cases [10], our model tested the effect of a cure rate due to treatment. This cure rate can be understood as a reduction in the number of parasites inside the host body. Treatment in chronic cases can reduce long-term complications caused by the disease [3, 34]. Nevertheless, treatment accessibility should be guaranteed for all of the diagnosed patients by eliminating existing barriers [29]. Regarding women in childbearing age, detection and treatment also prevent congenital transmission [35, 36].

Our model results are in accordance with this fact since the detection and treatment of infected people have an impact on the cumulative number of new infections (Figure 7). One important strategy to track infected people is by active surveillance in primary care and community action in order to identify pregnant women and follow up their children [37]. Even with a great effort to conduct this kind of strategy, in some cases, infected people can be lost. The simulations results show that there is a reduction in the number of total infected people by 52.76% if 25% of infected people are detected and treated when compared with a scenario without control. The detection and treatment also reduce the number of new cases when combined with treatment of infected newborns and surveillance on blood transfusions. For example, detecting 25% of infected individuals, treating 40% of infected newborns, and having a surveillance in blood banks 40% efficient, the number of new cases is almost 70% smaller when compared with a scenario without control. It is important that the control strategies are sustained; otherwise, the disease elimination will take even longer to be achieved. Figure 8 displays a result of a simulation where the control is applied for a limited period and it is then interrupted. During the period where control applications are performed, the number of new cases decreases, but it starts increasing again when control stops.

The model was applied to Spain, a country without the vector presence, but it could be similarly applied to other countries with vector absence in order to carry out a diagnosis of the current epidemiological situation and determine the order of magnitude of such control strategies' effects.

It should be recalled that a model is a simplified description of reality. Consequently, it entails necessary simplifications in order to focus on the stated aims. The proposed model was sufficient to show the importance of sustaining the control strategies considered in order to advance steadily towards the disease elimination. Otherwise, it will be present in a population for a long time causing long-term clinical manifestation and a burden on the public health system.

Other aspects can be also explored in future works as, for example, the introduction of migrations rates. Nevertheless, although migration flows have a straightforward effect on

Chagas disease dynamics in nonendemic countries, they are usually unpredictable and difficult to control. Therefore, *in silico* experiments could be used for exploring different scenarios and proposing possible actions to revert those negative epidemiological effects. Another control strategy that could be incorporated into the model for its testing is the screening of specific collectives in order to detect (and treat, if necessary) new asymptomatic cases among at-risk populations [38]. In the case of women in childbearing age, treating infected women before a future pregnancy would prevent congenital transmission [36].

Finally, it is also important to point out that the inter- and transdisciplinary work among modelers, health practitioners, community health workers, patients' associations, and other context-specific actors is essential for generating and implementing effective tools for decision making and public health control policies. In that sense, the development of simple models and user-friendly simulation platforms will guarantee that this necessary collaboration between modeling experts and nonexperts is feasible.

5. Conclusions

Mathematical models can be used as a valuable tool to explore different scenarios related to disease spread, as well as to estimate the epidemiological impact when control strategies are implemented. Interdisciplinary collaboration is extremely important in this context since it can improve decision making for the implementation of public policies in order to reduce the disease burden in public health.

Data Availability

The epidemiological and demographic data supporting this study are from previously reported studies and datasets, which have been cited. The processed data is available from the corresponding author upon request.

Conflicts of Interest

The authors declare that there are no conflicts of interest regarding the publication of this paper.

Acknowledgments

This research was partially funded by the Coordenação de Aperfeiçoamento de Pessoal de Nível Superior, Brasil (CAPES), Finance Code 001. Our best thanks are due to Dr. Pedro Albajar-Viñas for his important comments and suggestions. Preliminary results of this article were presented to XIV Workshop of Chagas Disease (XIV Taller sobre la Enfermedad de Chagas) and International Conference on Digital Health.

References

[1] *WHO, World Health Organization. Chagas Disease (American trypanosomiasis)*, 2017, http://www.who.int/mediacentre/factsheets/fs340/en/.

[2] "The importance of the multidisciplinary approach to deal with the new epidemiological scenario of Chagas disease (global health)," *Acta Tropica*, vol. 151, pp. 16–20, 2015.

[3] P. A. S. Junior, I. Molina, S. M. F. Murta et al., "Experimental and Clinical Treatment of Chagas Disease: A Review," *The American Journal of Tropical Medicine and Hygiene*, vol. 97, no. 5, pp. 1289–1303, 2017.

[4] E. Massad, "The Elimination of Chagas' Disease from Brazil," *Epidemiology and Infection*, vol. 136, pp. 1153–1164, 2008.

[5] A. Rassi Jr., A. Rassi, and J. A. Marin-Neto, "Chagas disease," *The Lancet*, vol. 375, no. 9723, pp. 1388–1402, 2010.

[6] C. Di Girolamo, C. Bodini, B. Marta, A. Ciannameo, and F. Cacciatore, "Chagas disease at the crossroad of international migration and public health policies: why a national screening might not be enough," *Eurosurveillance*, vol. 15, no. 37, 2011, Eurosurveillance.

[7] World Health Organization (WHO), *Chagas disease: control and elimination. Resolutions and Decisions WHA 63.20*, WHO, Geneva, 2010, http://www.who.int/neglected_diseases/mediacentre/WHA_63.20_Eng.pdf.

[8] A. Requena-Méndez, P. Albajar-Viñas, A. Angheben et al., "Health Policies to Control Chagas Disease Transmission in European Countries," *PLOS Neglected Tropical Diseases*, vol. 8, no. 10, p. e3245, 2014.

[9] A. Requena-Méndez, E. Aldasoro, E. de Lazzari et al., "Prevalence of Chagas Disease in Latin-American Migrants Living in Europe: A Systematic Review and Meta-analysis," *PLOS Neglected Tropical Diseases*, vol. 9, no. 2, p. e0003540, 2015.

[10] L. Basile, J. Jansa, Y. Carlier et al., "Chagas disease in European countries: the challenge of a surveillance system," *Chagas disease in Europe*, vol. 16, no. 37, 2011.

[11] Organización Panamericana de la Salud, *Estimación cuantitativa de la enfermedad de Chagas en las Américas. Spanish*, 2006, http://www.bvsops.org.uy/pdf/chagas19.pdf.

[12] G. A. Schmunis and Z. E. Yadon, "Chagas disease: a Latin American health problem becoming a world health problem," *Acta Tropica*, vol. 115, no. 1-2, pp. 14–21, 2010.

[13] M. Navarro, B. Navaza, A. Guionnet, and R. López-Vélez, "Chagas Disease in Spain: Need for Further Public Health Measures," *PLOS Neglected Tropical Diseases*, vol. 6, no. 12, 2012.

[14] M. Piron, M. Vergés, J. Muñoz et al., "Seroprevalence of *Trypanosoma cruzi* infection in at-risk blood donors in Catalonia (Spain)," *Transfusion*, vol. 48, no. 9, pp. 1862–1868, 2008.

[15] A. Angheben, L. Boix, D. Buonfrate et al., "Chagas disease and transfusion medicine: A perspective from non-endemic countries," *Blood Transfusion*, vol. 13, no. 4, pp. 540–550, 2015.

[16] C. Riera, R. Fisa, C. Martin, A. Guarro, M. Castro, J. M. Jorba et al., "Congenital transmission of *Trypanosoma cruzi* in Europe (Spain): a case report," *The American Journal of Tropical Medicine and Hygiene*, vol. 75, no. 6, pp. 1078–1081, 2006.

[17] J. Muñoz, M. Portús, M. Corachan, V. Fumadó, and J. Gascon, "Congenital *Trypanosoma cruzi* infection in a non-endemic area," *Transactions of the Royal Society of Tropical Medicine and Hygiene*, vol. 101, no. 11, pp. 1161-1162, 2007.

[18] J. X. Velasco-Hernández, "A model for Chagas disease involving transmission by vectors and blood transfusion," *Theoretical population biology*, vol. 46, pp. 1–31, 1994.

[19] H. Inaba and H. Sekine, "A mathematical model for Chagas disease with infection-age-dependent infectivity," *Mathematical Biosciences*, vol. 190, no. 1, pp. 39–69, 2004.

[20] S. M. Raimundo, E. Massad, and H. M. Yang, "Modelling congenital transmission of Chagas' disease," *Biosystems*, vol. 99, pp. 215–222, 2010.

[21] D. J. Coffield Jr., A. M. Spagnuolo, M. Shillor et al., "A Model for Chagas Disease with Oral and Congenital Transmission," *PLoS ONE*, vol. 8, no. 6, 2013.

[22] M. Fabrizio, N. J. Schweigmann, and N. J. Bartoloni, "Modelling inter-human transmission dynamics of Chagas disease: analysis and application," *Parasitology*, vol. 141, pp. 837–848, 2014.

[23] "The World Bank, Birth rate, crude (per 1,000 people)," https://data.worldbank.org/indicator/SP.DYN.CBRT.IN?locations=ES.

[24] J. Muñoz, O. Coll, T. Juncosa et al., "Prevalence and vertical transmission of *Trypanosoma cruzi* infection among pregnant latin american women attending 2 maternity clinics in Barcelona, Spain," *Clinical Infectious Diseases*, vol. 48, no. 12, pp. 1736–1740, 2009.

[25] "The World Bank, Death rate, crude (per 1,000 people)," https://data.worldbank.org/indicator/SP.DYN.CDRT.IN?locations=ESview=chart.

[26] Z. M. Cucunubá, O. Okuwoga, M.-G. Basáñez, and P. Nouvellet, "Increased mortality attributed to Chagas disease: a systematic review and meta-analysis," *Parasites & vectors*, vol. 9, p. 42, 2016.

[27] R. A. Gallastegui, C. C. Izaguirre, E. C. Brustenga et al., "Enfermedad de Chagas y Donación de Sangre," *Ministerio de Sanidad y Política Social*, 2009, Ministerio de Sanidad y Política Social.

[28] J. A. García-Erce, A. Campos, and M. Muñoz, "Blood donation and blood transfusion in Spain (1997-2007): the effects of demographic changes and universal leucoreduction," *Blood Transfusion*, vol. 8, p. 100, 2010.

[29] M. Navarro and J. J. de los Santos, "Access to Chagas disease treatment in non-endemic countries: the case of Spain," *The Lancet Global Health*, vol. 5, p. e577, 2017.

[30] "The World Bank, Population, total," https://data.worldbank.org/indicator/SP.POP.TOTL?locations=ES.

[31] J. Coura and P. Vinas, "Chagas disease: a new worldwide challenge," *Nature*, pp. 56-57, 2010.

[32] Y. Jackson and F. Chappuis, "Chagas disease in Switzerland: history and challenges," *Eurosurveillance*, vol. 16, 2011.

[33] K. Imai, T. Maeda, Y. Sayama et al., "Chronic Chagas disease with advanced cardiac complications in Japan: Case report and literature review," *Parasitology International*, vol. 64, no. 5, pp. 240–242, 2015.

[34] D. L. Fabbro, M. L. Streiger, E. D. Arias, M. L. Bizai, M. Del Barco, and N. A. Amicone, "Trypanocide treatment among adults with chronic Chagas disease living in Santa Fe City (Argentina), over a mean follow-up of 21 years: Parasitological, serological and clinical evolution," *Journal of the Brazilian Society of Tropical Medicine*, vol. 40, no. 1, pp. 1–10, 2007.

[35] S. Sosa-Estani, E. Cura, E. Velazquez, C. Yampotis, and E. L. Segura, "Etiological treatment of young women infected with *Trypanosoma cruzi*, and prevention of congenital transmission," *Journal of the Brazilian Society of Tropical Medicine*, vol. 42, no. 5, pp. 484–487, 2009.

[36] D. L. Fabbro, E. Danesi, V. Olivera et al., "Trypanocide Treatment of Women Infected with *Trypanosoma cruzi* and Its Effect on Preventing Congenital Chagas," *PLOS Neglected Tropical Diseases*, vol. 8, no. 11, p. e3312, 2014.

[37] A. Soriano-Arandes, L. Basile, H. Ouaarab et al., "Controlling congenital and paediatric Chagas disease through a community health approach with active surveillance and promotion of paediatric awareness," *BMC Public Health*, vol. 14, no. 1, 2014.

[38] A. Requena-Méndez, S. Bussion, E. Aldasoro et al., "Cost-effectiveness of Chagas disease screening in Latin American migrants at primary health-care centres in Europe: a Markov model analysis," *The Lancet Global Health*, vol. 5, no. 4, pp. e439–e447, 2017.

Hindawi
Complexity
Volume 2018, Article ID 4680140, 31 pages
https://doi.org/10.1155/2018/4680140

Research Article

Complexities in Financial Network Topological Dynamics: Modeling of Emerging and Developed Stock Markets

Yong Tang[1,2,3] **Jason Jie Xiong,**[4] **Zi-Yang Jia,**[5] **and Yi-Cheng Zhang**[3,6]

[1] *Center of Cyberspace and Security, School of Computer Science and Engineering, University of Electronic Science and Technology of China, Chengdu 610054, China*
[2] *School of Management and Economics, University of Electronic Science and Technology of China, Chengdu 610054, China*
[3] *Department of Physics, University of Fribourg, Chemin du Musée 3, CH-1700 Fribourg, Switzerland*
[4] *Department of Computer Information Systems and Supply Chain Management, Walker College of Business, Appalachian State University, Boone, NC 28608, USA*
[5] *Department of Computer Science, Rutgers University, Piscataway, NJ 08854, USA*
[6] *Institute of Fundamental and Frontier Sciences, University of Electronic Science and Technology of China, Chengdu 610054, China*

Correspondence should be addressed to Yong Tang; tangyong@uestc.edu.cn

Received 17 May 2018; Accepted 16 September 2018; Published 1 November 2018

Guest Editor: Claudio Tessone

Policy makings and regulations of financial markets rely on a good understanding of the complexity of financial markets. There have been recent advances in applying data-driven science and network theory into the studies of social and financial systems. Financial assets and institutions are strongly connected and influence each other. It is essential to study how the topological structures of financial networks could potentially influence market behaviors. Network analysis is an innovative method to enhance data mining and knowledge discovery in financial data. With the help of complex network theory, the topological network structures of a market can be extracted to reveal hidden information and relationships among stocks. In this study, two major markets of the most influential economies, China and the United States, are systematically studied from the perspective of financial network analysis. Results suggest that the network properties and hierarchical structures are fundamentally different for the two stock markets. The patterns embedded in the price movements are revealed and shed light on the market dynamics. Financial policymakers and regulators can gain inspiration from these findings for applications in policy making, regulations design, portfolio management, risk management, and trading.

1. Introduction

The visualization of networks and research of hierarchy structures are essential to study complex systems like financial markets. Thanks to the significant development of complex network science [1], quantitative methods and models have been applied in the studies of financial markets network structure. In financial network analysis, entities like assets, stocks, markets, companies, and institutions are modeled as vertices while their mutual relationships are abstracted as edges. This approach empowers industrial professionals and researchers to reveal hidden information embedded in the topological structures of financial networks, such as the market dynamics, trading activities, and investment sentiment. This information is essential to evaluate and monitor the financial market risks, contagions, distress propagation, as well as market mode shifts. Financial network analysis has been utilized in applications like portfolio management, trading, market regulation, stress testing, and risk management.

The USA and China are the top two dominating economies with influences over the global economies. The two economies are similar in market size. However, the US economy is well established and developed while the Chinese economy is emerging and still undertaking fast development. As the leading economic powerhouses, the health and stabilities of these two economies are vital for the prosperities of the world economy. During the past few years, both countries suffered a series of stock market disasters, such

as the 2008 US subprime crisis and the 2007 and 2015 Chinese stock market bubble bursts. These dramatic market crashes brought widespread and long-lasting negative impacts on economies and markets. The stock markets of both countries are also different regarding history, regulations, maturities, and scales. Thus, it is essential to understand the properties of these two markets by utilizing the data-driven science approach. Recently, various major markets in the world have been investigated using the financial network analysis approach. However, there is still a lack of systematical studies dedicating to compare the network structures and properties of the US and Chinese stock markets using the financial network analysis approach.

To understand how the two markets differ in the structures and topological properties, as well as the dynamics market properties, this research investigates the markets using a dataset spanning over nine years. In this research, the stock markets are modeled as multiple networks including hierarchical trees, minimum spanning trees, planar maximally filtered graphs, and assets graphs. Meanwhile, their detailed topological properties are analyzed and systematically compared. Through quantitative analysis and network visualization, results show the two markets are different in many ways. This provides insights for regulators on the structures and dynamics of stock markets from the perspective of network science.

This paper is organized as follows. First, Section 2 gives a background on the theory of complex networks, financial network analysis, and relevant complex network parameters are introduced. Then, in Section 3, the data and method used to construct networks are described. Section 4 presents the network properties. In Section 5, the detailed hierarchical structures of both stock networks are carefully investigated and compared. Finally, conclusions and discussions are presented in Section 6.

2. Literature Review of Financial Network Analysis

Network science has become an innovative tool widely used in studies of complex systems in a variety of engineering and scientific domains [2–4]. The network modeling methodologies and theoretical frameworks have revealed informative and useful empirical discoveries [5]. Studying the statistical properties such as degree distribution, average length, and clustering coefficient can help describe the networks topologies and the dynamics of network evolution. Furthermore, it is possible to study the information spreading, network stability, and phase changes and hopefully to predict and control the network dynamics [6].

Time series data can be modeled as networks [7, 8]. For price time series [9], calculation of correlation matrices for a group of assets is possible [10–12]. From the correlation matrices, financial network analysis could be applied to construct networks for further analysis and data mining [13–17]. In most existing literature, assets are treated as vertices, while the interconnectivity relationships are modeled as pairwise edges among assets. The correlation matrices are not only important for network analysis and topological visualization but also serve as a bridge between financial network analysis and traditional finance theories. This is similar to modern portfolio theory (MPT) [18, 19], which is based on the correlation relationships among assets. Network-based portfolio selection has been proposed for optimization and empirically proofed workable [20].

Since the minimum spanning tree approach is first used in the study of stock market structure [21], financial network analysis has grown into an essential tool of financial big data. However, this fast-growing field is still at an early stage [22]. Financial network analysis provides an unprecedented perspective shedding new insights on evaluating the market stability, market risk, shock propagation, and contagion [23–25]. The connectedness among assets plays the critical role of market contagion phase transition [26] which is similar to other tolerance properties of other nonfinancial complex networks [27]. Further research reveals that intermediate level of risk diversification can enhance the market robustness [28]. The importance and risk contribution of companies can be identified through the network analysis [29, 30]. The systemic risks and stability can also be evaluated according to the topological properties of the financial network, and providing implications for market regulations [22, 31, 32]. Through investigating the clustering of assets, portfolio optimization can be achieved with better predicted over realized risks [33]. Overlapping of portfolios is revealed by network analysis as one primary factor for market contagion [34]. In another approach, risk spillover networks are constructed to study the behaviors of financial institutions [35]. Instead of a single layer approach, by building multiple-layer network, the banking system risk is analyzed and quantified [36]. Regression models can also take network structure into consideration as factors for resilience and robustness of the markets [37]. This financial network approach opens more interesting new possibilities and dramatically enriches regression models in finance studies. Recently, there has been a thread of studies on major players in financial networks, such as 'too interconnected to fail' institutions [38], 'too central to fail' [39], and 'too big to fail' [40]. The research demonstrated that financial network analysis brings new insights to finance studies and benefits to finance practices.

In the rise of quantitative trading, the causality and lead/lag relationships revealed by financial network analysis can be particularly interesting for trading strategy design [41, 42]. Many researches have revealed stylized evidence that the network structure has a profound influence on the asset returns [43]. Taking risks into consideration, it has been found that investing in peripheries of financial networks might generate better returns over risks [44]. Furthermore, industry professionals would be inspired by financial network analysis to seek price movement signals for potential predictions [45].

While most existing financial network analysis literatures focus on the stock markets or specific economy sectors [46–48], a variety of financial systems have been studied as financial network such as global financial institutions [39, 40], world trade web [49, 50], interbank markets [51–54], exchanges [55], monetary market [56], corporate networks [57, 58], global banking [59], CDS market [60], and credit market [61].

Many major individual financial markets around the world have also been studied in network approach, such as US [62, 63], China [64–66], Germany [67, 68], EU [69–71], Brazil [33, 72], Italian [53, 56], Korea [73], Russia [74], and Mexico [36, 75]. Furthermore, there is literature focusing on the cross-board global markets [76, 77]. Using the partial data, networks of global markets are reconstructed, and methods are compared [56]. Bayesian graphical models are applied to identify groups of counties which are major contributors to systemic risks according to banking behaviors in the global banks [78]. For the European markets, the risk and contagion channels are studied, and results show the EU markets are vulnerable to risks [71]. Global stock exchange network is investigated to evaluate the attractions for IPOs [79]. A recent study has demonstrated the approach which uses transfer entropy to study a selection of major individual stocks around the world and reveals that stocks are clustered according to their countries and industries [80]. By looking into the network structures of the global financial network, it is possible to give new insights into the international business cycle [81]. The diversification and participation are investigated for various economies [82].

Considering a large number of assets in financial markets, the initial networks have massive edges. By filtering the noises of the networks, the financial networks can be significantly simplified to enable advanced analysis such as principal component analysis (PCA) [76] and random matrix theory (RMT) [83, 84] to further extract hidden patterns. Hierarchical tree (HT) [21, 68], minimum spanning tree (MST) [85], planar maximally filtered graphs (PMFG) [86], asset graph (AG) [87, 88], and partial correlation network [15, 89, 90] are major approaches applied in filtering financial networks. Mantegna [21] first introduces the minimum spanning tree method into the study of hierarchical structures in financial markets. With the network, we can study the topological structure of a market or a portfolio. In this research, we adopt the frameworks to study the correlations and the corresponding networks of stock markets both in China and the United States to systematically study how the two markets behave differently.

3. Data and Research Methods

3.1. Indices of CSI300 and S&P500. We study the stock markets of China and United States: the former is a typical representative of emerging countries with fast-growing GDP rate and influence on global economies, while the latter is the most established and developed economy in the world. To study the major stocks of each market, we focus on the component stocks of the major indices of the two stock markets, i.e., China Securities Index 300 (CSI300) for the Chinese stock market and Standard & Poor's 500 (S&P500) for the US market. In our study, we cover a period of nine years starting from 04/01/2007 and ending on 06/11/2015 with 2149 trading days for CSI300 and 2228 trading days for S&P500. The reason why the two markets have different numbers of trading dates is that the two markets have different trading calendars. Index and all component stocks daily price data of CSI300 are retrieved from the CSMAR Solution Database of Shenzhen GTA Education Tech. Ltd. We download the S&P500 index and component stocks daily prices data through Yahoo finance service. Since not all stocks are traded on each trading date, so we only select those CSI300 stocks with at least 2000 trading dates, and without continuous 100 nontrading dates, this selection results in a final set of 163 stocks. For S&P500, we select those stocks with at least 2100 trading dates, and in results, we get 468 stocks. After stocks selection, we take the prices on the available closest trading date to fill the nontrading dates. In Figures 1(a) and 1(b) we plot the daily close prices and the daily log returns for the index of CSI300 in the study period of 04/01/2007 and 06/11/2015 with 2149 trading days. In Figures 1(c) and 1(d), we plot the daily close prices and the daily log returns for the index of S&P500 in the same study period from 04/01/2007 to 06/11/2015 with 2228 trading days. From the figures, we see that the two markets show large fluctuations in the last nine years. CSI300 experienced huge market crashes in 2008 and 2015, while S&P500 kept climbing almost continuously after the 2008 financial crisis.

3.1.1. CSI300. China has two independent stock market exchanges, i.e., the Shanghai stock exchange and the Shenzhen stock exchange. Opened at the beginning of 1990s with only 25 years of trading history, the two markets have grown into important financial markets playing vital roles in China's financial markets and economy. Among the many stock market indices, the China Securities Index 300, or CSI300, was introduced by the China Securities Index Company, Ltd. in 2005 to a base of 1000 on 31/12/2004. In CSI300, a set of 300 stocks are included as the index components; all of them have the largest market values and are actively traded in Shanghai or Shenzhen stock exchanges. CSI300 has become a widely accepted benchmark to evaluate the whole stock markets behaviors in China as well as a good basis for other derivative products. Starting from 1000 points in the early of 2004, now CSI300 has reached 3793 points as of 06/11/2015 [91]. To give an image of the Chinese stock market, we plot the 2149 CSI300 index daily close prices and daily log returns in the study period between 04/01/2007 and 06/11/2015 in Figures 1(a) and 1(b). In the past nine years, CSI300 experienced two major market crashes in 2007-2008 and 2015, respectively, during which the market suffered huge losses and fluctuations. There are 163 stocks of CSI300 component stocks included in our dataset, as shown in Table 1, in which we summarize the numbers of these 163 stocks for all 20 industry sectors. As shown, all industry sectors from Agriculture to Comprehensive are represented. For convenience, we will refer to these 163 stocks as *CSI163* in the following parts.

3.1.2. S&P500. Compiled by Standard & Poor's in 1957, the S&P500 is an established American stock market index with more components, more risk diversification, and better reflection of the overall stock market performance than both the New York Stock Exchange (NYSE) and Nasdaq. All components are large stocks in capitalization with good liquidities and diversifications in different industry sectors. The S&P500 represents major parts of the market and is

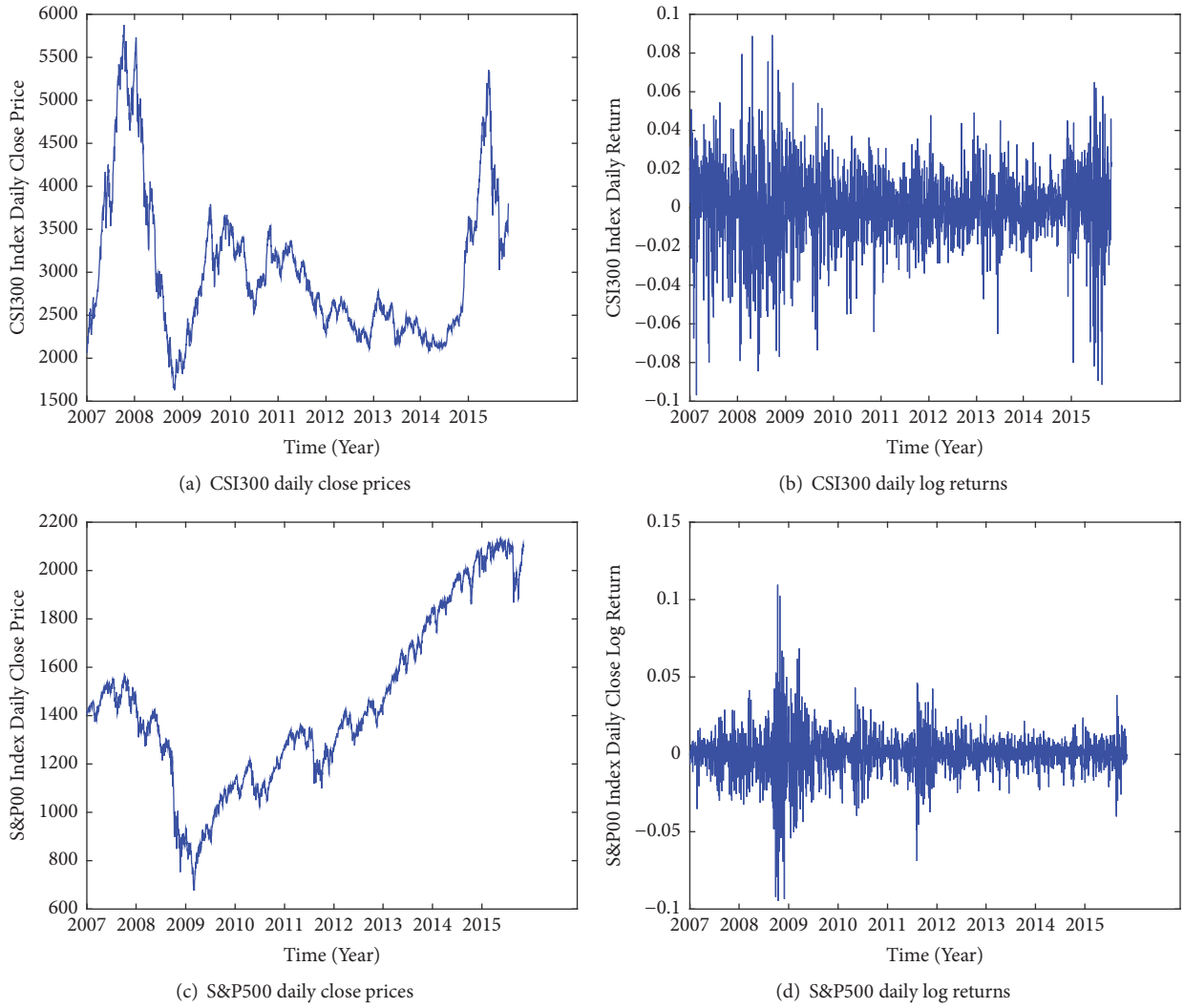

(a) CSI300 daily close prices

(b) CSI300 daily log returns

(c) S&P500 daily close prices

(d) S&P500 daily log returns

Figure 1: CSI300 index daily close prices (a) and log returns (b) in the study period between 04/01/2007 and 06/11/2015 with 2149 trading days. S&P500 index daily close prices (c) and log returns (d) in the study period between 04/01/2007 and 06/11/2015 with 2228 trading days.

considered as one of the best benchmarks for the US financial markets and economy. Starting from less than 100, after more than 50 years of development, the S&P500 reached 2099 on 06/11/2015 [92]. We plot 2228 daily close prices and log returns of the index of the S&P500 in our study period between 04/01/2007 and 06/11/2015 in Figures 1(c) and 1(d). We can observe that the S&P500 index suffered a major crash between 2008 and 2009 then recovered almost steadily with minor fluctuations. After the selection, there are 468 stocks of the S&P500 component stocks included in our dataset, as shown in Table 2. We summarize the numbers of these 468 stocks for all ten industry sectors. As shown, all industry sectors from Energy to Utilities are represented. For convenience, from now we will refer to these 468 stocks as *S&P468* in the following parts. Table 3 gives a summary of the two datasets of both CSI163 and S&P468; CSI163 has a larger standard deviation σ_r of the log returns, indicating larger fluctuations than S&P468. We use $\langle x \rangle$ to denote the average of variable x in this paper.

3.2. Construction of Stock Networks

3.2.1. Price Returns and Correlations. From the time-stamped price time series of a blanket of stocks, it is possible to calculate the correlations for any pair of stocks once a time window is given. $P_i(t)$ is the price at time t of stock s_i. It could be one of the daily prices of open, close, high, or low. Per most literature suggests, we choose the most used daily close price. To smooth the fluctuation without loss of generality, the logarithmic return for s_i in the period of $[t - \Delta t, t]$ is defined as

$$Y_i(t) = \ln P_i(t) - \ln P_i(t - \Delta t), \quad (1)$$

and usually used instead of $P_i(t)$ itself. In most cases, daily log returns are used where $\Delta t = 1$. For stock pair of s_i and s_j, we can extract the two price time series in a time window with a length or size of L, i.e., with L price values included in the window. The selection of L is expected to meet the requirement of $L/N > 1$. In a sliding window approach, we

Table 1: 163 component stocks of CSI300 are included in our dataset. In this table, we list the China Securities Regulatory Commission (CSRC) industry code, sector name, and numbers of stocks for each industry sector of these 163 stocks. All 20 industry sectors are represented.

Industry code	Industry Sector	Number of Stocks
A	Agriculture	1
B	Mining	6
C0	Food & Beverage	4
C1	Textiles & Apparel	4
C3	Paper & Printing	2
C4	Petrochemicals	9
C5	Electronics	7
C6	Metals & Non-metals	20
C7	Machinery	27
C8	Pharmaceuticals	15
D	Utilities	6
E	Construction	5
F	Transportation	10
G	IT	8
H	Wholesale & retail trade	10
I	Finance and insurance	10
J	Real estate	11
K	Social Services	3
L	Communication & Cultural Industry	2
M	Comprehensive	3

Table 2: 468 component stocks of S&P500 are included in the dataset. In this table, we list the Global Industry Classification Standard (GICS) code, sector name, and number of stocks for each industry sector in S&P500. All ten industry sectors are represented.

Industry code	Industry Sector	Number of Stocks
10	Energy	36
15	Materials	26
20	Industrials	63
25	Consumer Discretionary	78
30	Consumer Staples	33
35	Health Care	50
40	Financials	87
45	Information Technology	61
50	Telecommunication Services	5
55	Utilities	29

Table 3: Basic information of CSI163 and S&P468 datasets including the number of stocks, the number of trading days, the average log returns $\langle r \rangle$, and the standard deviation σ_r of the log returns is presented. Compared to the US market, the Chinese market has higher fluctuations in our study period between 04/01/2007 and 06/11/2015.

Dataset	Stocks	Days	$\langle r \rangle$	σ_r	$\langle r_{\min} \rangle$	$\langle r_{\max} \rangle$
CSI163	163	2149	1.4795e-04	0.0340	-0.4832	0.1002
S&P468	468	2228	1.4691e-04	0.0252	-0.3413	0.2168

can extract subsets of prices in a serial of sliding windows: $[1, L]$, $[2, L+1], \cdots$. For a given window, with the two time series of prices, it is possible to generate two log return time series using equation (1) for both stocks s_i and s_j. Thus, the correlation coefficient between two stocks can be calculated by using the Pearson correlation coefficient [21]

$$\rho_{ij} = \frac{\langle Y_i Y_j \rangle - \langle Y_i \rangle \langle Y_j \rangle}{\sqrt{\left(\langle Y_i^2 \rangle - \langle Y_i \rangle^2\right)\left(\langle Y_j^2 \rangle - \langle Y_j \rangle^2\right)}}, \tag{2}$$

where $\langle \cdots \rangle$ stands for the average. The value of ρ_{ij} ranges between -1 and 1, where a negative value of $\rho_{ij} < 0$ indicates the two stocks fluctuate in a noncorrelated manner, i.e., one falls down while another one climbs up. For a positive value of $\rho_{ij} > 0$, the two stocks fluctuate in a positively correlated way. In this case, they move in the same direction. If $\rho_{ij} \approx 0$, then they are not correlated. If $|\rho_{ij}| \approx 1$, then the two stocks are perfectly correlated or noncorrelated. In a stock market, the stocks from the same industry are more likely to be correlated.

For a portfolio of N stocks $s_1, s_2, \cdots, s_N$, we can calculate all $N \times N$ pairs of correlation coefficients ρ_{ij} for any s_i and s_j. These N^2 pairs of values can be expressed as a correlation coefficient matrix C with a size of $N \times N$.

Based on the correlation matrix C, we can define the distance d_{ij} between stock pair of s_i and s_j as

$$d_{ij} = \sqrt{2\left(1 - \rho_{ij}\right)}. \tag{3}$$

The values of d_{ij} form an adjacent symmetric matrix D, in which there are $N(N-1)/2$ different elements. It is verified that this definition satisfies the three rules of Euclidean distance: (1) $d_{ij} = 0$ if and only if $i = j$; (2) $d_{ij} = d_{ji}$;

(3) $d_{ij} \leq d_{ik}+d_{kj}$ [21]. Since $-1 \leq \rho_{ij} \leq 1$, we have $0 \leq d_{ij} \leq 2$. With this definition, the distance for two stocks has a value of 2 when they are completely anticorrelated ($\rho_{ij} = -1$), and a small distance close to 0 when they are positively and completely correlated ($\rho_{ij} \longrightarrow 1$). This makes it possible to compare the distances for any two pairs of stocks.

3.2.2. Network $N(V, E)$. With the adjacency matrix D, we can further construct the network $N(V, E)$ for the stocks, where stock s_i is represented as vertex $v_i \in V$, and $e_{ij} \in V$ represents the edge between v_i and v_j with a distance of d_{ij}. The network $N(V, E)$ is undirected in which only one edge exists between a pair of vertices. The size of the network is the number of stocks N. The possible maximum number of edges is $N(N-1)/2$ for an undirected complete network in which all vertex pairs are connected. For a portfolio with a large number of stocks N, the number of edges is a huge number. Thus it is necessary to simplify the network by filtering less important edges. In a simple threshold approach, by introducing a threshold value θ, we can reduce the network by chopping those edges whose distance are greater than θ and keeping the remaining edges. In other words, we only retain the connections which are strong enough, i.e., those with small distances, and all other weak edges with distances larger than the threshold θ are filtered as the following equation:

$$e_{ij} = \begin{cases} 1 & \text{if } d_{ij} < \theta, \\ 0 & \text{otherwise.} \end{cases} \tag{4}$$

Or in an edge ranking approach, we only keep a certain number of top edges with the strongest relationships, say $N-1$ edges. With this approach, the remaining edges are more likely to form loops in strongly connected vertices and are referred to as an *asset graph* [93].

3.2.3. Network Filtering. By filtering edges in a threshold approach, we may get isolated vertices or loops in the filtered network. To avoid this, tree approaches including *minimum spanning tree* (MST) can be used to chop edges but still keep all vertices connected as a tree. MST is introduced to investigate the hierarchical structure of stock networks first by Mantegna [21]. Many studies also use this approach, such as Jang et al., to investigate the foreign exchange market using in the periods of currency crises finding that the values of correlation coefficients decrease but the normalized tree length increase in crises [94]. Matteo et al. find that the dynamical *planar maximally filtered graphs* (PMFGs) can preserve same hierarchical structure as the dynamical MST, and the financial sector dominates the central role in the network [47]. As an application of network analysis in portfolio management, Onnela et al. suggest the assets of the classic Markowitz portfolio are always located on the outer leaves of the tree [88], and Pozzi et al. further suggest that even it is better to invest in the peripheries of the MST of a market [44]. In [85], MST networks extracted from real correlation data are compared with those generated from artificial random models. Results reveal that the properties of MST from real data cannot be reproduced, showing the uniqueness of real stock networks.

Based on the network $N(V, E)$, we can extract a tree connecting all vertices with $N-1$ edges with a minimum total distance also known as minimum spanning tree (MST) of the stocks. By only using the $N-1$ edges out of the maximum $N(N-1)/2$ edges, the network is dramatically simplified or filtered while keeping the most important shortest edges. To extract the MST, Kruskal's Algorithm was applied in three steps: (1) we rank all edges according to the distances from the shortest to the longest; (2) in each round, we choose the shortest edge into the MST while avoiding loops; (3) we repeat round #2 until all vertices and all $N-1$ shortest edges are added [95]. Bonanno et al. review the MST approach in revealing information of markets [96].

Using the MST, we can construct the *hierarchical tree* (HT) in which the subdominant ultrametric distance $d_{ij}^{<}$ is defined as the maximum distance of an edge along the path between v_i and v_j. The HT satisfies the first two rules with a stronger third one:

$$d_{ij}^{<} \leq \max\left(d_{ik}^{<}, d_{kj}^{<}\right), \tag{5}$$

With this ultrametric inequality, we can construct a hierarchical tree based on a MST and present a unique topological structure of the stocks [21, 97].

By loosening the requirements of MST up to 4 vertices, but forbid crossings, as many as $3(N-2)$ edges containing the MST as the subgraph including all the top $N-1$ shortest edges can be gathered. This new network can be drawn on a planar surface without link crossings is called *planar maximally filtered graphs* (PMFG) [47, 86, 98–101]. This makes PMFG different from MST, which also shows richer structures of the network. In a similar construction to MST, to construct PMFG, we firstly rank the edges in ascending orders according to the distances of edge pairs. Then we add the shortest edges into the PMFG but keeping the genus $g = k$, where the g is the largest number of simple closed curves one can draw on a planar surface without separating it. For the case of $g = 0$, when all edges are considered, PMFG can be gathered [86]. It has also been proved that an MST is a subgraph of a PMFG and the number of 3- and 4-cliques in a PMFG is $3n-8$ and $3n-4$, respectively [102].

Since PMFG contains more edges and allows loops and cliques, there is more information embedded in PMFG than in MST. After the introducing of PMFG into the study of network structures of stocks, PMFG has been used in studies of many stock markets, and more recently, PMFG is applied in investment strategy design [44]. Based on PMFG, a clustering approach called *Directed bubble hierarchical tree* (DBHT) is proposed and show good performance compared with other algorithms and also been applied to study financial data [103]. It has been reported that, in a running window approach, the PMFG shows stronger stability in a long run compared with MST [104].

4. Stock Network Topological Properties

A network $N = (V, E)$ is a graph composed of a set of vertices V and a set of edges E. In a network model, the participants are represented as the vertices V, and the

Table 4: For the CSI163 network, the maximum possible number of edges of $|e|_{\max}$ for $N = 163$ vertices, the existing edge number $|e|$, the edge density $|e|_{density}$, the average degree $\langle d \rangle$, the average distance $\langle d_{ij} \rangle$, the minimum distance $d_{ij}^{\min}$, and the maximum distance $d_{ij}^{\max}$ are presented for different θ from 0 to 1.5 in a step of 0.1.

θ	$\|e\|_{\max}$	$\|e\|$	$\|e\|_{density}$	$\langle d \rangle$	$\langle d_{ij} \rangle$	$d_{ij}^{\min}$	$d_{ij}^{\max}$
0.1	13203	0	0.0000	0.0000	0.0000	0.0000	0.0000
0.2	13203	0	0.0000	0.0000	0.0000	0.0000	0.0000
0.3	13203	2	0.0002	0.0245	0.0000	0.0049	0.0089
0.4	13203	30	0.0023	0.3681	0.0000	0.0010	0.0593
0.5	13203	91	0.0069	1.1166	0.0003	0.0003	0.2200
0.6	13203	276	0.0209	3.3865	0.0010	0.0003	0.3689
0.7	13203	1594	0.1207	19.5583	0.0038	0.0003	0.4291
0.8	13203	5620	0.4257	68.9571	0.0177	0.0004	0.5353
0.9	13203	10555	0.7994	129.5092	0.0666	0.0004	0.7098
1	13203	12816	0.9707	157.2515	0.1866	0.0005	0.7996
1.1	13203	13194	0.9993	161.8896	0.4052	0.0006	0.9443
1.2	13203	13203	1.0000	162.0000	0.6957	0.0902	1.0887
1.3	13203	13203	1.0000	162.0000	0.9637	0.3719	1.1910
1.4	13203	13203	1.0000	162.0000	1.0966	0.5515	1.2878
1.5	13203	13203	1.0000	162.0000	1.1141	0.5515	1.3230

relationship between any pair of two participants i and j is represented as the edge e_{ij} connecting the two vertices v_i and v_j. In this study, the following properties of financial markets are researched: (1) *Degree and Degree Distribution* which describes the connectivities of vertices; (2) *Clustering Coefficient* which is the indication of the transitivity and density of a network; (3) *Average Path Length*, which is a global property indicating how the network spans; (4) *Betweenness Centrality* which describe the global importance or centrality of vertices or edges; (5) *Components* which describe the grouping phenomena of substructures of the networks.

Based on how the correlations are calculated, there are two approaches, static or dynamic. In a static approach, the correlations are calculated over the whole period using all available prices. Thus we get a single static correlation matrix to describe the market regardless of the different market periods. When sliding windows are used in a dynamic approach, we get a sequence of correlation matrices. The static approach, which is the most used in literature, gives a static description of the structure of the market with details of different market periods like bear markets or bull markets. However, the dynamic approach can reveal the evolution of market structures and behaviors, which are especially useful for the comparisons of calm periods and crashes.

In this part, we present the topological properties of stock networks of the two markets, CSI163 and S&P468, in a dynamic approach. Considered to meet the requirement of $L/N > 1$, we set the sliding window size $L_{CSI163} = 170$ for CSI163 and $L_{S\&P468} = 500$ for S&P468. In total, there are 2149 windows for CSI163 and 2228 windows for S&P468. After calculating the log returns for both CSI163 and S&P468 by using equation (1), we calculate the correlation coefficient matrices over the period between 12/09/2007 and 06/11/2015 for CSI163, 26/12/2008 and 06/11/2015 for S&P468 using equation (2). Based on the correlation matrices, it is straight to get stock networks. For CSI163, we have a network of 163 vertices, and for the S&P468, we have a network of 468 vertices. The edge connecting two stocks indicates how the two stocks behave correlatively or anticorrelatively. For a positive correlation coefficient value, the two prices move in the same direction, while for a negative value, the two prices move in opposite directions, so to normalize all correlation coefficients to positive values as edge distances, we adopt the definition of distance based on equation (3). Through this definition, all negative values are transformed into positive distance values, and the order of values is preserved. All vertices in the networks for both markets are fixed. However, the edges vary in each sliding window as the correlation coefficients change. In the following parts, the statistical properties of both networks evolved in our study period are investigated.

4.1. Degree and Degree Distribution. For a network of N stocks, there are $N \times N$ edges, which is a huge number for a large N. So we normally filter the weakest edges to simplify the network. In the threshold approach, a threshold θ can be used to chop the edges, if $d_{ij} > \theta$. For a given network, different θ can lead to different structures with same vertices but different sets of remaining edges. Based on the correlation matrices, we first investigate the stock networks with different θ for both CSI163 and S&P468. In the sliding window approach, using daily log return time series, we first calculate the correlation matrices of 163×163 for CSI163 and 468×468 for S&P468; then we average all the correlation matrices over the study periods. After that, we get the averaged correlation matrices, with which we can apply the edge filtering process for different θ based on the equation (4). Based on the result, small θ closes to 0 will filter most edges while larger θ close to the maximum value two will keep most edges. We use an θ interval of $[0.1 - 1.5]$ with a step of 0.1. We present the basic network properties in Table 4 for

Table 5: For the S&P468 network, the max possible edges $|e|_{\max}$ for $N = 468$ vertices, the existing edge number $|e|$, the edge density $|e|_{density}$, the average degree $\langle d \rangle$, the average distance $\langle d_{ij} \rangle$, the minimum distance $d_{ij}^{\min}$, and the maximum distance $d_{ij}^{\max}$ are presented for different θ from 0 to 1.5 in a step of 0.1.

θ	$\lvert e\rvert_{\max}$	$\lvert e\rvert$	$\lvert e\rvert_{density}$	$\langle d \rangle$	$\langle d_{ij} \rangle$	$d_{ij}^{\min}$	$d_{ij}^{\max}$
0.1	109278	0	0.0000	0.0000	0.0000	0.0000	0.0000
0.2	109278	2	0.0000	0.0085	0.0000	0.0935	0.1094
0.3	109278	2	0.0000	0.0085	0.0000	0.1959	0.2033
0.4	109278	18	0.0002	0.0769	0.0000	0.0005	0.2033
0.5	109278	137	0.0013	0.5855	0.0001	0.0003	0.3265
0.6	109278	729	0.0067	3.1154	0.0007	0.0003	0.4980
0.7	109278	3571	0.0327	15.2607	0.0038	0.0004	0.6125
0.8	109278	16433	0.1504	70.2265	0.0213	0.0004	0.7255
0.9	109278	50364	0.4609	215.2308	0.0952	0.0005	0.8122
1	109278	88680	0.8115	378.9744	0.2739	0.0005	0.9264
1.1	109278	106179	0.9716	453.7564	0.5356	0.0006	1.0334
1.2	109278	108956	0.9971	465.6239	0.7994	0.0007	1.1486
1.3	109278	109277	1.0000	466.9957	0.9906	0.0044	1.2480
1.4	109278	109278	1.0000	467.0000	1.0711	0.1959	1.3465
1.5	109278	109278	1.0000	467.0000	1.0711	0.1959	1.3465

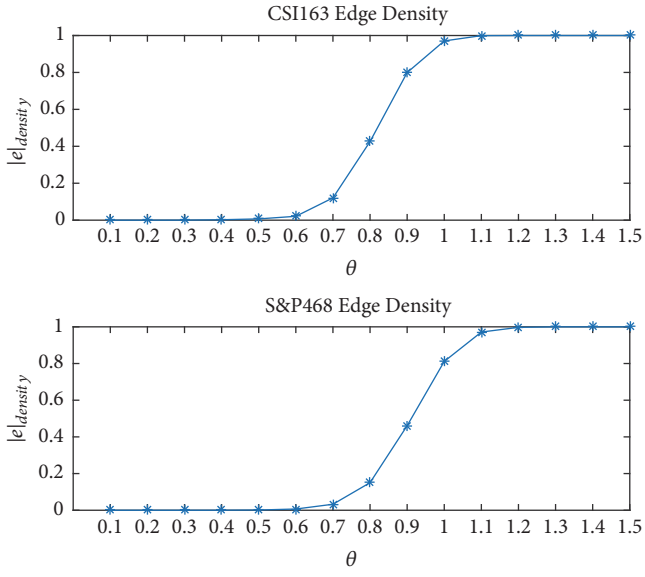

Figure 2: Edge densities of CSI163 and S&P468 for different thresholds θ from 0.1 to 1.5. It shows that the densities increase sharply from 0 to 1 in the θ interval of 0.6 and 1.

the CSI163 network and Table 5 with different θ between 0.1 and 1.5. The maximum possible edges are 13203 for CSI163 and 109278 for S&P468, respectively. For different distance thresholds θ, any edges whose distances are greater than the threshold are filtered. So with smaller θ, only a few edges remain in the network and this results a smaller edge density $|e|_{density}$, smaller average degree $\langle d \rangle$, average distance $\langle d_{ij} \rangle$, minimum distance $d_{ij}^{\min}$, and maximum distance $d_{ij}^{\max}$ as well.

In Figure 2, we plot the edge densities of CSI163 and S&P468 for different thresholds θ from 0.1 to 1.5. In the interval of 0.1 to 0.6, the densities for both networks are close to 0, meaning all edges are filtered. While in the interval of 1 to 1.5, the densities are close to 1, meaning that all edges are preserved. Between these two intervals, we see that the two curves have a similar shape with a slope when θ lies between 0.6 and 1. This indicates that most edges are within this interval. A similar edge density distribution is also reported in [65]. The study shows that stock networks also demonstrate a similar transforming interval.

We investigate the degree distributions of both networks with different θ. No matter if θ is too small or too large, the degree distributions are noisy, while in a narrow interval around 0.7, the distributions follow the power law. The regression fitting curve is a straight line in the plots of $\log P(k)$ against $\log(k)$, where the $\log P(k)$ is the $\log_{10}$ probability for a vertex with k degrees and the $\log(k)$ is the $\log_{10}$ degree. After running on the data, we plot the typical power law distributions in Figure 3(a) for CSI163 and Figure 3(b) for S&P468 respectively. For both distributions, we fit the $\log_{10}$-$\log_{10}$ distribution and get the power law exponents $\gamma = -0.9935$ for CSI163 and $\gamma = -1.2323$ for S&P468. In the plots, we use the same $bins = 20$ to calculate the probabilities for different degrees. As shown in Figure 3, we see that a large number of vertices have small degrees. Only a few vertices have large degrees. As the vertices are stocks, and the degrees are rooted in the correlations between stocks, for both CSI163 and S&P468 networks, only a few stocks are the highly correlated with the most parts of rest stocks. These stocks have a wider and larger influence over the whole networks, while other stocks with relatively smaller degrees are less correlated with other stocks. This presents limited influence over the network. The negative fitting slope value γ also indicates that both the CSI163 and S&P468 networks are scale-free networks in which a small portion of vertices have larger degrees while a large portion of

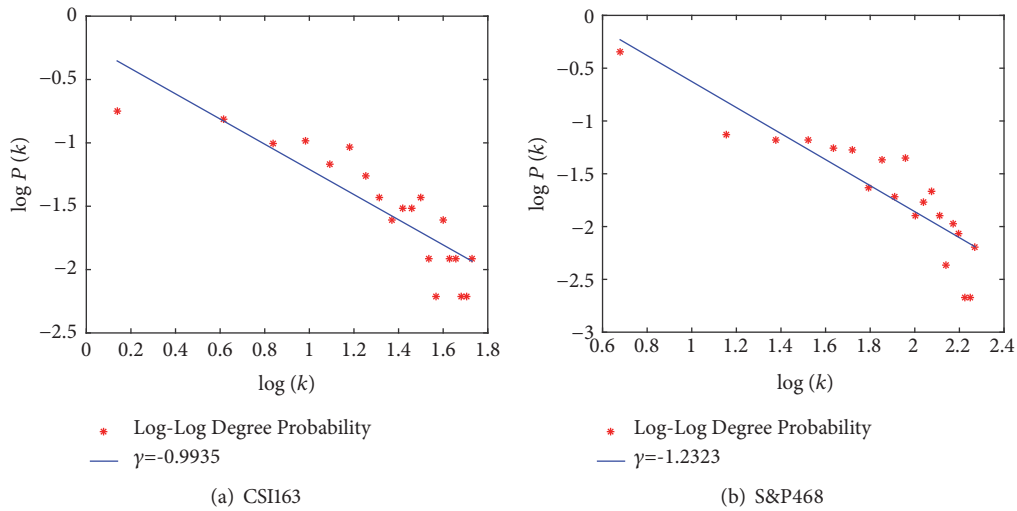

(a) CSI163 (b) S&P468

FIGURE 3: Log-Log degree distributions of CSI163 and S&P468 networks. By using different θ, we can filter out edges with larger distances. We find that not all the filtered networks can demonstrate the power law degree distributions. Only when θ falls within a narrow interval around 0.7, the filtered networks follow the power law degree distribution. In Figure 3(a), for the CSI163 network, we use $\theta = 0.68$ and we get a fitting line with a slope of $\gamma = -0.9935$. In Figure 3(b), for the S&P468 network, we use $\theta = 0.75$ and we get a fitting line with a slope of $\gamma = -1.2323$. This indicates that the degree distributions of both stock markets follow the power law in the form of $P(k) \sim k^{-\gamma}$, which also means the networks are scale free in which a small portion of vertices have larger degrees, while a large portion of vertices have small degrees.

vertices have smaller degrees this agree with previous studies [105].

4.2. Average Clustering Coefficient. Average clustering coefficient $\langle C \rangle$ is an average of all clustering coefficients $\langle C_i \rangle$ of all vertices. The clustering coefficient $\langle C_i \rangle$ indicates the transitivity for an individual vertex v_i, while the overall averaged clustering coefficient $\langle C \rangle$ is an indication of the transitivity and density of the whole network. In Figure 4, we present the average clustering coefficient $\langle C \rangle$ for both CSI163 and S&P468 networks comparing with random networks. The $\langle C \rangle$ gets larger with the θ when larger θ will preserve more edges, while it remains almost unchanged with a slight increase in both random networks. Comparing with random networks of same sizes of 163×163 for CSI163 and 468×268 for S&P468, $\langle C \rangle$ of both two stock networks are significantly larger than that of the corresponding random networks. For CSI163, $\langle C \rangle$ is 4.9574 times larger than that of the random networks on average with a maximum of 11.8903 times. For S&P468 the average multiple is 5.2305 times, and maximum multiple is 10.4180 times compared with the random networks. This shows that both stock networks are well connected with better transitivity. This result agrees with many other previous studies.

4.3. Average Path Length. Unlike clustering coefficient which is a local property, for any two vertices v_i and v_j in a network, the number of edges covering the shortest route linking the two vertices is defined as the characteristic path length, l_{ij}, in [2] which is a typical global property. By averaging the lengths of all possible pairs, we can calculate the average path length $\langle L \rangle$. As an indication of how the network is connected, many real networks have small $\langle L \rangle$ compared with random networks. In Figure 5, we plot the average path length $\langle L \rangle$ of both CSI163 and S&P468 networks with comparisons of random networks in same sizes. The two stock networks are significantly different from the corresponding random networks with the same sizes of 163×163 and 468×468. While the flat curves of $\langle L \rangle$ of random networks stay almost unchanged with θ, this is a result of the universal homogeneous edge distribution on the whole network. There are peaks for the stock networks. On the left hand of the peak, there is a decline of $\langle L \rangle$ with the decrease of θ, since when θ gets too small, most edges are filtered, and the giant networks break into small parts and $\langle L \rangle$ in small parts are decreasing significantly. However, for the right hand of the peak, $\langle L \rangle$ gets smaller with the increase of θ due to the increasing connectivity when more and more edges are preserved. This shows the stock networks of both CSI163 and S&P468 are different from random networks.

4.4. Betweenness Centrality. The betweenness b_{v_i} of vertex v_i is defined as the number of shortest paths passing v_i, which is an indication of the importance of an individual vertex in the contribution to the global connectivity. By averaging over the betweenness of all vertices, we can compare the betweenness for any two vertices. Larger betweenness means great global influence of the stock networks. This is the same to the edges. The betweenness $b_{e_{ij}}$ is the number of shortest paths passing the edge e_{ij} indicating the importance of this edge for its contribution to the global connectivity. In this study, we focus on the vertex betweenness. In the calculation of the shortest paths, we can use the original distance d_{ij} defined in equation (3) or simplify the network as a binary network according to

$$e_{ij} = \begin{cases} 1 & d_{ij} > 0, \\ 0 & d_{ij} = 0. \end{cases} \quad (6)$$

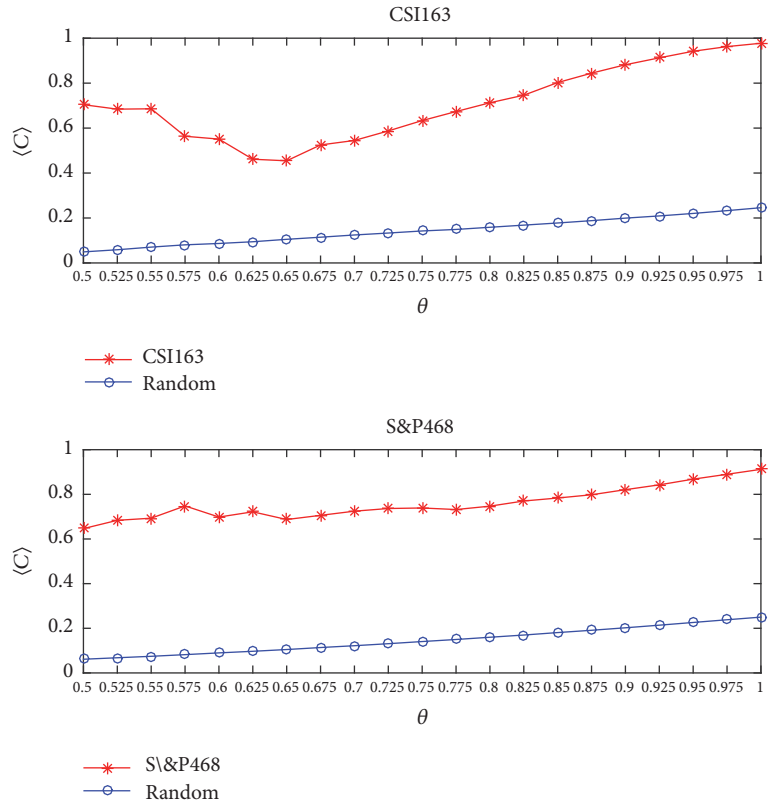

Figure 4: Average clustering coefficient $\langle C\rangle$ of CSI163 and S&P468 for different thresholds θ. It shows that $\langle C\rangle$ gets larger with θ. To compare with random networks, we plot the corresponding average clustering coefficients under the same interval of θ. As is shown, for both CSI163 and S&P468 networks, $\langle C\rangle$ values are significantly larger than the random networks of the same size. This indicates the stock markets are far from random and the stocks are comparatively clustered.

In the former, edges with different distances have different contributions to the paths, while, for the latter, all edges of nonzero distance are normalized as 1 and treated equally with great scarifying of original distance information. As shown in Figure 6, we plot the average betweenness $\langle B\rangle$ of CSI163 and S&P468 for both binary case and weighted case under different θ in Figures 6(a) and 6(b) respectively. For binary network case, all edges with positive distances are normalized as unit 1, while, in weighted networks, the original distances are directly used in the calculation of shortest paths. The shapes for binary and weighted networks are different. There are peaks for both stock networks in binary networks, while $\langle B\rangle$ gets larger with θ from almost zero to large numbers in weighted networks.

We visualize the stock networks of CSI163 and S&P468 with different θ of 0.6, 0.7, 0.8, 0.9 in Figures 7(a)–7(d) and 8(a)–8(d), respectively. It shows that the networks can be dramatically simplified using small values of θ and the edges are preserved in larger values of θ. As listed in Table 4, the edge density of CSI163 grows dramatically from 0.0209 (θ = 0.6) to 0.7994 (θ = 0.9), while, for S&P468 as shown in Table 5, the edge density of S&P468 grows also dramatically from 0.0067 (θ = 0.6) to 0.4609 (θ = 0.9). All networks in this paper are generated using the *Pajek* complex network software [106].

4.5. Components. A component *Com* is a subnetwork of the whole network with connected vertices. For a given network with a set of N vertices, the possible size of *Com* can range from 1 for an isolated vertex to N for all connected vertices. When an individual vertex v_i is disconnected from any other vertices, v_i itself forms the smallest component with a single vertex. When all the vertices are connected without any isolated vertices, the network is a single giant component. For a stock network, the stocks are correlated with each other, while stocks belonging to different components are not correlated. The component structures of stock networks have great implications for risk management of a portfolio. Since the stocks fall in the same component are correlated, so it is a bad idea to invest in most stocks from the same components. We should invest stocks from different components to diverse the risk of the whole portfolio. When θ is small, most edges are filtered leaving many vertices isolated. As a result, we see the emerging of a large number of small components. However, with the growth of θ, more and more edges are preserved. This allows the connectivity increase resulting in the appearing of larger components. In Figure 9, the properties of components of CSI163 and S&P468 networks with different θ is presented. For the two networks, the number of components $N_{components}$ (red), the max component size S_{max} (green), and the average component size $\langle S\rangle$ (blue)

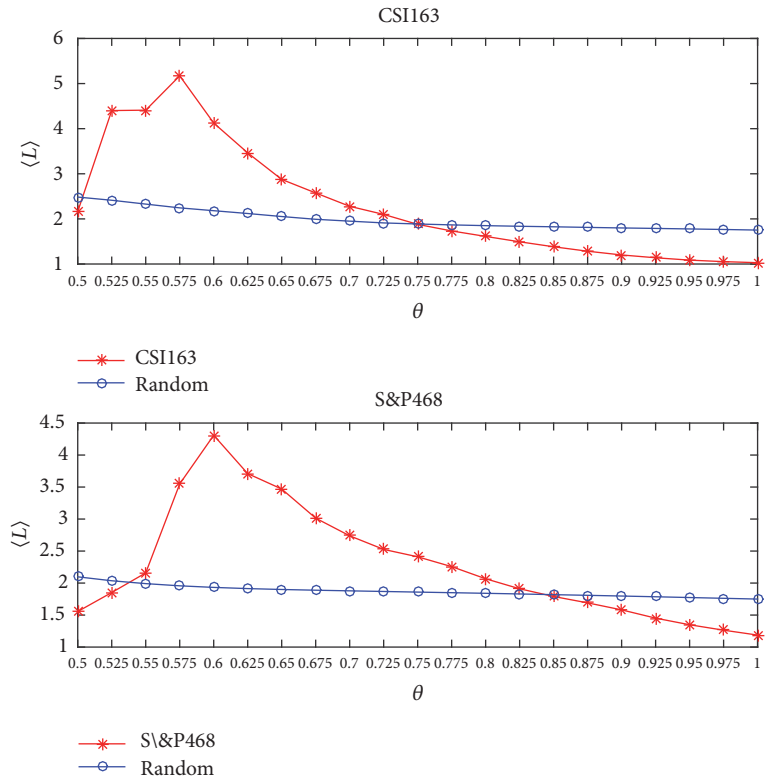

Figure 5: Average path lengths $\langle L\rangle$ for CSI163 and S&P468 under different θ compared with values for random networks in same sizes of 163×163 and 468×468. It shows that for the two networks, there are peaks of $\langle L\rangle$ above the curve of the corresponding random networks. At first, θ is small, most edges are filtered, and the whole networks are broken into parts; thus the disconnected vertices and edges are also filtered. So on the left hand, starting from the peak, with the decrease of θ, we see that $\langle L\rangle$ decreases too, while starting from the peak, with the increase of θ, we see a constant decline of $\langle L\rangle$, for more edges remained resulting in decreasing of $\langle L\rangle$. For the random networks, $\langle L\rangle$ stay almost unchanged because of the homogeneous edge distributions across the whole networks.

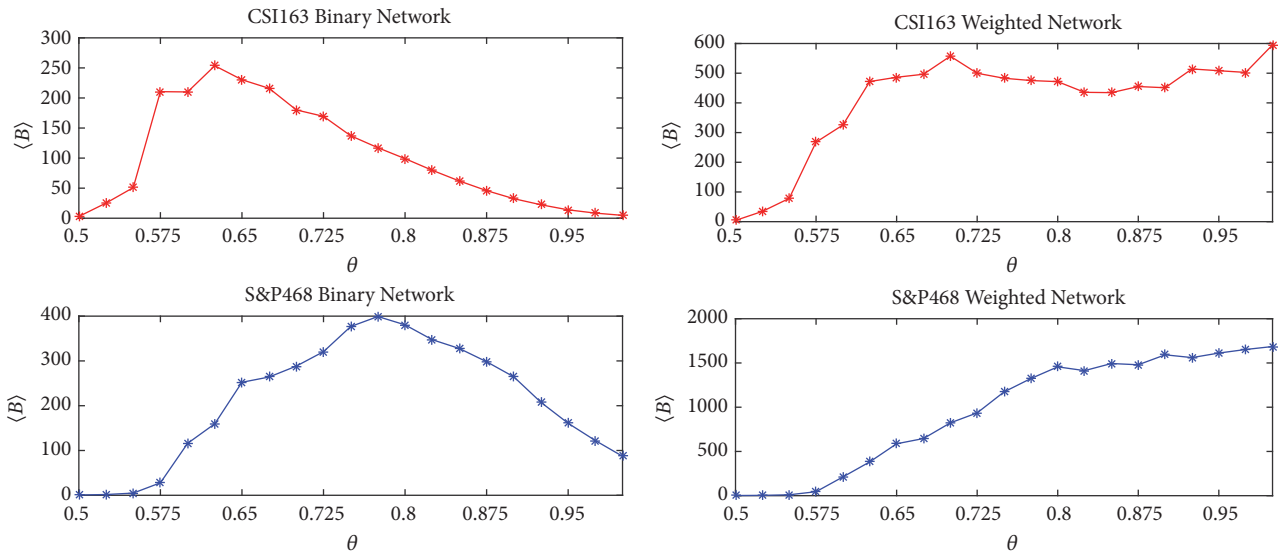

(a) Binary Network (b) Weighted Network

Figure 6: Average betweenness $\langle B\rangle$ of CSI163 and S&P468 is calculated for both the original weighted approach and binary simplification approach under different θ. The average betweenness for binary networks is different from the weighted network. For binary networks, the curves for CSI163 and S&P468 share a similar shape. On the left hand of the peak, the $\langle B\rangle$ gets larger with the increase of θ, for more edges and more vertices are preserved, and this leads to a growing number of paths, while on the right hand of the peak, large connected network emerges leading to a small value of averaged $\langle B\rangle$. In other words, the importance of a single individual vertex or edge is weakened in well-connected networks (large θ).

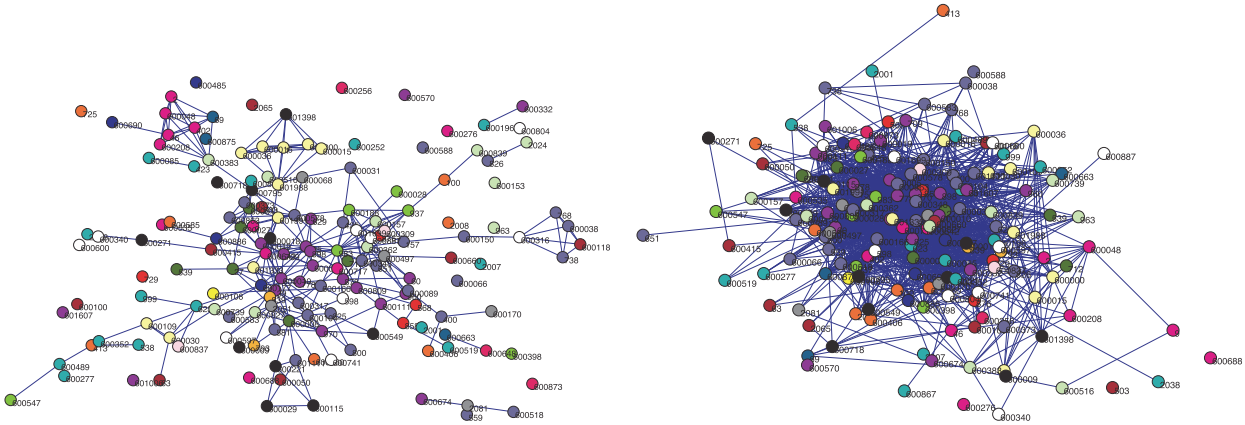

(a) CSI163 network $\theta = 0.6$

(b) CSI163 network $\theta = 0.7$

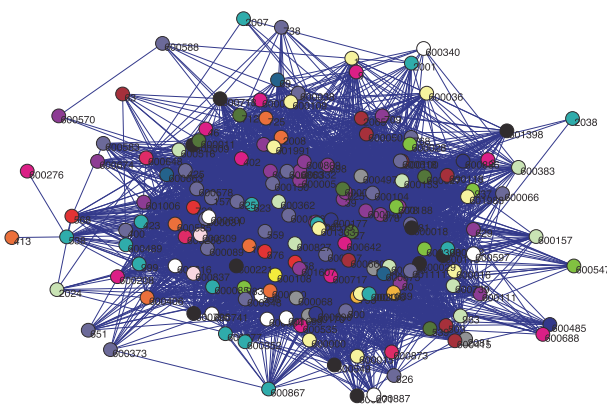

(c) CSI163 network $\theta = 0.8$

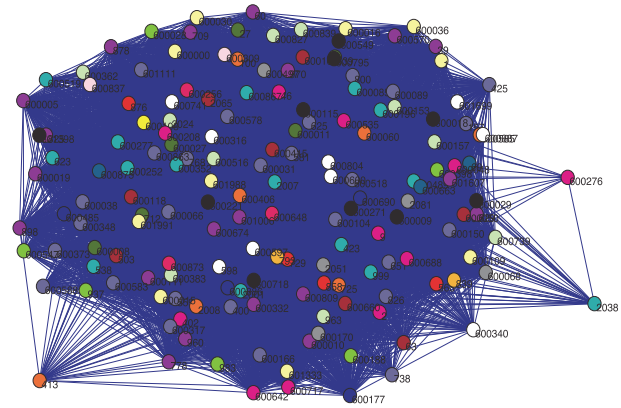

(d) CSI163 network $\theta = 0.9$

FIGURE 7: CSI163 networks with different θ of 0.6 (a), 0.7 (b), 0.8 (c), 0.9 (d). It shows that the network is relatively sparser with small θ while denser with large θ, for small θ greatly simplifies the network by filtering most edges with larger distance. As a result, the edge density when $\theta = 0.9$ is about 38.25 times to that when $\theta = 0.6$. Different vertex colors indicate different industry sectors.

shows similar pattern and changes with the values of θ. Critical changes are obvious for both networks in the θ interval about $[0.3 - 0.8]$ for CSI163 and in $[0.5 - 1.1]$ for S&P468, respectively. Before the transition interval, most vertices are isolated when the whole network breaks into small components, and both of the maximum and average component sizes are small. In the transition interval, the number of components decreases with both maximum and average component sizes. After the transition interval, the three properties stay unchanged when the giant connected component appear with maximum and average size equal to the number of total vertices. The similar component properties transition under different of θ phenomena is also observed in the study of a set of Chinese stocks [65] with a reported transition critical value about $\theta = 0.17$.

To investigate how industry sectors are connected in the stock network, we summarize the properties of both CSI163 and S&P468 networks with $\theta = 1.0$ listed in Tables 6 and 7, respectively. As it shows, in the CSI163 network, the industry sectors are all most the same in average degree $\langle d \rangle$ and average clustering coefficient $\langle C \rangle$, while with significantly different values of average betweenness coefficient $\langle B \rangle$. The difference of average degree $\langle d \rangle$ and average clustering coefficient $\langle C \rangle$ are not significant among the industry sectors. This indicates that all sectors have similar degrees and clustering coefficients. The difference between the average betweenness coefficient $\langle B \rangle$ shows that the sectors contribute to the global connectivity differently. It is worth mentioning that the finance and insurance sector has the largest average clustering coefficient $\langle C \rangle$ of 0.9829 but with a relatively small value of average betweenness coefficient $\langle B \rangle$ which is only 118.4000. For the S&P468 network, as shown in Table 7, we observe that Financials sector has the largest value of $\langle d \rangle$ of 421.7471 and the 3rd largest value of $\langle B \rangle$ of 1297.8161, with a smaller value of the average clustering coefficient $\langle C \rangle$ of 0.8975, which are very different from the CSI163 network. Furthermore, the Energy and Industrials have the largest values of $\langle d \rangle$ and $\langle B \rangle$, while Consumer Staples and Telecommunication Services have the smallest $\langle d \rangle$ and $\langle B \rangle$. From this, we also observe that, for the S&P468 network, the sectors with larger $\langle B \rangle$ are likely to have smaller values of $\langle C \rangle$ and vise verse. The findings indicate that the US market is dominated by Financials while the finance and insurance in Chinese stock markets play relatively less influential roles.

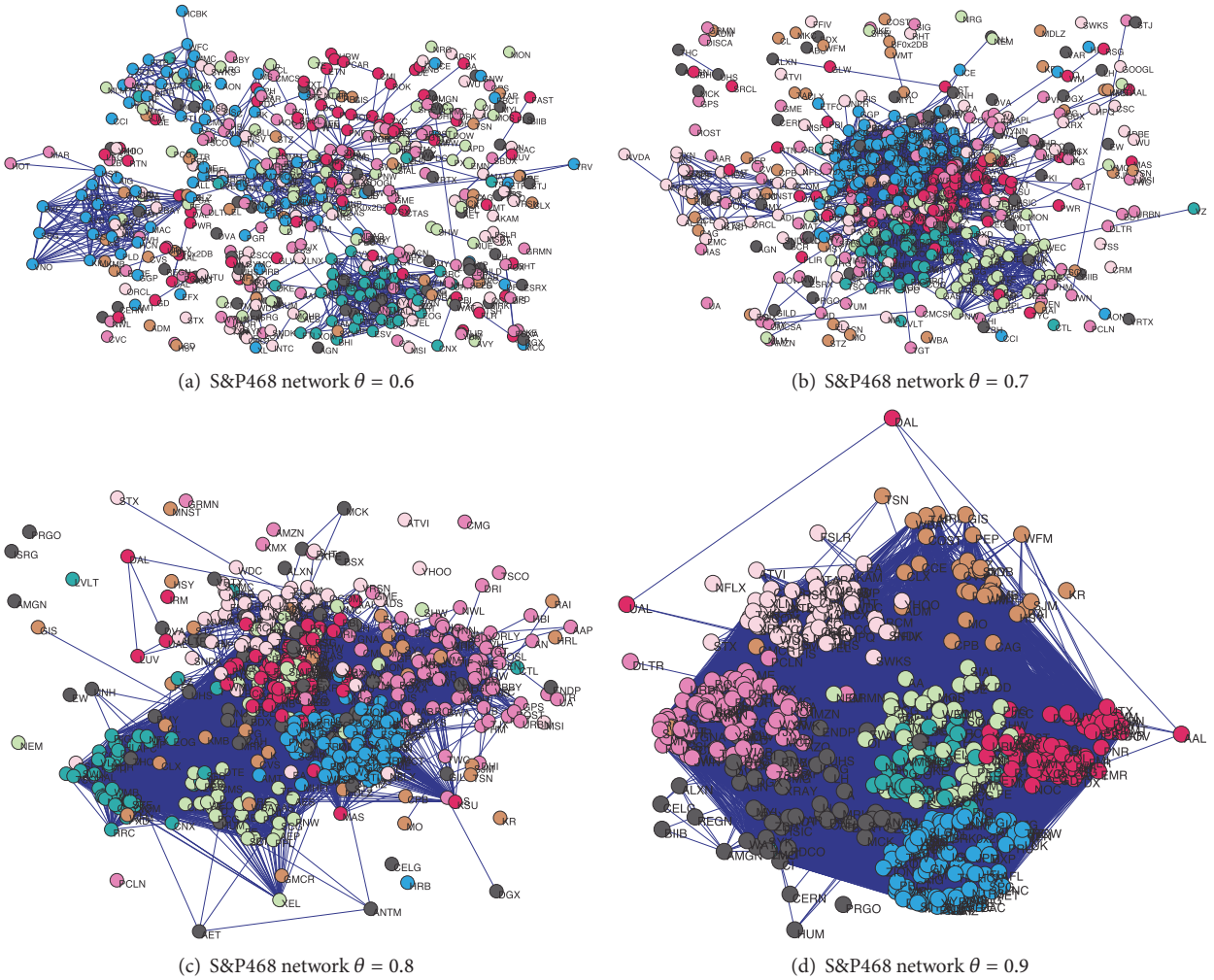

(a) S&P468 network $\theta = 0.6$

(b) S&P468 network $\theta = 0.7$

(c) S&P468 network $\theta = 0.8$

(d) S&P468 network $\theta = 0.9$

FIGURE 8: S&P468 networks with different θ of 0.6 (a), 0.7 (b), 0.8 (c), and 0.9 (d). It also shows that the edge densities with different θ change dramatically. We find that the edge density when $\theta = 0.9$ is 68.79 times to that when $\theta = 0.6$. Different vertex colors indicate different industry sectors.

By focusing on the top stocks, it is possible to look into the details of the networks. In Table 8, for the CSI163 network with $\theta = 0.8$, we present the top 10 stocks with the largest values of degree d_i and betweenness b_i ranked in descending order in the upper part and the lower part, respectively. The stock code, company name, industry name, and values of d_i, c_i, and b_i are listed. Younger Group, which is a leading fashion brand in China, has the largest degree of $d_i = 133$, and HuDong Heavy Machinery, which is a major machinery manufacturer in China, has the largest betweenness coefficient of $b_i = 5444$. While, in the S&P468 network, as shown in Table 9, T. Rowe Price Group has the largest degree of 266, and Loews Corp. has the largest betweenness coefficient value of 13202, both stocks are in the Financials sector. For both stock networks, the two lists based on d_i and b_i are similar. In other words, top stocks with largest degree values also appear as top stocks with largest betweenness coefficients b_i. It is worth noting that the list based on the ranking of clustering coefficients c_i are dramatically different those based on degrees or betweenness coefficients. This indicates that degree d_i and the betweenness b_i are consistent in describing the importance of an individual vertex, since the higher degree a vertex has, the more likely it is on the shortest paths. As indicated in the two tables, the stocks with codes labeled in bold appear on both top 10 lists, and in fact, the rest of the stocks on one list also can be found appearing in a similar ranking position on another list. We can also observe that stocks belong to Industries of Metals & Nonmetals, Machinery, and Pharmaceuticals are dominant the two top 10 lists in the CSI163 network. However, for S&P468 network, Financials, Industrials, and Materials are major stocks in the two lists. As an emerging market, Industrials sector has great influence in Chinese stock market, while the Financials sector has greater influence in US stock market which agrees with [10]. The significant difference between the two stock markets confirms the previous studies with similar results indicating that Industrials is the most influential sector among all industry sectors, while the financial sector has weaker influence [107]. This is consistent with our previous results revealed Tables 6 and 7.

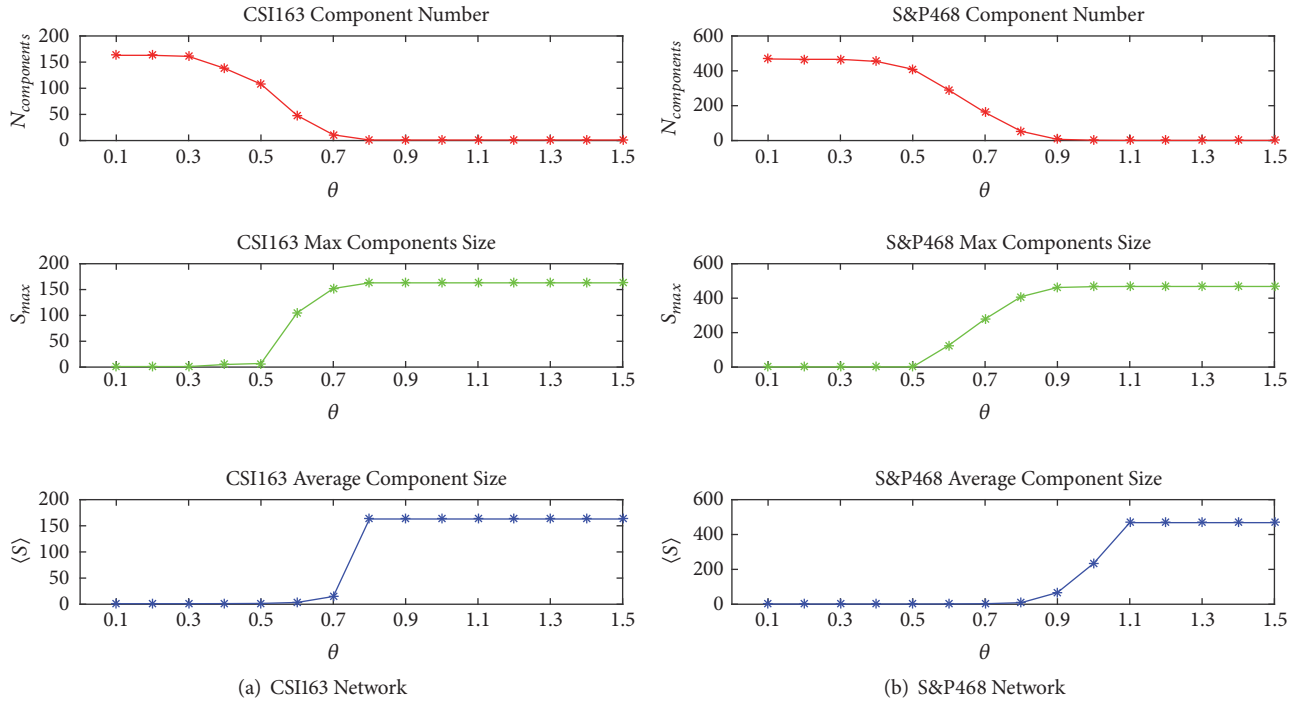

(a) CSI163 Network (b) S&P468 Network

FIGURE 9: The component properties of the components number $N_{components}$ (red), the max component size S_{max} (green), and the average component size $\langle S \rangle$ (blue) are plotted for CSI163 and S&P468 with different thresholds θ in (a) and (b), respectively. Both networks show similar transitions when the networks transform from a large number of small isolated components into a connected giant network. Before the transition interval, edges are filtered leaving isolated vertices are not correlated. After the transition interval, edges are preserved making most vertices connected to form a single giant network in which all vertices are correlated.

TABLE 6: In this table, we list the China Securities Regulatory Commission (CSRC) industry code, the sector name and the numbers of stocks, the average degree $\langle d \rangle$, the average clustering coefficient $\langle C \rangle$, and the average betweenness coefficient $\langle B \rangle$ for each industry sector of these 163 stocks. The values are calculated from the CSI163 network with $\theta = 1.0$.

Code	Industry Sector	Number	$\langle d \rangle$	$\langle C \rangle$	$\langle B \rangle$
A	Agriculture	1	162.0000	0.9703	754.0000
B	Mining	6	154.3333	0.9803	974.6667
C0	Food & Beverage	4	160.2500	0.9738	770.0000
C1	Textiles & Apparel	4	159.2500	0.9764	437.5000
C3	Paper & Printing	2	159.0000	0.9757	343.0000
C4	Petrochemicals	9	157.4444	0.9776	417.5556
C5	Electronics	7	157.1429	0.9783	176.8571
C6	Metals & Non-metals	20	159.9500	0.9756	808.0000
C7	Machinery	27	157.5926	0.9772	664.7407
C8	Pharmaceuticals	15	151.6000	0.9764	324.2667
D	Utilities	6	159.6667	0.9770	199.6667
E	Construction	5	160.2000	0.9768	945.2000
F	Transportation	10	157.9000	0.9792	426.2000
G	IT	8	156.3750	0.9775	444.0000
H	Wholesale & retail trade	10	158.8000	0.9775	341.2000
I	Finance and insurance	10	155.8000	0.9829	118.4000
J	Real estate	11	153.2727	0.9791	302.3636
K	Social Services	3	161.0000	0.9726	109.3333
L	Communication	2	160.0000	0.9775	821.0000
M	Comprehensive	3	159.6667	0.9777	582.6667

Table 7: In this table, we list the industry code, the sector name, the numbers of stocks, the average degree $\langle d \rangle$, the average clustering coefficient $\langle C \rangle$, and the average betweenness coefficient $\langle B \rangle$ for each industry sector of S&P468 stocks. The values are calculated for the S&P468 network with $\theta = 1.0$.

Code	Industry Sector	Number	$\langle d \rangle$	$\langle C \rangle$	$\langle B \rangle$
10	Energy	36	419.6944	0.8948	1264.6111
15	Materials	26	404.2692	0.8948	1717.8462
20	Industrials	63	415.8571	0.8894	1937.0476
25	Consumer Discretionary	78	376.0256	0.9194	786.8205
30	Consumer Staples	33	269.0303	0.9194	37.8182
35	Health Care	50	309.6000	0.9135	213.8000
40	Financials	87	421.7471	0.8975	1297.8161
45	Information Technology	61	373.9344	0.9245	363.6721
50	Telecommunication	5	293.2000	0.9456	124.8000
55	Utilities	29	375.3448	0.9142	579.2414

Table 8: Top stocks with highest values of degree d_i, and betweenness b_i ranked in descending order of d_i and b_i when the $\theta = 0.8$ for CSI163 network. Stock codes in bold indicate the stocks appear at both top 10 stocks.

Code	Name	Industry	$d_i \downarrow$	c_i	b_i
600177	Youngor Group	Textiles & Apparel	133	0.5416	2154
600642	Shanghai Wanye Enterprises	Real estate	131	0.5732	2362
39	China International Marine Containers (Group)	Metals & Non-metals	127	0.5929	2276
600010	Inner Mongolia Baotou Steel Union	Metals & Non-metals	125	0.5738	1112
600166	Beiqi Foton Motor	Machinery	123	0.6047	72
825	Shanxi Taigang Stainless Steel	Metals & Non-metals	122	0.6005	2644
623	Jilin Aodong Medicine Industry (Groups)	Pharmaceuticals	121	0.6058	60
600362	Beijinghualian Hypermarket	Wholesale and retail trade	121	0.6127	1552
600717	Qinhuangdao Yaohua Glass	Real estate	119	0.6095	1354
600005	Wuhan Iron And Steel	Metals & Non-metals	118	0.6009	532
Code	Name	Industry	d_i	c_i	$b_i \downarrow$
600150	HuDong Heavy Machinery	Machinery	110	0.6155	5444
898	Angang Steel	Metals & Non-metals	114	0.6367	4560
600398	Anyuan Industrial	Mining	95	0.6710	4140
2051	China CAMC Engineering	Construction	114	0.6226	4136
601607	Aluminum Corporation of China Limited	Metals & Non-metals	116	0.6304	2766
825	Shanxi Taigang Stainless Steel	Metals & Non-metals	122	0.6005	2644
600031	Sany Heavy Industry	Machinery	85	0.7300	2584
600642	Shanghai Wanye Enterprises	Real estate	131	0.5732	2362
39	China International Marine Containers (Group)	Metals & Non-metals	127	0.5929	2276
600177	Youngor Group	Textiles & Apparel	133	0.5416	2154

5. Hierarchical Structures of Stock Networks

Mantegna introduced the minimum spanning tree and hierarchical clustering methods into the study of financial networks [21], in which a distance matrix D is built from the correlation matrix for all stocks. Based on the distance matrix, the minimum spanning tree is extracted. Since the minimum spanning tree contains the information of edges connecting all vertices in a single spanning tree with the shortest total length, it is also possible to extract the hierarchical clustering tree from the minimum spanning tree, where the distance for vertex v_i and v_j is subdominant *ultrametric* distance $d^<(i, j)$ as the maximum value of distance along the shortest path between the two vertices v_i and v_j [108]. However, the subdominant ultrametric distance approach will lose much edge distance information, for two separated vertices which are indirectly connected on the minimum spanning tree with a specific larger subdominant ultrametric distance might be directly linked in the original distance matrix. Vertices which should be clustered together might be separated in a hierarchical clustering tree based on ultrametric distance. To preserve the hierarchical structure of the minimum spanning tree as well as more information allowing loops and cliques, Planar Maximally Filtered Graph (PMFG) is proposed in [86]. Based on PMFG, the influence of different sectors of CSI300 is studied revealing that the industrial sector is

Table 9: Top stocks with highest values of degree d_i, and betweenness b_i ranked in descending order of d_i and b_i when the $\theta = 0.8$ for S&P468 network. Stock codes in bold indicate the stocks appear at both top 10 stocks.

Code	Name	Industry	$d_i \downarrow$	c_i	b_i
TROW	T. Rowe Price Group	Financials	266	0.3882	4536
L	Loews Corp.	Financials	263	0.4069	13202
SNA	Snap-On Inc.	Consumer Discretionary	263	0.3894	8350
IVZ	Invesco Ltd.	Financials	261	0.4016	2868
BEN	Franklin Resources	Financials	259	0.4074	7836
HON	Honeywell Int'l Inc.	Industrials	256	0.4151	1790
AMG	Affiliated Managers Group Inc	Financials	255	0.4128	2042
DD	Du Pont (E.I.)	Materials	255	0.4163	4966
SIAL	Sigma-Aldrich	Materials	254	0.4186	7020
ROP	Roper Industries	Industrials	247	0.4326	8626
Code	Name	Industry	d_i	c_i	$b_i \downarrow$
L	Loews Corp.	Financials	263	0.4069	13202
HST	Host Hotels & Resorts	Financials	223	0.4938	12510
OKE	ONEOK	Energy	174	0.5329	9978
ROP	Roper Industries	Industrials	247	0.4326	8626
SNA	Snap-On Inc.	Consumer Discretionary	263	0.3894	8350
BEN	Franklin Resources	Financials	259	0.4074	7836
FLS	Flowserve Corporation	Industrials	202	0.5271	7726
JPM	JPMorgan Chase & Co.	Financials	124	0.7409	7614
UTX	United Technologies	Industrials	217	0.4746	7590
SIAL	Sigma-Aldrich	Materials	254	0.4186	7020

the dominant part of the whole market [107]. In [109], the hierarchical tree structure of multiple industry indices in China are investigated before and after a crisis showing the structure changes around the crisis period. A similar study of global financial crisis impact on stock market shows that the Turkish market is less influenced [110]. Authors propose to use *Kullback-Leibler* distance for the filtering procedures in [11]. International real estate market networks in different countries are studied in [99] revealing that markets are clustered according to geographical locations. Instead of using the methods of [21], a typical approach is applied to extract the hierarchical structure of the German stock market in [68]. Using the industry classification information as the benchmark, authors compared the methods used to extract the clusters in financial networks [103]. In [111], *Neighbor-Net* approach is applied in which more distance information is used in the construction of the tree compared to the hierarchical clustering.

Since a sliding window approach with a window size of L is utilized, in a study period of total P trading days, we can get a sequence of $P - L + 1$ trading windows. We have $P_{csi163} = 2149$ for CSI163 and $P_{s\&p468} = 2228$ for S&P468 trading dates in our study period between 04/01/2007 to 06/11/2015, respectively. As we adapted in previous parts, we set the sliding window size as $L_{csi163} = 170$ for CSI163 and $L_{S\&P468} = 500$ for S&P468. We have $W_{csi163} = 1980$ windows for CSI163 and $W_{S\&P468} = 1729$ for S&P468 respectively. For each sliding window at time t, we can get the distance matrices $D_{csi163}(t)$ and $D_{S\&P468}(t)$ where $t = 1, \cdots, W$. To investigate the structures of the two markets taking the whole study period as a whole, we calculate the averaged distance matrix by averaging all elements overall sliding windows as

$$\langle D \rangle = \frac{1}{W} \sum_t D_t. \tag{7}$$

With this averaged distance matrix, we construct the hierarchical trees, minimum spanning trees, and asset graphs and study the evolvement of the properties of minimum spanning trees and asset graphs for both CSI163 and S&P468.

5.1. Hierarchical Tree. In the study of the stock market or a portfolio, a set of individual stocks belonging to different economic sectors behavior correlated together. Based on the prices information, the correlation matrix can be formed. Based on that, a distance matrix can be derived. Using the distance matrix, clustering algorithms can be further applied to extract the clustering structures of the stocks. For the stocks falling in the same cluster, they behave similar sharing correlated price fluctuations, while, for the stocks coming from different clusters, they are less similar than the ones of the same clusters. The main objective of clustering algorithms is to minimize the dissimilarity for stocks in the same cluster and maximize the dissimilarity for stocks in different clusters meanwhile. Since the dissimilarity is naturally measured by the distance, the selection of definition of distance between clusters is important for clustering algorithms. Four distance definitions as shown in equations (8)-(11) are used in extracting of hierarchical clustering trees. The distance between two clusters, c_m and c_n, is defined as the minimum distance for

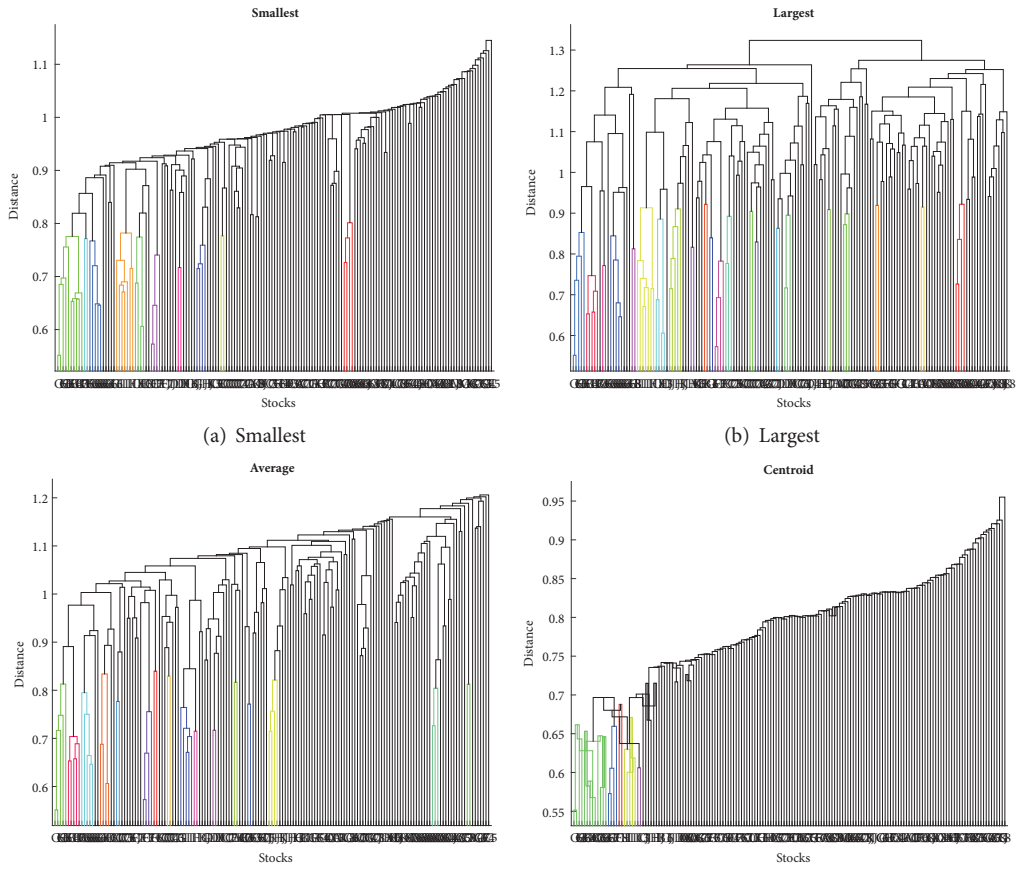

(a) Smallest (b) Largest

(c) Average (d) Centroid

Figure 10: CSI163 dendrogram hierarchical cluster trees extracted with different distance definitions in (a) smallest distance for stock pairs, equation (8); (b) largest distance for stock pairs, equation (9); (c) average distance for stock pairs, equation (10); (d) distance between centroids for clusters, equation (11). The color threshold is 0.7. All stocks whose linkage values are less than this threshold would be colored with a unique color. As shown in the figures, different distance definitions extract different dendrogram hierarchical cluster trees whereas the same color threshold generates different results. We see that the largest distance definition reveals more details of network.

all pairs as in equation (8), the maximum distance for all pairs as in equation (9), the average distance for all pairs as in equation (10), and the distance between average centroids of the two clusters as in equation (11), respectively.

$$d_{m,n} = \min\left(d_{o_m^i, o_n^j}\right) \tag{8}$$

$$d_{m,n} = \max\left(d_{o_m^i, o_n^j}\right) \tag{9}$$

$$d_{m,n} = \frac{1}{N_m N_n} \sum_i \sum_j d_{o_m^i, o_n^j} \tag{10}$$

$$d_{m,n} = d\left(\overline{o_m}, \overline{o_n}\right) \tag{11}$$

In our study, we use all these four definitions of cluster distance. For CSI163 network, we present the dendrogram hierarchical cluster trees in Figures 10(a)–10(d). For S&P468 network, we present the trees in Figures 11(a)–11(d). In these trees, the leaf nodes are individual stocks, and the height of two merged branches indicates the distance or dissimilarity between two clusters or stocks. The higher they merge, the larger the distance is. For similar clusters or stocks, they merge in a lower value of height. To color the similar stocks, a color threshold of $0.7 \times \max(d_{o_m^i, o_n^j})$ is used. Thus all similar clusters or stocks are colored with the same colors. By adjusting this color threshold, we can get the clusters from the dendrogram hierarchical cluster trees. As shown in the figures, using different definitions, we can get different hierarchical cluster trees and it is obvious that Figures 10(b) and 10(c) reveal more details of the structures, in which the distance between clusters is the largest of all pairs and the average distance of all pairs, respectively. The similar effect is also observed in Figures 11(b) and 11(c) for S&P468 networks. These clustering results are found to agree with the classifications of stocks very well. The colored clusters are composed of stocks mostly from the same economy sectors. Though there are exceptions that some stocks from different sectors are clustered together, or stocks from the same sector are clustered in different clusters. It is still astonishing to see that stocks can be clustered which agree with the economy sectors classification only from the prices information. These results indicate that hierarchical cluster trees constructed from price correlation matrix can reveal economy sectors and this has potential applications in portfolio selection and risk management.

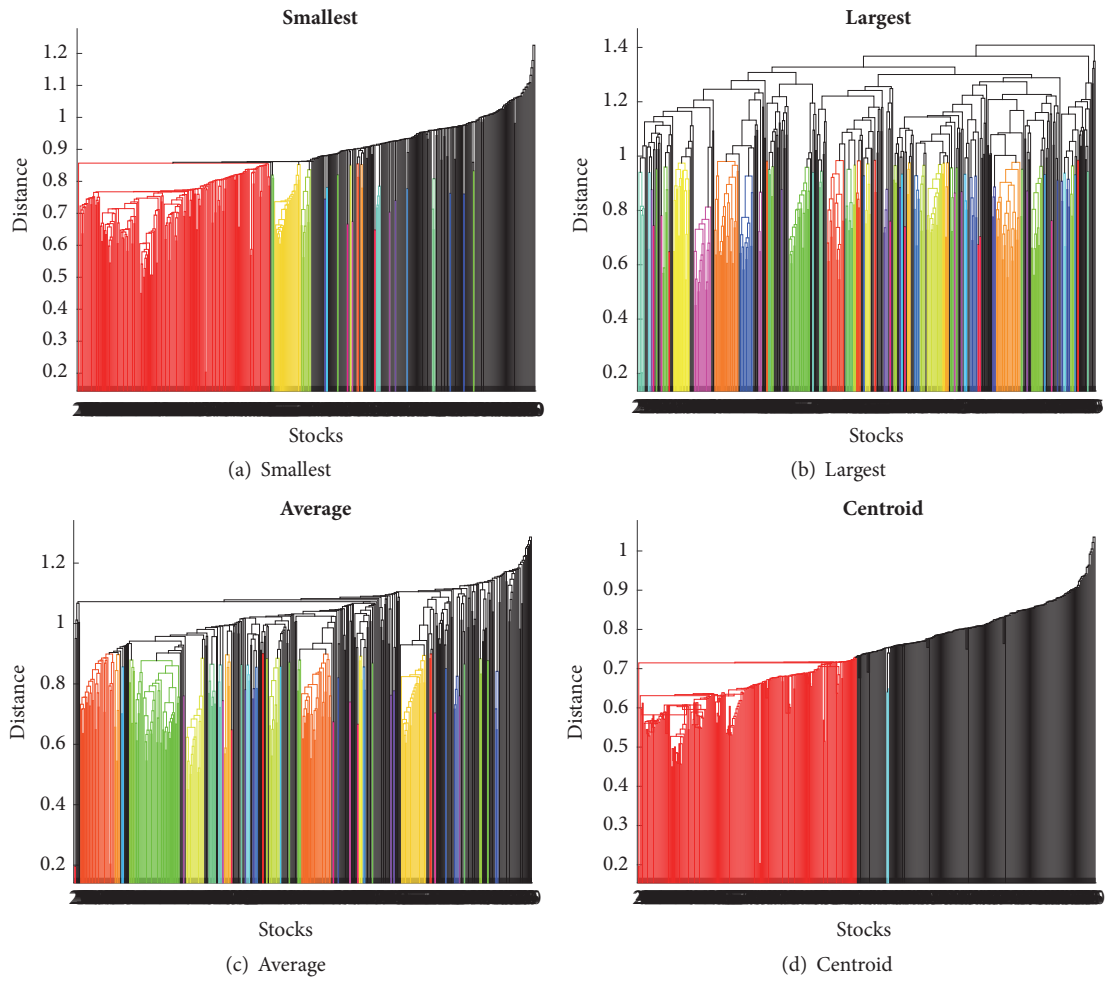

FIGURE 11: S&P468 dendrogram hierarchical cluster trees extracted with different distance definitions in (a) smallest distance for stock pairs, equation (8); (b) largest distance for stock pairs, equation (9); (c) average distance for stock pairs, equation (10); (d) distance between centroids for clusters, equation (11). The color threshold is 0.7. All stocks whose linkage values are less than this threshold would be colored with a unique color. As shown in the figures, different distance definitions extract different dendrogram hierarchical cluster trees whereas the same color threshold generates different results. Again, the largest distance definition reveals more details of network.

5.2. Minimum Spanning Tree. For a given undirected weighted network with N vertices, we can simplify the network by extracting the backbone of the network connecting all vertices, but with a minimum total length of edges, this backbone is called minimum spanning tree, or MST for short. Since loops or circles are not allowed to connect vertices, a MST has a topological structure of tree with $N - 1$ edges which is dramatically simplified from the original network which might have a maximum of $N(N-1)/2$ edges. This brings huge advantages to the study of networks of stocks by reducing noises and simplifying the computation as well.

To construct a minimum spanning tree from a given network, it is easy to be achieved by using *Kruskal's Algorithm* [95], in which all edges are ranked in ascending order. Starting from the shortest edge on the edges ranking list, we add edges to the tree by keeping the tree in spanning form without introducing circles. When all edges are considered, we get a final minimum spanning tree comprising all connected N vertices with a minimum total length of $N - 1$ edges. For a network in which all edges are with distinct lengths, the extracted MST is unique. In Figure 12, we demonstrate the

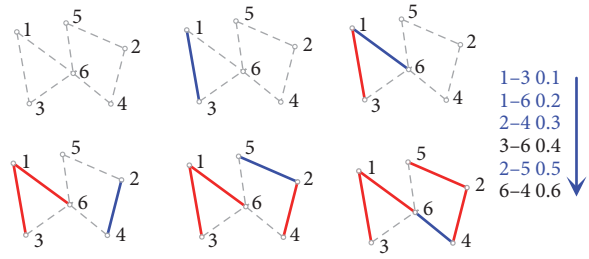

FIGURE 12: The extraction of a minimum spanning tree from a six vertices network using Kruskal's MST Algorithm. We rank all edges in descending order according to the edge lengths. Starting from the shortest edge and add the edges into the tree but avoiding loops or circles, after considering all edges, we get a final tree connecting all vertices with the minimum total edge lengths. In our example, after adding $e_{1,3}$, $e_{1,6}$, $e_{2,4}$, $e_{2,5}$, and $e_{6,4}$, we finally extract a tree of $T_{3,1,6,4,2,5}$ with a total length of 1.1.

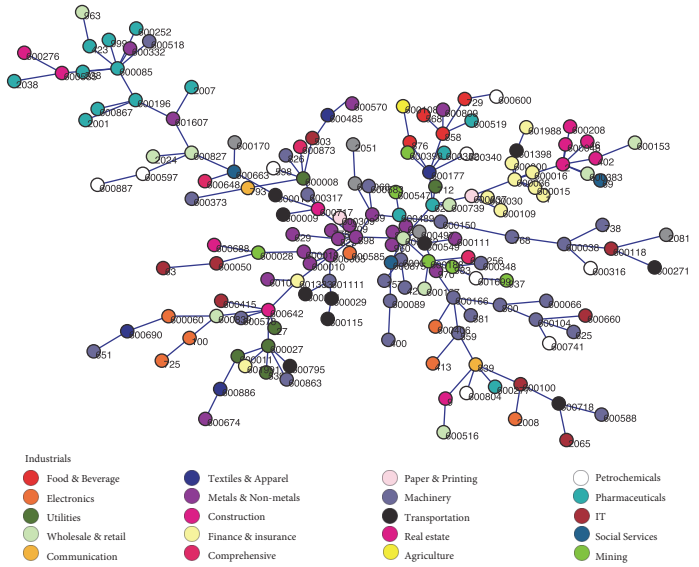

Figure 13: Minimum spanning tree of CSI163. Vertices are colored to indicate different industry sectors.

Table 10: In this table, we present the top 10 stocks with the largest degrees in the MST of CSI163. As is shown, the top 10 stocks are diverse in industry sectors which represents 1 Wholesale & retail stock, 1 Metals & Non-metals stock, 2 Pharmaceuticals stocks, 2 Real estate stocks, 1 Finance & insurance stock, 2 Utilities stocks, and 1 Textiles & Apparel stock.

Degree	Code	Name	Industry
11	600362	Beijinghualian Hypermarket	Wholesale & retail
9	898	Angang Steel	Metals & Non-metals
8	600085	Beijing Tongrentang	Pharmaceuticals
7	2	China Vanke	Real estate
7	600036	China Merchants Bank	Finance & insurance
6	600008	Beijing Capital	Utilities
6	600027	Huadian Power	Utilities
6	600177	Youngor Group	Textiles & Apparel
6	600642	Shanghai Wanye Enterprises	Real estate
5	623	Jilin Aodong Medicine Industry	Pharmaceuticals

process of extracting the minimum spanning tree from a six vertices network following Kruskal's MST Algorithm. The edges are ranked in descending order, and we start from the shortest ones and add them into the tree but omit the edges which might introduce loops; after considering all edges, we get a minimum spanning tree with a minimum total length. In this example, edge (3,6) and (6,4) are omitted because that $e_{3,6}$ might bring a loop of (3,6,1) and $e_{6,4}$ might bring a loop of (6,4,2,5). Another widely used algorithm is *Prim's Algorithm* [112] which begins with a starting vertex and adds the shortest one to the existing tree from all edges connected to the tree. By repeating this greedily, we can extract the minimum spanning tree of the given network. In this research, we apply Kruskal's Algorithm to analyze the network structures of CSI163 and S&P468.

To extract the minimum spanning trees of the stock networks of CSI163 and S&P468, we average all correlation matrices over the investigated time windows, presented in Figures 13 and 14 for CSI163 and S&P468, respectively. We see that the stocks of the same industry sectors are clustered in the MSTs for both CSI163 and S&P468, and this clustering effect is much more obvious for S&P468 in which stocks are well clustered according to the industry sectors of S&P500.

We further look into the connectivities of MSTs for both CSI163 and S&P468; we find that after the edge filtering process, some stocks are still well connected with other stocks. These stocks are the key stocks in the contribution of connectivities of the MSTs, while most stocks are poorly connected with the degree of only one or two. In Tables 10 and 11, we present the top 10 stocks according to their degrees in MST of CSI163 and S&P468, respectively. We find that the most connected stocks of CSI163 are diverse, while, for the MST of S&P468, 3 Financials stocks appear in the top 10. This agrees with other analysis that the Chinese stock market is much more diverse and Financials stocks play important roles in the US market.

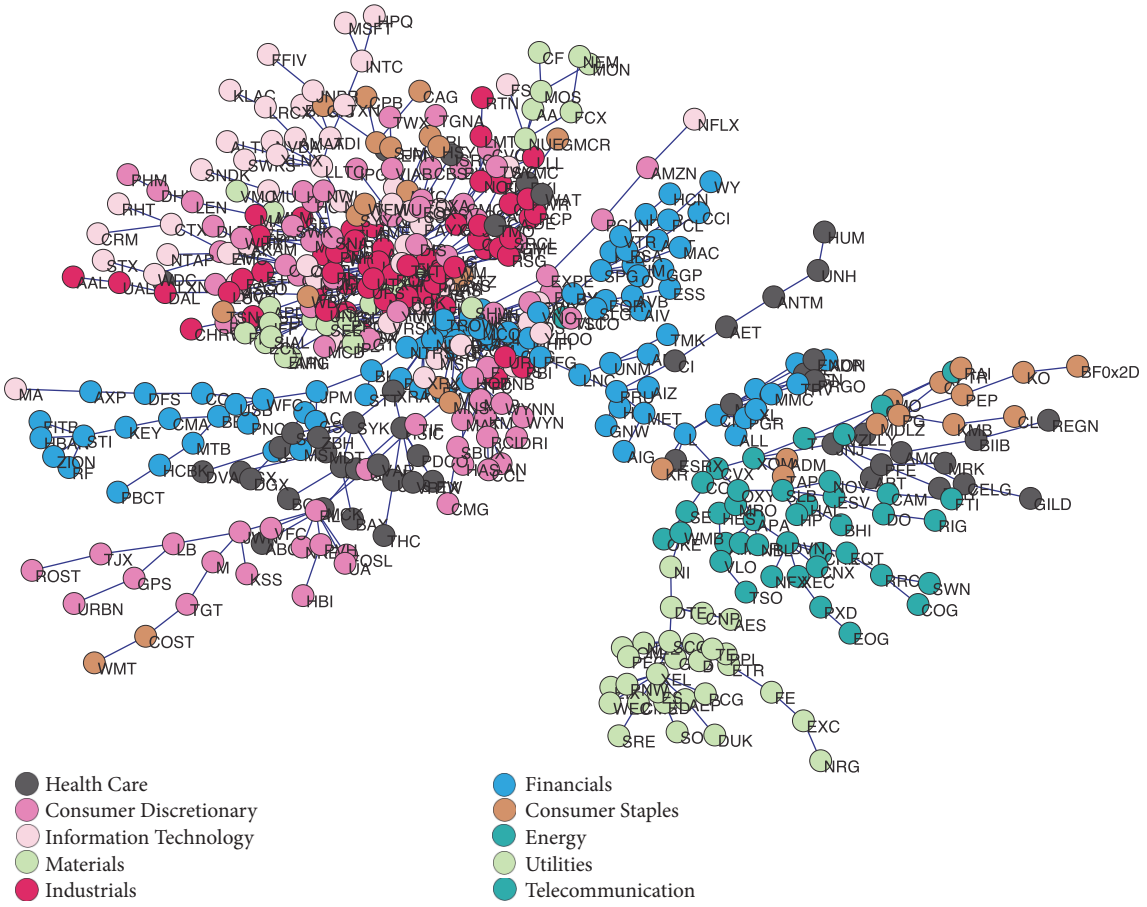

Figure 14: Minimum spanning tree of S&P468. Vertices are colored to indicate different industry sectors.

Table 11: In this table, we present the top 10 stocks with the largest degrees in the MST of S&P468. As is shown, Honeywell Intl. is the most connected stock in the MST with a degree of 38. The top 10 stocks are composed of 2 Industrials stocks, 3 Financials stocks, 2 Utilities stocks, 1 Health Care stock, and 1 Consumer Discretionary stock.

Degree	Tick	Stock Name	Industry
38	HON	Honeywell Intl.	Industrials
18	TROW	T. Rowe Price Group	Financials
11	SCG	SCANA Corp	Utilities
10	ITW	Illinois Tool Works	Industrials
9	ADP	Automatic Data Processing	IT
9	XEL	Xcel Energy Inc	Utilities
8	JNJ	Johnson & Johnson	Health Care
8	SPG	Simon Property	Financials
8	SNA	Snap-On Inc.	Consumer Discretionary
7	AMG	Affiliated Managers	Financials

5.3. Planar Maximally Filtered Graph. Like the minimum spanning tree (MST) approach, planar maximally filtered graphs, PMFG, is also an edge filtering method but the allowance of cliques up to 4 vertices shows much richer structure information of a network rather than a single tree. Based on the correlation matrix, the PMFG spans on a planar surface without crossing of edges but with loops and holes. It is believed that a PMFG might reveal more details of the networks. After the introduction of PMFG by Tumminello et al. in the study of 100 stocks of NYSE [86], PMFG has been applied in many studies of financial networks. In [67], the authors study the PMFG networks of DAX 30 stocks. Instead of using the correlation matrix, a p-values matrix of EngleGranger cointegration test is used to extract the PMFG for Chinese stocks in [98]. The stability and robustness of PMFG for 300 NYSE stocks are compared with MST in a

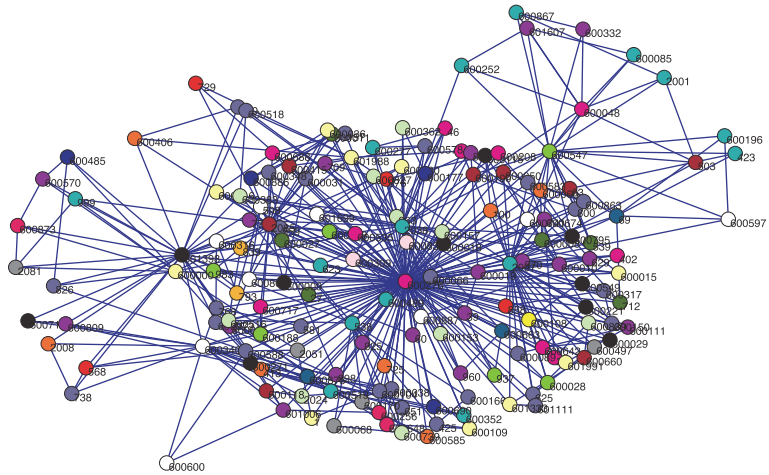

Figure 15: PMFG of CSI163.

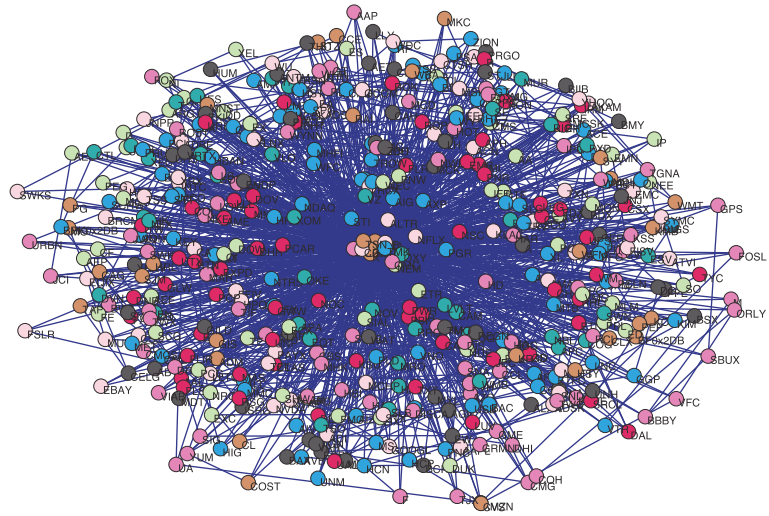

Figure 16: PMFG of S&P468.

running window approach, and the results reveal that PMFG is stabler than MST [104]. In [47], the same authors of [104] confirm that PMFG provides stronger robustness and stability in revealing network structures of stock markets. It has also been proven that the PMFG always contains an MST for the same distance matrix [86].

The PMFGs of CSI163 and S&P468 networks are plotted in Figures 15 and 16, respectively. We see that PMFGs have much more edges compared to MSTs. Further, we use another layout to plot the two PMFGs in Figures 17 and 18, from which, we find that PMFGs also produce good clusters for stocks of different industry sectors.

5.4. Asset Graph. In the minimum spanning tree (MST), a connected tree structure connecting all vertices with a minimum total length of edges is extracted. The selection process of adding edges in generating an MST out of a distance matrix is presented in Figure 12; an MST is always a connected single tree without disconnected parts. By connecting the N vertices, a total of $N - 1$ edges are needed, where N is the number of vertices in the original network. It is obvious that an MST does not guarantee to be with the possible minimum total lengths of the $N - 1$ edges. By changing the strategy of how edges are selected and allowing disconnected parts, the asset graph (AG) approach is proposed in [87, 88]. Similar to MST, to generate an AG, we start the distance matrix containing all pairwise distances information of the network; we first rank all edges in ascending order from the shortest to the longest. Without considering the requirement of keeping a tree connected, we choose the top $N - 1$ edges to form an AG. It has been found that AG extracts similar structures as MST can do with smaller normalized length and with better stable structure over time. In this section, we show the AG networks for both markets. In Figures 19 and 20, we present AG structures for CSI163 and S&P468 networks, respectively. Compared with Figures 13 and 14 of the minimum spanning trees of CSI163 and S&P468 networks, we see that AG structures are more complex than MST and there are many isolated vertices in AG. The connected cliques in AG are the most correlated

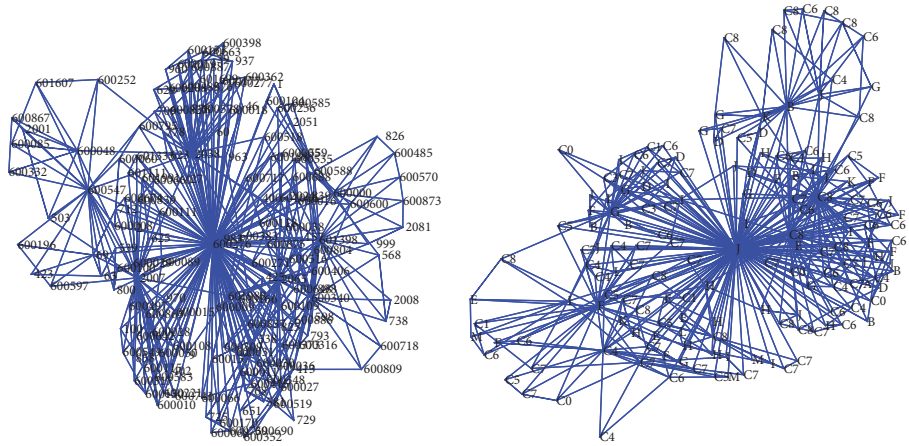

(a) Stock (b) Industry

Figure 17: CSI163 PMFG. We label the vertices with stock codes in (a) and industry codes in (b).

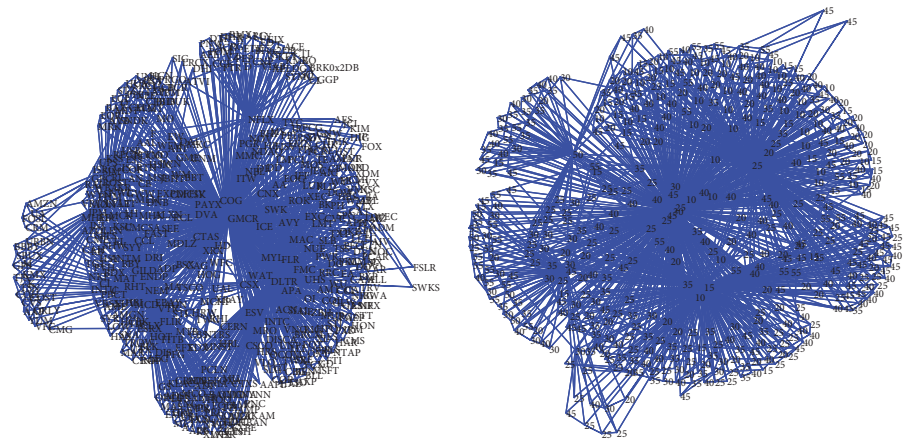

(a) Stock (b) Industry

Figure 18: S&P468 PMFG. We label the vertices with stock codes in (a) and industry codes in (b).

stocks connected by the shortest possible edges; in other words, by connecting the most correlated stocks, AG omits the less correlated stocks. We also observe that many cliques emerge in AG and this reveals more information about the structures than in MST where no loops or cliques are allowed. We see that AG is a simple but effective network simplification approach in extracting the most correlated stocks. However, the sacrifice is also obvious, as shown in Figures 19 and 20, the clustering is poor in AG compared with MST for both markets.

We have shown that AG allows isolated vertices and not all vertices are connected in one giant tree. To generate an AG, we can use different numbers of edges; with the increase in edge number, we can see that the portion of isolated vertices declines. It is interesting to investigate how the vertices are related to the edge numbers. In the original distance matrix, the maximum possible number of edges is $N(N-1)/2$. The percentage of the fraction of AG is the top edges added to AG networks to the total possible edges. When we increase this edge percentage, more and more vertices are connected. We calculate the percentage of connected vertices as the number of connected to the total vertices number of N. We plot these results in Figures 21(a) and 21(b) for CSI163 and S&p468 networks, respectively. As the figures show, with a small fraction of edges being included, more and more vertices are connected; it requires only 0.0123 and 0.0043 of the total edges for all vertices to be connected in CSI163 and S&P468, respectively. This indicates that the top edges are very effective in connecting vertices for S&P468 than CSI163.

In the previous section, all structures are extracted from the average distance matrices over the whole study periods which is defined in equation (7) as $\langle D \rangle = (1/W)\sum_t D_t$, where W is the number of sliding windows. In this part, we investigate the dynamic structures of the filtered networks with a focus on the AG and MST. For each sliding window, at time t, we get a series of distance matrices D_t based on the returns data on the interval of $[t, t-1, \ldots, t-L+1]$ where L is the length of a sliding window. For each sliding window, using the distance matrix D_t, we construct the corresponding original network N_t, the asset graph AG_t, and the minimum

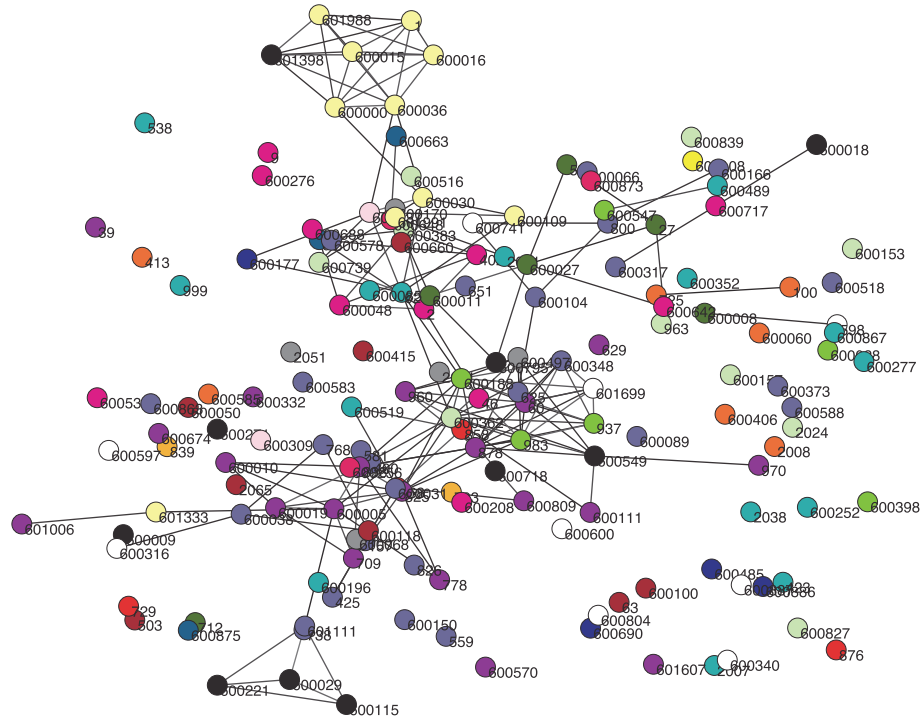

FIGURE 19: Asset graph of CSI163 with $N - 1$ shortest edges.

spanning tree MST_t. Using our dataset, we get $W_{csi163} = 1980$ windows for CSI163 and $W_{S\&P468} = 1729$ for S&P468 in the study period between 04/01/2007 and 06/11/2015.

In Figure 22, we present the distance distributions of original distance matrices N_t, asset graphs AG_t, and minimum spanning trees MST_t for both of CSI163 and S&P468 in the study period between 04/01/2007 and 06/11/2015. In the original network N_t, a number of $N(N-1)/2$ edges are considered, while, for AG_t and MST_t, $N-1$ edges are considered. Since the sliding window sizes are $L_{csi163} = 170$ and $L_{S\&P468} = 500$, we should keep in mind that a slice of distribution is a result of the past L dates, i.e., about half of a year for CSI163 and two years for S&P468. The shapes of these distributions are influenced by the lengths of L. We choose the same set of lengths by considering the requirements of random matrix theory approach which we shall discuss later. The similar plots are reported in [87] in the study of 477 stocks from NYSE which is in a similar size of our S&P468 dataset in which 468 stocks are included. We add more evidence by comparing two markets of CSI163 and S&P468. In Figures 22(a) and 22(b), we observe obvious shifts of the distribution centers for both markets. In these shifts, positive shifts to the mean value of $\langle d_{ij} \rangle = \sqrt{2}$ roughly correspond to the normal market periods, while negative shifts to the mean value correspond to the bear or collapsing market periods. This indicates that the stocks behave synchronized in bad periods and this agrees with many previous studies. This also provides a potential market measurement for investors and regulators to watch how market shift behaviors. In Figures 22(c) and 22(d), the distributions of distances of AG for CSI163 and S&P468 are plotted. Since AG is a subgraph of the original network and is composed of the top $N-1$ shortest edges, we expect the distributions show a left shift to the mean center of $\langle d_{ij} \rangle = \sqrt{2}$ compared to the original networks, and this is well shown in the plots for both CSI163 and S&P468, more precisely, the distributions of AG are zoom-in of the left tails of original networks. The MST, as shown in Figures 22(e) and 22(f), has a relatively wider distribution which is positively shifted compared to AG but negatively shifted to the original network. Also, we find that, in AG and MST networks, the most parts of the distributions stay on the left hand of the center $\sqrt{2}$ which means the network is correlated on average; in other words, for periods when the mean center stays on the left hand, the network backbones of AG and MST are on average correlated, and rarely anticorrelated. A potential implication is that, for the whole market, the network provides a diversified portfolio when the market is normal or in a bull state, but for the top edges in AG and MST, the network moves together with less diversification when the market falls into bear markets or crisis periods.

The distance d_{ij} indicates how the two stocks correlate with each other. Larger d_{ij} means smaller correlation and vice versa. For an original network N at time t, the total distance can be introduced as

$$d_{total} = \sum_{i,j} d_{ij}, \tag{12}$$

and the average distance for the original network can be defined as

$$\left\langle d_{ij} \right\rangle = \frac{1}{N(N-1)/2} \sum_{i,j} d_{ij}. \tag{13}$$

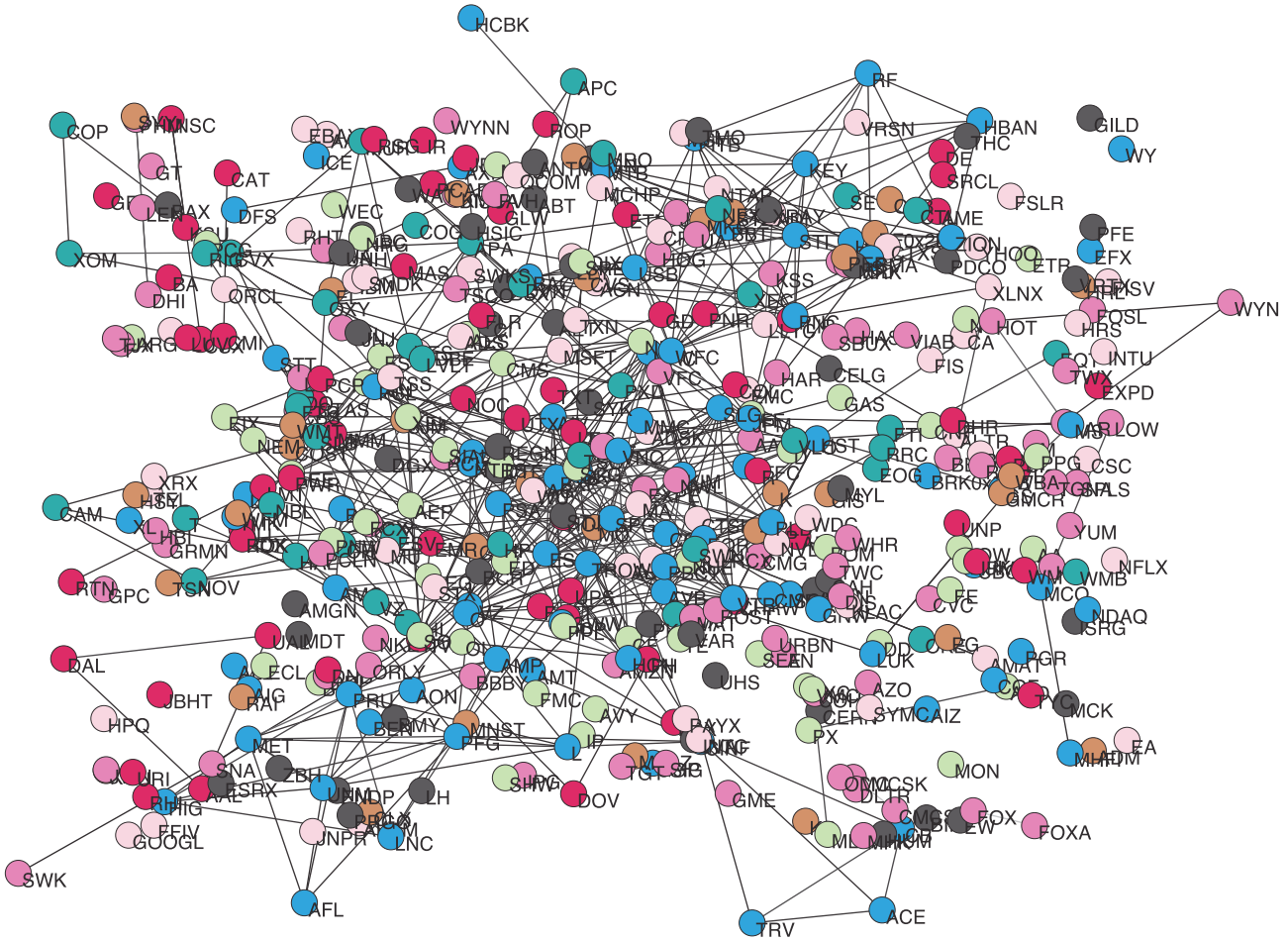

Figure 20: Asset graph of S&P468 with $N - 1$ shortest edges.

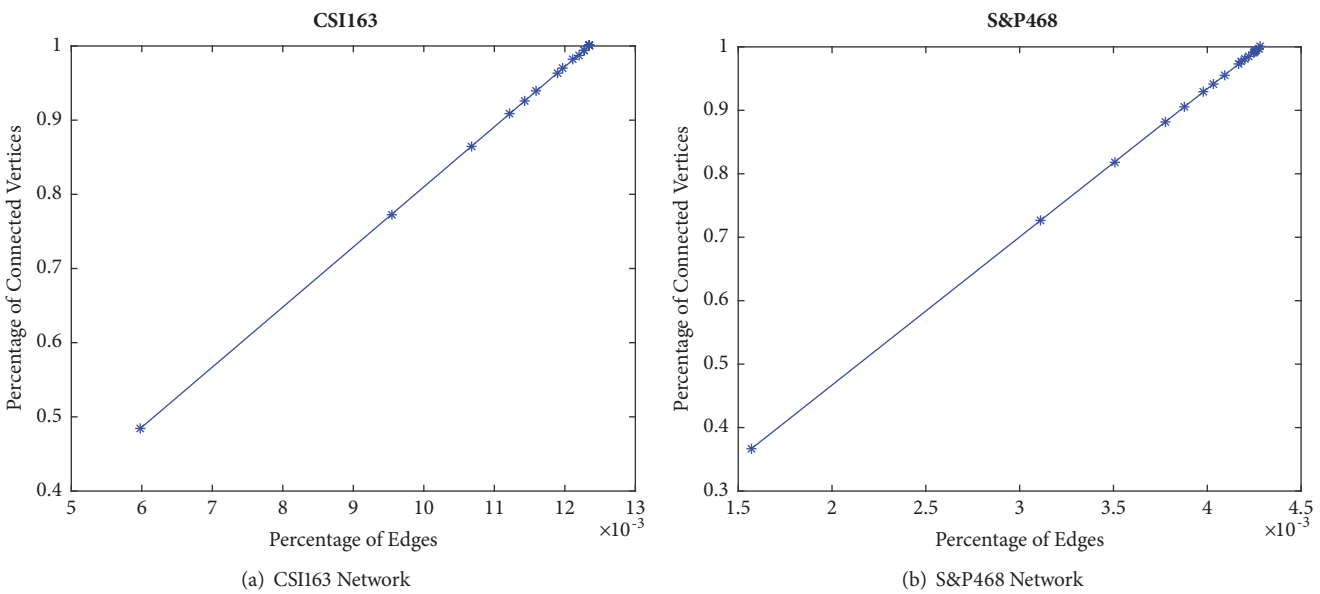

(a) CSI163 Network

(b) S&P468 Network

Figure 21: Percentages of connected vertices of AG against edge densities for CSI163 and S&P468 networks.

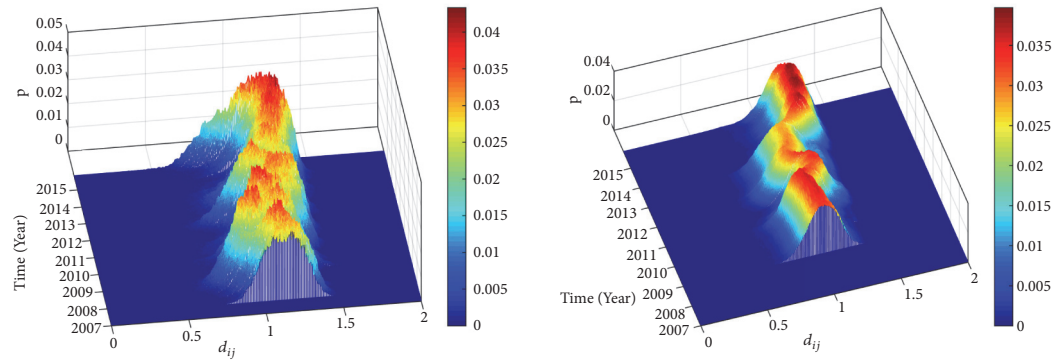

(a) CSI163 Original

(b) S&P468 Original

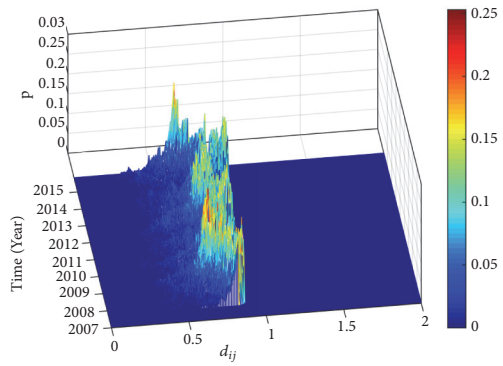

(c) CSI163 AG

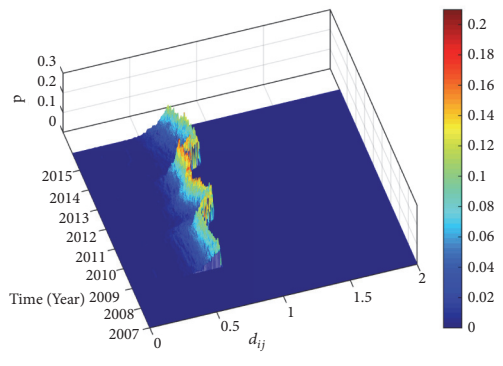

(d) S&P468 AG

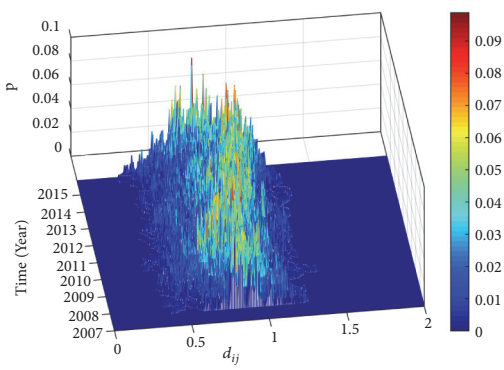

(e) CSI163 MST

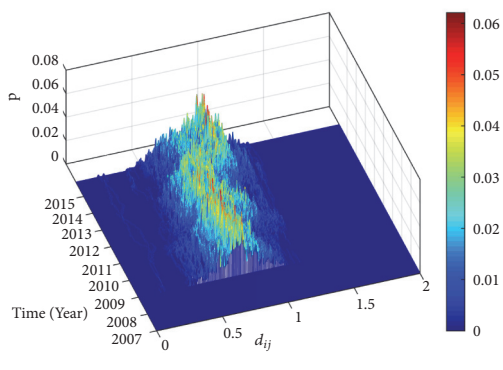

(f) S&P468 MST

Figure 22: Probability distributions of all distances d_{ij} of N_t, AG_t, and MST_t of CSI163 and S&P468 over the years in our study period between 04/01/2007 and 06/11/2015. The total number of edges is $N(N-1)/2$ for N_t, and $N-1$ for AG_t and MST_t, respectively. Since the sliding window size $L_{CSI163} = 170$ and $L_{S\&P468} = 500$, so the data only starts after a period of L.

In the same way, we can calculate the total distances for AG_t and MST_t using equation (12), but considering the edge number for AG_t and MST_t is $N-1$, we normalize the average distance for them as

$$\langle d_{ij} \rangle = \frac{1}{N-1} \sum_{i,j} d_{ij}. \tag{14}$$

To investigate the tightness of the network, the total distance d_{total} and average distance $\langle d_{ij} \rangle$ for the original network N_t, AG_t, and MST_t in our study periods for both networks are investigated. We plot the results in Figure 23 for d_{total} and Figure 24 for $\langle d_{ij} \rangle$, respectively. For each stock market, total distance d_{total} and average distance $\langle d_{ij} \rangle$ show similar shapes. For both stock markets, the values are in this order: $N_t > MST_t > AG_t$; i.e., the original networks have the largest values of d_{total} and $\langle d_{ij} \rangle$ compared to MST_t and AG_t, while AG_t has the smallest values.

By comparing the total distance d_{total} plotted in Figure 23(a) and the average distance $\langle d_{ij} \rangle$ plotted in

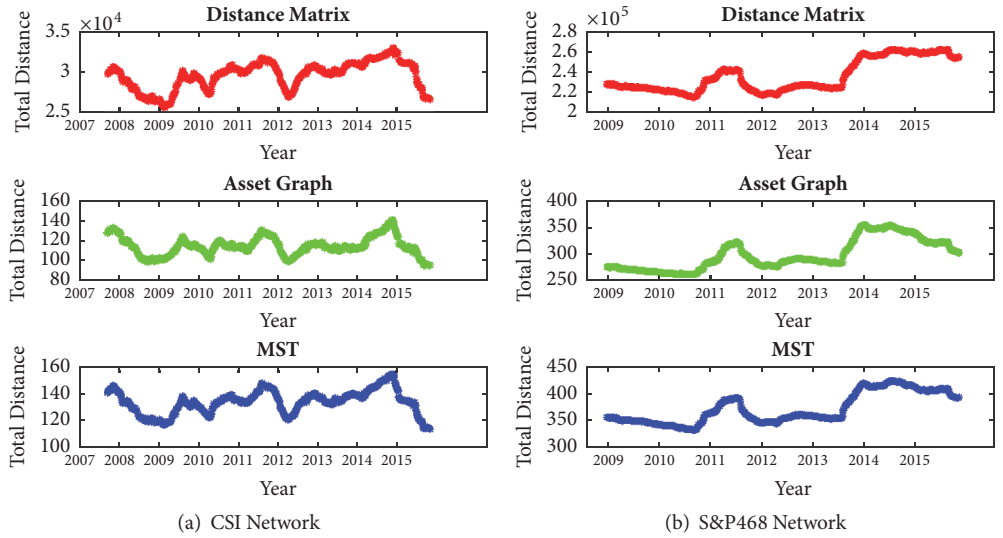

(a) CSI Network (b) S&P468 Network

FIGURE 23: The evolving of total distances d_{total} of original network N_t, asset graph AG_t, and minimum spanning tree MST_t for CSI163 and S&P468 over time in the study period.

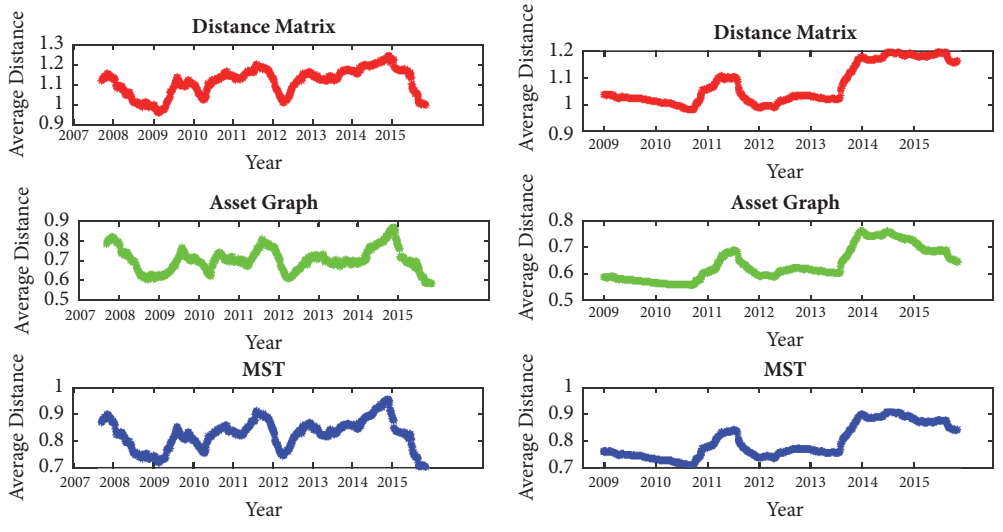

(a) CSI Network (b) S&P468 Network

FIGURE 24: The evolving of average distances $\langle d_{ij} \rangle$ of original network N_t, asset graph AG_t, and minimum spanning tree MST_t for CSI163 and S&P468 over time in the study period.

Figure 24(a) for CSI163 over the study period, we find the six plots share similar shapes. The same similarities are also observed in Figures 23(b) and 24(b) for the S&P468 network. This indicates that the AG and MST are both good backbones of the whole original market networks, and this tracking stays robust over time. For both networks, we also find that the curve of MST_t is above AG_t which means the total and average distances are slightly larger in MST than in AG. Our findings agree with the results reported in [87]. Since the two stock markets datasets have different stock numbers, we compare the average distance between the two markets, and as shown in Figure 24, we see that the CSI163 is slightly sparser than S&P468, which indicates that the CSI163 which is a developing market is more diversified than S&P468 which is a developed market; this also agrees with many previous research.

In Table 12, we summary the average $\langle\langle d_{ij} \rangle\rangle$, minimum $\langle d_{ij} \rangle_{\min}$, maximum $\langle d_{ij} \rangle_{\max}$, and standard deviation $\langle d_{ij} \rangle_{\sigma}$ of CSI163 and S&P468 networks for three kinds networks: original, AG, and MST. We can see that the values are in the order of $N > MST > AG$ for average, minimum, and maximum. Also the three networks have similar standard deviations. We find that the values of $\langle\langle d_{ij} \rangle\rangle$ and minimum $\langle d_{ij} \rangle_{\min}$ for CSI163 are slightly larger than S&P468 which indicates stocks in CSI163 are less likely to correlated than in S&P468. To visualize the distributions of these three kinds of networks, we plot the probability density function (PDF) for the original network, AG, and MST for CSI163 and S&P468

Table 12: Average $\langle\langle d_{ij}\rangle\rangle$, minimum $\langle d_{ij}\rangle_{\min}$, maximum $\langle d_{ij}\rangle_{\max}$, and standard deviation $\langle d_{ij}\rangle_{\sigma}$ of CSI163 and S&P468 networks. The values of first row belong to the original network N, those of the second row belong to the AG, and those of the third row belong to MST.

CSI163				S&P468			
$\langle\langle d_{ij}\rangle\rangle$	$\langle d_{ij}\rangle_{\min}$	$\langle d_{ij}\rangle_{\max}$	$\langle d_{ij}\rangle_{\sigma}$	$\langle\langle d_{ij}\rangle\rangle$	$\langle d_{ij}\rangle_{\min}$	$\langle d_{ij}\rangle_{\max}$	$\langle d_{ij}\rangle_{\sigma}$
1.1145	1.2445	0.9619	0.0650	1.0754	1.1968	0.9816	0.0731
0.7049	0.8708	0.5868	0.0578	0.6377	0.7607	0.5579	0.0623
0.8251	0.9565	0.7017	0.0540	0.7971	0.9092	0.7113	0.0615

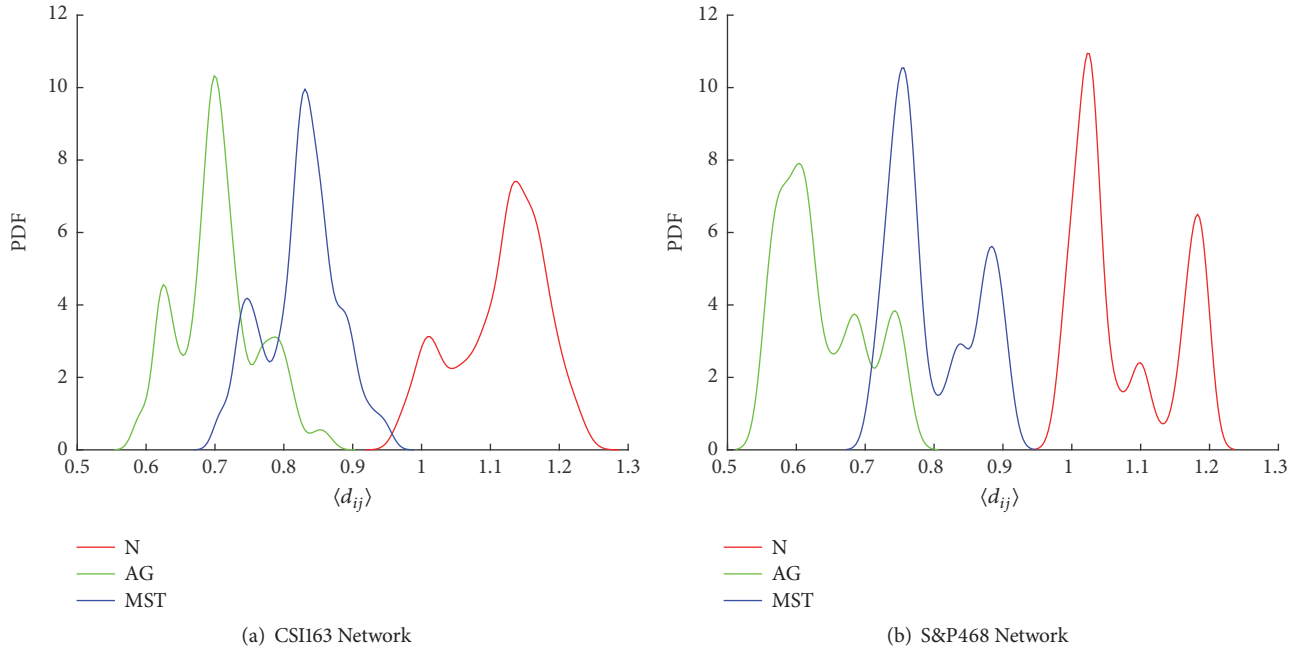

(a) CSI163 Network (b) S&P468 Network

Figure 25: Probability density function (PDF) of average distance $\langle d_{ij}\rangle$ of original network N, asset graph AG, and minimum spanning tree MST for CSI163 and S&P468.

in Figures 25(a) and 25(b), respectively. We see that the distributions of all three networks share similar shapes but with different mean centers; as shown in the figures, the AG locates on the left, MST locates in the center, and original locates on the right.

6. Conclusion and Discussion

In this research, we investigated the properties and models of the complex network theory and its applications from data science perspective. Using the daily close prices of two sets of stocks from CSI300 and S&P500, we constructed the correlation matrices for both the whole study periods and all sliding windows. Based on these correlation matrices, we build the networks with stocks as the vertices and correlation relationships as the edges. We systematically applied network filtering methods like hierarchical tree, minimum spanning tree, planar maximally filtered graph, and asset graph to simplify the networks. For each filtered network, the network properties are discussed. Financial markets are complex systems, and it is important to extract useful information from the noise background by applying methods like complex networks. We find that, for the stock markets, CSI300 and S&P500, the former is an emerging market while the latter is a mature well-developed market. They share similar properties in many ways and also vary in many aspects. The revealed properties and robustness might provide sights of the structures and dynamics of the two stock markets for practitioners and regulators. Furthermore, it is interesting to develop trading strategies with the information revealed from the topological networks of stocks or indices. For instance, the pair trading [113–116] is a basic and market neutral strategy considering the movement of a correlated stock pair, in which if the spread widens, then traders can short one and long another one to gain the spread. One might use the information of the networks to identify the pairs and evaluate the reliabilities. Also, considering pairs between groups of stocks rather than only two stocks, we might use the component or cluster information revealed in the networks to build the trading groups. Furthermore, the directed networks built with Granger causalities or lagged correlations might give more lead/lag details of stock pairs on the time factors asynchronously. Second, with the help of network edge filtering, we can significantly simplify the networks, but most studies focus on the topological simplification without concerns of the original portfolio returns. What if

we consider the returns with the topology of the networks to optimize the portfolio selection? The topological structure can give us information on how diverse the portfolio is but this is not enough to design the portfolio without return information. A possible way is to adjust the portfolio selection by considering measurements like the ratio of returns over total distances of a portfolio or other approaches combining both topological and return information. Also, the techniques of network modeling and analysis can enhance the ability in policy modeling and decision making. We hope this work can inspire policymakers and researchers in applying network theories in wider applications.

Data Availability

The data used to support the findings of this study are available from the corresponding author upon request.

Conflicts of Interest

The authors declare that they have no conflicts of interest.

Supplementary Materials

An online appendix file containing all tick information is available on the publisher website. *(Supplementary Materials)*

References

[1] M. E. J. Newman, "The structure and function of complex networks," *SIAM Review*, vol. 45, no. 2, pp. 167–256, 2003.

[2] D. J. Watts and S. H. Strogatz, "Collective dynamics of "small-world" networks," *Nature*, vol. 393, no. 6684, pp. 440–442, 1998.

[3] A.-L. Barabási and R. Albert, "Emergence of scaling in random networks," *Science*, vol. 286, no. 5439, pp. 509–512, 1999.

[4] B. Albert-László, *Linked: The New Science of Networks*, Perseus, 2002.

[5] L. D. F. Costa, O. N. Oliveira Jr., G. Travieso et al., "Analyzing and modeling real-world phenomena with complex networks: a survey of applications," *Advances in Physics*, vol. 60, no. 3, pp. 329–412, 2011.

[6] S. Boccaletti, V. Latora, Y. Moreno, M. Chavez, and D. W. Hwang, "Complex networks: Structure and dynamics," *Physics Reports*, vol. 424, no. 4-5, pp. 175–308, 2006.

[7] Z. Gao, M. Small, and J. Kurths, "Complex network analysis of time series," *EPL (Europhysics Letters)*, vol. 116, no. 5, Article ID 50001, 2016.

[8] M. Barigozzi and M. Hallin, "A network analysis of the volatility of high dimensional financial series," *Journal of the Royal Statistical Society: Series C (Applied Statistics)*, vol. 66, no. 3, pp. 581–605, 2017.

[9] S. An, X. Gao, M. Jiang, and X. Sun, "Multivariate financial time series in the light of complex network analysis," *Physica A: Statistical Mechanics and its Applications*, vol. 503, pp. 1241–1255, 2018.

[10] C. K. Tse, J. Liu, and F. C. M. Lau, "A network perspective of the stock market," *Journal of Empirical Finance*, vol. 17, no. 4, pp. 659–667, 2010.

[11] M. Tumminello, F. Lillo, and R. N. Mantegna, "Correlation, hierarchies, and networks in financial markets," *Journal of Economic Behavior & Organization*, vol. 75, no. 1, pp. 40–58, 2010.

[12] M. Lin, G. Wang, C. Xie, and H. E. Stanley, "Cross-correlations and influence in world gold markets," *Physica A: Statistical Mechanics and its Applications*, vol. 490, pp. 504–512, 2018.

[13] V. Boginski, S. Butenko, and P. M. Pardalos, "Statistical analysis of financial networks," *Computational Statistics & Data Analysis*, vol. 48, no. 2, pp. 431–443, 2005.

[14] V. Boginski, S. Butenko, and P. M. Pardalos, "Mining market data: A network approach," *Computers & Operations Research*, vol. 33, part Special Issue: Operations Research and Data Mining, no. 11, pp. 3171–3184, 2006.

[15] G.-J. Wang, C. Xie, and H. E. Stanley, "Correlation Structure and Evolution of World Stock Markets: Evidence from Pearson and Partial Correlation-Based Networks," *Computational Economics*, vol. 51, no. 3, pp. 607–635, 2018.

[16] G.-J. Wang, C. Xie, and S. Chen, "Multiscale correlation networks analysis of the US stock market: a wavelet analysis," *Journal of Economic Interaction and Coordination*, vol. 12, no. 3, pp. 561–594, 2017.

[17] Nicolò Musmeci, Vincenzo Nicosia, Tomaso Aste, Tiziana Di Matteo, and Vito Latora, "The Multiplex Dependency Structure of Financial Markets," *Complexity*, vol. 2017, Article ID 9586064, 13 pages, 2017.

[18] H. Markowitz, "Portfolio selection," *The Journal of Finance*, vol. 7, no. 1, pp. 77–91, 1952.

[19] V. Kalyagin, A. Koldanov, P. Koldanov, and V. Zamaraev, "Market graph and Markowitz model," in *Optimization in Science And Engineering*, T. M. Rassias, C. A. Floudas, and S. Butenko, Eds., pp. 293–306, Springer, New York, USA, 2014.

[20] V. Boginski, S. Butenko, O. Shirokikh, S. Trukhanov, and J. Gil Lafuente, "A network-based data mining approach to portfolio selection via weighted clique relaxations," *Annals of Operations Research*, vol. 216, no. 1, pp. 23–34, 2014.

[21] R. N. Mantegna, "Hierarchical structure in financial markets," *The European Physical Journal B - Condensed Matter and Complex Systems*, vol. 11, no. 1, pp. 193–197, 1999.

[22] S. Battiston, J. D. Farmer, A. Flache et al., "Complexity theory and financial regulation," *Science*, vol. 351, no. 6275, pp. 818-819, 2016.

[23] X.-G. Yan, C. Xie, and G.-J. Wang, "Stock market network's topological stability: evidence from planar maximally filtered graph and minimal spanning tree," *International Journal of Modern Physics B*, vol. 29, no. 22, Article ID 1550161, 2015.

[24] X.-G. Yan, C. Xie, and G.-J. Wang, "The stability of financial market networks," *EPL (Europhysics Letters)*, vol. 107, no. 4, Article ID 48002, 2014.

[25] P. Glasserman and H. P. Young, "How likely is contagion in financial networks?" *Journal of Banking & Finance*, vol. 50, Supplement C, pp. 383–399, 2015.

[26] D. Acemoglu, A. Ozdaglar, and A. Tahbaz-Salehi, "Systemic risk and stability in financial networks," *American Economic Review*, vol. 105, no. 2, pp. 564–608, 2015.

[27] R. Albert, H. Jeong, and A.-L. Barabási, "Error and attack tolerance of complex networks," *Nature*, vol. 406, no. 6794, pp. 378–382, 2000.

[28] S. Battiston, D. Delli Gatti, M. Gallegati, B. Greenwald, and J. E. Stiglitz, "Liaisons dangereuses: increasing connectivity, risk sharing, and systemic risk," *Journal of Economic Dynamics and Control*, vol. 36, no. 8, pp. 1121–1141, 2012.

[29] N. Hautsch, J. Schaumburg, and M. Schienle, "Financial network systemic risk contributions," *Review of Finance*, vol. 19, no. 2, pp. 685–738, 2015.

[30] G. Cimini, T. Squartini, D. Garlaschelli, and A. Gabrielli, "Systemic Risk Analysis on Reconstructed Economic and Financial Networks," *Scientific Reports*, vol. 5, Article ID 15758, 2015.

[31] E. Nier, J. Yang, T. Yorulmazer, and A. Alentorn, "Network models and financial stability," *Journal of Economic Dynamics and Control (JEDC)*, vol. 31, no. 6, pp. 2033–2060, 2007.

[32] K. Anand, P. Gai, S. Kapadia, S. Brennan, and M. Willison, "A network model of financial system resilience," *Journal of Economic Behavior & Organization*, vol. 85, Supplement C, pp. 219–235, 2013.

[33] B. M. Tabak, T. R. Serra, and D. O. Cajueiro, "Topological properties of stock market networks: the case of Brazil," *Physica A: Statistical Mechanics and its Applications*, vol. 389, no. 16, pp. 3240–3249, 2010.

[34] F. Caccioli, M. Shrestha, C. Moore, and J. D. Farmer, "Stability analysis of financial contagion due to overlapping portfolios," *Journal of Banking & Finance*, vol. 46, Supplement C, pp. 233–245, 2014.

[35] G.-J. Wang, C. Xie, K. He, and H. E. Stanley, "Extreme risk spillover network: application to financial institutions," *Quantitative Finance*, vol. 17, no. 9, pp. 1417–1433, 2017.

[36] S. Poledna, J. L. Molina-Borboa, S. Martínez-Jaramillo, M. van der Leij, and S. Thurner, "The multi-layer network nature of systemic risk and its implications for the costs of financial crises," *Journal of Financial Stability*, vol. 20, Supplement C, pp. 70–81, 2015.

[37] T. Kauê Dal'Maso Peron, L. da Fontoura Costa, and F. A. Rodrigues, "The structure and resilience of financial market networks," *Chaos: An Interdisciplinary Journal of Nonlinear Science*, vol. 22, no. 1, 2012.

[38] M. Gofman, "Efficiency and stability of a financial architecture with too-interconnected-to-fail institutions," *Journal of Financial Economics*, vol. 124, no. 1, pp. 113–146, 2017.

[39] S. Battiston, M. Puliga, R. Kaushik, P. Tasca, and G. Caldarelli, "DebtRank: too central to fail? financial networks, the FED and systemic risk," *Scientific Reports*, vol. 2, article no. 541, 2012.

[40] C. Zhou, "Are Banks Too Big to Fail? Measuring Systemic Importance of Financial Institutions," *International Journal of Central Banking*, vol. 6, no. 34, pp. 205–250, 2010, https://ideas.repec.org/a/ijc/ijcjou/y2010q4a10.html.

[41] C. Brooks, A. G. Rew, and S. Ritson, "A trading strategy based on the lead–lag relationship between the spot index and futures contract for the FTSE 100," *International Journal of Forecasting*, vol. 17, no. 1, pp. 31–44, 2001.

[42] C. Curme, M. Tumminello, R. N. Mantegna, H. E. Stanley, and D. Y. Kenett, "Emergence of statistically validated financial intraday lead-lag relationships," *Quantitative Finance*, vol. 15, no. 8, pp. 1375–1386, 2015.

[43] K. Chen, P. Luo, B. Sun, and H. Wang, "Which stocks are profitable? A network method to investigate the effects of network structure on stock returns," *Physica A: Statistical Mechanics and its Applications*, vol. 436, pp. 224–235, 2015.

[44] F. Pozzi, T. Di Matteo, and T. Aste, "Spread of risk across financial markets: better to invest in the peripheries," *Scientific Reports*, vol. 3, Article ID 1665, 2013, http://dx.doi.org/10.1038/srep01665.

[45] W. Zhang, C. Li, Y. Ye, W. Li, and E. W. T. Ngai, "Dynamic Business Network Analysis for Correlated Stock Price Movement Prediction," *IEEE Intelligent Systems*, vol. 30, no. 2, pp. 26–33, 2015.

[46] M. Billo, M. Getmansky, A. W. Lo, and L. Pelizzon, "Econometric measures of connectedness and systemic risk in the finance and insurance sectors," *Journal of Financial Economics*, vol. 104, no. 3, pp. 535–559, 2012.

[47] T. Di Matteo, F. Pozzi, and T. Aste, "The use of dynamical networks to detect the hierarchical organization of financial market sectors," *The European Physical Journal B*, vol. 73, no. 1, pp. 3–11, 2010.

[48] X. F. Jiang, T. T. Chen, and B. Zheng, "Structure of local interactions in complex financial dynamics," *Scientific Reports*, vol. 4, Article ID 5321, 2014, http://dx.doi.org/10.1038/srep05321.

[49] L. De Benedictis and L. Tajoli, "The World Trade Network," *The World Economy*, vol. 34, no. 8, pp. 1417–1454, 2011.

[50] J. He and M. W. Deem, "Structure and response in the world trade network," *Physical Review Letters*, vol. 105, Article ID 198701, 2010.

[51] D. in't Veld and I. van Lelyveld, "Finding the core: Network structure in interbank markets," *Journal of Banking & Finance*, vol. 49, pp. 27–40, 2014.

[52] Y. Luo, J. Xiong, L. G. Dong, and Y. Tang, "Statistical correlation properties of the SHIBOR interbank lending market," *China Finance Review International*, vol. 5, no. 2, pp. 91–102, 2015.

[53] M. Affinito and A. F. Pozzolo, "The interbank network across the global financial crisis: Evidence from italy," *Journal of Banking & Finance*, vol. 80, no. Supplement C, pp. 90–107, 2017.

[54] C.-P. Georg, "The effect of the interbank network structure on contagion and common shocks," *Journal of Banking & Finance*, vol. 37, no. 7, pp. 2216–2228, 2013.

[55] D. J. Fenn, M. A. Porter, P. J. Mucha et al., "Dynamical clustering of exchange rates," *Quantitative Finance*, vol. 12, no. 10, pp. 1493–1520, 2012.

[56] G. Iori, G. De Masi, O. V. Precup, G. Gabbi, and G. Caldarelli, "A network analysis of the Italian overnight money market," *Journal of Economic Dynamics and Control (JEDC)*, vol. 32, no. 1, pp. 259–278, 2008.

[57] C. Piccardi, L. Calatroni, and F. Bertoni, "Communities in Italian corporate networks," *Physica A: Statistical Mechanics and its Applications*, vol. 389, no. 22, pp. 5247–5258, 2010.

[58] S. Vitali, J. B. Glattfelder, and S. Battiston, "The network of global corporate control," *PLoS ONE*, vol. 6, no. 10, Article ID 0025995, pp. 1–6, 2011.

[59] C. Minoiu and J. A. Reyes, "A network analysis of global banking: 1978–2010," *Journal of Financial Stability*, vol. 9, no. 2, pp. 168–184, 2013.

[60] T. A. Peltonen, M. Scheicher, and G. Vuillemey, "The network structure of the CDS market and its determinants," *Journal of Financial Stability*, vol. 13, Supplement C, pp. 118–133, 2014.

[61] L. Marotta, S. Miccichè, Y. Fujiwara et al., "Backbone of credit relationships in the Japanese credit market," *EPJ Data Science*, vol. 5, no. 1, 2016.

[62] F. X. Diebold and K. Yılmaz, "On the network topology of variance decompositions: measuring the connectedness of financial firms," *Journal of Econometrics*, vol. 182, no. 1, pp. 119–134, 2014.

[63] S. Saavedra, L. J. Gilarranz, R. P. Rohr, M. Schnabel, B. Uzzi, and J. Bascompte, "Stock fluctuations are correlated and amplified across networks of interlocking directorates," *EPJ Data Science*, vol. 3, no. 1, Article ID 30, 2014.

[64] H. Chen, Y. Mai, and S.-P. Li, "Analysis of network clustering behavior of the Chinese stock market," *Physica A: Statistical Mechanics and its Applications*, vol. 414, pp. 360–367, 2014.

[65] W.-Q. Huang, X.-T. Zhuang, and S. Yao, "A network analysis of the Chinese stock market," *Physica A: Statistical Mechanics and its Applications*, vol. 388, no. 14, pp. 2956–2964, 2009.

[66] F. Ren and W.-X. Zhou, "Dynamic evolution of cross-correlations in the chinese stock market," *PLoS ONE*, vol. 9, no. 5, Article ID e97711, 2014.

[67] J. Birch, A. A. Pantelous, and K. Soramäki, "Analysis of Correlation Based Networks Representing DAX 30 Stock Price Returns," *Computational Economics*, vol. 47, no. 4, pp. 501–525, 2016.

[68] J. G. Brida and W. A. Risso, "Hierarchical structure of the German stock market," *Expert Systems with Applications*, vol. 37, no. 5, pp. 3846–3852, 2010.

[69] P. Caraiani, "Characterizing emerging European stock markets through complex networks: from local properties to self-similar characteristics," *Physica A: Statistical Mechanics and its Applications*, vol. 391, no. 13, pp. 3629–3637, 2012.

[70] K. Kosmidou, D. Kousenidis, A. Ladas, and C. Negkakis, "Determinants of risk in the banking sector during the European Financial Crisis," *Journal of Financial Stability*, vol. 33, pp. 285–296, 2017.

[71] N. Paltalidis, D. Gounopoulos, R. Kizys, and Y. Koutelidakis, "Transmission channels of systemic risk and contagion in the european financial network," *Journal of Banking & Finance*, vol. 61, Supplement 1, pp. S36–S52, 2015.

[72] M. F. Da Silva, É. J. De Area Leão Pereira, A. M. Da Silva Filho, A. P. N. De Castro, J. Garcia Vivas Miranda, and G. F. Zebende, "Quantifying cross-correlation between Ibovespa and Brazilian blue-chips: The DCCA approach," *Physica A: Statistical Mechanics and its Applications*, vol. 424, pp. 124–129, 2015.

[73] J. Lee, J. Youn, and W. Chang, "Intraday volatility and network topological properties in the Korean stock market," *Physica A: Statistical Mechanics and its Applications*, vol. 391, no. 4, pp. 1354–1360, 2012.

[74] A. Vizgunov, B. Goldengorin, V. Kalyagin, A. Koldanov, P. Koldanov, and P. M. Pardalos, "Network approach for the Russian stock market," *Computational Management Science*, vol. 11, no. 1-2, pp. 45–55, 2014.

[75] S. Martinez-Jaramillo, B. Alexandrova-Kabadjova, B. Bravo-Benitez, and J. P. Solórzano-Margain, "An empirical study of the Mexican banking system's network and its implications for systemic risk," *Journal of Economic Dynamics and Control (JEDC)*, vol. 40, Supplement C, pp. 242–265, 2014.

[76] E. Jondeau, E. Jurczenko, and M. Rockinger, "Moment component analysis: An illustration with international stock markets," *Journal of Business & Economic Statistics*, pp. 1–23, 2017, https://doi.org/10.1080/07350015.2016.1216851.

[77] R. Kali and J. Reyes, "The architecture of globalization: a network approach to international economic integration," *Journal of International Business Studies*, vol. 38, no. 4, pp. 595–620, 2007.

[78] P. Giudici and A. Spelta, "Graphical network models for international financial flows," *Journal of Business & Economic Statistics*, vol. 34, no. 1, pp. 128–138, 2016.

[79] N. Cetorelli and S. Peristiani, "Prestigious stock exchanges: A network analysis of international financial centers," *Journal of Banking & Finance*, vol. 37, no. 5, pp. 1543–1551, 2013.

[80] L. Sandoval, "Structure of a Global Network of financial companies based on transfer entropy," *Entropy*, vol. 16, no. 8, pp. 4443–4482, 2014.

[81] P. Caraiani, "Using complex networks to characterize international business cycles," *PLoS ONE*, vol. 8, no. 3, Article ID e58109, 2013.

[82] T. C. Silva, S. R. S. de Souza, and B. M. Tabak, "Structure and dynamics of the global financial network," *Chaos, Solitons & Fractals*, vol. 88, Supplement C, pp. 218–234, 2016.

[83] L. Laloux, P. Cizeau, M. Potters, and J.-P. Bouchaud, "Random matrix theory and financial correlations," *International Journal of Theoretical and Applied Finance*, vol. 03, no. 03, pp. 391–397, 2000.

[84] I. I. Dimov, P. N. Kolm, L. Maclin, and D. Y. C. Shiber, "Hidden noise structure and random matrix models of stock correlations," *Quantitative Finance*, vol. 12, no. 4, pp. 567–572, 2012.

[85] G. Bonanno, G. Caldarelli, F. Lillo, and R. N. Mantegna, "Topology of correlation-based minimal spanning trees in real and model markets," *Physical Review E: Statistical, Nonlinear, and Soft Matter Physics*, vol. 68, no. 4, Article ID 046130, 2003.

[86] M. Tumminello, T. Aste, T. di Matteo, and R. N. Mantegna, "A tool for filtering information in complex systems," *Proceedings of the National Acadamy of Sciences of the United States of America*, vol. 102, no. 30, pp. 10421–10426, 2005.

[87] J.-P. Onnela, A. Chakraborti, K. Kaski, J. Kertsz, and A. Kanto, "Asset Trees and Asset Graphs in Financial Markets," *Physica Scripta*, vol. 2003, no. T106, p. 48, 2003.

[88] J.-P. Onnela, A. Chakraborti, K. Kaski, J. Kertész, and A. Kanto, "Dynamics of market correlations: Taxonomy and portfolio analysis," *Physical Review E: Statistical, Nonlinear, and Soft Matter Physics*, vol. 68, no. 5, Article ID 056110, 2003.

[89] D. Y. Kenett, M. Tumminello, A. Madi, G. Gur-Gershgoren, R. N. Mantegna, and E. Ben-Jacob, "Dominating clasp of the financial sector revealed by partial correlation analysis of the stock market," *PLoS ONE*, vol. 5, no. 12, Article ID e15032, 2010.

[90] D. Y. Kenett, X. Huang, I. Vodenska, S. Havlin, and H. E. Stanley, "Partial correlation analysis: applications for financial markets," *Quantitative Finance*, vol. 15, no. 4, pp. 569–578, 2015.

[91] L. China Securities Index Company, *China Securities Index 300 Index*, 2017, http://www.csindex.com.cn/sseportal_en/csiportal/zs/jbxx/report.do?code=000300.

[92] "S&p 500 index," 2017, http://us.spindices.com/indices/equity/sp-500.

[93] J.-P. Onnela, *Complex Networks in The Study of Financial And Social Systems*, Helsinki University of Technology, 2006.

[94] W. Jang, J. Lee, and W. Chang, "Currency crises and the evolution of foreign exchange market: evidence from minimum spanning tree," *Physica A: Statistical Mechanics and its Applications*, vol. 390, no. 4, pp. 707–718, 2011.

[95] J. B. Kruskal, "On the shortest spanning subtree of a graph and the traveling salesman problem," *Proceedings of the American Mathematical Society*, vol. 7, no. 1, pp. 48–50, 1956.

[96] G. Bonanno, G. Caldarelli, F. Lillo, S. Micciché, N. Vandewalle, and R. N. Mantegna, "Networks of equities in financial markets," *The European Physical Journal B - Condensed Matter and Complex Systems*, vol. 38, no. 2, pp. 363–371, 2004.

[97] R. N. Mantegna and H. E. Stanley, *An Introduction to Econophysics: Correlations and Complexity in Finance*, Cambridge University Press, New York, NY, USA, 2000.

[98] C. Tu, "Cointegration-based financial networks study in Chinese stock market," *Physica A: Statistical Mechanics and its Applications*, vol. 402, no. 3, pp. 245–254, 2014.

[99] G.-J. Wang and C. Xie, "Correlation structure and dynamics of international real estate securities markets: A network perspective," *Physica A: Statistical Mechanics and Its Applications*, vol. 424, pp. 176–193, 2015.

[100] M. Eryiğit and R. Eryiğit, "Network structure of cross-correlations among the world market indices," *Physica A: Statistical Mechanics and its Applications*, vol. 388, no. 17, pp. 3551–3562, 2009.

[101] T. Di Matteo and T. Aste, "Extracting the correlation structure by means of planar embedding," in *Proceedings of the SPIE*, vol. 6039, p. 60390P, Brisbane, Australia, 2005.

[102] J. Birch, A. A. Pantelous, and K. Zuev, "The maximum number of 3- and 4-cliques within a planar maximally filtered graph," *Physica A: Statistical Mechanics and its Applications*, vol. 417, pp. 221–229, 2015.

[103] N. Musmeci, T. Aste, and T. Di Matteo, "Relation between financial market structure and the real economy: Comparison between clustering methods," *PLoS ONE*, vol. 10, no. 3, 2015, http://dx.doi.org/10.1371.

[104] F. Pozzi, T. Aste, G. Rotundo et al., "Dynamical correlations in financial systems," in *Proceedings of the SPIE*, vol. 6802, p. 68021E, Canberra, ACT, Australia, 2007.

[105] J. Liu, C. K. Tse, and K. He, "Fierce stock market fluctuation disrupts scalefree distribution," *Quantitative Finance*, vol. 11, no. 6, pp. 817–823, 2011.

[106] V. Batagelj and A. Mrvar, "Pajek-program for large network analysis," *Connections*, vol. 21, no. 2, pp. 47–57, 1998.

[107] Y. Mai, H. Chen, and L. Meng, "An analysis of the sectorial influence of CSI300 stocks within the directed network," *Physica A: Statistical Mechanics and its Applications*, vol. 396, pp. 235–241, 2014.

[108] R. Rammal, G. Toulouse, and M. A. Virasoro, "Ultrametricity for physicists," *Reviews of Modern Physics*, vol. 58, no. 3, pp. 765–788, 1986.

[109] R. Yang, X. Li, and T. Zhang, "Analysis of linkage effects among industry sectors in China's stock market before and after the financial crisis," *Physica A: Statistical Mechanics and its Applications*, vol. 411, pp. 12–20, 2014.

[110] E. Kantar, M. Keskin, and B. Deviren, "Analysis of the effects of the global financial crisis on the Turkish economy, using hierarchical methods," *Physica A: Statistical Mechanics and its Applications*, vol. 391, no. 7, pp. 2342–2352, 2012.

[111] A. Rea and W. Rea, "Visualization of a stock market correlation matrix," *Physica A: Statistical Mechanics and its Applications*, vol. 400, pp. 109–123, 2014.

[112] R. C. Prim, "Shortest connection networks and some generalizations," *Bell System Technical Journal*, vol. 36, no. 6, pp. 1389–1401, 1957.

[113] R. J. Elliott, J. van der Hoek, and W. P. Malcolm, "Pairs trading," *Quantitative Finance*, vol. 5, no. 3, pp. 271–276, 2005.

[114] E. Gatev, W. N. Goetzmann, and K. G. Rouwenhorst, "Pairs trading: performance of a relative-value arbitrage rule," *Review of Financial Studies*, vol. 19, no. 3, pp. 797–827, 2006.

[115] S. Mudchanatongsuk, J. A. Primbs, and W. Wong, "Optimal pairs trading: A stochastic control approach," in *Proceedings of the 2008 American Control Conference, ACC*, pp. 1035–1039, USA, June 2008.

[116] J. Wang, C. Rostoker, and A. Wagner, "A high performance pair trading application," in *Proceedings of the 2009 IEEE International Symposium on Parallel & Distributed Processing (IPDPS)*, pp. 1–8, Rome, Italy, May 2009.

Hindawi
Complexity
Volume 2018, Article ID 8283919, 9 pages
https://doi.org/10.1155/2018/8283919

Research Article

SOSerbia: Android-Based Software Platform for Sending Emergency Messages

Mihailo Jovanovic,[1] Ivan Babic,[2] Milan Cabarkapa,[3] Jelena Misic,[4] Sasa Mijalkovic,[1] Vojkan Nikolic,[1] and Dragan Randjelovic[1]

[1]*Department for Informatics and Computing, Criminalistics and Police University, Belgrade 11000, Serbia*
[2]*Department for Postgraduate Studies, Singidunum University, Belgrade 11000, Serbia*
[3]*School of Electrical Engineering, University of Belgrade, Belgrade 11000, Serbia*
[4]*Faculty of Electronic Engineering, University of Nis, Nis 18000, Serbia*

Correspondence should be addressed to Milan Cabarkapa; cabmilan@etf.rs

Received 18 May 2018; Accepted 3 September 2018; Published 23 October 2018

Guest Editor: Miguel Fuentes

This paper presents Android-based SOS platform named SOSerbia for sending emergency messages by citizens in Serbia. The heart of the platform is SOS client Android application which is an easy and simple solution for sending SOS messages with unique combination of volume buttons. The proposed platform solves a lot of safety, security, and emergency problems for people who can be in dangerous situations. After a person presses a correct combination of buttons, a message with his or her location is sent to the operating center of the Serbian Police. The platform merges several appropriately combined advanced Android technologies into one complete solution. The proposed solution also uses the Google location API for getting user's location and Media Player broadcast receiver for reading pressed buttons for volume. This logic can be also customized for any other mobile operating system. In other words, the proposed architecture can be also implemented in iOS or Windows OS. It should be noted that the proposed architecture is optimized for different mobile devices. It is also implemented with simple widget and background process based on location. The proposed platform is experimentally demonstrated as a part of emergency response center at the Ministry of Interior of the Republic of Serbia. This platform overcomes real-life problems that other state-of-the-art solutions introduce and can be applied and integrated easily in any national police and e-government systems.

1. Introduction

Nowadays, IT technologies grow rapidly and constantly. Our daily life cannot be imagined without using these technologies. An accelerated development of the mobile OS, such as Android and iOS, has changed the main point of using mobile phones. A mobile phone is not used only for telephoning and sending messages but also is used for many new and smart features. Some of these features allow location sharing and tracking, which denotes a powerful and efficient tool that should be used carefully because of the private information, such as location [1]. On the other hand, in recent years, people live faster. In general, people could experience a lot of unexpected situations like accidents, hijacking, and criminal rate on a daily basis. Fortunately, people have their mobile phones next to them at any moment, so they can feel more protected. Thus, they can act in emergency situations quickly and save their lives. Due to the fact that Android is the most commonly used OS for mobile [2–5], there are many applications developed and specialized for its easy use (please see [1] and references therein). In other words, nowadays, the problem of emergency, dangerous situations can be potentially solved to the certain extent. According to statistics of the Ministry of Interior of the Republic of Serbia, in the Republic of Serbia, in the last 10 years, there were 139 kidnapping, 791 rapes, 257 rape attempts, 43,482 cases of home violence, 1446 thieveries, 32,584 robberies, 426 trafficking, 4 terrorism actions, 791 cases of school violence, 439,368 car accidents, and 216,041 fire accidents. This paper suggests an approach to the security problem in Serbia

through the implementation of modern mobile architecture, to address the mentioned issues of emergency and dangerous situations for people who are in trouble. The main aim is to enable people to send in an easy and unnoticeable way a SMS message containing their location to the Police Operating Center. To the best knowledge of the authors, this appropriate combination of advanced Android technologies proposed in this paper for the first time constructs unique, complete, and operatively usable software platform for sending emergency messages. The source code of Android application can be pulled from https://bitbucket.org/bicba90/sos_android/. The proposed platform clearly overcomes the problems introduced in previously proposed solutions described in literature.

The rest of the paper is organized as follows. In Related Work, the related works and applications are presented. In The Architecture of the Proposed Platform, the architecture and operation of the proposed solution are presented. A description of implementation of the proposed platform is presented in Implementation. The next section, Experimental Usage and Evaluation, is provided and discussed. Finally, the Conclusion is given in last section.

2. Related Work

Mobile applications and mobile services are becoming one of the technology mainstreams in recent years. Android-based applications are becoming a proper tool in order to solve different everyday life problems [1, 6, 7]. Recently, many researchers have tried to find a proper solution to address the security issue in the case of emergency [8–13], but there has been no proper solution.

In [8], an Android application that offers SOS message sending using the GPS location via a WhatsApp messenger to predefine recipient was proposed. To activate an SOS message sending, user has to shake his Android phone while the application is running. The main idea the author had was to enable sending of user's location via some of the modern services such as WhatsApp. However, if the application is not running, and the user is in a situation where he cannot pull out his or her phone from a pocket or a bag, this application is of no use.

Similar application intended for the cases where there is no operation of mobile communication systems was presented in [9]. The proposed application is used in a way that a group of phones, which have this application installed, create an ad hoc, a peer-to-peer-like, wireless network. On the one hand, this application is very good because in many cases, such as earthquake and other natural disaster cases, due to the damages, there is no proper operation of standard communication systems. On the other hand, this is not a good solution because it relies on a fact that each user has an installed proposed application, which could not be the case and which surely decreases the effectiveness of the proposed application. This application is also convenient for the places when there is no mobile communication signal, such as rural places. However, in this modern society, there is almost no place where there is no mobile communication signal. Due to the all abovementioned options, it can be concluded that the proposed application is good to be used in some situations but it cannot address the problem that we try to solve here. If other Android phones near us do not use this application, then this is useless, and the messages go as far as the network of phones goes, and apart from all that, in most cases when there is an emergency, the mobile network is available, so there is no need for this application.

The application that addresses the problem of the location on the roads is presented in [10]. Namely, it was concluded that road accidents are the factors that increase the mortality level. So the basic idea of the application is to warn a driver that he is approaching dangerous corner and help him slow down and prepare for the corner. The application is notifying a driver about the dangerous corner within 700 meters before the sharp corner. The warning is realized by playing "buzz" sound as the alert, to tell the driver that there are dangerous corners ahead. Besides, this system will give suggestions to the closest emergency places by only refreshing the list of the places and pin point the emergency places on map. The localization technique used in this application is very similar to those we use in our application. Both the application presented in [10] and our application use the GPS service to obtain accurate user position. However, the application [10] is customized for road transport and cannot solve several different kinds of dangerous situations.

Furthermore, there is a similar application is *bSafe* Android application [11]. This application provides more than one option to the user; namely, four services are provided: *bSafe Alarm*, *Follow me*, *Timer Alarm*, and *Fake call*. The first one is intended for sending an SMS with the user location, but besides the location, both audio and video data can be sent together with the information about the location. When this option is activated, an automatic recording is triggered and the recorded data is sent to the desired number or numbers. In this application, user can define a friend cycle containing as mush numbers as the user wants, and these numbers can be edited unlimited number of times. The second option allows tracking of the user's location on the map in real time. The third option allows user to set the time he thinks he will reach some location, and if he does not reach the location in defined period, SMS message with his current location will be sent. The last, but not the least, option provides a face call. When user activates this option, the face call is performed, which can be beneficial in the case when user wants to divert attacker's attention by letting him know that there is someone who could hear if attack happens, which could be used as a kind of evidence. However, this app is not integrated with any centralized system and is not useful in several dangerous situations where there is no time for active usage of mobile phone.

The application *GoSuraksheit* [12] is also one of the similar applications. This application is also intended for sending of the SMS with the user's location. The operation principle is the similar to the presented applications [10, 11]. The user's location is obtained by using the GPS and then forwarded to the desired numbers (up to five numbers). The main advantage of this application is that it provides a possibility to share the location on a popular social network, Facebook.

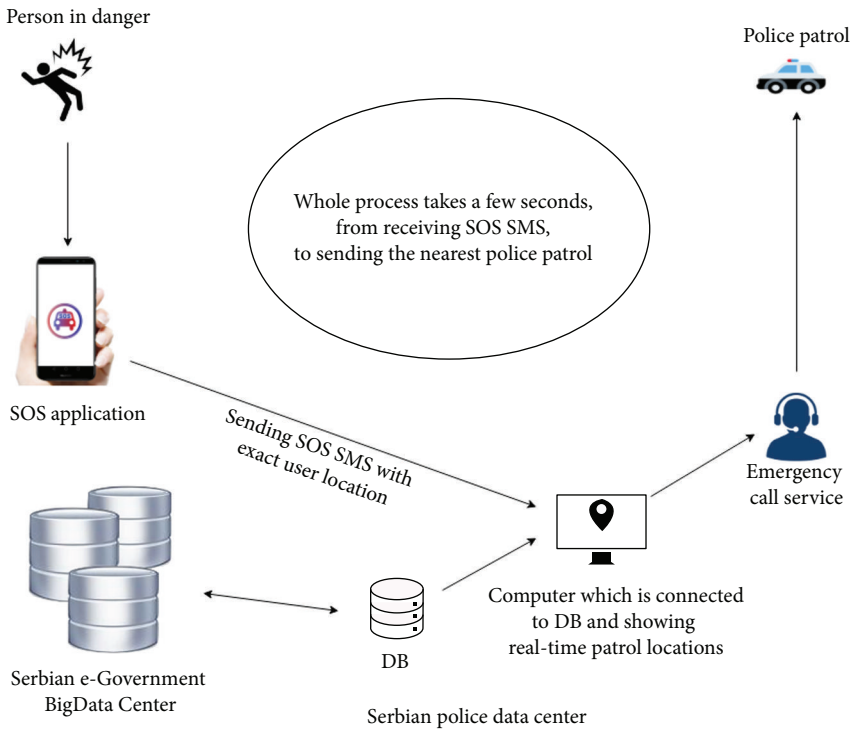

Figure 1: The architecture of the proposed platform.

The main disadvantages of the service presented in paper [12] are as follows:

(i) The service does not include any centralized logic and integration into government system

(ii) The client mobile app is not applicable in many dangerous situations

The application presented in [13] allows mobile phone user in an emergency to send the SMS to the police or rescue center. With each request, user's location coordinates are sent to the police center number. This application can operate in two modes, network mode and GPS mode. All the details of a user, such as description, priority, and current location report, are sent to the server. In other words, this app solves the problem of integration with the centralized system in order to help the citizens, but it is also inapplicable in several dangerous situations when the victim cannot actively use mobile phone.

To summarize, in order to trigger previously listed applications, it is necessary to open the application on a mobile phone which is sometimes impossible to do. The shortcomings of these applications is that there is no emergency button or trigger for fast and silent alert, even if the application has some sort of silent switch, such as phone shaking or detection of user running, which is not good because the application can be triggered accidently. In addition, some of the presented applications do not have the widget. Moreover, there is no any information about experimental usage of the proposed app [8–13] and its reaction time measurements in real-life situation. These services also cannot give any useful analytics after long-time operative usage of client app.

On the other hand, the application we propose here effectively works in the situations when the victim cannot easily and actively use mobile phone. It can even work if the screen is broken and the device is locked, and it sends messages directly to the Police Data Center. This center is integrated with Serbian e-Government BigData Center and it will be possible to apply advanced analytics solutions after the proposed service generates a sufficiently large amount of data.

3. The Architecture of the Proposed Platform

The architecture of the proposed application and its operation is presented in Figure 1. As it can be seen, the first step is sending of the SOS message when the user is in danger. The second one is processing of sent data at the police computer center that has a DB connected to Serbian e-Government BigData Center. This DB has a list of users and exact real-time locations of police patrols, so it can be easily calculated the nearest patrol distance. After this step, patrol is informed by the dispatch center about location where they should go. The main purpose of this process is to minimize the time from sending the SMS to getting a help from the police. By using the proposed application, in only few steps, of which the first one is triggering SMS with buttons, the second one is related to the DB with users where we already know who is sending the SMS, and the third is a determination the closest police patrol according to the obtained information on user's location (each patrol is

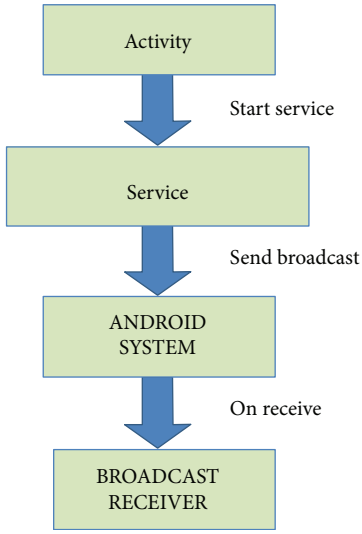

Figure 2: The architecture of the client Android application.

equipped with a GPS transmitter). The patrol should be informed where to go by the operator from Police Data Center, and that is the only part that is not automated.

The proposed architecture of the client Android application is shown in Figure 2. Three components properly combined are necessary to provide a good operation flow of suggested solution: activity, service, and broadcast receiver [14]. An activity interacts with user so it creates a window to place UI (user interface) elements. An Android application can contain several activities, which means that many different screens can interact with each other [15]. In proposed approach, user via view in activity sends a request for starting service that is responsible for getting current location. To explain, *service* is a component which runs in the background without direct interaction with the user and it is used for repetitive and potentially long running operations. As the service has no user interface, it is not bound to the lifecycle of an activity [14]. In the proposed client app, broadcast receiver is responsible for registering system events and allows reading pressed buttons for default combination as an Android component which allows you to register for system or application events. All registered receivers for an event are notified by the Android runtime once this event happens.

To sum up, implemented client solution is consisted of these three components. For release stage, SOS application also uses Google API Client library for locations ("com.google.android.gms:play-services-location:10.2.6") for getting user's location. Google Location Services API is the most popular service for adding location awareness with automated location tracking, geofencing, and activity recognition.

The proposed architecture of the client Android application also allows implementation of multiple options, such as

(i) emergency trigger—for emergency SMS sending to the emergency services

(ii) widget trigger—same as previous, but only for sending when phone is unlocked

(iii) pattern/pin—for opening and activating application

(iv) time locker—for setting application's active hours

(v) SMS remote control—if application receives a message from predefined number with certain code (#123backup), for example, it will trigger data backup (SMS, images, videos, and documents), user will be able to select what he wants to save or upload to cloud

(vi) restore/factory reset—in case the device is stolen or lost

(vii) app icon hidden in whole user system—in case the phone is stolen

(viii) camera remote control—again trigger feature remotely, this time turn camera on, take a picture with front and rear camera, and send it to predefined number

For the first release of the service, we have selected first two options to implement, emergency trigger and widget trigger. In other words, our SOS application is developed for working in two ways. First, service is implemented to have listener for buttons that user needs to press (default combination for sending SOS message). Second, service is implemented when widget has occurred. When user presses widget, it automatically sends message with its own location and any other information if the service is customized for different users.

4. Implementation

4.1. Release Stage. SOS application for sending emergency messages uses Android platform. This is an offline app, which means that it can work without access to the Internet. What this essentially means is that it gives a better experience to the users, and it can even be a key factor for them in order to retain or uninstall application. Further, the main reasons for using Android as a client platform are as follows:

(i) Open source (can be leveraged without having to worry about the licensing costs)

(ii) Dissociation of the user's interface from the business logic

(iii) Asynchronous calls (easy to code client-side multithreading)

(iv) Customizable user interface (create custom interfaces for different business)

(v) Reusable and responsive components (support for Android material)

(vi) Portability (can easily be ported to other mobile operating systems)

The list of features and advantages embedded in *Android OS* is quite long. The core release-stage functionality is to send message, prompted by the users, based on existing

Figure 3: Main screen implementation.

services implemented for listening and getting location. This client-side module provides integration of *Google Service API Location* and JSON for parsing model.

On the one hand, with the listener services used on the UI side, SOS client communicates with this service that has been started in background and performs location task and starts broadcast receiver for media. On the other hand, there is a widget, which user presses and triggers service during this process.

4.2. User Interface. In one word, user interface is everything that the user can see and interact with. User interface of the proposed client Android application is shown in Figure 3. Android provides a variety of prebuilt UI components, such as structured layout objects and UI controls that allow to build the graphical user interface (see Figure 4). UI in SOS application is implemented in XML, using primarily LinearLayout [15]. LinearLayout is a view group that aligns all children in a single direction, vertically or horizontally and also supports assigning a weight to individual child with the android: layout_weight attribute. This attribute assigns an "importance" value to a view in terms of how much space it should occupy on the screen.

4.3. Widget. App Widgets are miniature application views that can be embedded in other applications (such as the home screen) and receive periodic updates [15]. These views are referred to as widgets in the user interface, and it can be published one with an App Widget provider. An application component that is able to hold other App Widgets is called an App Widget host. Figure 5 shows implemented SOS App Widget.

As mentioned, SOS application uses App Widget declared in manifest file (see Figure 6) implemented in class *CustomAppWidgetProvider* which extends class AppWidgetProvider. The AppWidgetProvider class extends BroadcastReceiver as a convenience class to handle the App Widget broadcasts. The AppWidgetProvider receives only the event broadcasts that are relevant to the App Widget, such as when the App Widget is updated, deleted, enabled, and disabled. When these broadcast events occur, the AppWidgetProvider receives method calls such as OnUpdate() and OnReceive() method.

The proposed client application calls OnUpdate() method when the user adds the App Widget, so it should perform the essential setup, such as to define event handlers for views and to start a temporary service, if necessary. However, if you have declared a configuration activity, this method is not called when the user adds the App Widget, but is called for the subsequent updates. It is the responsibility of the configuration activity to perform the first update when configuration is done (see Figure 7).

The proposed client application calls OnReceive() method for every broadcast and before each of the rest callback methods. This method checks if location is turned on. If yes, service is starting. If not, it shows toast message for warning to turn the location on in settings (see Figure 8).

4.4. Service. A service is an application component representing either an application's desire to perform a longer-running operation while not interacting with the user or to supply functionality for other applications to use [14]. Each service class must have a corresponding <service> declaration in its package's AndroidManifest.xml. Services can be started with Context.startService() and Context.bindService(). Services run in the main thread of their hosting process. In this work, two services are implemented: volume service and widget service.

4.5. Volume Service. A volume service is one of two applications services, as we can see in Figure 9. Service can be started and stopped by the user, by pushing one of those two buttons *Pokreni servis* (eng. *Start service*) and *Zaustavi servis* (eng. *Stop service*). It is called volume service mainly because this service is working in background and waiting to capture right the combination of volume buttons sequentially pressed (at this particular implementation case that combination is set to up-down-up-down). This combination of volume buttons pressed triggers the SMS sending (see Figure 10). After service is started, location services must be enabled so that volume service can send user's location in message. Basic principle is that after user triggers the right combination, service starts with gathering information about user's location which usually takes between 1 and 5 seconds (mainly depends on connection quality at the moment of sending SOS SMS message) and immediately after that it sends message with map link. After sending the message, volume service remains active if there is need for a new send.

```
<LinearLayout xmlns:android="http://schemas.android.com/apk/res/android"
    xmlns:tools="http://schemas.android.com/tools"
    android:layout_width="match_parent"
    android:layout_height="match_parent"
    android:background="@color/colorBlue"
    android:orientation="vertical"
    android:padding="16dp">

    <ImageView
        android:id="@+id/imageView"
        android:layout_width="match_parent"
        android:layout_height="match_parent"
        android:layout_weight="2"
        android:scaleType="fitCenter"
        android:src="@drawable/logo"
        tools:ignore="ContentDescription" />

    <LinearLayout
        android:layout_width="match_parent"
        android:layout_height="wrap_content"
        android:orientation="vertical">

        <LinearLayout
            android:layout_width="match_parent"
            android:layout_height="wrap_content"
            android:orientation="horizontal">

            <Button
                android:id="@+id/start_button"
                style="?android:attr/buttonBarButtonStyle"
                android:layout_width="match_parent"
                android:layout_height="50dp"
                android:layout_marginEnd="8dp"
                android:layout_marginRight="8dp"
```

Figure 4: Main screen implemented in XML.

Figure 5: SOS widget.

4.6. Widget Service. A widget service implementation shown in Figure 11 has almost the same logic as volume service; the difference between them is that the widget service is triggered by widget button, after which is not listening for volume button-pressed combination, but instead it starts location services and sends message after finding the right location. Also, widget service is destroyed after sending message, because its only purpose is to send message in the shortest way. So, the implemented principle is that the service sends a message on location change, as we can see in Figure 12. When service finds a location, it sends a message, stops the location updates, and destroys the widget service.

4.7. Presentation of Solution. Final result generated by proposed client is shown in Figure 13. We can see a message which contains link to the Google maps with user's coordinates shown as a pin. Message contains text in this form—"SOS my location is *Google maps link*." With this location, user who sends an SOS message can be rescued in the short period of time. The form of SOS message can be easily customized to different kinds of app users.

5. Experimental Usage and Evaluation

For evaluation purposes, the platform has been tested multiple times in different real-life situations. Application is working as intended and sends a message every time after a given command.

During the period of experimental usage, the shortest reaction time was less than a minute that includes period from sending SOS SMS until the arrival of police patrol, and the longest period was 3 minutes, and that was the situation where police patrol was on the other side of their patrolling area; in other words, they were at furthest possible location from the accident (approximately 4 km). These specific numbers are roughly measured using few simulation attempts as well as some real-life situations and statistical data from the Ministry of Interior, Republic of Serbia, and they highly depend on internal police organization.

Drawbacks of the app are the locations, which are not correct in closed spaces or not even shown at all, and it is because of device's inability to find GPS satellites. Also, other issue is the high buildings with lots of floors, where the coordinates are the same for the whole building and there are lots of apartments in it, but that can be almost fixed by sending the elevation of device. However, we will still have a problem with multiple apartments, for example. So those are the few things that we have to look back at, during further development of the proposed platform.

```
<receiver android:name="com.sosService.CustomAppWidgetProvider">
    <intent-filter>
        <action android:name="android.appwidget.action.APPWIDGET_UPDATE" />
    </intent-filter>

    <meta-data
        android:name="android.appwidget.provider"
        android:resource="@xml/widget_info" />
</receiver>
```

Figure 6: CustomAppWidgetProvider declared in manifest file.

```
@Override
public void onUpdate(Context context, AppWidgetManager appWidgetManager, int[] appWidgetIds) {
    final int count = appWidgetIds.length;
    this.context = context;
    for (int i = 0; i < count; i++) {
        int widgetId = appWidgetIds[i];

        remoteViews = new RemoteViews(context.getPackageName(),
                R.layout.layout_widget);
        remoteViews.setTextViewText(R.id.textView, text: "");

        Intent intent = new Intent(context, CustomAppWidgetProvider.class);
        intent.setAction(AppWidgetManager.ACTION_APPWIDGET_UPDATE);
        intent.putExtra(AppWidgetManager.EXTRA_APPWIDGET_IDS, appWidgetIds);
        PendingIntent pendingIntent = PendingIntent.getBroadcast(context,
                requestCode: 0, intent, PendingIntent.FLAG_UPDATE_CURRENT);

        remoteViews.setOnClickPendingIntent(R.id.start_button,
                getPendingSelfIntent(context, BUTTON_SOS));

        appWidgetManager.updateAppWidget(widgetId, remoteViews);
    }
```

Figure 7: OnUpdate method in CustomAppWidgetProvider class.

```
public void onReceive(Context context, Intent intent) {
    super.onReceive(context, intent);

    if (BUTTON_SOS.equals(intent.getAction())) {

        final LocationManager manager = (LocationManager) context.getSystemService(Context.LOCATION_SERVICE);
        if (!manager.isProviderEnabled(LocationManager.GPS_PROVIDER)) {
            context.startActivity(new Intent(Settings.ACTION_LOCATION_SOURCE_SETTINGS));
            Toast.makeText(context, "Uključite GPS/Lokacijske servise i pritisnite dugme ponovo", Toast.LENGTH_LONG).show();
        } else {
            context.stopService(new Intent(context, WidgetService.class));

            context.startService(new Intent(context, WidgetService.class));
        }

    }
}
```

Figure 8: OnReceive() method in CustomAppWidgetProvider class.

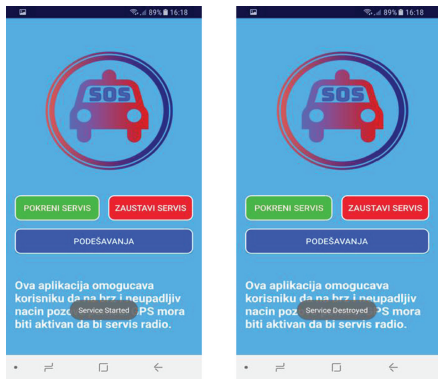

Figure 9: Main screen with start and stop buttons for service and settings button for the app.

6. Conclusion

In this paper, an Android-based SOS software platform has been presented. The client SOS application is designed in a way to enable user to send his location in a simple and unnoticeable way. The performance of the proposed application has been verified experimentally. The application is shown to be very useful in a large number of life-threatening situations. Moreover, this kind of applications is very suitable for children monitoring during many of their activities, such as going to the school, for a run, or during travelling, and in the situation where children find themselves in an unknown place or dangerous situation.

One of the main advantages of the proposed application is that it is directly connected to the police system and its

```
private BroadcastReceiver broadcastReceiver = (context, intent) → {
        if ("android.media.VOLUME_CHANGED_ACTION".equals(intent.getAction())) {
            int volume = intent.getIntExtra( name: "android.media.EXTRA_VOLUME_STREAM_VALUE",  defaultValue: 0);
            if (b == 0) {
                if (volumePrev < volume) {
                    b++;
                    vreme = System.currentTimeMillis();
                }
            } else {
                if (volumePrev < volume) {
                    if (tacnaKombinacija[b]) {
                        b++;
                    } else {
                        b = 0;volumePrev = 0;
                    }
                } else {
                    if (!tacnaKombinacija[b]) {
                        b++;
                    } else {
                        b = 0;volumePrev = 0;}}
            if (b == 7) {
                if (System.currentTimeMillis() - vreme < 5000) {
                    final LocationManager manager = (LocationManager) context.getSystemService(Context.LOCATION_SERVICE);
                    if (!manager.isProviderEnabled(LocationManager.GPS_PROVIDER))
                        Toast.makeText(context, "Uključite GPS/Lokacijske servise i pritisnite dugme ponovo", Toast.LENGTH_LONG).show(
                    else {
                        createLocationRequest();
                        mGoogleApiClient = new GoogleApiClient.Builder( context: VolumeService.this)
                                .addApi(LocationServices.API)
                                .addConnectionCallbacks(VolumeService.this)
                                .addOnConnectionFailedListener(VolumeService.this)
                                .build();
                        mGoogleApiClient.connect();}}
                b = 0;
                volumePrev = 0;}
            Log.i(TAG,  msg: "You have pressed " + b + " prosli " + volumePrev + " sadasnji" + volume);
            volumePrev = volume;}
    };
```

Figure 10: Implemented volume service logic.

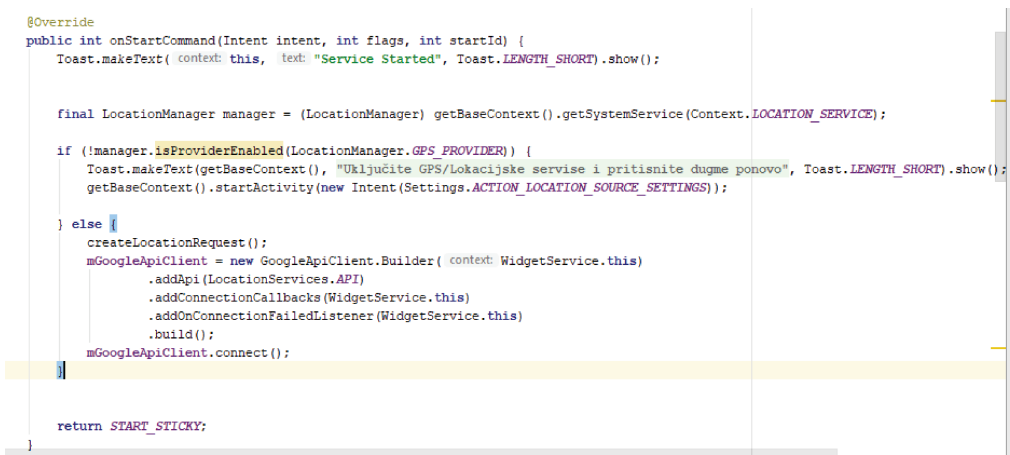

```
@Override
public int onStartCommand(Intent intent, int flags, int startId) {
    Toast.makeText( context: this,  text: "Service Started", Toast.LENGTH_SHORT).show();


    final LocationManager manager = (LocationManager) getBaseContext().getSystemService(Context.LOCATION_SERVICE);

    if (!manager.isProviderEnabled(LocationManager.GPS_PROVIDER)) {
        Toast.makeText(getBaseContext(), "Uključite GPS/Lokacijske servise i pritisnite dugme ponovo", Toast.LENGTH_SHORT).show();
        getBaseContext().startActivity(new Intent(Settings.ACTION_LOCATION_SOURCE_SETTINGS));

    } else {
        createLocationRequest();
        mGoogleApiClient = new GoogleApiClient.Builder( context: WidgetService.this)
                .addApi(LocationServices.API)
                .addConnectionCallbacks(WidgetService.this)
                .addOnConnectionFailedListener(WidgetService.this)
                .build();
        mGoogleApiClient.connect();
    }


    return START_STICKY;
}
```

Figure 11: Implemented widget service logic.

```
@Override
public void onLocationChanged(Location location) {
    loc = location;

    //  String phoneNo = "+381652222796";
    String phoneNo =  SharedPreferencesUtil.getSettings(getBaseContext()).getPhone();
    String msg = "SOS moja lokacija je";

    String myLocation = " http://www.google.com/maps/place/lat,lon/@lat,lon,14z";
    myLocation = myLocation.replaceAll( regex: "lat", String.valueOf(loc.getLatitude())).replaceAll( regex: "lon", String.valueOf(loc

    SmsManager smsManager = SmsManager.getDefault();
    smsManager.sendTextMessage(phoneNo,  scAddress: null,  text: msg + myLocation,  sentIntent: null,  deliveryIntent: null);
    Toast.makeText( context: this, "SOS poruka poslata!", Toast.LENGTH_SHORT).show();
    stopLocationUpdates();

}

protected void startLocationUpdates() {
    PendingResult<Status> pendingResult = LocationServices.FusedLocationApi.requestLocationUpdates(
            mGoogleApiClient, mLocationRequest,  locationListener: this);
}

protected void createLocationRequest() {
    mLocationRequest = new LocationRequest();
    mLocationRequest.setInterval(INTERVAL);
    mLocationRequest.setFastestInterval(FASTEST_INTERVAL);
    mLocationRequest.setPriority(LocationRequest.PRIORITY_BALANCED_POWER_ACCURACY);
}
```

Figure 12: Implemented location update logic.

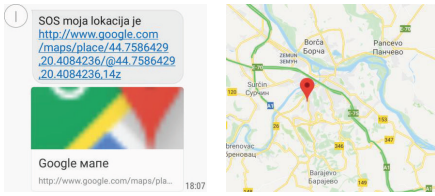

Figures 13: Example of SOS emergency message.

database, which means that a needed and necessary help can be obtained as soon as possible. Besides, the police have the information on all mobile phone users and real-time locations of all police patrols and there are a large number of highly experienced people who can help a victim. The other advantage is that almost the entire process is automated; the only thing that should be done manually by an operator at the Police Operation Data Centre is to determine which of the police patrols is the closest to the victim and to direct them to go the sent location to help a victim. This way, the time needed to react is decreased significantly, which can save many lives.

Data Availability

The source code of the proposed application used to support the findings of this study is included within the article. Executable installation file with installation instruction can be found (https://drive.google.com/drive/folders/1WI-4KDNrd9cX49Cf3BS6qJC2f9xMr30Y). This file can be easily generated from the source code included in the article. This app can be easily integrated and tested in any police or similar system.

Conflicts of Interest

The authors declare that they have no conflicts of interest.

Acknowledgments

The authors would like to thank the people from the Sector for Analytics, Telecommunication and Information Technologies, Ministry of Interior, Republic of Serbia, as well as people from Government Office of Information Technology and e-Government, Republic of Serbia, for their support and constructive comments during the implementation and experimental testing.

References

[1] G. Athanasopoulou and P. Koutsakis, "eMatch: an android application for finding friends in your location," *Mobile Information Systems*, vol. 2015, Article ID 463791, 11 pages, 2015.

[2] Y. Yan, S. Cosgrove, V. Anand et al., "RTDroid: a design for real-time android," *IEEE Transactions on Mobile Computing*, vol. 15, no. 10, pp. 2564–2584, 2016.

[3] Y. Yan, K. Dantu, S. Y. Ko, J. Vitek, and L. Ziarek, "Making android run on time," in *2017 IEEE Real-Time and Embedded Technology and Applications Symposium (RTAS)*, pp. 25–36, Pittsburgh, PA, USA, 2017.

[4] M. N. Soorki, M. H. Manshaei, W. Saad et al., "Collaborative real-time content download application for wireless device-to-device communications," in *GLOBECOM 2017 - 2017 IEEE Global Communications Conference*, pp. 1–6, Singapore, 2017.

[5] K. Dantu, S. Y. Ko, and L. Ziarek, "RAINA: reliability and adaptability in android for fog computing," *IEEE Communications Magazine*, vol. 55, no. 4, pp. 41–45, 2017.

[6] D. Bucerzan, C. Ratiu, and M. J. Manolescu, "SmartSteg: a new android based steganography application," *International Journal of Computers, Communications & Control*, vol. 8, no. 5, pp. 681–688, 2013.

[7] K. Bahadoor and P. Hosein, "Application for the detection of dangerous driving and an associated gamification framework," in *2016 IEEE 4th International Conference on Future Internet of Things and Cloud Workshops (FiCloudW)*, pp. 276–281, Vienna, Austria, 2016.

[8] H. Akshay Kumar, N. Divyashree, A. Nithu, R. Revathi, and Y. Suresh, "Anuti — an application to aid during emergency," in *2016 International Conference on Circuits, Controls, Communications and Computing (I4C)*, pp. 1–6, Bangalore, India, 2016.

[9] V. Tundjungsari and A. Sabiq, "Android-based application using mobile adhoc network for search and rescue operation during disaster," in *2017 International Conference on Electrical Engineering and Computer Science (ICECOS)*, pp. 16–21, Palembang, Indonesia, 2017.

[10] A. Z. Zulkafi, S. Basri, L. T. Jung, and R. Ahmad, "Android based car alert system," in *2016 3rd International Conference on Computer and Information Sciences (ICCOINS)*, pp. 501–506, Kuala Lumpur, Malaysia, 2016.

[11] "bSafe Android app," October 2018, https://play.google.com/store/apps/details?id=com.bipper.app.bsafe&hl=en.

[12] "GoSuraksheit Android app," October 2018, https://go-suraksheit.soft112.com/.

[13] R. Jadhav, J. Patel, D. Jain, and S. Phadhtare, "Emergency management system using android application," *International Journal of Computer Science and Information Technologies*, vol. 5, no. 3, pp. 2803–2805, 2014.

[14] D. MacLean, S. Komatineni, and G. Allen, *Pro Android 5*, Apress, 2015.

[15] W. Jackson, *Pro Android UI*, Apress, 2014.

Hindawi
Complexity
Volume 2018, Article ID 5806827, 12 pages
https://doi.org/10.1155/2018/5806827

Research Article

Enhancing Countries' Fitness with Recommender Systems on the International Trade Network

Hao Liao,[1] **Xiao-Min Huang**,[1] **Xing-Tong Wu**,[1] **Ming-Kai Liu**,[1] **Alexandre Vidmer**,[1] **Ming-Yang Zhou**,[1] **and Yi-Cheng Zhang**[1,2]

[1]*National Engineering Laboratory for Big Data System Computing Technology, Guangdong Province Key Laboratory of Popular High Performance Computers, College of Computer Science and Software Engineering, Shenzhen University, Shenzhen 518060, China*
[2]*Department of Physics, University of Fribourg, 1700 Fribourg, Switzerland*

Correspondence should be addressed to Ming-Yang Zhou; zhoumy2010@gmail.com

Received 17 May 2018; Revised 23 August 2018; Accepted 4 October 2018; Published 18 October 2018

Guest Editor: Miguel Fuentes

Prediction is one of the major challenges in complex systems. The prediction methods have shown to be effective predictors of the evolution of networks. These methods can help policy makers to solve practical problems successfully and make better strategy for the future. In this work, we focus on exporting countries' data of the International Trade Network. A recommendation system is then used to identify the products that correspond to the production capacity of each individual country but are somehow overlooked by the country. Then, we simulate the evolution of the country's fitness if it would have followed the recommendations. The result of this work is the combination of these two methods to provide insights to countries on how to enhance the diversification of their exported products in a scientific way and improve national competitiveness significantly, especially for developing countries.

1. Introduction

International trade plays a considerable role in the exchange channels between countries [1, 2]. It is also becoming more important as time goes on. In 1960, international trade accounted for roughly 25% of a country's total Gross Domestic Product (GDP). Nowadays it accounts for nearly 60% of countries GDP [3]. Historically, various classic economic models were developed to evaluate the dissimilarity of wealth resulting from the exportation of diverse goods [4]. Models based on the gravity equation were also developed and showed to be adequate to explain many of the features of the international trade [5]. Another approach, the Product Space, attempted to illustrate how the nations will develop in the future by projecting the exports data onto a two-dimensional map and observing the diffusion of the export process [6]. Economic models mainly consist of commodity profits, geographical relations, comprehensive productivity, economic structure [7], and a series of macroeconomic elements. In practice, numerous complex external factors, e.g., national policies, religious beliefs, and the country's current production capacity, are key components in the international trade. Here, we also recognize that plenty of sociologists have constructed grand theories on the empirical study of global economic development [8–10]. These methods and theories were developed by David Snyder and Edward L. Kick [11]; it was the first study of international trade and world economic growth using a network framework in the American Journal of Sociology, 1979. In [12], the authors emphasized the importance of the global trade, and the structure of the modern world system was addressed by multiple-network analysis. The complex network approach was also used in [13], and it was shown that the International Trade Network and the World Wide Web both have collaborative characteristics [14]. Indeed, the International Trade Network is a complex network in terms of structure. With this is in mind, we apply recommendation algorithms that are usually applied on e-commerce systems in order to predict the evolution of the International Trade Network [15–17].

Two methods were proposed to assign scores to countries and products using the complex network approach. The basis

of these methods is to analyze the relation between countries and their exports and then to rank the countries according to their economic competitiveness and the exported good with the economic advantage they bring to the exporting countries. The first method, the Method of Reflection (MR), proposed the Economic Complexity Index (ECI) to account for the production characteristics of countries. The countries are ranked according to their exporting capacity. The authors pointed out that the method is able to predict the future economic expansion of countries and that the scores obtained with MR indicate which products should be exported in order to maximize the countries' performance [18]. In [19], a method based on the Markov chain was proposed. The method showed the need to take into account the nonlinear interactions between exported commodities and national diversity. This led to the development of the Fitness and Complexity metric [20]. It is an iterative method based on the nonlinearity of the system. This method was shown to be conceptually more grounded than the previous ones and a better predictor of the economic evolution [21, 22]. This method was applied to forecast the GDP growth in a recent work. The authors reported that their estimates were on average 25 percent more accurate than were those made by the International Monetary Fund [23].

In this paper, we start with a detailed definition of the used algorithms, namely, the Probabilistic Spreading algorithm [24], the Heat Spreading algorithm [25], the Degree Increase algorithm [26], and the Time-Aware Probabilistic Spreading algorithms [27]. We then apply these four algorithms to the International Trade Network and compare their performance on two different aspects. The first one is the evaluation of the accuracy of the recommendation, which is a standard evaluation of the recommendation algorithms. The second aspect is the evaluation of the algorithms on their ability to recommend products that would improve the countries' fitness. This is obtained by the combination of the recommendation results with the Fitness and Complexity scores to simulate the changes in rankings and fitness values of countries after exporting recommended products. The experimental results confirm the validity of the recommendation algorithm on this task and show the validity of our approach to tackle this problem.

2. Materials and Methods

2.1. International Trade Network

2001 to 2015. This dataset was cleaned using *harmonization* techniques in [28] and the similar categories were merged together. Additionally, the countries that had no entries recorded for exportation between 2001 and 2015 were removed. After cleaning procedure, the International Trade Network was comprised of 192 countries and 786 commodities. We use the bipartite network approach to represent the data. In this approach, one set of nodes represents the countries, and the second set of nodes represents the commodities. If a country is considered as an exporter of a commodity, a link connects the country's node and the commodity node.

RCA. The data of the International Trade Network includes country nodes and commodity nodes. These two types of nodes form a bipartite network. One important aspect of our network representation is that it is binary. Either two nodes are connected, or they are not. We then need a criterion to define if a country can be considered as an exporter of a commodity or not. Indeed, even if countries cannot produce a specific commodity, they might export a very small amount of it. Therefore it should not be considered as an exporter of the commodity. In order to quantify the advantage of a country on a commodity, we use the "Revealed Comparative Advantage" (RCA) as a clear constraint to determine whether a country can be considered as an exporter of certain commodities [29].

$$RCA_{i\alpha} = \frac{e_{i\alpha} / \sum_j e_{j\alpha}}{\sum_\beta e_{i\beta} / \sum_{j\beta} e_{j\beta}}, \quad (1)$$

where $e_{i\alpha}$ is the total amount of export α for country i. If the country i is regarded as an exporter of the commodity α, the export amount of the commodity α should occupy a larger proportion in the total amount of the export goods of the country i. We set the RCA value to 1 and the country-commodity will have links when this pair of nodes satisfies the condition of $RCA_{i\alpha} \geq 1$. These nodes and links together constitute the bipartite network of the international trade activities.

2.2. Methods

2.2.1. Recommendation System. Recommendation systems aim at recommending the most adequate items for users. In comparison with traditional link prediction, the focus is put on individual nodes rather than individual links. In our case, the main focus of the recommendation process is the countries nodes. For each country node in the system, the algorithms compute a score for every product in the network. If the country is already considered as an exporter of an item, the score corresponding to the product is set to 0 (i.e., a product that is already exported is not recommended). The recommendation list for each country is composed by the top L products with the highest score for the particular country. We now describe the algorithms used in this work. Note that L is set to 20 in this work and it has been shown to have no impact on the significance of the accuracy [17].

In order to compare the performance of the five recommender algorithms, we choose a year T and predict which additional product the countries export at year $T + 5$ (the testing set) based solely on the data up to year T (the training set).

Probabilistic Spreading (ProbS). For target user i, the initial resources are first distributed evenly on the item side and then propagated to the user side through a random walk process [24]. In the same way, the resources are then returned to the item side. Both steps are used to allocate resources among neighbors and then spread to the other side. Finally, the score of each item for country i is obtained. The initial resource

vector is represented as $f^{(i)}$ and its elements are represented as $f_\alpha^{(i)} = a_{i\alpha}$. The final resource values $s_\alpha^{(i)}$ can be written as

$$s_\alpha^{(i)} = \sum_{\beta=1}^{I} W_{\alpha\beta} f_\beta^{(i)}. \quad (2)$$

The elements of the redistribution matrix W are derived from Probabilistic Spreading process.

$$W_{\alpha\beta} = \frac{1}{k_\beta} \sum_{j=1}^{U} \frac{a_{j\alpha} a_{j\beta}}{k_j}, \quad (3)$$

where I denotes the number of products and U the number of countries. $a_{j\alpha}a_{j\beta}$ represents path from item β to item α through country j in two random walks. The ProbS algorithm employs a column-normalized transition matrix. The partition of k_β and k_j corresponds to the uniform partition of resources between all links from nodes β and j [30].

Heat Spreading (HeatS). The HeatS spreading algorithm evolved from the Probabilistic Spreading algorithm. These two methods are similar in structure and both use random walk processes to the redistribute initial resources. Compared with the ProbS algorithm, resources spread more evenly in the HeatS spreading method and items with only few connections usually benefit from a higher score than with the ProbS algorithm [25].

The initial resource vector is set to $f^{(i)}$ according to user's item collection; the elements $f_\alpha^{(i)} = a_{i\alpha}$ can be regarded as the temperature value of the item. Unlike the ProbS algorithm, which uses column normalization transformation matrix, the HeatS algorithm uses row normalization. The spreading process is represented by a matrix as follows, where $W' = W^T$:

$$W'_{\alpha\beta} = \frac{1}{k_\alpha} \sum_{j=1}^{U} \frac{a_{j\alpha} a_{j\beta}}{k_j}. \quad (4)$$

Resource received by the user i is equal to the average resource owned by the user's collected item. Similarly, item side receives resources transmitted from the user through the averaging process. The item's score is calculated as

$$h_\alpha^{(i)} = \sum_{\beta=1}^{I} W'_{\alpha\beta} f_\beta^{(i)}. \quad (5)$$

Degree Increase (DI). The time information is often overlooked in the evolution of complex networks. In fact, time plays a crucial role in the evolution of information networks [31–33]. The combination of recommendation systems with time dynamics improves the recommendation and allows performing better predictions. It has been proven that the Degree Increase (DI) method can accurately predict the prevalence of items in the future. The increase in popularity of item α within time window τ is

$$\Delta k_\alpha (t, \tau) = k_\alpha (t) - k_\alpha (t - \tau), \quad (6)$$

where item degree $k_\alpha(t) = \sum_i A_{i\alpha}(t)$ corresponds to the number of users who have collected item α. The final item score is expressed as

$$\Delta k'_\alpha (t, \tau) = \Delta k_\alpha (t, \tau) + \varepsilon k_\alpha (t). \quad (7)$$

In practice, the value of ε must be small enough to ensure that the ranking of commodity popularity growth $\Delta k_\alpha(t, \tau)$ does not change.

Time-Aware Probabilistic Spreading (TProbS). The ProbS method is characterized by the fact that spread of resources is cumulative; that is, the more popular items are more likely to get high scores and get recommended to users. The Time-Aware Probabilistic Spreading method integrates the ProbS method with the DI method. It is written mathematically as

$$u_\alpha^{(i)} = s_\alpha^{(i)} \left(\frac{\Delta k'_\alpha (t, \tau)}{k_\alpha (t)} \right)^\theta, \quad (8)$$

where the parameter θ is an additional parameter to define the length of past time window.

2.2.2. Fitness and Complexity Metrics. The Fitness and Complexity metrics are used to measure the competitiveness of countries and the quality of exported products. The algorithm consists of two nonlinear coupling equations [20, 34], which eventually reach a fixed value through iterative methods and the equations are defined as

$$F_i^n = \sum_{\alpha=1}^{I} a_{i\alpha} Q_\alpha^{n-1} \quad (9)$$

$$Q_\alpha^n = \frac{1}{\sum_{i=1}^{U} a_{i\alpha} 1/F_i^{n-1}}, \quad (10)$$

where F_i^n indicates the fitness of country i after n iterations. In [35], the convergence of the algorithm and its stopping condition were demonstrated. The higher the fitness value, the more advantageous the variety and complexity of the goods exported by the country. The study [36] shows that the weak economies can analyze how to get out of the poverty trap and increase the diversification of their exports via fitness metrics. Complexity Q_α^n cannot simply be calculated from the average of countries' fitness. Successful countries export almost all products and it is unable to infer the complexity of each product from their export data (for example, our data shows that a total of 786 products were included in the International Trade Network from 2001 to 2015, and the United States exported a total of 775 kinds of products). Therefore, the complexity of product should be measured in a nonlinear way; namely, it is essential to reduce contribution of successful countries. Assuming that product α possesses two exporters i and j with fitness values of 0.2 and 15, respectively, the complexity of the product would be 0.197. If the two exporters i and j have fitness values of 10 and 15, the complexity would be 6. These two examples verify the fact that the value of complexity depends mainly on the worst exporter.

2.2.3. Precision and Recall Metrics. In general, recommendation algorithms are compared in their ability to predict the future. In order to evaluate their accuracy, we use two metrics, namely, the Precision and the Recall metrics. We are not interested in the accuracy of the algorithms per se, but the accuracy of the recommendation results is an important evaluation indicator. A higher accuracy indicates that the exporting countries possess the capacity to produce the recommended commodities. Indeed, the countries should be able to produce the recommended commodities in the near future; otherwise the recommendation process would be meaningless.

Precision. For each country, the individual Precision is measured as the fraction of recommended products that are eventually exported. If n_i is the number of products that are eventually exported by country i and that are actually recommended, then the Precision for country i is $P_i = n_i/L$. The Precision P is the average of P_i over every country. *Recall*. Recall is similar to Precision, but we use the number of newly exported goods instead of the fixed recommendation list L. If country i exports E_i additional items in the testing set, the individual Recall reads $R_i = n_i/E_i$. The Recall is the average of R_i over every country.

2.3. Addition of Products to Countries' Export Basket. After having obtained the recommendation list from the previously described recommendation methods, we add the goods that are at the top of the recommendation lists to the respective countries' exports baskets. Then, the fitness value of each country is reevaluated and its change is recorded. However, the calculations of fitness are an iterative nonlinear process, which is coupled with the complexity of the products. Thus, in order to evaluate the changes brought by adding the products to the country's export basket, only one country is modified at a time. In other words, for a given country i, only its recommendation list is added to its exports basket and the rest of the network is left untouched. For instance, if we have a high complexity product to the export basket of a low fitness country, the complexity of the product might be greatly reduced, which will have a strong impact on the rest of the Fitness and Complexity values. The simulation process is described as below. For each country, we add the L products in its recommendation list to its export basket. For each product α in the top L part of the recommendation list of country i, we add a link between the country i and the product α in the data. The export volume of product α from country i must satisfy the condition of $RCA \geq 1$.

3. Results

3.1. Accuracy of the Recommendation Algorithms. The first step in the comparison of the algorithms is to compare their accuracies. We perform the predictions from years 2001 to 2010. The results are shown in Figure 1. First, we see that the top performing method is the TProbS method. This is not surprising as this is the one including both the strength of ProbS and time information. The parameter $\theta = 0.2$ is constantly the one giving the highest Recall in our simulation and thus is fixed to this value. Obviously, this lessens the impact of degree increase on the network, which is compatible with the expected behavior of countries development. They should not all focus on the same products, but they still follow the ongoing trends. As noted in [17], the HeatS method performs surprisingly well. This method usually performs poorly in online e-commerce networks [25] but has the advantage of recommending products with lower degree. DI and Degree both perform poorly, which is expected as they do not take into account the production capabilities of countries.

3.2. Tier Division. An interesting study is to investigate the impact of the methods on countries with different fitness rank. It is not certain that a country that belongs to the top of the fitness list will behave the same to a country that belongs at the bottom of the list. In order to study this effect, we divide the countries into three different categories according to their fitness rank. The three categories hold the same number of countries and thus are denoted as top tier, middle tier, and low tier. For each category, we compute the average increased ranking and increased fitness after the addition of the recommended exports. The results are shown in Figure 2. The countries that benefit the most from these recommendations are middle and low tier countries. In panel (a), the most interesting result is in HeatS. The increased rankings by following its recommendation are much higher than those of TProbS. This is especially true with top tier countries, as following the recommendation of TProbS would even lower a country's fitness. This comes from the fact that top tier countries need to innovate and produce goods for which there are only a few competitors, while, for middle and low tier countries, it is sufficient to produce additional items. Note that we try adding time to HeatS: the Recall improved to the level of TProbS, but the improvement of fitness was lower than that of HeatS. So we decided to keep only HeatS and TProbS for simplicity.

From panel (b), we see that the fitness of top tier countries is the one improving the most, which shows that the recommendation algorithm indeed recommends different complex products in line with the ability of the country. For top tier countries, the difference of fitness between two countries is large, while, for lower tier countries, the fitness difference between two countries is much smaller. This fact explains the result that top tier countries' fitness improvement is significant but their ranking is only slightly improved, while the low tier countries can increase the ranking a lot in the case of less improvement in fitness. To illustrate better our recommendation results, we select three countries in each tier. Due to the limit of the page size, we only choose the five products with the highest score according to TProbS and HeatS for each country. The products recommended by TProbS and HeatS are shown in Tables 1 and 2, respectively. Both tables show the products with different complexity for various tier countries.

3.3. Evolution of Countries' Fitness. In order to directly study the effect of each algorithm on the country's fitness value, we randomly select 30 countries in the middle tier and compare

Table 1: The top five recommended products by TProbS algorithms for three randomly selected countries in different tiers.

Tier	Country	Recommended products (top 5)
Low tier	Vanuatu	Cigarettes
		Fruit, fresh or dried
		Plants and parts of trees used in perfumery; in pharmacy; etc.
		Sawlogs and veneer logs, of non-coniferous species
		Non-alcoholic beverages
	Tonga	Spices, except pepper and pimento
		Sugar confectionery and preparations, non-chocolate
		Fish, dried, salted or in brine; smoked fish
		Cement
		Wood, simply shaped
	Dominica	Meal and flour of wheat and flour of meslin
		Cask, drums, etc., of iron, steel, aluminium, for packing goods
		Packing containers, box files, etc., of paper, used in offices
		Beer made from malt
		Plastic packing containers, lids, stoppers and other closures
Middle tier	Norway	Animals, live (including zoo animals, pets, insects, etc.)
		Fuel wood and wood charcoal
		Bovine and equine hides, raw, whether or not split
		Bones, ivory, horns, coral, shells and similar products
		Soaps, organic products and preparations for use as soap
	Mauritius	Skirts
		Vegetable products roots and tubers, fresh, dried
		Leather of other hides or skins
		Footwear
		Other outer garments
	Kyrgyzstan	Oil seeds and oleaginous fruits
		Fish, fresh or chilled, excluding fillet
		Eggs, birds, and egg yolks, fresh, dried or preserved, in shell
		Fruit or vegetable juices
		Jams, jellies, marmalades, etc., as cooked preparations
Top tier	Germany	Iron, steel, aluminium reservoirs, tanks, etc., capacity 300 lt plus
		Non-domestic refrigerators and refrigerating equipment, parts
		Insulated electric wire, cable, bars, etc.
		Bottles etc. of glass
		Railway or tramway sleepers
	Italy	Refined sugar etc.
		Fuel wood and wood charcoal
		Sugar confectionery and preparations
		Manufactures of mineral materials (other than ceramic)
		cotton, not elastic nor rubberized
	Switzerland	Structures and parts of, of iron, steel; plates, rods, and the like
		Manufactures of mineral materials (other than ceramic)
		Other furniture and parts thereof
		Organic surface-active agents
		Miscellaneous articles of base metal

Table 2: The top five recommended products by HeatS algorithms for three randomly selected countries in different tiers.

Tier	Country	Recommended products (top 5)
Low tier	Vanuatu	Sugars, beet and cane, raw, solid
		Natural rubber latex; natural rubber and gums
		Jute, other textile bast fibers, raw, processed but not spun
		Ores and concentrates of uranium and thorium
		Nuts edible, fresh or dried
	Tonga	Manila hemp, raw or processed but not spun
		Coconut (copra) oil
		Cocoa beans, raw, roasted
		Waxes of animal or vegetable origin
		Palm nuts and kernels
	Dominica	Potassium salts, natural, crude
		Distilled alcoholic beverages
		Surveying, navigational, compasses, etc., instruments, nonelectrical
		Figs, fresh or dried
		Beer made from malt
Middle tier	Norway	Crustaceans and molluscs, fresh, chilled, frozen, salted
		Asbestos
		Radio-active chemical elements, isotopes etc.
		Ships, boats and other vessels
		Iron ore agglomerates
	Mauritius	Fabrics, woven
		Fish, dried, salted or in brine; smoked fish
		Articles of apparel, clothing accessories of plastic or rubber
		Household appliances, decorative article, etc., of base metal
		Headgear and fitting thereof
	Kyrgyzstan	Meat of sheep and goats, fresh, chilled or frozen
		Iron ore and concentrates, not agglomerated
		Coffee green, roasted; coffee substitutes containing coffee
		Cut flowers and foliage
		Railway or tramway sleepers (ties) of wood
Top tier	Germany	Photographic and cinematographic apparatus and equipment
		Organo-sulfur compounds
		Parts of the pumps and compressor
		Orthopedic appliances, hearing aids, artificial parts of the body
		Phenols and phenol-alcohols, and their derivatives
	Italy	Digital central storage units, separately consigned
		Children's toys, indoor games, etc.
		Optical instruments and apparatus
		Fabrics of glass fiber (including narrow, pile fabrics, lace, etc.)
		Printing presses
	Switzerland	Electro-medical equipment
		Chemical products and preparations
		Parts of steam power units
		Spectacles and spectacle frames
		Other chemical derivatives of cellulose; vulcanized fiber

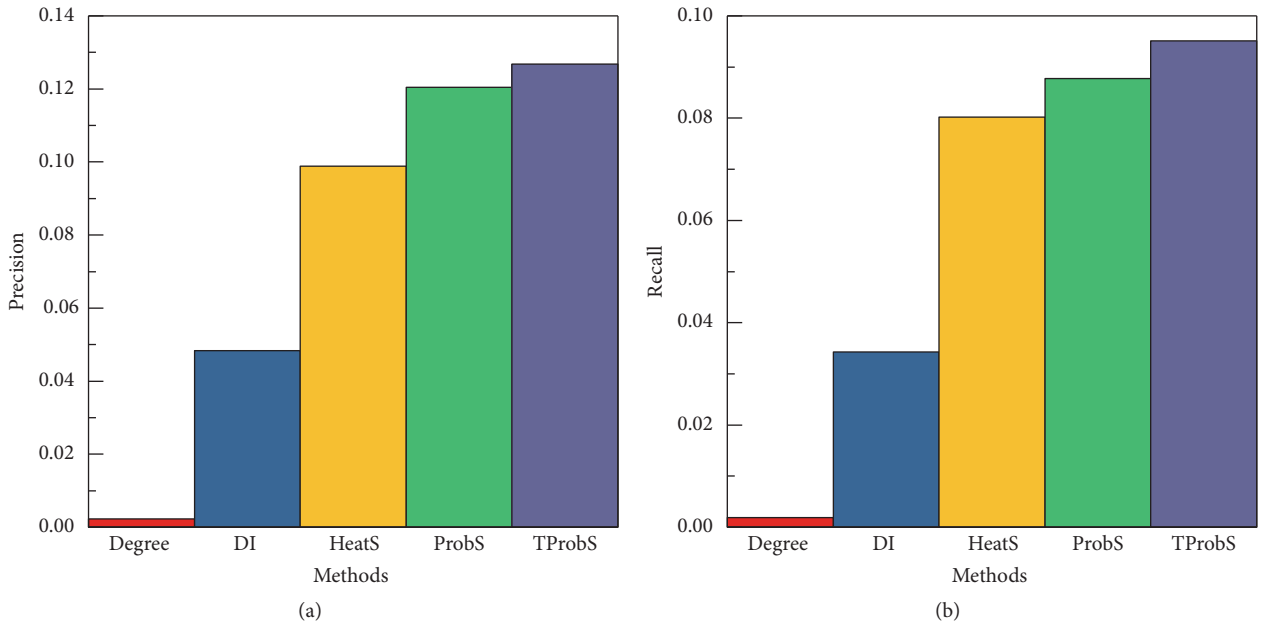

FIGURE 1: A comparison of Recall and Precision for the five algorithms. The recommendation is performed at year T for year $T + 5$, with T ranging from year 2001 to 2010. The results shown are averaged over this time period. For TProbS, we set a value of $\theta = 0.2$. The Degree method simply ranks the products according to their degree. All subsequent experiments were based on this recommendation.

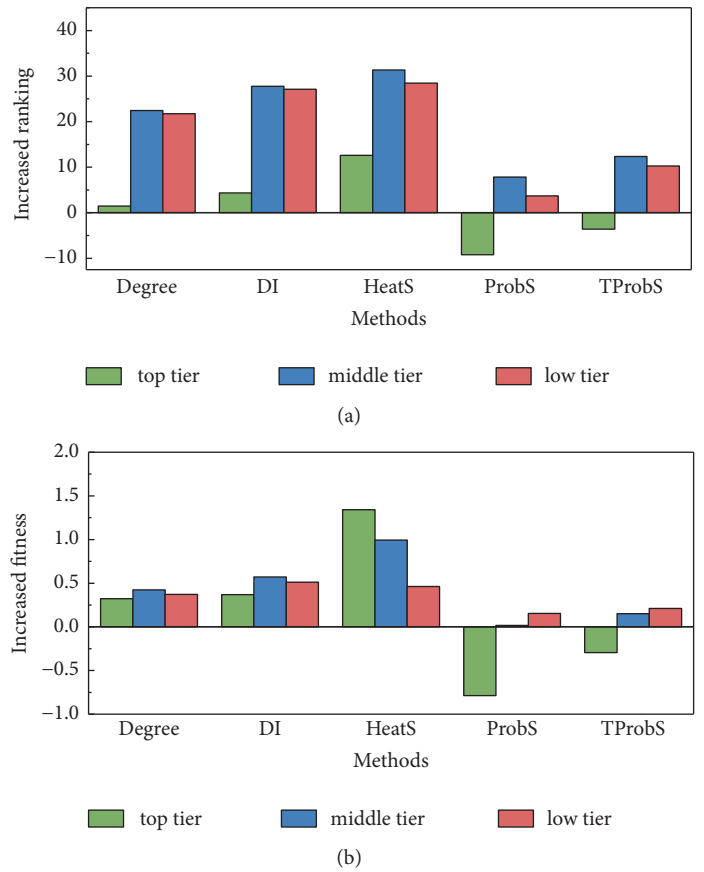

FIGURE 2: Panel (a) is the average increase of fitness ranking for the three different tiers of countries for the time period 2008–2015. The number of goods added for each country is set to $L = 20$. Panel (b) is the average increased fitness value of those three tiers.

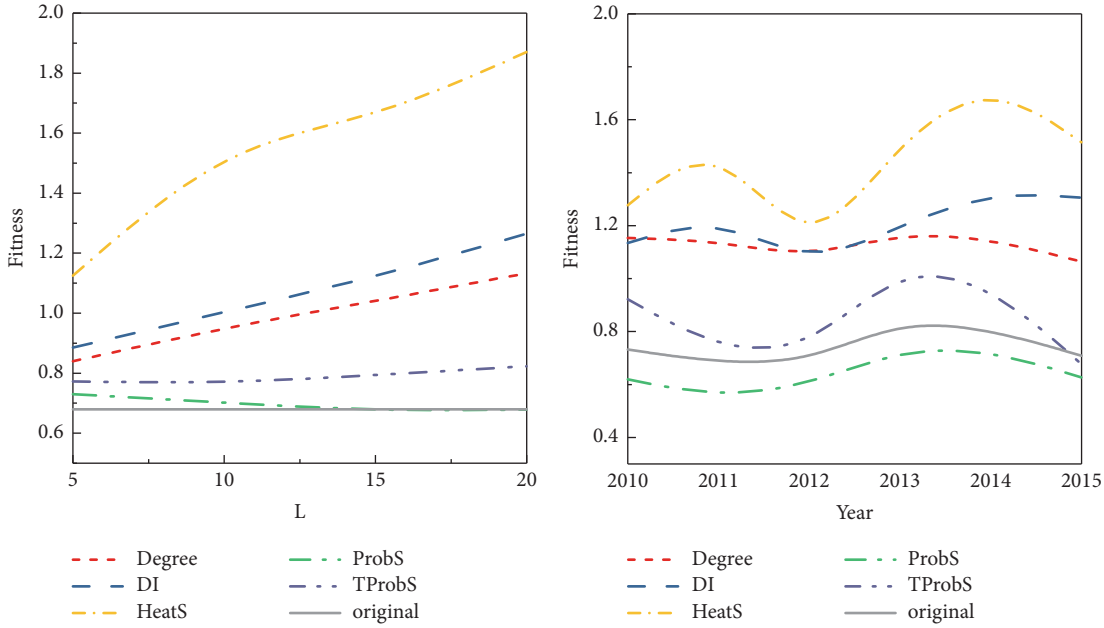

FIGURE 3: Panel (a) shows fitness values as a function of the length of the recommendation list L. The results are average over 30 randomly selected countries and over the 15 years spanned by the data. Time evolution of fitness for the thirty selected middle tier countries that are shown in panel (b). The length of the recommendation list is set to $L = 20$.

the evolution in the average fitness of these countries for the different methods. We compare the normal evolution of countries and the one recommended by these algorithms. The results are shown in Figure 3 (panel (a)). For any length of the recommendation list L, HeatS is the top performing by a great margin compared to other methods. For all methods, ranking is consistent for every choice of L, and so the choice of the value is not meaningful, as long as it is reasonably small compared to the total number of items. By looking at the evolution with the length of the recommendation list L, we find that the results are consistent and if the country should follow the recommendation, even if it can add only few products to its export basket. Following the recommendation made by HeatS seems to be adequate in terms of technological requirements (i.e., the countries have the required technology) as well as the best path to increase the country's fitness. In Figure 3 (panel (b)), the results are shown for different years and for fixed L. Though some methods are better in a specific year than others, it is clear that HeatS is always the top performing method, followed by Degree and DI and then TProbS. This is good news as it shows the robustness of our method, both in the isolated case and in the real evolution of countries' exports.

We are also interested in the individual behavior of the fitness evolution. We randomly select four countries and study the effect of the method on the evolution of the fitness values. The comparison of the five methods as a function of L and the original fitness is shown in Figure 4. Again, HeatS is the top performing method, except for Kazakhstan. For this country, DI and Degree are the top performing methods due to the low fitness of this country. The original fitness values corresponding to the four countries Croatia, Kazakhstan, Poland, and Colombia are 2.0563, 0.7234, 3.7678, and 1.0714, respectively. While we saw in Figure 3 that HeatS is always best on average, it is different when considering individual countries with especially low production. The impact of the recommendation on the increased ranking of the four countries is shown in Figure 5. We see in Figure 5 (panel (b)) that even if HeatS is not the best method, the difference in ranking is quite small, while in other panels it clearly outperforms other methods.

3.4. Real Production Ability. In the previous results, we fixed a parameter L and assigned the same number of new products to every country. However, in reality some countries produce many new products in a specific year, while some others struggle more. To reflect this, we use a dynamic length of the recommendation L_i, where L_i is the length of the recommendation list for country i, equal to its number of new products between times $T + 5$ and T. We build a "virtual network" corresponding exactly to the real one at $T + 5$, except for one country i, for which we replace the links that appear between T and $T + 5$ by those of the recommendation list. This ensures that the network is of constant size. The results for HeatS are shown in Figure 6. We see that HeatS improves greatly the fitness of most countries that follow its recommendation. Only a few countries see their fitness decreasing compared to their original evolution. As a comparison, we see in Figure 7 that TProbS is of no use for top tier countries, but for middle and especially low tier countries they might benefit from it. While lower than for HeatS, the recommendations of TProbS are made of more widespread technologies and so might be easier to follow for the low fitness countries.

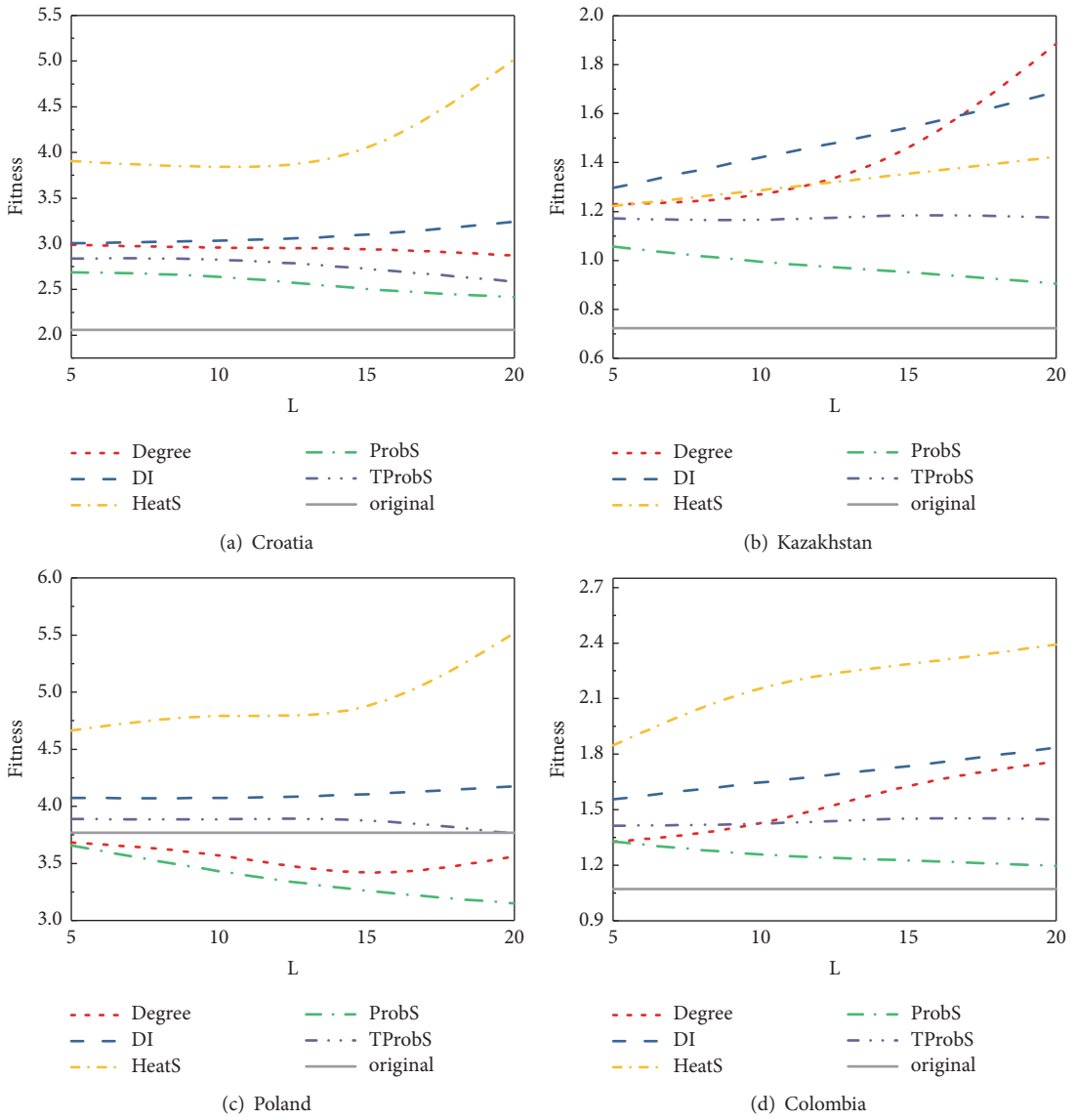

FIGURE 4: Detailed view of the fitness as a function of the length of the recommendation list L for four randomly selected countries. The original fitness values of four countries Croatia, Kazakhstan, Poland, and Colombia are 2.0563, 0.7234, 3.7678, and 1.0714, respectively.

4. Conclusion

In this study, we extended the traditional recommendations, which are usually applied on social networks, to the international trade. Thanks to recent advances in measuring the potential countries' evolution based solely on the network structure, we designed a method which aims to help countries to find a suitable evolution path among all the possible ones. The study suffers two main limitations. The first one is that the exports categories are roughly defined. Only about 786 categories are present in the dataset. This leads to some categories containing very varied products, such as *iron based goods*. The second one is that there are important restrictions, or conversely support, to the trade between countries. For instance, USA, Canada, and Mexico recently signed an agreement to open the market of dairy and car parts. On the opposite side, countries might limit their sensitive exports, such as military goods, to specific countries. While the first limitation is difficult to address due to the data limitations, the second one can be added by weighting differently the relationships between countries on specific products.

At the same time, the recommendation proved to grasp the countries technological evolution by being able to correctly predict the future, and the method of Fitness and Complexity has been shown in [37–39] to uncover hidden features of the countries' evolution. It is important to note that the recommendation method should agree with the similar capabilities of a country [40]. Those two ingredients together mixed with our results show remarkable evidence that our methods as supplementary message could help to

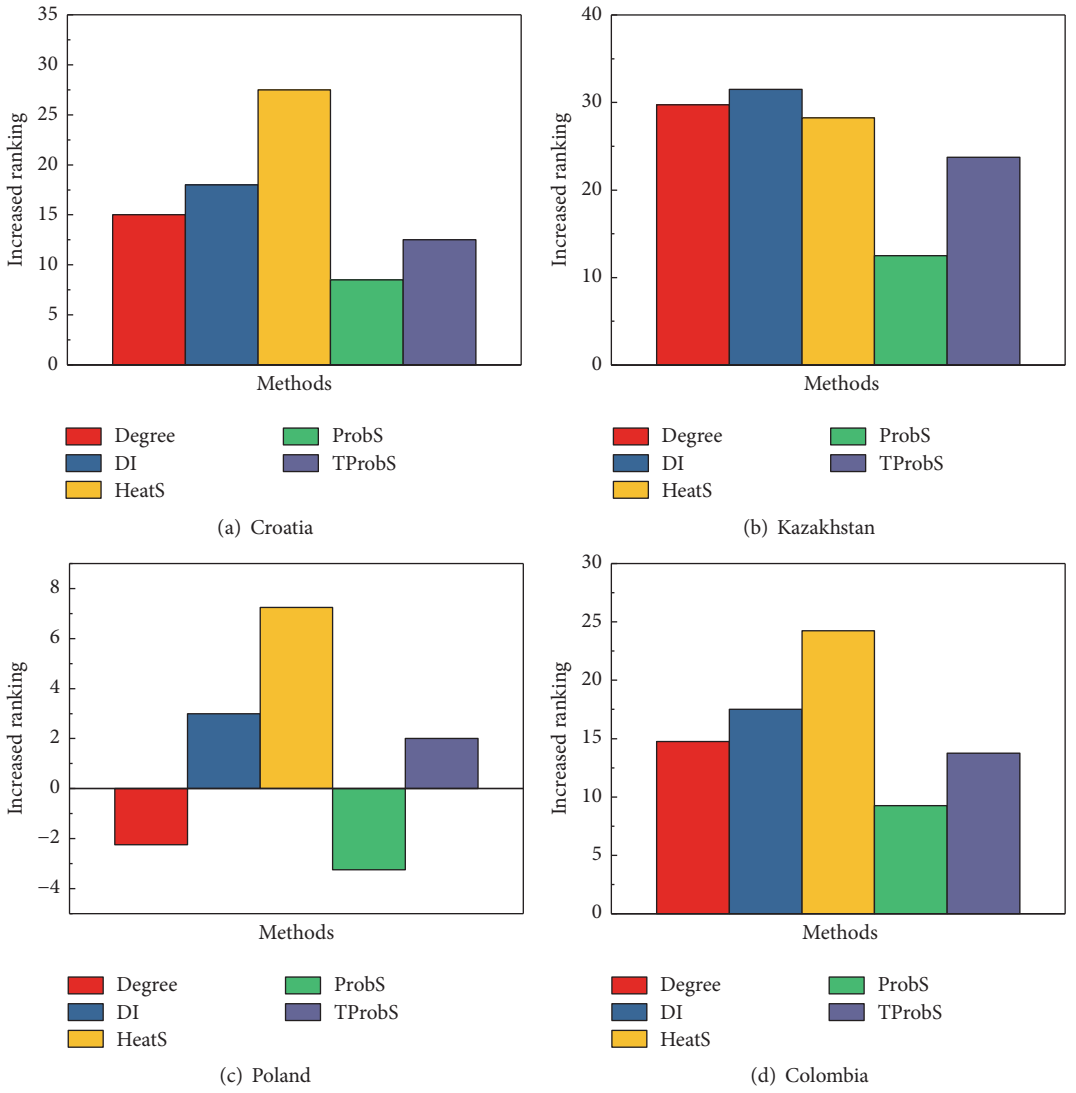

Figure 5: Comparison of the increased rankings of the four selected countries. The increased ranking of each method is averaged over different lengths of the recommendation list L.

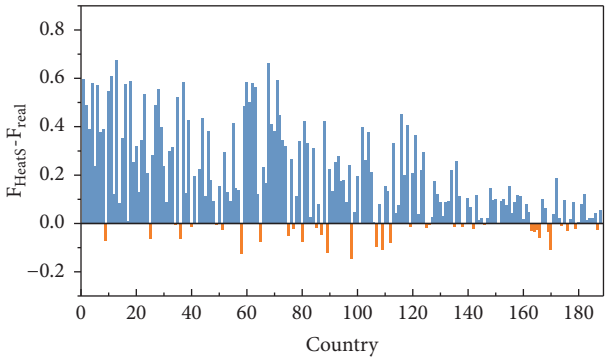

Figure 6: Difference of fitness resulting from following recommendation of HeatS and real evolution. The countries are sorted according to their fitness value, country 0 being the one with the highest average fitness. Each bar represents a country. The recommendation is performed at year T for year $T + 5$, with T ranging from year 2001 to 2010. 143 countries of the 181 countries would see their fitness improve by following the recommendation of HeatS.

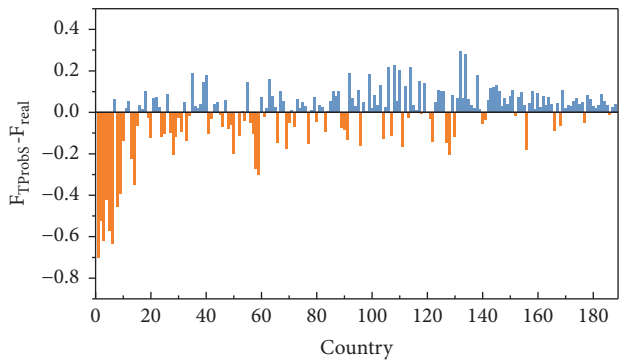

FIGURE 7: Difference of fitness resulting from following recommendation of TProbS and real evolution. The countries are sorted according to their fitness value, country 0 being the one with the highest average fitness. Each bar represents a country. The recommendation is performed at year T for year $T + 5$, with T ranging from year 2001 to 2010. 120 countries of the 181 countries would see their fitness improve by following the recommendation of TProbS.

design objective metrics in order to facilitate the work of policy makers and encourage the development of technology towards the better economic goal.

Data Availability

The data used to support the findings of this study are available from the corresponding author upon request.

Conflicts of Interest

The authors declare that they have no conflicts of interest.

Acknowledgments

We acknowledge financial support from the National Natural Science Foundation of China grants number 61803266, 11547040, 61873171, and 61703281; the Guangdong Province Natural Science Foundation of China grants number 2016A030310051 and 2017A030310374; the Foundation for Distinguished Young Talents in Higher Education of Guangdong grant number 2015KONCX143; the Shenzhen Fundamental Research Foundation grants number JCYJ20150529164656096 and JCYJ20170302153955969; the Natural Science Foundation of SZU grant number 2016-24; and the Guangdong Pre-National Project grant number 2014GKXM054.

References

[1] A. Almog, T. Squartini, and D. Garlaschelli, "The double role of GDP in shaping the structure of the International Trade Network," *International Journal of Computational Economics and Econometrics*, vol. 7, 2015.

[2] H. Liao, M. S. Mariani, M. s. Medo, Y.-C. Zhang, and M.-Y. Zhou, "Ranking in evolving complex networks," *Physics Reports*, vol. 689, pp. 1–54, 2017.

[3] The World Bank, Trade, data retrieved from World Bank national accounts data, (2018). https://data.worldbank.org/indicator/NE.TRD.GNFS.ZS.

[4] D. Hummels and P. J. Klenow, "The variety and quality of a nation's exports," *American Economic Review*, vol. 95, no. 3, pp. 704–723, 2005.

[5] G. Fagiolo, "The international-trade network: Gravity equations and topological properties," *Journal of Economic Interaction and Coordination*, vol. 5, no. 1, pp. 1–25, 2010.

[6] C. A. Hidalgo, B. Winger, A.-L. Barabási, and R. Hausmann, "The product space conditions the development of nations," *Science*, vol. 317, no. 5837, pp. 482–487, 2007.

[7] M. V. Tomasello, N. Perra, C. J. Tessone, M. Karsai, and F. Schweitzer, "The role of endogenous and exogenous mechanisms in the formation of R&D networks," *Scientific Reports*, vol. 4, pp. 5679-5679, 2014.

[8] A. Portes and J. Sensenbrenner, "Embeddedness and immigration: notes on the social determinants of economic action," *American Journal of Sociology*, vol. 98, no. 6, pp. 1320–1350, 1993.

[9] I. Wallerstein, *The modern world-system I: Capitalist agriculture and the origins of the European world-economy in the sixteenth century*, vol. 1, Univ of California Press, 2011.

[10] S. Sassen, *Cities in a world economy*, Sage Publications, 2018.

[11] D. Snyder and E. L. Kick, "Structural position in the world system and economic growth, 1955-1970: a multiple-network analysis of transnational interactions," *American Journal of Sociology*, vol. 84, no. 5, pp. 1096–1126, 1979.

[12] E. L. Kick, L. A. McKinney, S. McDonald, and A. Jorgenson, "A multiple-network analysis of the world system of nations, 1995-1999," *Sage Handbook of Social Network Analysis*, pp. 311–327, 2011.

[13] M. Á. Serrano and M. Boguñá, "Topology of the world trade web," *Physical Review E: Statistical, Nonlinear, and Soft Matter Physics*, vol. 68, no. 2, p. 015101, 2003.

[14] D. Garcia, C. J. Tessone, P. Mavrodiev, and N. Perony, "The digital traces of bubbles: Feedback cycles between socio-economic signals in the Bitcoin economy," *Journal of the Royal Society Interface*, vol. 11, no. 99, article no. 0623, 2014.

[15] L. Lü and T. Zhou, "Link prediction in complex networks: a survey," *Physica A: Statistical Mechanics and its Applications*, vol. 390, no. 6, pp. 1150–1170, 2011.

[16] D. Liben-Nowell and J. Kleinberg, *The link-prediction problem for social networks*, John Wiley & Sons, Inc., 2007.

[17] A. Vidmer, A. Zeng, M. Medo, and Y.-C. Zhang, "Prediction in complex systems: The case of the international trade network," *Physica A: Statistical Mechanics and its Applications*, vol. 436, pp. 188–199, 2015.

[18] C. A. Hidalgo and R. Hausmann, "The building blocks of economic complexity," *Proceedings of the National Acadamy of Sciences of the United States of America*, vol. 106, no. 26, pp. 10570–10575, 2009.

[19] G. Caldarelli, M. Cristelli, A. Gabrielli, L. Pietronero, A. Scala, and A. Tacchella, "A network analysis of countries' export flows: firm grounds for the building blocks of the economy," *PLoS ONE*, vol. 7, no. 10, Article ID e47278, 2012.

[20] A. Tacchella, M. Cristelli, G. Caldarelli, A. Gabrielli, and L. Pietronero, "A new metrics for countries' fitness and products' complexity," *Scientific Reports*, vol. 2, pp. 723–730, 2012.

[21] L. Pietronero, M. Cristelli, A. Gabrielli, D. Mazzilli et al., "Economic complexity: "buttarla in caciara" vs a constructive approach," https://arxiv.org/abs/1709.05272.

[22] M. Cristelli, A. Gabrielli, A. Tacchella, G. Caldarelli, and L. Pietronero, "Measuring the intangibles: A metrics for the economic complexity of countries and products," *PloS one*, vol. 8, no. 8, p. e70726, 2013.

[23] A. Tacchella, D. Mazzilli, and L. Pietronero, "A dynamical systems approach to gross domestic product forecasting," *Nature Physics*, vol. 14, no. 8, pp. 861–865, 2018.

[24] T. Zhou, J. Ren, M. Medo, and Y. Zhang, "Bipartite network projection and personal recommendation," *Physical Review E: Statistical, Nonlinear, and Soft Matter Physics*, vol. 76, no. 4, Article ID 046115, 2007.

[25] T. Zhou, Z. Kuscsik, J. Liu, M. Medo, J. R. Wakeling, and Y. Zhang, "Solving the apparent diversity-accuracy dilemma of recommender systems," *Proceedings of the National Acadamy of Sciences of the United States of America*, vol. 107, no. 10, pp. 4511–4515, 2010.

[26] A. Zeng, S. Gualdi, M. Medo, and Y.-C. Zhang, "Trend prediction in temporal bipartite networks: the case of Movielens, Netflix, and Digg," *Advances in Complex Systems. A Multidisciplinary Journal*, vol. 16, no. 4-5, 1350024, 15 pages, 2013.

[27] A. Vidmer and M. Medo, "The essential role of time in network-based recommendation," *EPL (Europhysics Letters)*, vol. 116, no. 3, p. 30007, 2016.

[28] G. Gaulier and S. Zignago, "BACI: International Trade Database at the Product-Level (the 1994-2007 Version)," *SSRN Electronic Journal*, Working Papers 2010-2023, CEPII (October 2010). URL http://www.cepii.fr/CEPII/fr/publications/wp/abstract.asp?NoDoc=2726.

[29] B. Balassa, "Trade Liberalisation and "Revealed" Comparative Advantage," *The Manchester School*, vol. 33, no. 2, pp. 99–123, 1965.

[30] F. Yu, A. Zeng, S. Gillard, and M. Medo, "Network-based recommendation algorithms: a review," *Physica A: Statistical Mechanics and its Applications*, vol. 452, pp. 192–208, 2016.

[31] R. Crane and D. Sornette, "Robust dynamic classes revealed by measuring the response function of a social system," *Proceedings of the National Acadamy of Sciences of the United States of America*, vol. 105, no. 41, pp. 15649–15653, 2008.

[32] G. Szabo and B. A. Huberman, "Predicting the popularity of online content," *Communications of the ACM*, vol. 53, no. 8, pp. 80–88, 2010.

[33] Z.-M. Ren, Y.-Q. Shi, and H. Liao, "Characterizing popularity dynamics of online videos," *Physica A: Statistical Mechanics and its Applications*, vol. 453, pp. 236–241, 2016.

[34] H. Liao and A. Vidmer, "A Comparative Analysis of the Predictive Abilities of Economic Complexity Metrics Using International Trade Network," *Complexity*, vol. 2018, Article ID 2825948, 12 pages, 2018.

[35] E. Pugliese, A. Zaccaria, and L. Pietronero, "On the convergence of the Fitness-Complexity algorithm," *The European Physical Journal Special Topics*, vol. 225, no. 10, pp. 1893–1911, 2016.

[36] E. Pugliese, G. L. Chiarotti, A. Zaccaria, and L. Pietronero, "Complex economies have a lateral escape from the poverty trap," *PLoS ONE*, vol. 12, no. 1, p. e0168540, 2017.

[37] A. Tacchella, M. Cristelli, G. Caldarelli, A. Gabrielli, and L. Pietronero, "Economic complexity: conceptual grounding of a new metrics for global competitiveness," *Journal of Economic Dynamics & Control*, vol. 37, no. 8, pp. 1683–1691, 2013.

[38] G. Cimini, A. Gabrielli, and F. S. Labini, "The scientific competitiveness of nations," *PLoS ONE*, vol. 9, no. 12, p. e113470, 2014.

[39] M. S. Mariani, A. Vidmer, M. Medo, and Y.-C. Zhang, "Measuring economic complexity of countries and products: which metric to use?" *The European Physical Journal B*, vol. 88, no. 11, article 293, pp. 1–9, 2015.

[40] E. Pugliese, G. Cimini, A. Patelli, A. Zaccaria, L. Pietronero, and A. Gabrielli, "Unfolding the innovation system for the development of countries: co-evolution of science, technology and production," https://arxiv.org/abs/1707.05146.

Hindawi
Complexity
Volume 2018, Article ID 7032402, 8 pages
https://doi.org/10.1155/2018/7032402

Research Article

A Novel Decision-Making Approach to Fund Investments Based on Multigranulation Rough Set

Xima Yue and Xiang Su

School of Economics and Management, Jiangsu University of Science and Technology, Zhenjiang 212003, China

Correspondence should be addressed to Xima Yue; ximayue@126.com

Received 11 July 2018; Accepted 2 September 2018; Published 14 October 2018

Guest Editor: Bernardo A. Furtado

Fund investment is a hot issue in today's society. How to choose a project for investment is affected by many factors. In view of this problem, this paper starts from the granular computing point of view and combines the multigranulation rough set decision-making method to construct a fund investment decision information system; then, the fund investment decision information system is reduced under different thresholds, and the decision rules are extracted through reduction. And from the aspects of decision accuracy and rule accuracy, the rules are analyzed. Finally, decision rules are used to give the decision of the fund investment project. This study provides a new approach to fund management.

1. Introduction

Fund investment management [1] is a hot issue in today's society. How to choose a better one from some of the possible fund projects or to find some direction from the existing successful fund project before investment is a problem that every decision maker needs to think about. At present, many scholars have studied how to carry out project selection and malpractice from the pension fund industry and social insurance industry [2–6].

In order to enable investors to better invest in projects, many scholars have carried out many researches on investment methods in recent years. Lu [7] uses mathematical methods to analyze the major Reynolds index, SHARP index, Jansen index, and M2 index, which are mainly used in the performance evaluation of the fund, and deduces the relationship between each other by mathematical methods. It also expounds the conditions for the use of indicators in the performance evaluation of funds. Peng [8] systematically introduced the theories and methods of performance evaluation of open-end funds and summarized the research results of fund performance evaluation both at home and abroad. Then, according to the scientific, systematic, and feasible principles, we select 9 indicators that can reflect the performance level of the open-end fund and use the analytic hierarchy process to construct the system of the performance evaluation of the open-end fund in China. Then, we evaluated the index factors of sample funds in the sample period, respectively. Finally, combined with fuzzy comprehensive evaluation method and grey comprehensive evaluation method, we get the overall evaluation results of an open-end fund performance. From the quantitative and qualitative point of view, Xu [9] selected the VaR method combining the GARCH model and the fuzzy comprehensive evaluation method using the analytic hierarchy process to further construct the risk assessment system of China's open fund.

Rough set theory [10, 11] is a mathematical method proposed by Professor Pawlak in 1982 to effectively analyze and deal with inaccurate, inconsistent, and incomplete information. After nearly thirty years of development, rough set theory has been widely used in the fields of pattern recognition, machine learning, decision analysis, knowledge acquisition, and data mining. The classical rough set is an equivalent class derived from a single undiscernible two-element relation on a domain. The following and upper approximation sets are used to rough the unknown concept. Granular computing is a new discipline with rapid development. It integrates many theoretical research achievements

such as rough set, fuzzy set, and artificial intelligence. At present, rough set theory has become an important tool for granular computing. Literatures [12–14] from the angle of granular computing (parallel multiple grain structures), the knowledge particles (equivalent classes) derived from a single indiscernible two-element relation, are analyzed to approximate the inadequacies of the rough sets of the unknown concepts. Furthermore, the concept of multigranulation rough sets is proposed. An optimistic multigranulation rough set and a pessimistic multigranulation rough set model are given. The Pawlak rough set is extended from a single grain structure to a number of granular structures, and it is proved that the classic rough set model of Pawlak is a special case of the multigranularity rough set. In addition, many researchers have extended the multigranularity rough set. Xu et al. have done a lot of work on multigranulation rough sets [15–20]. Yang and others studied the multigranularity rough set [21–25] based on incomplete information system, test cost sensitivity, and hierarchical structure.

In order to solve the problem of project investment fund, this paper constructs the fund investment decision information system from the perspective of granular computing and combined with multigranular rough set decision method. Then reduce the information table, extract the rules from the simplified information table, and perform the rule analysis. Finally, the decision conclusions of the fund investment are given. The main contributions of this article are as follows:

(1) This paper proposes a method for constructing a project fund investment decision information system, which is the premise that we use rough sets to solve project investment problems

(2) In this paper, the generalized multigranularity rough set model is used to reduce the fund project information system, and then the rules are extracted on the simplified information system. Finally, the fund investment decision is given from these rules

The remaining structure of this paper is shown as follows: in the second part, the related knowledge of multigranularity rough sets is introduced. In the third part, the cleaning information system of the fund investment project is constructed. In the fourth part, the fund investment decision based on the multigranularity rough set is studied. Finally, the conclusion is given in the fifth part.

2. Preliminaries

The section recalls necessary concepts and preliminaries required in the sequel of our work. Detailed description of the theory can be found in [12, 13, 26–29].

An information system with decisions is an ordered quadruple $\mathscr{F} = (U, A \cup D, F, G)$, where

(i) $U = \{x_1, x_2, \cdots, x_n\}$ is a nonempty finite set of objects

(ii) $A \cup D$ is a nonempty finite attribute set

(iii) $A = \{a_1, a_2, \cdots, a_p\}$ denotes the set of condition attributes

(iv) $D = \{d_1, d_2, \cdots, d_q\}$ denotes the set of decision attributes and $A \cap D = \varnothing$

(v) $F = \{f_k \mid U \longrightarrow V_k, k \le p\}$, $f_k(x)$ is the value of a_k on $x \in U$, V_k, the domain of a_k, $a_k \in A$

(vi) $G = \{g_{k'} \mid U \longrightarrow V_{k'}, k' \le q\}$, $g_{k'}(x)$ is the value of $d_{k'}$ on $x \in U$, $V_{k'}$, the domain of $d_{k'}$, $d_{k'} \in D$

In an information system, the equivalence class of an object with respect to an attribute subset of A is a granularity from the viewpoint of granular computing. A partition of the universe is a granular structure. Rough set proposed by Pawlak is a single granularity rough set model, and the granular structure in this model is induced by the indiscernibility relation of the attribute set. In general, the above cases cannot always be satisfied or required in practical problems. In the three cases referred in [12], there are limitations in single granularity rough set for addressing practical problems with multiple partitions, and multigranulation rough set can now be used to effectively solve these problems. Under those circumstances, we must describe a target concept through multiple binary relations on the universe according to user's requirements or targets of problem solving. In the literatures [12, 13, 26, 27], to apply rough set theory to practical problems widely, multigranulation rough set model has been studied based on multiple equivalence relations.

Let $\mathscr{F} = (U, A \cup D, F, G)$ be an information system, $X \subseteq U$ and $P = \{P_1, P_2, \cdots, P_t\} P_i \subseteq A (i = 1, 2, \cdots, l)$. Then P_i or U/P_i is referred to as a granularity. The equivalence class of an object x with respect to P_i is defined as

$$[x]_{Pi} = \{y \in U | f(x, a) = f(y, a)\}, \quad (a \in P_i). \tag{1}$$

The lower and upper approximation sets of X with respect to single P_i are defined as follows:

$$\begin{aligned} \underline{P_i}(X) &= \left\{x \in U \mid [x]_{P_i} \subseteq X\right\}, \\ \overline{P_i}(X) &= \left\{x \in U \mid [x]_{P_i} \bigcap X \neq \varnothing\right\}. \end{aligned} \tag{2}$$

Considering further studies on multigranulation rough set, we now review the two basic forms of multigranulation rough set model.

Definition 1 (see [12]). Let $\mathscr{F} = (U, A \cup D, F, G)$ be an information system, $X \subseteq U$ and $P = \{P_1, P_2, \cdots, P_t\}$, $P_i \subseteq A (i = 1, 2, \cdots, l)$. The optimistic multigranulation lower and upper approximation sets of X with respect to single P are defined as follows:

$$\begin{aligned} \underline{P}(X)_{OM} &= \left\{x \in U \mid \vee\left([x]_{P_i} \subseteq X\right), i \le l\right\}, \\ \bar{P}(X)_{OM} &= \left\{x \in U \mid \wedge\left([x]_{P_i} \bigcap X \neq \varnothing\right), i \le l\right\} \end{aligned} \tag{3}$$

where "∨" means the logical operator "or," which represents that the alternative conditions are satisfied, and "∧" means the logical operator "and," which represents that all of the conditions are satisfied.

The set X is definable if and only if $\underline{P}(X)_{OM} = \overline{P}(X)_{OM}$. Otherwise, X is rough. $\underline{P}(X)_{OM}$ and $\overline{P}(X)_{OM}$ are referred to as optimistic lower and upper approximation sets, respectively.

From the above definition, the operators "∨" and "∧" can be exchanged between the optimistic lower approximation set and the optimistic upper approximation set. Corresponding to optimistic multigranulation rough set, pessimistic multigranulation rough set model can be defined in the following.

Definition 2 (see [12]). Let $\mathcal{I} = (U, A \cup D, F, G)$ be an information system, $X \subseteq U$ and $P = \{P_1, P_2, \cdots, P_t\}$, $P_i \subseteq A$ $(i = 1, 2, \cdots, l)$. The optimistic multigranulation lower and upper approximation sets of X with respect to single P are defined as follows:

$$\begin{aligned} \underline{P}(X)_{\mathrm{PM}} &= \left\{ x \in U \mid \wedge \left([x]_{P_i} \subseteq X \right), i \le l \right\}, \\ \overline{P}(X)_{\mathrm{PM}} &= \left\{ x \in U \mid \vee \left([x]_{P_i} \bigcap X \neq \varnothing \right), i \le l \right\}. \end{aligned} \tag{4}$$

The set X is definable when and only when $\underline{P}(X)_{\mathrm{PM}} = \overline{P}(X)_{\mathrm{PM}}$. Otherwise, X is rough. $\underline{P}(X)_{\mathrm{PM}}$ and $\overline{P}(X)_{\mathrm{PM}}$ are referred to as pessimistic lower and upper approximation sets, respectively.

The uncertainty of a concept in a multigranulation rough set model is also due to the existence of a boundary region. The greater the boundary of a concept is, the lower its accuracy is, and the coarser the concept is. Similar to the measures in the Pawlak rough set model, the accuracy and roughness measures in optimistic multigranulation rough set and pessimistic multigranulation rough set were defined in the same way [12]. As generalizations of the Pawlak rough set model, we only show the relations among optimistic multigranulation rough set, pessimistic multigranulation rough set, and single granularity rough set in the following.

Proposition 1 (see [12]). *Let $\mathcal{I} = (U, A \cup D, F, G)$ be an information system, $X \subseteq U$ and $P = \{P_1, P_2, \cdots, P_t\}$, $P_i \subseteq A$ $(i = 1, 2, \cdots, l)$. The following properties hold:*

(1) $\underline{P}(X)_{\mathrm{OM}} = \bigcup_{i=1}^{l} \underline{P_i}(X)$

(2) $\overline{P}(X)_{\mathrm{OM}} = \bigcap_{i=1}^{l} \overline{P_i}(X)$

(3) $\underline{P}(X)_{\mathrm{PM}} = \bigcap_{i=1}^{l} \underline{P_i}(X)$

(4) $\overline{P}(X)_{\mathrm{PM}} = \bigcup_{i=1}^{l} \overline{P}_i(X)$

(5) $\underline{P}(X)_{\mathrm{PM}} \subseteq \underline{P}(X)_{\mathrm{OM}}$

(6) $\overline{P}(X)_{\mathrm{OM}} \subseteq \overline{P}(X)_{\mathrm{PM}}$

In addition, there are many related properties as well as proof, please refer to [12, 28].

In order to express generalized multigranulation rough sets, we first introduce a characteristic function, which is called support feature function.

Definition 3 (see [30]). Let $\mathcal{I} = (U, A \cup D, F, G)$ be an information system, $X \subseteq U$ and $P = \{P_1, P_2, \cdots, P_t\}$, $P_i \subseteq A$ $(i = 1, 2, \cdots, l)$, suppose

$$S_X^{P_i}(x) = \begin{cases} 1, & [x]_{P_i} \subseteq X \\ 0, & \text{else} \end{cases} \quad (i \le l). \tag{5}$$

$S_X^{P_i}(x)$ is called x's support feature function for X, which is used to describe the inclusion relation between equivalence class $[x]_{P_i}$ and concept X, which indicates whether object x accurately supports X by P_i.

The optimistic multigranular rough set and the pessimistic multigranular rough set are generalizations of two multigranular rough set models. We will propose a new multigranular rough set model with the parameter $\beta \in (0.5, 1]$. We have introduced this parameter to implement the conceptual description of objects that support the concept at the most granular levels. Objects that may portray the concept are ignored below the corresponding level. The new model is expressed as follows.

Definition 4 (see [30]). Let $\mathcal{I} = (U, A \cup D, F, G)$ be an information system, $X \subseteq U$ and $P = \{P_1, P_2, \cdots, P_t\}$, $P_i \subseteq A (i = 1, 2, \cdots, l)$, $S_X^{P_i}(x)$ is called x's support feature function for X. For any $\beta \in (0.5, 1]$, the lower approximation and upper approximation of X for P are defined as follows:

$$\begin{aligned} \underline{P}(X)_{\beta} &= \left\{ x \in U \mid \frac{\sum_{i=1}^{l} S_X^{P_i}(x)}{l} \ge \beta \right\}, \\ \overline{P}(X)_{\beta} &= \left\{ x \in U \mid \frac{\sum_{i=1}^{l} \left(1 - S_{\sim X}^{P_i}(x) \right)}{l} > 1 - \beta \right\}. \end{aligned} \tag{6}$$

The set X is definable if $\underline{P}(X)_{\beta} = \overline{P}(X)_{\beta}$; otherwise, X is a rough set. We denote this generalized multigranulation rough set model as GMGRS, and β as the information level for P.

The multigranulation rough set is a generalization of the classical rough set. Since several attributes in the information system can have different effects on the decision-making

effect, when these effects cannot be performed simultaneously, but separately and independently, we cannot use classical rough set theory to treat these attributes as a whole through an indistinguishable relationship for system reduction and rule extraction. Therefore, according to the general process of rough set decision, we can get the specific steps of multigranular rough set decision and provide a theoretical model for decision analysis of fund project investment in multigranular environment.

3. Construction of Decision Information System for Fund Investments

Fund has become an increasingly important source of financing for people. For a decision maker, one may need to adopt a better one from some possible fund projects or find some directions from existing successful fund projects before investing. How to do it? We will propose a novel decision-making fund investments based on multigranulation rough set. This section mainly focuses to build fund investment decision information system.

The flow chart of our multigranulation decision-making model for fund investment is shown in Figure 1.

As can be seen from the flow chart, the investment decision system model based on the multigranulation rough set fund is constructed according to the following steps.

Step 1. Select condition attributes of the decision system. Before investing in the fund project, we first carry out the essential project evaluation for each project. In this paper, we through the project interviews, questionnaires, and other methods to determine project evaluation factors, which are *Market environment*, *Science and technology level*, *Education level*, *Management level*, and *Cultural level*, respectively. There are five aspects to measure every fund project. These evaluation factors consists of a conditional attribute set of the fun investment decision-making system based on multigranulation rough sets.

Step 2. Determine the value of the every condition attribute. According to the performance of market environment level, science and technology level, education level, management level, and culture level, a comprehensive overall evaluation of the items was conducted to be evaluated. In order to study conveniently, we only have a small research. So, we can simplify attribute values, which is divided into A, B, C, D, and E five grades for each factor. Moreover, five grades A, B, C, D, and E present mainly *outstanding*, *good*, *general*, *poor*, and *very poor*, respectively.

Step 3. Determine the decision attribute of the decision system. According to the above analysis, the decision attribute is divided into *good* and *common* decision results. Of course, depending on the situation, the decision attribute can also be set to three or more attribute values.

Step 4. Knowledge representation of the decision system based on multigranulation rough set. According to the knowledge of multigranulation rough sets and the above analysis, we

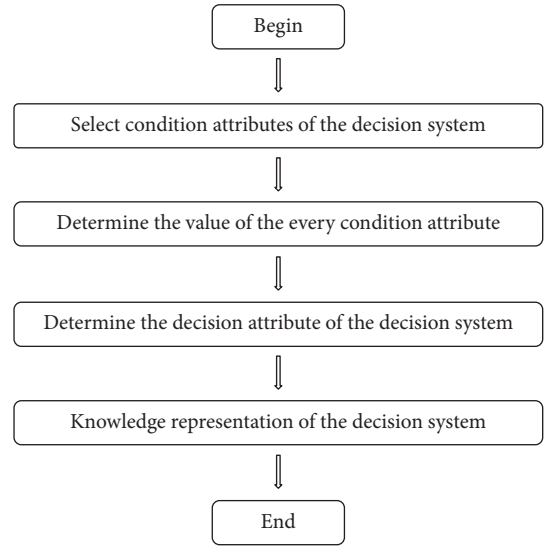

Figure 1: The flow chart of multigranulation decision-making model for fund investment.

Table 1: A fund investment information decision system.

U	P_1	P_2	P_3	P_4	P_5	d
x_1	A	A	C	B	C	G
x_2	B	A	C	C	D	Co
x_3	C	D	E	B	D	Co
x_4	B	B	A	B	A	G
x_5	A	B	D	A	B	G
x_6	C	C	C	D	E	Co

regard these five conditional attributes as five granularities, i.e., $P_1 = \{a_1\}$, $P_2 = \{a_2\}$, $P_3 = \{a_3\}$, $P_4 = \{a_4\}$, $P_5 = \{a_5\}$. At the same time, we randomly selected six experts. These experts are familiar with every project comparison by a long period of research and questionnaire. Thus, the evaluation result can be thought to constitute a small expert system.

Through this evaluation form, we obtained 6 valid data and formed 6 objects into the decision-making information system in Table 1.

Remark. We mainly check the reduction and decision rule by designing multiple granularity rough set decision steps, and we can get more granular rough set decision-making application. In the paper, we do not set on a large scale data in detail and do not set testing for the rules, which will be our future research work.

4. Decision Making for Fund Investments Based on Multigranulation Rough Set

In this section, based on the previous theories, the fund investment decisions are made with multigranulation rough sets. Firstly, generalized multigranulation rough set model

is used to fund investment decision-making information system, and then some important rules are extracted based on the reduction of the information system. Finally, results of fund investment decision can be given from the obtained conclusion.

Starting from the data of the fund investment decision-making information system in Table 1, funds are classified according to different granularities. The classification results are as follows:

$$\begin{aligned}
\frac{U}{P_1} &= \{\{x_1, x_5\}, \{x_2, x_4\}, \{x_3, x_6\}\},\\
\frac{U}{P_2} &= \{\{x_1, x_2\}, \{x_3\}, \{x_4, x_5\}, \{x_6\}\},\\
\frac{U}{P_3} &= \{\{x_1, x_2, x_6\}, \{x_3\}, \{x_4\}, \{x_5\}\},\\
\frac{U}{P_4} &= \{\{x_1, x_3, x_4\}, \{x_2\}, \{x_5\}, \{x_6\}\},\\
\frac{U}{P_5} &= \{\{x_1\}, \{x_2, x_3\}, \{x_4\}, \{x_5\}, \{x_6\}\},\\
\frac{U}{d} &= \{\{x_1, x_4, x_5\}, \{x_2, x_3, x_6\}\}.
\end{aligned} \tag{7}$$

If we take information level $\beta = 0.7$ $(0.6 < \beta \leq 1)$ and $\beta = 0.6$ $(0.5 < \beta \leq 0.6)$, then we can obtain the support feature matrix tables of lower approximation and upper approximation for every decision class in Tables 2–5.

So, we can calculate the lower approximation and upper approximation of D_1 and D_2.

$$\begin{aligned}
&\underline{P}(D_1)_{0.7} = \{x_5\},\\
&\bar{P}(D_1)_{0.7} = \{x_1, x_2, x_4, x_5\},\\
&\underline{P}(D_2)_{0.7} = \{x_3, x_6\},\\
&\bar{P}(D_1)_{0.7} = \{x_1, x_2, x_3, x_4, x_6\},\\
&\underline{P}(D_1)_{0.6} = \{x_4, x_5\},\\
&\bar{P}(D_1)_{0.6} = \{x_1, x_2, x_4, x_5\},\\
&\underline{P}(D_2)_{0.6} = \{x_3, x_6\},\\
&\bar{P}(D_2)_{0.6} = \{x_1, x_2, x_3, x_6\}.
\end{aligned} \tag{8}$$

In keeping the classification unchanged, all the reductions of the decision-making information system are obtained by MATLAB calculation as follows.

If we take information level $\beta = 0.7$ $(0.6 < \beta \leq 1)$, then the reduction is $\{a_1, a_2, a_3, a_4, a_5\}$. Moreover, if we take information level $\beta = 0.6$ $(0.5 < \beta \leq 0.6)$, then the reduction is $\{a_1, a_2, a_3, a_5\}$ and $\{a_2, a_3, a_4, a_5\}$.

In the next, we extract the rules from two cases according to the reduction obtained above and give the quantitative results for the decision precision and rule precision of the rules.

Table 2: The support feature matrix table of lower approximation ($\beta = 0.7$).

	D_1	D_2
x_1	0	0
x_2	0	0
x_3	0	1
x_4	0	0
x_5	1	0
x_6	0	1

Table 3: The support feature matrix table of upper approximation ($\beta = 0.7$).

	D_1	D_2
x_1	1	1
x_2	1	1
x_3	0	1
x_4	1	1
x_5	1	0
x_6	0	1

Table 4: The support feature matrix table of upper approximation ($\beta = 0.6$).

	D_1	D_2
x_1	1	1
x_2	1	1
x_3	0	1
x_4	1	0
x_5	1	0
x_6	0	1

Table 5: The support feature matrix table of lower approximation ($\beta = 0.6$).

	D_1	D_2
x_1	0	0
x_2	0	0
x_3	0	1
x_4	1	0
x_5	1	0
x_6	0	1

Case 1. The information level is $\beta = 0.7$ $(0.6 < \beta \leq 1)$, and the reduction is $\{a_1, a_2, a_3, a_4, a_5\}$.

In this case, rule can be carried out in accordance with the system. In fact, each object is a decision rule,

and the information cannot be simplified attributes in the system. So, we extract the rules directly, and the rules are in the following.

$$\begin{aligned}
&r_1 : (P_1, A)\wedge(P_2, A)\wedge(P_3, C)\wedge(P_4, B)\wedge(P_5, C) \longrightarrow (d, G, (0.6, 1]),\\
&r_2 : (P_1, B)\wedge(P_2, A)\wedge(P_3, C)\wedge(P_4, C)\wedge(P_5, D) \longrightarrow (d, Co, (0.6, 1]),\\
&r_3 : (P_1, C)\wedge(P_2, D)\wedge(P_3, E)\wedge(P_4, B)\wedge(P_5, D) \longrightarrow (d, Co, (0.6, 1]),\\
&r_4 : (P_1, B)\wedge(P_2, B)\wedge(P_3, A)\wedge(P_4, B)\wedge(P_5, A) \longrightarrow (d, G, (0.6, 1]),\\
&r_5 : (P_1, A)\wedge(P_2, B)\wedge(P_3, D)\wedge(P_4, A)\wedge(P_5, B) \longrightarrow (d, G, (0.6, 1]),\\
&r_6 : (P_1, C)\wedge(P_2, C)\wedge(P_3, C)\wedge(P_4, D)\wedge(P_5, E) \longrightarrow (d, Co, (0.6, 1]).
\end{aligned} \tag{9}$$

These rules are always valid and unique in decision information system of Table 1. Moreover, we can find that the decision accuracy of each rule is all 1/3 and the rule accuracy is 1. In this case, the evaluation requires all the information of a fund project, which is not very useful for us to simplify the decision-making process and deal with unknown information.

Case 2. The information level is $\beta = 0.6$ $(0.5 < \beta \leq 0.6)$, and the reduction is $\{a_1, a_2, a_3, a_5\}$ and $\{a_2, a_3, a_4, a_5\}$.

In the case, from the reductions, we can find that the decision system can be presented by partial not all attributes.

Thus, the decision system can be simplified in the following two decision tables which are Tables 6 and 7.

From Table 6, we can have some rules as follows:

$$\begin{aligned}
&r_1 : (P_1, A)\wedge(P_2, A)\wedge(P_3, C)\wedge(P_5, C) \longrightarrow (d, G, (0.5, 0.6]),\\
&r_2 : (P_1, B)\wedge(P_2, A)\wedge(P_3, C)\wedge(P_5, D) \longrightarrow (d, Co, (0.5, 0.6]),\\
&r_3 : (P_1, C)\wedge(P_2, D)\wedge(P_3, E)\wedge(P_5, D) \longrightarrow (d, Co, (0.5, 0.6]),\\
&r_4 : (P_1, B)\wedge(P_2, B)\wedge(P_3, A)\wedge(P_5, A) \longrightarrow (d, G, (0.5, 0.6]),\\
&r_5 : (P_1, A)\wedge(P_2, B)\wedge(P_3, D)\wedge(P_5, B) \longrightarrow (d, G, (0.5, 0.6]),\\
&r_6 : (P_1, C)\wedge(P_2, C)\wedge(P_3, C)\wedge(P_5, E) \longrightarrow (d, Co, (0.5, 0.6]).
\end{aligned} \tag{10}$$

From Table 7, we can have some rules as follows:

$$\begin{aligned}
&r_7 : (P_2, A)\wedge(P_3, C)\wedge(P_4, B)\wedge(P_5, C) \longrightarrow (d, G, (0.5, 0.6]),\\
&r_8 : (P_2, A)\wedge(P_3, C)\wedge(P_4, C)\wedge(P_5, D) \longrightarrow (d, Co, (0.5, 0.6]),\\
&r_9 : (P_2, D)\wedge(P_3, E)\wedge(P_4, B)\wedge(P_5, D) \longrightarrow (d, Co, (0.5, 0.6]),\\
&r_{10} : (P_2, B)\wedge(P_3, A)\wedge(P_4, B)\wedge(P_5, A) \longrightarrow (d, G, (0.5, 0.6]),\\
&r_{11} : (P_2, B)\wedge(P_3, D)\wedge(P_4, A)\wedge(P_5, B) \longrightarrow (d, G, (0.5, 0.6]),\\
&r_{12} : (P_2, C)\wedge(P_3, C)\wedge(P_4, D)\wedge(P_5, E) \longrightarrow (d, Co, (0.5, 0.6]).
\end{aligned} \tag{11}$$

Table 6: Fund investment decision system after the reduction (I).

U	P_1	P_2	P_3	P_5	d
x_1	A	A	C	C	G
x_2	B	A	C	D	Co
x_3	C	D	E	D	Co
x_4	B	B	A	A	G
x_5	A	B	D	B	G
x_6	C	C	C	E	Co

Table 7: Fund investment decision system after the reduction (II).

U	P_2	P_3	P_4	P_5	d
x_1	A	C	B	C	G
x_2	A	C	C	D	Co
x_3	D	E	B	D	Co
x_4	B	A	B	A	G
x_5	B	D	A	B	G
x_6	C	C	D	E	Co

As a result of our data on a smaller scale, the reduction of information system data has no duplication, so that we get 12 decision rules. When the data size is larger, reduction can make a lot of duplicate data merging, effectively reduce the number of decision rules, and improve the decision accuracy and precision of rules.

According to the calculation, the accuracy of the above 12 decision rules is 1/6 and the accuracy of the rules is 1. Although the decision-making accuracy is reduced, the rule accuracy does not decrease. So, we can have that reduction that simplifies the test of the data validation rules; decision conclusion can be obtained without a large scale of data validation.

From the rules obtained above, the conclusion of the decision making for fund investments can be got about the decision information system in Table 1. According to the representation form of decision rules, each decision result is shown in Table 8. The symbol means that the corresponding value is arbitrary, that is, any value taken under the specified conditions in the table has no influence on the decision result indicated in the table.

5. Conclusions

In this paper, a multigranulation rough set decision method is used to construct the fund investment decision information system; then, the fund investment decision information system is reduced at different thresholds, the decision rules are extracted by reduction and the rules are analyzed, and finally the decision rules are given using fund investment

Table 8: Decision results of the fund investment information system.

The serial number	Decision factors	Decision results	Decision accuracy	Information level β
1	a_1—outstanding, a_2—outstanding, a_3—general, a_4—good, a_5—general	G	1	(0.6,1]
2	a_1—good, a_2—outstanding, a_3—general, a_4—general, a_5—poor	Co	1	(0.6,1]
3	a_1—general, a_2—poor, a_3—very poor, a_4—good, a_5—poor	Co	1	(0.6,1]
4	a_1—good, a_2—good, a_3—outstanding, a_4—good, a_5—outstanding	G	1	(0.6,1]
5	a_1—outstanding, a_2—good, a_3—poor, a_4—outstanding, a_5—good	G	1	(0.6,1]
6	a_1—general, a_2—general, a_3—general, a_4—poor, a_5—very poor	Co	1	(0.6,1]
7	a_1—outstanding, a_2—outstanding, a_3—general, a_4—*, a_5—general	G	1	(0.5,0.6]
8	a_1—good, a_2—outstanding, a_3—general, a_4—*, a_5—poor	Co	1	(0.5,0.6]
9	a_1—general, a_2—poor, a_3—very poor, a_4—*, a_5—poor	Co	1	(0.5,0.6]
10	a_1—good, a_2—good, a_3—outstanding, a_4—*, a_5—outstanding	G	1	(0.5,0.6]
11	a_1—outstanding, a_2—good, a_3—poor, a_4—*, a_5—good	G	1	(0.5,0.6]
12	a_1—general, a_2—general, a_3—general, a_4—*, a_5—very poor	Co	1	(0.5,0.6]
13	a_1—*, a_2—outstanding, a_3—general, a_4—good, a_5—general	G	1	(0.5,0.6]
14	a_1—*, a_2—outstanding, a_3—general, a_4—general, a_5—poor	Co	1	(0.5,0.6]
15	a_1—*, a_2—poor, a_3—very poor, a_4—good, a_5—poor	Co	1	(0.5,0.6]
16	a_1—*, a_2—good, a_3—outstanding, a_4—good, a_5—outstanding	G	1	(0.5,0.6]
17	a_1—*, a_2—good, a_3—poor, a_4—outstanding, a_5—good	G	1	(0.5,0.6]
18	a_1—*, a_2—general, a_3—general, a_4—poor, a_5—very poor	C_O	1	(0.5,0.6]

decision making. This study provides a new approach to fund management, enriching the application of multigranulation rough sets.

Data Availability

The data used to support the findings of this study are included within the article.

Conflicts of Interest

The authors declare no conflict of interest.

Authors' Contributions

XY is the principal investigator of this work. He performed the experiments and wrote this manuscript. XS contributed to the framework and provided several suggestions for improving the quality of this manuscript. All authors revised and approved the publication.

References

[1] Y. Li, *Fund Investment Management*, Economic Science Press, 2002.

[2] D. Blake, A. G. Rossi, A. Timmermann, I. Tonks, and R. Wermers, "Decentralized investment management: evidence from the pension fund industry," *The Journal of Finance*, vol. 68, no. 3, pp. 1133–1178, 2013.

[3] D. L. Luskin and L. G. Tint, *Investment Fund Management Method and System*, 2002.

[4] A. Andonov, P. Eichholtz, and N. Kok, "Intermediated investment management in private markets: evidence from pension fund investments in real estate," *Journal of Financial Markets*, vol. 22, pp. 73–103, 2015.

[5] Z. Wei and Y. Lin, *Investment Management Mode of Social Insurance Fund and Getting Rid of the Predicament*, 2014, Reform.

[6] Y. Zhang, "Analysis of China's social security fund investment management under the background of financial crisis," *Science and Technology Economy Market*, vol. 31, no. 1, pp. 106-107, 2016.

[7] Z. Lu, "Analysis of the relationship between performance evaluation indicators of securities investment funds," *Economic Mathematics*, vol. 22, no. 3, pp. 235–239, 2005.

[8] J. Peng, *Research on Performance Evaluation of Open Fund in China Based on Fuzzy Mathematics*, Jiangxi University of Science and Technology, 2012.

[9] X. Xu, *Research on the Risk Assessment of Open End Funds in China – Based on the Application of VaR–GARCH Model and Fuzzy Mathematics Method*, Hefei Polytechnic University, 2015.

[10] Z. Pawlak, "Rough sets," *International Journal of Computer & Information Sciences*, vol. 11, no. 5, pp. 341–356, 1982.

[11] Z. Pawlak, "Rudiments of rough sets," *Information Sciences*, vol. 177, no. 1, pp. 3–27, 2007.

[12] Y. Qian, J. Liang, Y. Yao, and C. Dang, "MGRS: a multigranulation rough set," *Information Sciences*, vol. 180, no. 6, pp. 949–970, 2010.

[13] Y. Qian, J. Liang, and C. Dang, "Incomplete multigranulation rough set," *IEEE Transactions on Systems, Man, and Cybernetics - Part A: Systems and Humans*, vol. 40, no. 2, pp. 420–431, 2010.

[14] Y. Qian, J. Liang, and W. Wei, "Pessimistic rough decision," in *Proceedings of the 2nd International Workshop on Rough Sets Theory*, pp. 440–449, Zhoushan, China, 2010.

[15] W. Xu, W. Sun, X. Zhang, and W. Zhang, "Multiple granulation rough set approach to ordered information systems," *International Journal of General Systems*, vol. 41, no. 5, pp. 475–501, 2012.

[16] W. Xu, Q. Wang, and S. Luo, "Multi-granulation fuzzy rough sets," *Journal of Intelligent & Fuzzy Systems*, vol. 26, no. 3, pp. 1323–1340, 2014.

[17] W. Xu, Q. Wang, and X. Zhang, "Multi-granulation fuzzy rough sets in a fuzzy tolerance approximation space," *International Journal of Fuzzy Systems*, vol. 13, no. 4, pp. 246–259, 2011.

[18] W. Xu, Q. Wang, and X. Zhang, "Multi-granulation rough sets based on tolerance relations," *Soft Computing*, vol. 17, no. 7, pp. 1241–1252, 2013.

[19] W. Xu and W. Li, "Granular computing approach to two-way learning based on formal concept analysis in fuzzy datasets," *IEEE Transactions on Cybernetics*, vol. 46, no. 2, pp. 366–379, 2016.

[20] W. Li and W. Xu, "Multigranulation decision-theoretic rough set in ordered information system," *Fundamenta Informaticae*, vol. 139, no. 1, pp. 67–89, 2015.

[21] X. Yang, Y. Qi, X. Song, and J. Yang, "Test cost sensitive multigranulation rough set: model and minimal cost selection," *Information Sciences*, vol. 250, no. 11, pp. 184–199, 2013.

[22] X. Yang, Y. Qi, H. Yu, X. Song, and J. Yang, "Updating multigranulation rough approximations with increasing of granular structures," *Knowledge-Based Systems*, vol. 64, no. 1, pp. 59–69, 2014.

[23] X. Yang, "Hierarchical structures on multigranulation spaces," *Journal of Computer Science and Technology*, vol. 27, no. 6, pp. 1169–1183, 2012.

[24] X. Yang, "On multigranulation rough sets in incomplete information system," *International Journal of Machine Learning and Cybernetics*, vol. 3, no. 3, pp. 223–232, 2012.

[25] L. Wang, X. Yang, and J. Yang, "A new incomplete multi granularity rough set," *Journal of Nanjing University (Natural Science)*, vol. 48, no. 4, pp. 436–444, 2012.

[26] Y. Qian, J. Liang, and C. Dang, "Knowledge structure, knowledge granulation and knowledge distance in a knowledge base," *International Journal of Approximate Reasoning*, vol. 50, no. 1, pp. 174–188, 2009.

[27] Y. Yao, "Information granulation and rough set approximation," *International Journal of Intelligent Systems*, vol. 16, no. 1, pp. 87–104, 2001.

[28] Y. Qian and J. Liang, "Rough set method based on multi-granulations," in *2006 5th IEEE International Conference on Cognitive Informatics*, pp. 297–304, Beijing, China, July 2006.

[29] W. Xu, X. Zhang, and Q. Wang, "A generalized multi-granulation rough set approach," in *Bio-Inspired Computing and Applications. ICIC 2011*, Lecture Notes in Computer Science, D. S. Huang, Y. Gan, P. Premaratne, and K. Han, Eds., pp. 681–689, Springer, Berlin, Heidelberg, 2011.

[30] W. Xu, W. Li, and X. Zhang, "Generalized multigranulation rough sets and optimal granularity selection," *Granular Computing*, vol. 2, no. 4, pp. 271–288, 2017.

Hindawi
Complexity
Volume 2018, Article ID 9672849, 15 pages
https://doi.org/10.1155/2018/9672849

Research Article

The Resilience of Public Policies in Economic Development

Gonzalo Castañeda[1] **and Omar A. Guerrero**[2,3,4]

[1]*Centro de Investigación y Docencia Economica (CIDE), Mexico*
[2]*The Alan Turing Institute, London, UK*
[3]*Department of Economics and STEaPP, University College London, UK*
[4]*CABDyN Complexity Centre, University of Oxford, UK*

Correspondence should be addressed to Omar A. Guerrero; oguerrer@gmail.com

Received 3 April 2018; Accepted 2 August 2018; Published 2 October 2018

Academic Editor: Claudio Tessone

This paper studies the resilience of public policies that governments design for catalyzing economic development. This property depends on the extent to which behavioral heuristics and spillover effects allow policymakers to attain their original goals when a particular policy cannot be funded as originally planned. This scenario takes place, for example, when unanticipated events such as natural disasters or political turmoil obstruct the use of resources to advance certain policy issues, *e.g.,* infrastructure or labor reforms. Here, we analyze how the adaptive capacity of the policy-making process generates resilience in the face of disruptions. In order to estimate the allocation of resources across policies, we employ a computational model that accounts for diverse social mechanisms, for example, coevolutionary learning and network interdependencies. In our simulations, we use a data set of 117 countries on 79 development indicators over an 11-year period. Then, we calculate a resilience score corresponding to each development indicator via counter-factual analysis of policy disruptions. Next, we assess whether some development strategies produce resilient/fragile policy profiles. Finally, by studying the relationship between policy resilience and policy priority, we determine which issues are bottlenecks to economic development.

1. Introduction

Most economists are largely concerned with designing efficient policies for firms and the public sector but much less preoccupied of why certain strategies fail when facing adverse situations. Their focus on the optimal allocation of resources has, on one hand, an ontological explanation since—in the neoclassical view—governments and firms are assumed to have the capacity to control the performance of a system or organization [1]. On the other hand, there is an epistemological explanation since economic theories are deductive constructions built on agents maximizing objective functions that are specified in well-defined problems. These features become evident in the most well-known textbook definition of economics, *e.g., "the study of rational behaviors dealing with multiple objectives and limited resources that can be used for alternative purposes"* [rephrasing [2]].

Unfortunately, the rational conception of economics—where consumers, firms, and governments are centrally coordinated through equilibria—does not allow for a clear understanding of why firms, policies, and economies fail. That is, the study of resilience in human-made systems is not possible without a decentralized systemic view. The concept of resilience has different connotations depending on the field of inquiry (*e.g.*, physics, ecology, economics, sociology, or psychology). In this paper, we use a definition that is compatible with the problem of policy-making and development: "*Resilience is the [adaptive] capacity of a system, enterprise, or a person to maintain its core purpose and integrity in the face of dramatically changed circumstances*" ([3], p. 7).

Under the lens of complexity science, explanations for the failure of economies and their resilience come to light. This is so because complexity builds on the idea that agents within a system and systems themselves are interconnected;

hence, they are not fully decomposable [4, 5]. Thus, it is possible for a moderate perturbation on a subpopulation to permeate throughout the system and influence its overall performance with—sometimes—catastrophic consequences. Complexity, however, is not only about connectivity but also about diversity and adaptation. These properties stem from the evolutionary nature of economic systems. With these properties, economies are equipped to respond to adverse events or failures of their components. On one hand, diversity allows a system to generate alternative solutions to the ones impaired by a failure. On the other, adaptation allows agents to react by updating their objectives and strategies when the environment changes.

In this paper, we study the resilience of transformative public policies. A policy is transformative when it is designed to generate a change in a specific issue in order to reach a goal. For example, if the goal is to decrease infant mortality by 50%, a transformative public policy is the construction of hospitals in marginalized communities, while a nontransformative one is the expenditure to maintain the current health infrastructure. When countries attempt to reach a large set of goals simultaneously, resilience arises from the evolutionary nature of the process where policies are designed and implemented. The work of [6] (hereon refer to as CCG) provides a framework to model such process as a behavioral game between a central authority (government) and public functionaries (bureaucrats) on a network of policy spillovers. For a country, the estimated "allocation profile"—i.e., the evolved distribution of resources across policy issues—can be thought of as a consistent (or relatively efficient) package. In this political economy game, the government tries to make the best use of its budget, while bureaucrats may divert some of the allocated funds for a personal gain (*i.e.*, corruption). Hence, rather than modelling agents designing an optimal budgetary allocation, we estimate the emergent allocation profile.

In order to study resilience, we estimate the alternative allocation profiles that emerge in the pretense of adverse events. The intuition is that it is not always feasible to implement the allocation profile estimated for an economic setting that is free of unexpected adversities. These adversities occur when resources initially intended for a transformative policy have to be reassigned to a different purpose. For instance, improving health facilities is put on hold because fighting an epidemic outbreak consumes a large share of resources from the ministry of health; a labor reform has to be postponed when the affected unions sabotage its implementation; an expansion of the highway system is cancelled because recovering from a natural disaster requires substantial resources for repairing damaged infrastructure.

An estimated allocation profile depends on the goals of the government. Consistent with the literature of economic development, we assume that those targets are drawn from exemplary countries. That is, a government determines its goals by imitating the development indicators of a more advanced nation. We term these adopted targets a *development mode*. Resilience is measured by estimating the allocation profile of a development mode when one of its public policies is exogenously suspended, which we call a *disruption*. Therefore, resilience is the capacity of the system to maintain the evolution of socioeconomic indicators in line with a prespecified development mode. For a single country, the allocation profiles corresponding to each development mode allow estimating the expected time of convergence to targets. Significant deviations from the expectation indicate whether a policy is resilient or fragile. In this sense, resilience is not the property of being able to recover the initial condition of a system but rather its capability of continuing to fulfill its goals when facing adverse circumstances.

Resilience analysis allows us to compare not only policy issues but also allocation profiles. For example, a country like Mexico may have different options of development modes (Canada, Singapore, France, etc.); however, some allocation profiles may be more resilient than others. Therefore, assessing the feasibility of a development mode is not only an exercise about costs and benefits but also of endurance to adverse events. This analysis is significantly enriched when considering the priority that governments assign to specific policy issues (*i.e.*, the amount of resources allocated). For instance, a policy issue that is not resilient may hinder the possibility of reaching the targets set by the government. If such a policy receives a low priority from the government, the outcomes in terms of economic development may be worse than expected. In other words, policies with poor resilience and low priority act as bottlenecks to economic development. Identifying these bottlenecks is paramount to development studies. Ironically, due to the rational-equilibrium epistemology of neoclassical economics, there are no adequate quantitative tools for this purpose. Our work fills this gap and provides a well-suited analytic tool.

The rest of the paper is structured with five more sections. In the second section, we frame our approach in the literature of policy resilience. In the third section, we present the data used to calibrate our model. In the fourth section, we provide an overview of the CCG model for analyzing the policy-making process and explain how allocation profiles and their resilience are estimated. In the fifth section, we show the results of our estimations for three country cases and a more detailed description of aggregate outcomes for the entire database. Finally, in the sixth section, we discuss the benefits of complexity tools for studying resilience and summarize our main findings.

2. On the Nature of Resilience and Policy-Making

This paper studies the resilience of public policies that are formulated through a process of adaptation and learning. (It is neither about a system's architecture nor of policy tools that can improve the resilience of a particular system (e.g., ecological, environmental, transportation, regional, social, financial, urban, organizational, productive, and business).) It explores the likelihood of failure in the pursuit of specific development modes, independently of how this mode was originally established (*e.g.*, internal political agreements, imitating successful countries, through international consensus, or from pressures of the civil society). This is a relevant and intriguing question since the evaluation of society's (or

government's) aspirations requires to estimate the reachability of alternative standards. In the related literature, this approach falls under the umbrella of policy resilience at the process level. This literature refers to the institutional and procedural features of policy-making that are in place when an unanticipated shock disrupts a socioeconomic system [7]. In this respect, resilience should be of great concern in setting a societal agenda (development modes) and in formulating an allocation profile that is coherent with such agenda.

The policy process relates to three mechanisms. First, it has to do with the governance of decision-making (*e.g.*, stakeholder participation, institutional accountability, and multilevel and polycentric architectures). Second, it relates to the functionaries' capability of harnessing information for producing workable policies (*e.g.*, involvement of nonstate actors with specialized expertise, a culture of evidence-based decision-making). Third, it deals with the administrative capacity of public officials at the local (or agency) level so that policies can be implemented rapidly and with certain degree of flexibility (*e.g.*, well-designed protocols, use of transparent rules, mechanisms for conflict resolution among agencies, and a well-functioning system for the monitoring and sanctioning of corruption).

The political economy game developed by CCG incorporates important aspects of this policy-making process, emphasizing the distinction between design and implementation. For example, it specifies the mechanisms for the misuse of budgetary allocations by bureaucrats. Accordingly, we employ this model to study how the disruption of a public policy modifies the distribution of resources allocated to the remaining policies, while maintaining the original set of goals. This is a resilience problem because the policy-making process is able to readjust the allocation profile without losing its ability to fulfill the government's agenda (i.e., it is a dynamic property of the system). A related but different concept is robustness. In the literature of complexity, robustness refers to the ability of a system to keep working when some components fail (e.g., an edge in a network). Sometimes, robustness occurs due to the redundancy of components, paths, and functions [8]. Clearly, robustness is a static property of the system since it is not intended to capture the adaptive nature of an economy (it only considers connectivity and diversity).

In recent years, we have witnessed an explosion of quantitative methodologies for analyzing the resilience and robustness of socioeconomic systems [9, 10]. However, the literature of policy analysis at the process level is mainly qualitative [11–13]. Consequently, the tools and recommendations in this line of research are based solely on case studies and on an informal treatment of complexity. In order to develop a quantitative framework at the process level, it is convenient to construct a calibrated model on how policies are endogenously designed and implemented. This is precisely our approach. First, we build a computational political economy game. Then, we perform Monte Carlo simulations to estimate allocation profiles and resilience scores. Finally, we analyze the outcomes in terms of countries, socioeconomic indicators, development modes, and bottlenecks.

3. Data

The data consist of annual observations of 79 policy indicators for 117 countries, covering the 2006–2016 period. Three secondary sources are used to build this database: the Global Competitiveness Report produced by the World Economic Forum, the World Development Indicators, and the World Governance Indicators, being the latter two assembled by the World Bank. Following CCG, we normalize these indicators so that the worst possible outcome takes a value of 0, while the best value is 1 across countries and years.

We synthesize this information by grouping the 79 development indicators in 13 commonly used pillars. To illustrate the data structure, we pool countries into four clusters by similarity in their development indicators (with cluster 1 being the most advanced and cluster 4 the least). We identify the clusters of countries by applying Ward's method with the L2 (Euclidean) norm as the distance metric across the 79 indicators. Figure 1 shows that, in general, more advanced nations have higher levels of development indicators. The large gap between the clusters 1 and 2 denotes the middle-income development trap.

3.1. Spillover Network. An important component of the CCG model is a network of spillovers between public policies that accounts for well-known interdependencies between policy issues [14–16]. Empirically, this network is estimated from partial correlations between development indicators at the level of each country. Therefore, we estimate one network for each country. Arguably, a network topology reflects the socioeconomic conditions in a specific nation. We employ a two-step empirical strategy developed in the estimation of neural networks from functional magnetic resonance imaging data [17, 18]. First, we apply the method of triangulated maximally filtered graphs (TMFG) [19] to estimate which pairs of indicators have significant relationships. Then, we determine the edges' directions (inferred causality) through the likelihood-ratios method developed by [20]. The field of network estimation has various different methods, without a broad consensus on a gold standard. Each method assumes a specific underlying model and is designed for data with certain properties. Our methodological choice is based on the applicability of this strategy to high-dimensional time series of short length. However, as new and better methods emerge, we expect further improvements to our estimations.

4. Methods

We use the CCG model in order to simulate the policy-making process through a behavioral game with two types of agents: a central authority (government) and public servants (functionaries or bureaucrats). Firstly, the government allocates resources to different public policies, with the aim of improving the indicators associated to their respective policy issues. Secondly, functionaries in charge of implementing these policies have incentives to divert public funds for personal gain. This game takes place on a spillover network. These spillovers encourage free-riding and reinforce a misalignment between the government's and functionaries'

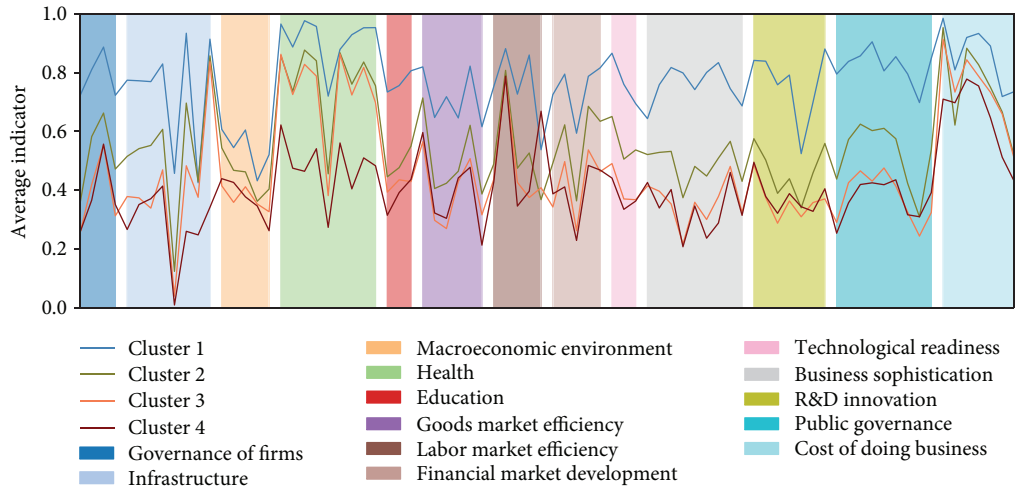

FIGURE 1: Gaps in socioeconomic indicators between development clusters in 2016. The X-axis corresponds to development indicators, organized by development pillar. The wider the shaded area, the more development indicators within the corresponding pillar. For countries without observations for 2016, we take the most recent one.

incentives. (See [6] for a detailed interpretation of the model's equations and different validation tests).

4.1. Evolution of Development Indicators. There are N policy issues in the economy, each one with an indicator that measures its level of development. As a government invests $P_i \in [0, 1]$ resources in a policy issue, its indicator grows, *i.e.*, the investment accumulates. This means that, when the government sets a target T_i for policy issue i, indicator I_i will reach T_i after a number of periods. Hence, the dynamics describing the evolution of I_i are given by

$$I_{i,t} = I_{i,t-1} + \gamma(T_i - I_{i,t-1})\left(C_{i,t} + \sum_j C_{j,t}A_{j,i}\right), \quad (1)$$

where γ captures the effectiveness of policy-making in a specific country; $C_{i,t} \in [0, P_i]$ is the contribution of bureaucrat i (see explanation in next section), and $\mathbb{A}$ is the adjacency matrix of the spillovers network (a weighted directed graph).

4.2. The Learning Process of Public Servants. In a given period t, a public servant i receives $P_{i,t}$ resources from the central authority and uses $C_{i,t}$ effectively in the implementation of the public policy. Hence, $P_{i,t} - C_{i,t}$ is the level of corruption of i, while the level of i's indicator gives him (or her) political status. Then, in order to determine the impact of this contribution, the bureaucrat evaluates the change in benefits F_i expressed through

$$F_{i,t} = (I_{i,t} + P_{i,t} - C_{i,t})(1 - \theta_{i,t}f_{R,t}), \quad (2)$$

where $\theta_{i,t}$ is an indicator function derived from the supervision of the central authority, and $f_{R,t}$ is a map from the indicator of *rule of law* to a probability. In the CCG model, a period should not be interpreted as time, since the method does not aim at reproducing time series. Instead, it should be interpreted as the realization of events such as budgetary readjustments. Hence, if it takes more periods to reach one set of goals than another, we say that the former are more difficult to attain than the latter.

We assume that the government cannot observe the functionaries' contributions directly, although larger diversions of funds are more difficult to hide. Hence, we model government supervision as a random variable $\theta_{i,t}$. The outcome $\theta_{i,t}$ is 1 if the public servant in policy issue i is caught diverting public funds and zero otherwise. Then, the probability mass function of θ_i at time t is

$$\theta_{i,t} = \begin{cases} 1 & \text{with probability } f_{C,t}\dfrac{(P_{i,t} - C_{i,t})}{\sum_{j=1}^{N}(P_{j,t} - C_{j,t})}, \\ 0 & \text{with probability } 1 - f_{C,t}\dfrac{(P_{i,t} - C_{i,t})}{\sum_{j=1}^{N}(P_{j,t} - C_{j,t})}, \end{cases} \quad (3)$$

where $f_{C,t}$ is a function mapping the indicator of *control of corruption* to a probability.

Note that $f_{C,t}$ captures the efforts from the central authority to detect corrupt officials. Meanwhile, $f_{R,t}$ reflects the capability of the state to punish officials involved in these activities. These two mechanisms describe different constraints that governments face when fighting corruption. To be more specific, $f_{R,t}$ and $f_{C,t}$ take the form

$$f_{X,t} = \frac{I_{X,t}}{e^{1-I_{X,t}}}, \quad (4)$$

where $X = R$ for the rule of law, or $X = C$ for control of corruption.

The contribution of functionary i is determined by

$$C_{i,t} = \min\left\{P_{i,t}, \max\left(0, C_{i,t-1} + d_{i,t}\left|\Delta F_{i,t}\right|\frac{C_{i,t-1} + C_{i,t-2}}{2}\right)\right\}, \quad (5)$$

where $\Delta F_{i,t}$ is the most recent change in benefits, and $d_{i,t}$ is the sign function

$$d_{i,t} = \text{sgn}\,(\Delta F_{i,t} \cdot \Delta C_{i,t}), \tag{6}$$

such that

$$\begin{aligned} \Delta F_{i,t} &= F_{i,t-1} - F_{i,t-2}, \\ \Delta C_{i,t} &= C_{i,t-1} - C_{i,t-2}. \end{aligned} \tag{7}$$

That is, functionaries' contributions increase when higher (or lower) past benefits coincide with higher (or lower) past contributions. Therefore, as time goes by, bureaucrats learn the level of corruption that gives them certain confidence of keeping the benefits derived from their public post.

4.3. The Adaptive Behavior of the Central Authority. The government's problem consists in deciding how to allocate its limited resources to a large set of policies. Its objective is to reduce the gap between the current indicators (I_i) and their targets (T_i), where the latter come from a previously selected development mode. Formally, the government's multidimensional problem is

$$\min \quad \left(\sum_{i=1}^{N} (I_{i,t} - T_i)^2 \right). \tag{8}$$

Resource allocations $P_{1,t}, \ldots, P_{N,t}$ are the control variables of the central authority. We call a specific configuration of these variables an *allocation profile*. These packages of policies are the key endogenous variables to be simulated by the model. The amount of resources that the government can invest per period in a profile is restricted by

$$\sum_{i}^{N} P_{i,t} \leq B \forall t, \tag{9}$$

where B denotes *noncommitted* resources of the central authority. It is important to clarify that the resources involved in this problem are those destined to transformative policies, not public expenditure committed to previously established purposes (*e.g.*, highway maintenance, agricultural subventions, and payment of public debt).

Each time step, the central authority determines an allocation profile and evaluates the gap between targets and observed indicators. The amount of resources allocated to policy issue i is determined by

$$p_{i,t} = \frac{q_{i,t}}{\sum_{j}^{N} q_{i,t}}, \tag{10}$$

where $q_{i,t}$ is the propensity of assigning resources to policy i, defined as

$$q_{i,t} = (T_i - I_{i,t})(K_i + 1)\left(1 - \theta_{i,t} f_{R,t}\right), \tag{11}$$

where K_i is the number of outgoing connections of node i, also known as its out-degree. Here, the out-degree captures the centrality or importance of a policy issue for the country. Hence, the government does not know the structure of the network but has a proxy of the relevance of each policy issue.

Finally, the amount of resources allocated to policy i is

$$P_{i,t} = p_{i,t} B. \tag{12}$$

This component of the policy-making process indicates that the government's behavior is adaptive. That is, resources are redistributed when undesired events such as the detection of corruption materialize.

4.4. Algorithm. Once the political economy game is formulated mathematically, an agent-based model is programmed with Algorithm 1. Note that, for each simulation, four endogenous variables are obtained: public servants' contributions and benefits, government's allocations, and society's development indicators. A simulation halts when a convergence criterion is met for all indicators. The combination of a coevolutionary learning process, the diversity of conditions that bureaucrats face, and the network of policy spillovers requires computational simulation.

4.5. Estimation of Allocation Profiles. Each country in the data set can adopt development modes of nations with (1) a higher GDP per capita (adjusted for purchasing power parity) and (2) a higher average level of development indicators. This means that, for the sample of 117 countries, there are more than 6000 combinations of country-mode pairs (*e.g.*, RUS-CAN stands for Russia adopting the Canada development mode). We estimate the allocation profiles of each of these pairs, assuming no policy disruptions. For a given pair, a single allocation profile consists of the intertemporal averages $P = \{1/\ell \sum_{t=0}^{\ell} P_{i,t}\}_{i=1}^{N}$, where ℓ is the number of periods before converging to the targets. For the same pair, we perform m Monte Carlo simulations and compute the average allocation profile $\bar{P} = \{1/M \sum_{m=1}^{M} P_i^m\}_{i=1}^{N}$. Each simulation is calibrated by imputing the empirical values of the country's development indicators in 2016 (the initial conditions), the estimated network of spillovers, the values of the adopted mode's development indicators in 2016 (the targets), and the budget constrain B obtained from an indicator on public expenditure as a fraction of GDP.

In order to provide inference on aggregate metrics, we calibrate parameter γ to fit our endogenous variable of corruption ($P_i - C_i$) to the observed levels of an empirical indicator on the diversion of public funds. This is done through a clustering algorithm that classifies all countries into different categories of γ (see details in [6]). Once the model has been calibrated, we obtain the average allocation profile for a set of Monte Carlo simulations. The purpose of estimating these profiles is to obtain the relative priorities that governments give to different policies under

Input: $\mathbb{A}$, T, B, γ
for each *time* t **do**
  for each *public servant* i **do**
    update contribution $C_{i,t}$;
    update benefits $F_{i,t}$;
  for each *node* i **do**
    update indicator $I_{i,t}$;
  for each *node* i **do**
    central authority updates $P_{i,t}$;
  if $|I_{i,t} - I_{i,t-1}| < \epsilon$ *for every* i **then**
    halt;

Algorithm 1: Computation implementation.

each development mode, which we use in this paper to identify bottlenecks.

For illustration purposes, Figure 2 presents the estimated policy profiles for three different country-mode pairs. From this example, we infer that policy priorities depend on the specific pair, which highlights the relevance of context in the design and implementation of policies. Likewise, we can conclude that the coherence of the allocation profile, and not the strength of isolated policies, is what really matters to achieve development goals.

4.6. Estimation of Resilience. The strategy to assess the resilience of an individual policy is to measure the effect of disrupting its budgetary allocation. This exercise describes a scenario where the central authority of a country is forced to put off the implementation of a transformative policy due to an unexpected event. In the context of our behavioral game, the disruption of a transformative policy in issue i precludes it from receiving sustained allocations. Aware of this disruption, the government adapts and modifies its policy priorities in an attempt to reach the targets specified by the chosen development mode. In other words, this "change of plans" alters the coevolutionary learning process between central authority and functionaries, and, hence, the dynamics through which the indicators reach all their targets. More formally, assume that policy i has been disrupted ($P_{i,t} = 0$ for all t). Let $\mathcal{T}^i_j$ denote the time it takes for indicator j to converge to its target while i has been disrupted. Then, the adjusted convergence time induced by a disruption of i is

$$\mathcal{T}^i = \frac{(T_i - I_{i,0})}{N-1} \sum_{j \neq i}^{N-1} \mathcal{T}^i_j, \tag{13}$$

where $T_i - I_{i,0}$ takes into account the fact that, by disrupting an indicator with a large initial gap, the average convergence time becomes shorter. The fact that a policy issue is not receiving direct investments does not inhibit the possibility that the level of its associated indicator can increase. On the contrary, this is likely to happen because there are spillover effects among policies.

As we previously discussed, resilience is a dynamic property of a system. This means that the effect of disrupting a particular public policy needs to be measured beyond the budgetary consequences of setting $P_{i,t} = 0$. In other words, a policy is said to be resilient if the corresponding adjusted convergence time is lower than the expectation from removing direct investments from i. In contrast, the policy is said to be fragile if its adjusted convergence time is higher. (A direct comparison of convergence times between the complete and the disrupted models is not informative. This is so because it is not possible to isolate the effect of the disrupted policy due to the adaptive nature of the model. That is, the complete model has N objectives and the disrupted has N-1, rendering any comparison useless without a normalization that accounts for the effect of the disrupted policy.)

Our proxy to measure the direct budgetary effects on convergence time is $\bar{P}_i$, the average allocation to policy issue i obtained from the model without disruptions. Note that, by (11), $\bar{P}_i$ and $T_i - I_{i,0}$ are positively correlated. Therefore, if the model was purely driven by budgetary effects, a relationship between $\bar{P}_i$ and $\mathcal{T}^i$ would be almost perfect (although not necessarily linear). Deviations from the expectation of such relationship denote evidence of resilience and fragility. Allow us to illustrate this with a hypothetical example. Figure 3 shows artificial data about the positive relationship between $\mathcal{T}^i$ and $\bar{P}_i$. The solid line represents the estimated relationship, *i.e.*, the expected budgetary effect on the adjusted convergence time. The dots above the confidence interval denote fragile policy issues because their disruption increase convergence time more than expected. The dots under the interval correspond to resilient policies. Finally, the policy issues inside the interval are undefined because they are explained by the budgetary effect.

Figure 3 exemplifies the importance of a systemic approach to public policy. The points away from the expectation capture the effects derived from the coevolutionary dynamics of the model and the network. Given that each country can choose between multiple development modes and that it has a unique combination of network topology, initial conditions, and institutional factors, the relationship to be estimated for each country is

$$\widehat{\mathcal{T}}^{\,i} = a\bar{P}_i^b + \varepsilon_i, \tag{14}$$

where a and b are the parameters to be estimated via nonlinear least squares. Then, we construct our resilience score of policy i as follows

$$\mathcal{R}^i = \begin{cases} \widehat{\mathcal{T}}^i_l - \mathcal{T}^i & \text{if } \mathcal{T}^i < \widehat{\mathcal{T}}^i_l, \\ \widehat{\mathcal{T}}^i_u - \mathcal{T}^i & \text{if } \mathcal{T}^i < \widehat{\mathcal{T}}^i_u, \\ 0 & \text{otherwise,} \end{cases} \tag{15}$$

where $\widehat{\mathcal{T}}^i_l$ and $\widehat{\mathcal{T}}^i_u$ denote the lower and upper bounds of the estimated confidence interval. For clarity in the exposition of our results, the positive value of this score indicates that the corresponding policy is resilient (below the curve), while the negative value denotes that the policy is fragile (above the curve).

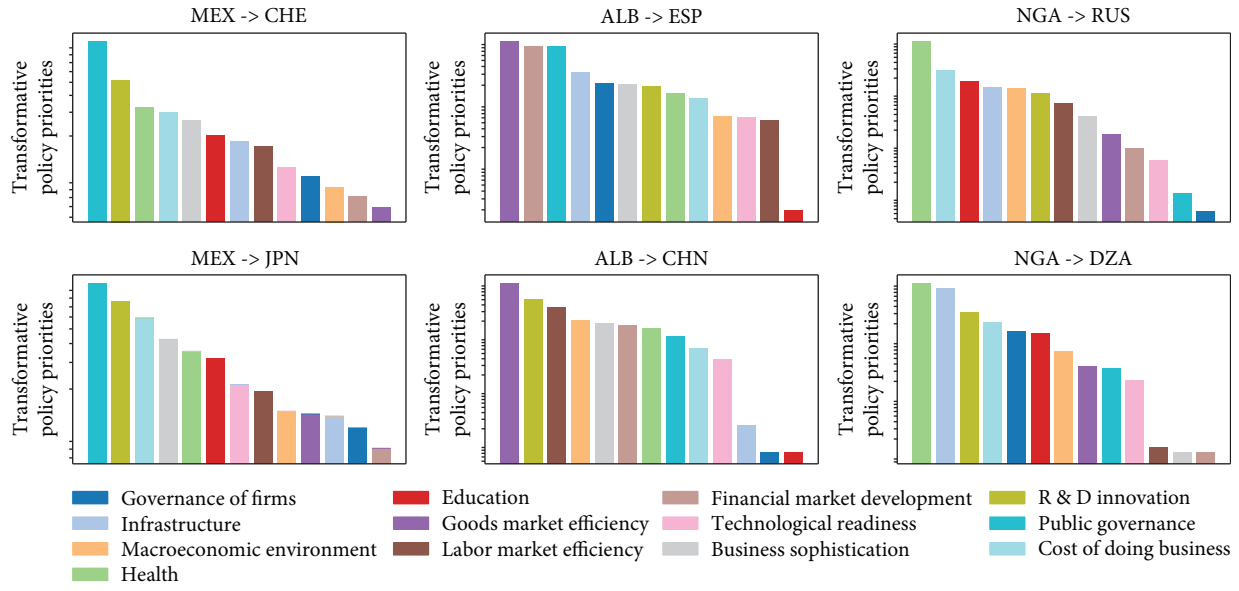

Figure 2: Average allocation profiles of three country cases.

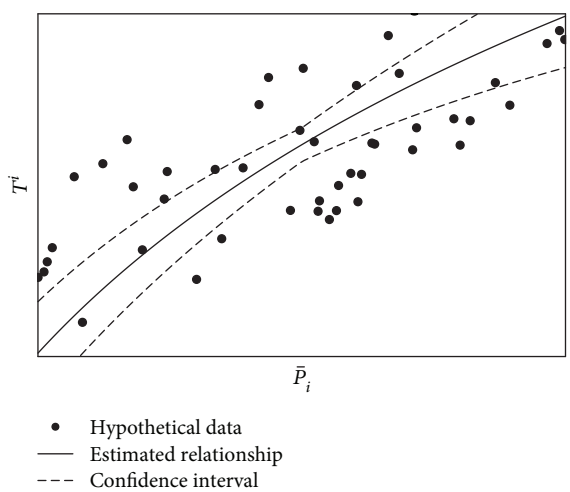

Figure 3: Hypothetical identification of resilient/fragile policies.

5. Results

We estimate the 79 disrupted allocation profiles of each country-mode pair (for each of the 79 cases of disruption in a country-mode pair, we performed 30 Monte Carlo simulations). For an individual country x, we pool all the outputs from simulating the adoption of all the development modes that x can follow. Then, we fit the curve in (14) to these outputs. Although we do not display confidence intervals in our plots (due to their narrowness), all our results were calculated considering an interval of 95% confidence. This curve provides the expected adjusted convergence time when x cuts its budget allocation to a disrupted policy with certain level of priority. When the convergence time from disrupting a policy deviates significantly from this expectation, it suggests resilience or fragility.

First, we provide an aggregate example in Figure 4 by fitting (14) to the pooled outputs of all the country-mode pairs. (The time variable in the vertical axis is normalized by the sum of adjusted convergence times of all perturbations in the profile, while the priorities in the horizontal axis are normalized by the country's budget B.) This aggregate exercise is useful to show the general structure of convergence times and relative priorities. Note that the simulated points produce a nonlinear fit, so resilient policies are those below the curve, while fragile ones lie above it. Many policies exhibit low relative priorities and short convergence times when disrupted. On the other hand, fewer have large budgetary allocations while, at the same time, produce long convergence times. The inset panel shows the distribution of deviations from the curve. This shows that most of the points are well explained by budgetary effects.

5.1. The Importance of Spillovers. Our next aggregate result highlights the importance of spillover effects on the simulation outcomes. Network effects on node-level dynamic were already identified by [6], who showed that more incoming spillovers induce lower contributions. Then, in the context of resilience, a straightforward demonstration of these effects is through the adjusted convergence time when the allocation on issue i is disrupted. Figure 5 shows this metric aggregated by countries (Figure 5(a)) and by indicators (Figure 5(b)). That is, the dots represent average values across simulation runs and development modes for all indicators and for all countries, respectively. In each panel, the estimates have been obtained from the full model, incorporating spillover effects, and from an incomplete version where we deactivate all interactions among policy issues.

Figure 5(a) shows that the simulations generate significantly different convergence times for most countries when we remove spillovers. Notice that, in most cases, the adjusted convergence time is lower when countries have spillover effects. This indicates that network effects tend to be

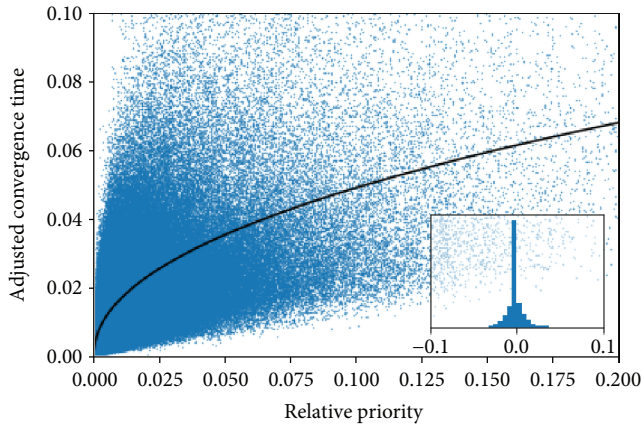

FIGURE 4: Expected convergence time from budgetary effects for all country-modes pairs. The inset panel shows the deviations from the fitted curve.

beneficial for reaching development goals, independently of disrupted public policies. In some cases, however, this does not occur due to different mechanisms. In our view, an intuitive explanation for an increase in convergence time due to spillover effects has to do with the reallocation of resources. For example, it is possible that—for some countries and development modes—redistributing resources from a disrupted issue to other policies generates biases in favor of nodes with relatively fewer outgoing spillovers. Under these circumstances, it may seem as if the presence of spillovers is detrimental for reaching the targets. Interestingly, we find that these cases tend to be advanced nations, suggesting that spillover effects are more beneficial (at least in a more direct way) in developing countries. Of course, second order effects might also contribute to this phenomenon.

In Figure 5(b), we can see that, by removing the spillovers, the adjusted convergence time varies modestly between indicators. This is expected since, in the absence of a network, indicators evolve only through the contributions of their bureaucrats. In this case, most of the empirical variation comes from the different budget constraints across countries. Since indicator-level aggregations include all countries, this variation is not observed across indicators. Therefore, spillovers provide an important source of heterogeneity to study resilience at the aggregate level of each indicator.

5.2. Simulation Results for Three Countries. Out of the 117 countries in the data set, we select three to estimate (14). These countries are in significantly different stages of development, for example, Mexico is considered a high-middle income country (cluster 2), Albania is lower-middle (cluster 3), and Nigeria is low (cluster 4).

Figure 6 shows the pooled outputs of all the country-mode pairs for each of the three cases. To be more precise, each dot in Figure 6(a) corresponds to $\mathcal{T}^i$ and $\bar{P}_i$ when i is disrupted in a specific development mode that Mexico can adopt. That is, there are 79 dots for each development mode. Here, we highlight the dots corresponding to the most resilient development mode (in blue) and to the least one (in orange). The resilience of a country-mode pair is measured through the average resilience score from its 79 disrupted policies. High resilience at the level of an allocation profile does not imply that all policies are resilient. It means that a country adopting a particular development mode has better chances at reaching its targets below the expected time.

Figure 7 shows the outcome of a similar exercise, this time, highlighting the indicators with the highest and the lowest average resilience scores across development modes. The blue (orange) dots highlight the most (least) resilient indicator across different development modes. In the Mexican case, the most fragile issue falls into the pillar of *public governance*, while the most resilient belongs to the pillar of *cost of doing business*. For Albania, the most resilient indicator corresponds to the *R&D innovation* pillar and the most fragile to the *financial market development* pillar. In the case of Nigeria, the most fragile issue relates to the pillar of *infrastructure* while the most resilient is part of the *health* pillar. These findings illustrate two important facts: (i) a disaggregated analysis is very important because some policy issues within a development mode can be very resilient while others can be extremely fragile, and (ii) a particular policy issue can be highly resilient (or fragile) for a country, no matter which development mode is adopted.

Finally, Figure 8(a)–8(c) show which ones are the most and the least resilient development pillars. The resilience of a pillar measures the average score of its corresponding indicators (or policy issues) across all development modes adoptable by a country. For the Mexican case, *public governance* is the most fragile pillar while *infrastructure* is the most resilient. Interestingly, the most resilient (fragile) pillar contains indicators that are rather fragile (resilient), highlighting the importance of disaggregation. This also occurs in the other two cases but with different pillars. For Albania, the most fragile pillar is *health*, and the most resilient is *R&D innovation*. This picture is completely reversed for Nigeria. This is an interesting result since, intuitively, one would expect *health* to be fragile. The Nigerian case is special because the effect on convergence time is largely dominated by the gap between initial conditions and targets. In fact, Nigeria exhibits a disproportionate indicator-target gap of its health-related indicators, which makes it a high-priority pillar (due to (11)), as shown in Figure 2. In contrast, for example, Mexico's top pillar—*public governance*—is the most fragile. This highlights the importance of context specificity and the interactions between initial conditions, targets, and spillovers.

5.3. A Global View of Resilience. In this section, we provide a global perspective of resilience by computing average scores at the level of development pillars and indicators. The purpose of this section is to understand how, across all the countries in the sample, certain policy issues tend to be fragile or resilient. These global averages are obtained from all the country-mode estimations. In other words, these results should be interpreted as the level of resilience that we should expect if we were to study a policy issue in a hypothetical country with the average characteristics of the population.

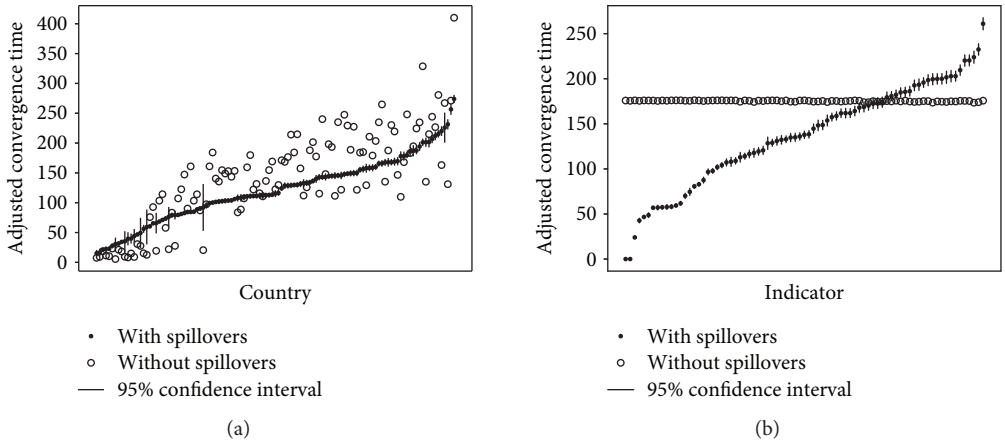

Figure 5: Estimations for the adjusted convergence times in models with and without spillovers. (a) Aggregation by country (sorted by $\mathcal{T}$). (b) Aggregation by indicator (sorted by $\mathcal{T}$).

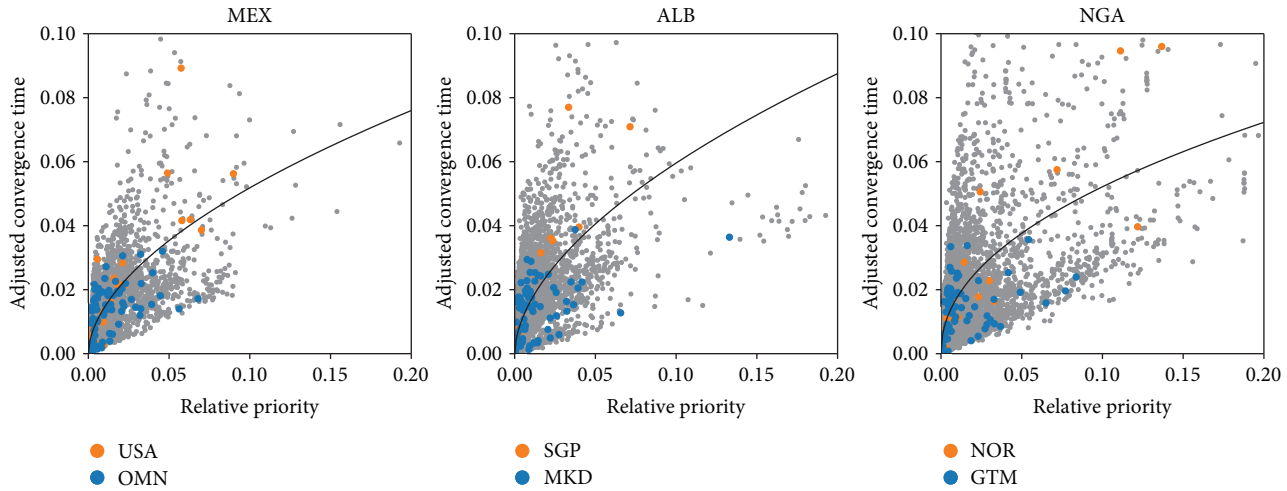

Figure 6: The most (blue) and the least (orange) resilient development modes for three countries. The majority of orange dots are not visible because they are covered by the blue ones. Gray dots refer to other development modes.

Figure 9 shows the average resilience scores at the level of development pillars. The top three most resilient pillars are *governance of firms*, *technological readiness*, and *cost of doing business*. In contrast, the three most fragile pillars (negative resilience scores) are *infrastructure*, *macroeconomic environment*, and *business sophistication*. Note that, due to the dominance of laggard economies in the country population, these estimates are biased towards developing countries. Nevertheless, if we pick a country at random, these are the expected levels of resilience to be found in each development pillar.

Figure 10 presents the average resilience scores at the level of each development indicator. Once more, the bar diagram highlights the importance of a disaggregated analysis. For instance, Figure 9 indicates that the *macroeconomic environment* pillar is rather fragile, yet in Figure 10, we can see that the *inflation* indicator is resilient. This is particularly interesting given the generalized notion that controlling inflation is central for economic development. This result, in contrast, suggests that this policy issue is not critical to attain the rest of the development goals. This is coherent with the idea of incorporating more diverse development goals in the international agenda. For example, one of the drivers behind the Sustainable Development Goals has been a critical position towards the narrow scope of the Millennium Development Project, which focused almost exclusively in economic outcomes. In fact, most development pillars have at least one indicator with the opposite classification (resilient/fragile). The top five most resilient indicators are *time to resolve insolvency*, *time required to enforce a contract*, *government procurement of advanced tech. products*, *survival to age 65 (male)*, and *adolescent fertility rate*, with two of them belonging to the pillar of *cost of doing business* and two more to *health*. The top five most fragile indicators are *business cost of crime and violence*, *infant mortality rate*, *tuberculosis cases*, *quality of port infrastructure*, and *quality of roads*, with two of them belonging to the *health* pillar and two more to *infrastructure*.

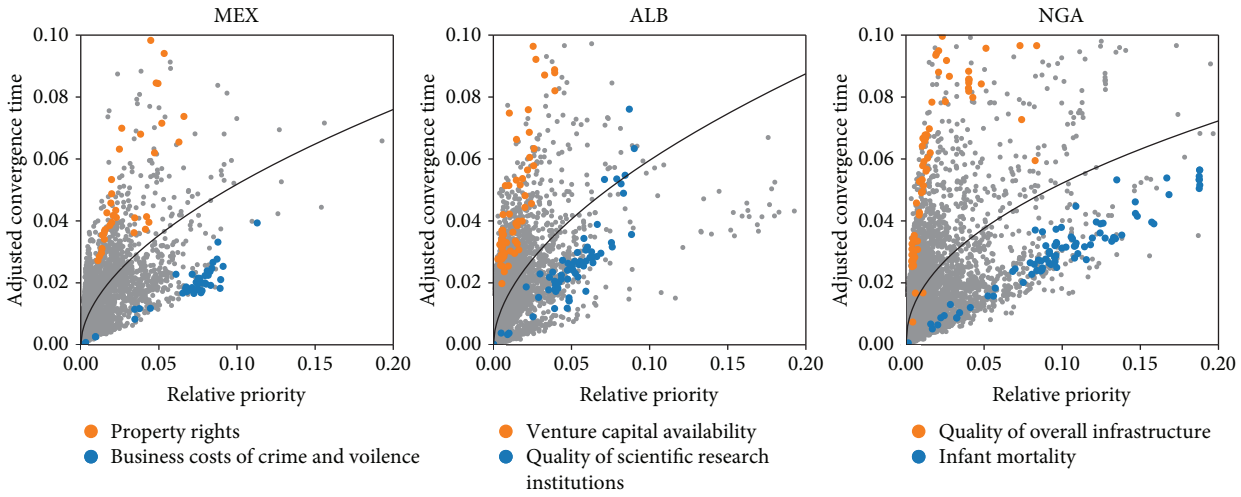

Figure 7: The most (blue) and the least (orange) resilient development indicators for three countries.

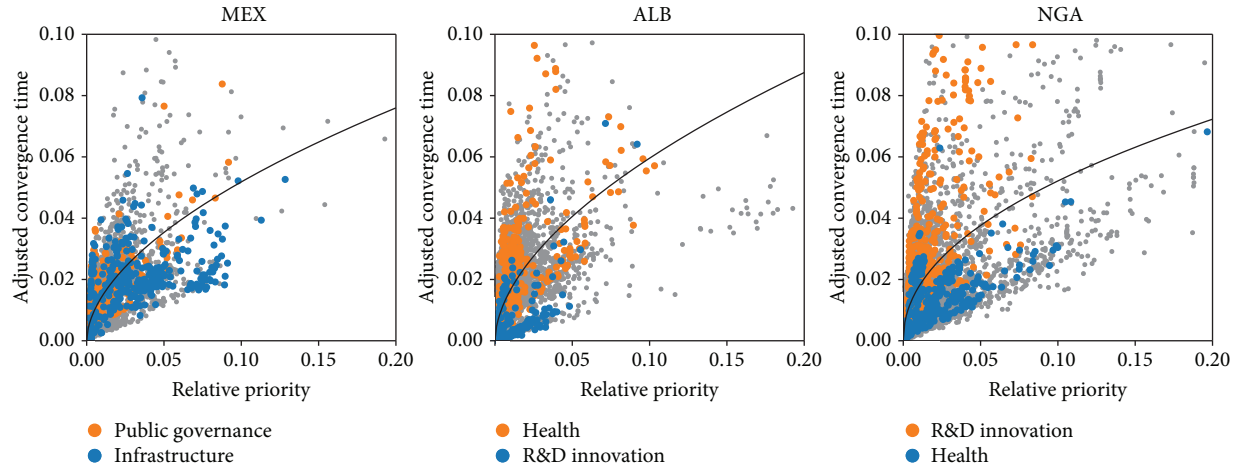

Figure 8: The most (blue) and the least (orange) resilient development pillars for three countries.

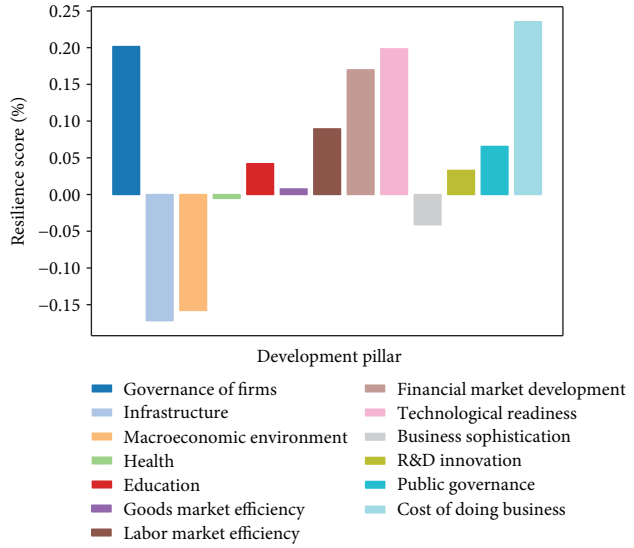

Figure 9: Average resilience by development pillar.

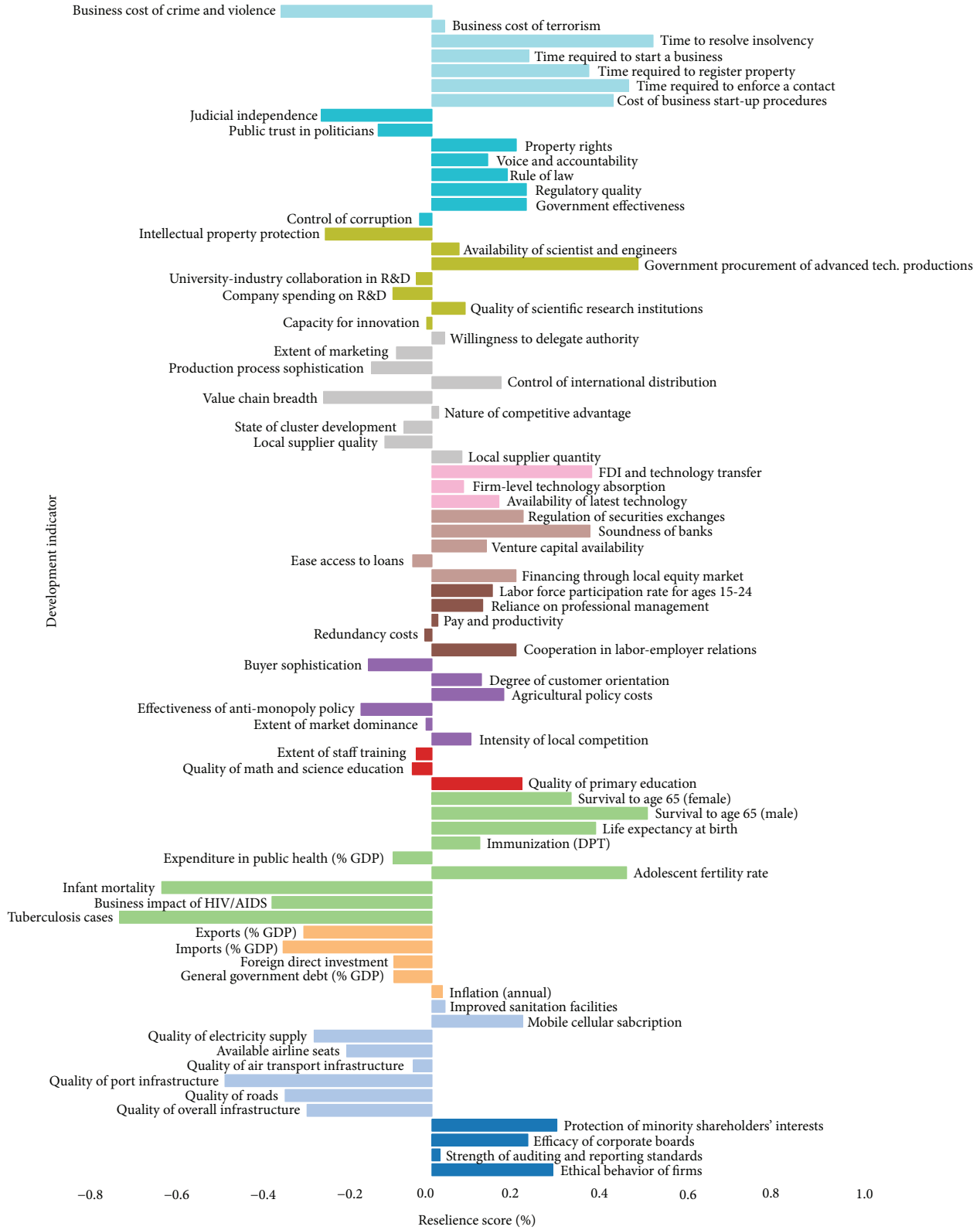

Figure 10: Average resilience by development indicator.

5.4. Bottlenecks and Sturdy Policy Issues. One of the key challenges in development is the identification of policy issues that act as binding constraints to development [21–23]. In other words, there exist certain policy issues that act as bottlenecks, so their identification can make policy design substantially more effective. In our context, bottlenecks are

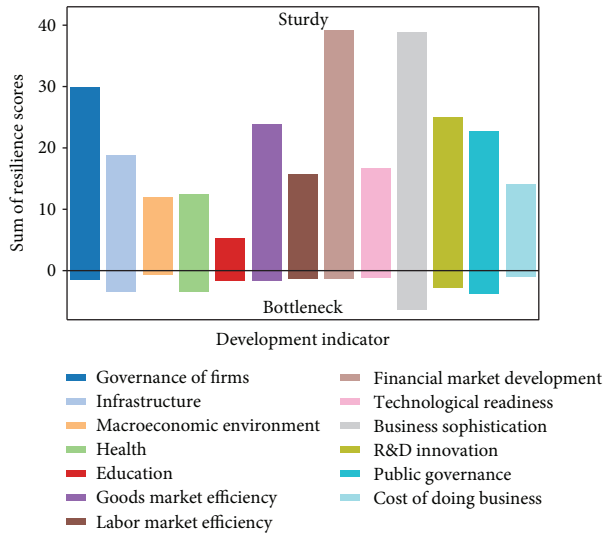

FIGURE 11: Bottlenecks and sturdy policy overall scores by development pillars. Bottlenecks: fragile policies in the 5th percentile of relative priorities. Sturdy: resilient policies in the 95th percentile of relative priorities.

fragile policy issues that receive a low relative priority by the central authority. Put it differently, these are policies where the central authority does not invest large sums, and, ironically, their disruption lowers the chances of attaining the goals of a chosen development mode.

Another important concept is *sturdiness*. We say that a policy issue is sturdy when it is a prime objective of the central authority, and, nonetheless, it is very resilient to disruptions. This paradoxical scenario is explained by two important features of the policy-making process. On the one hand, the adaptability of the agents involved in the design and implementation of policies (governments and public functionaries) allows a proper reallocation of resources from the original priorities to alternative policies which, in turn, mitigate negative impacts. On the other hand, the network of interdependent policies helps to improve the performance of an indicator even if it does not receive direct contributions from the general budget.

In order to identify bottlenecks and sturdy policies, we isolate those points that fall in the 5th and 95th percentiles of relative priorities. Bottlenecks are fragile policies in the 5th percentile, while sturdy ones are resilient issues in the 95th. Once isolated, we calculate the overall score of the bottlenecks (which is negative) and sturdy policies (positive) at the levels of pillars and development indicators. The overall score consists of summing the indicator-level scores. The reason for a sum, and not an average, is that the sum takes into account the frequency with which a policy appears in bottleneck or sturdy issues across all country-mode pairs. Figure 11 shows the overall scores of bottlenecks and sturdy policies in each development pillar.

The first thing to notice in Figure 11 is the large difference in the number of cases between bottlenecks and sturdy policies, being the latter much more frequent. This pattern emerges from the learning and adaptive behavior of the agents. It means that the adaptive nature of the policy-making process reduces the number of scenarios where adverse events hinder economic development. The second feature is that the sturdiest indicators belong to the pillars of *business sophistication*, *financial market development*, and *governance of firms*. On the other hand, the most critical bottlenecks belong to the pillars of *business sophistication*, *public governance*, *health*, and *infrastructure*.

Figure 12 presents a similar visualization, disaggregated by development indicators. Here, the sturdiest policy issues are *control of international distribution*, *venture capital availability*, *financing through local equity market*, *buyer sophistication*, and *ethical behavior of firms*. In contrast, the most critical bottlenecks are *production process sophistication*, *value chain breadth*, *extent of staff training*, *university-industry collaboration*, and *business impact of HIV/AIDS*. The reason why an indicator can be sturdy and a bottleneck at the same time is that resilience scores may be differ significantly between country-mode pairs. Figure 13 in the appendix presents another visualization at the level of the development pillars but disaggregated into countries.

6. Conclusions

The quantitative study of prioritization and resilience of public policies demands a systemic approach in order to provide rigorous guidelines for policy advice. Traditional methods such as regression analyses, growth diagnostics, and benchmarking are severely limited for this purpose because they neglect the fundamental systemic qualities of any economy. These include the interdependencies between policies, the importance of societal context (*i.e.*, initial conditions, structure, and development modes to pursue), the multiobjective goal-seeking behavior of governments, and political economy considerations that produce misaligned incentives. In this paper, we develop a complexity approach that overcomes these limitations and use it to understand the phenomenon of resilience in public policy.

Our framework allows identifying the allocation profiles that an adaptive government selects—through a behavioral game—in an attempt to reach the multiple targets of a prespecified development mode. These profiles are established in an environment where public functionaries in charge of implementing policies learn how to divert public funds. Thus, by modelling the policy-making process, our methodology is capable of analyzing the adaptive nature of resilience in policy issues when facing adverse events.

By disturbing the resource allocation to specific policy issues, we obtain multiple results that help us to understand policy resilience. First, some policy issues are resilient (*i.e.*, the development goals are reached earlier than expected) while others are fragile. Second, context matters because the level of resilience or fragility depends on the country's initial conditions and the adopted development mode. Third, for specific countries, some policy issues prove to be resilient across development modes. Fourth, although some development pillars tend to be resilient for specific countries, it is common to find that at least one of its indicators is fragile.

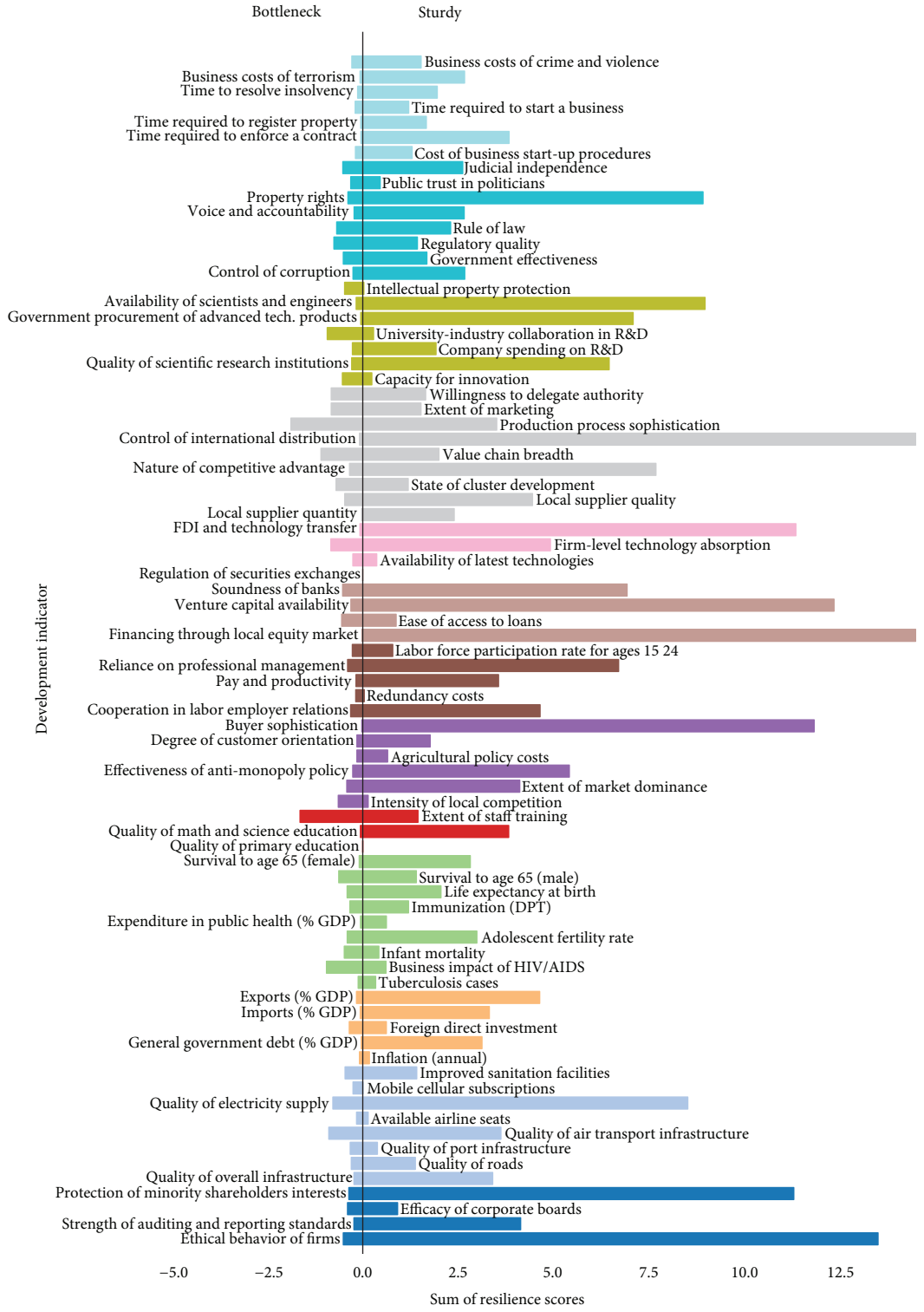

Figure 12: Sturdy policies and bottlenecks by development indicators. Bottlenecks: fragile policies in the 5th percentile of relative priorities. Sturdy: resilient policies in the 95th percentile of relative priorities.

Fifth, there is a set of sturdy policy issues that combine high levels of resilience with large budget allocations. In contrast, fragile policies with low budgetary priority are identified as the bottlenecks to development. Overall, there are more sturdy policies than bottlenecks. However, the latter should raise some flags in the development strategies of governments, since they represent major impairments to the economic development of their nations.

Appendix

Country-Level Analysis

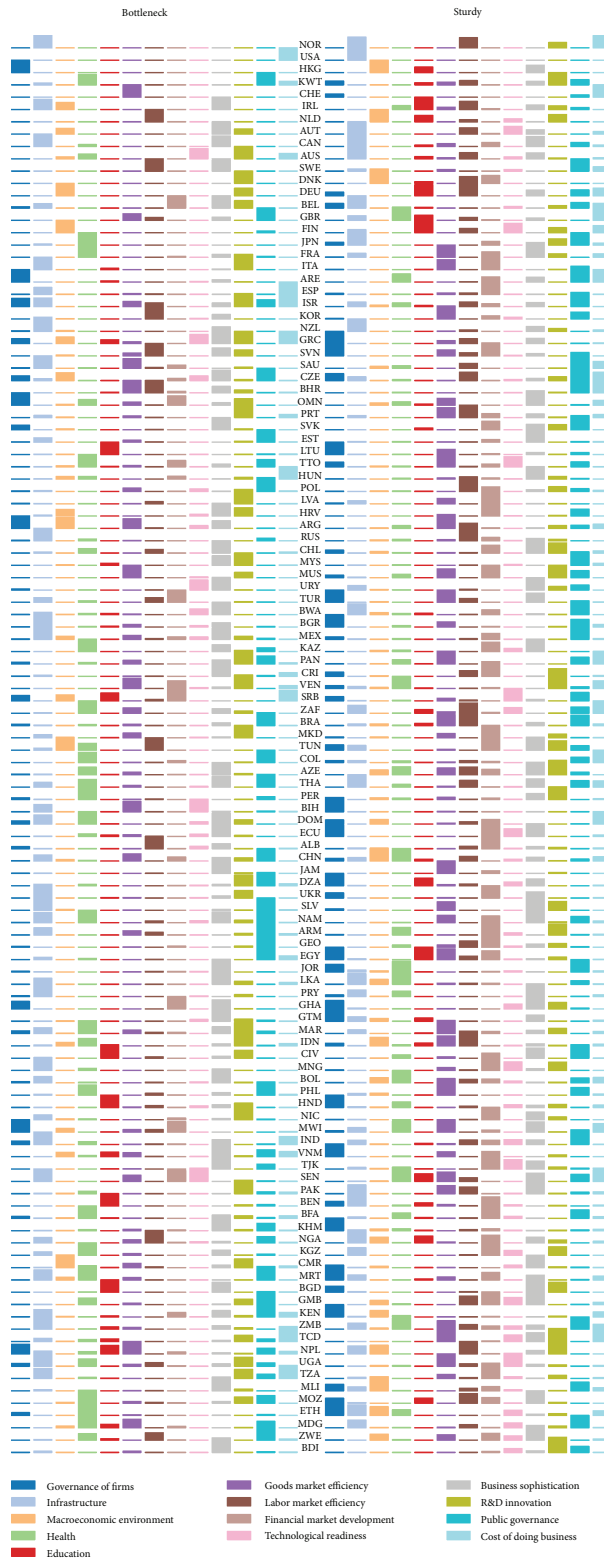

Figure 13: Sturdy policies and bottlenecks by development indicators by country (sorted by purchasing power parity income per capita). Bottlenecks: fragile policies in the 5th percentile of relative priorities. Sturdy: resilient policies in the 95th percentile of relative priorities.

Data Availability

The data was obtained from public datasets from the World Bank and the World Economic Forum.

Conflicts of Interest

The authors declare that they have no conflicts of interest.

References

[1] D. Colander and R. Kupers, *Complexity and the Art of Public Policy: Solving Society's Problems from the Bottom Up*, Princeton University Press, 2014.

[2] L. Robbins, *An Essay on the Nature and Significance of Economic Science*, McMillan, London, UK, 2014.

[3] A. Zolli and A. Healy, *Resilience: Why Things Bounce Back*, Free Press, New York, NY, USA, 2012.

[4] H. Simon, "The architecture of complexity," *Proceedings of the American Philosophical Society*, vol. 106, no. 6, pp. 467–482, 1962.

[5] H. Simon, *The Sciences of the Artificial*, MIT Press, Cambridge, MA, USA, 1996.

[6] G. Castañeda, F. Chávez-Juárez, and O. A. Guerrero, "How do governments determine policy priorities? Studying development strategies through spillover networks," *Journal of Economic Behavior & Organization*, vol. 154, pp. 335–361, 2018.

[7] G. Capano and J. J. Woo, "Resilience and robustness in policy design: a critical appraisal," *Policy Sciences*, vol. 50, no. 3, pp. 399–426, 2017.

[8] A. Barabási and M. Pósfai, *Network Science*, Cambridge University Press, Cambridge, UK, 2016.

[9] K. Anand, P. Gai, S. Kapadia, S. Brennan, and M. Willison, "A network model of financial system resilience," *Journal of Economic Behavior & Organization*, vol. 85, pp. 219–235, 2013.

[10] D. Grigat and F. Caccioli, "Reverse stress testing interbank networks," *Scientific Reports*, vol. 7, no. 1, article 15616, 2017.

[11] K. Chmutina, G. Lizarralde, A. Dainty, and L. Bosher, "Unpacking resilience policy discourse," *Cities*, vol. 58, pp. 70–79, 2016.

[12] A. Duit, "Resilience thinking: lessons for public administration," *Public Administration*, vol. 94, no. 2, pp. 364–380, 2016.

[13] N. Galea, A. Powell, M. Loosemore, and L. Chappell, "Designing robust and revisable policies for gender equality: lessons from the Australian construction industry," *Construction Management and Economics*, vol. 33, no. 5-6, pp. 375–389, 2015.

[14] L. Ceriani and C. Gigliarano, "Multidimensional well-being: a Bayesian networks approach," Technical Report 399, ECINEQ, Society for the Study of Economic Inequality, 2016.

[15] E. N. Cinicioglu, G. Ulusoy, Ş. Önsel Ekici, F. Ülengin, and B. Ülengin, "Exploring the interaction between competitiveness of a country and innovation using Bayesian networks," *Innovation and Development*, vol. 7, no. 2, pp. 175–209, 2017.

[16] M. Czyżewska and T. Mroczek, "Bayesian approach to the process of identification of the determinants of innovativeness," *e-Finanse: Financial Internet Quarterly*, vol. 10, no. 2, pp. 44–56, 2014.

[17] P. Hoyer, A. Hyvärinen, R. Scheines et al., "Causal discovery of linear acyclic models with arbitrary distributions," in *Proceedings of the Twenty-Fourth Conference on Uncertainty in Artificial Intelligence, UAI'08*, pp. 282–289, Arlington, Virginia, USA, 2008.

[18] S. M. Smith, K. L. Miller, G. Salimi-Khorshidi et al., "Network modelling methods for FMRI," *NeuroImage*, vol. 54, no. 2, pp. 875–891, 2011.

[19] G. Massara, T. Di Matteo, and T. Aste, "Network filtering for big data: triangulated maximally filtered graph," *Journal of Complex Networks*, vol. 5, no. 2, pp. 161–178, 2017.

[20] A. Hyvärinen and S. Smith, "Pairwise likelihood ratios for estimation of non-Gaussian structural equation models," *Journal of Machine Learning Research*, vol. 14, pp. 111–152, 2013.

[21] R. Hausmann, B. Klinger, and R. Wagner, "Doing growth diagnostics in practice: a'mindbook'," Technical Report 177, Center for International Development at Harvard University, 2008.

[22] P. Rondo-Brovetto and I. Saliterer, "Comparing regions, cities, and communities: local government benchmarking as an instrument for improving performance and competitiveness," *The Innovation Journal: The Public Sector Innovation Journal*, vol. 12, no. 3, 2007.

[23] H. Werlin, "Bottlenecks to developments: studies from the World Bank's Economic Development Institute," *Public Administration and Development*, vol. 11, no. 3, pp. 189–191, 1991.

Hindawi
Complexity
Volume 2018, Article ID 7409397, 5 pages
https://doi.org/10.1155/2018/7409397

Research Article

Instability in Stable Marriage Problem: Matching Unequally Numbered Men and Women

Gui-Yuan Shi,[1,2] **Yi-Xiu Kong**,[1,2] **Bo-Lun Chen**,[1] **Guang-Hui Yuan**,[3] **and Rui-Jie Wu**[2]

[1]*Faculty of Computer and Software Engineering, Huaiyin Institute of Technology, Huaian 233003, China*
[2]*Department of Physics, University of Fribourg, Fribourg 1700, Switzerland*
[3]*Fintech Research Institute, Shanghai University of Finance and Economics, Shanghai 200433, China*

Correspondence should be addressed to Rui-Jie Wu; ruijie.wu@unifr.ch

Received 12 June 2018; Accepted 8 August 2018; Published 5 September 2018

Academic Editor: Claudio Tessone

The goal of the stable marriage problem is to match by pair two sets composed by the same number of elements. Due to its widespread applications in the real world, especially the unique importance to the centralized matchmaker, a very large number of questions have been extensively studied in this field. This article considers a generalized form of the stable marriage problem, where different numbers of men and women need to be matched pairwise and the emergence of single men or women is inevitable. Theoretical analysis and numerical simulations confirm that even a small deviation on the number of men and women from the equality condition can have a large impact on the matching solution of the Gale-Shapley algorithm. These results provide insights to many of the real-world applications when matching two sides with an unequal number.

1. Introduction

The stable marriage problem (SMP) consists in matching men and women by pairs. By extension, this problem can consist in the matching of two groups composed of different elements. For instance, there are extensive applications in college admissions [1], labor markets [2], and many other social systems [3]. The recent advances in Internet technology have introduced the SMP into new applications: assigning a large number of users to internet server [4], matching peers in a P2P network according to preference [5], the resource allocation in 5G networks [6], or the matching mechanism of real-world dating website [7].

Many researchers studied the algorithms and properties on this fascinating and practical problem. The study of the SMP started in 1962 with the Gale-Shapley (G-S) algorithm [1]. This algorithm matches men and women with the guarantee that there is always a stable match for an equal number of men and women [8]. In 2012, the Nobel Prize in Economics was awarded to Lloyd S. Shapley and Alvin E. Roth for "the theory of stable allocations and the practice of market design." In this algorithm, each man ranks women separately, from his favorite to his least favorite. Then, each man who is still single issues a proposal to the highest woman in his list who has not rejected him yet. The woman then decides to accept or reject him, by retaining only the man who is the most desirable to her. This solution is proved to be one of the stable men-optimal solutions.

Besides mathematicians and computer scientists, statistical physicists are also interested in this issue [9, 10]. Indeed, statistical physics is used to treat the problem with a large number of particles, which is also well-suited to treat the SMP. The mean field theory was applied to calculate satisfaction of both men and women in the stable marriage problem, and it was found that men, who are the active side, were far happier than women [11]. This method can also be used to estimate the number of stable solutions [12, 13]. The replica method used in spin glass was applied to study the global optimal solution in bipartite matching, although this is not a stable solution [14–17]. In addition, some interesting varied

variations have been studied, such as the impact of matching on the matching of partial information [18, 19], spatial distribution, intrinsic fitness [20], and acceptance threshold [13].

So far, mainstream research has been focusing on the matching of the equal number of the two sides. In fact, however, real-world matching problems are seldom a match of a precisely equal size of two sides. We have seen many examples in daily life, the student admission, job market, the recent "one to one poverty alleviation program" policy promoted by the Chinese government, or even the real application of SMP: the marriage matching on dating website [7]. These problems are mostly matching between different numbers of elements on both sides. We are curious to know whether the original stable solution of the Gale-Shapley algorithm can be applied to these unequal size-matching problems and, if not, how would the stable solution of matching be changed? What is the overall happiness of all agents in the stable solution? Here, in this paper, we extend the stable marriage problem to a generalized stable marriage problem (GSMP), which represents a matching between any given sizes of the two sides. Dzierzawa and Oméro [13] implemented the numerical simulation to test the matching result of $N + 1$ men and N women, and their simulation shows that in this case, women are far happier than men according to the Gale-Shapley algorithm. This is hugely different from what the original SMP stable solution suggests. This is crucial because it reveals that the Gale-Shapley solution is very sensitive to even the smallest variation in the number of people and actually cannot be directly used to analyze many unequal size-matching problems. We further thoroughly study the stable solution in GSMP, a matching between any number of men and women. We carry out a theoretical analysis of the stable solution for GSMP and obtain the average happiness for men and women for any given population, and the result is in perfect match with the numerical simulations.

2. Methods

We start with the classical scenario with N male and M females to match pairwise. Here, we assume that everyone knows all people from the opposite gender and that there is a wish list for each person which represents the ranking of all persons from the other gender to her/his preference. Following previous research models [11, 13, 17], a reasonable and simple assumption is that all wish lists are randomly established and irrelevant. We define an energy function for each person, which is equal to the ranking of their eventual partner in their wish list. The lower energy one has, the happier the person is. When $N = M$, it is the conventional SMP. Here, we extend the SMP to groups with different sizes. When $N \neq M$, obviously, there will be some people who will remain single. For these persons, their energy is defined as one worse than the bottom of the wish list; that is to say, the energy is $M + 1$ for single men and $N + 1$ for women. Since the number of single persons is obvious, the result of the calculation can be simply converted for other definitions. Here, we use Greek letters to represent men and Latin letters to represent women. Their energy is denoted as e_m and e_w for men and women, respectively.

The G-S algorithm runs as follows: unengaged men will continue to send proposals to women, and women keep the one she prefers between the suitor and her provisional partner. The process stops when no man issues proposal again, either all men are engaged or the unengaged men are rejected by everyone. For $N \leq M$, this means that all men are engaged. For the case of $N > M$, M men are engaged and the remaining $N - M$ men are still single.

3. Result and Discussion

The stable marriage problem of the equal size of the two sides has been thoroughly studied by many previous researches. For $M = N$, several studies have proved that in the stable solution of G-S the algorithm, the average energy of men is $\overline{\epsilon_m} = \log(N)$, and the average energy of women is $\overline{\epsilon_w} = N/\log(N)$.

3.1. Matching for $M > N$

3.1.1. The Average Energy of Men. First, let us consider the situation that the number of women M is larger than the number of men N. During the process of men proposing to women, we notice the following: (1) the total energy of men is equal to the number of proposals men have already sent. (2) Once a woman is engaged, she will remain engaged (perhaps with different men) forever; that is to say, the number of partners will never decrease.

Now, we focus on the number of matched pairs in the proposing process; when it reaches to N, every man has already been assigned to a partner and the proposal process stops. When the number of matched pairs is K, there are $M - K$ women who remain unengaged. If one proposal is sent to an engaged woman, no matter the suitor or the woman's current provisional partner wins, the number of matched pairs will not change. If a proposal is sent to an unengaged woman, which has a probability of $(M - K)/M$, the number of matched pairs will increase to $K + 1$. It is easy to deduce that on average $M/(M - K)$, proposals have to be sent to match one more pair.

Thus, in order to increase the number of matched pairs from 0 to N, the expected total number of proposals men have to send is

$$L_{N,M} = \sum_{K=0}^{N-1} \frac{M}{M-K} = M\left(\sum_{i=1}^{M} \frac{1}{i} - \sum_{j=1}^{M-N} \frac{1}{j}\right). \quad (1)$$

Hence, the average energy of men when $M > N$ is

$$\overline{\epsilon_m} = \frac{L_{N,M}}{N} = \frac{M}{N} \ln \frac{M}{M-N}. \quad (2)$$

3.1.2. The Average Energy of Women. To obtain the average energy of women $\overline{\epsilon}_w$, let us consider the final stable solution, in which everyone's partner has been determined. Let us assume a chosen woman who was finally paired with the man ranked β in her list, so men who ranked higher than β in her list did not issue a proposal to her. According to the ranking of the men in the women's list, let us denote the

men's energy as follows: $\overline{\epsilon}_m(\alpha), \alpha \in \{1, 2, \cdots, N\}$. The men who ranked in the top $\beta - 1$ in the woman's list must have a better partner than the woman, which means the energy of the woman is higher than that of the assigned partners of these men. This is because if the rank of the lady in a certain men's list is less than the energy value of the man, then he must have already issued a proposal to the woman according to the G-S Algorithm, thus causing a conflict. We can compute the probability of a woman matched with the man ranked β in her list:

$$P_\beta = \coprod_{\alpha=1}^{\beta-1}\left(1 - \frac{\epsilon_m(\alpha)}{M}\right) * \frac{\epsilon_m(\beta)}{M}. \tag{3}$$

The energy of the single women is equal to $N + 1$. They did not receive any proposal; the probability is:

$$P_{N+1} = \prod_{\alpha=1}^{N}\left(1 - \frac{\epsilon_m(\alpha)}{M}\right). \tag{4}$$

Similarly, we use $\overline{\epsilon_m}$ to replace $\epsilon_m(\alpha)$; then we have

$$\begin{aligned} P_\beta &= \left(1 - \frac{\overline{\epsilon_m}}{M}\right)^{\beta-1} * \frac{\overline{\epsilon_m}}{M}, \\ P_{N+1} &= \left(1 - \frac{\overline{\epsilon_m}}{M}\right)^{N}. \end{aligned} \tag{5}$$

Consider $\overline{\epsilon_w} = \sum \beta * p_\beta$; we can estimate the average energy of women:

$$\overline{\epsilon_w} = \frac{\overline{\epsilon_m}}{M}\sum_{i=1}^{N} i * \left(1 - \frac{\overline{\epsilon_m}}{M}\right)^{i-1} + (N+1) * \left(1 - \frac{\overline{\epsilon_m}}{M}\right)^{N}. \tag{6}$$

The summation of the series gives

$$\epsilon_w = \frac{\overline{\epsilon_m}}{M}\frac{1 - ((1 - \overline{\epsilon_m})/M)^N}{(\overline{\epsilon_m}/M)^2} + \left(1 - \frac{\overline{\epsilon_m}}{M}\right)^{N}. \tag{7}$$

Since we have $\overline{\epsilon_m} = (M/N)\ln(M/(M-N))$, $(1 - (\overline{\epsilon_m}/M))^N$ approximately is equal to $(M-N)/M$.

$$\overline{\epsilon_w} = \frac{N}{\overline{\epsilon_m}} + \frac{M-N}{M}, \tag{8}$$

and also we can see

$$\overline{\epsilon_w} * \overline{\epsilon_m} \simeq N. \tag{9}$$

3.2. Matching for $M < N$

3.2.1. The Average Energy of Women. While $M < N$, let us denote the energy of each woman as ϵ_i, and the average of ϵ_i is denoted by $\overline{\epsilon_w}$.

In the final matching state, all the women are matched but $N - M$ men are left single. The probability of a man being single is $\prod_{i=1}^{M}(1 - (\epsilon_i/N))$; i.e., he is ranked lower than any of the current partner in women's lists. In total, we have $N - M$ men who are single, which means the probability of being single is $(N-M)/N$, so we have

$$\coprod_{i=1}^{M}\left(1 - \frac{\epsilon_i}{N}\right) = \frac{N-M}{N}. \tag{10}$$

Approximately, we use $\overline{\epsilon_w}$ to replace ϵ_i,

$$\left(1 - \frac{\overline{\epsilon_w}}{N}\right)^{M} = \frac{N-M}{N}, \tag{11}$$

by taking the logarithm of both sides; we have

$$\overline{\epsilon_w} = \frac{N}{M}\ln\frac{N}{N-M}. \tag{12}$$

3.2.2. The Average Energy of Men. Let us consider the final stable state of matching which we know the exact matching result of everyone. For any chosen man, we denote the energy of women in his list as $\epsilon_w(j), j \in \{1, 2, \ldots, M\}$. Then we have the probability that he was accepted by the woman ranked i^{th} in his list:

$$Q_i = \prod_{j=1}^{i-1}\left(1 - \frac{\epsilon_w(j)}{N}\right)\frac{\epsilon_w(i)}{N}. \tag{13}$$

And the probability that he was rejected by all women is (we assume the energy of each single men is $M + 1$)

$$Q_{M+1} = \prod_{j=1}^{M}\left(1 - \frac{\epsilon_w(j)}{N}\right). \tag{14}$$

We can approximate $\epsilon_w(j)$ with the mean value $\overline{\epsilon_w}$, when N is large. By averaging over i, we obtain:

$$\begin{aligned} \overline{\epsilon_m} &= \sum_{i=1}^{M} i\left(1 - \frac{\overline{\epsilon_w}}{N}\right)^{i-1}\frac{\overline{\epsilon_w}}{N} + (M+1)\left(1 - \frac{\overline{\epsilon_w}}{N}\right)^{M}, \\ \overline{\epsilon_m} &= \frac{\overline{\epsilon_w}}{N}\frac{1 - (1 - (\overline{\epsilon_w}/N))^M}{(\overline{\epsilon_w}/N)^2} + \left(1 - \frac{\overline{\epsilon_w}}{N}\right)^{M}, \end{aligned} \tag{15}$$

since $(1 - (\overline{\epsilon_w}/N))^M = (N-M)/N$; we have

$$\overline{\epsilon_w}\left(\overline{\epsilon_m} - \frac{N-M}{M}\right) = M. \tag{16}$$

3.3. Numerical Simulations. The simulation result is shown in Figure 1. Without the loss of generality, we fix the number of men equal to 1000 and vary the number of women M from 1 to 2000. Under our definition of single's energy, as our theoretical result predicted, the average energy of men increases in the beginning and almost

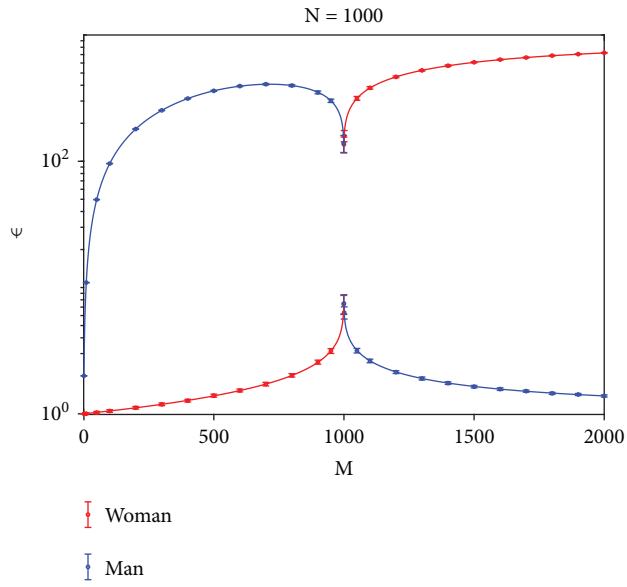

FIGURE 1: The average energy of N men and M women versus the number of women M, where N is set to 1000. The result is obtained by averaging over 100 realizations. The dots and their error bars represent the simulations results and the standard deviation, respectively. The solid lines represent our theoretical predictions.

saturate when M reaches around 700. The energy plateau is mainly caused by the fact that we set the energy of single men at $M + 1$. Although other definitions may apply, we choose this definition out of many reasonable ones to make the theoretical analysis easier. It is notable that the average energy is low when M is close to 1. It is instructive to many social phenomena. When there are too few women (M close to 1), most men end up single in the matching. But the feeling of happiness, as written by sociologist Ruut Veenhoven [21], "results from comparison" may come from the relative comparison among surroundings, so that the overall happiness which is low may not be a surprising outcome.

The energies of both men and women have dramatic changes when M approaches 1000. The energy of men has a sharp drop in this region while the energy of women experiences a big rise. The energies of the active side and passive side exchange their positions. As M increases, the energy of men continues to decrease; at the meantime, the energy of women keeps growing which is natural for the situation that more women compete for a certain number of men. In total, our simulation result verified our previous theoretical analysis.

For many of the actual matching problems, the change in the number of people's happiness is not as sensitive to the theoretical predictions. This may be due to some intrinsic factors: appearance, test scores, university rankings, work ability, salary level, and so on, which will cause the wish list to become relevant. One of our studies recently [22] reveals that the correlation of the people's wish lists can significantly reduce the inherent instability of the G-S algorithm in the generalized group size case.

4. Conclusion

In summary, we extend the study of the conventional stable marriage problem to groups with different numbers of persons. This study has a realistic impact because the numbers of matching parties are often different in many scenarios in the real world and the losers of the competition are widespread. For the traditional N men-M women matching problem, it is widely accepted that the Gale-Shapley algorithm leads to a matching result in which the active side occupies a huge advantage. However, we find that even by reducing only one woman, the men of the active side become obviously disadvantageous, which means that original stable matching solution is super sensitive to changes in the number of matching members.

In this paper, we thoroughly study the matching solution of unequally sized stable marriage problem and provide both a theoretical solution and numerical simulations. These findings help to further understand the structure and properties of the SMP solution; it also sheds a light on the matching process of matchmakers or resource allocators who deal with many of the real bipartite matching problems with scarcity of one side.

Data Availability

The data used to support the findings of this study are available from the corresponding author upon request.

Conflicts of Interest

The authors declare no conflict of interest.

Acknowledgments

We would like to thank Prof. Yi-Cheng Zhang, Alexandre Vidmer, and Wen-Yao Zhang for helpful discussions. This research is supported in part by the Chinese National Natural Science Foundation under grant no. 61602202 and Natural Science Foundation of Jiangsu Province under grant nos. BK20160428 and BK20161302. GYS and YXK acknowledge the support from China Scholarship Council (CSC).

References

[1] D. Gale and L. S. Shapley, "College admissions and the stability of marriage," *The American Mathematical Monthly*, vol. 69, no. 1, pp. 9–15, 1962.

[2] A. E. Roth, "The evolution of the labor market for medical interns and residents: a case study in game theory," *Journal of Political Economy*, vol. 92, no. 6, pp. 991–1016, 1984.

[3] A. E. Roth and M. A. O. Sotomayor, *Two-Sided Matching: A Study in Game-Theoretic Modeling and Analysis (No. 18)*, Cambridge University Press, 1992.

[4] B. M. Maggs and R. K. Sitaraman, "Algorithmic nuggets in content delivery," *ACM SIGCOMM Computer Communication Review*, vol. 45, no. 3, pp. 52–66, 2015.

[5] D. Lebedev, F. Mathieu, L. Viennot, A. T. Gai, J. Reynier, and F. De Montgolfier, "On using matching theory to understand

P2P network design," in *INOC 2007, International Network Optimization Conference*, Spa, Belgium, 2007.

[6] M. Hasan and E. Hossain, "Distributed resource allocation in 5G cellular networks," in *Towards 5G: Applications, Requirements and Candidate Technologies*, pp. 245–269, Wiley, 2015.

[7] G. J. Hitsch, A. Hortaçsu, and D. Ariely, "Matching and sorting in online dating," *American Economic Review*, vol. 100, no. 1, pp. 130–163, 2010.

[8] A. E. Roth, "The economics of matching: stability and incentives," *Mathematics of Operations Research*, vol. 7, no. 4, pp. 617–628, 1982.

[9] Y.-C. Zhang, "The information economy," in *Non-Equilibrium Social Science and Policy*, Springer, Cham, 2017.

[10] A. Chakraborti, D. Challet, A. Chatterjee, M. Marsili, Y. C. Zhang, and B. K. Chakrabarti, "Statistical mechanics of competitive resource allocation using agent-based models," *Physics Reports*, vol. 552, pp. 1–25, 2015.

[11] M. J. Oméro, M. Dzierzawa, M. Marsili, and Y. C. Zhang, "Scaling behavior in the stable marriage problem," *Journal de Physique I*, vol. 7, no. 12, pp. 1723–1732, 1997.

[12] B. Pittel, "The average number of stable matchings," *SIAM Journal on Discrete Mathematics*, vol. 2, no. 4, pp. 530–549, 1989.

[13] M. Dzierzawa and M. J. Oméro, "Statistics of stable marriages," *Physica A: Statistical Mechanics and its Applications*, vol. 287, no. 1-2, pp. 321–333, 2000.

[14] M. Mézard and G. Parisi, "Replicas and optimization," *Journal de Physique Lettres*, vol. 46, no. 17, pp. 771–778, 1985.

[15] M. Mézard and G. Parisi, "On the solution of the random link matching problems," *Journal de Physique*, vol. 48, no. 9, pp. 1451–1459, 1987.

[16] V. S. Dotsenko, "Exact solution of the random bipartite matching model," *Journal of Physics A: Mathematical and General*, vol. 33, no. 10, pp. 2015–2030, 2000.

[17] G. Y. Shi, Y. X. Kong, H. Liao, and Y. C. Zhang, "Analysis of ground state in random bipartite matching," *Physica A: Statistical Mechanics and its Applications*, vol. 444, pp. 397–402, 2016.

[18] Y. C. Zhang, "Happier world with more information," *Physica A: Statistical Mechanics and its Applications*, vol. 299, no. 1-2, pp. 104–120, 2001.

[19] P. Laureti and Y. C. Zhang, "Matching games with partial information," *Physica A: Statistical Mechanics and its Applications*, vol. 324, no. 1-2, pp. 49–65, 2003.

[20] G. Caldarelli and A. Capocci, "Beauty and distance in the stable marriage problem," *Physica A: Statistical Mechanics and its Applications*, vol. 300, no. 1-2, pp. 325–331, 2001.

[21] R. Veenhoven, "Is happiness relative?," *Social Indicators Research*, vol. 24, no. 1, pp. 1–34, 1991.

[22] Y. X. Kong, G. H. Yuan, L. Zhou, R. J. Wu, and G. Y. Shi, "Competition may increase social happiness in bipartite matching problem," 2018, http://arxiv.org/abs/1805.09088v2.